

## **VOLUME I**

### **BUDGET PERIOD I TOPICAL REPORT**

#### **DESIGN AND IMPLEMENTATION OF A CO<sub>2</sub> FLOOD UTILIZING ADVANCED RESERVOIR CHARACTERIZATION AND HORIZONTAL INJECTION WELLS IN A SHALLOW SHELF CARBONATE APPROACHING WATERFLOOD DEPLETION**

<b>Cooperative Agreement Number:</b>	<b>DE-FC22-94BC14991</b>	
<b>Participant Organization:</b>	<b>Phillips Petroleum Company 4001 Penbrook Odessa, Texas 79762</b>	
<b>Date of Report:</b>	<b>02/01/2001</b>	
<b>Award Date:</b>	<b>06/03/94</b>	
<b>Anticipated Completion Date:</b>	<b>01/02/01</b>	
<b>Program Manager:</b>	<b>Don R. Wier</b>	<b>(06/94–12/95)</b>
	<b>John S. Chimahusky</b>	<b>(12/95–12/97)</b>
	<b>Kirk L. Czirr</b>	<b>(12/97–01/01)</b>
<b>Project Co-ordinator:</b>	<b>Larry Hallenbeck</b>	<b>(06/94–12/95)</b>
	<b>Matthew G. Gerard</b>	<b>(12/95–06/96)</b>
	<b>Kim B. Dollens</b>	<b>(06/96–10/98)</b>
	<b>Rex Owen</b>	<b>(10/98–01/01)</b>
<b>Principal Investigators:</b>	<b>K. J. Harpole R. L. King</b>	
	<b>Ed G. Durrett B. A. Baldwin</b>	
	<b>Susan Snow</b>	<b>D. Wegener</b>
	<b>J. S. Bles</b>	<b>M. Navarrette</b>
	<b>Carlton Robertson</b>	
	<b>C. D. Caldwell</b>	
	<b>D. J. Harms</b>	
<b>Contracting Officer's Representative (COR):</b>	<b>Jerry F. Casteel</b>	<b>(to 9/98)</b>
	<b>Daniel Ferguson</b>	<b>(9/98–01/01)</b>

**Reporting Period:**

**06/03/94 - 6/30/96**



## LEGAL NOTICE / DISCLAIMER

This report was prepared by Phillips Petroleum Company pursuant to a Cooperative Agreement partially funded by the U. S. Department of Energy, and neither Phillips Petroleum Company nor any of its subcontractors nor the U. S. Department of Energy, nor any person acting on behalf of either:

- (A) Makes any warranty or representation, express or implied, with respect to the accuracy, completeness, or usefulness of the information contained in this report, or that the use of any information, apparatus, method, or process disclosed in this report may not infringe privately-owned rights; or
- (B) Assumes any liabilities with respect to the use of, or for damages resulting from the use of, any information, apparatus, method or process disclosed in this report.

Reference herein to any specific commercial product, process, or service by trade name, trademark, manufacturer, or otherwise, does not necessarily constitute or imply its endorsement, recommendation, or favoring by the U. S. Department of Energy. The views and opinions of authors expressed herein do not necessarily state or reflect those of the U. S. Department of Energy.

## **REPORT TABLE OF CONTENTS**

	<b>Figure*</b>
<b>Introduction</b>	
<b>General Information</b>	<b>I</b>
<b>3-D Reservoir Description</b>	<b>II</b>
<b>Field Development History</b>	<b>III</b>
<b>Field Production Constraints and Design Logic</b>	<b>IV</b>
<b>Evaluation of Cost-Share Project Results</b>	<b>V</b>
<b>Supporting Data</b>	<b>VI</b>
<b>Environmental Information</b>	<b>VII</b>

\* - The information required by the cooperative agreement is defined by Figures I through VII on pages C-8 through C-13 in Exhibit C of the co-operative agreement signed on June, 1994 by Phillips Petroleum Company and the Department of Energy (DOE).

## INTRODUCTION

The cooperative agreement signed in June, 1994 by Phillips Petroleum Company and the Department of Energy (DOE) requires two Topical Reports to establish a minimum dataset and data collection for this Class II activity. The first report is due at the end of Budget Period I and should include preliminary data and permit the DOE to review such data before the project is completed. The second Topical Report is due at the end of Budget Period II. Budget Period I was completed on June 30, 1996. The report presented here fulfills the requirement for the first Topical Report.

The information required by the cooperative agreement is that outlined in Figures I through VII on pages C-8 through C-13 in Exhibit C of the agreement. The major topics covered by these Figures are:

Figure I	General Information;
Figure II	3-D Reservoir Description;
Figure III	Field Development History;
Figure IV	Field Production Constraints and Design Logic;
Figure V	Evaluation of Cost-Share Project Results;
Figure VI	Supporting Data;
Figure VII	Environmental Information.

A copy of the Figure for a given major topic is given directly behind the tab for that major topic.

# **FIGURE I**

## FIGURE I

### GENERAL INFORMATION

**Field Name:** South Cowden

**Reservoir Name:** Grayburg

**State:** Texas

**County(s):** Ector

**Formation(s):** Grayburg and San Andres

**RRC District (If Texas):** 8

**Field Discovery data:** November 28, 1932

**Current Operator:** Phillips Petroleum Company

**Current (6/1996) working interest ownership (names and percentages of all those > 10%):**

H. A. De Compeigne Jr.	.02667570
Fina Oil & Chemical	.10997580
McRae Management Trust	.00469110
Autry C. Stephens	.04019890
Patoil Corp.	.03864420
W. F. Pennebaker	.00469110
Nancy Sealy Thompson	.00469110
Violent Graves Stubbeman	.00469110
Phillips Petroleum Company	.76574100

**Project description (approximately 500 - 1000 words - from public abstract):**

### ABSTRACT

The work reported here covers Budget Phase I of the project. The principal tasks in Budget Phase I are the Reservoir Analysis and Characterization Task and the Advanced Technology Definition Task. Completion of these tasks have enabled an optimum carbon dioxide (CO<sub>2</sub>) flood project to be designed and evaluated from an economic and risk analysis standpoint. Field implementation of the project has

been recommended to the working interest owners of the South Cowden Unit (SCU) and approval has been obtained.

The project focused on reducing initial investment cost by utilizing horizontal injection wells and concentrating the project in the best productivity area of the field. An innovative CO<sub>2</sub> purchase agreement (no take or pay requirements, CO<sub>2</sub> purchase price tied to West Texas Intermediate (WTI) crude oil price) and gas recycle agreements (expensing cost as opposed to large capital investments for compression) were negotiated to further improve project economics.

A detailed San Andres reservoir characterization study was completed by an integrated team of geoscientists and engineers. The study consisted of detailed core description, integration of log response to core descriptions, mapping of the major flow units, evaluation of porosity and permeability relationships, geostatistical analysis of permeability trends, and direct integration of reservoir performance with the geological interpretation. The study methodology fostered iterative bidirectional feedback between the reservoir characterization team and the reservoir engineering/simulation team to allow simultaneous refinement and convergence of the geological interpretation with the reservoir model. The fundamental conclusion from the study was that South Cowden exhibited favorable enhanced oil recovery characteristics, particularly reservoir quality and continuity.

Detailed San Andres core descriptions were made of two full cores and several partial cores from the South Cowden Unit. Core information from the contiguous Emmons and Moss Units were also incorporated into the study. The core study concluded that reservoir quality in the South Cowden Unit is controlled primarily by the distribution of a bioturbated and diagenetically altered rock type with a distinctive “chaotic” texture. The “chaotic” modifier derives from the visual effect of pervasive, small-scale intermixing of tan oil-stained reservoir rock with tight gray non-reservoir rock.

The San Andres section was divided into multiple zones, A through G, based on the core study and gamma ray markers that correlate wells across the unit. Each zone was mapped as continuous across the field. The “chaotic” reservoir rock extends from Zone C to the lower part of Zone F. Zones D and E are considered the main floodable zones, though Zone F is also productive and Zone C is productive above the oil-water contact.

Repeat Formation Tester (RFT) measurements indicated good vertical pressure communication between Zones D and E, fair communication with Zone F, and poor communication with Zone C. The lower parts of Zone F is separated from Zone E by a thin silty dolomite layer, which may hinder efficient vertical sweep between the two zones. Zone C is effectively isolated from the zones above. Open-hole hydraulic fracture tests indicate a strong tendency for induced fractures to grow downward from the productive zones to Zone A, a high permeability, normally water bearing grainstone layer.

Understanding of reservoir rock distribution, identification of vertical pressure barriers within the reservoir (especially relative to the oil-water contact), and recognition of the nature of hydraulic fracture propagation in the reservoir were critical to the formulation of the CO<sub>2</sub> flood development plan: Horizontal water alternating gas (WAG) injection wells placed downstructure in Zones D and E, which

are above the oil-water contact throughout the project area and do not have internal vertical pressure barriers. Vertical WAG injection wells placed upstructure, where Zone C is above the oil-water contact but isolated by a vertical pressure barrier from the CO<sub>2</sub> sweep in Zones D and E. Perforation of the lower part of Zone F in vertical injectors will compensate for vertical sweep inefficiency across the weak pressure barrier between Zone F and E. Injection pressures in both horizontal and vertical WAG injectors will be kept below the fracture gradient (0.58 psi/ft) to minimize CO<sub>2</sub> losses to deeper, nonproductive zones.

A full-field reservoir simulation model was constructed covering all of South Cowden Unit (SCU) , Emmons Unit and a portion of the Moss Unit, both of which border SCU to the north. Model grid and layering were designed to conform to the geological configuration of the reservoir. Porosity, permeability, and flow properties of the major reservoir facies identified by the reservoir characterization team were incorporated into the model. An iterative, “predictive” history matching approach was employed whereby the team were involved in making refinements to reservoir description until the model was able to accurately predict historical waterflood performance. This predictive approach provides added confidence in future performance forecasts.

Critical laboratory data on CO<sub>2</sub>/oil phase behavior, minimum miscibility pressure, and oil recovery efficiency were matched and incorporated into the model. The model was then used to evaluate alternative CO<sub>2</sub> project developments, including the optimum use of horizontal CO<sub>2</sub> injection wells. The most attractive project development incorporated both horizontal and vertical CO<sub>2</sub> injection wells to conform to the reservoir geology and maximize sweep efficiency. This configuration was presented as the Authority for Expenditure (AFE) “Base Case” development plan.

**Project team members:**

Don R. Wier	Larry Hallenbeck
John S. Chimahusky	Matthew G. Gerard
K. L. Czirr	Kim B. Dollens
R. Owen	K. J. Harpole
R. L. King	Ed G. Durrett
B. A. Baldwin	S. Snow
D. Wegener	J. S. Bles
M. Navarrette	C. R. Robertson
C. D. Caldwell	D. J. Harms

**Technical contracts (name, affiliation, phone, address):**

Contract No. DE-FC22-94BC14991

**Primary Drive Mechanism:**

Solution gas and fluid expansion

**Estimated primary recovery factor (%):**

15%

**Estimated incremental Secondary Recovery Factor (%):**

20%

**Estimated Total of Primary and Secondary Recovery Factor (%):**

40%

**Date of first production:**

June 9, 1948

**Number of wells drilled in Field (to 6/96):**

104

**Well Patterns (5-Spot, 9-spot, line drive, etc.):**

Modified inverted 5-spot, peripheral

**Number of wells penetrating reservoir (to 6/96):**

**Total completions to date in field (to 6/96):**

69

**Total current completions, each reservoir (to 6/96):**

40

**Total current producers, each reservoir (to 6/96):**

29

**Total current injection wells, each reservoir (to 6/96):**



**Number of flowing wells (to 6/96):**

None – all have pumping equipment

**Summary field history (approximately 500 words):**

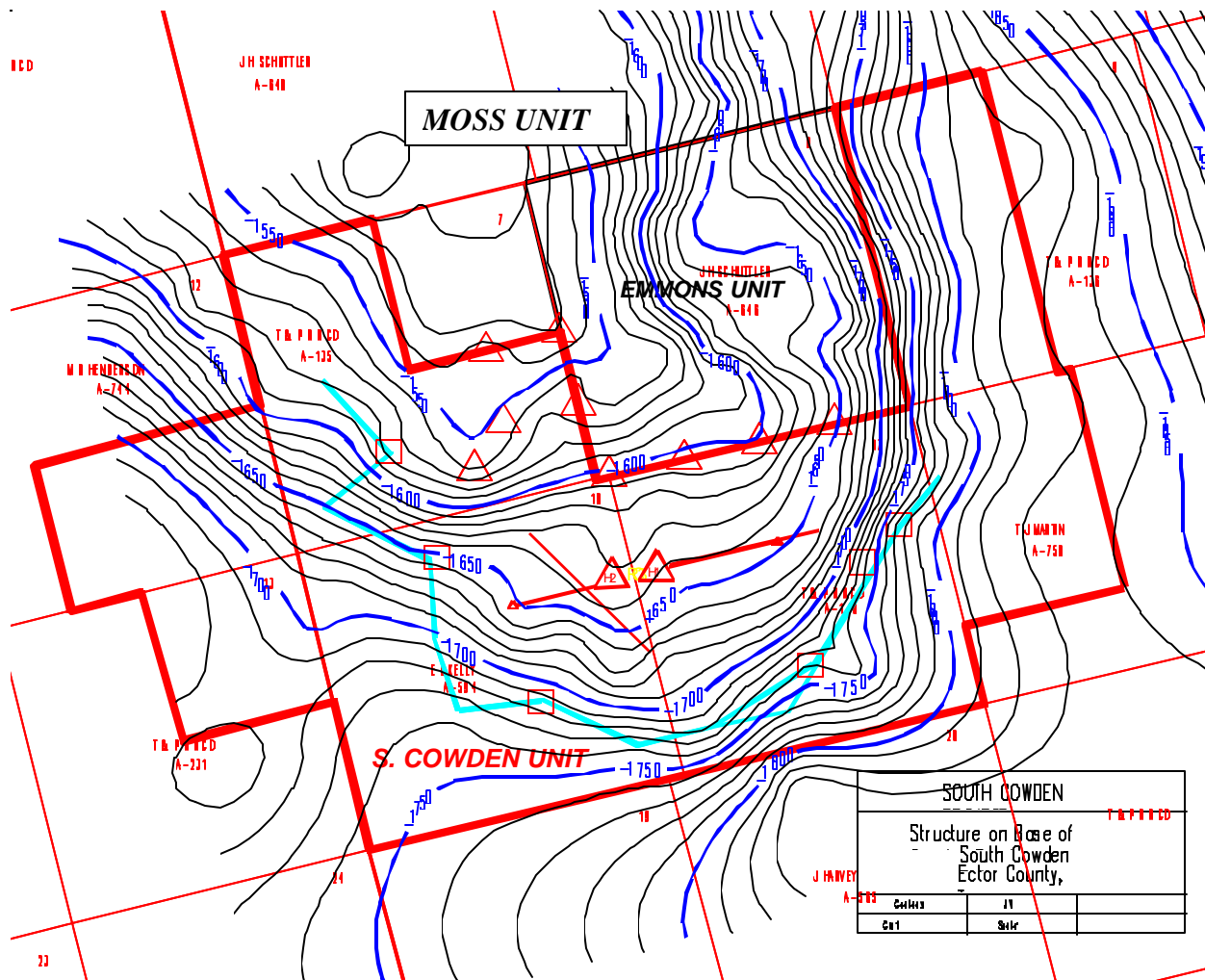
The South Cowden Unit is part of the South Cowden Field of Ector County, Texas. Production is from the Grayburg and San Andres dolomite formations of Permian Age, at an approximate depth of 4550 feet. These formations were deposited in shallow carbonate shelf environments along the eastern margin of the Central Basin Platform. The primary target of CO<sub>2</sub> flood development under the proposed project is a 150-200 foot gross interval within the San Andres. The original oil-in-place was estimated at 86.5 million barrels. The field was discovered in 1932, with production commencing in the project area June 9, 1948. Unitization occurred during 1965, when waterflood operations were initiated. The Unit was approaching its economic limit under secondary recovery, producing about 370 barrels of oil per day (BOPD) at a watercut in excess of 90% from 42 active producers and 15 active water injectors. Ultimate primary plus secondary recovery was expected to be 35 million stock tank barrels (STB), or approximately 40% of the original oil-in-place (OOIP).

In June of 1994, Phillips Petroleum and the Department of Energy (DOE) signed a contract for the development of the South Cowden CO<sub>2</sub> flood. The DOE would provide funds for the detailed reservoir characterization of South Cowden and, if approved, would participate in the actual demonstration of the project. In return, Phillips Petroleum would make public any technology gained from the project and would make strong efforts to publish the results. Technology transfer would be an integral part of the project.

The DOE project performance forecasts were based on a 40% hydrocarbon pore volume (HCPV) total CO<sub>2</sub> injection volume. All produced gas assumed mixed with purchased CO<sub>2</sub> and reinjected through a central facility. No natural gas liquid (NGL) recovery was premised in the preliminary forecasts. Ultimate CO<sub>2</sub> flood incremental oil recovery above continued waterflood operations in the DOE project area was forecasted to be 12.4% of the OOIP within the project area. CO<sub>2</sub> utilization efficiency is forecast to be 8.5 MCF/STB incremental oil. These performance projections are typical for CO<sub>2</sub> floods in the San Andres in west Texas.

**Project Locations:**

The Phillips Petroleum operated South Cowden Unit (SCU) is located 10 miles south of the city of Odessa in Ector County, Texas. The South Cowden Unit is directly offset by two other San Andres units. Phillips' Emmons Unit (purchased from Fina in 1996) and Unocal's Moss Unit. Figure I.1 displays a structure map of South Cowden and surrounding units.



**Figure I.1**

## **FIGURE II**

## **FIGURE II**

### **3-D DESCRIPTION OF RESERVOIR**

#### **AREAL AND VERTICAL DESCRIPTION:**

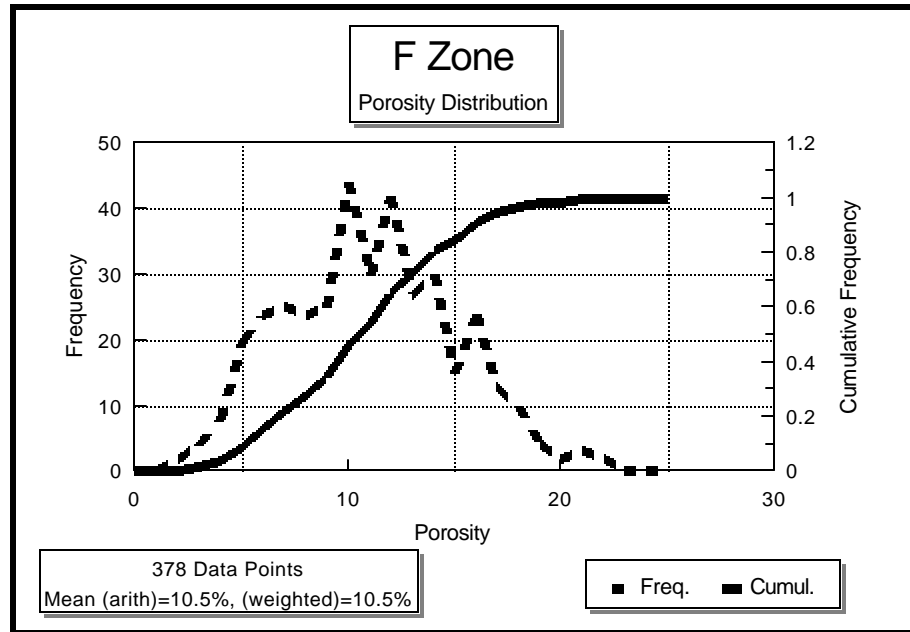
Simulation maps are taken from the original model used to forecast the authority for expenditure (AFE) base case. Note the original model had six layers. One layer each for the F, D and C zones and three layers for the E zone. Porosity and permeability distribution plots are taken from all available core data. Geological maps taken from geological model used for AFE generation.

#### **Areal Extent:**

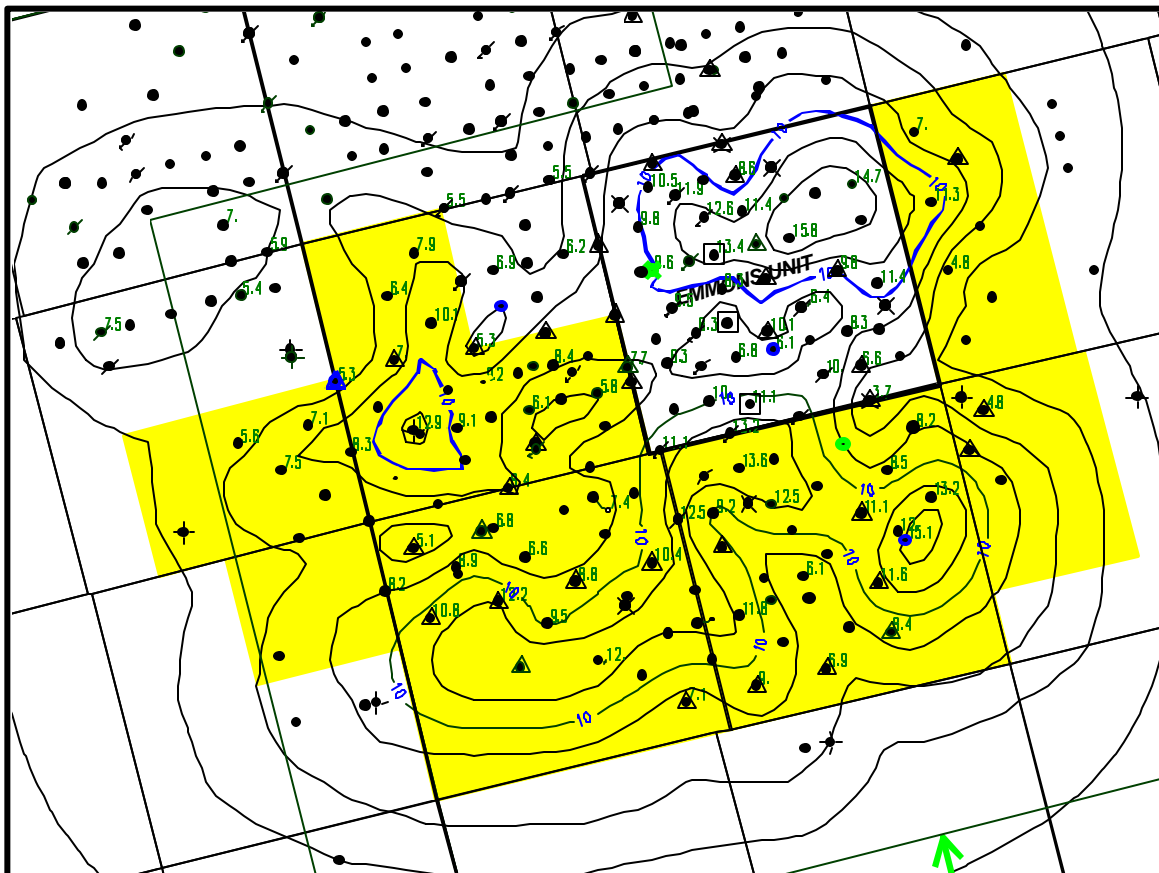
2050 acres

# Porosity mean, distribution and map:

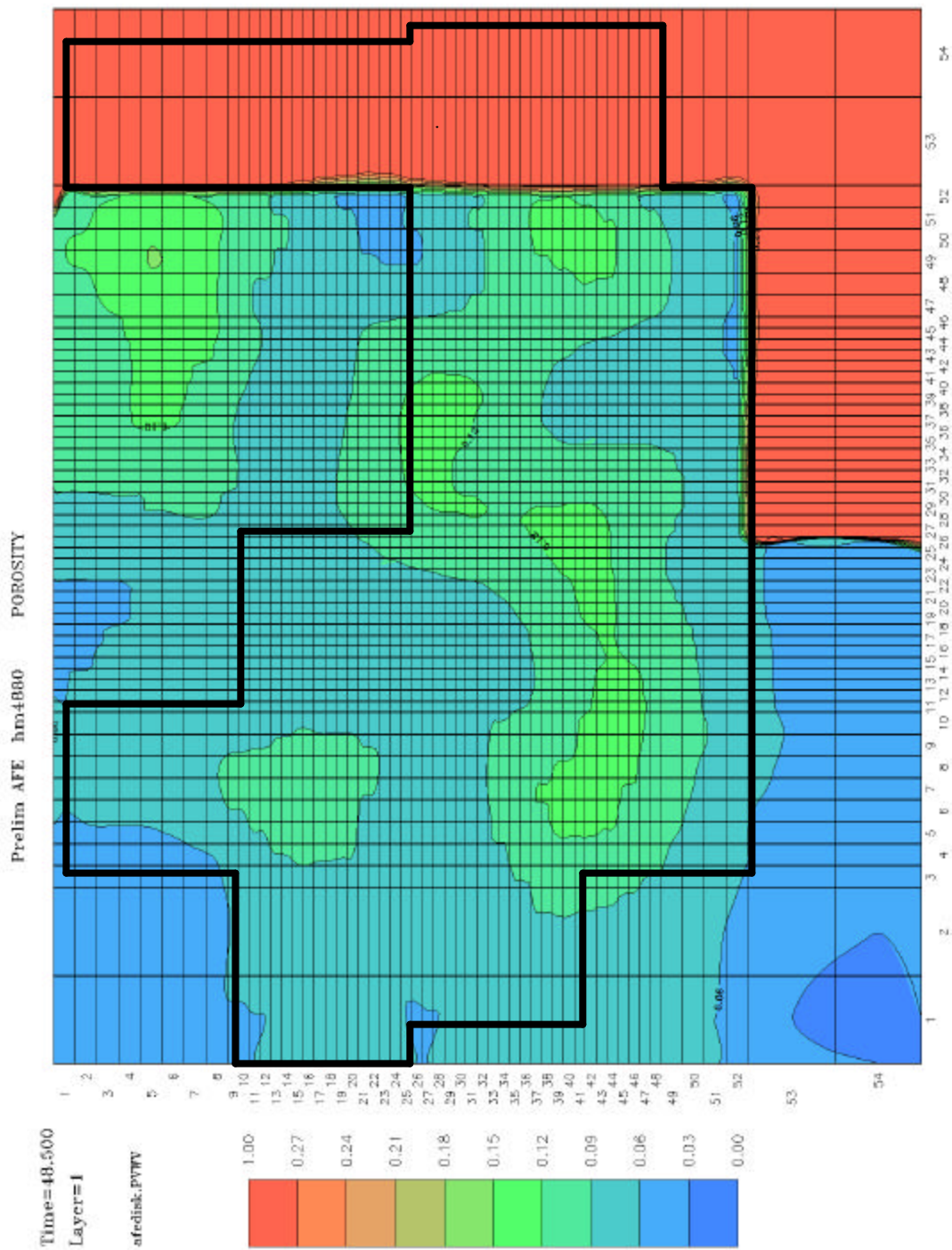
F Zone Distribution and Mean



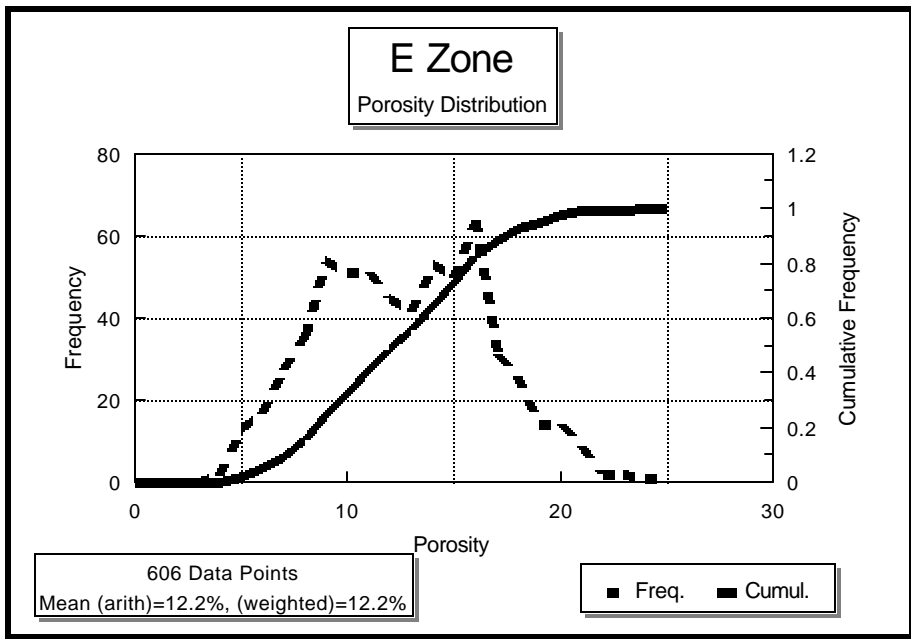
Average Porosity Map (San Andres zone F – geological mapping)



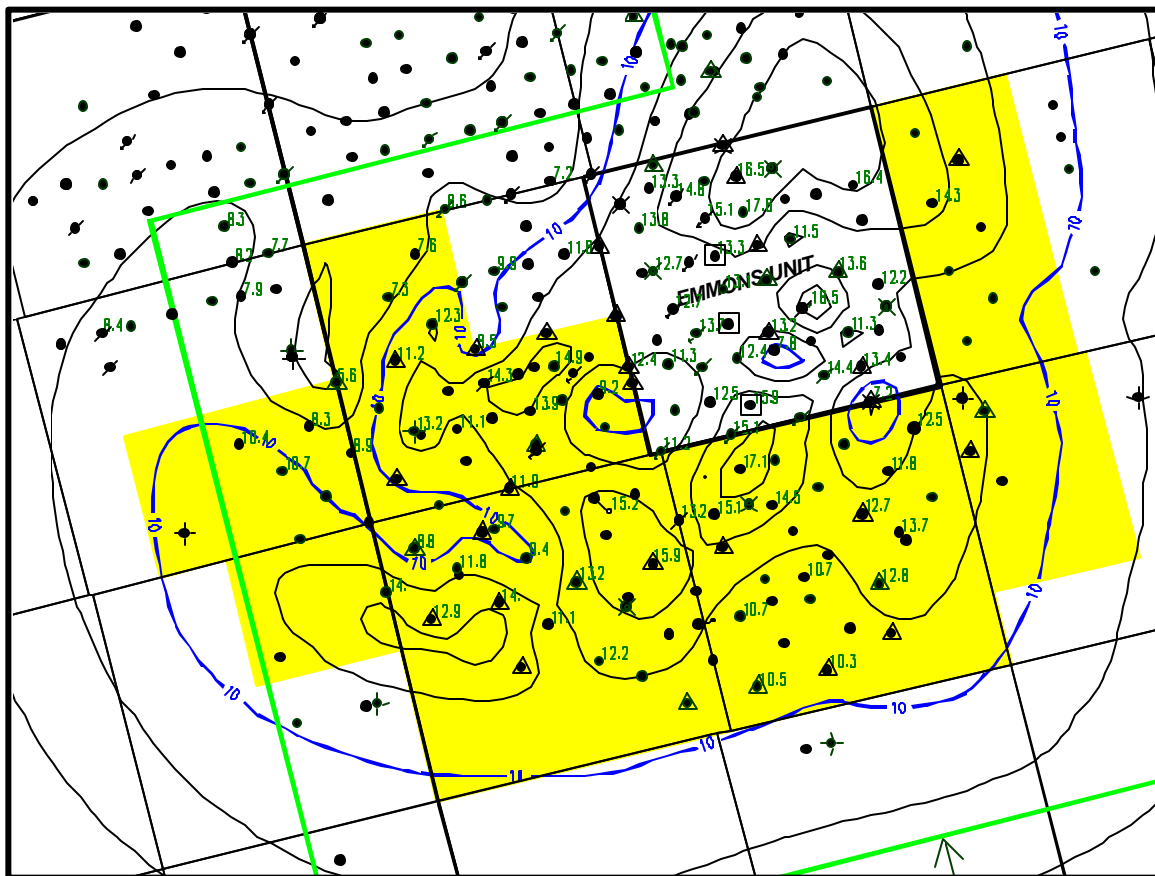
Average Porosity Map (San Andres zone F – simulation model)



## E Zone Distribution and Mean

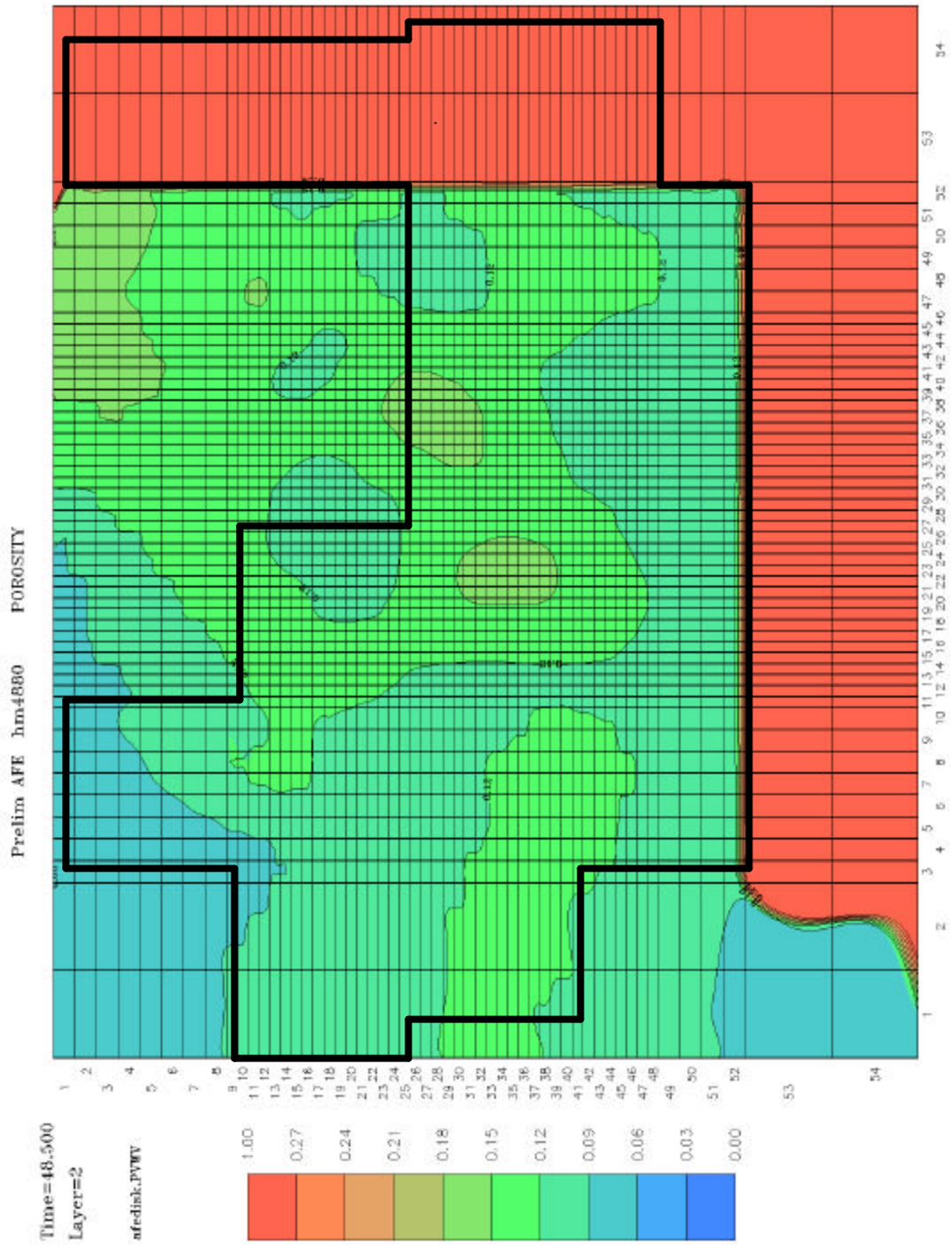


### Average Porosity Map (San Andres zone E – geological mapping)

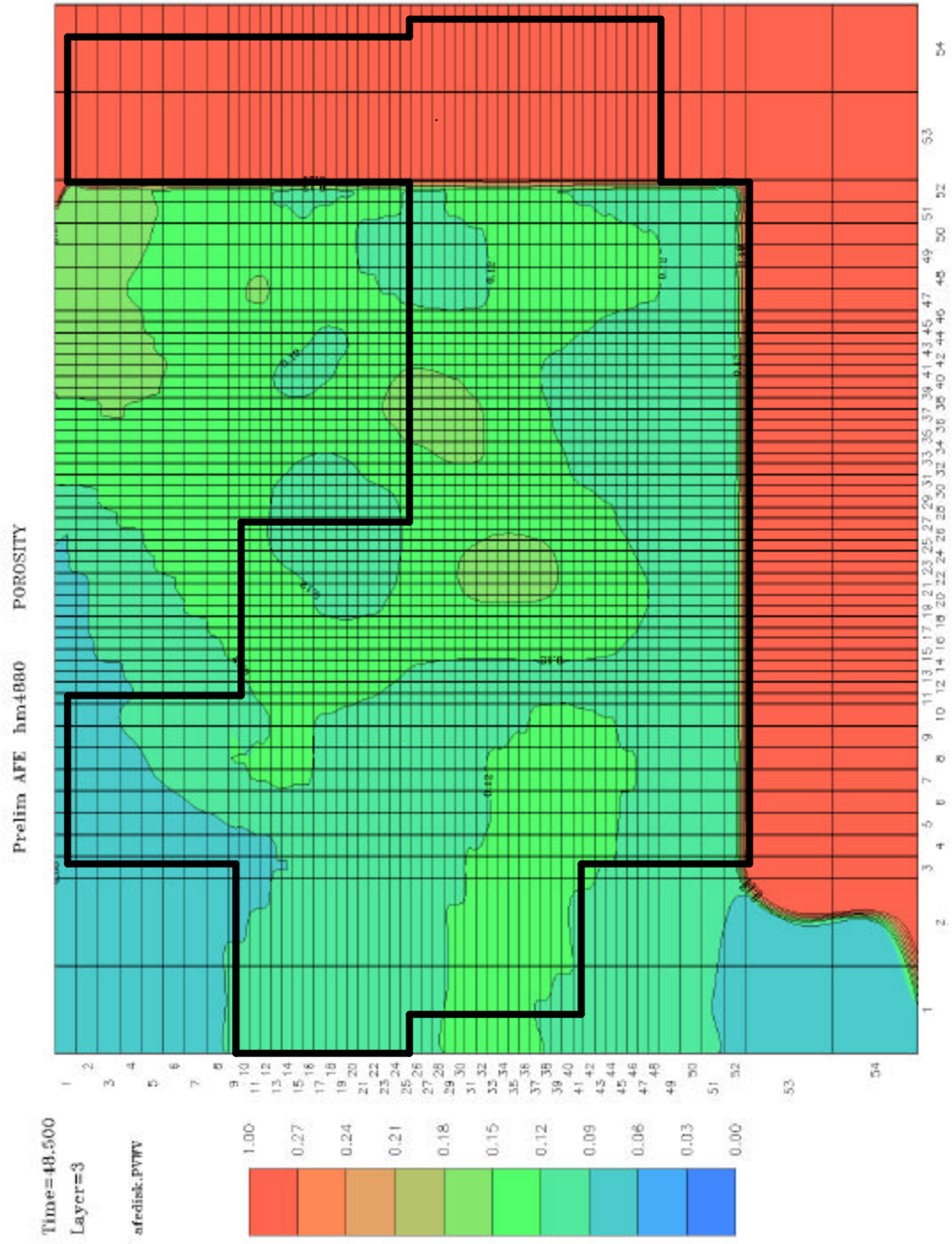




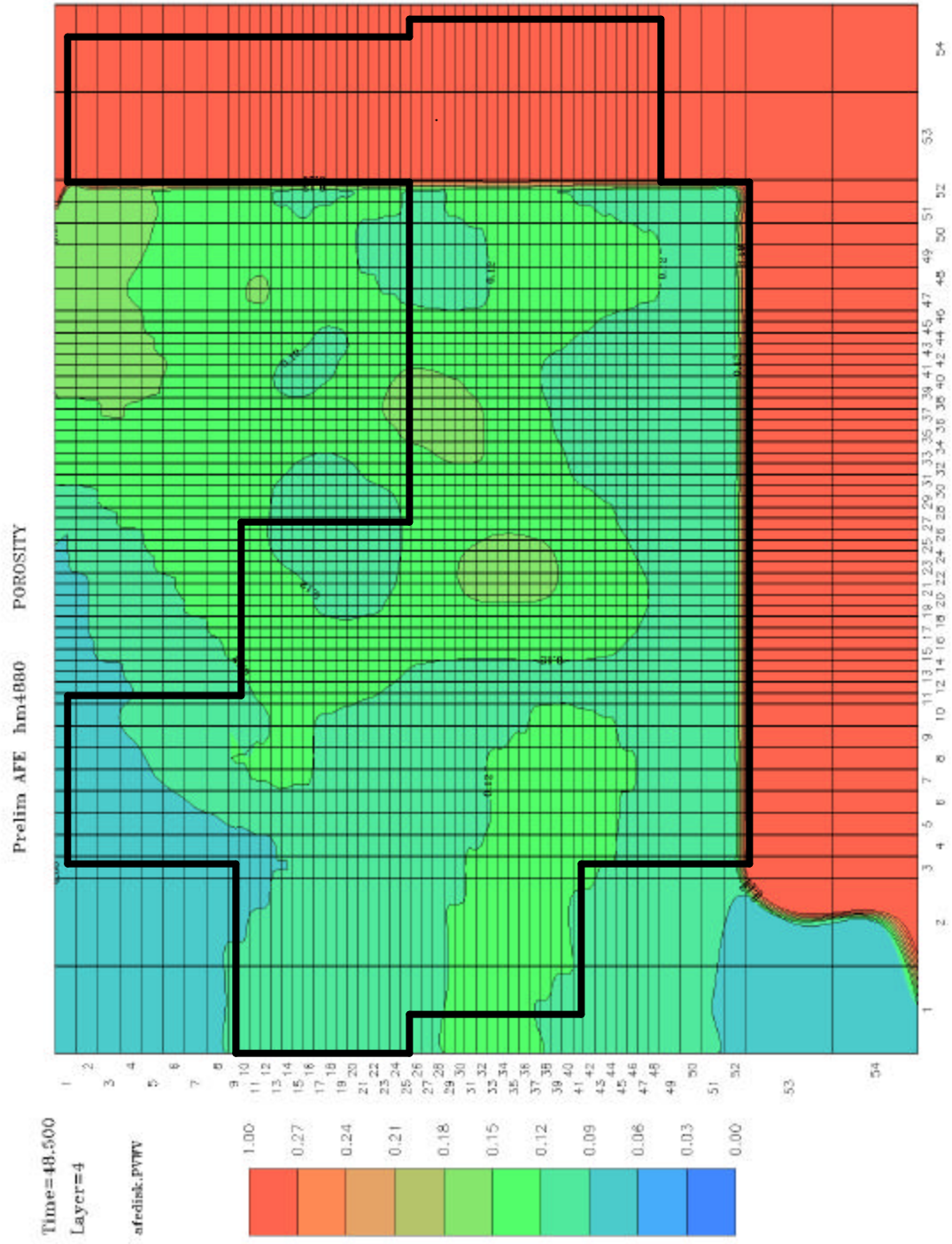
- Average Porosity Map (San Andres zone E1 – simulation model)



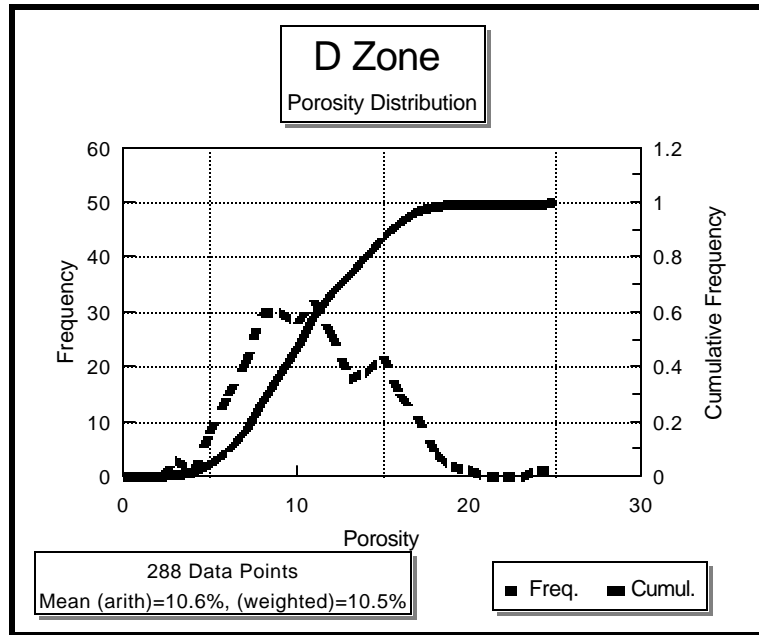
- Average Porosity Map (San Andres zone E2 – simulation model)



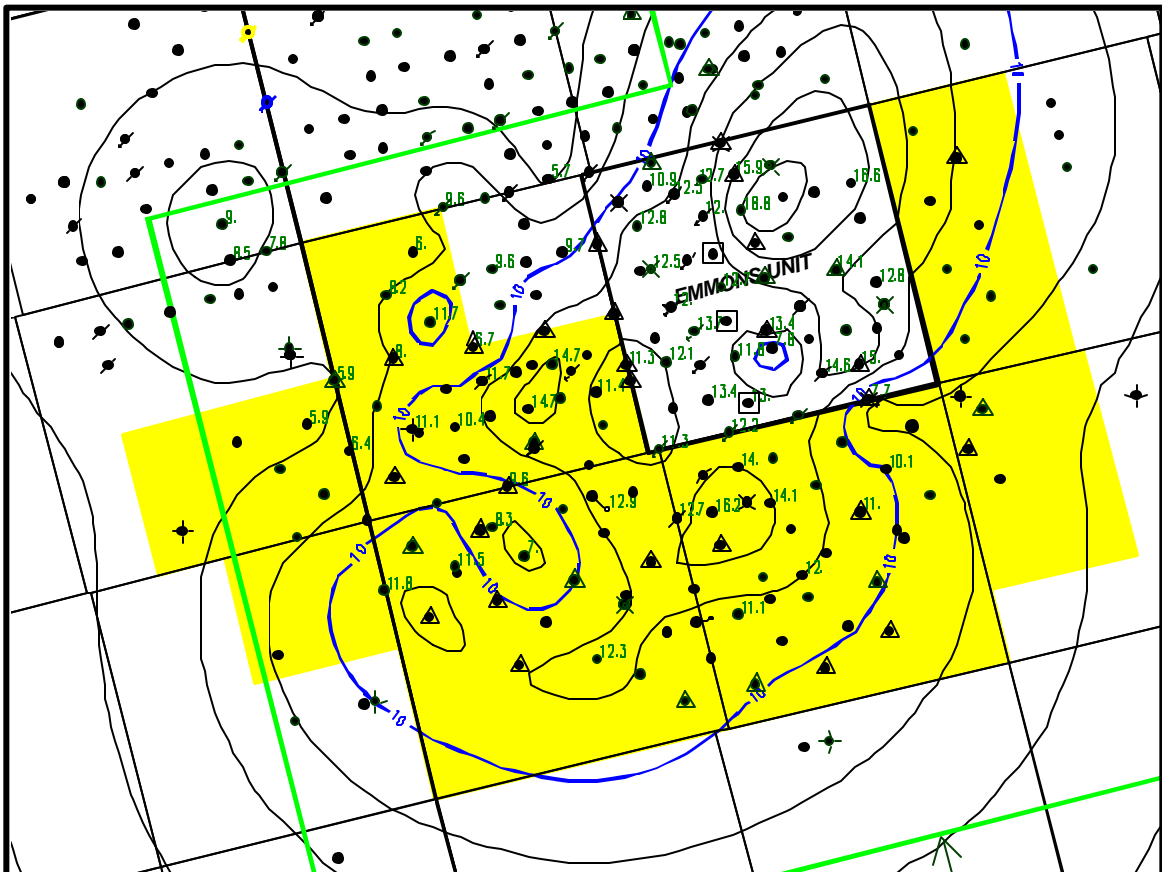
- Average Porosity Map (San Andres zone E3 – simulation model)



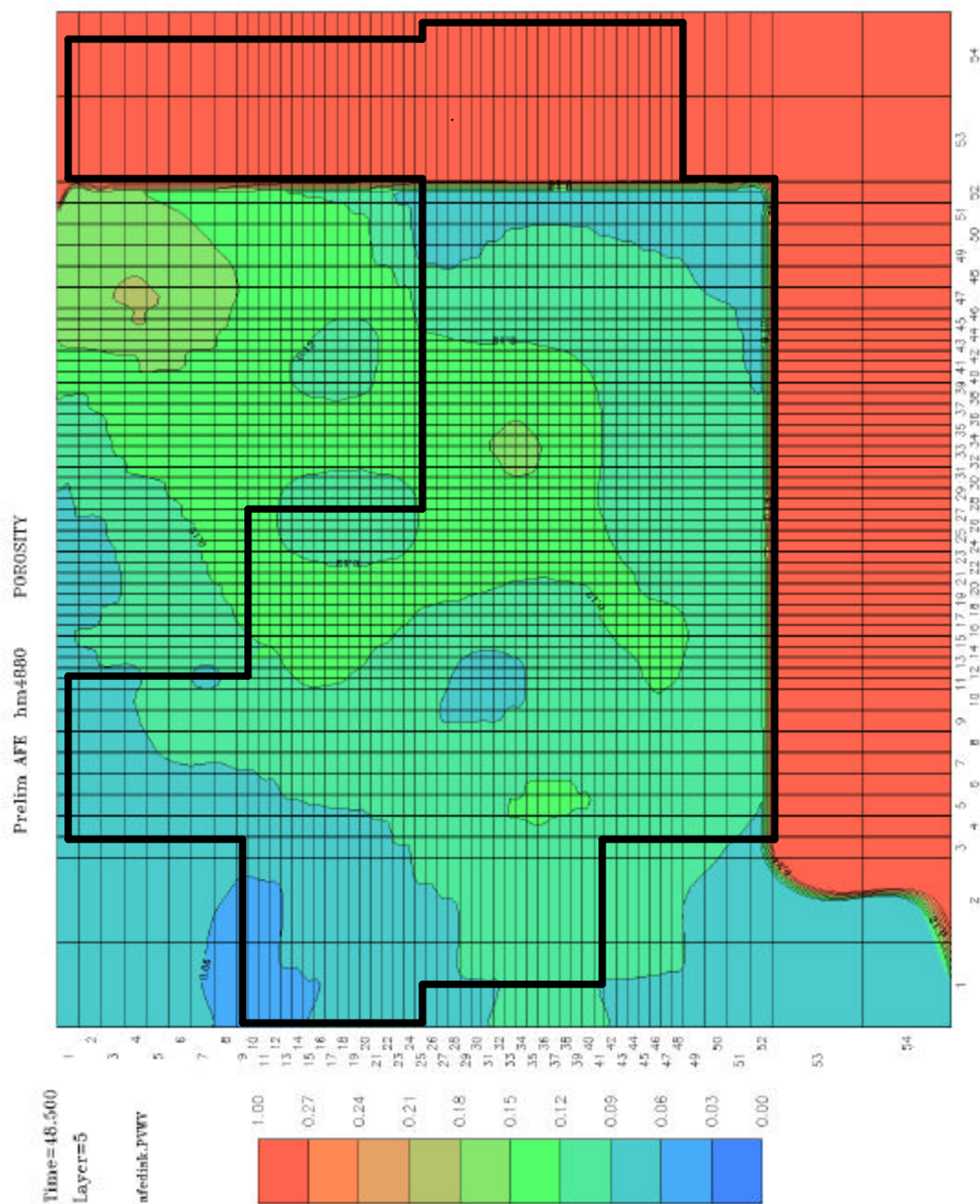
## D Zone Distribution and Mean



## Average Porosity Map (San Andres zone D – geological mapping)

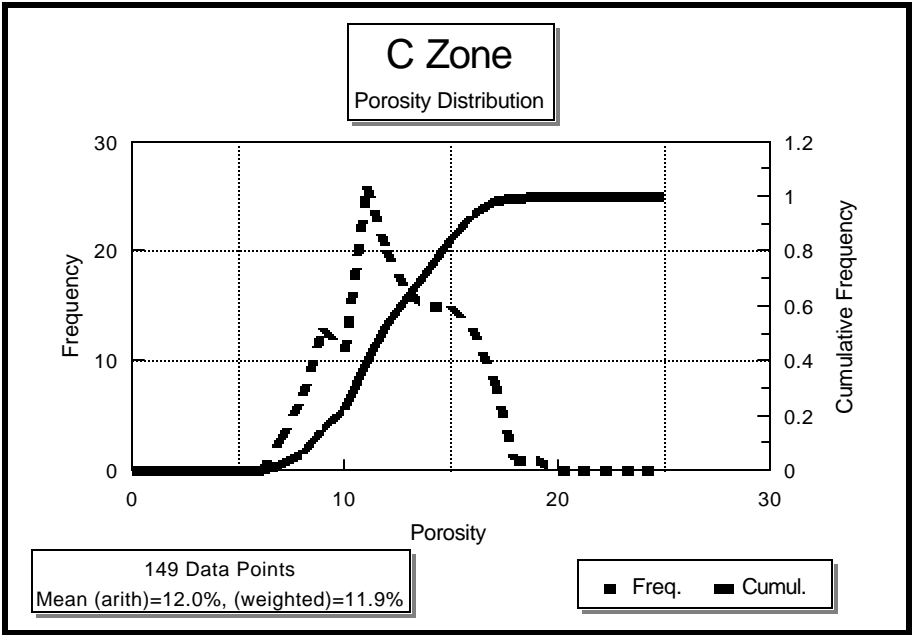


- Average Porosity Map (San Andres zone D – simulation model)

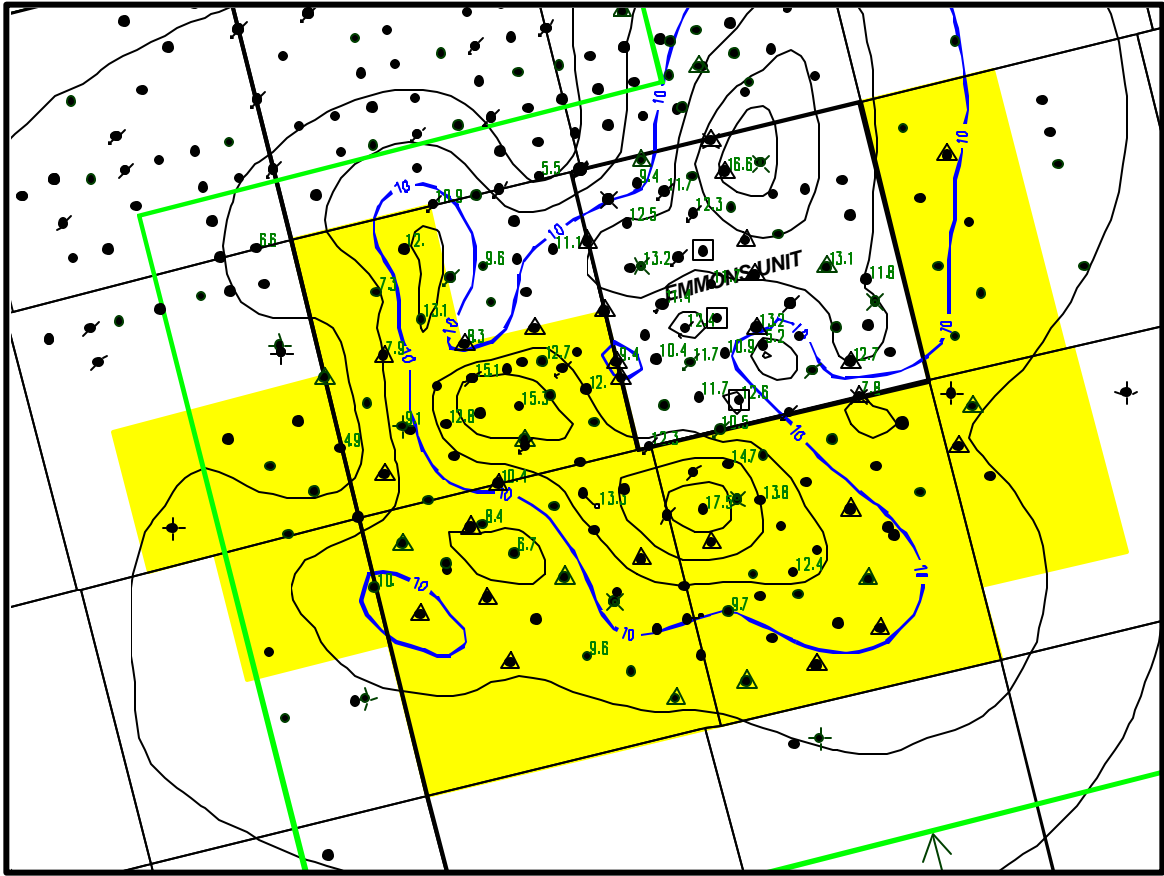




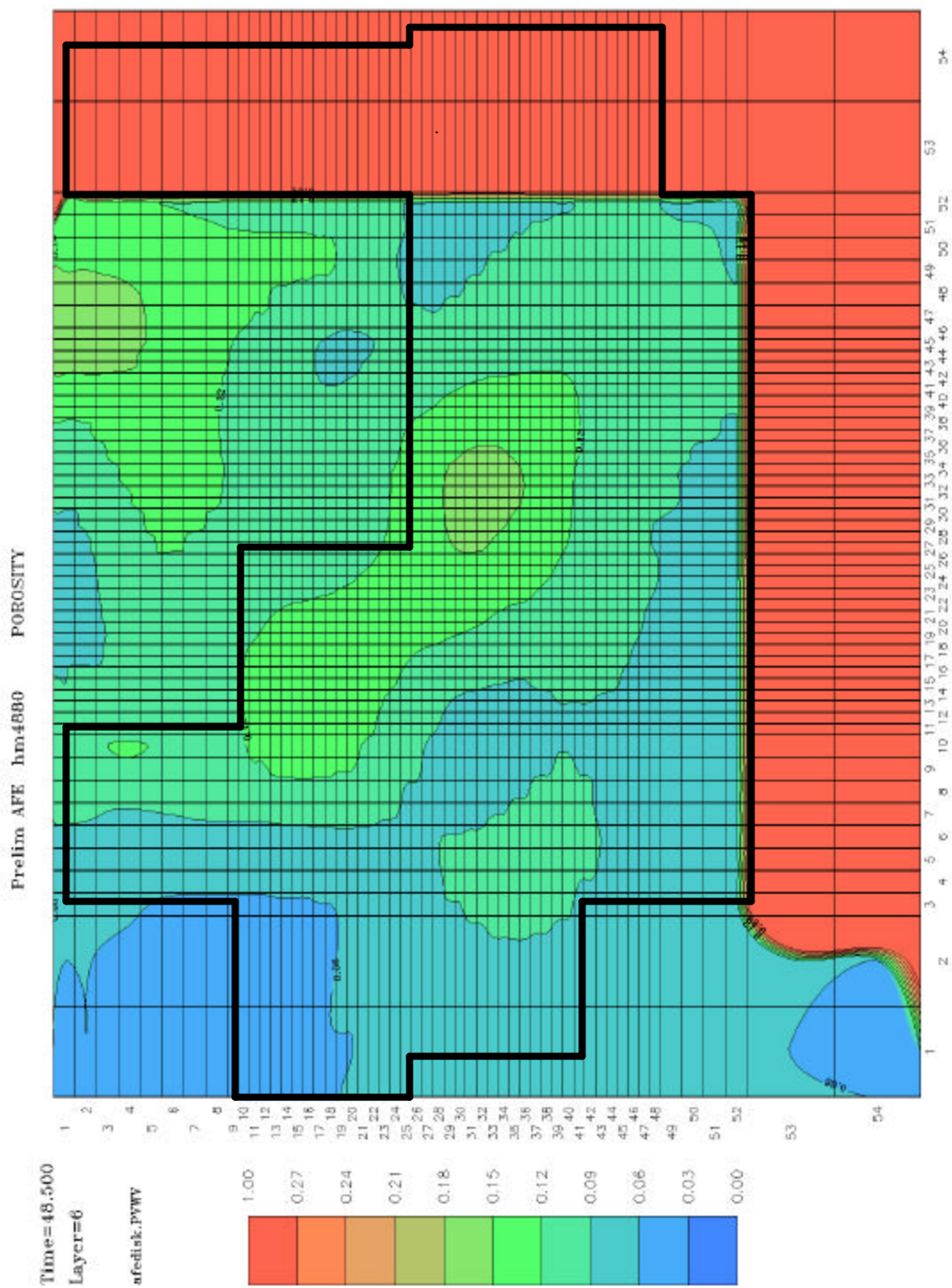
### C Zone Distribution and Mean



### Average Porosity Map (San Andres zone C – geological mapping)



Average Porosity Map (San Andres zone C – simulation model)

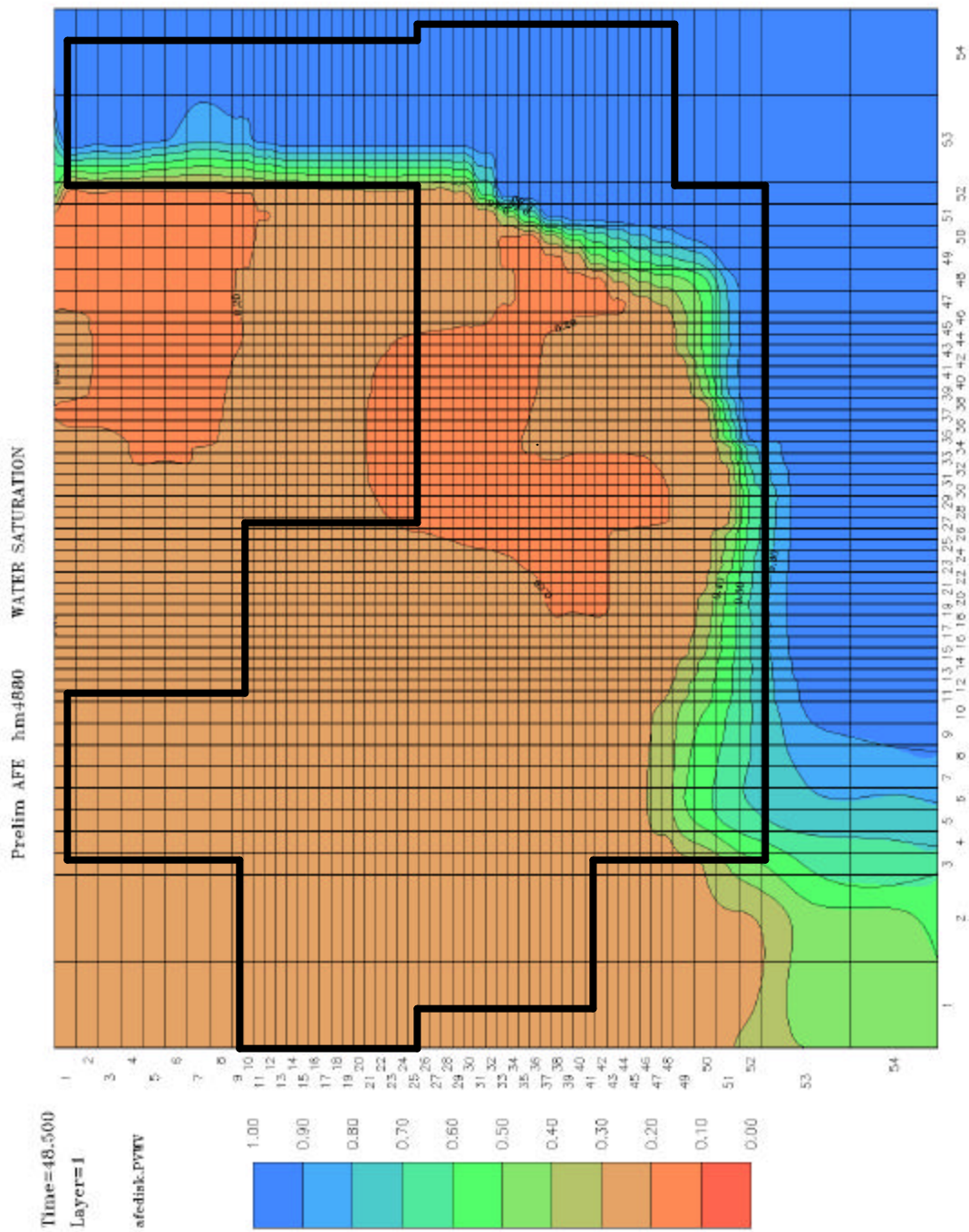


## **Original saturation mean, distribution and map:**

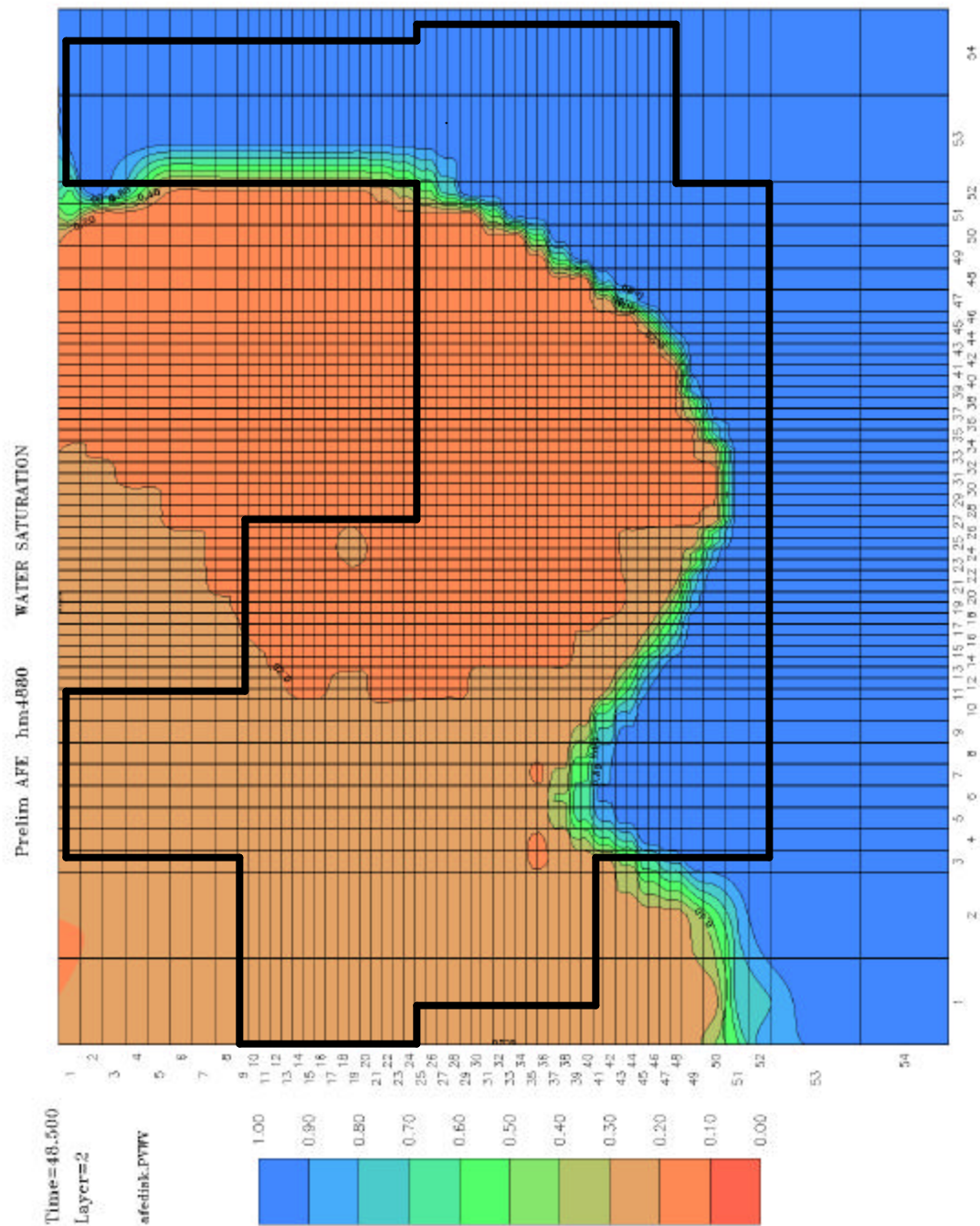
- Initial oil saturations for each simulation model layer are 100% less initial water saturation (there are only two phases initially in the model)



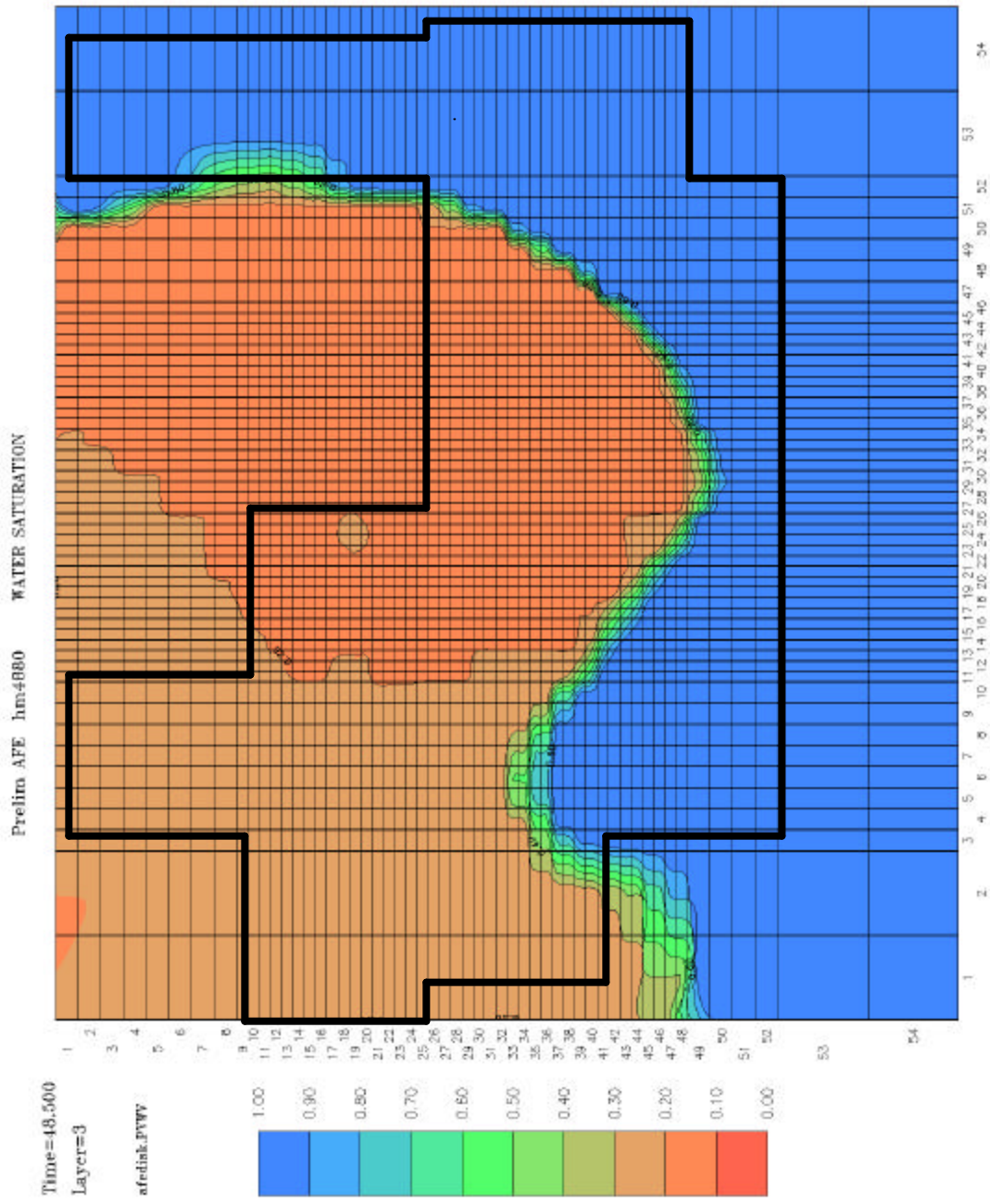
Original Water Saturation (Taken from simulation layer 1 = San Andres zone F)



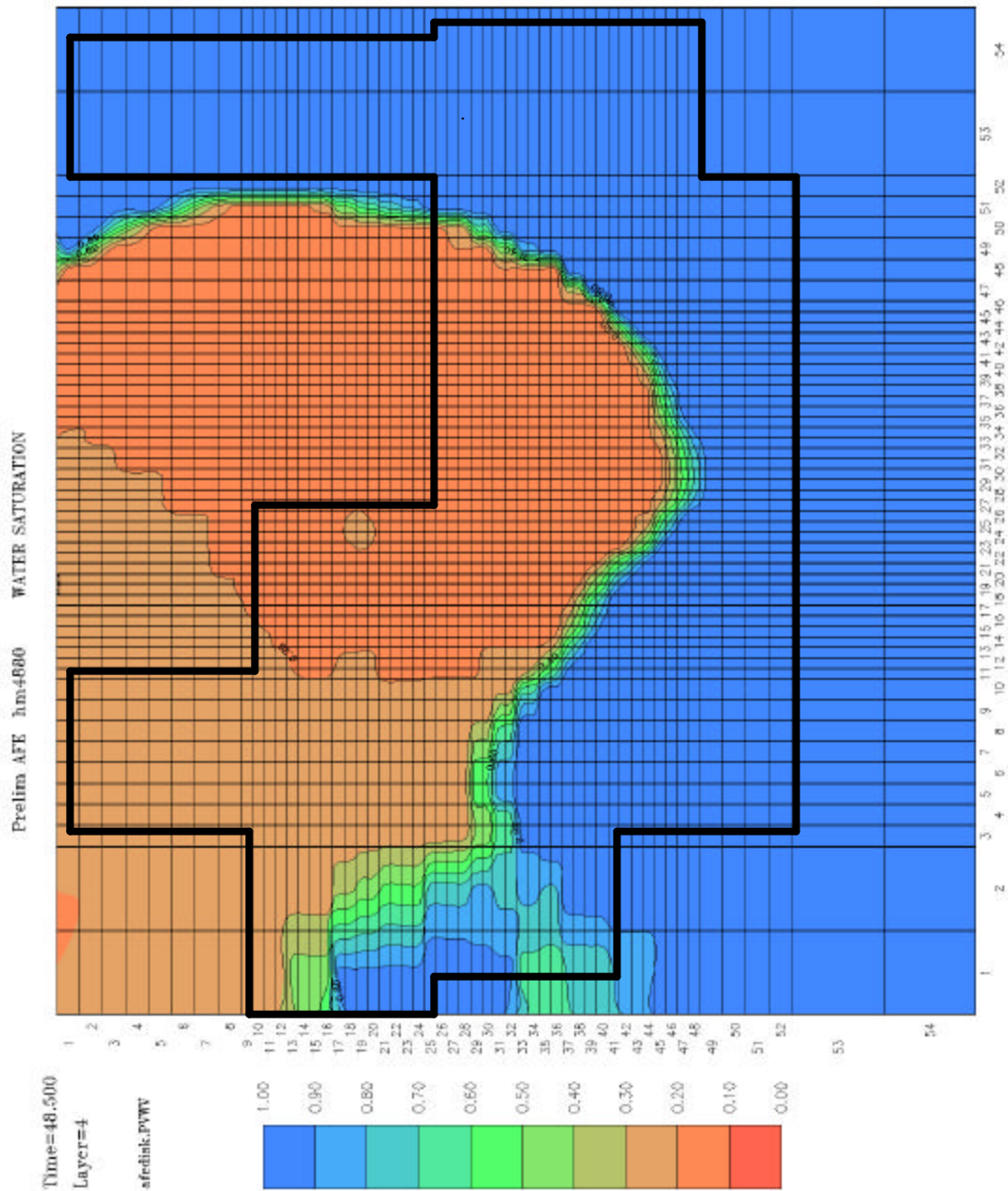
Original Water Saturation (Taken from simulation layer 2 = San Andres zone E1)



Original Water Saturation (Taken from simulation layer 3 = San Andres zone E2)

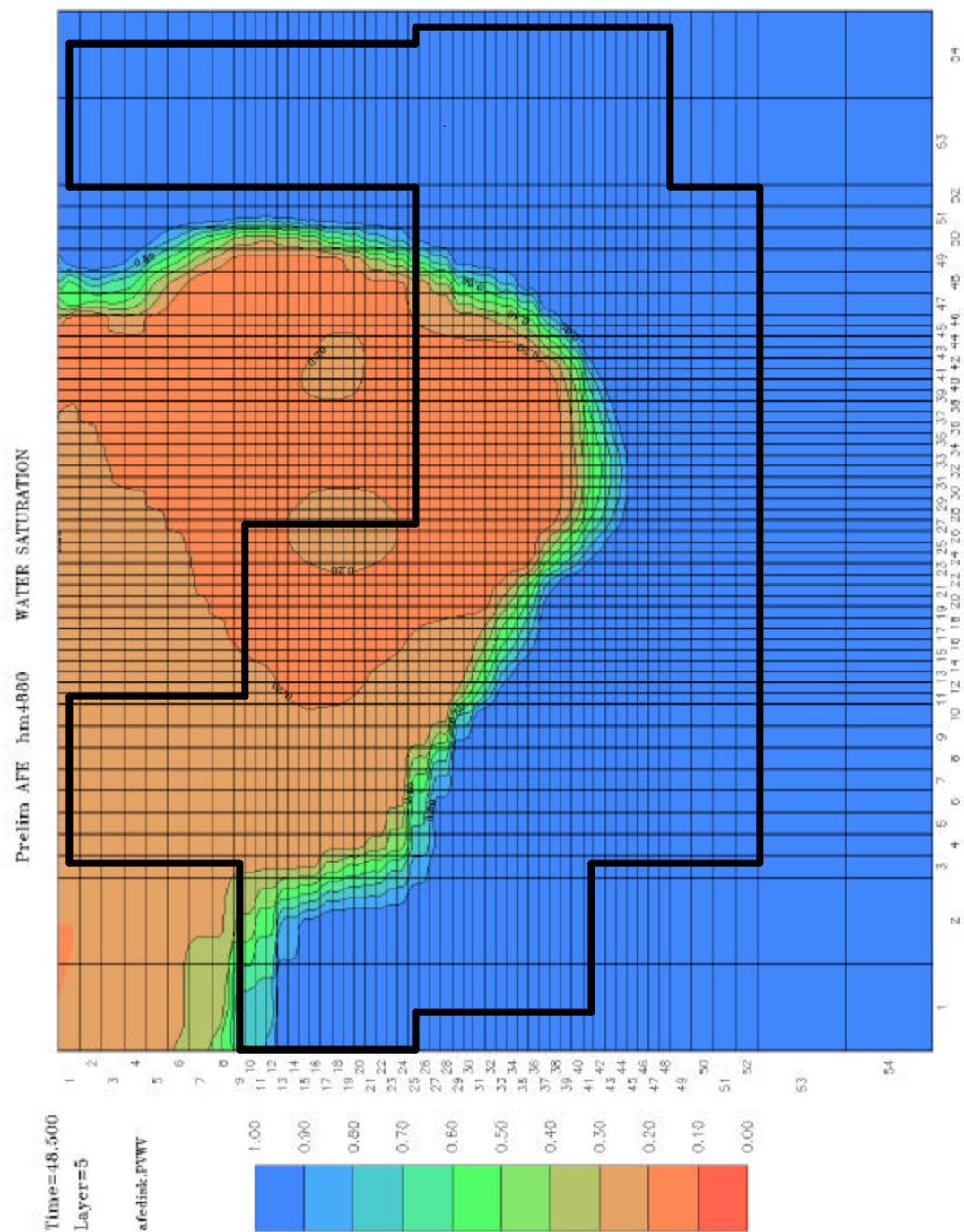


Original Water Saturation (Taken from simulation layer 4 = San Andres zone E3)

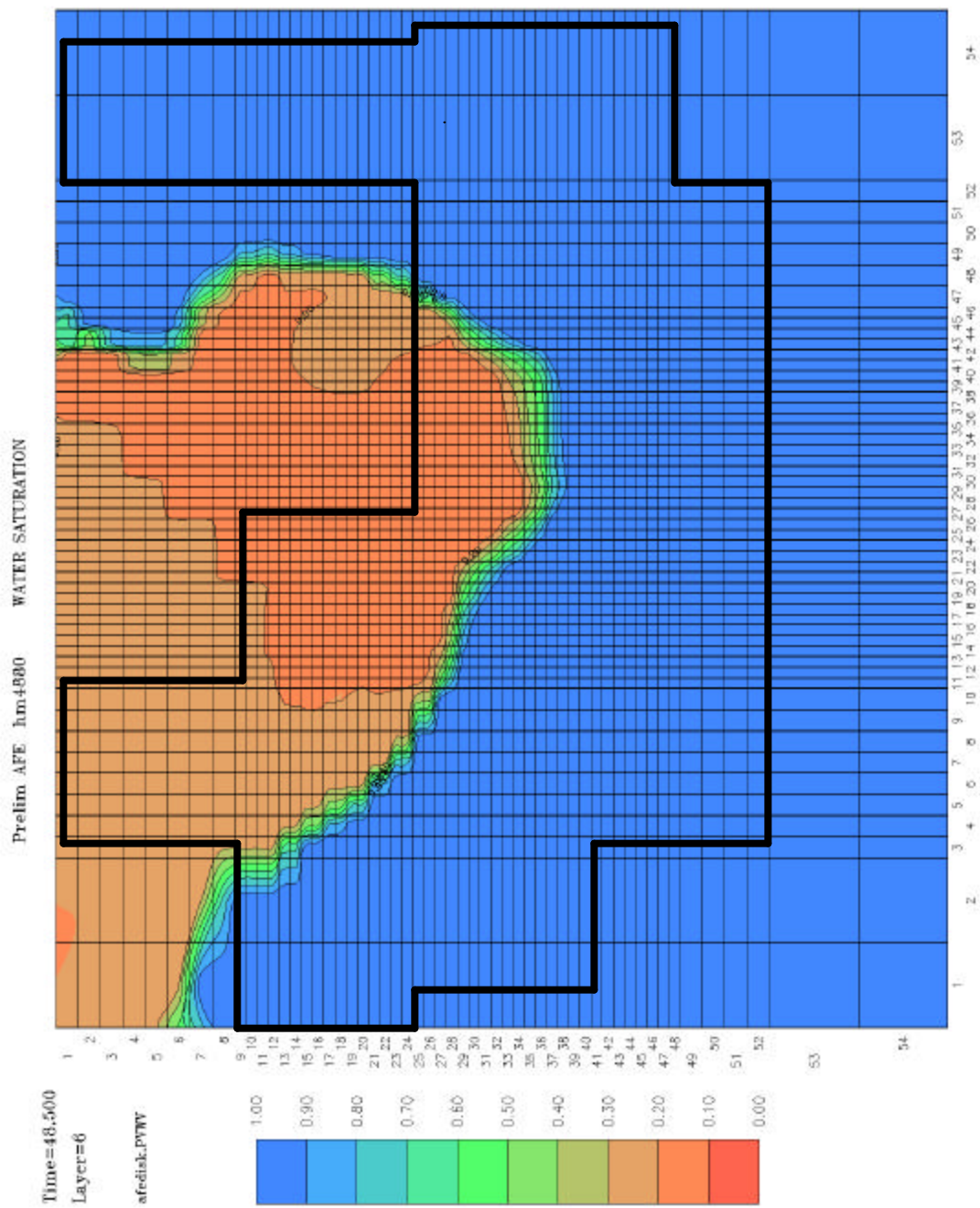




Original Water Saturation (Taken from simulation layer 5 = San Andres zone D)



# Original Water Saturation (Taken from simulation layer 6 = San Andres zone C)

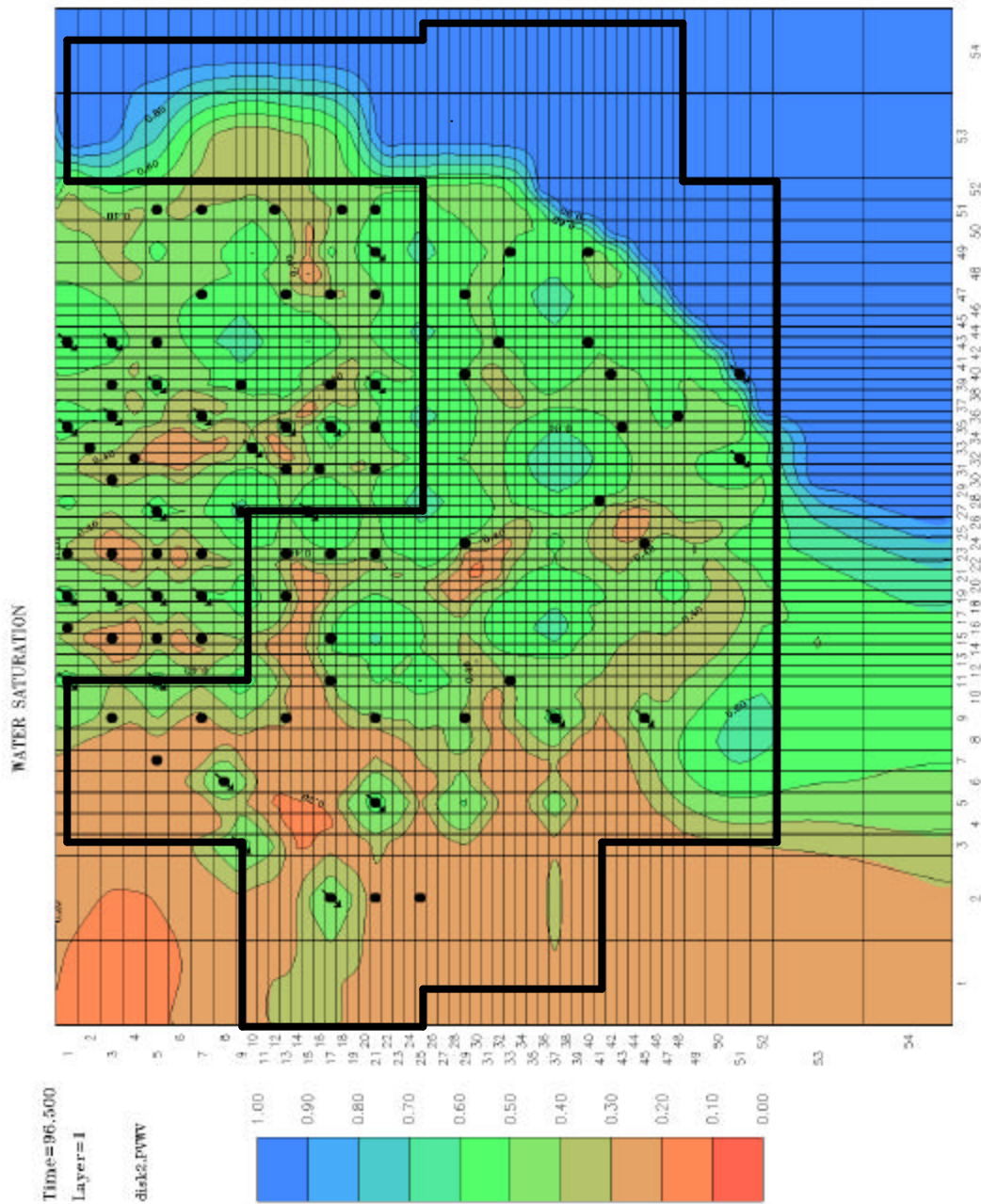


**- Gas**

Gas Saturation zero initially

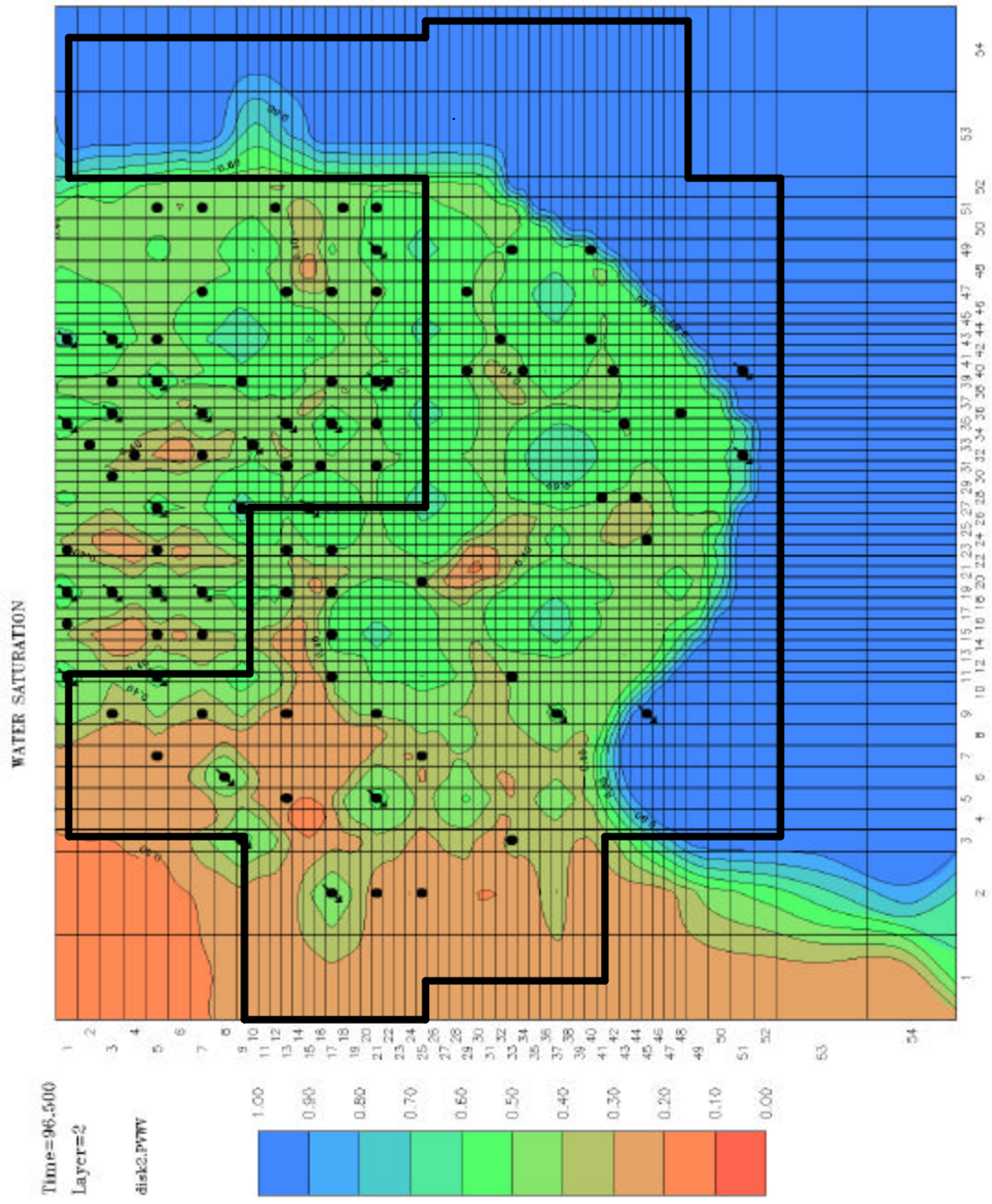
# Saturation distribution map at the inception of cost-share project: Maps shown are at year 1996.5

Water Saturation (Taken from simulation layer 1 = San Andres zone F)

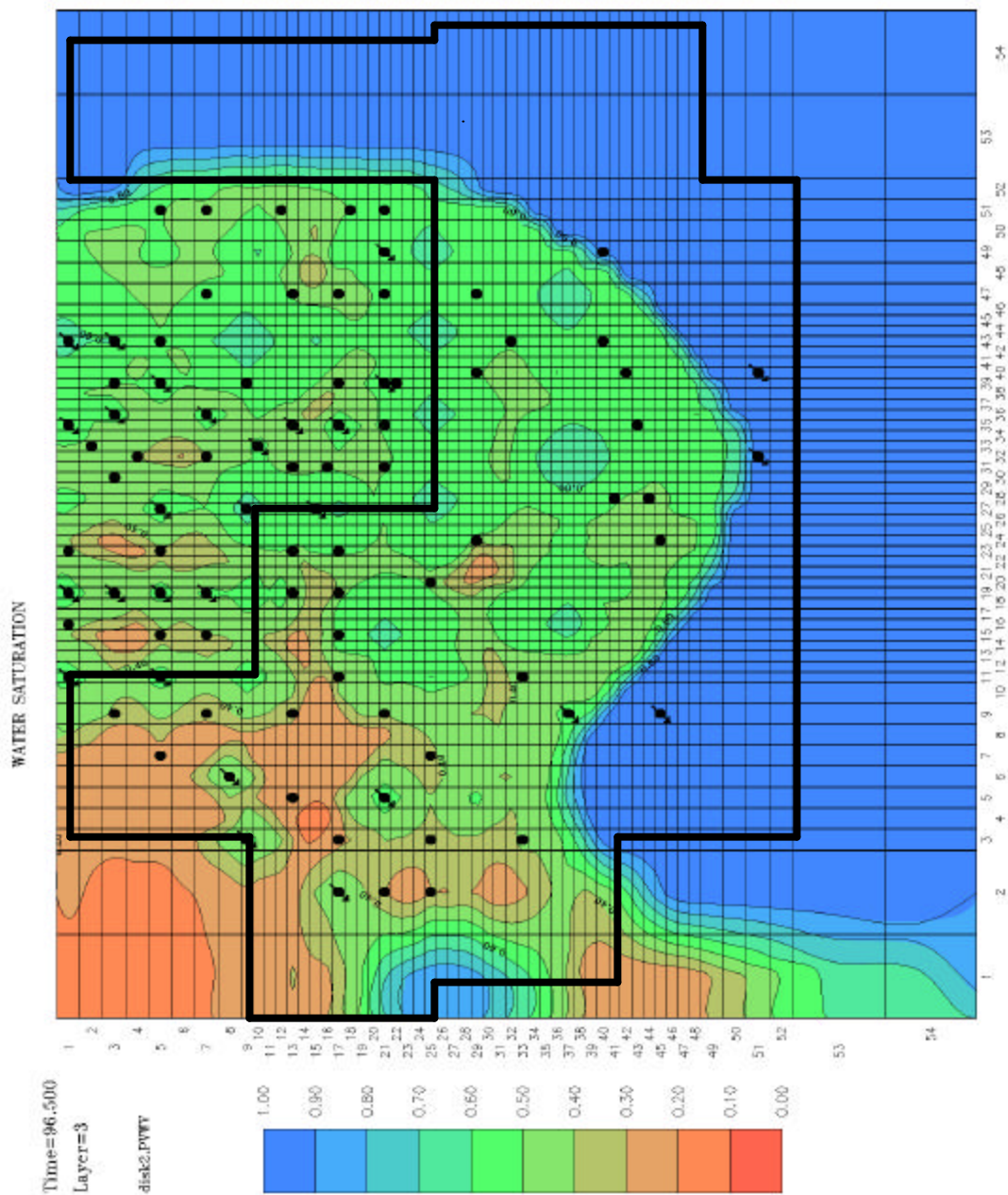




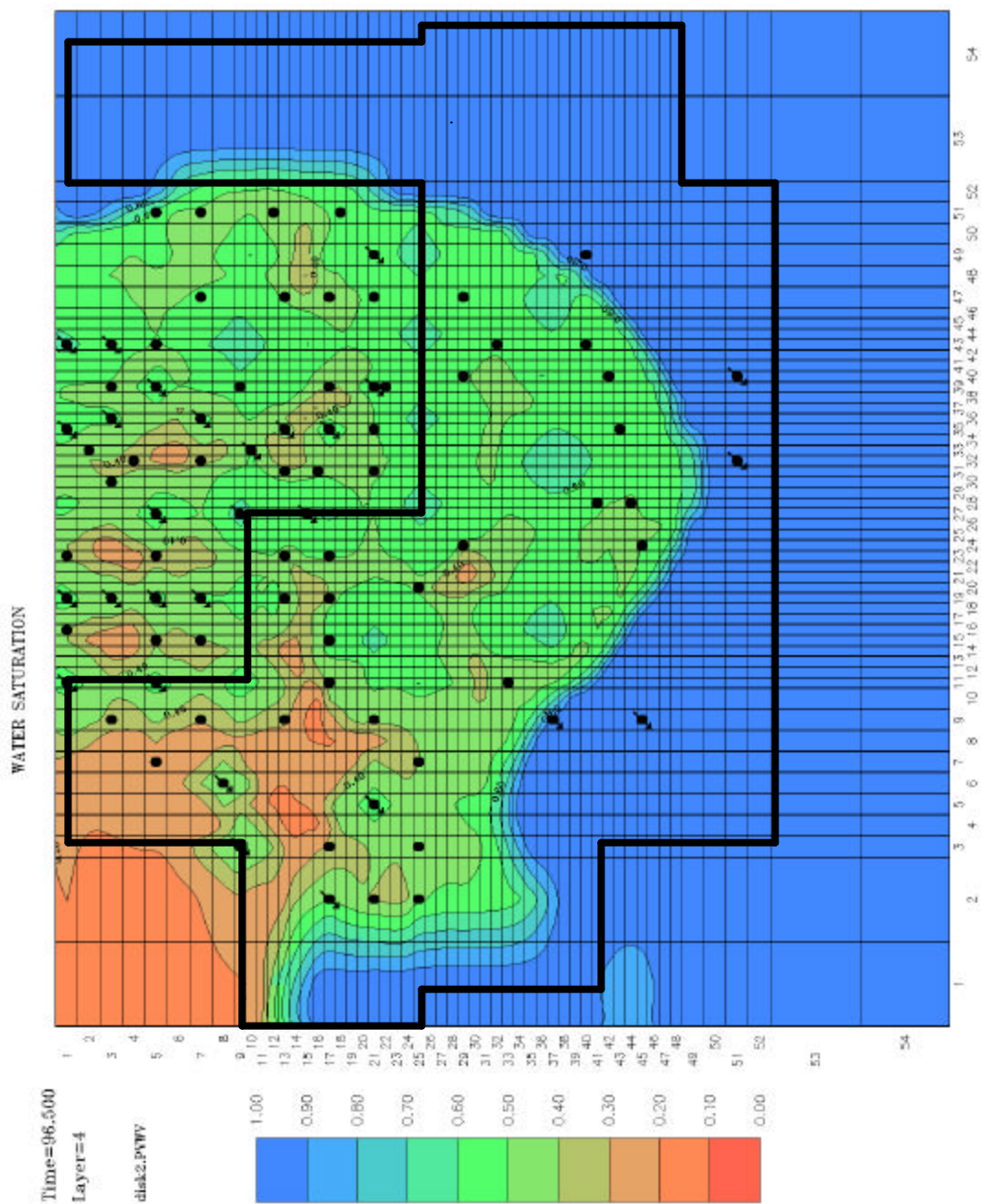
# Water Saturation (Taken from simulation layer 2 = San Andres zone E1)



# Water Saturation (Taken from simulation layer 3 = San Andres zone E2)

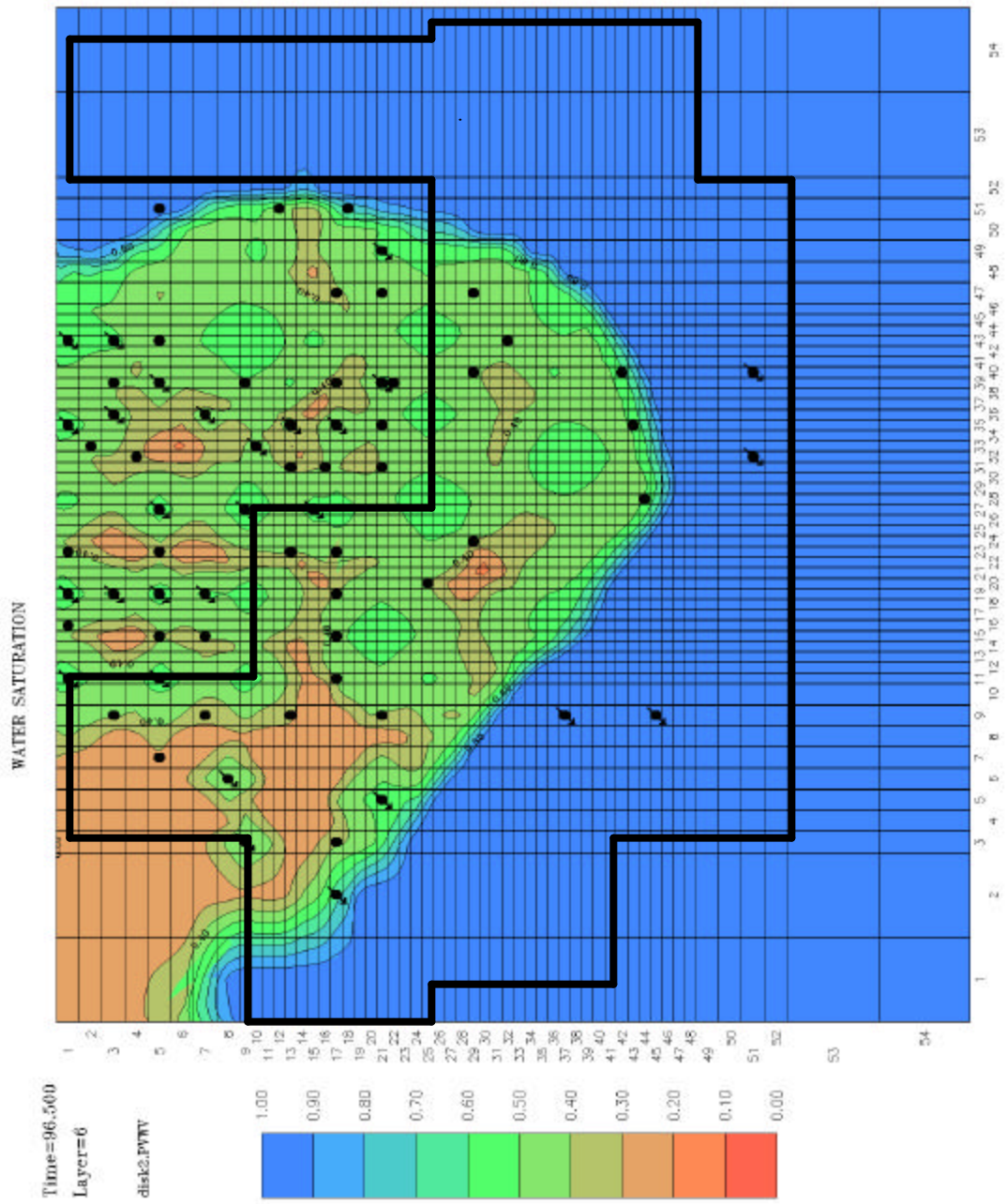


# Water Saturation (Taken from simulation layer 4 = San Andres zone E3)

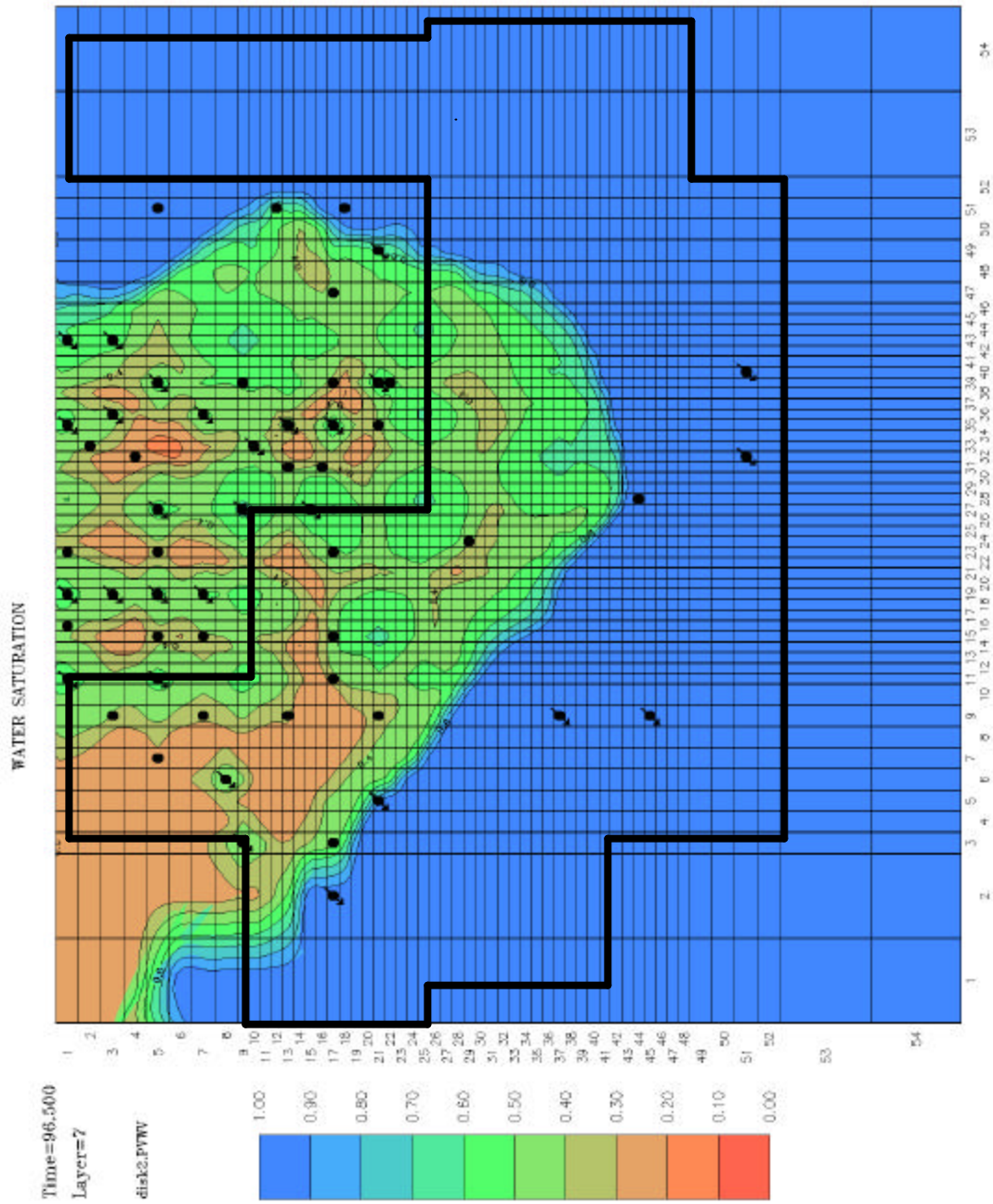




# Water Saturation (Taken from simulation layer 5 = San Andres zone D)



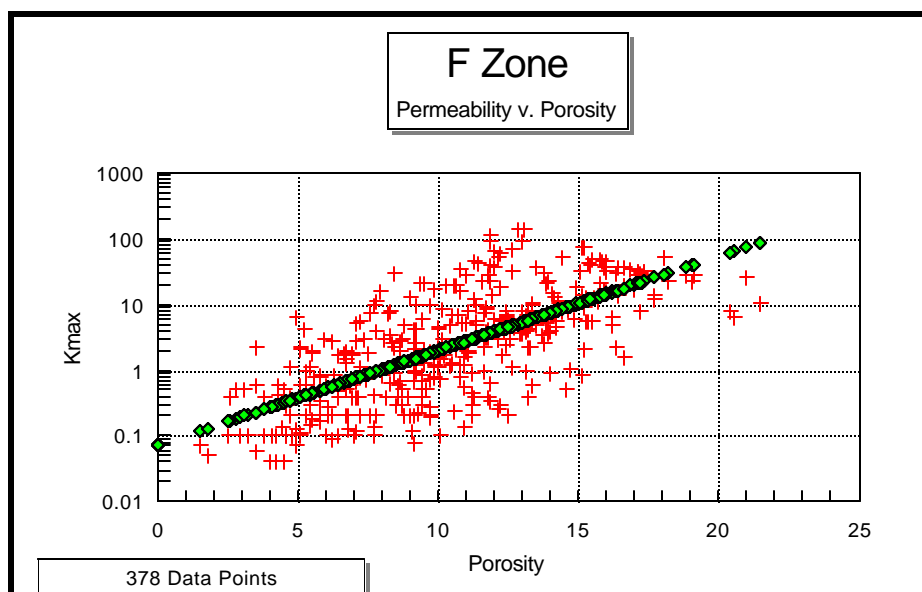
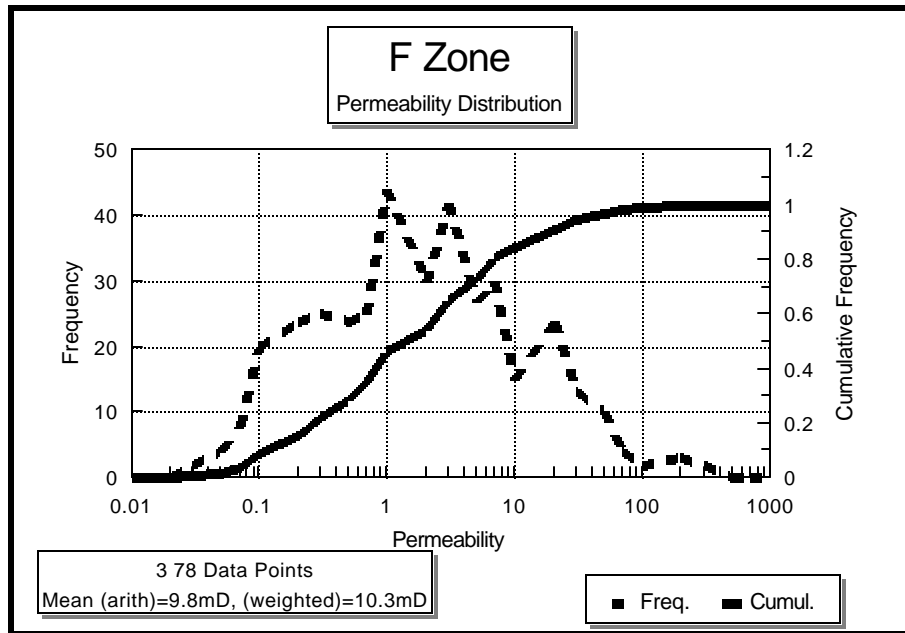
# Water Saturation (Taken from simulation layer 6 = San Andres zone C)



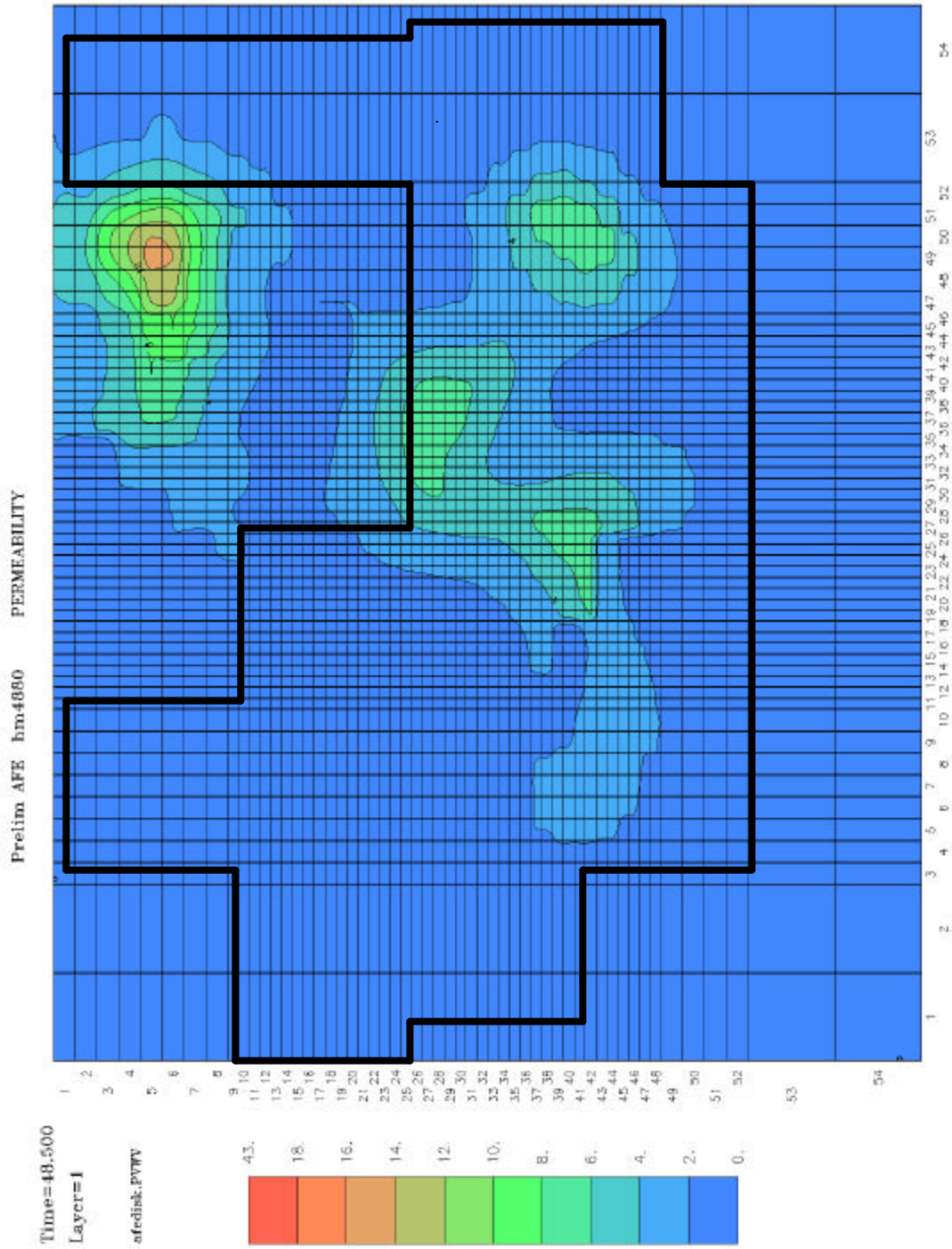
## **Permeability mean, distribution and map:**

(Note : simulation model maps use the scale 0 mD minimum to 20 mD maximum. Greater than 20 mD is one color/shade)

## F zone core data distribution and mean

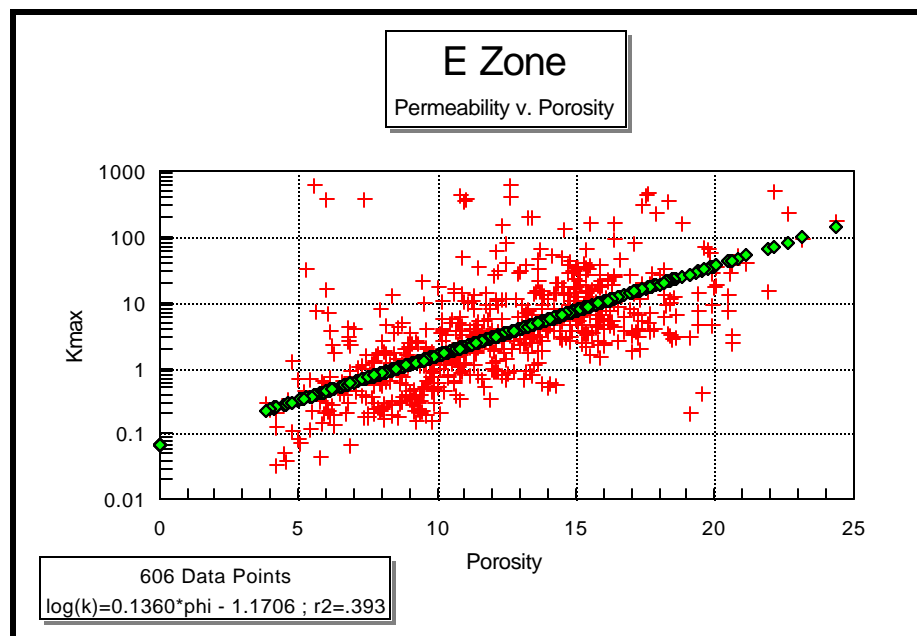
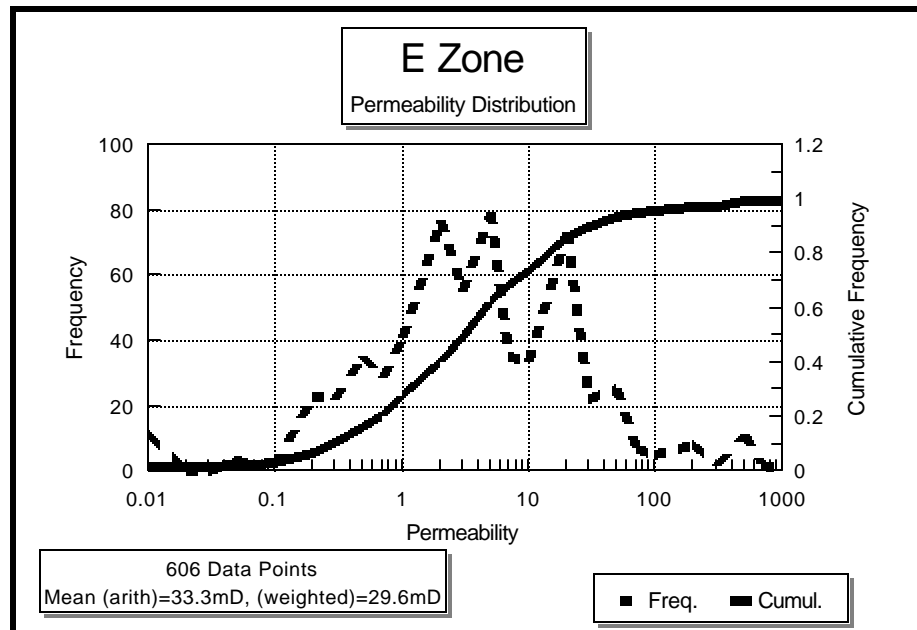


Permeability Map (Taken from simulation layer 1 = San Andres zone F)

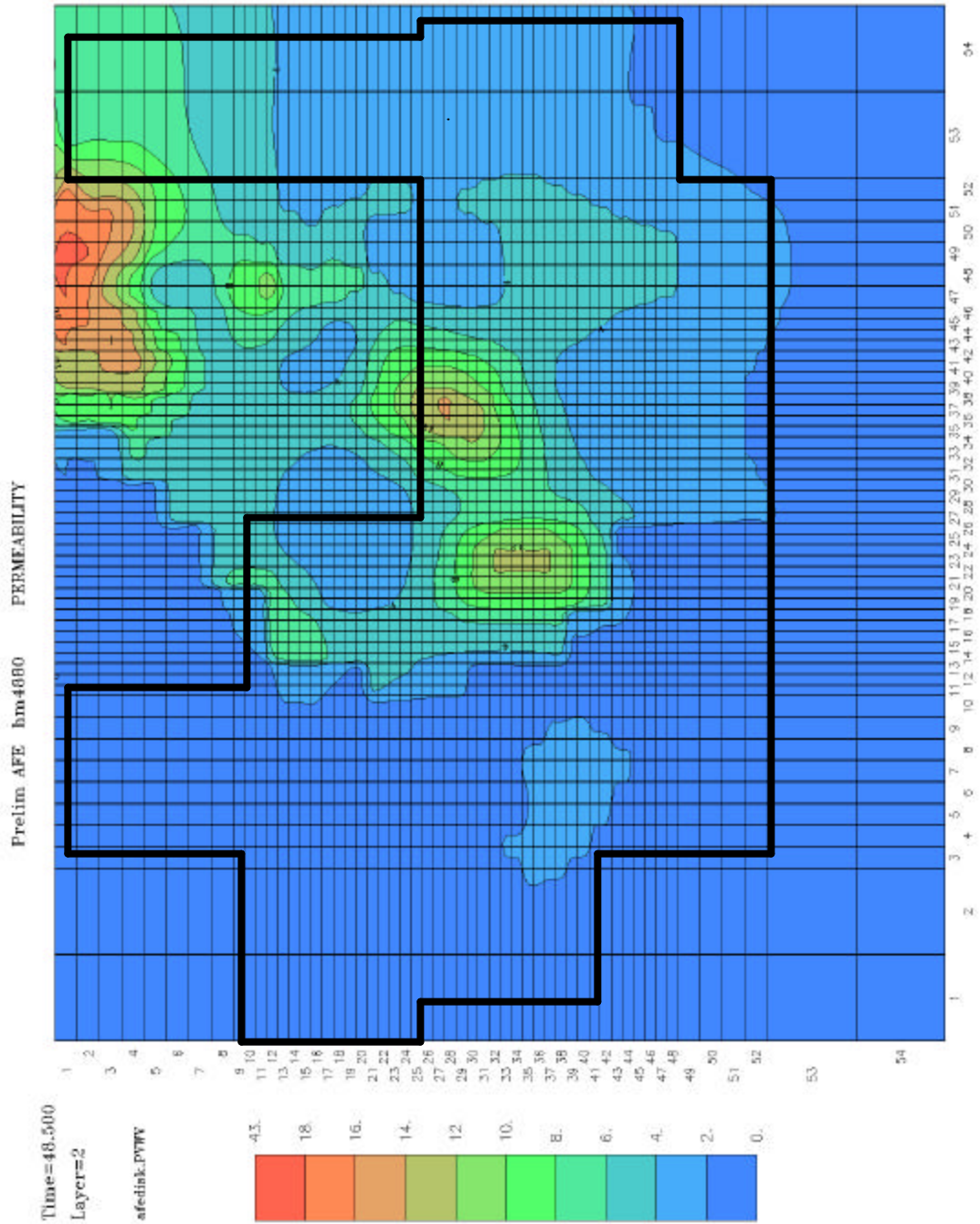




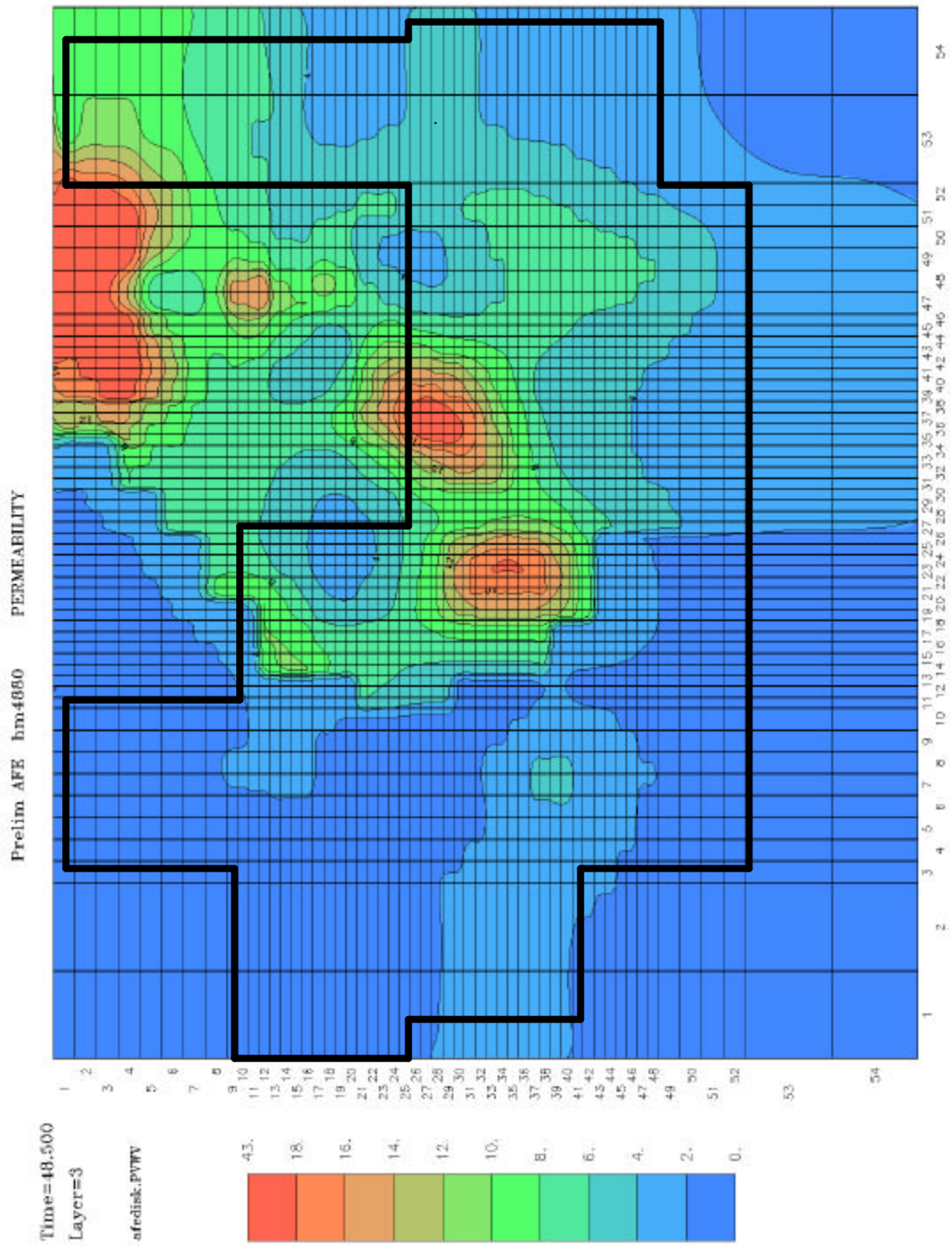
## E zone core data distribution and mean



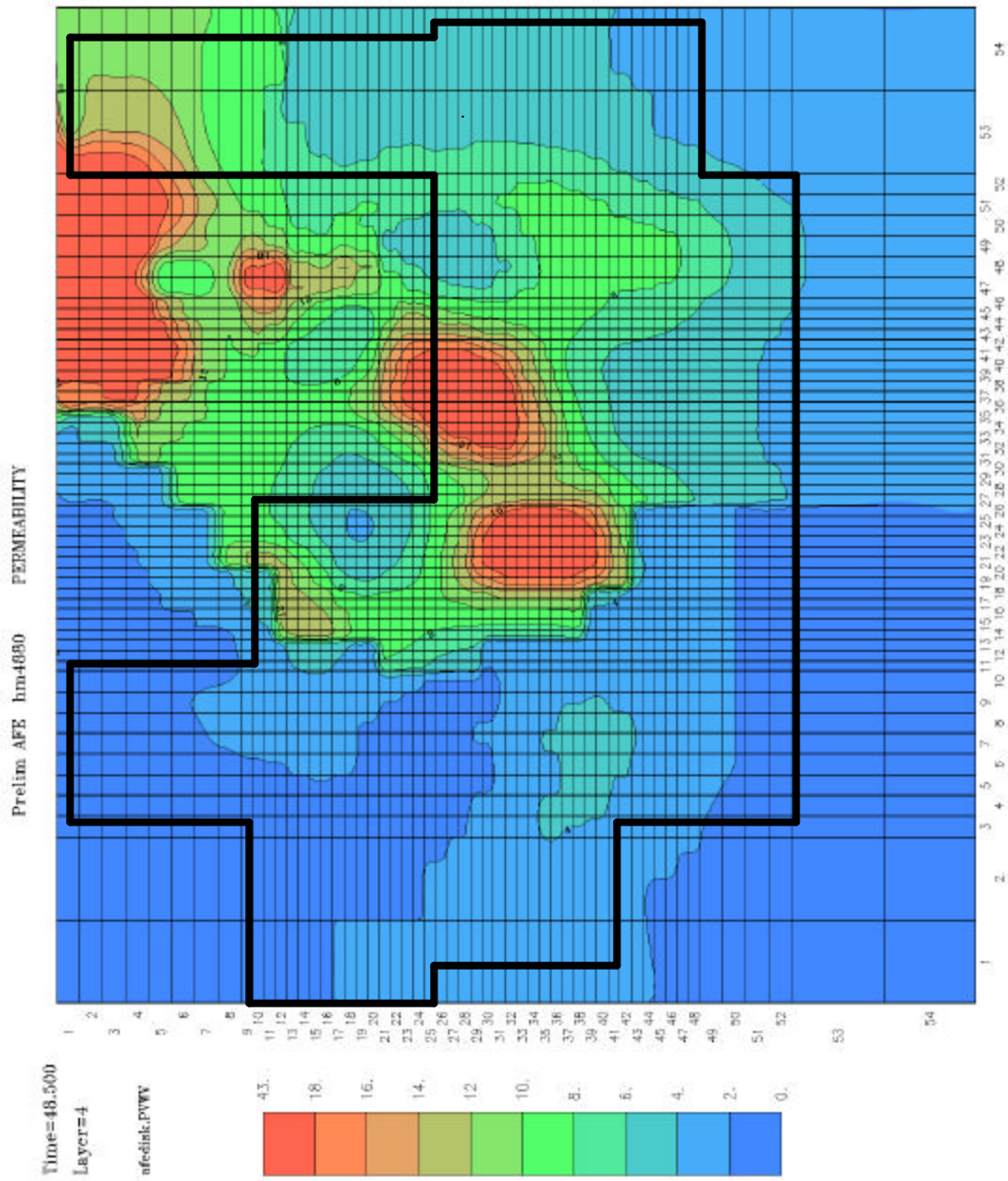
# Permeability Map (Taken from simulation layer 2 = San Andres zone E1)



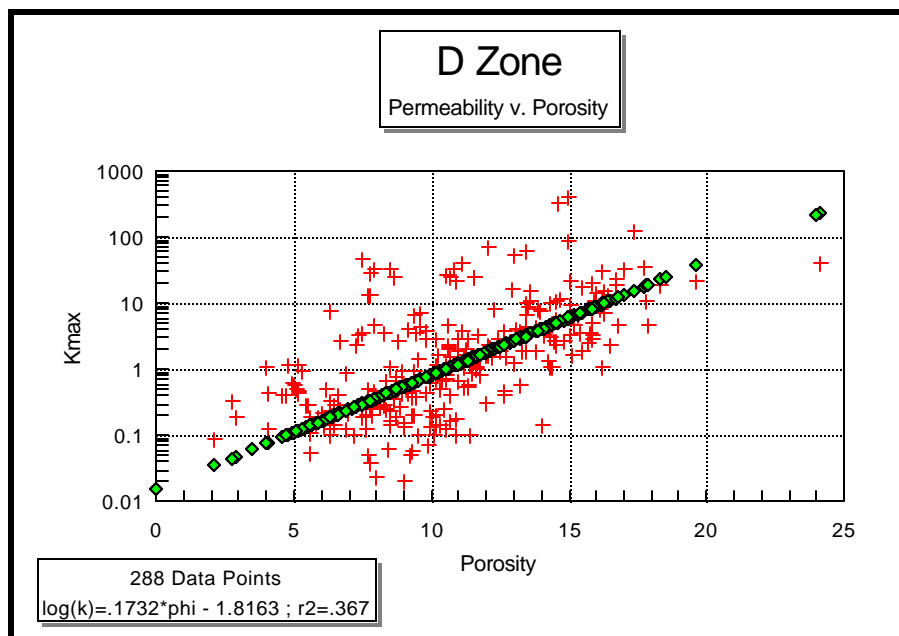
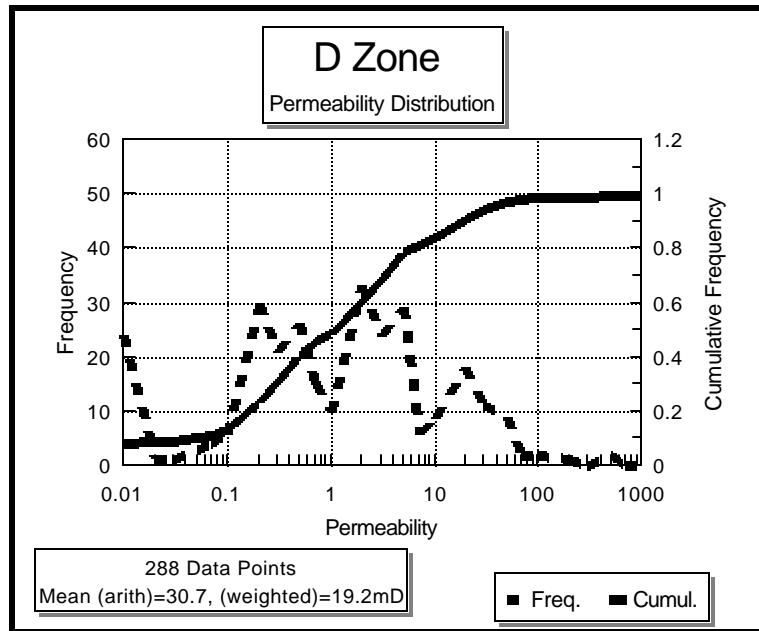
# Permeability Map (Taken from simulation layer 3 = San Andres zone E2)



# Permeability Map (Taken from simulation layer 4 = San Andres zone E3)

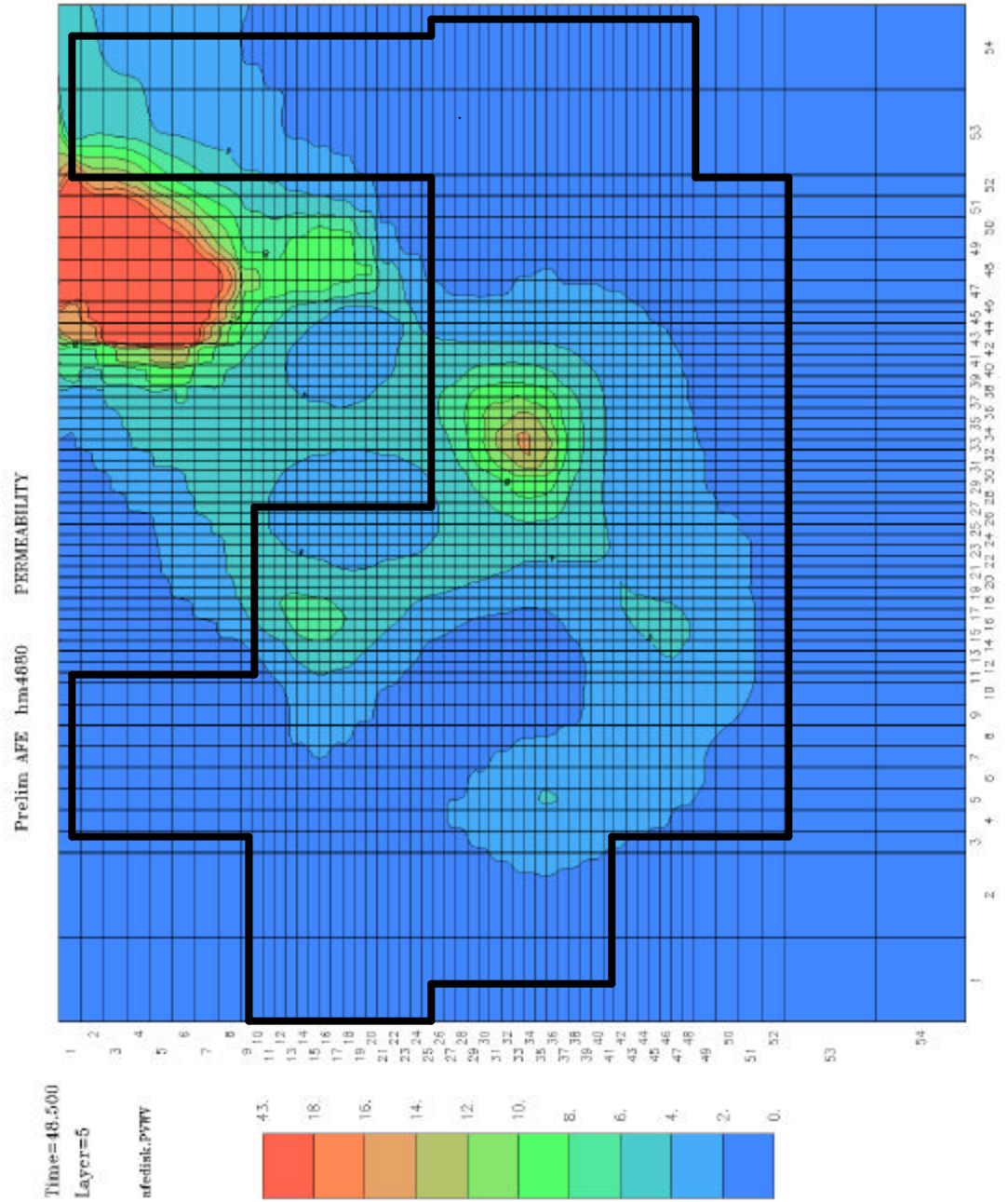


## D zone core data distribution and mean

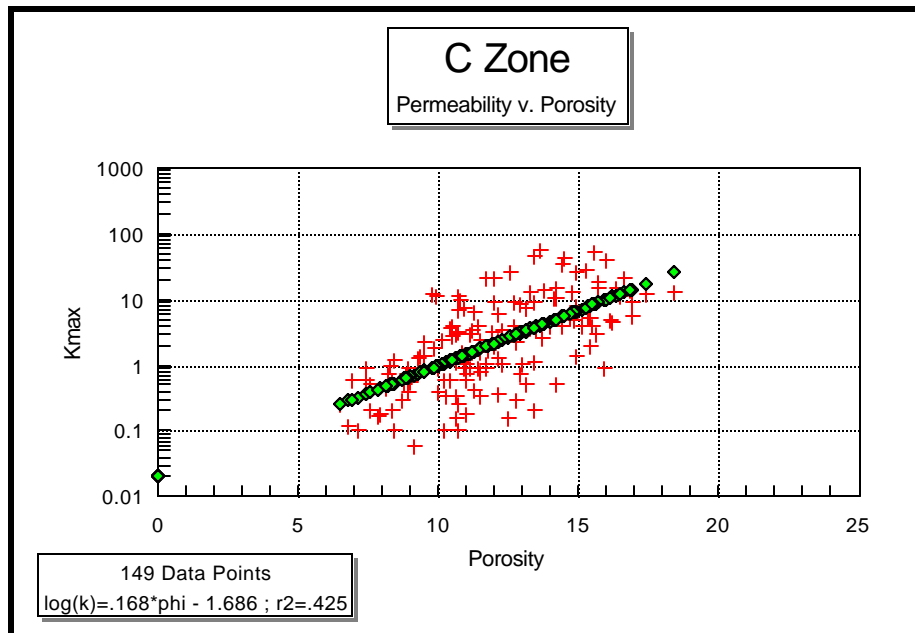
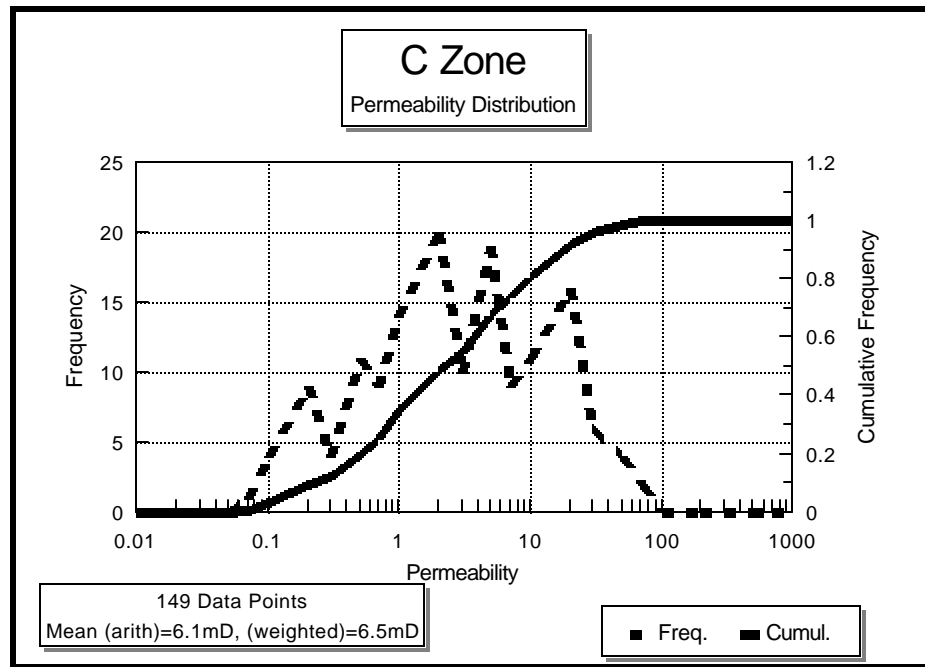




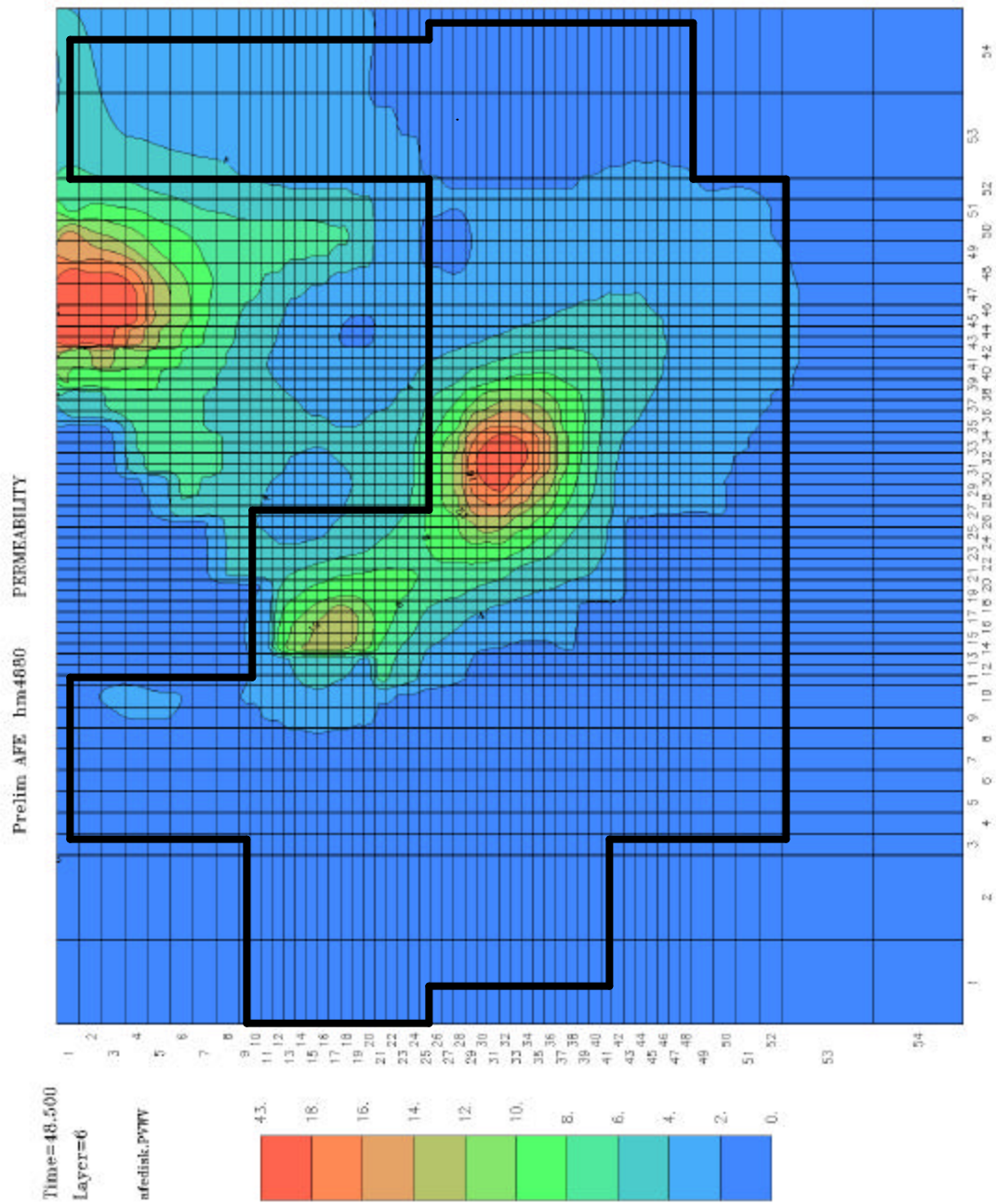
# Permeability Map (Taken from simulation layer 5 = San Andres zone D)



## C zone core data distribution and mean



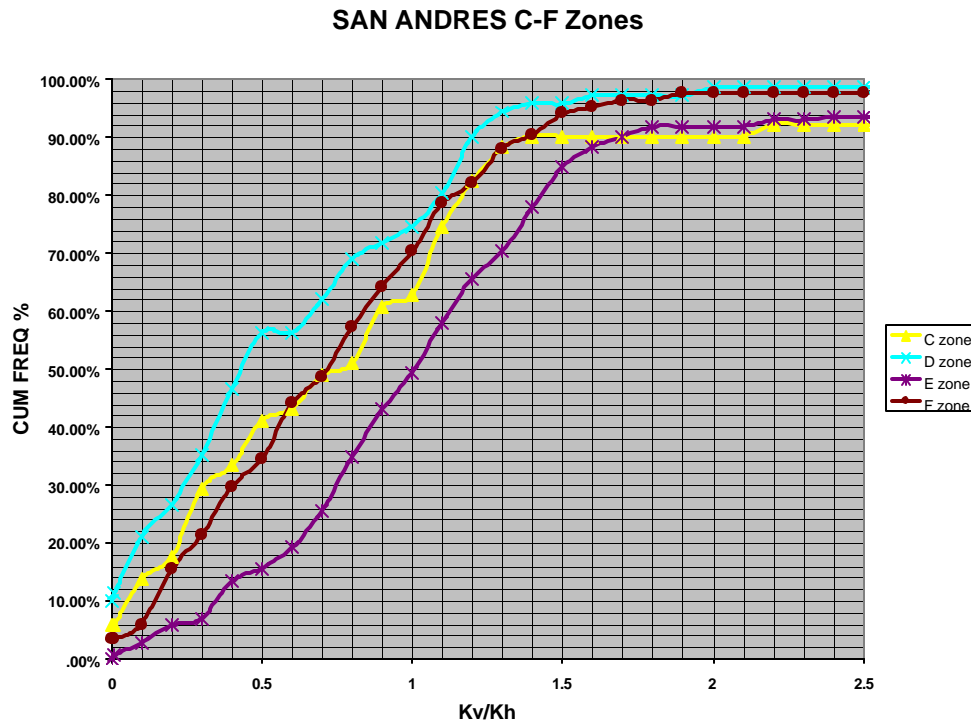
# Permeability Map (Taken from simulation layer 6 = San Andres zone C)





### Directional permeability ( $k_y/k_x$ ):

Core data from 5 wells that have vertical permeability measurements are summarized below in a statistical distribution plot for the upper San Andres layers.



The above plot illustrates core scale vertical to horizontal permeability ratios within the San Andres layers. Below are the simulation vertical to horizontal permeability ratios used at the end of the history match process to match waterflood performance.

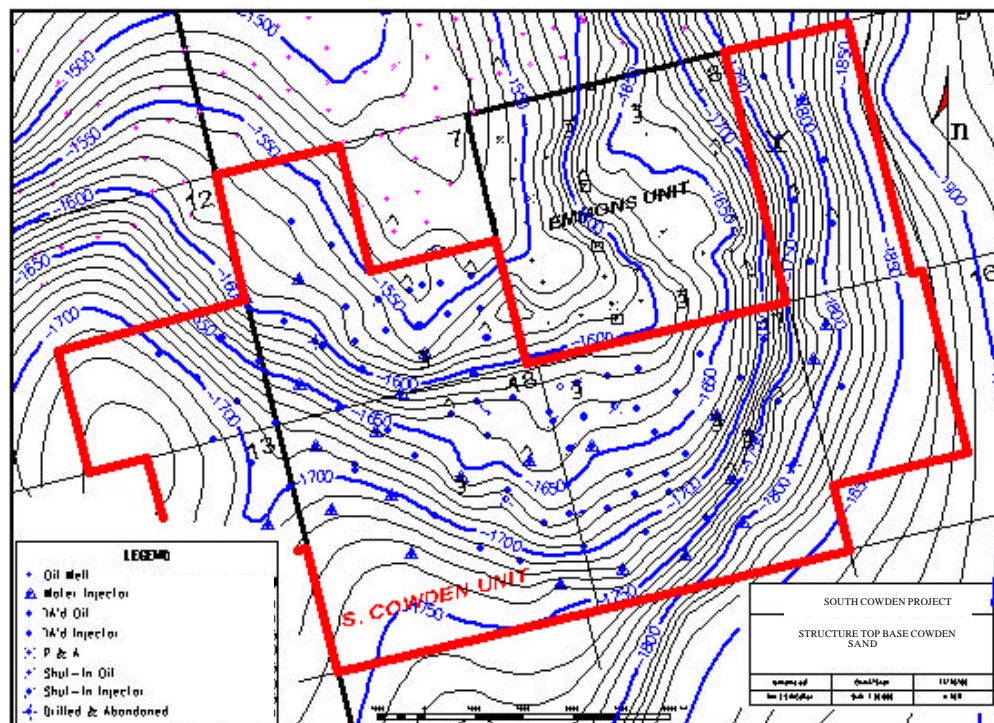
Simulation Layer	Geological Layer	Kv/Kh
Layer 1	San Andres Zone F	0.0 (no communication above F zone)
Layer 2	San Andres Zone E1	0.1
Layer 3	San Andres Zone E2	0.1
Layer 4	San Andres Zone E3	0.1
Layer 5	San Andres Zone D	0.01
Layer 6	San Andres Zone C	0.001

### Pay continuity as a function of well-spacing:

The San Andres intervals A through G are correlate over the entire lease, and are independent of well spacing.

### Reservoir dip (angle and direction):

The lease dips slightly down to the South East over the majority of the field. To the southern and eastern extremities lies a steeper dip down into the Central Basin. This is illustrated below with the Base Of the Cowden Sand, the interval immediately above the San Andres.



**Location and extent of faults or other flow barriers (if applicable):**

The San Andres is believed not to have any naturally occurring fractures. As discussed in the reservoir characterization sections the top C zone is believed to form a vertical communication barrier. The tight Cowden Sand forms the seal above the San Andres reservoir interval.

**Location and extent of salt domes (if applicable):**

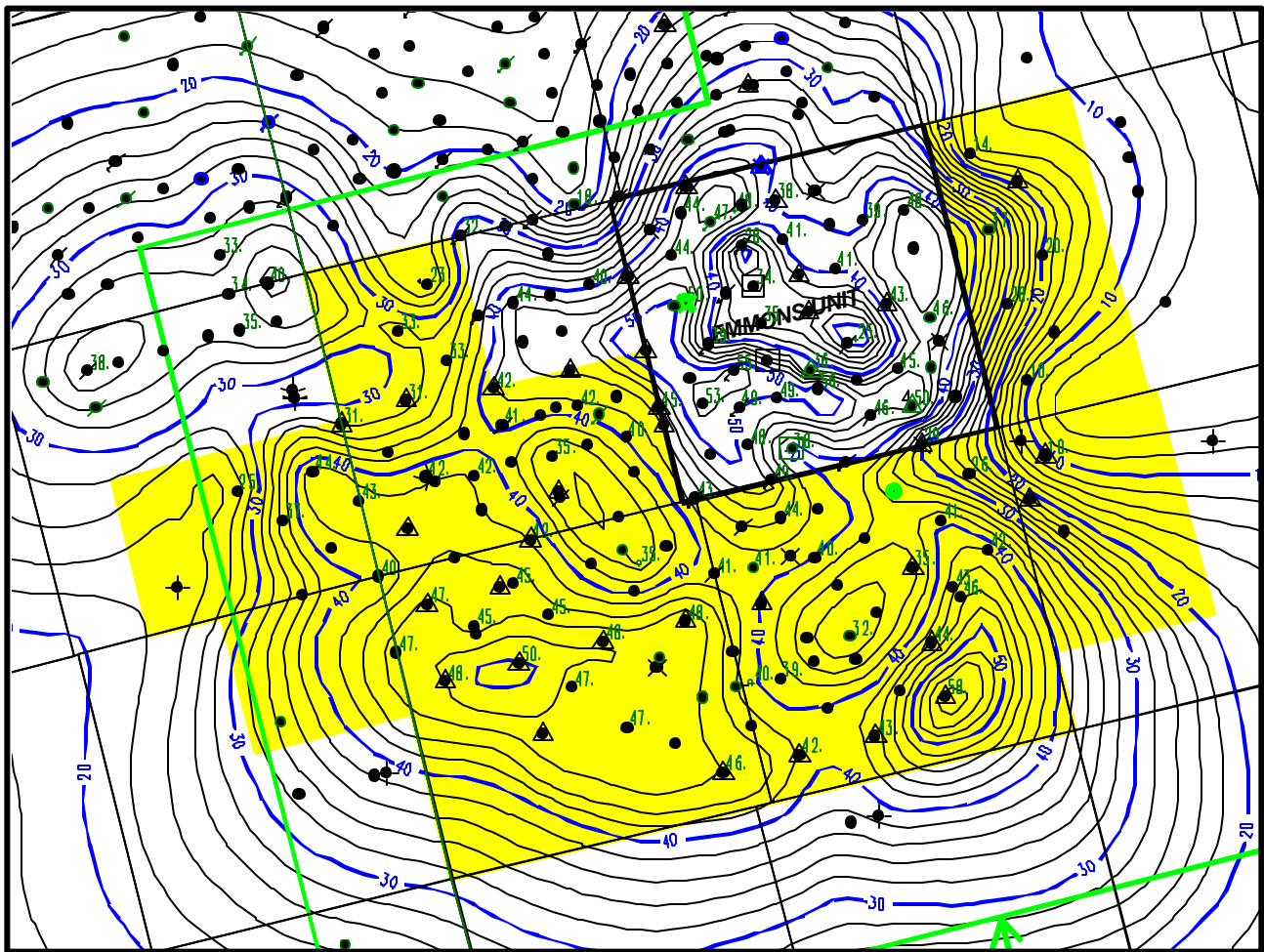
None

**Measure of cross flow among reservoir layers:**

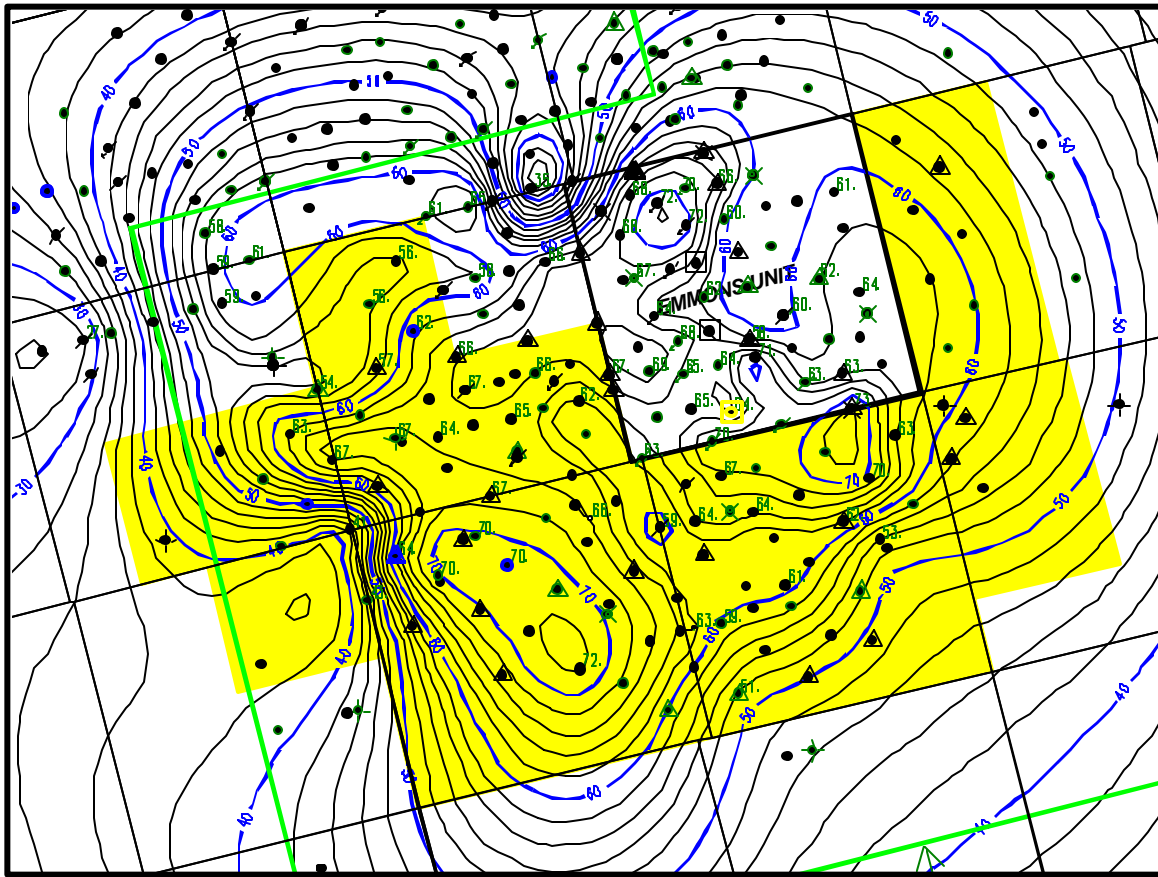
None

# Average net pay thickness, distribution and map:

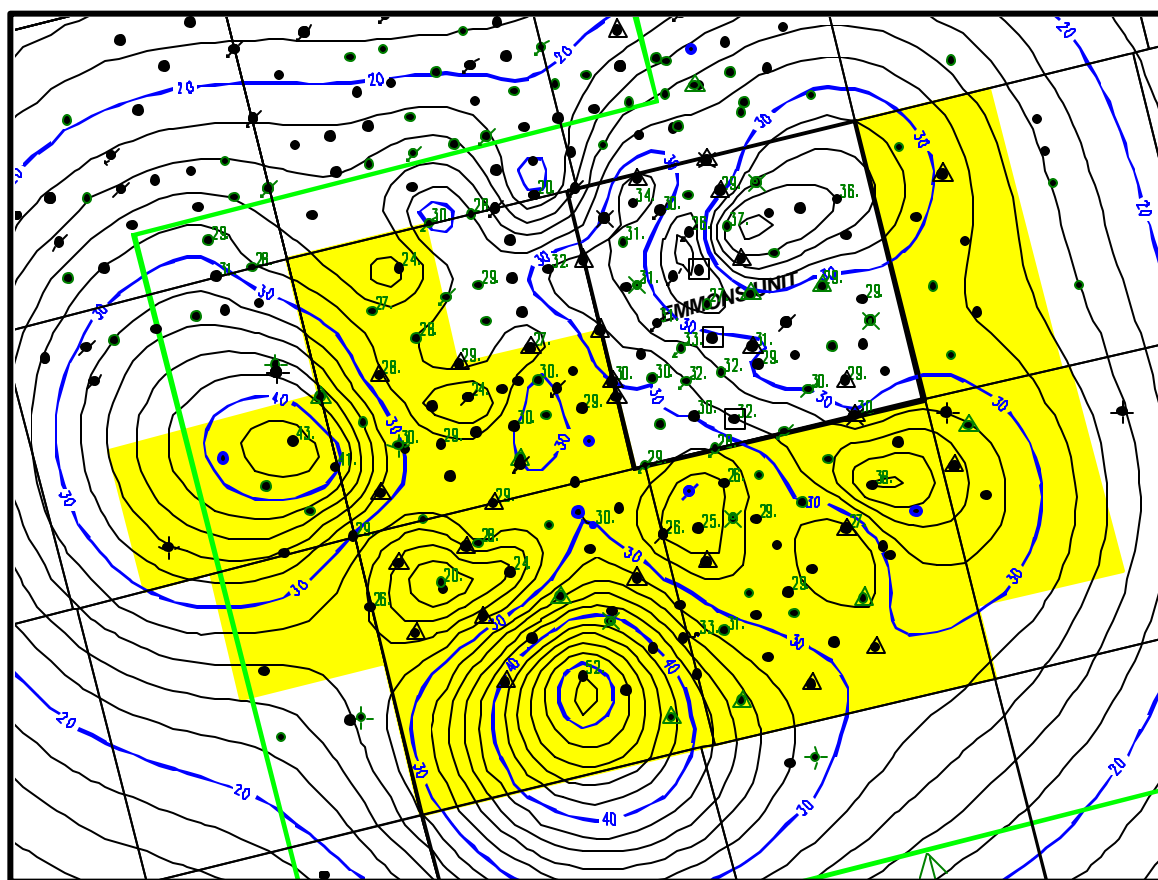
Net Isopach Map (Taken from Geological Model San Andres zone F)  
(contour 2' interval)



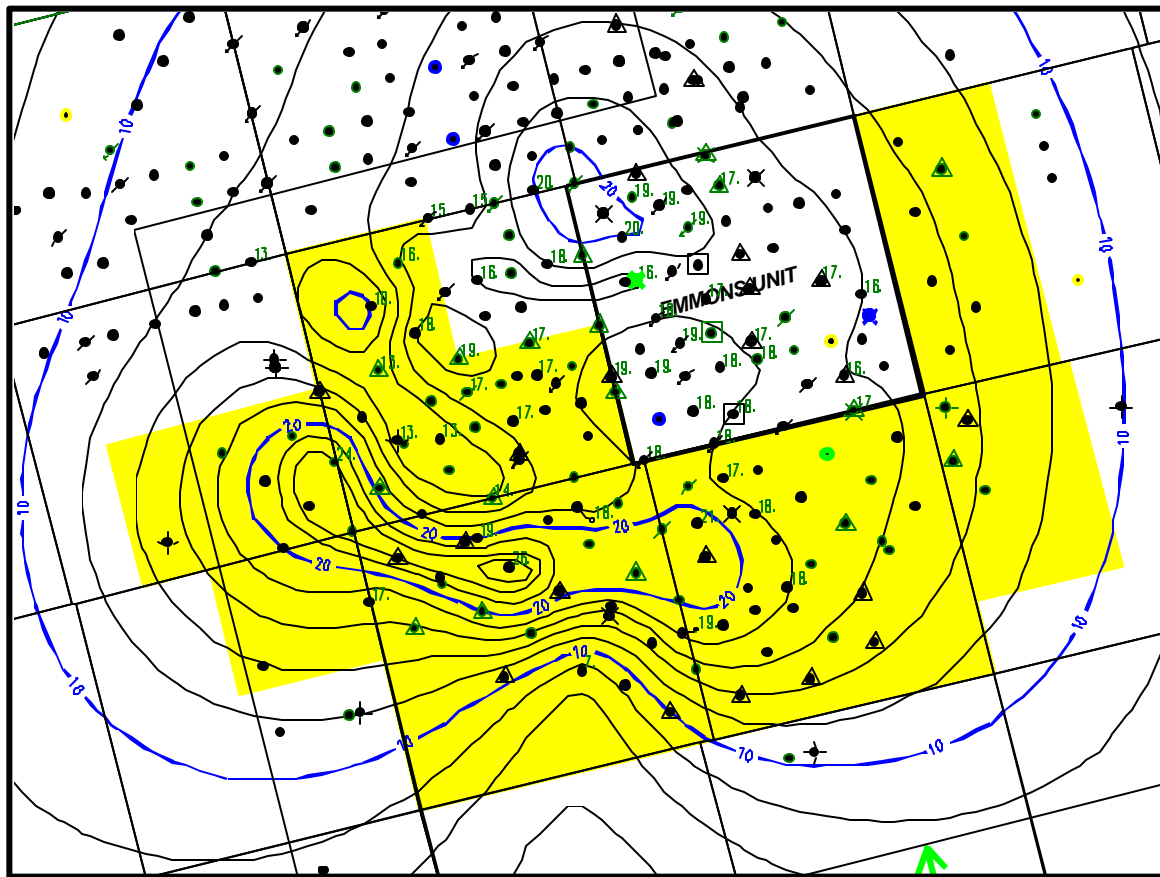
Net Isopach Map (Taken from Geological Model San Andres zone E)  
(contour 2' interval)



**Net Isopach Map (Taken from Geological Model San Andres zone D)**  
(contour 2' interval)

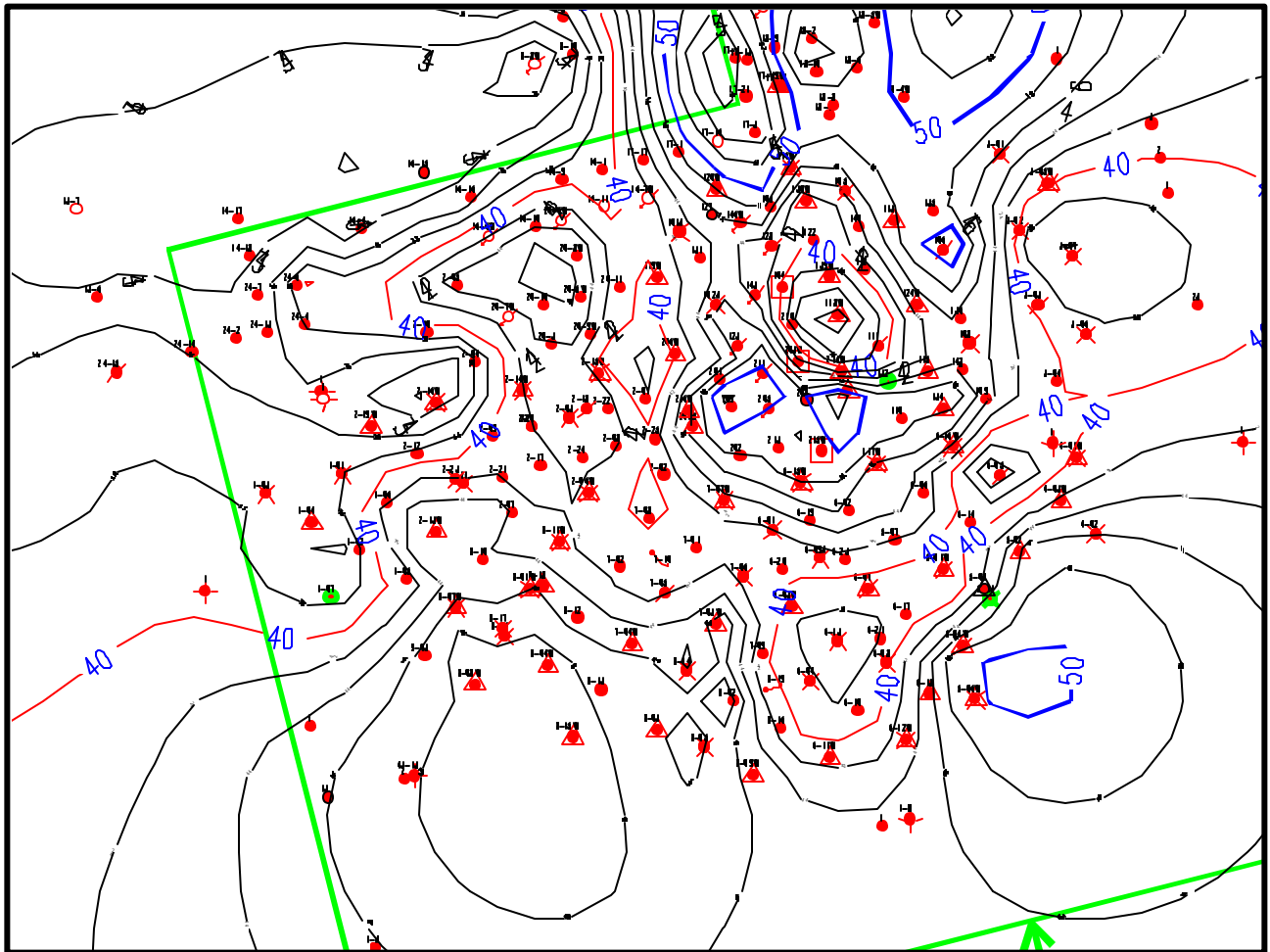


Net Isopach Map (Taken from Geological Model San Andres zone C)  
(contour 2' interval)



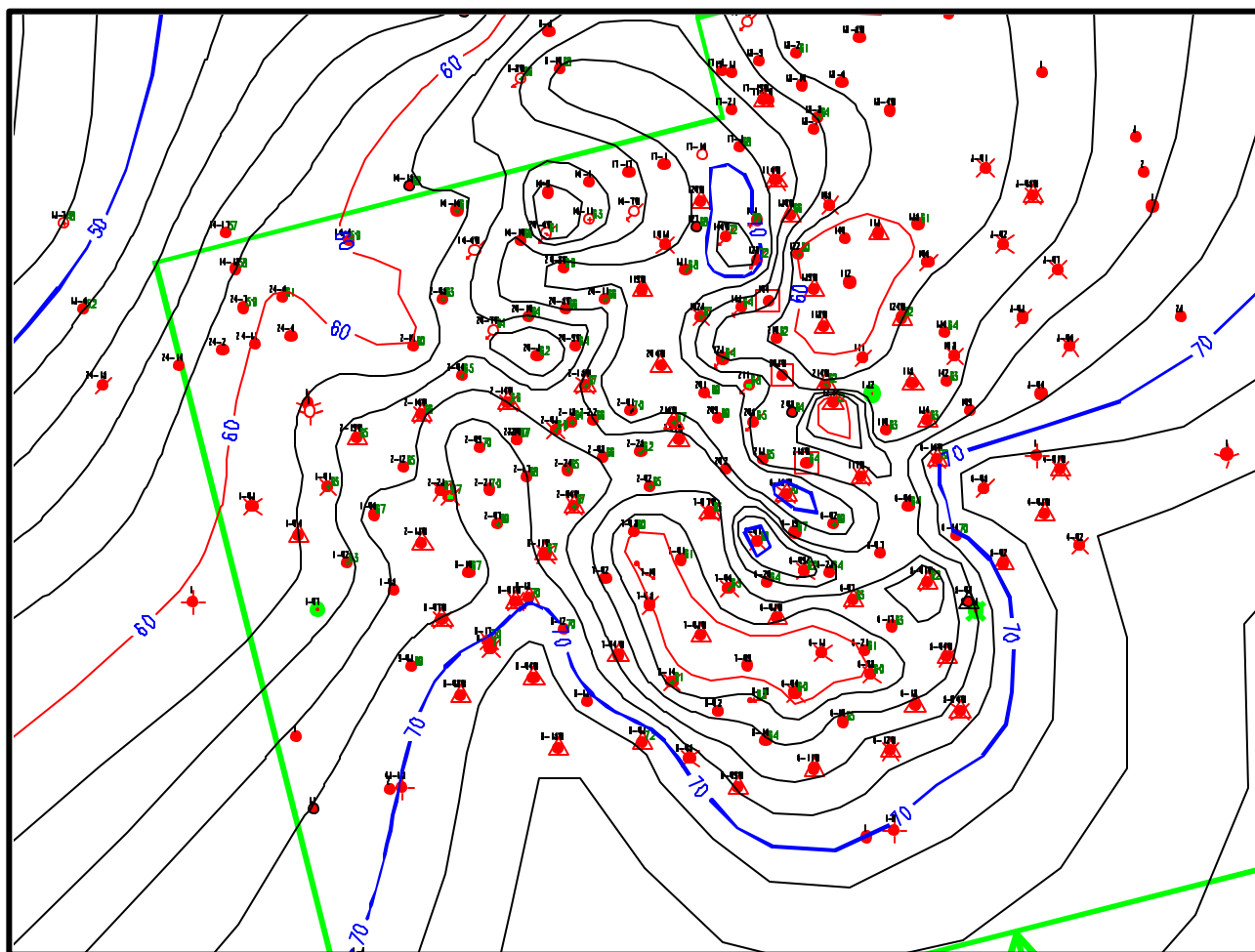
# Average gross pay thickness, distribution and map:

Gross Isopach Map (Taken from Geological Model San Andres zone F)  
(contour 2' interval)

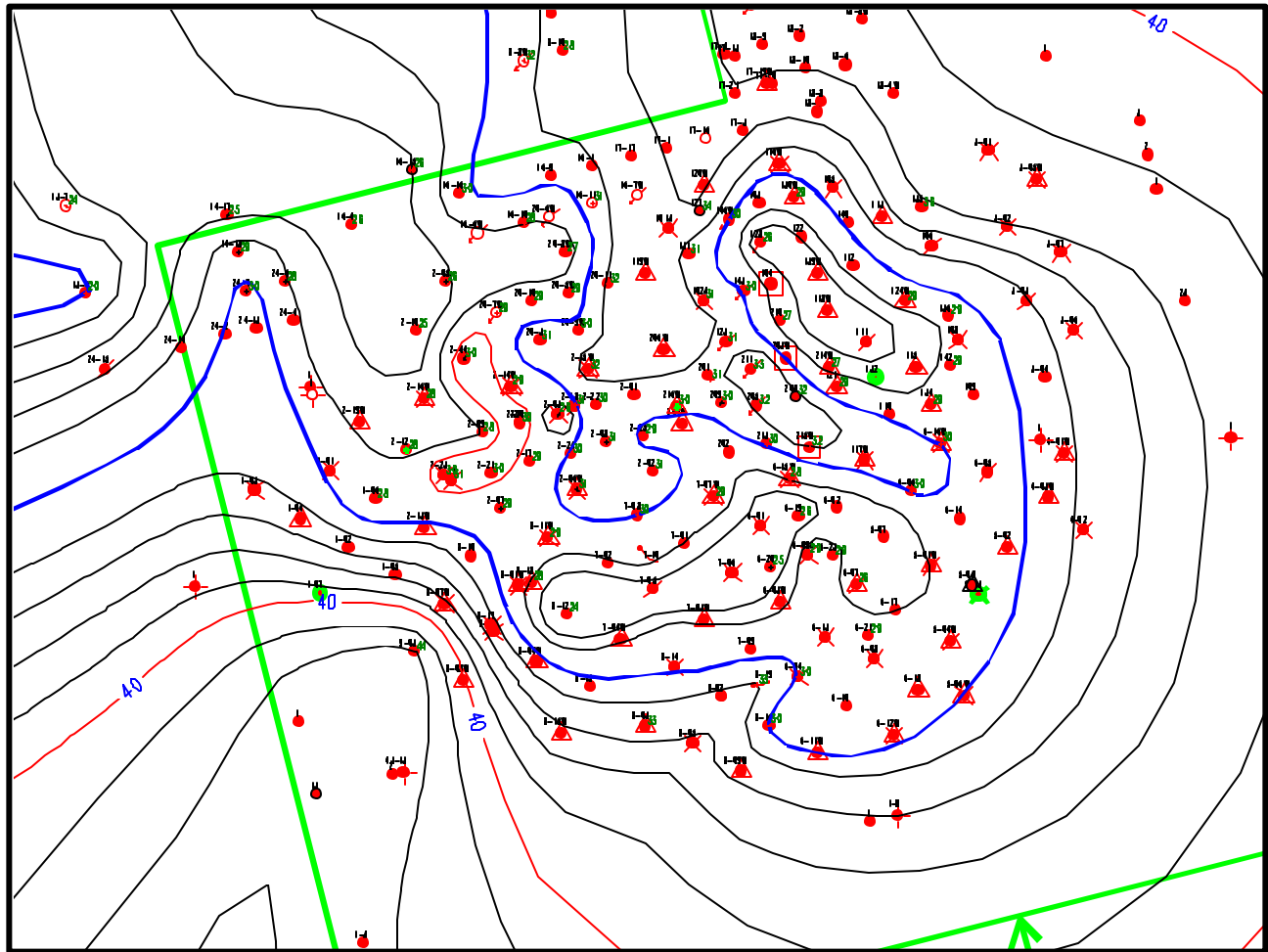




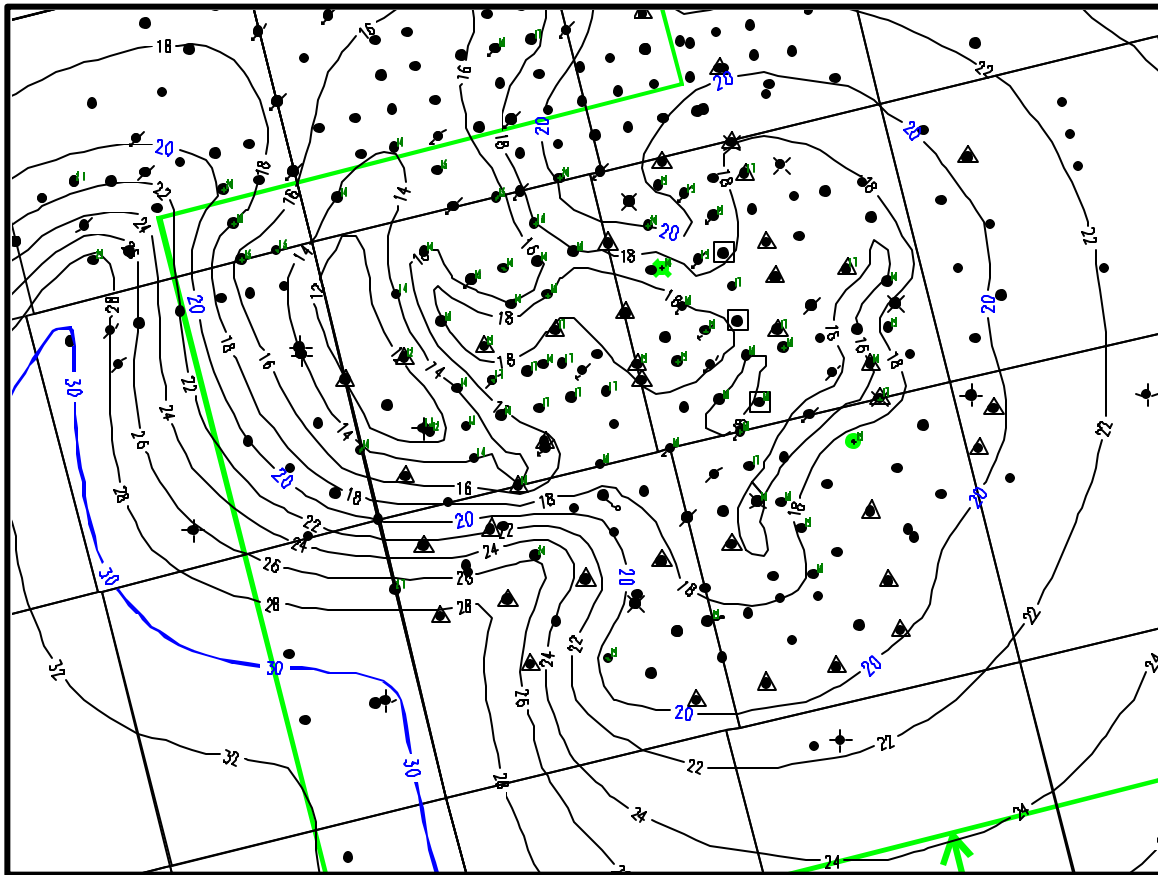
**Gross Isopach Map (Taken from Geological Model San Andres zone E)**  
 (contour 2' interval)



Gross Isopach Map (Taken from Geological Model San Andres zone D)  
(contour 2' interval)



**Gross Isopach Map (Taken from Geological Model San Andres zone C)**  
(contour 2' interval)



**Number of reservoir layers:**

The San Andres was split up into 7 layers, A through G. The main target for the CO<sub>2</sub> flood being layers C through F.

**Vertical porosity profile(s):**

None

**If gas cap is present:** None

- **Gas/Oil contact:**

- **Gas cap area:**

- **Gas cap bulk volume**

- **Gas-in-place**

**If aquifer is present:**

- **Initial oil-water contact:**

1800 TVD ft ss

- **Current oil-water contact:**

1800 TVD ft ss

- **Aquifer size:**

There is believed to be some aquifer support coming from the Central Basin to the East and South of the flood.

The original geological mapping of South Cowden Unit (SCU) showed pore volume (PV) going to zero outside of the well control to the East and South of the field. During the history matching phase of simulation modeling, with only the geologically mapped oil volume, producing well rates and pressures fell very rapidly during the early depletion period (prior to 1965).

This indicated either original oil in place (OOIP) needed to be larger or some additional source of pressure support prior to water injection. Several possibilities were evaluated including increasing PV in the outside row of aquifer cells (below oil water contact) to get a better match

with early performance. Increasing aquifer volume was judged the most reasonable explanation for extra reservoir energy. The calculated aquifer to oil pore volume ratio was estimated at 6.3 and was consistent with seismic data showing continuity of thickness and porosity in the zone down-dip to the East and South.

**- Water influx rate:**

No aquifer influx function was used

**GEOLOGICAL CHARACTERISTICS**

**Lithology:**

Grayburg and San Andres dolomite formations. These formations were deposited in shallow carbonate shelf environments along the eastern margin of the Central Basin Platform.

**Geologic Age:**

Permian Age

**Facies analysis for each reservoir:**

Detailed San Andres core descriptions were made of two full cores and several partial cores from the South Cowden Unit. Core information from the contiguous Emmons and Moss Units were also incorporated into the study. The core study concluded that reservoir quality in the South Cowden Unit is controlled primarily by the distribution of a bioturbated and diagenetically altered rock type with a distinctive “chaotic” texture. The “chaotic” modifier derives from the visual effect of pervasive, small-scale intermixing of tan oil-stained reservoir rock with tight gray non-reservoir rock.

**- Description of depositional facies:**

Refer to attached Core Analysis Report in supporting data.

**- Distribution of facies across the project area:**

Refer to attached Core Analysis Report in supporting data.

**- Distribution of porosity, permeability, oil saturation, and net pay by facies:**

Refer to attached Core Analysis Report in supporting data.

**- Cross-plot of permeability vs. porosity by facies:**

Refer to attached Core Analysis Report in supporting data. Also refer to section describing layer permeability properties for cross plots of porosity and permeability by layer.

**- Wireline log response to depositional facies:**

Refer to attached Core Analysis Report in supporting data.

**- Horizontal continuity and vertical communication of facies:**

Refer to attached Core Analysis Report in supporting data.

**Description of geologic elements:**

**- Depositional environment:**

Refer to attached Core Analysis Report in supporting data.

**- Reservoir diagenesis:**

Refer to attached Core Analysis Report in supporting data.

**- Structural style:**

Refer to attached Core Analysis Report in supporting data.

**Evaluation of reservoir heterogeneity:**

**- Microscopic heterogeneity; pore throat size distribution:**

Refer to attached Core Analysis Report in supporting data.

**- Microscopic heterogeneity; features at interwell scale:**

Refer to attached Core Analysis Report in supporting data.

**- Megascopic heterogeneity; features at field/reservoir level:**

Refer to attached Core Analysis Report in supporting data.

**FLUID CHARACTERISTICS:**

**Initial reservoir pressure:**

1730 psia @ -1625 ft. Ss Datum

**Log of reservoir pressure vs. production (or time):**Reservoir pressure history:

<u>Date</u>	<u>Pressure</u>	<u>Datum</u>	<u>Comments / Source</u>
1960	545 psia	-1600 ft ss	average of 33 well survey
1965	500 psig	unkown	from correspondence
1967	617 psia	-1625 ft ss	range (<500 psi to > 1500 psi) (from pressure map)
1992	2247 psia		(avg of 11 RFT pressures taken in SCU 8-19)**
1994	2360 psia		(avg of 7 RFT pressures taken in SCU 6-23)**
1994	2350 psia	-1800 ft ss (est)	P* from buildup in SCU 6-23 **
	2090 psia	-1796 ft ss	P* from buildup in SCU 6-21 **

(\*\* NOTE: Pressure buildup and RFT data included with supporting data)

**Reservoir temperature:**

98 F

**Oil gravity:**

36 API

**Oil viscosity at standard condition:**

4.2 cp

**Oil viscosity at In-situ reservoir condition:**

2.0 cp

**Initial oil formation volume factor (Bo):**

1.12 RB / STB

**Bubble point pressure:**

625 psia

**Initial gas in solution (Rs):**

217 SCF / STB

**Fluid composition test (CO<sub>2</sub>, N<sub>2</sub>, H<sub>2</sub>, Hydrocarbons):**

South Cowden Reservoir Fluid Composition  
Normalized Feed Mole Fractions

Component	Number	
N <sub>2</sub>	1	0.0047
CO <sub>2</sub>	2	0.0066
H <sub>2</sub> S	3	0.0209
C <sub>1</sub>	4	0.1150
C <sub>2</sub>	5	0.0575
C <sub>3</sub>	6	0.0704
IC <sub>4</sub>	7	0.0156
C <sub>4</sub>	8	0.0447
IC <sub>5</sub>	9	0.0249
C <sub>5</sub>	10	0.0239
C <sub>6</sub>	11	0.0699
C <sub>7</sub>	12	0.5459
SUM:		1.0000

C<sub>7+</sub> Molecular Weight 228.00

C<sub>7+</sub> Specific Gravity 0.8784

Reservoir Temperature 98 F

**Gas gravity:**

0.839

**Gas viscosity:**

0.0152 cp

**Initial gas formation volume factor (Bg):**

0.000497 RB/SCF



**Log of Bo, Rs, Bg as a function of reservoir pressure:**

Complete laboratory PVT reports are included with Supporting Data. Additional information on reservoir fluid characterization is presented in the sections on Reservoir Simulation.

**Water density:**

1.056 gm / cc (65.9 lb / ft<sup>3</sup>)

**Water viscosity:**

0.80 cp

**Water salinity:****South Cowden Water Analyses**

Water Sample	%TDS	Na	K	Ca	Mg	Sr	Cl	SO <sub>4</sub>
					ppm			
Tract2-Trans,Pump	7.27	22800	388	2500	619	55.8	36200	3593
Tract 6-FWKO	7.84	25100	441	2490	633	55.0	39900	3238
Tract6-IPD	7.84	25200	513	2490	650	55.3	39400	3237
Tract6-FWKO (Aerated and filtered)	7.72	24900	442	2420	636	53.4	40500	4173

## **FIGURE III**

## FIGURE III

### FIELD DEVELOPMENT HISTORY

#### RECOVERY TECHNIQUES UTILIZED

**Primary:** Solution gas drive and fluid expansion

**Secondary:** Waterflood

**Tertiary:** Alternating CO<sub>2</sub> / water miscible flood

**Advanced secondary (including horizontal drilling):**

#### FOR EACH RECOVERY TECHNIQUE

##### Primary

**Start date:**

1940

**Project life:**

25 years

**Estimated incremental recovery:**

10 MMSTB

**Monthly production by well:**

Individual well production data is supplied in the Oilfield Manager (OFM) database.

**Type of injectant:**

N/A

**Injection schedule (Bbl/day/well):**

N/A

**Number and timing of new wells drilled (producer, injection, disposal):**

33 producers were drilled between 1940 and April 1965.

A total of 57 producers were drilled between 1940 and June 1965.

**Number and timing of wells converted (producer to injection or to disposal):**

N/A

**Secondary**

**Start date:**

June 1965

**Project life:**

31 years

**Estimated incremental recovery:**

25.4 MMSTB above primary

**Monthly production by well:**

Individual well production data is supplied in the OFM database.

**Type of injectant:**

Water

**Injection schedule (Bbl/day/well):**

Individual well production data is supplied in the OFM database

**Number and timing of new wells drilled (producer, injection, disposal):**

**SCU WELL HSITORY (1959 Onwards)**

	Wells	Wells	Wells
	Prod.	Injecting	Injecting
	Oil	Water	Gas
Date	wells	wells	wells
3/1/1959	33	0	0
4/1/1959	33	0	0
5/1/1959	33	0	0
6/1/1959	33	0	0
7/1/1959	33	0	0
8/1/1959	33	0	0
9/1/1959	33	0	0
10/1/1959	33	0	0
11/1/1959	33	0	0
12/1/1959	33	0	0
1/1/1960	33	0	0
2/1/1960	33	0	0
3/1/1960	33	0	0
4/1/1960	33	0	0
5/1/1960	33	0	0
6/1/1960	33	0	0
7/1/1960	33	0	0
8/1/1960	33	0	0
9/1/1960	33	0	0
10/1/1960	33	0	0
11/1/1960	33	0	0
12/1/1960	33	0	0
1/1/1961	33	0	0
2/1/1961	33	0	0
3/1/1961	33	0	0
4/1/1961	33	0	0
5/1/1961	33	0	0
6/1/1961	33	0	0
7/1/1961	33	0	0
8/1/1961	33	0	0
9/1/1961	33	0	0
10/1/1961	33	0	0
11/1/1961	33	0	0
12/1/1961	33	0	0

1/1/1962	33	0	0
2/1/1962	33	0	0
3/1/1962	33	0	0
4/1/1962	33	0	0
5/1/1962	33	0	0
6/1/1962	33	0	0
7/1/1962	33	0	0
8/1/1962	33	0	0
9/1/1962	33	0	0
10/1/1962	33	0	0
11/1/1962	33	0	0
12/1/1962	33	0	0
1/1/1963	33	0	0
2/1/1963	33	0	0
3/1/1963	33	0	0
4/1/1963	33	0	0
5/1/1963	33	0	0
6/1/1963	33	0	0
7/1/1963	33	0	0
8/1/1963	33	0	0
9/1/1963	33	0	0
10/1/1963	33	0	0
11/1/1963	33	0	0
12/1/1963	33	0	0
1/1/1964	33	0	0
2/1/1964	33	0	0
3/1/1964	33	0	0
4/1/1964	33	0	0
5/1/1964	33	0	0
6/1/1964	33	0	0
7/1/1964	33	0	0
8/1/1964	33	0	0
9/1/1964	33	0	0
10/1/1964	33	0	0
11/1/1964	33	0	0
12/1/1964	33	0	0
1/1/1965	33	0	0
2/1/1965	33	0	0
3/1/1965	33	0	0
4/1/1965	57	0	0
5/1/1965	56	0	0
6/1/1965	57	0	0
7/1/1965	53	3	0
8/1/1965	53	3	0
9/1/1965	54	3	0
10/1/1965	52	4	0

11/1/1965	52	4	0
12/1/1965	51	4	0
1/1/1966	52	4	0
2/1/1966	49	7	0
3/1/1966	45	10	0
4/1/1966	44	11	0
5/1/1966	44	11	0
6/1/1966	44	11	0
7/1/1966	46	11	0
8/1/1966	46	11	0
9/1/1966	44	11	0
10/1/1966	45	11	0
11/1/1966	45	11	0
12/1/1966	45	10	0
1/1/1967	45	10	0
2/1/1967	46	10	0
3/1/1967	45	10	0
4/1/1967	45	10	0
5/1/1967	45	10	0
6/1/1967	46	10	0
7/1/1967	46	10	0
8/1/1967	46	10	0
9/1/1967	46	10	0
10/1/1967	46	10	0
11/1/1967	46	10	0
12/1/1967	46	10	0
1/1/1968	46	10	0
2/1/1968	45	10	0
3/1/1968	44	10	0
4/1/1968	44	10	0
5/1/1968	42	11	0
6/1/1968	42	11	0
7/1/1968	42	11	0
8/1/1968	41	12	0
9/1/1968	41	12	0
10/1/1968	42	13	0
11/1/1968	42	13	0
12/1/1968	42	13	0
1/1/1969	42	13	0
2/1/1969	42	12	0
3/1/1969	42	12	0
4/1/1969	42	12	0
5/1/1969	42	12	0
6/1/1969	42	12	0
7/1/1969	40	12	0
8/1/1969	40	13	0

9/1/1969	41	13	0
10/1/1969	41	13	0
11/1/1969	41	13	0
12/1/1969	41	13	0
1/1/1970	41	14	0
2/1/1970	40	14	0
3/1/1970	40	14	0
4/1/1970	40	14	0
5/1/1970	40	14	0
6/1/1970	40	14	0
7/1/1970	41	14	0
8/1/1970	41	14	0
9/1/1970	41	14	0
10/1/1970	41	14	0
11/1/1970	41	14	0
12/1/1970	41	14	0
1/1/1971	41	14	0
2/1/1971	41	14	0
3/1/1971	41	14	0
4/1/1971	41	14	0
5/1/1971	41	14	0
6/1/1971	41	14	0
7/1/1971	40	14	0
8/1/1971	40	14	0
9/1/1971	40	14	0
10/1/1971	42	14	0
11/1/1971	42	14	0
12/1/1971	41	14	0
1/1/1972	43	14	0
2/1/1972	43	14	0
3/1/1972	42	14	0
4/1/1972	43	14	0
5/1/1972	42	15	0
6/1/1972	42	15	0
7/1/1972	42	15	0
8/1/1972	42	16	0
9/1/1972	43	16	0
10/1/1972	43	15	0
11/1/1972	41	15	0
12/1/1972	42	15	0
1/1/1973	42	15	0
2/1/1973	42	17	0
3/1/1973	42	17	0
4/1/1973	44	17	0
5/1/1973	44	17	0
6/1/1973	44	17	0



7/1/1973	44	17	0
8/1/1973	44	17	0
9/1/1973	44	17	0
10/1/1973	44	17	0
11/1/1973	42	19	0
12/1/1973	43	19	0
1/1/1974	43	19	0
2/1/1974	45	19	0
3/1/1974	45	19	0
4/1/1974	45	19	0
5/1/1974	45	19	0
6/1/1974	47	19	0
7/1/1974	51	19	0
8/1/1974	51	19	0
9/1/1974	51	19	0
10/1/1974	51	19	0
11/1/1974	50	19	0
12/1/1974	50	19	0
1/1/1975	50	20	0
2/1/1975	51	20	0
3/1/1975	54	20	0
4/1/1975	54	20	0
5/1/1975	54	20	0
6/1/1975	54	20	0
7/1/1975	54	20	0
8/1/1975	54	20	0
9/1/1975	54	20	0
10/1/1975	55	20	0
11/1/1975	55	20	0
12/1/1975	55	20	0
1/1/1976	55	20	0
2/1/1976	55	20	0
3/1/1976	54	21	0
4/1/1976	54	21	0
5/1/1976	54	21	0
6/1/1976	54	21	0
7/1/1976	54	21	0
8/1/1976	54	21	0
9/1/1976	54	21	0
10/1/1976	54	21	0
11/1/1976	54	21	0
12/1/1976	54	21	0
1/1/1977	53	21	0
2/1/1977	54	21	0
3/1/1977	53	21	0
4/1/1977	53	21	0

5/1/1977	53	21	0
6/1/1977	53	21	0
7/1/1977	53	21	0
8/1/1977	53	22	0
9/1/1977	53	22	0
10/1/1977	53	22	0
11/1/1977	53	22	0
12/1/1977	53	22	0
1/1/1978	53	22	0
2/1/1978	53	22	0
3/1/1978	53	22	0
4/1/1978	53	22	0
5/1/1978	53	22	0
6/1/1978	53	22	0
7/1/1978	53	22	0
8/1/1978	53	22	0
9/1/1978	53	22	0
10/1/1978	53	22	0
11/1/1978	53	22	0
12/1/1978	53	22	0
1/1/1979	53	22	0
2/1/1979	53	22	0
3/1/1979	53	22	0
4/1/1979	52	22	0
5/1/1979	51	21	0
6/1/1979	51	21	0
7/1/1979	52	21	0
8/1/1979	54	22	0
9/1/1979	55	22	0
10/1/1979	54	22	0
11/1/1979	53	22	0
12/1/1979	53	22	0
1/1/1980	53	22	0
2/1/1980	53	22	0
3/1/1980	54	22	0
4/1/1980	54	17	0
5/1/1980	54	16	0
6/1/1980	54	22	0
7/1/1980	53	22	0
8/1/1980	53	22	0
9/1/1980	54	22	0
10/1/1980	52	22	0
11/1/1980	54	22	0
12/1/1980	52	22	0
1/1/1981	53	22	0
2/1/1981	54	22	0

3/1/1981	54	22	0
4/1/1981	54	22	0
5/1/1981	54	22	0
6/1/1981	54	22	0
7/1/1981	53	22	0
8/1/1981	54	22	0
9/1/1981	52	22	0
10/1/1981	53	22	0
11/1/1981	52	22	0
12/1/1981	51	22	0
1/1/1982	52	22	0
2/1/1982	52	22	0
3/1/1982	52	22	0
4/1/1982	53	22	0
5/1/1982	53	22	0
6/1/1982	51	19	0
7/1/1982	55	22	0
8/1/1982	55	23	0
9/1/1982	55	23	0
10/1/1982	55	23	0
11/1/1982	56	23	0
12/1/1982	55	23	0
1/1/1983	55	23	0
2/1/1983	55	23	0
3/1/1983	56	24	0
4/1/1983	56	24	0
5/1/1983	56	24	0
6/1/1983	56	24	0
7/1/1983	56	24	0
8/1/1983	56	24	0
9/1/1983	55	24	0
10/1/1983	56	23	0
11/1/1983	55	23	0
12/1/1983	54	24	0
1/1/1984	54	24	0
2/1/1984	55	24	0
3/1/1984	55	24	0
4/1/1984	55	24	0
5/1/1984	54	24	0
6/1/1984	54	24	0
7/1/1984	54	24	0
8/1/1984	54	24	0
9/1/1984	54	24	0
10/1/1984	54	24	0
11/1/1984	56	24	0
12/1/1984	56	24	0

1/1/1985	55	24	0
2/1/1985	56	24	0
3/1/1985	54	26	0
4/1/1985	54	26	0
5/1/1985	53	26	0
6/1/1985	54	26	0
7/1/1985	54	26	0
8/1/1985	54	26	0
9/1/1985	54	26	0
10/1/1985	54	26	0
11/1/1985	54	26	0
12/1/1985	55	26	0
1/1/1986	54	25	0
2/1/1986	54	26	0
3/1/1986	54	25	0
4/1/1986	54	26	0
5/1/1986	54	26	0
6/1/1986	55	26	0
7/1/1986	55	26	0
8/1/1986	53	26	0
9/1/1986	55	26	0
10/1/1986	53	26	0
11/1/1986	54	26	0
12/1/1986	54	26	0
1/1/1987	55	26	0
2/1/1987	56	26	0
3/1/1987	55	26	0
4/1/1987	55	26	0
5/1/1987	54	26	0
6/1/1987	54	26	0
7/1/1987	54	26	0
8/1/1987	54	26	0
9/1/1987	54	26	0
10/1/1987	54	26	0
11/1/1987	54	26	0
12/1/1987	54	26	0
1/1/1988	53	26	0
2/1/1988	53	26	0
3/1/1988	52	26	0
4/1/1988	53	26	0
5/1/1988	53	26	0
6/1/1988	53	26	0
7/1/1988	53	26	0
8/1/1988	53	26	0
9/1/1988	53	26	0
10/1/1988	53	25	0
11/1/1988	53	25	0

12/1/1988	53	25	0
1/1/1989	52	25	0
2/1/1989	52	25	0
3/1/1989	51	25	0
4/1/1989	52	25	0
5/1/1989	52	25	0
6/1/1989	52	26	0
7/1/1989	52	26	0
8/1/1989	52	25	0
9/1/1989	52	26	0
10/1/1989	52	26	0
11/1/1989	52	26	0
12/1/1989	52	26	0
1/1/1990	52	26	0
2/1/1990	53	23	0
3/1/1990	53	26	0
4/1/1990	53	23	0
5/1/1990	53	21	0
6/1/1990	52	21	0
7/1/1990	52	22	0
8/1/1990	52	24	0
9/1/1990	53	22	0
10/1/1990	51	21	0
11/1/1990	50	19	0
12/1/1990	53	24	0
1/1/1991	53	23	0
2/1/1991	52	22	0
3/1/1991	52	22	0
4/1/1991	51	20	0
5/1/1991	51	20	0
6/1/1991	52	20	0
7/1/1991	52	19	0
8/1/1991	51	20	0
9/1/1991	51	20	0
10/1/1991	51	20	0
11/1/1991	51	20	0
12/1/1991	51	20	0
1/1/1992	50	20	0
2/1/1992	48	20	0
3/1/1992	52	20	0
4/1/1992	50	19	0
5/1/1992	52	20	0
6/1/1992	52	20	0
7/1/1992	52	20	0
8/1/1992	52	20	0
9/1/1992	52	19	0

10/1/1992	52	20	0
11/1/1992	52	19	0
12/1/1992	52	19	0
1/1/1993	52	19	0
2/1/1993	53	19	0
3/1/1993	51	18	0
4/1/1993	51	18	0
5/1/1993	51	17	0
6/1/1993	50	17	0
7/1/1993	50	18	0
8/1/1993	49	18	0
9/1/1993	47	18	0
10/1/1993	46	18	0
11/1/1993	46	18	0
12/1/1993	45	18	0
1/1/1994	41	18	0
2/1/1994	39	17	0
3/1/1994	39	17	0
4/1/1994	38	19	0
5/1/1994	38	16	0
6/1/1994	39	16	0
7/1/1994	39	16	0
8/1/1994	38	16	0
9/1/1994	39	17	0
10/1/1994	38	17	0
11/1/1994	39	11	0
12/1/1994	39	12	0
1/1/1995	39	13	0
2/1/1995	39	12	0
3/1/1995	39	12	0
4/1/1995	39	12	0
5/1/1995	39	12	0
6/1/1995	39	12	0
7/1/1995	39	12	0
8/1/1995	39	12	0
9/1/1995	39	13	0
10/1/1995	39	11	0
11/1/1995	39	10	0
12/1/1995	41	11	0
1/1/1996	42	14	0
2/1/1996	42	13	0
3/1/1996	42	12	0
4/1/1996	40	14	0
5/1/1996	40	12	0
6/1/1996	40	12	0

Number and timing of wells converted (producer to injection or to disposal):

SCU CONVERTED WELLS	
FROM PRODUCER TO INJECTION	
	1st Month
	Date
Number	Injection
Well	on
005W06	7/1/1965
008W05	7/1/1965
001W04	7/1/1965
003W05	10/1/1965
008W08	2/1/1966
007W04	2/1/1966
006W03	2/1/1966
005W01	3/1/1966
006W11	3/1/1966
002W13	3/1/1966
002W06	3/1/1966
008W04	5/1/1968
005W04	5/1/1972
008W07	2/1/1973
008W01	2/1/1973
008W09	11/1/1973
002W16	3/1/1976
008W11	6/1/1979
004W01	3/1/1983
008W15	3/1/1985
009W02	3/1/1985
004W03	6/1/1989

### Tertiary

Start date:

July 1996

Project life:

Expected 25 years + , dependent on oil pricing and operating expense.

**Estimated incremental recovery:**

12.4 MMSTB above waterflood recovery

**Monthly production by well:**

Individual expected well production data is supplied in the simulation output.

**Type of injectant:**

CO<sub>2</sub>

**Injection schedule (Bbl/day/well):**

Individual expected well injection data is supplied in the simulation output.



**Number and timing of new wells drilled (producer, injection, disposal):**

**SCHEDULE OF WORK  
(WELLS)**

1995

Drill Well RC-3 (6-24)

1996

Drill Wells H-1 and H-2

Drill vertical wag injector 206C (2-26W)

Drill two lease line vertical wag injectors 707 and M17C

Equip 615W as wag injector

Drill producing wells 798, 7-12, 6-22 and 799

Reactivate producers 705 and 620

Convert to water injection wells 2-21, 8-18, 8-03, 6-18  
and 5-02

1997

Reactivate 6-16W as lease line water injector

Reactivate producers 6-19, 7-02, 7-08 and 8-13

Drill vertical wag injector 208C (2-27W)

1998

Drill producing wells 203A and 699

Reactivate producers 2-20 and 6-05

1999+

Drill four replacement producers (locations to be  
determined)

Convert to wag injection: RC3 and 224C

**Number and timing of wells converted (producer to injection or to disposal):**

See above

**SUMMARY OF WELLS: FOR EACH WELL IN THE PROJECT AREA**

**Well Name, Existing well or Project well, API Reference No., Completion Data, Formation top (MD & TVD), Formation base (MD & TVD), Total depth (MD & TVD), Vertical or Horizontal, Horizontal: radius, lateral, TVD, MD, Status (producing; flowing or artificial lift; Type of artificial lift), Perforated intervals (MVD), Cored intervals, Completion Type (openhole, gravel pack, cased and perforated, etc), Stimulation type (acid, fracture treatment).**

South Cowden Unit Field Development History													
Operator / Lease Name	Ending or Project Well No.	API No.	Completion Date	MD Above Sea	Top (BGS)	E Top	E Top	D Top	C Top	R Top	A Top	A Mid	A Base
Well No.	Well	API No.	Completion Date	MD Above Sea	Top (BGS)	E Top	E Top	D Top	C Top	R Top	A Top	A Mid	A Base
IFCO South Cowden Unit	101	Existing	4213504769	2947	4595	4582?	4545	4712					
	102	Existing	4770	2958	4546								
	103	Existing	4771	2948	4582	4571?	4709	4776					
	104	Existing	4772	2946	4545	4561?	4701	4758					
	105	Existing	31384	2965	4547	4565	4705	4746					
	106	Existing	31402	2961	4595	4575	4545	4716	4744	4758	4733?		
	107	Existing	31383	2969	4583								
	201	Project	48304	2940	4481	4502	4539	4575	4635				
	202	Project	48305	2960	4526	4542	4582	4647	4678				
	203	Project	48306	2936	4476	4480	4533	4599	4625	4542			
	204	Existing	48307	2921	4479	4488	4531	4596	4626	4544			
	205	Existing	48308	2927	4477	4487	4532?	4595	4621	4537	4602?		
	206	Project	48309	2949	4508								
	207	Project	48310	2944	4540	4503	4542	4600	4627				
	208	Project	48311	2938	4492	4507	4550	4616	4647	4634	4689	4735	
	209	Project	48312	2933	4511	4521?	4564	4624	4662	4678	4718	4758	
	210	Existing	48313	2924	4493	4501	4542	4600	4627	4541	4607	4699	4733
	211	Existing	48314	2944	4550	4561?	4604	4671	4702	4737	4743?	4793?	
	212	Existing	48315	2938	4544	4554?	4601	4668	4694				
	20913	Project	48316	2956	4588	4619	4669	4738					
	20914	Project	21514	2930	4476	4488	4529	4595	4624	4543	4671	4708	4740?
	20915	Project	30920	2930	4480	4500	4520	4596	4624	4543	4671	4708	4740?
	20916	Project	30878	2932	4511	4531?	4563	4629	4657	4567			
	217	Project	31389	2942	4506	4519	4558	4621	4655	4571	4704	4735	
	218	Project	21191	2938	4483	4493	4534?	4597	4629	4546	4672?	4702?	
	20919	Existing	3396	2941	4533	4551?	4587	4645	4675	4543	4690		
	220	Project	33999	2932	4495	4505	4548	4615	4645	4562	4690		
	221	Project	34656	2966	4531	4542	4584	4654	4684	4597	4733		
	222	Project	34922	2936	4481	4495	4537	4603	4633	4599	4719	4737	
	223	Existing	35381	2943	4554	4565	4607	4674	4704	4717	4745?		
	224	Project	35153	2941	4490	4502	4546	4611	4641	4598	4698	4718	
	225	Project	35682	2947	4518	4530	4571	4633	4662	4579	4738	4755	
	301	Existing	2689	2945	4575	4605	4744						
	302	Existing	2681	2931	4563	4602?	4719						
	303	Existing	2651	2905	4543	4582							
	304	Existing	2682	2902	4578	4705							
	30405	Existing	2883	2985									
	305	Existing	3584	2901	4705								
	307	Existing	3585	2903	4598	4725							
	40601	Existing	2611	2902	4585	4715?							
	402	Existing	2610	2909	4721	4635							
	4003	Project	33910	2899	4578								
	5001	Project	5718	2902	4598	4601?	4641	4703					
	5002	Project	5719	2892	4570	4683	4730?	4787					
	503	Existing	5720	2907	4652	4684	4699	4731					
	5004	Project	5721	2922	4599	4600	4724	4754					
	505	Existing	5722	2901	4580	4672							
	5006	Existing	5723	2922	4587	4672							
	507	Project	30526	2924	4584	4679	4821	4888					
	508	Project	35362	2900	4551	4664	4707	4759					

South Cowden Unit Field Development History																										
Well No.	Operator / Lease Name	Project Well	API No.	Completion Date	R/O Acres	Top (BGS)	E Top	Fertigation Tops				A Top	A Mid	A Base	ID	Vertical or Horizontal	Status	Perforation Intervals	Cased Intervals	Completion Type	Simulation Type	Simulation Size Gals./Lbs. Sulf				
								D Top	C Top	B Top																
601	PFCO South Cowden Unit	Project	5797	Oct-48	2599	4586									4700	Vertical	Abandoned	4658-4700		Open-Hole	MHO	280 Cts				
602		Project	5798	Dec-48	2593	4551									4694	Vertical	Pumping	4653-4694		Open-Hole	Acid	1000				
603		Project	5799	Feb-49	2590	4507									4699	Vertical	Shut-In	4656-4699		Open-Hole	MHO	300 Cts				
604		Project	5800	Jun-49	2598	4517	46317	4669	4729	4759					4770	Vertical	Abandoned	4659-4770		Open-Hole	MHO	460 Cts				
605		Project	5801	Dec-49	2593	4504	46307	4682	4736						4738	Vertical	Abandoned	4653-4728		Open-Hole	MHO	440 Cts				
606		Project	5802	Feb-50	2591	4500									4738	Vertical	Pumping	4658-4738		Open-Hole	MHO	430 Cts				
607		Project	5803	Mar-50	2597	4575									4759	Vertical	Shut-In	4654-4759		Open-Hole	MHO	550 Cts				
608		Project	5804	Apr-50	2593	4523									4759	Vertical	Abandoned	4654-4759		Open-Hole	MHO	520 Cts				
609		Project	5805	Jun-50	2598	4570									4752	Vertical	Abandoned	4651-4752		Open-Hole	MHO	438 Cts				
610		Project	5806	Jul-50	2596	4590									4778	Vertical	Pumping	4655-4778		Open-Hole	MHO	431 Cts				
611		Project	5807	Oct-54	2598	4588	4671	4713	4773						4758	Vertical	Injecting	4653-4749		Open-Hole	First	3000 / 4500				
612		Existing	5808	May-55	2590	4590	4702	4745							4737	Vertical	Injecting			Open-Hole	MHO	260 Cts				
613		Project	31388	Aug-74	2544	4599									4718	Vertical	Abandoned	4659-4713		Cut & Perd	Acid	4000				
614		Project	31392	Aug-74	2511	4583	4656	4637	4707	4737					4770	Vertical	Pumping	4656-4657		Cut & Perd	Acid	4000				
615		Project	31400	Jul-75	2544	4547	4660	4689	4719	4726	4751				4651	Vertical	Injecting	4658-4718		Cut & Perd	Acid	6000				
616		Project	32189	Aug-77	2505	4555	45717	4612	4655	4715	4732				4625	Vertical	Shut-In	4630-4724		Cut & Perd	Acid	5000				
617		Project	33179	Jul-79	2508	4593									4720	Vertical	Pumping	4659-4618		Cut & Perd	Acid	5100				
618		Project	33895	Jul-82	2593	4576	4693	4731							4736	Vertical	Abandoned	4622-4711		Cut & Perd	Acid	4000				
619		Project	34621	Nov-84	2598	4598	4673	4612	4684	4710	4727				4775	Vertical	Abandoned	4670-4679		Cut & Perd	Acid	6000				
620		Project	36152	Sep-90	2548	4590	4694	4635	4698	4724	4737				4800	Vertical	Pumping	4650-4729		Cut & Perd	Acid	12000				
621	Project	36347	Sep-94	2598	4510	4625	4664	4725	4754	4772	4805			4800	Vertical	Abandoned	4658-4808	4800-4775	Cut & Perd	Acid	3000					
623	Project	36941	Sep-94	2593	4572	4595	4636	4690	4719	4737	4762			4800	Vertical	Pumping	4673-4672		Cut & Perd	Acid	2000					
701	Project	36535	Sep-94	2544	4574									4707	Vertical	Pumping	4694-4697		Open-Hole	Acid	3000					
702	Project	36536	Oct-98	2546	4584									4830	Vertical	Abandoned			Open-Hole	Acid	2500					
703	Project	36537	Nov-98	2598	4573	4591	4639	4705						4890	Vertical	Shut-In			Open-Hole	Acid	3000					
704	Project	36538	Nov-98	2553	4595	4619	4667	4737						4835	Vertical	Shut-In	4650-4835		Open-Hole	Acid	5900					
705	Project	36539	Dec-98	2548	4588									4730	Vertical	Abandoned	4670-4830		Open-Hole	Acid	2900					
706	Project	36540	Sep-99	2566	4590	4694	4636	4698	4723					4730	Vertical	Abandoned	4694-4715		Cut & Perd	Acid	3000					
707	Project	36541	Jan-00	2548	4554	4655	4688	4621	4700	4718				4750	Vertical	Abandoned	4650-4707		Cut & Perd	Acid	2000					
708	Project	36539	Jul-00	2548	4594									4770	Vertical	Pumping	4673-4737		Cut & Perd	Acid	3000					
709	Project	36537	Nov-01	2546	4586	4605	4647	4713	4743	4761	4793			4730	Vertical	Pumping	4651-4656	4830-4730	Cut & Perd	Acid	4000					
710	Project	36538	Jul-03	2596	4591	4605	4647	4713	4743	4761	4793			4774	Vertical	Abandoned	4648-4670	4830-4835	Cut & Perd	Acid	9100					
801	Existing	3516	Feb-49	2552	4511									4774	Vertical	Abandoned			Open-Hole	MHO	220 Cts					
802	Project	3517	Mar-49	2544	4511									4840	Vertical	Pumping	4649-4759		Open-Hole	MHO	220 Cts					
803	Project	3518	Apr-49	2591	4560	4601	4728	4830	4853	4902				4900	Vertical	Shut-In	4700-4792		Open-Hole	MHO	240 Cts					
804	Project	3519	Jul-49	2596	4561	4675	4725	4797						4790	Vertical	Injecting			Open-Hole	MHO	240 Cts					
805	Project	3520	Jul-50	2565	4588									4791	Vertical	Abandoned	4654-4738		Open-Hole	MHO	240 Cts					
806	Existing	3521	Jun-52	2598	4590									4820	Vertical	Abandoned	4658-4820		Open-Hole	MHO	250 Cts					
807	Existing	3522	Feb-55	2562	4563	4664	4711	4752						4790	Vertical	Abandoned	4654-4650		Open-Hole	MHO	268 Cts					
808	Existing	3523	Mar-55	2560	4593	4664	4743							4799	Vertical	Injecting	4627-4757		Open-Hole	MHO	220 Cts					
809	Project	3524	Jun-55	2546	4584	4702	4748							4791	Vertical	Injecting			Open-Hole	MHO	147 Cts					
810	Project	30665	Apr-73	2596	4512									4790	Vertical	Pumping	4654-4738		Cut & Perd	Acid	5000					
811	Project	30666	May-73	2548	4599	4674	4616	4683	4712	4726	4726			4750	Vertical	Abandoned	4658-4830	4830-4830	Cut & Perd	Acid	5000					
812	Project	31481	Mar-75	2567	4623	4635	4681	4751	4775	4801				4830	Vertical	Pumping	4654-4650		Cut & Perd	Acid	4000					
813	Project	31302	Feb-74	2599	4598	4675	4723							4830	Vertical	Abandoned	4673-4757		Cut & Perd	Acid	4000					
814	Project	31391	Jul-74	2562	4528									4790	Vertical	Abandoned	4610-4759		Cut & Perd	Acid	4000					
815	Project	31301	Feb-74	2562	4598									4800	Vertical	Injecting	4653-4791		Cut & Perd	Acid	4000					
816	Project	31480	Feb-75	2547	4538									4835	Vertical	Pumping	4651-4738		Cut & Perd	Acid	7900					
817	Existing	33180	Sep-79	2569	4590									4830	Vertical	Abandoned	4651-4650		Cut & Perd	Acid	4000					
818	Project	33178	Aug-79	2599	4599	4621	4666	4736	4764					4730	Vertical	Pumping	4628-4724		Cut & Perd	Acid	4200					
819	Project	36541	May-92	2548	4530	4644	4684	4747	4780	4799	4842	4940		5172	Vertical	Pumping	4678-4670		Cut & Perd	Acid	12000					
901	Existing	9304	Apr-54	NL										4830	Vertical	Shut-In			Open-Hole	MHO	544 Cts					
902	Existing	5595	Aug-54	NL										4830	Vertical	Abandoned			Open-Hole	Glycoline	30 Cts					
903	Existing	31479	May-75	2597	4571	4683	4730	4798	4843	4916				4830	Vertical	Pumping	4674-4733		Cut & Perd	Acid	4000					

## **FIGURE IV**

## **FIGURE IV**

### **FIELD PRODUCTION CONSTRAINTS AND DESIGN LOGIC**

#### **Qualitative Review of Reservoir Description and Development History**

The South Cowden Unit (SCU) produces from the Grayburg and San Andres Formations of Permian age. These formations were deposited in shallow carbonate shelf environments along the eastern margin of the Central Basin Platform. The primary target for carbon dioxide (CO<sub>2</sub>) flood development under the proposed project is a 150 - 200 foot gross interval within the San Andres at an average depth of 4550 feet.

South Cowden was discovered in 1940 and unitized for secondary recovery waterflood operations beginning in 1965. The Unit was nearing its economic limit, producing about 400 BOPD at a water-cut of 95% from 38 active producers and 15 active water injectors. Ultimate primary plus secondary recovery was expected to be about 35 million STB or approximately 40 percent of the original oil-in-place. The original oil-in-place for the South Cowden Unit is estimated to be 86.5 million barrels.

CO<sub>2</sub> flood potential at South Cowden was first evaluated in 1982. The study concluded South Cowden reservoir is an excellent technical candidate for CO<sub>2</sub> flooding. Plans were made in the early 1980's to implement a CO<sub>2</sub> miscible WAG project using a conventional 40-acre five-spot pattern development. These plans were postponed following the oil price collapse in the mid-1980's. A second full feasibility study was conducted in 1991. The study indicated excellent incremental CO<sub>2</sub> oil recovery potential; however the project did not meet minimum economic guidelines using a conventional CO<sub>2</sub> development approach.

The Budget Phase 1 project focused on reducing initial investment cost by utilizing horizontal injection wells and concentrating the project in the best productivity area of the field. An innovative CO<sub>2</sub> purchase agreement (no take or pay requirements, CO<sub>2</sub> purchase price tied to WTI oil price) and gas recycle agreements (expensing cost as opposed to large capital investments for compression) were negotiated to further improve project economics.

A detailed reservoir characterization study was completed by an integrated team of geoscientists and engineers. The study consisted of detailed core description, integration of log response to core descriptions, mapping of the major flow units, evaluation of porosity and permeability relationships, geostatistical analysis of permeability trends, and direct integration of reservoir performance with the geological interpretation. The study methodology fostered iterative bi-directional feedback between the reservoir characterization team and the reservoir engineering/simulation team to allow simultaneous refinement and convergence of the geological interpretation with the reservoir model. The fundamental

conclusion from the study was that South Cowden exhibits favorable enhanced oil recovery characteristics, particularly reservoir quality and continuity.

Detailed core descriptions were made of two full cores and several partial cores from the South Cowden Unit. Core information from the contiguous Emmons and Moss Units were also incorporated into the study. The core study concluded reservoir quality at South Cowden Unit was controlled primarily by the distribution of a bioturbated and diagenetically altered rock type with a distinctive “chaotic” texture. The “chaotic” modifier derives from the visual effect of pervasive, small-scale intermixing of tan oil-stained reservoir rock with tight gray non-reservoir rock.

The San Andres section is divided into multiple zones based on the core study and gamma ray markers that correlated across the unit. The type log for South Cowden Unit Well No. 8-19 is shown as Figure IV.1. Each zone is mapped as continuous across the field. The “chaotic” reservoir rock extends from Zone C to the lower part of Zone F. Zones D and E are considered the main floodable zones, with Zone F also productive in some areas and Zone C productive above the oil-water contact, in the structurally higher parts of the lease.

RFT measurements indicated good vertical pressure communication between Zones D and E, fair communication with Zone F, and poor communication with Zone C. The lower part of Zone F is separated from Zone E by a thin silty dolomite layer, which may hinder efficient vertical sweep between the two zones. Zone C is effectively isolated from the zones above. Open-hole hydraulic fracture tests indicated a strong tendency for induced fractures to grow downward from the productive zones to Zone A, a high permeability, water bearing grainstone layer.

Understanding of reservoir rock distribution, identification of vertical pressure barriers within the reservoir (especially relative to the oil-water contact), and recognition of the nature of hydraulic fracture propagation in the reservoir were critical to the formulation of the CO<sub>2</sub> flood development plan: Horizontal WAG injection wells placed downstructure in Zones D and E, which are above the oil-water contact throughout the project area and do not have internal vertical pressure barriers. Vertical WAG injection wells placed upstructure, where Zone C is above the oil-water contact but isolated by a vertical pressure barrier from the CO<sub>2</sub> sweep in Zones D and E. Perforation of the lower part of Zone F in vertical injectors will compensate for the vertical sweep inefficiency across the weak pressure barrier between Zone F and E. Injection pressures in both horizontal and vertical WAG injectors will be kept below the fracture gradient (0.58 psi/ft) to minimize CO<sub>2</sub> losses to deeper, nonproductive zones.

A full-field reservoir simulation model was constructed covering all of the South Cowden Unit (SCU), Emmons Unit and a portion of Unocal’s Moss Unit, both of which border SCU to the north. Model grid and layering were laid out to conform to the geological configuration of the reservoir. Porosity, permeability, and flow properties of the major reservoir facies identified by the reservoir characterization team were incorporated into the model. An iterative, “predictive” history matching approach was employed whereby the team were involved in making refinements to reservoir description until the

model was able to accurately predict historical waterflood performance. This predictive approach provides added confidence in future performance forecasts.

Critical laboratory data on CO<sub>2</sub>/oil phase behavior, minimum miscibility pressure, and oil recovery efficiency were matched and incorporated into the model. The model was then used to evaluate alternative CO<sub>2</sub> project developments, including the optimum use of horizontal CO<sub>2</sub> injection wells. The most attractive project development incorporated both horizontal and vertical CO<sub>2</sub> injection wells to conform to the reservoir geology and maximize sweep efficiency. This configuration is presented as the AFE “Base Case” development plan.

## **Problem Statement - Constraints On Further Producibility**

### **Technological and Economical**

Many United States oil fields in shallow shelf carbonate (SSC) reservoirs have been producing for 40 years or more, are fully developed, and have produced large volumes of oil through successful primary and secondary (waterflooding) operations. Increasingly these fields are approaching their economic limit and face abandonment within the next decade despite having one-half to two-thirds of the original oil-in-place in these fields will remain in the reservoir (Bebout et al, 1987). Carbon dioxide (CO<sub>2</sub>) miscible flooding has been demonstrated to be a technically viable tertiary enhanced oil recovery process to extend producing life and significantly increase ultimate recovery. However, many of these SSC reservoirs nearing economic limit will soon face an abandonment decision and will probably not be developed as tertiary (CO<sub>2</sub>) enhanced oil recovery projects.

There are several key producibility problems, both technical and economic, which prevent more widespread application of tertiary (CO<sub>2</sub>) miscible flooding in these reservoirs:

1. Under-utilization of existing reservoir characterization technology, particularly by operators of smaller fields. A practical, multi-disciplinary reservoir characterization approach is essential to understand the internal architecture of the reservoir, delineate the high potential portions of the field, and guide the successful application of any advanced technology (Bebout et al, 1987).
2. One of the most significant obstacles to implementing a tertiary CO<sub>2</sub> flood project is that only old wellbores and surface facilities are available. Often, most of the existing wellbores and facilities are not suitable for use in a CO<sub>2</sub> injection project. Application of a tertiary CO<sub>2</sub> flood requires a large investment in new wells, surface facilities, gas processing plants, etc. Conventional CO<sub>2</sub> project development practices have been directed primarily toward large projects where sizable economies of scale can significantly improve economics. If the industry restricts itself to using existing, conventional approaches to development, projects will not be economically viable in most smaller SSC reservoirs.
3. Limitations in the effectiveness of the CO<sub>2</sub> flood process itself, resulting primarily from poor sweep efficiency obtained with a low viscosity, high mobility injectant. Problems with sweep



efficiency result in using a water-alternating-gas (WAG) process for mobility control in most CO<sub>2</sub> floods. This increases time required to recover incremental oil and reduces project economics. Research work into various chemical methods (CO<sub>2</sub>/surfactant foams, direct thickening agents for CO<sub>2</sub>, polymers, etc.) to improve mobility control in CO<sub>2</sub> floods is continuing. Phillips conducted a field trial of CO<sub>2</sub> mobility control foam in the East Vacuum Grayburg-San Andres Unit in Lea County, New Mexico. However, Phillips also believes there is significant potential to improve sweep efficiency and reduce costs in CO<sub>2</sub> flood projects through use of horizontal injection wells rather than existing pattern development using vertical injection wells.

Phillips Petroleum proposed to address these producibility problems by demonstrating economic viability of an innovative reservoir management and development strategy : multiple horizontal CO<sub>2</sub> injection wells drilled from a central location, and a comprehensive reservoir characterization study by an integrated, multi-disciplinary team determining optimum location, orientation, and completion configurations. The use of horizontal wells drilled from a centralized location: (1) reduces the number of new injection wells and equipment; (2) allows concentration of surface reinjection facilities; and (3) minimizes costs associated with CO<sub>2</sub> distribution system. This significantly reduces initial investment to implement a tertiary CO<sub>2</sub> flood project. In addition, use of horizontal CO<sub>2</sub> injection wells provides better areal sweep efficiency when compared with CO<sub>2</sub> injection into vertical wellbores. As a consequence this should allow a larger initial slug CO<sub>2</sub> before a water-alternating-gas (WAG) process is implemented for mobility control. Also, with improved areal sweep, optimum WAG ratio will lower and this should consequently improve project economics.

## **Safety, Property Loss and Environmental Risks**

Below is a preliminary risk assessment for the South Cowden CO<sub>2</sub> Injection Project. This assessment provides an initial review of safety, property loss and environmental risks associated with the project. Additional reviews will be conducted as considered prudent.

The most significant potential hazard, public hydrogen sulfide (H<sub>2</sub>S) exposure, was reviewed in detail. Dispersion modeling results indicated the worst case release would not result in public exposure to hazardous concentrations of H<sub>2</sub>S. Reasonable precautions are planned to protect the public from accidental H<sub>2</sub>S release.

A review of the risks and precautions are given below:

### **Risks**

#### **A. Safety**

The primary safety risk relates to release of hydrogen sulfide. There are four main scenarios for which a release of H<sub>2</sub>S may occur.

1. Blowout of Injection Well
2. Rupture of ReInjection System
3. Blowout of Producing Well
4. Rupture of Field Production Header
5. Rupture of Production Flowline

Of these, only blowout of a CO<sub>2</sub> injection well is considered serious. Both “horizontal” injectors will be able to inject approximately 5 MMCFD maximum injection rate. Although the potential of the wells was unknown, a conservative estimate of 7.5 MMCFD was used for worst case calculation of 100 parts per million (ppm) radius of exposure for an uncontrolled blowout. Mark Deese of Phillips safety department, Bartlesville ran TRACE dispersion modeling and calculated a 100 ppm radius of exposure (ROE) of 928 feet. Since surface injection well locations are more than 2000 feet from the nearest residence, public exposure to hydrogen sulfide should not be hazardous. Additional modeling for rupture of CO<sub>2</sub> and production headers was found to be of significantly less concern than blowout of an injector well.

Producing well rates closest to residential areas were reviewed. It was determined existing gas production rates were so low that flowline rupture would present little potential for 100 ppm H<sub>2</sub>S public exposure. The scenario of a producing well blowout was considered unlikely because of low oil and gas production rates and very high water production rates for the wells located in proximity to the residential areas. None of the producing wells were flowing wells and all produced through pumping units. Existing producers in and near the residential area were planned to be converted into a “ring” of water injection wells. This conversion is intended to eliminate concerns of H<sub>2</sub>S exposure due to wellhead/flowline leaks near the residential area.

## B. Property Damage

The primary cause of property damage would be a tank battery fire. The consequences of a tank battery fire would generally be cost of replacement tanks and/or process equipment and production delay while reconstructing facilities. In the event of a battery fire, surplus tanks and vessels are available at low cost. Also, temporary tanks and production equipment could be utilized to minimize down time associated with a fire loss.

Fire risk to the public is minimal considering the distance from the tank batteries to public property. The risk to operating personnel is minimal, since Phillips North America Production (NAP) hot work and hot tapping procedures preclude operations, which would present fire hazards. Also, incipient fire training is periodically provided to operations personnel.

Following a tank battery fire, some environmental remediation would be required. However, this would likely involve the standard practice of aerating and fertilizing the contaminated soil until oil content is within Texas Railroad Commission limits.

### C. Environmental

Oil spill represents the greatest risk of environmental damage. However, the South Cowden Field is not located in an environmentally sensitive area. There are no waterways, wetlands, endangered species habitats or other sensitive areas, which would be affected by an oil spill. The field is not considered to fall under SPCC requirements. Spills would be remediated according to Texas Railroad Commission requirements.

### **Precautions**

#### A. Hydrogen Sulfide

Fixed H<sub>2</sub>S monitors will be installed at the tank battery, production headers and along the property line between the field and the residential areas. These monitors will alarm upon detection of H<sub>2</sub>S and will automatically “call out” to notify appropriate personnel of H<sub>2</sub>S detection. Additionally, fixed CO<sub>2</sub> monitors will be installed at the injector wells and at the CO<sub>2</sub> header and will also be connected to an alarm/call out system.

A written Hydrogen Sulfide Contingency Plan will be prepared for the project.

#### B. Reinjection System Safety Devices

The CO<sub>2</sub> reinjection system is being equipped with appropriate safety sensors and shut down devices which will isolate the system in the event of an undesirable event such as a leak. Dupont’s TRACE model was used to determine chemical concentrations and cloud dynamics for this spill. The model simulates a theoretical release of carbon dioxide. Several release scenarios were modeled to determine the maximum distance where 4900 ppm occurs, which is approximately equivalent to 100 ppm of H<sub>2</sub>S. Various emission rates were used based on the data supplied. Each emission rate was modeled with different wind speeds of 5 mph, 10 mph, and 15 mph. Also, each emission rate was modeled with different temperatures of 30 F, 70 F, and 110 F.

Year	Mass Available (lbs/sec)	5 MPH 30 F	5 MPH 70 F	5 MPH 110 F	10 MPH 30 F	10 MPH 70 F	10 MPH 110 F	15 MPH 30 F	15 MPH 70 F	15 MPH 110 F
1995	.0018	66'	132'	132'	264'	264'	264'	396'	396'	396'
1998	1.057	281'	269'	268'	304'	256'	253'	264'	344'	320'
2001	2.292	418'	393'	380'	349'	358'	347'	398'	389'	343'

2005	3.224	501'	471'	559'	387'	397'	393'	357'	391'	374'
2010	4.278	578'	544'	528'	447'	449'	455'	457'	466'	398'
2015	5.274	656'	656'	585'	513'	498'	489'	493'	502'	430'
MAX	9.86	890'	928'	798'	704'	657'	628'	636'	630'	556'

The worst case showed the furthest distance where 4900 ppm of CO<sub>2</sub> occurs was 928 feet downwind from source. From this modeling, if light winds are present during an accidental release, reasonable precautions should be taken to protect the community surrounding this facility. Modeling results are “best guess” and usually conservative.

#### Land Purchase Premise

The acreage under Section 17 Block 42, which is the location of the Tract 6 Battery and the future location of the injection facilities will be purchased. The acreage will extend from the north boundary of the section to the 385 Highway, then to the diagonal line of the 385 Ranch West Estates, then to the west line of the section, then back to the north line. Some additional lots south of the diagonal line will be purchased as well.

The intent of this purchase is as follows:

1. Reduce the cost of payment of damages.
2. Reduce the safety hazards from CO<sub>2</sub> or H<sub>2</sub>S.
3. Allow uninhibited development of the main CO<sub>2</sub> flooded area.

See attached Figure IV.2 for map of estimated area of CO<sub>2</sub> exposure and land purchase.

#### Method of Problem Detection

#### Application of New Tools or Techniques

The purpose of the project is to design an optimum CO<sub>2</sub> flood project utilizing advanced reservoir characterization and CO<sub>2</sub> horizontal injection wells, demonstrate the performance of this project and transfer the information to the public so it can be used to avoid premature abandonment of other fields. The Unit's producibility problem is that it is a mature flood with watercut exceeding 95%. Oil must be mobilized through the use of miscible or near-miscible fluid in order to recover significant additional reserves. As the unit is relatively small, it does not have the benefit of economies of scale inherent in large scale projects. Thus, new and innovative methods are required to reduce the investment and operating costs.

The project focused on reducing initial investment by utilizing horizontal injection wells and concentrating the project in the best productivity area of the field. An innovative CO<sub>2</sub> purchase agreement (no take or pay requirements, CO<sub>2</sub> purchase price tied to WTI oil price) and gas recycle agreements (expensing cost as opposed to large capital investments for compression) were negotiated to further improve project economics.

A detailed reservoir characterization study was completed by an integrated team of geoscientists and engineers. The study consisted of detailed core description, integration of log response to core descriptions, mapping of major flow units, evaluation of porosity and permeability relationships, geostatistical analysis of permeability trends, and direct integration of reservoir performance with the geological interpretation. The study methodology fostered iterative bi-directional feedback between the reservoir characterization team and the reservoir engineering/simulation team to allow simultaneous refinement and convergence of the geological interpretation with the reservoir model. The fundamental conclusion from the study is that South Cowden exhibits favorable enhanced oil recovery characteristics, particularly reservoir quality and continuity.

Understanding of reservoir rock distribution, identification of vertical pressure barriers within the reservoir (especially relative to the oil-water contact), and recognition of the nature of hydraulic fracture propagation in the reservoir were critical to the formulation of the CO<sub>2</sub> flood development plan. Horizontal WAG injection wells placed downstructure in Zones D and E, which are above the oil-water contact throughout the project area and do not have internal vertical pressure barriers. Vertical WAG injection wells placed upstructure, where Zone C is above the oil-water contact but isolated by a vertical pressure barrier from the CO<sub>2</sub> sweep in Zones D and E. Perforation of the lower part of Zone F in vertical injectors will compensate for the vertical sweep inefficiency across the weak pressure barrier between Zone F and E. Injection pressures in both horizontal and vertical WAG injectors will be kept below the fracture gradient (0.58 psi/ft) to minimize CO<sub>2</sub> losses to deeper, nonproductive zones.

A full-field reservoir simulation model was constructed covering all of the South Cowden Unit (SCU), Emmons Unit and a portion of Unocal's Moss Unit, both of which border the SCU to the north. Model grid and layering were laid out to conform to geological configuration of the reservoir. Porosity, permeability, and flow properties of the major reservoir facies identified by the reservoir characterization team were incorporated into the model. An iterative, "predictive" history matching approach was employed whereby the team were involved in making refinements to the model reservoir description until the model was able to accurately predict historical waterflood performance. This predictive approach provides added confidence in future performance forecasts.

Critical laboratory data on CO<sub>2</sub>/oil phase behavior, minimum miscibility pressure, and oil recovery efficiency were matched and incorporated into the model. The model was then used to evaluate alternative CO<sub>2</sub> project developments, including the optimum use of horizontal CO<sub>2</sub> injection wells. The most attractive project development incorporated both horizontal and vertical CO<sub>2</sub> injection wells to

conform to the reservoir geology and maximize sweep efficiency. This configuration is presented as the AFE “Base Case” development plan.

### **Inconsistency Between the Design and Actual Performance**

This issue will be addressed in the Topical Report at the end of Budget Period II.

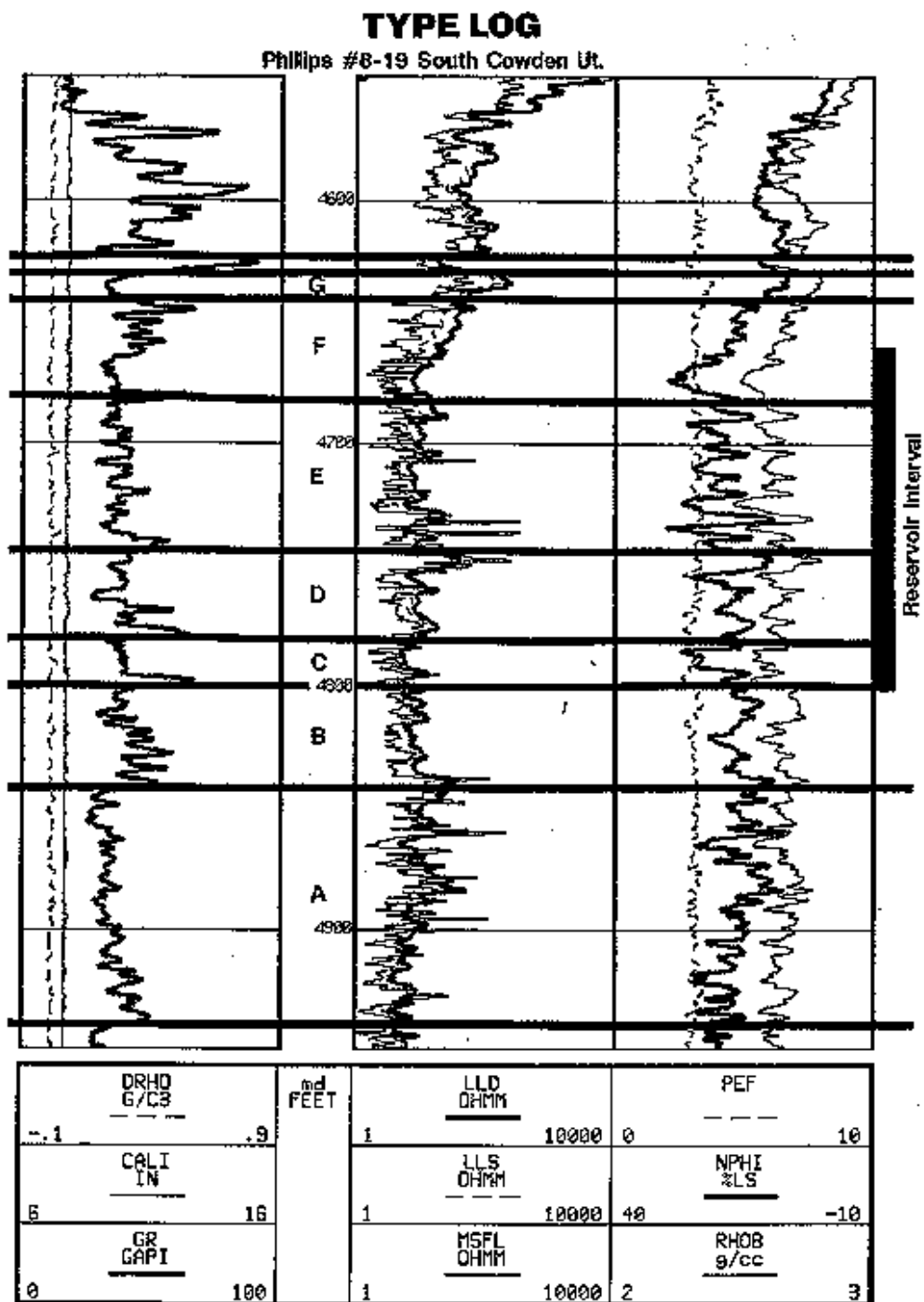


Figure IV.1. Type log for South Cowden Unit Well No. 8-19

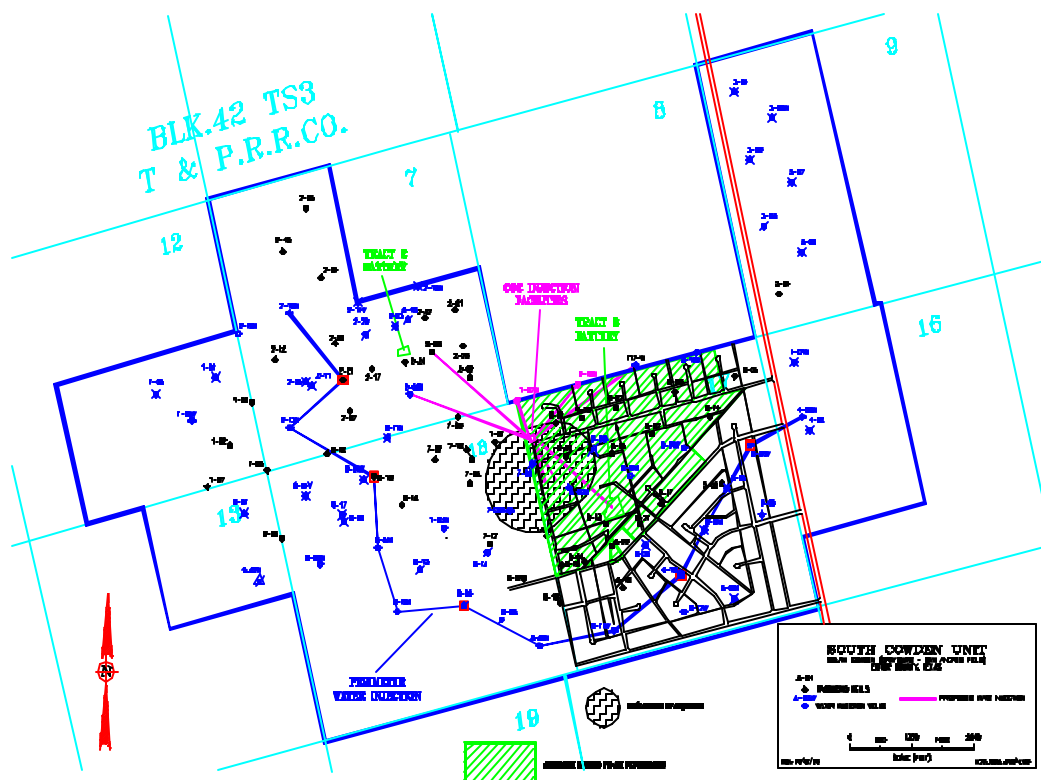


Figure IV.2 Map of CO2 Radius of Exposure Area



## **FIGURE V**

## FIGURE V

### EVALUATION OF COST-SHARE PROJECT RESULTS

#### **Type of Project**

The South Cowden cost-share project is designed as a tertiary, miscible carbon dioxide (CO<sub>2</sub>) injection project. The South Cowden Unit (SCU) is an example of a mature waterflood, rapidly reaching its economic limit. Performance of the waterflood has been very good, however field average watercut approached 95 percent. Selective infill drilling over the past few years has met with limited success, leaving tertiary enhanced oil recovery as the remaining prospect for extending field life. The demonstration project at South Cowden will use horizontal CO<sub>2</sub> injection wells drilled and operated from a centralized facilities area. The most effective well configuration for South Cowden utilizes horizontal CO<sub>2</sub> injectors in downdip locations, in combination with vertical injection wells in updip locations.

#### **Injection Program**

#### **Type of Injectant**

The tertiary injectant in the South Cowden project will be carbon dioxide. The injected CO<sub>2</sub> will be multi-contact miscible with reservoir crude at reservoir conditions expected during the project operations. Simulation modeling forecasts, discussed in following sections, show significant advantages in oil recovery efficiency when using a WAG (water-alternating-gas) injection scheme vs. continuous CO<sub>2</sub> injection. The WAG process improves mobility control for the CO<sub>2</sub> injection process and increases sweep efficiency. WAG injection would be started after injection gas breakthrough has occurred at several producing wells.

#### **Injection Schedule**

The project development plan calls for CO<sub>2</sub> injection into two horizontal wells and five vertical wells. The existing well configuration and plans for development under the cost-share project are illustrated below. The horizontal wells (1650 feet and 2400 feet lateral sections) are forecast to inject 4.7 and 5.1 MMCFPD/well, respectively. The five vertical injection wells are forecast to average about 1.4 MMCFPD/well (ranging from 0.9 to 1.8 MMCFPD). Thus, the horizontal wells are expected to average about 3.5 times the injection rate of an average vertical well. Figure V.1 is a map indicating the project area, and location of proposed WAG injection wells.

#### **Injection Pattern (prior to inception of the cost-share project)**

There was no well-established waterflood injection pattern in the South Cowden Unit prior to inception of the cost-share project. Water injection at the Unit began in 1965 with peripheral injection into wells around the edge of the producing structure, near the oil/water contact. Leaseline cooperative water

injection was added in the mid-1970's along the northern boundary of the Unit with the Emmons and Moss Units. In the late 1970's through the mid-1980's, several additional water injection wells were added at selected locations in the interior of the Unit without any formal pattern development.

### **Number and Schedule of New Producers Drilled**

The planned project development included drilling a total of seven additional producing wells. Five of these were planned as replacement wells for existing producers known to have poor mechanical integrity. Three producing wells were scheduled to be drilled in late 1995, two more in 1996, and the remaining two wells drilled in 1997-1998.

### **Number and Schedule of New Injectors Drilled**

The planned project development included drilling of two horizontal CO<sub>2</sub> injection wells and four vertical CO<sub>2</sub> injection wells. Two vertical CO<sub>2</sub> injection wells were scheduled to be drilled in late 1995 and the two horizontal CO<sub>2</sub> injection wells and two additional vertical injectors for 1996.

### **Number and Schedule of Conversion Wells**

There were no plans for conversions of producing wells to CO<sub>2</sub> injection in the project because of mechanical integrity and safety concerns, as well as the potential for out-of-zone losses of expensive CO<sub>2</sub> injectant. There were plans for one existing water injection well, which shows a good "in-zone" injection profile, to be equipped for CO<sub>2</sub> injection service. Six existing producing wells around the perimeter of the CO<sub>2</sub> project area were planned for conversion to water injection. This would create a ring of water injectors around the CO<sub>2</sub> flood project area to provide containment of the injected CO<sub>2</sub>.

## **Simulation Study**

### **Type of Simulator Used**

Both fully compositional and modified black-oil mixing parameter simulations were used in the South Cowden project evaluation and design study. Compositional simulation was used for process mechanism and reservoir characterization sensitivity studies. A modified black-oil, mixing parameter simulator was used for full-field modeling studies, but only after being tuned in benchmarking studies with the compositional model, as discussed below.

Compositional simulators have the advantage of allowing a more rigorous and realistic treatment of phase behavior and mass transfer effects during the multi-contact CO<sub>2</sub>/oil displacement process. However, they require much more computational effort and computing time - particularly when simulating complex phase behavior. These factors can be major limitations when very large, full-field simulations are needed to model effects of heterogeneity and sweep efficiency in cases where irregular well patterns or horizontal wells are used, such as in the South Cowden project.

Modified black-oil, mixing parameter simulators have the advantage of requiring less computational effort and computing time because they assume a simplified, first-contact miscible phase behavior, adjusted or modified with empirical mixing rules to describe the effective transport and displacement characteristics. These empirical parameters must be correctly specified either by history matching of field performance or by matching the CO<sub>2</sub> flood process performance against a compositional simulator. This approach allows incorporation of more detailed heterogeneity into the reservoir model and is more practical for simulation of large-scale problems. In many cases, correct representation of reservoir heterogeneity has a larger impact on CO<sub>2</sub> flood performance than does the degree of rigor used in representing the phase behavior.

A five-spot pattern model with reservoir properties representative of the "sweet spot" in the proposed South Cowden project area was set up and run on both the compositional and mixing parameter simulators. Empirical parameters in the mixing parameter model were adjusted until its performance matched that obtained with the fully compositional simulator using a 16-component EOS to represent fluid phase behavior. Parallel runs were made on the two simulators during reservoir characterization sensitivity studies to assess the response to changes in layering, Kv/Kh, grid size, etc. and ensure that comparable performance was obtained with the mixing parameter model under a wide range of displacement conditions.

The mixing parameter model initially produced optimistic results compared with the compositional simulations. Several factors were identified as contributing to this difference. First, unadjusted CO<sub>2</sub> injectivity was higher in the mixing parameter model. Apparently, compositional phase behavior effects resulted in a lower CO<sub>2</sub>-rich phase mobility. Code changes were made in the mixing parameter simulator to allow adjustments to the solvent phase relative permeability to better match both experimental data and compositional model injectivity. Secondly, additional code changes were made to incorporate CO<sub>2</sub> solubility in the aqueous phase in the mixing parameter simulator. Correctly modeling this effect reduced incremental CO<sub>2</sub> flood oil recovery by 8-10%, depending on WAG strategy, and resulted in increased gas production during the later project life. Third, the compositional model produced a significant fraction (7-8%) of the total incremental hydrocarbons as NGL's in the separator gas stream. This compositional behavior could not be simulated with the simplified phase behavior used in the mixing parameter model. Oil recovery predictions from the mixing parameter simulations were adjusted to account for this effect. Finally, areal and vertical sweep efficiency comparisons showed the displacement to be slightly less efficient in the compositional simulations than in the mixing parameter simulations. The value of the mixing parameter ( $\omega$ ) was adjusted until the mixing parameter model performance matched the compositional model results. With these adjustments to the empirical parameters in the mixing parameter model, comparable performance forecasts were obtained from the two simulation models over a wide range of conditions of heterogeneity and WAG strategy.

Grid size sensitivity studies were conducted to aid in selecting a full-field model grid. The fivespot pattern model was used for these studies. The sensitivity of waterflood response to areal grid size and numerical dispersion is shown in Figure V.2. Too coarse an areal grid resulted in early water breakthrough and lower waterflood oil recovery. The compositional and mixing parameter models

produced comparable primary depletion and waterflood forecasts. Cumulative oil production vs. time for the two models is shown in Figure V.3. Areal sweep and displacement characteristics were also similar, as shown by the saturation profiles at the end of waterflood (Figure V.4).

Incremental CO<sub>2</sub> flood oil recovery was also affected by numerical effects due to areal grid size. Figure V.5 shows the effect of areal model grid cell size on incremental oil recovery for both the compositional and mixing parameter models. The two models converge to the same value as grid cell size is reduced and numerical effects are eliminated. Incremental recovery appears to be more sensitive to grid size effects in the mixing parameter model than in the compositional model in this case.

Grid size sensitivities were also run to look at the impact of vertical grid resolution, or number of layers, on CO<sub>2</sub> flood performance. Figures V.6 and V.7 show some sensitivity of performance to layer thickness (number of layers). Incremental oil recovery was reduced about 5% as layer thickness was reduced from 20 feet to 2 feet (from 3 layers to 30 layers used to represent the main reservoir interval). Gas production response was more sensitive to vertical grid resolution; gas production increased approximately 12% as layer thickness was decreased. These results show that using too great a layer thickness in the model will tend to underestimate gravity override effects.

### **Complete Set of Rock and Fluid data Used in the Simulator**

#### **1. Historical Production Data by Well**

This data is provided in an Oil Field Manager (OFM) database for the project. Oilfield Manager (OFM) is a commercially available PC-based software product widely used by both major and independent operators in the Permian Basin. The OFM digital database is included with the supporting data for this report.

#### **2. Historical Injection Data by Well**

This data is provided in an Oil Field Manager (OFM) database for the project.

#### **3. PVT Data**

A recombined separator fluid sample was taken from the South Cowden reservoir. The laboratory fluid PVT analyses are included with the supporting data for this report. The recombined reservoir fluid composition is given in Table V.1. A Peng-Robinson equation with a sixteen component fluid description was chosen to initially characterize the South Cowden reservoir fluid. Five pseudo components were chosen to characterize the C<sub>7+</sub> fraction of the oil. The EOS was tuned to match laboratory fluid analysis data with volume translation used to improve the fluid density match.

The experimental data set used for tuning the EOS included differential liberation data; pure component injection gas density, viscosity, and Z-factor data; and vapor-liquid equilibrium data from CO<sub>2</sub>/reservoir

oil swelling tests at 15, 30, 41, and 68 mole percent injection gas. A satisfactory match to all experimental data was obtained with the sixteen component fluid description given in Table V.2. The quality of the match obtained between experimental and EOS predicted fluid properties is shown graphically in Figures V.8 - V.18.

The pressure vs. composition diagram for this fluid description is shown in Figure V.19. Emphasis was placed on matching vapor and liquid phase properties and compositions in both the low pressure (634 psia flash of 41 mol% injection gas) and high pressure (2514 psia flash of 68 mol% injection gas) regions of the pressure-composition space investigated by the experimental data. A comparison of experimental vs. EOS predicted phase relative volumes, compositions, and intensive properties is presented in Table V.3 and Figures V.20 and V.21. Measured saturation pressures were matched to within about 150 psi at the lower CO<sub>2</sub> concentrations.

After the sixteen component EOS had been tuned to obtain a satisfactory match of the experimental data, the number of components was reduced using a stepwise regression procedure to generate a more tractable fluid characterization for use in compositional reservoir simulation. A comparable match with the experimental data (maximum deviation in any property vs. 16-component characterization about 7%) was obtained after reduction to an eight component fluid description. The eight component EOS fluid characterization is shown in Table V.4.

The final EOS fluid characterizations (both the sixteen component and eight component fluid descriptions) were incorporated into a one-dimensional compositional simulation model to predict laboratory slim tube displacement behavior. A satisfactory match of laboratory slim tube oil recovery and gas-oil ratio behavior was obtained using both fluid characterizations (Figures V.22 and V.23). Further prediction runs were made to characterize the recovery efficiency vs. pressure for CO<sub>2</sub> with the South Cowden crude (Figure V.24). The minimum miscibility pressure (MMP, defined as the pressure where oil recovery efficiency exceeds 90% OOIP at 1.2 PV injection) was determined to be approximately 1200 psia. This compares favorably with slim tube displacement experiments conducted in the early 1980's using South Cowden stock tank oil which indicated MMP to be approximately 1140 psig. Current reservoir pressure at the South Cowden Unit is above 2000 psi and substantially above the required MMP.

#### **4. Relative Permeability Data**

Relative permeability and rock property data were based on special core analysis (SCAL) data from five wells in the South Cowden field; these included conventional, oil-base native state, and sponge cores. Copies of the SCAL laboratory data and reports are included with the supporting data for this report. Data were available for 21 water-oil relative permeability tests (both steady-state and unsteady-state tests were run); 32 water-oil relative permeability endpoint tests; 15 gas-oil relative permeability tests; and eight CO<sub>2</sub>/oil coreflood tests. Four of the CO<sub>2</sub>/oil corefloods were special tests designed to measure CO<sub>2</sub> trapped gas saturation, residual oil to CO<sub>2</sub> displacement, and endpoint CO<sub>2</sub> and water relative permeabilities in a WAG process. Magnetic resonance imaging was used to screen many of the core plugs prior to testing to ensure that no "hidden" internal heterogeneities were present in the plugs to

add scatter to the data. These data were all normalized and correlated by geologic lithofacies and by reservoir zone. This resulted in three major rock types being identified for use in field-wide simulation modeling work. Simulator output, including these data and other simulation model input data, is included in digital form with the supporting data for this report.

## **5. Three-dimensional Grid of Porosity, Permeability, and Fluid Saturation**

A three-dimensional simulation model of the South Cowden Unit was built using a 54 x 54 areal grid with six layers to describe the CO<sub>2</sub> flood target interval covering Zones C, D, E, and F described in the reservoir characterization work. This simulation model grid contains 17,500 active cells and covers a 7.5 square mile area incorporating approximately 170 wells. Greater areal grid definition was used in the "sweet spot" of the reservoir - identified as the most attractive potential project area within the Unit. The vertical grid was refined within the main reservoir interval (Zone E). This provided the ability to incorporate the details of reservoir heterogeneity within the E Zone, allow simulation of vertical movement of fluids due to gravity segregation, evaluate alternative placement of horizontal injection wells within the reservoir section and to make sensitivity runs to evaluate variations in permeability stratification and effective Kv/Kh ratio.

Individual layer structure, isopach, and porosity maps were digitized and incorporated into the reservoir simulation model. Simulator model input data is included in digital form with the supporting data for this report.

Porosity vs. permeability relationships, capillary pressure and initial water saturation distribution functions, and relative permeability data were input based on the distribution of the three major rock types identified in the reservoir characterization work. Initial water saturation varied from approximately 10% PV in the best reservoir quality rock in the project area to almost 30% PV in the poor reservoir quality areas on the western margin of the Unit. The original oil-in-place (OOIP) for the Unit was calculated to be 86.5 MMSTB.

Vertical permeability measurements were available on a foot-by-foot basis for whole core analyses from three wells in the project area. The measured vertical permeabilities were generally greater than the measured horizontal permeabilities in the E Zone in these three wells. Initial Kv/Kh ratios in the model were estimated by using harmonic averages for the vertical permeability and using geometric means for the areal permeability. This resulted in an average Kv/Kh ratio of 0.21 for the E Zone. In addition, the vertical transmissibility was further restricted across several layer boundaries which had been identified in the geologic studies as depositional sequence boundaries extending over much of the field area.

## **6. Rock Compressibility Factor**

Average formation rock compressibility for the South Cowden reservoir interval was measured as  $4.25 \times 10^{-6}$  psi<sup>-1</sup>.

## **Simulation of Performance for Oil , Gas, Water and Reservoir Pressures**

## 1. History Match Reservoir Performance prior to Cost-shared Project

An interactive, "predictive" history matching approach was used to match field performance. In this approach, wells are not "forced" to produce or inject at their historical oil production or water injection rates. Rather, actual well constraints (operational, facility, and regulatory) are applied to each well along with the well's completion and stimulation history, and the wells are allowed to produce or inject as much fluid as these constraints and the model reservoir description will allow. For example, constraints applied to the South Cowden producing wells include the individual well completion and stimulation history, artificial lift constraints governing liquid lifting capacity and producing bottomhole pressure, and any regulatory allowable limits which were in effect during early field life. Injection well constraints included the completion and stimulation history, and the wellhead injection pressure vs. time.

During history matching, the model reservoir description was adjusted until a satisfactory prediction of both primary depletion and waterflood performance was obtained with the model. Prior to major history match iterations, several sensitivity cases were often run in which key parameters (e.g. porosity, permeability, Kv/Kh, completion efficiency, etc.) were varied in order to demonstrate the magnitude of influence of each parameter at this point in the matching process. This approach allowed the entire reservoir characterization team to be involved in making decisions as to which model parameters were best candidates to adjust to obtain the desired performance and still keep the model consistent with all reservoir characterization data. Successful prediction of oil production rate vs. time was the primary criterion chosen to determine that a satisfactory history match had been obtained. The key parameters which had to be adjusted to match historical performance were the aquifer influx during early producing life, effective Kv/Kh ratio, and the permeability vs. porosity transforms used to estimate the three-dimensional permeability distribution.

The resulting final prediction of oil recovery vs. time for the historical production period is shown in Figure V.25. Note that at least some of the wells were constrained by regulatory allowable limits until about 1970; after that time all wells were producing at capacity. The corresponding prediction of water injection rate vs. time is shown in Figure V.26. The predicted water injection matches actual performance very well during the period 1965-1976 when the reservoir is filling up and being repressured. After the Unit reaches peak oil production rates in the mid-1970's, measured water injection exceeds the simulator predictions by about 25 percent. A review of injection profile surveys run in the mid-1980's and available on all but two injectors shows an average of about 30% out-of-zone injection. Microfracturing tests run in the two reservoir characterization wells drilled in 1994 indicated that fractures in this reservoir tend to initiate in the lower part of the section and grow downward toward a high permeability grainstone interval below the oil-water contact. Further evidence of substantial out-of-zone injection comes from a single-zone production test of the grainstone interval in the SCU 8-19 well in 1992. The grainstone interval had sufficient pressure to flow 100% water to the surface.

Over the past two years, wellhead injection pressures have been decreased and in November of 1994, a number of injectors with poor injection profiles were shut in. Over this period (1993-1995), the actual water injection rate has approached the predicted rate and the two curves match very well after the



shut-in of several problem wells in November 1994 (Figure V.26). Figure V.27 compares simulator predictions of watercut performance vs. measured field data. The model predictions show a reasonably good overall match with historical field performance, however during the period from 1989-1994, the predicted watercuts were 90-92% compared with observed watercuts of 94-95%+. This difference is substantial, representing about 4000-5000 barrels more water being produced from the field than is predicted by the simulation model history match. Much of this excess water was being produced from one well (SCU 6-13). This well had been hydraulically fractured and was equipped with an electrical submersible pump, producing 4000+ barrels of fluid per day at a 95+% watercut. After the SCU 6-13 well was shut-in in late 1994, along with several other high watercut producing wells and offsetting injection wells, the field watercut and the model predictions agree very well (Figure V.27). This indicates that much of the injected water during this period was probably being ineffectively cycled through the reservoir.

The final model predictions also matched individual zone RFT pressures measured in recent project area infill wells (SCU 8-19 and 6-23). This pressure match confirmed that the overall material balance in the project area was satisfied, and gave additional confidence that effective  $K_v/K_h$  ratios between reservoir zones was modeled adequately. Besides matching zone-by-zone RFT pressures, the production rate and water cut performance of these two wells, plus two additional infill wells drilled in the past few years were matched. This provided additional confidence that the current saturation and pressure distribution in the model should approximate actual reservoir conditions at the start of CO<sub>2</sub> flood operations.

## **2. Projection of Performance of Cost-shared Project**

Numerous full-field simulation runs were made to evaluate CO<sub>2</sub> flood performance under various configurations of horizontal and vertical wells. Initial runs evaluated the impact of horizontal well length, placement, and completion efficiency on CO<sub>2</sub> flood performance. Several alternative project development options were simulated. These were evaluated for oil recovery efficiency, areal and vertical sweep efficiency and CO<sub>2</sub> utilization efficiency. Several prediction runs were made for each of the more promising cases to evaluate the effect of uncertainties in the geologic reservoir description and well completion efficiency on project performance. A primary focus in this work was on the placement and completion strategy for horizontal CO<sub>2</sub> injection wells under various reservoir description cases.

Simulation runs were also made to evaluate CO<sub>2</sub> process performance under various alternative pattern configurations and project development scenarios. CO<sub>2</sub> injection rate and wellhead injection pressure requirements were calculated and provided to the facilities design team for use in sizing and design of the CO<sub>2</sub> distribution system and injection well facilities. Compositional simulation runs were made to provide initial estimates of produced gas rates under various development scenarios. CO<sub>2</sub> purchase volumes and recycle volumes were forecast for several different CO<sub>2</sub> injection and recycle strategies.

Compositional simulation modeling also provided estimates of produced gas composition and potential NGL yield vs. time. Figure V.28 shows typical composition vs. time profiles computed for a five-spot pattern model. This analysis showed that 7-8% of the total incremental hydrocarbons produced by the CO<sub>2</sub> flood process would be produced as natural gas liquids (NGL's) in the separator gas stream. This

volume was judged to be insufficient to warrant significant investment in gas processing facilities for the project.

Based on full-field simulations to evaluate various combinations of horizontal and vertical CO<sub>2</sub> WAG injection wells, it was determined that the most effective well configuration for the South Cowden project utilizes horizontal CO<sub>2</sub> WAG injectors in downdip locations oriented approximately parallel to structural strike, in combination with vertical WAG injection wells in updip locations. Vertical permeability restrictions in the lower portion of the main reservoir interval limit the vertical distribution of injected CO<sub>2</sub> into these lower intervals if only horizontal injection wells are used. In the downdip locations, much of the reservoir pore volume in the lower intervals lies below the original oil-water contact.

Sensitivity studies were conducted to investigate the effects of CO<sub>2</sub> WAG injection strategy on project performance. Incremental oil recovery vs. WAG ratio results from these simulations showed that WAG operations produced significant increases in oil recovery efficiency compared with continuous CO<sub>2</sub> injection. Maximum oil recovery was obtained at a WAG ratio of approximately 2:1, however the time required to inject a given total volume of CO<sub>2</sub> was significantly longer at this higher WAG ratio. A variable WAG ratio injection scheme, using a 7-12% HCPV initial CO<sub>2</sub> slug followed by increasing water/gas ratio as the flood matures, is premised in the preliminary project design. This provides an economic compromise of increased oil recovery efficiency vs. continuous CO<sub>2</sub> injection, while accelerating incremental oil response and reducing overall project life vs. a straight 2:1 WAG process.

Performance forecasts were generated for a Base Case project development plan. The AFE Base Case performance oil forecast is shown in Figures V.29. Incremental oil recovery forecasted for the Base Case project is 10.4% OOIP. The full-field simulator was also used to assess the effect of uncertainties in key input and operating parameters on production profiles and recoverable reserves for use in project risk analysis. The project team identified major elements of uncertainty having the largest impact on performance forecasts. These grouped into three major categories - reservoir characterization/heterogeneity/sweep efficiency; CO<sub>2</sub> process efficiency/target oil volume; and well completion efficiency/injectivity (with the greatest focus on horizontal well completion effectiveness).

### **3. Comparison of Actual With Projected Performance**

These comparisons will be discussed in the Topical Report at the end of Budget Phase II.

#### **Project Economics**

##### **Incremental non-drilling capital costs (compressors, etc.)**

Non-drilling incremental investments are shown in Table V.5. These costs are also given in columns 3, 4, 5, 6, 7, 8, 9, and 10 of Table V.6.

#### **Fixed operating costs (lifting costs, etc.)**

These costs are given in columns 7 and 9 of Table V.7. Column 7 gives the project area wellcost and column 9 gives the well cost outside the project area.

#### **Process dependent operating costs (\$/well/month)**

##### **1) Injectant purchase cost**

The price negotiations are confidential and the CO<sub>2</sub> price will not be divulged in this report.

##### **2) Injection and recycling cost**

The injection cost is included in the recycle costs. These costs are given in column 4 of Table V.7.

##### **3) Treatment and disposal costs**

Treatment costs are included in the recycle costs. Disposal costs are included within the total lease expense (see column 10 in Table V.7).

#### **Drilling and completion costs (\$/well)**

Costs for drilling, completion, reactivating and “re-equipping” existing injectors are shown in Table V.8. These costs are also given in column 2 of Table V.6.

#### **Reservoir Description costs (data gathering and processing, reservoir simulation study and other costs).**

The costs for Budget Period I work through March 1997 are given in Table V.9.

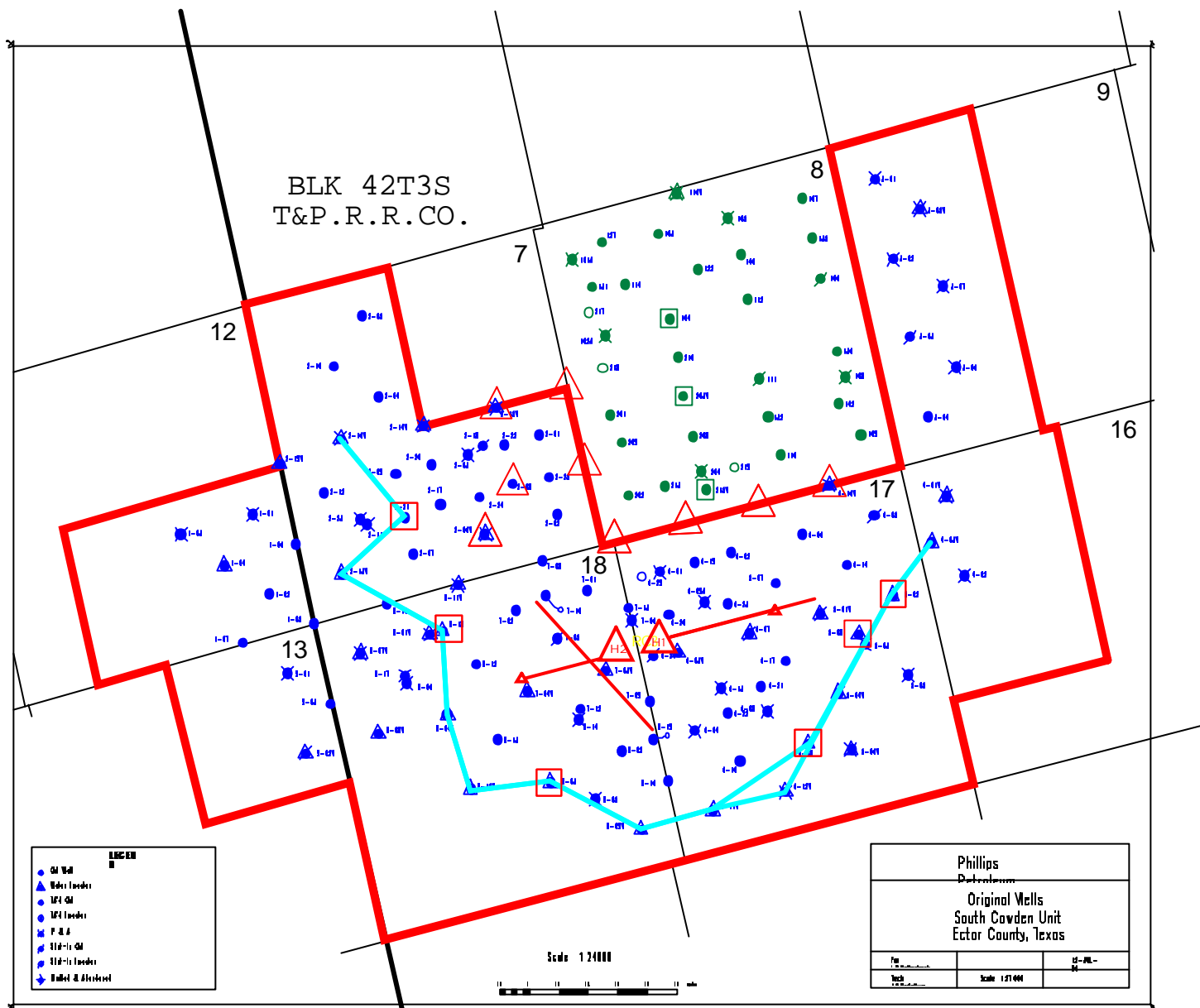


Figure V.1 Map of project area and proposed WAG injection wells

## Oil Recovery vs. Grid Size - Waterflood

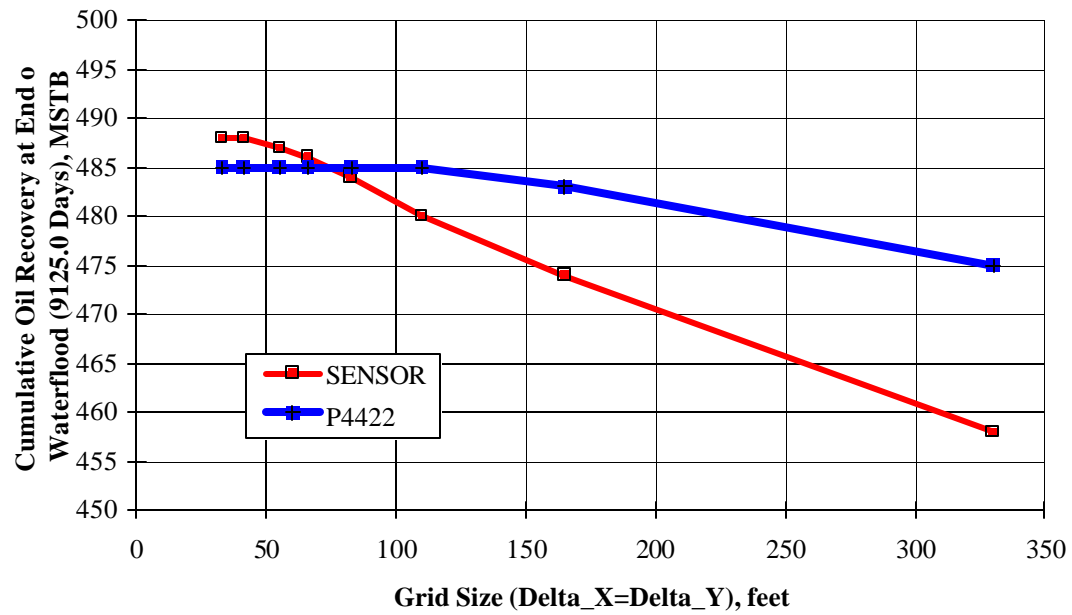


Figure V.2. Sensitivity of WF Response to areal grid size and numerical dispersion

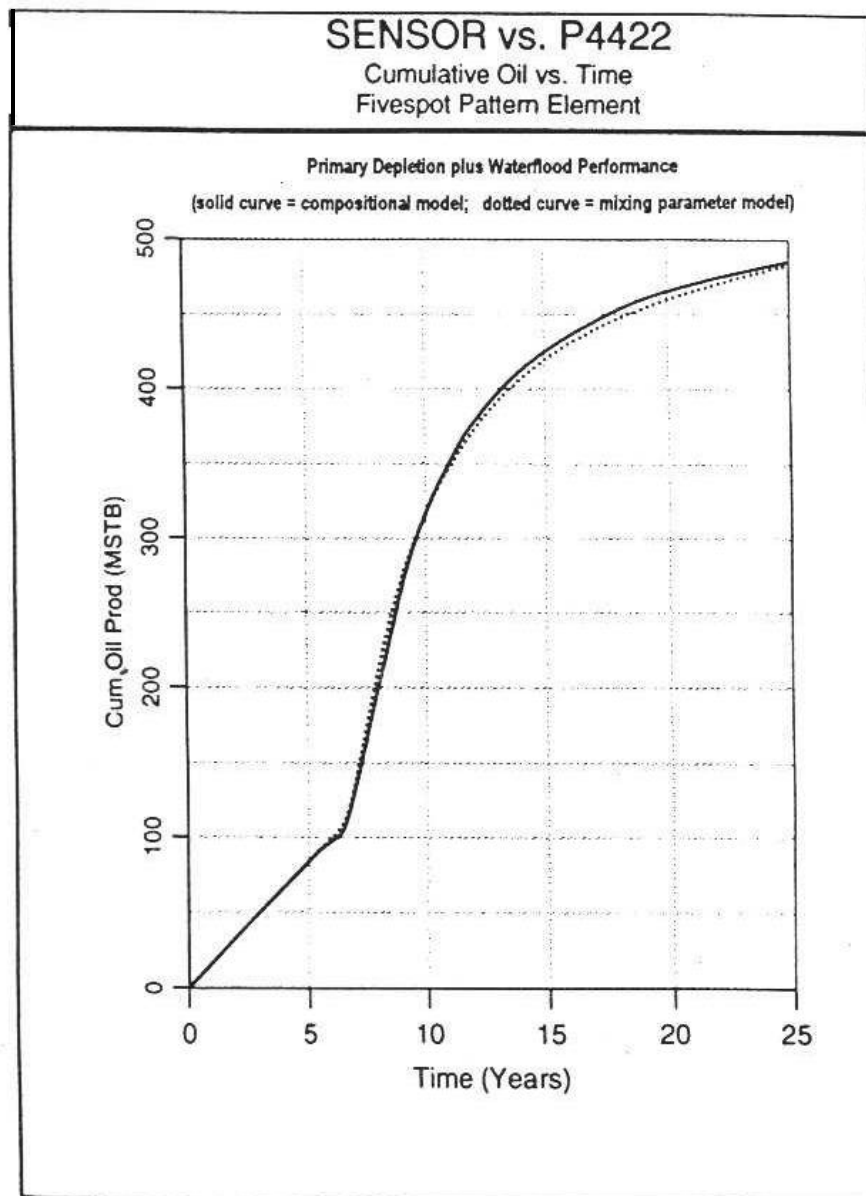


Figure V.3 Cumulative oil production vs time for the two models

### Saturation Profile Between Injector and Producer in Fivespot Pattern Models

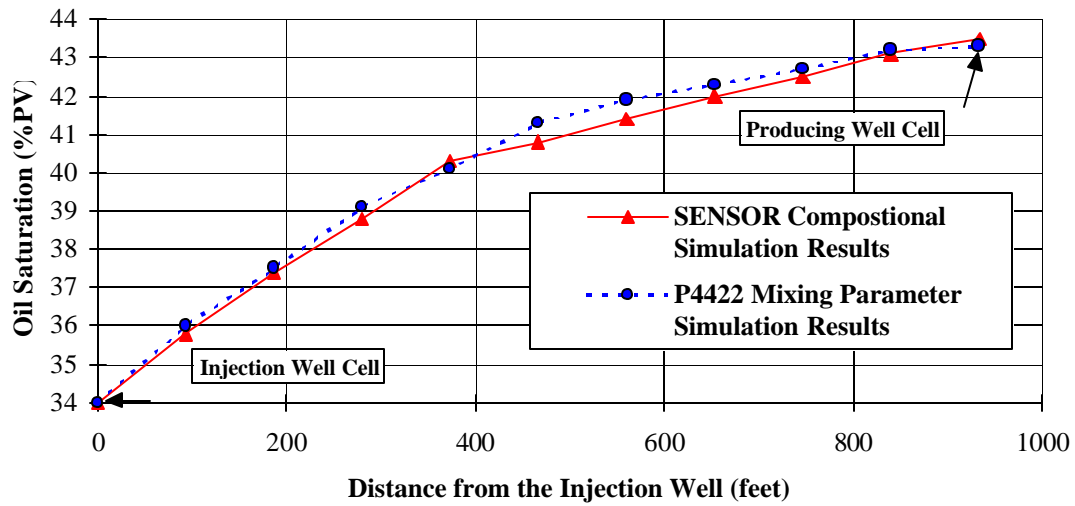


Figure V.4. Saturation profile at end of waterflood

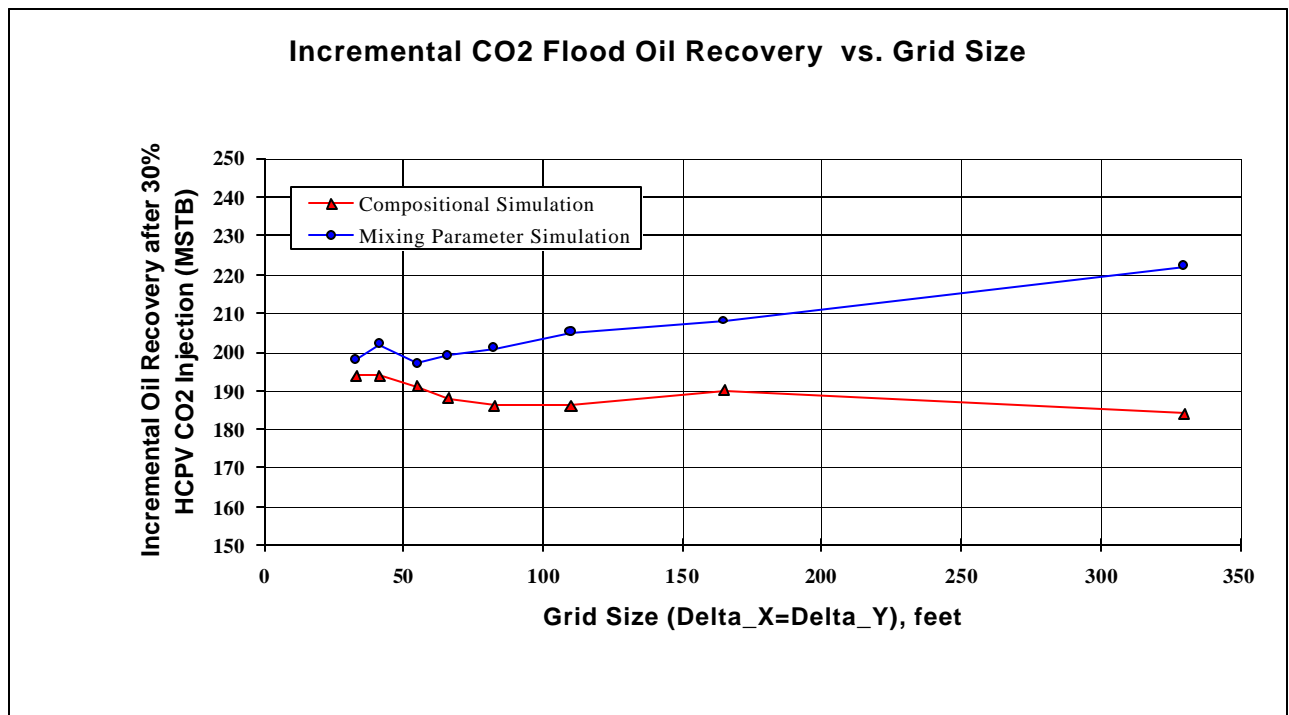


Figure V.5 Effect of areal model grid cell size on incremental oil recovery

## CO2 Flood Oil Recovery vs. Layer Thickness

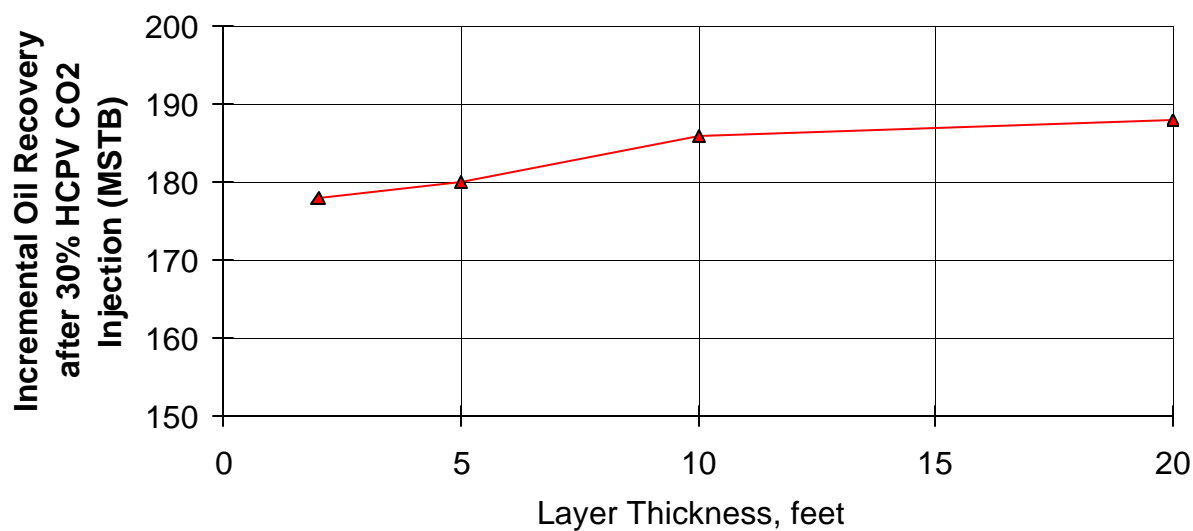


Figure V.6 Sensitivity of performance to layer thickness

## CO2 Flood Gas Production vs. Layer Thickness

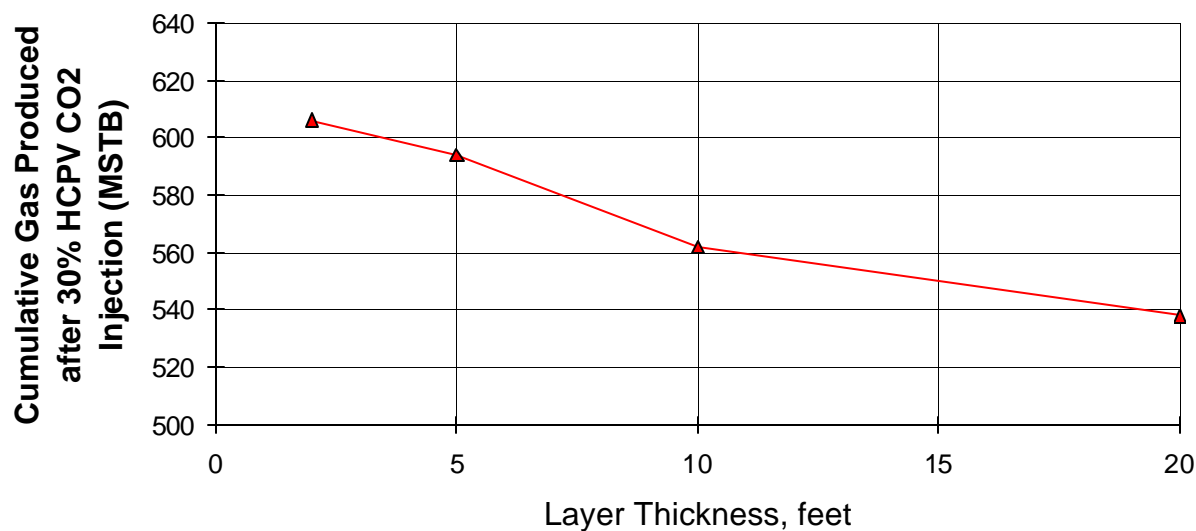


Figure V.7 Sensitivity of performance to layer thickness



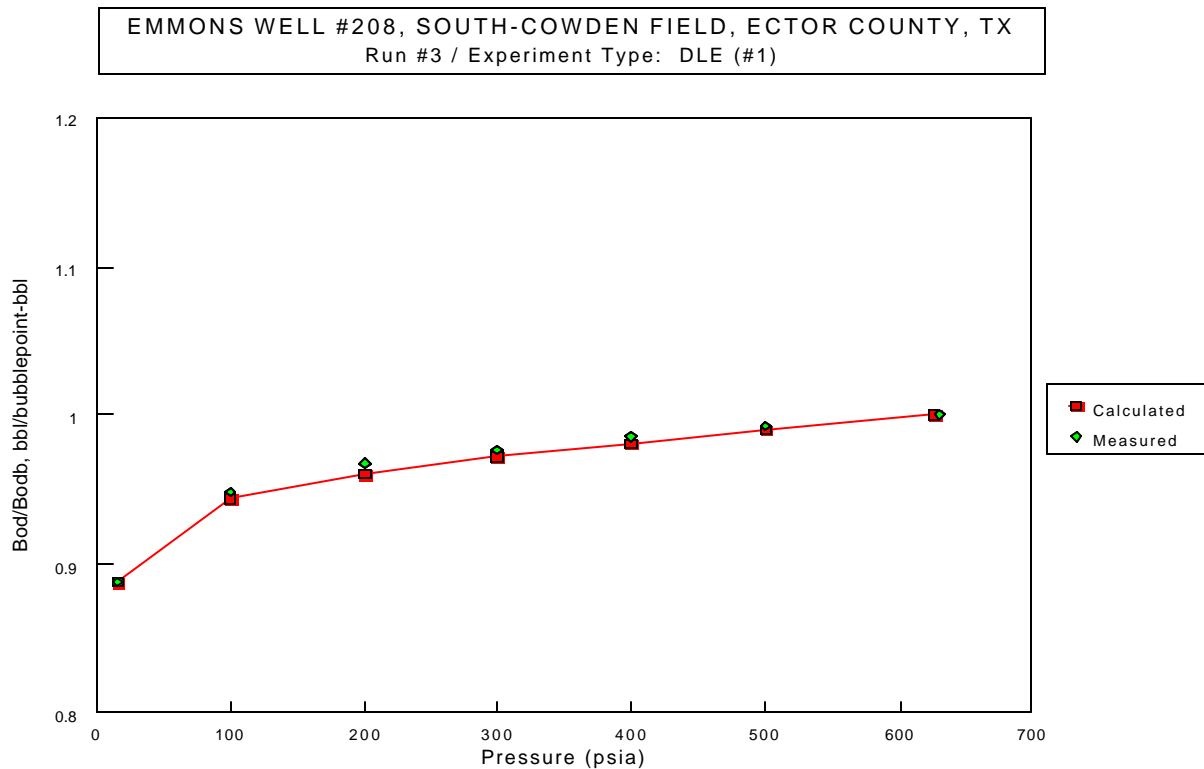


Figure V.8 Matches of experimental and EOS-predicted fluid pressure

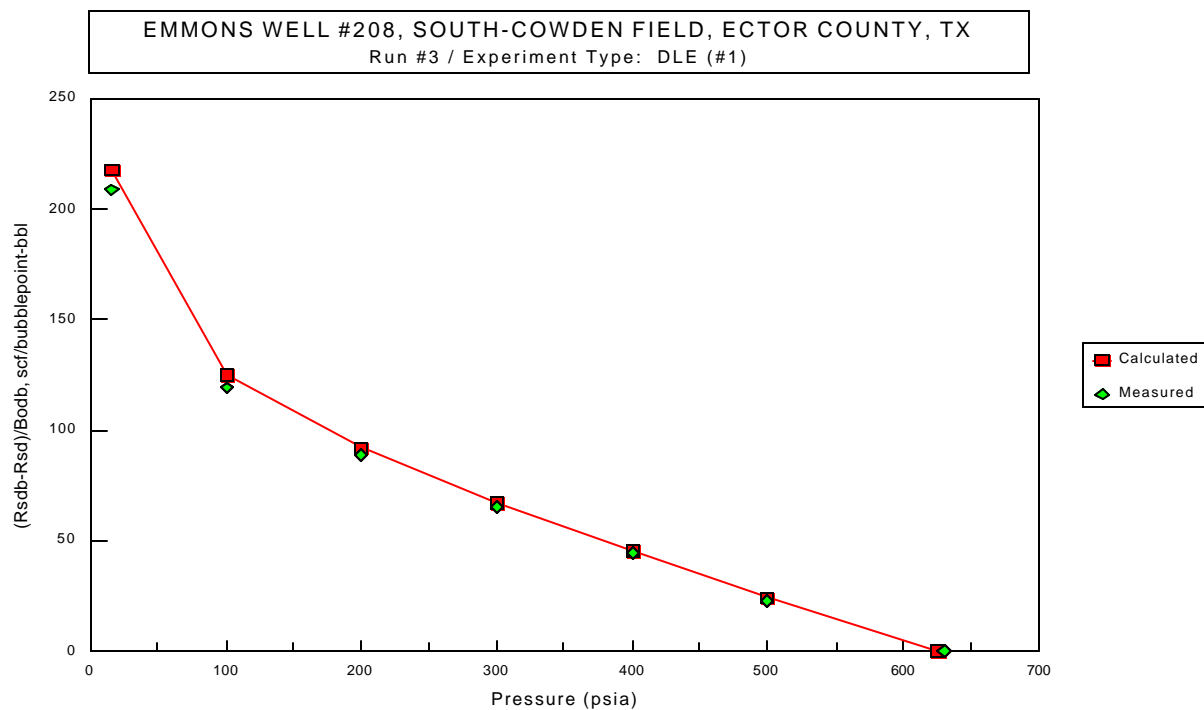


Figure V.9 Matches of experimental and EOS-predicted fluid pressures

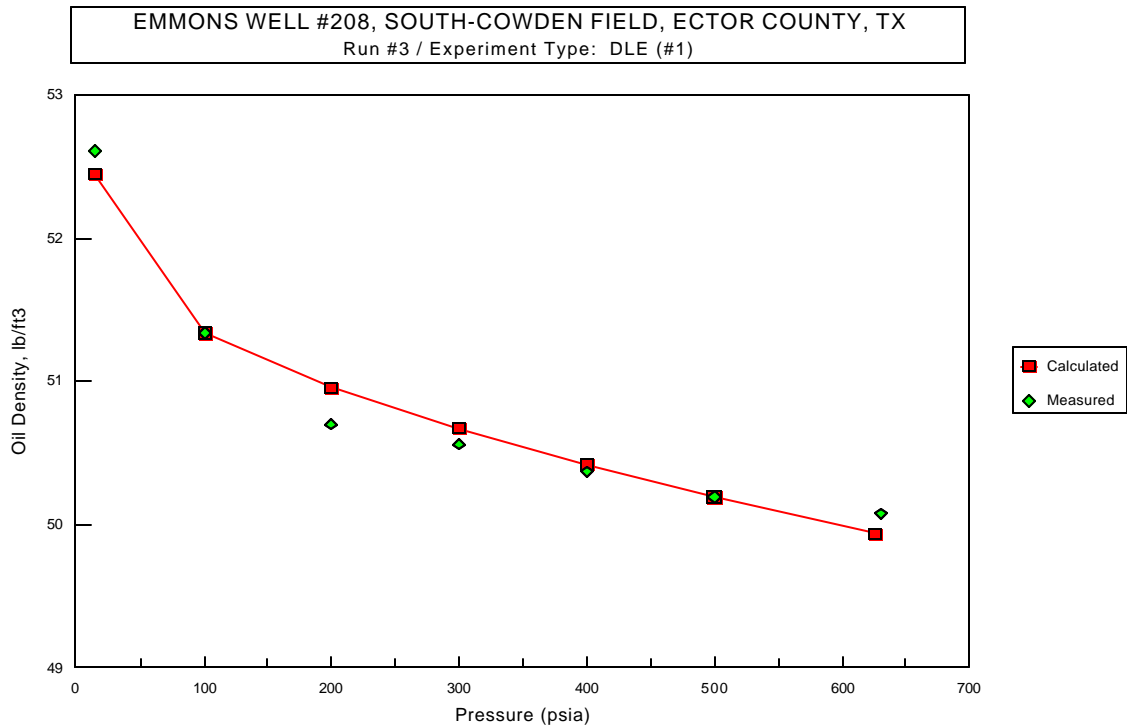


Figure V.10 Matches of experimental and EOS-predicted fluid pressure

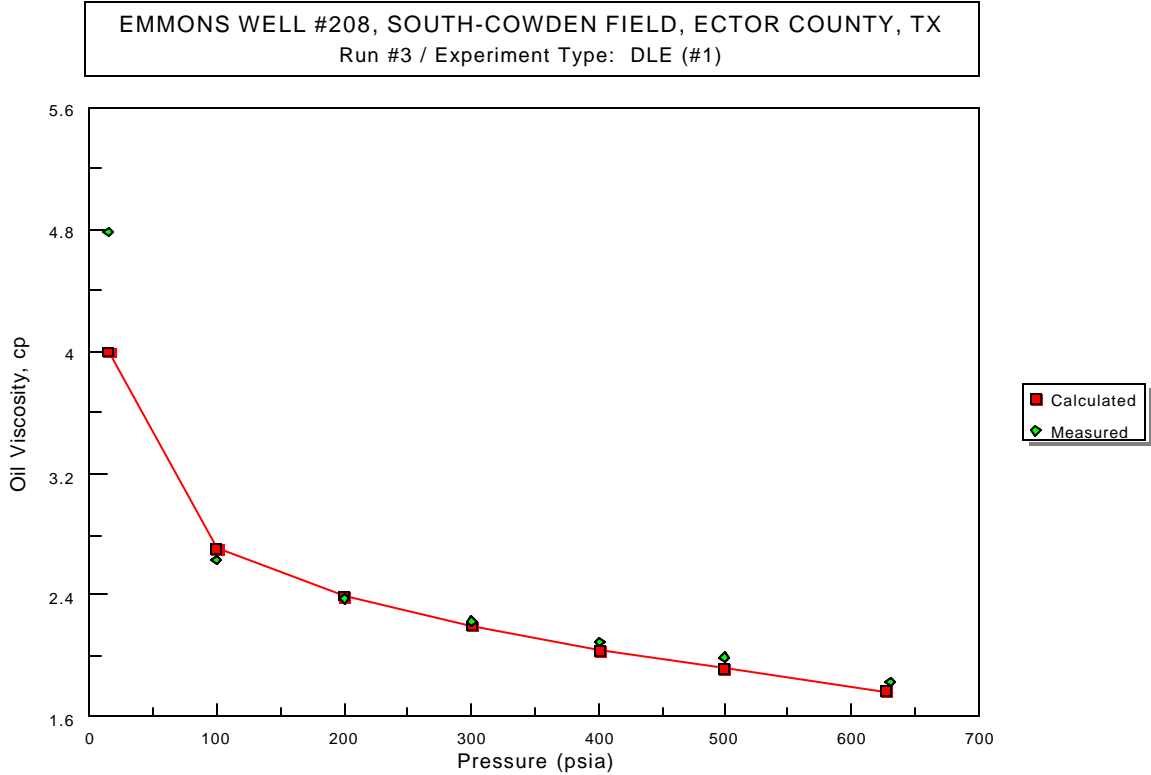


Figure V.11 Matches of experimental and EOS-predicted fluid pressures.

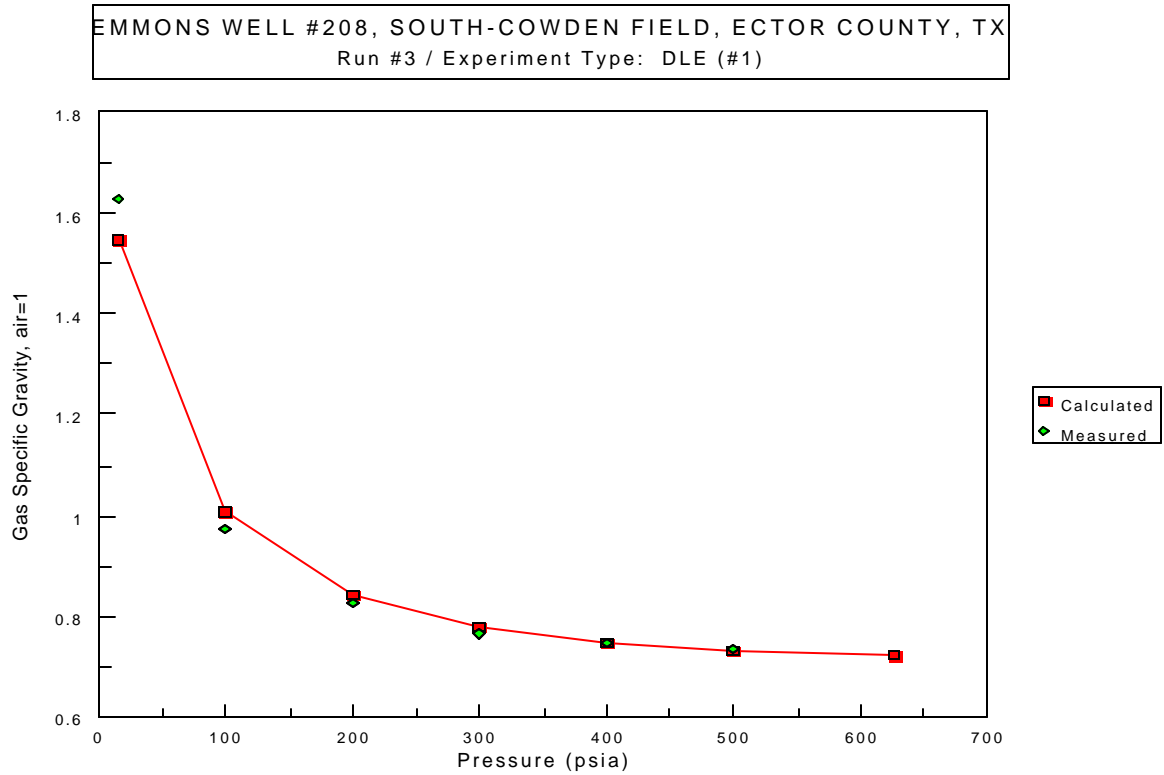


Figure V.12 Matches of experimental and EOS-predicted fluid pressures.

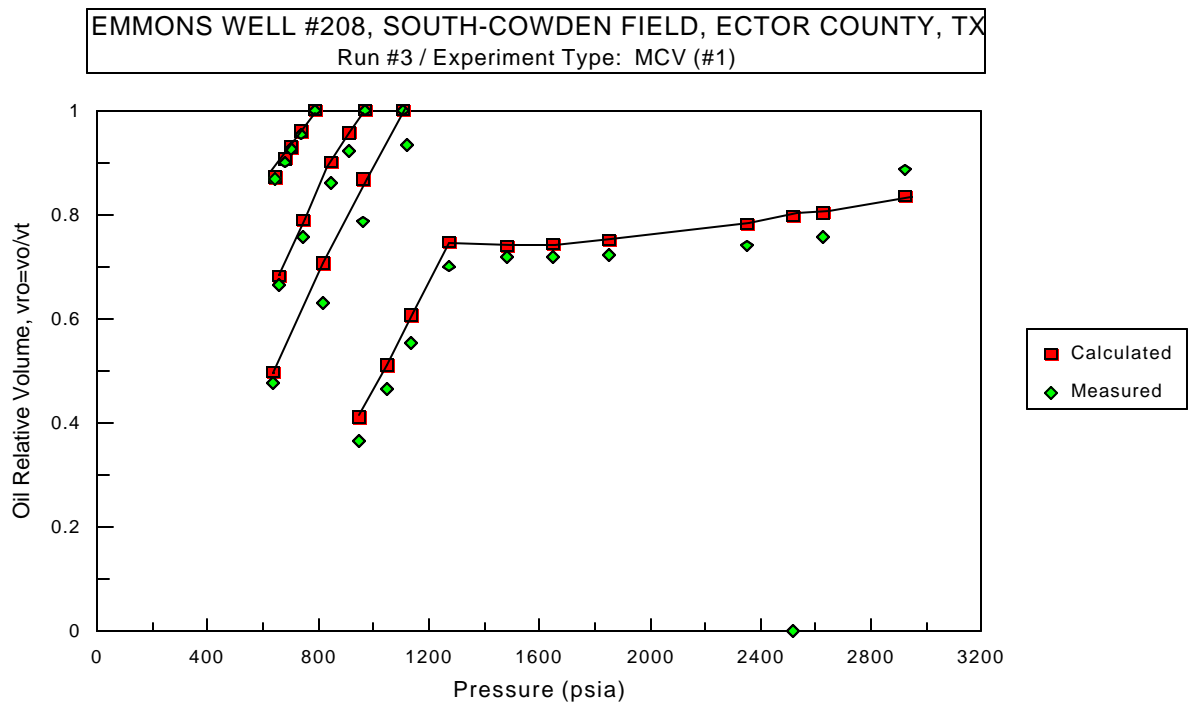


Figure V.13 Matches of experimental and EOS-predicted fluid pressures.

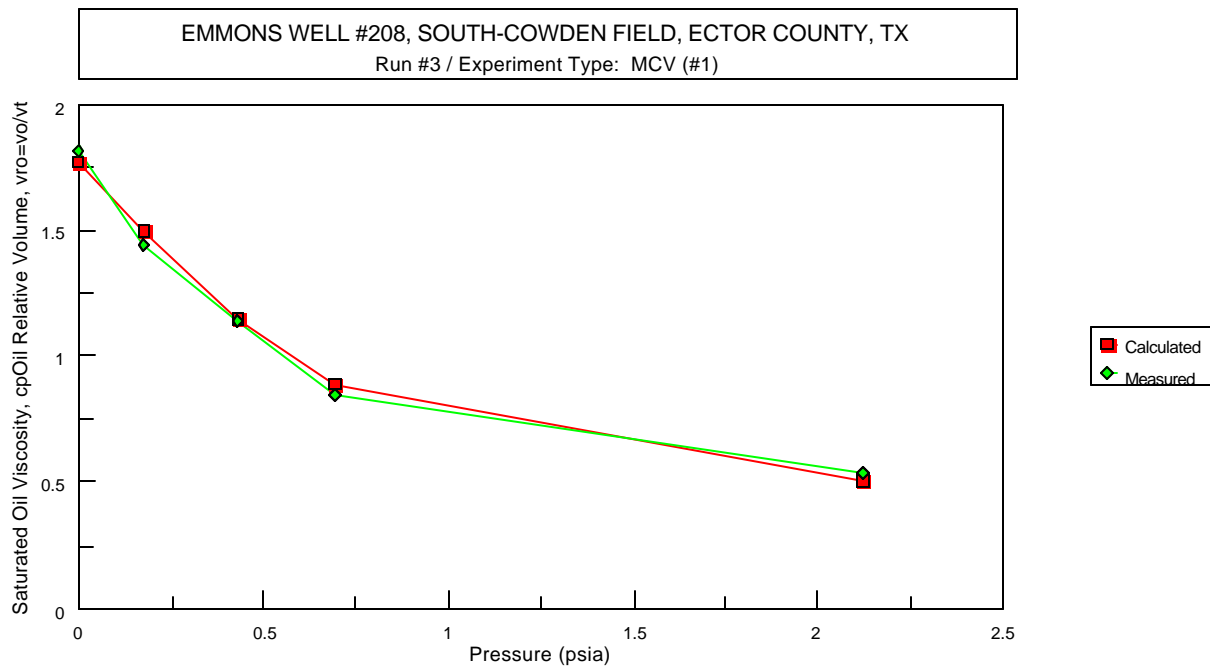


Figure V.14 Matches of experimental and EOS-predicted fluid pressures.

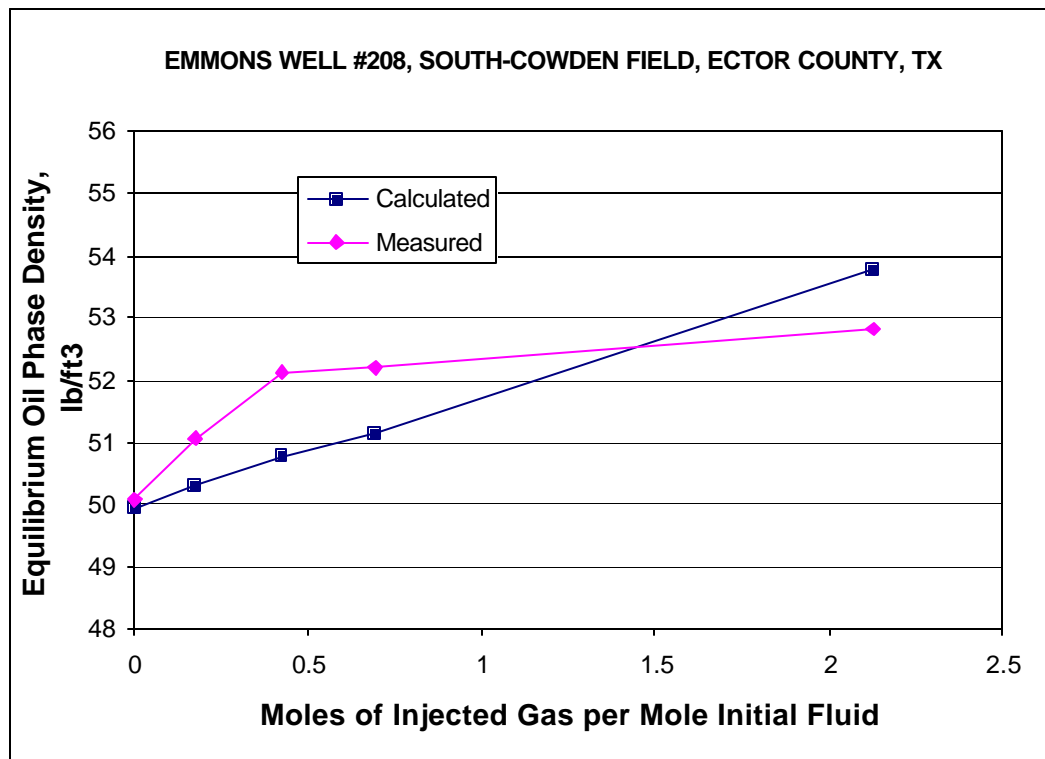


Figure V.15 Matches of experimental and EOS-predicted fluid pressures.

EMMONS WELL #208, SOUTH-COWDEN FIELD, ECTOR COUNTY, TX  
Run #3 / Experiment Type: CCE (#1)

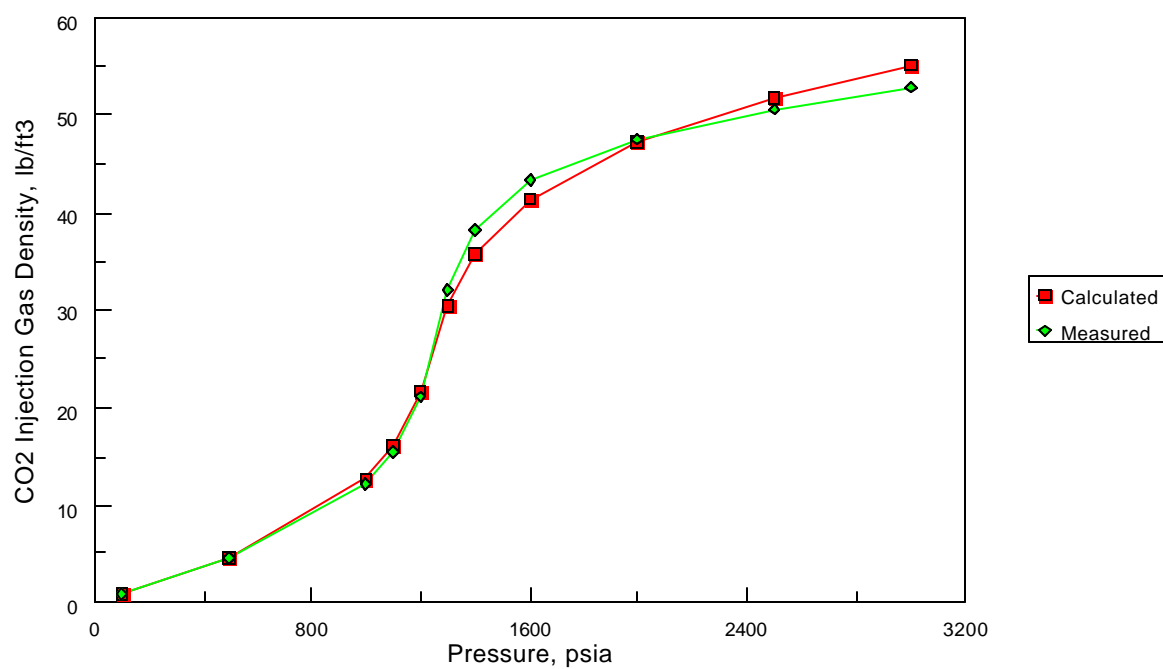


Figure V.16 Matches of experimental and EOS-predicted fluid pressures.

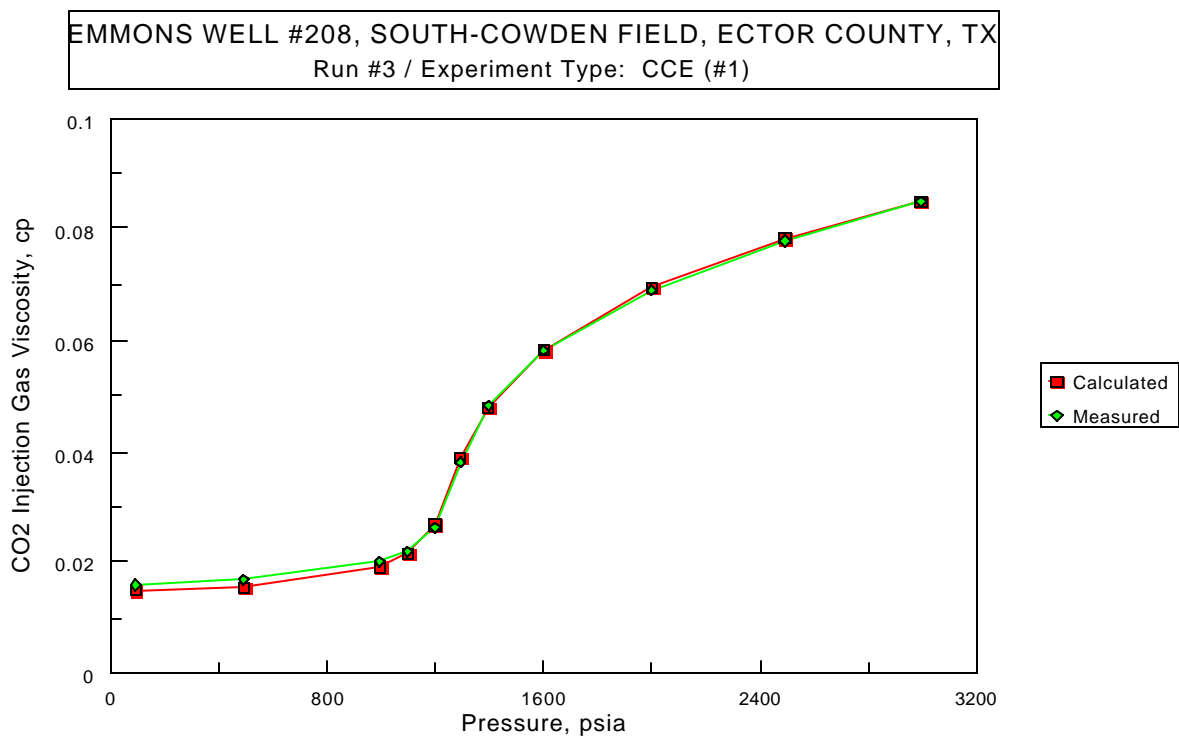


Figure V.17 Matches of experimental and EOS-predicted fluid pressures.

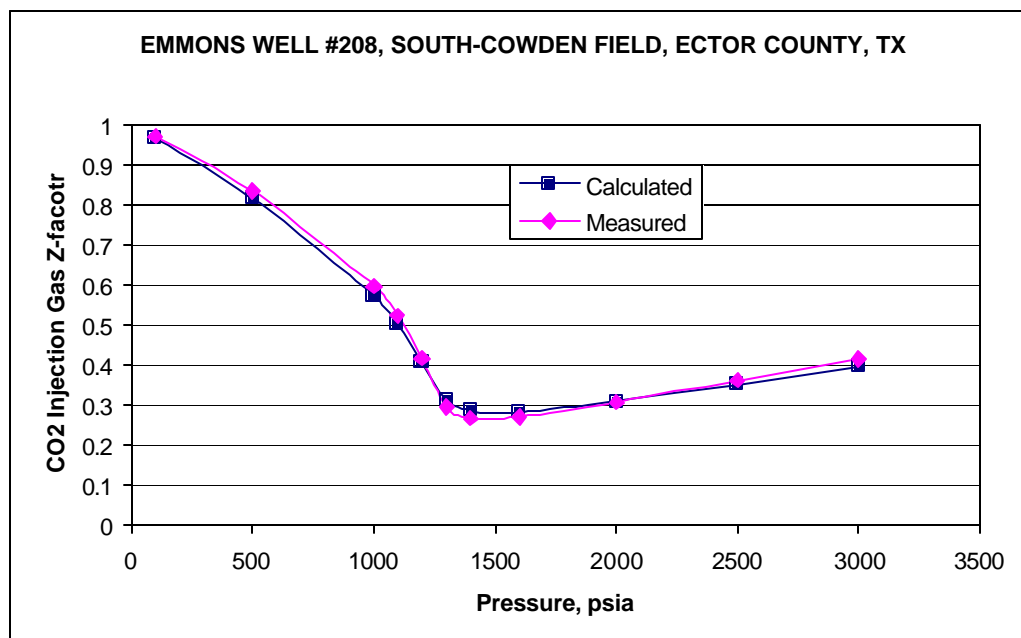


Figure V.18 Matches of experimental and EOS-predicted fluid pressures.

# South Cowden Pressure vs. Composition

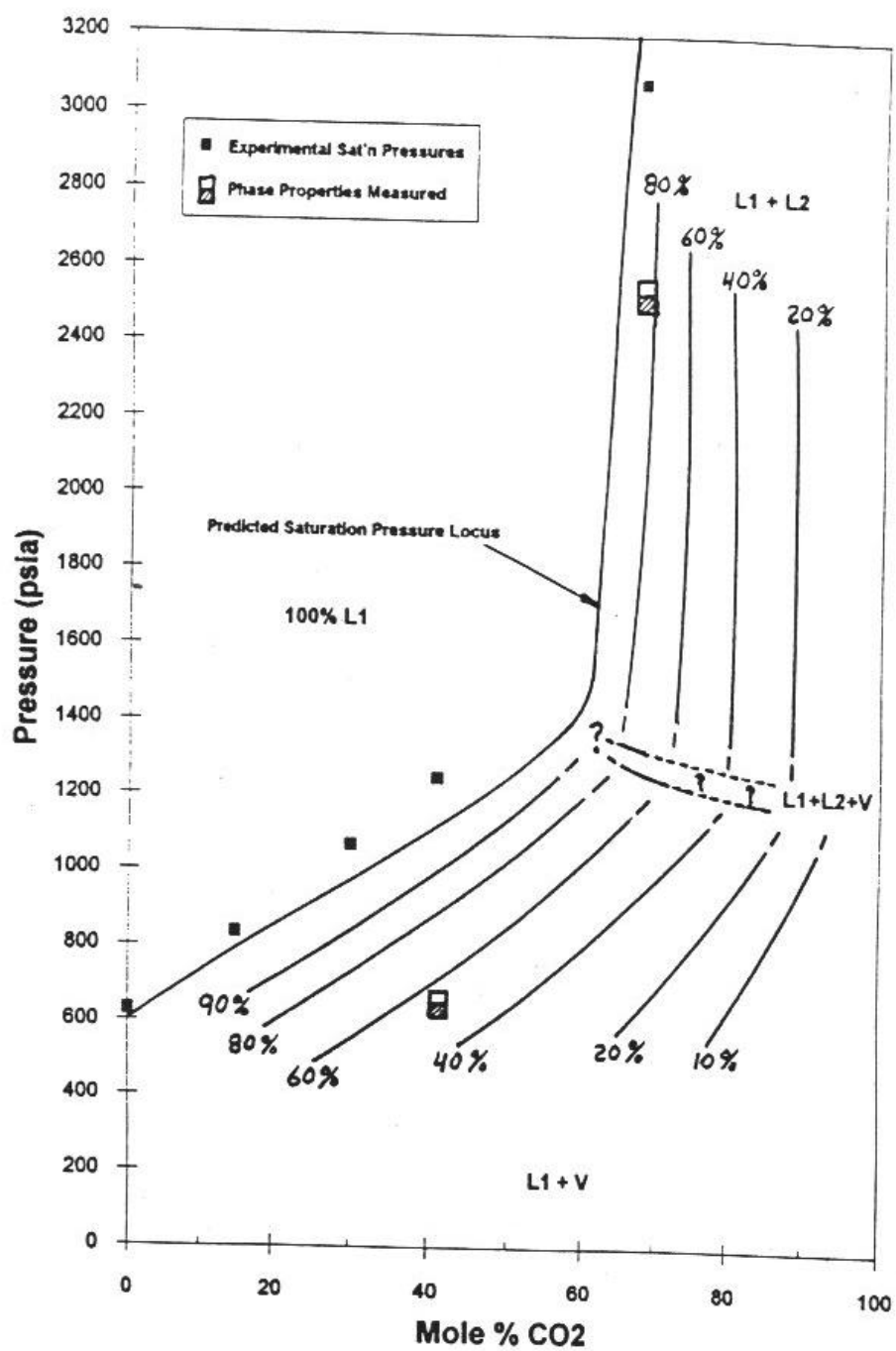


Figure V.19 Pressure vs Composition Diagram

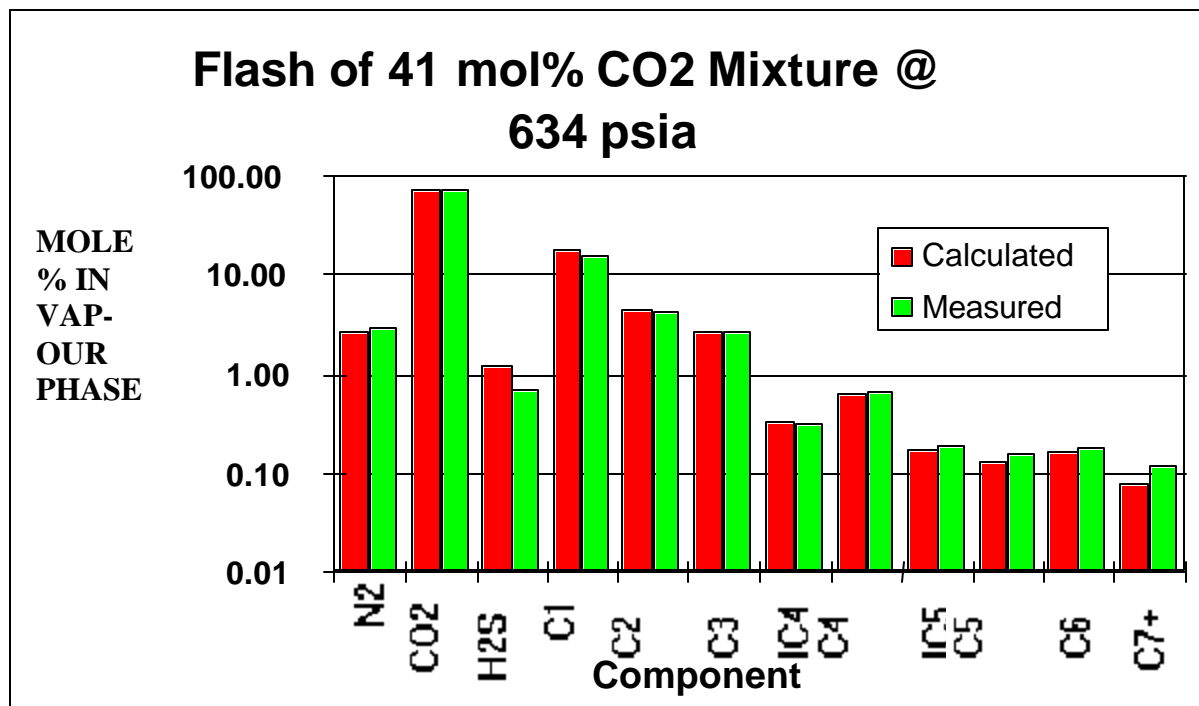


Figure V.20 EOS predicted fluid data

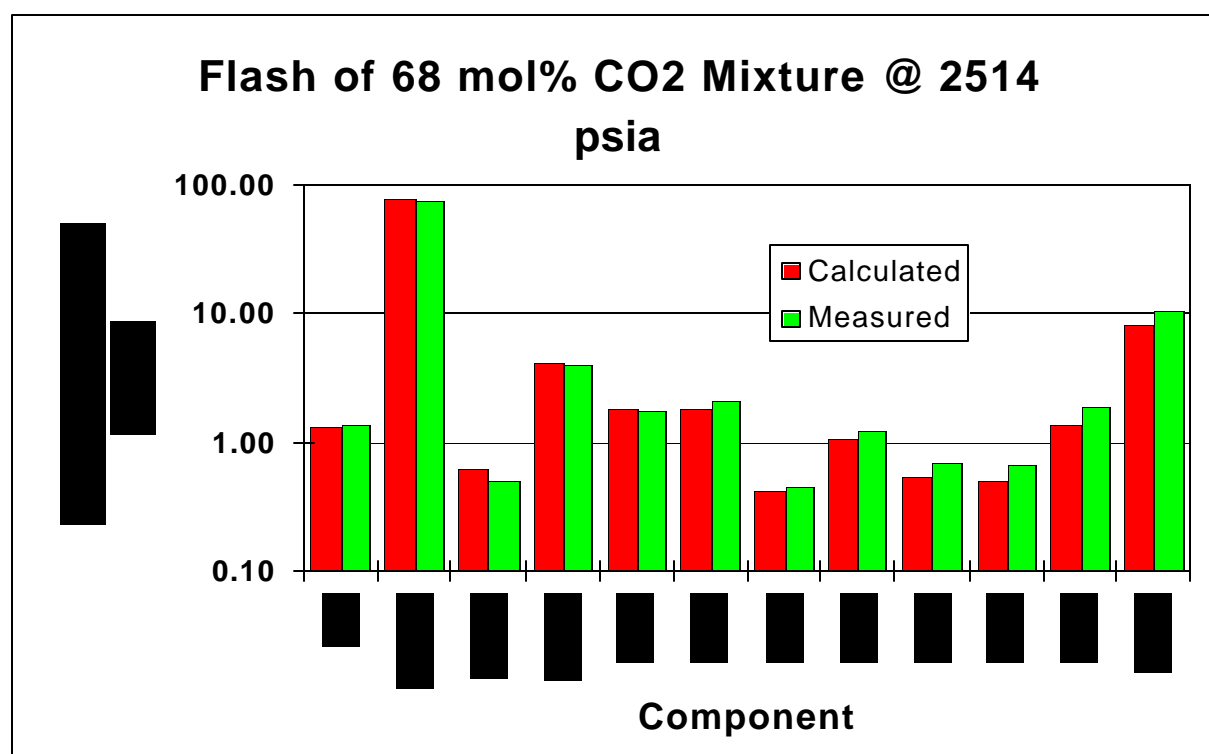


Figure V.21 EOS predicted fluid data



## SENSOR Slim Tube Simulation vs. Lab Data

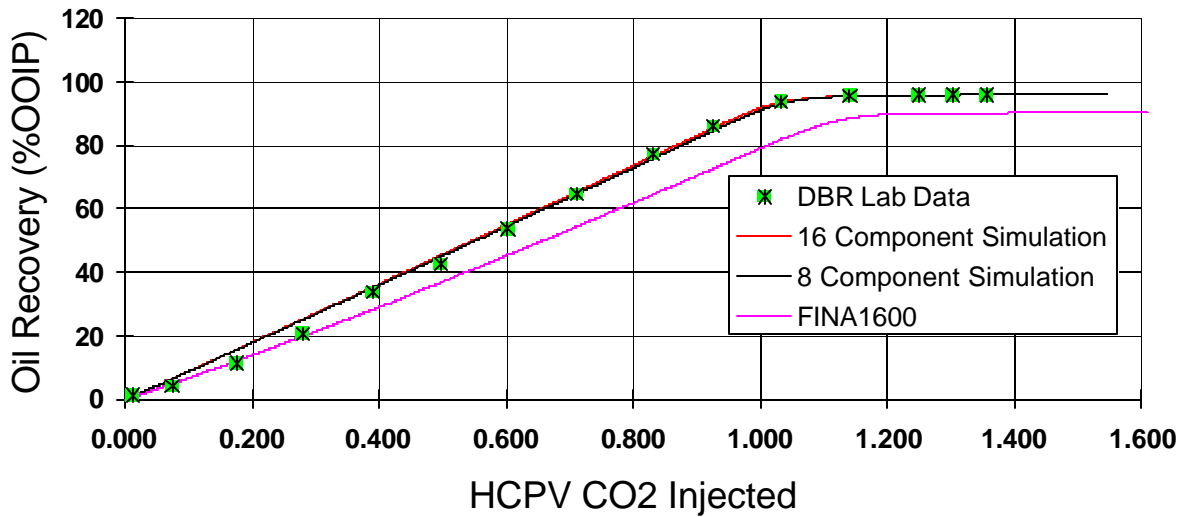


Figure V.22 Slim tube oil recovery.

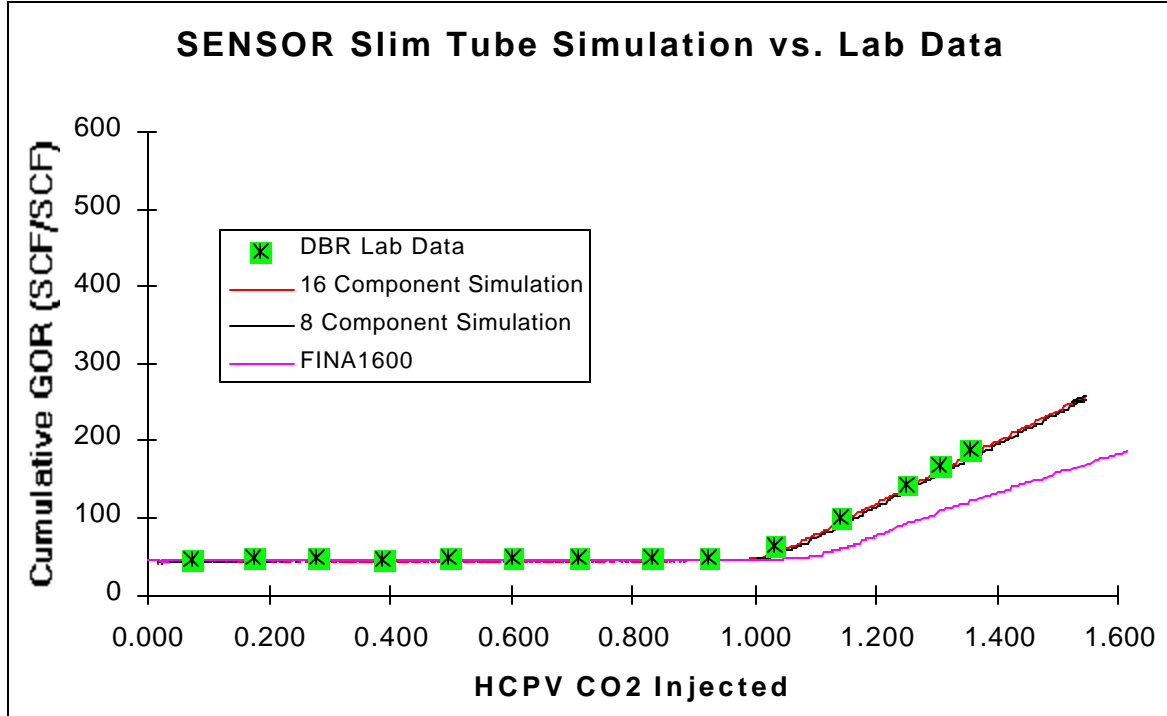


Figure V.23 Slim tube GOR behavior

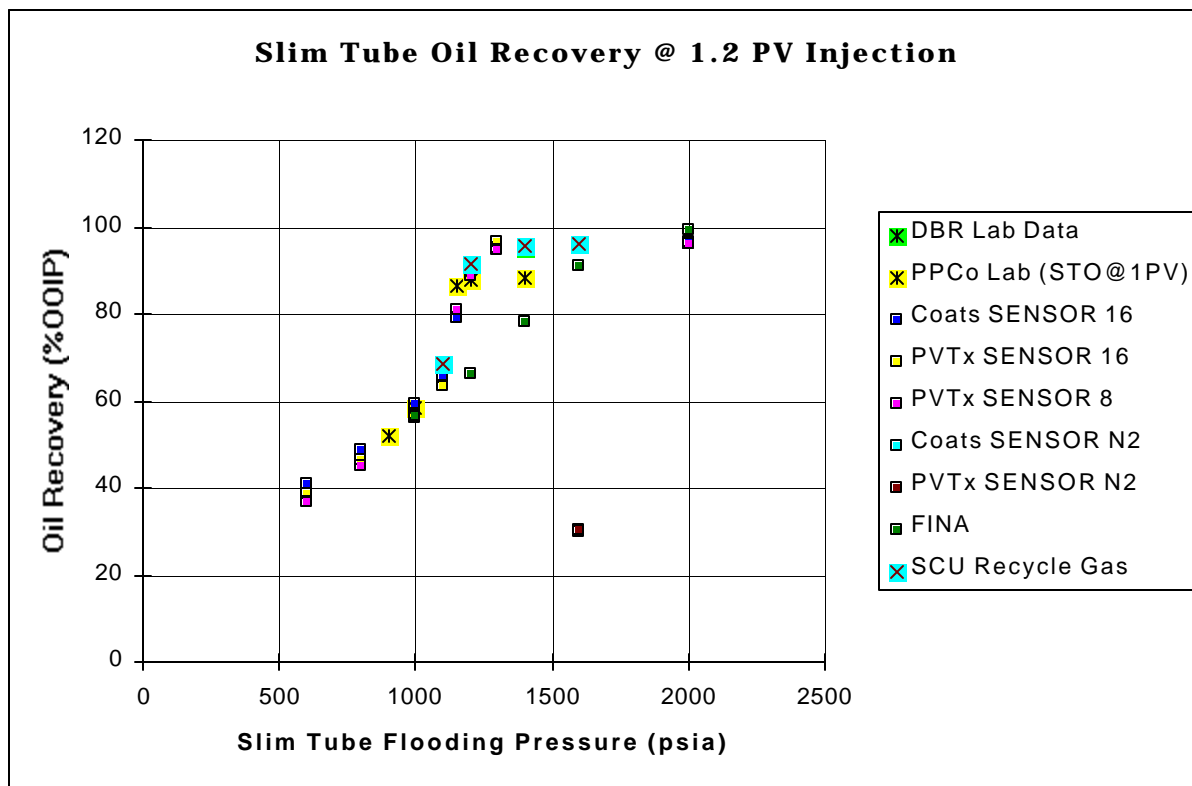


Figure V.24 Recovery efficiency vs pressure for CO<sub>2</sub>

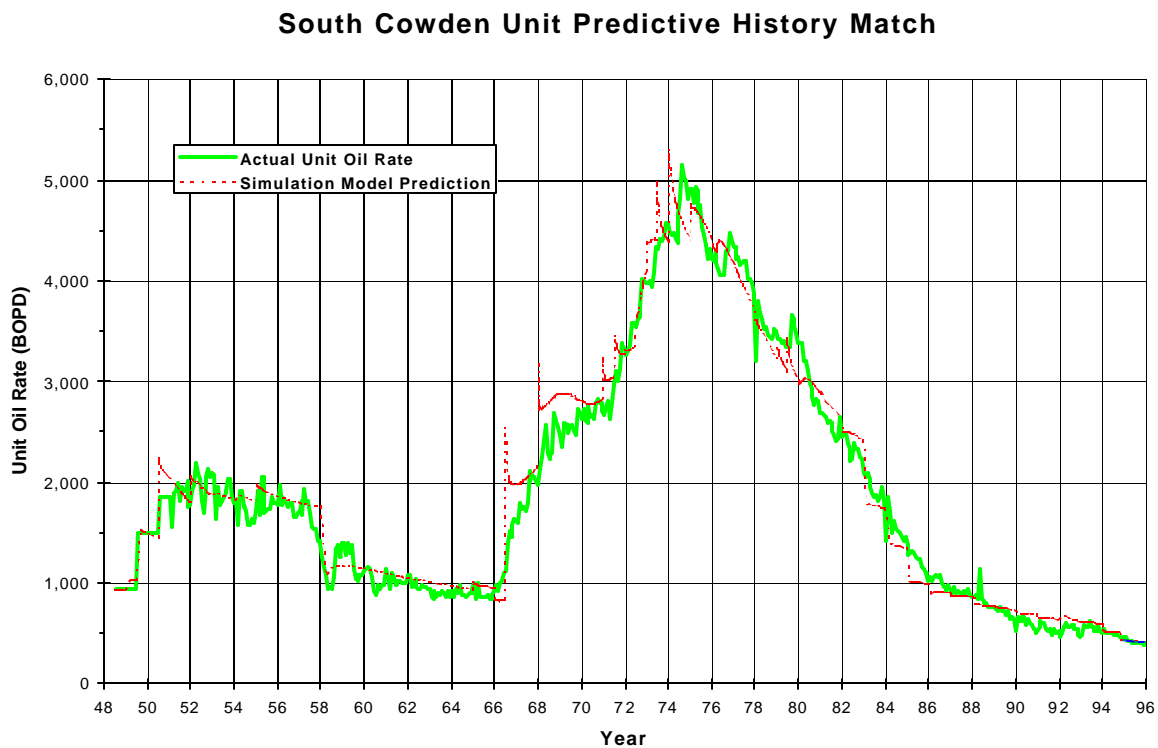


Figure V.25 Final prediction of oil recovery vs time

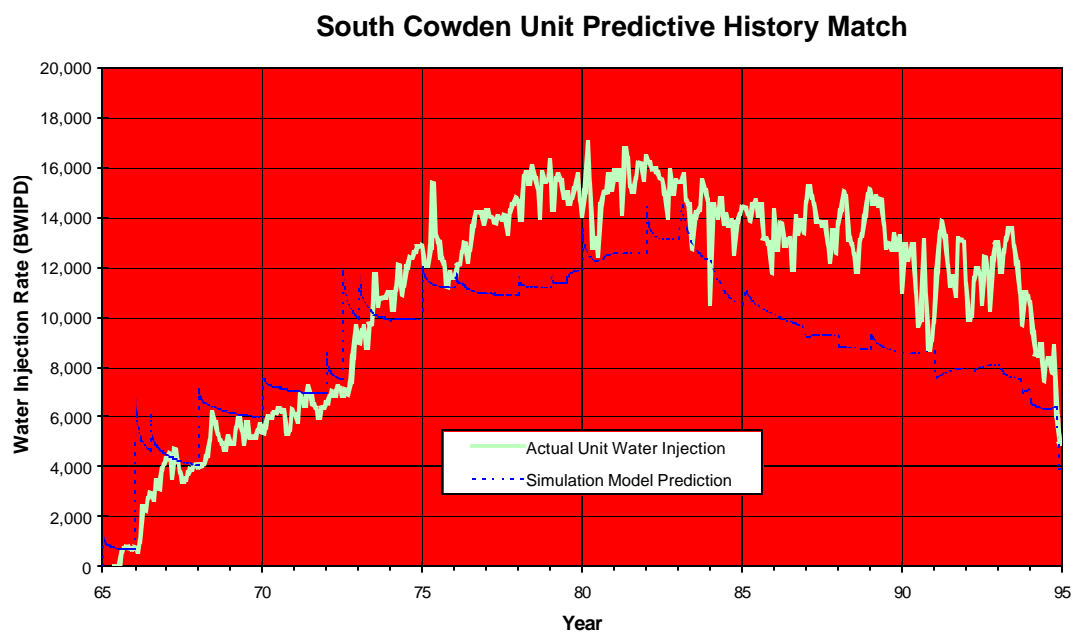


Figure V.26 Final prediction of water injection rate vs time

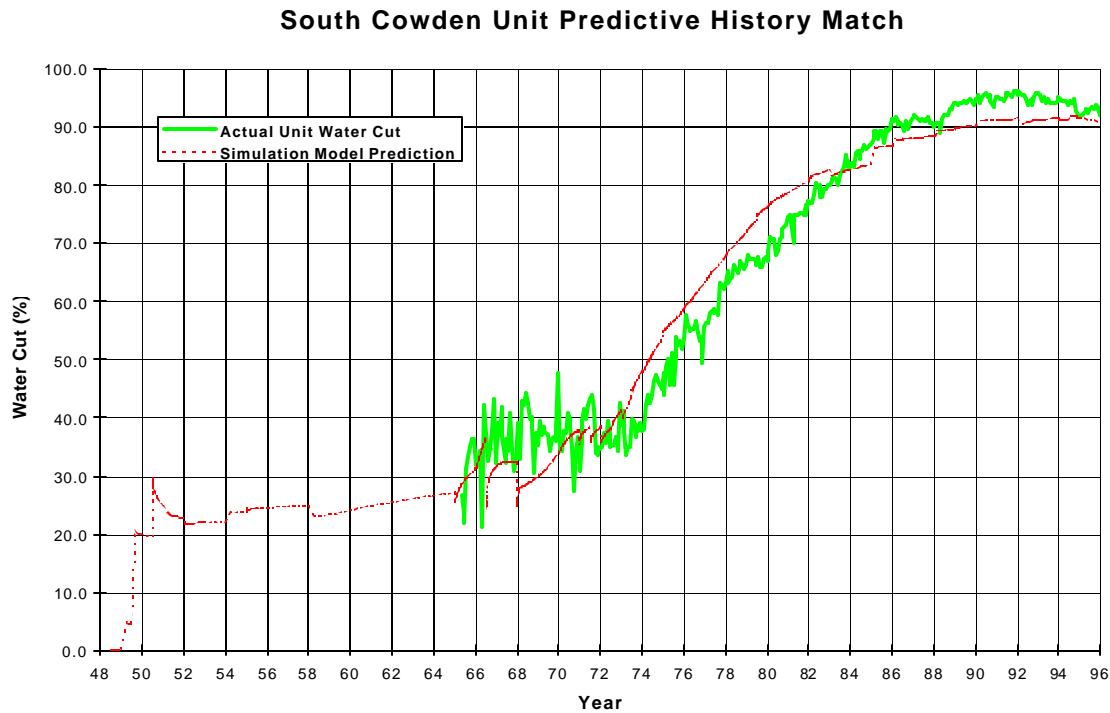


Figure V.27 Historical watercut match.

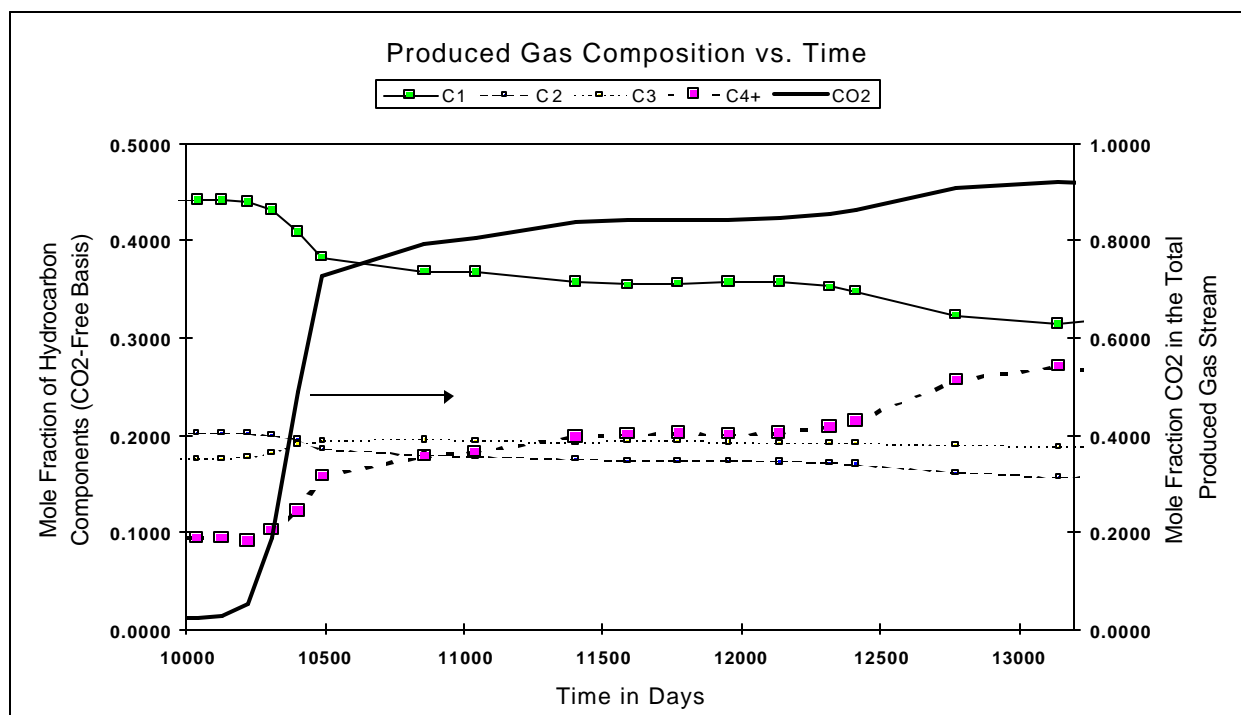


Figure V.28 Comp vs time for 5 spot pattern

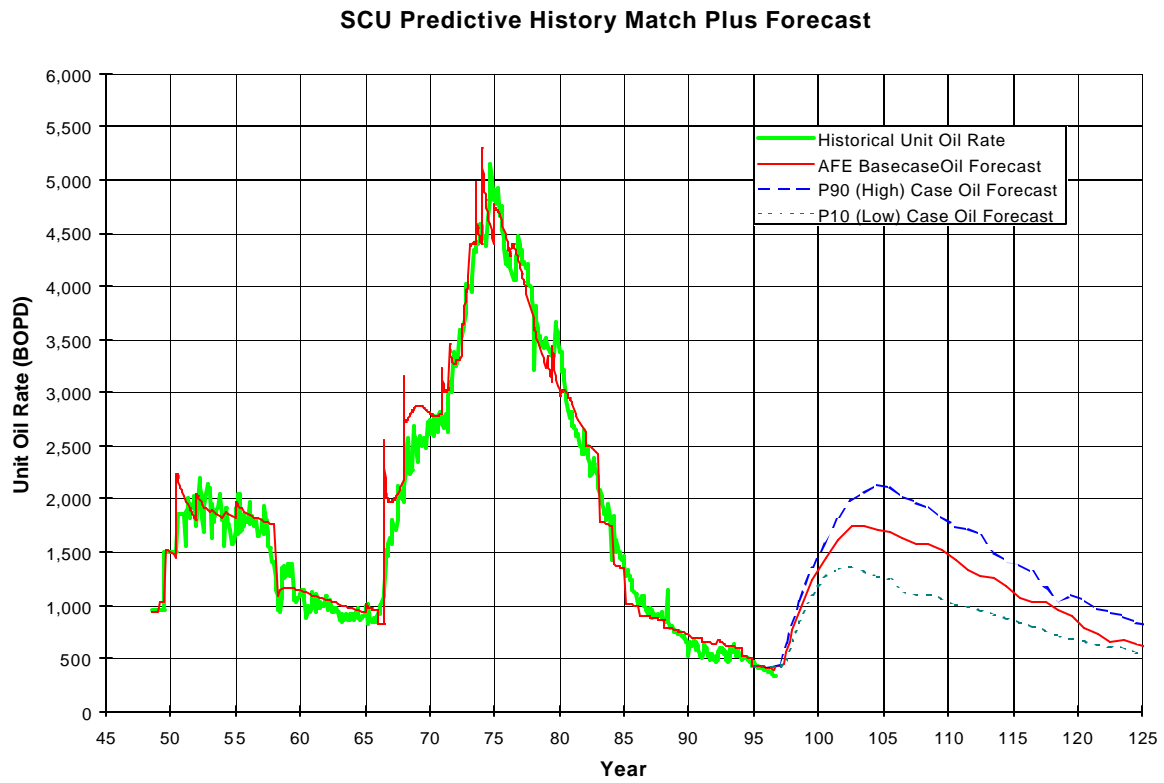


Figure V.29 Base case performance forecast

# RECOMBINED RESERVOIR FLUID COMPOSITION

TABLE V.1

## South Cowden Reservoir Fluid Composition

### Normalized Feed Mole Fractions

Component	Number	
N <sub>2</sub>	1	0.0047
CO <sub>2</sub>	2	0.0066
H <sub>2</sub> S	3	0.0209
C <sub>1</sub>	4	0.1150
C <sub>2</sub>	5	0.0575
C <sub>3</sub>	6	0.0704
IC <sub>4</sub>	7	0.0156
C <sub>4</sub>	8	0.0447
IC <sub>5</sub>	9	0.0249
C <sub>5</sub>	10	0.0239
C <sub>6</sub>	11	0.0699
C <sub>7+</sub>	12	0.5459
	Sum:	1.0000
C <sub>7+</sub> Molecular Weight		228.00
C <sub>7+</sub> Specific Gravity		0.8784
Reservoir Temperature		98 °F

# SIXTEEN COMPONENT EQUATION OF STATE FLUID DESCRIPTION

TABLE V.2

## SOUTH COWDEN 16-COMPONENT EOS FLUID DESCRIPTION

Revised Component Property Data (Field Units):

Component	No.	Mol Weight	Critical Temp. (K)	Critical Pressure (psia)	Acentric Factor	Critical Volume (ft <sup>3</sup> /mol)	Specific Gravity	Boiling Point (K)	EOS Constant - Correction Factors - Omega A	Omega B
N2	1	28.01	227.3	493.0	0.0450	1.4427	0.4700	139.3	1.0000	1.0000
CO2	2	44.01	311.0	1070.6	0.2310	1.5051	0.5072	350.4	1.0000	1.0000
H2S	3	34.08	372.4	1306.0	0.1000	1.5641	0.5000	383.1	1.0000	1.0000
C1	4	16.04	343.0	667.8	0.0115	1.5899	0.3300	301.0	1.0000	1.0000
C2	5	30.07	549.8	707.8	0.0908	2.3695	0.4500	332.2	1.0000	1.0000
C3	6	44.10	685.7	616.3	0.1454	3.2499	0.5077	416.0	1.0000	1.0000
IC4	7	58.12	734.7	529.1	0.1756	4.2082	0.5631	470.6	1.0000	1.0000
C4	8	58.12	785.3	550.7	0.1528	4.0803	0.5844	490.8	1.0000	1.0000
IC5	9	72.15	826.8	490.4	0.2273	4.8991	0.6247	541.8	1.0000	1.0000
C5	10	72.15	845.4	488.6	0.2510	4.8702	0.6310	556.6	1.0000	1.0000
C6	11	86.18	913.4	436.9	0.2957	5.9290	0.6640	615.4	1.0000	1.0000
C7+	(F1)	100.01	1022.0	461.1	0.2772	6.3118	0.7637	681.4	1.0000	1.0000
C7+	(F2)	143.67	1175.7	369.4	0.3953	8.6332	0.8178	822.1	1.0000	1.0000
C7+	(F3)	226.56	1367.5	270.7	0.5986	12.8241	0.8705	1018.4	1.0000	1.0000
C7+	(F4)	359.06	1557.3	199.3	0.8707	18.1942	0.9181	1228.8	1.0000	1.0000
C7+	(F5)	570.00	1740.6	154.3	1.1880	23.6228	0.9642	1436.8	1.0000	1.0000

Revised Component Property Data (SI Units):

Component	No.	Critical Temp. (K)	Critical Pressure (kPa)	Critical Volume (m <sup>3</sup> /kmol)	Critical Z-factor	Boiling Point (K)	Parachor	Vol. Trans. Shift (m <sup>3</sup> /g)	EOS Zc
N2	1	126.3	3399.1	0.0901	0.2916	77.4	41.0	-0.19300	0.3074
CO2	2	304.2	7381.5	0.0940	0.2742	194.7	70.0	-0.09842	0.3074
H2S	3	373.5	9004.6	0.0976	0.2831	212.8	41.0	-0.12900	0.3074
C1	4	190.5	4604.3	0.0993	0.2884	111.7	77.0	-0.15900	0.3074
C2	5	305.4	4886.1	0.1479	0.2843	184.6	108.0	-0.11300	0.3074
C3	6	389.8	4749.2	0.2029	0.2804	231.1	150.1	-0.08600	0.3074
IC4	7	406.1	3648.0	0.2627	0.2824	261.4	181.5	-0.08400	0.3074
C4	8	425.2	3796.9	0.2547	0.2736	272.7	189.9	-0.06700	0.3074
IC5	9	460.4	3381.2	0.3058	0.2701	301.0	225.0	-0.06700	0.3074
C5	10	469.7	3588.8	0.3040	0.2623	309.2	231.5	-0.06100	0.3074
C6	11	507.4	3012.3	0.3701	0.2643	341.9	271.0	-0.03900	0.3074
C7+	(F1)	567.8	3179.3	0.3940	0.2654	378.5	312.4	-0.01706	0.3074
C7+	(F2)	653.2	2546.9	0.5390	0.2528	456.7	430.0	0.04564	0.3074
C7+	(F3)	759.7	1866.6	0.8006	0.2366	565.8	630.3	0.07905	0.3074
C7+	(F4)	865.1	1374.4	1.1358	0.2170	682.7	887.5	0.08352	0.3074
C7+	(F5)	967.0	1064.2	1.4747	0.1952	798.2	1137.7	0.02383	0.3074

Normalized Feed Mole Fractions:

Feed Identifier		
Component	No.	1
N2	1	0.0047000
CO2	2	0.0066000
H2S	3	0.0209000
C1	4	0.1150000
C2	5	0.0575000
C3	6	0.0704000
IC4	7	0.0156000
C4	8	0.0447000
IC5	9	0.0249000
C5	10	0.0239000
C6	11	0.0699000
C7+	(F1)	0.0915369
C7+	(F2)	0.1633763
C7+	(F3)	0.1558047
C7+	(F4)	0.0972604
C7+	(F5)	0.0379218
Sum:	16	1.0000000
Plus Molecular Weight		228.00
Plus Specific Gravity		0.8784

COMPARISON EXPERIMENTAL vs EQUATION OF STATE  
PREDICTION

TABLE V.3

**EOS Predicted vs. Laboratory Measured Phase Properties**

	(41 mol% CO <sub>2</sub> @ 634 psia)		(68 mol% CO <sub>2</sub> @ 2514 psia)	
	<u>Laboratory</u> <u>Measurement</u>	<u>EOS</u> <u>Prediction</u>	<u>Laboratory</u> <u>Measurement</u>	<u>EOS</u> <u>Prediction</u>
$V_r$ <sub>HC-RICH</sub>	47.4%	49.4%	75%(est.)	79.5%
$\mu_{CO_2-RICH}$	.017 cp	.015 cp	0.17 cp	0.16 cp
$\mu_{HC-RICH}$	1.41 cp	1.57 cp	0.54 cp	0.56 cp
$\rho_{CO_2-RICH}$	0.080 gm/cc	0.081 gm/cc	0.797 gm/cc	0.817 gm/cc
$\rho$ <sub>HC-RICH</sub>	0.828 gm/cc	0.828 gm/cc	0.846 gm/cc	0.855 gm/cc
$MW_{CO_2-RICH}$	38.9	38.0	58.2	57.0
$MW_{HC-RICH}$	128.1	125.2	81.2	83.2
$X_{CO_2/CO_2-RICH}$	72.3%	69.0%	74.9%	75.5%
$X_{CO_2/HC-RICH}$	27.7%	31.5%	64.3%	64.2%
$X_{C_7+CO_2-RICH}$	0.11%	0.08%	10.5%	10.1%
$X_{C_7+HC-RICH}$	46.1%	42.7%	20.2%	20.1%



# EIGHT COMPONENT EQUATION OF STATE FLUID CHARACTERIZATION

TABLE V.4

## SOUTH COWDEN 8-COMPONENT EOS FLUID DESCRIPTION

Revised Component Property Data (Field Units):

Component	No.	Mol Weight	Critical Temp. (R)	Critical Pressure (psia)	Acentric Factor	Critical Volume (ft <sup>3</sup> /mol)	Specific Gravity	Boiling Point (R)	EOS Constant - Correction Factors - Omega A	Omega B
C02	1	44.01	547.6	1070.6	0.2310	1.5240	0.5072	350.4	1.0000	1.0000
C1N2	2	17.14	363.6	708.4	0.0336	1.2123	0.3420	216.1	0.9040	0.9966
C2	3	30.07	549.8	707.8	0.0908	1.7597	0.4500	332.2	1.0000	1.0000
C3C5	4	56.44	756.9	547.6	0.1928	3.9078	0.5698	486.3	0.9574	0.9804
C6F1	5	94.02	978.9	451.5	0.2845	7.7368	0.7207	655.2	0.9907	0.9972
F2	6	143.67	1175.7	369.4	0.3953	11.1685	0.8178	822.1	1.0000	1.0000
F3	7	226.56	1367.5	270.7	0.5986	17.4082	0.8705	1018.4	1.0000	1.0000
F4F5	8	418.23	1627.4	182.1	0.9920	29.9614	0.9352	1308.3	0.9567	0.9832

Revised Component Property Data (SI Units):

Component	No.	Critical Temp. (K)	Critical Pressure (kPa)	Critical Volume (m <sup>3</sup> /kmol)	Critical Z-factor	Boiling Point (K)	Parachor	Vol. Trans. Shift s=c/b	EOS Zc
C02	1	304.2	7381.5	0.0951	0.2776	194.7	70.0	0.09842	0.3074
C1N2	2	202.0	4884.2	0.0757	0.2201	120.1	76.7	-0.14989	0.3074
C2	3	305.4	4880.1	0.1099	0.2111	184.6	108.0	-0.11300	0.3074
C3C5	4	420.5	3775.6	0.2440	0.2634	270.2	184.0	-0.07343	0.3074
C6F1	5	543.8	3113.0	0.4830	0.3325	364.0	294.5	-0.00641	0.3074
F2	6	653.2	2546.9	0.6972	0.3270	456.7	430.0	0.04564	0.3074
F3	7	759.7	1866.4	1.0868	0.3211	565.8	630.3	0.07905	0.3074
F4F5	8	904.1	1255.5	1.8704	0.3124	726.8	957.7	0.05733	0.3074

Normalized Feed Mole Fractions:

Feed Identifier		
Component	No.	1
C02	1	0.0275000
C1N2	2	0.1197000
C2	3	0.0575000
C3C5	4	0.1795000
C6F1	5	0.1614369
F2	6	0.1633763
F3	7	0.1558047
F4F5	8	0.1351822
Sum:	8	1.0000000

**SCHEDULE OF WORK  
(FACILITIES)**

**TABLE V.5**

		<u>EXPENDITURE, \$M</u>
1995	Purchase land and build fence	\$320
1996	Construct injection facilities Start battery modifications Prepare for compression Replace water injection system Install cathodic protection Starat automation installation	\$2,390
1997	Continue battery modifications Start flowline replacement Continue automation installation	\$250
1998	Finish battery modification Continue flowline replacement Upgrade compression Continue automation	\$450
1999+	Finish flowline replacement Finish automation installation	\$300
	TOTAL	\$3,710

**INVESTMENT SUMMARY  
(UNESCALATED GROSS)**

**TABLE V.6**

Col 1	Col 2	Col 3	Col 4	Col 5	Col 6	Col 7	Col 8	Col 9	Col 10	Col 11
Year	Well Costs	CO2 Facilities	Production Facilities	Flowlines	Compression Installation	Land Acquisition	Replace W.I. Lines	Cathodic Protection	Automation	Total Investments
1996	\$4,222	\$663	\$203	\$75	\$555	\$322	\$395	\$406	\$87	\$6,928
1997	\$512		\$30	\$142	\$1			\$0	\$80	\$764
1998	\$722		\$180	\$142	\$50				\$80	\$1,173
1999	\$608			\$142					\$80	\$829
2000	\$304			\$0	\$25					\$329
2001	\$304									\$304
2002					\$50					\$50
2003										\$0
2004										\$0
2005										\$0
2006										\$0
2007										\$0
2008										\$0
2009										\$0
2010										\$0
2011										\$0
2012										\$0
2013										\$0
2014					\$25					\$25
2015										\$0
2016										\$0
2017										\$0
2018										\$0
2019										\$0
2020										\$0
2021										\$0
2022					\$15					\$15
2023										\$0
2024										\$0
2025										\$0
Total	\$6,670	\$663	\$413	\$502	\$721	\$322	\$395	\$406	\$326	\$10,418

**INVESTMENT SUMMARY  
(UNESCALATED GROSS)**

**TABLE V.7**

Col 1	Col 2	Col 3	Col 4	Col 5	Col 6	Col 7	Col 8	Col 9	Col 10	Col 11
Year	Total CO2 Cost	DOE Share CO2	Recycle Costs	DOE Share Recycle	Project Area Well Count	Project Area Well Cost	Other SCU Well Count	Other SCU Well Cost	Total Lease Expense	Total Minus CO2 Expense
1996	*	*	0	0	34	782	13	299	1081	1081
1997			61	20	34	782	12	276	1058	1119
1998			215	69	34	782	11	253	1035	1250
1999			250	80	34	782	10	230	1012	1262
2000			318		34	860	9	207	1067	1386
2001			332		34	860	8	184	1044	1376
2002			556		34	860	8	184	1044	1601
2003			575		34	860	8	184	1044	1620
2004			591		33	835	8	184	1019	1610
2005			593		33	835	8	184	1019	1612
2006			579		33	835	8	184	1019	1598
2007			570		33	835	8	184	1019	1589
2008			591		33	835	8	184	1019	1609
2009			618		33	835	8	184	1019	1637
2010			636		33	835	8	184	1019	1655
2011			629		31	784	8	184	968	1597
2012			618		31	784	8	184	968	1586
2013			627		31	784	8	184	968	1595
2014			688		31	784	8	184	968	1657
2015			709		30	759	8	184	943	1652
2016			660		29	734	8	184	918	1578
2017			657		29	734	8	184	918	1575
2018			675		28	708	8	184	892	1567
2019			684		28	708	8	184	892	1576
2020			701		27	683	8	184	867	1568
2021			673		25	633	8	184	817	1490
2022			417		25	633	8	184	817	1234
2023			398		24	607	8	184	791	1189
2024			397		23	582	8	184	766	1163
2025			384		22	557	8	184	741	1125
Total	*	*	15401			22887		5865	28752	44154

\* - Confidential Information

**SCHEDULE OF WORK  
(WELLS)**

**TABLE V.8**

	<u>EXPENDITURE, \$M</u>
1995	
Drill Well RC-3 (6-24)	\$350
1996	
Drill Wells H-1 and H-2	\$3,870
Drill vertical wag injector 206C (2-26W)	
Drill two Leaseline vertical wag injectors 707 and M17C	
Equip 615W as wag injector	
Drill producing wells 798, 7-12, 6-22 and 799	
Reactivate producers 705 and 620	
Convert to water injection wells 2-21, 8-18, 8-03, 6-18 and 5-02	
1997	
Reactivate 6-16W as Leaseline water injector	\$510
Reactivate producers 6-19, 7-02, 7-08 and 8-13	
Drill vertical wag injector 208C (2-27W)	
1998	
Drill producing wells 203A and 699	\$720
Reactivate producers 2-20 and 6-05	
1999+	
Drill four replacement producers (locations to be determined)	\$1,210
Convert to wag injection: RC3 and 224C	
TOTAL	\$6,660

# BUDGET PHASE I RESERVOIR DESCRIPTION COSTS

TABLE V.9

SOUTH COWDEN DOE PROJECT BUDGET PHASE 1									
SUB TASK	AFE NO.	DESCRIPTION	1,994	1,995	TO 6/1996	TOTAL TO DATE	Federal Share	Gross Amount	(Over) / Under
I.1	P-CJ54	Process & interpret 3-D Seismic Data	107	0	0	107	46	30,199	30,092
I.2	P-CJ59	Update injection well condition database	0	663	0	663	282	12,047	11,384
I.3	P-CL48	Drill core, complete, & equip. to produce Well #6-21	385,182	1,940	0	387,122	122,027	493,890	206,768
I.4	P-CN46	Drill core, complete & equip. to produce Well #5-23	329,877	33,023	0	362,900	154,233	474,866	111,766
I.5	P-CJ60	Evaluate unit production history and waterflood response	2,812	1,161	0	3,973	1,698	36,904	32,931
I.6	P-CJ65	Perform core description and petrographic studies	37,846	49,220	(22,131)	64,935	27,997	57,155	(7,780)
I.7	P-CJ66	Geological-petrophysical interpretation of stratigraphic framework	25,471	17,675	0	43,046	18,295	104,848	61,800
I.8	P-CJ57	Conduct preparatory/conceptual reservoir simulation studies characterization	15,242	16,685	(6,173)	25,954	11,030	29,954	4,000
I.9	P-CJ61	Integrate geological, petrophysical & seismic data in 3-D geologic reservoir description				0	0	48,886	48,886
II.1	P-CJ62	Special Laboratory Studies	2,105	254,101	(139,818)	116,388	49,465	155,045	38,657
II.2	P-CJ63	Advanced Geostatistical Studies	0	1,015	(560)	455	193	37,444	36,989
II.3	P-CJ64	Reservoir Simulation Studies	0	151,634	(79,707)	71,927	30,969	85,773	14,846
II.4	P-CJ65	Horizontal well scheme and finalize project development plan	0	20,662	1,900	22,452	9,542	32,266	9,813
II.5	P-CJ72	Design Upgrade & Addition to producing well equipment, production gathering system & prod. Facilities for DOE project	0	2,751	12,091	14,842	6,308	34,302	19,460
II.6	P-CJ73	Design Upgrades & additions to injection well equipment, water & CO2 recycle & reinjection facilities on the South Cowden DOE Project	0	13,319	3,864	17,183	7,303	49,954	32,771
II.7	P-CJ68	Finalize AFE - Quality Cost Estimates and Forecast Operating Expense on the DOE Project	0	3,341	0	3,341	1,420	25,170	21,829
II.1	P-CJ66	Technical paper presentation and publications	1,214	7,468	20	8,702	3,696	78,230	69,528
II.2	P-CJ67	Quarterly newsletter	0	0	0	0	0	5,103	5,103
II.4	P-CJ68	Host core workshop	0	0	0	0	0	18,096	18,096
II.5	P-CJ69	Press releases or summary articles	0	0	0	0	0	7,855	7,855
II.6	P-CJ70	Project management, reporting, & activities for project continuation	1,389	39,364	6,270	47,013	19,981	237,106	190,092
		TOTALS	701,245	614,001	(224,244)	1,091,002	463,676	2,065,490	964,488

## **FIGURE VI**

**FIGURE VI**  
**SUPPORTING DATA**



## **PVT ANALYSIS REPORTS**



**PETROLEUM  
TESTING  
SERVICE, INC.**

12051 RIVERA RD. • SANTA FE SPRINGS, CA 90670-2289

TELEPHONE (213) 698-0081 • PANAFAX (213) 693-0947

**FINA OIL AND CHEMICAL COMPANY  
RESERVOIR FLUID ANALYSIS  
FINAL REPORT**

**UNIT 208  
EMMONS FIELD  
ECTOR COUNTY, TEXAS**

**MAY 1990 FILE NO. 13518**

**REVISED DECEMBER 1990**



PETROLEUM  
TESTING  
SERVICE, INC.

12051 RIVERA ROAD  
SANTA FE SPRINGS, CA 90670-2289

May 4, 1990

Mr. P.K. Pande  
Fina Oil & Chemical Company  
6 Desta Drive  
Midland, TX 79702

Dear P.K.:


Re: Reservoir Fluid Analysis  
Emmons Unit #208  
Emmons Field  
File No. 13518

Enclosed is a reservoir fluid analysis report on separator samples collected from your well Unit #208, Emmons Field, Ector County, Texas and delivered to our laboratory in Santa Fe Springs, California for analysis. Laboratory procedures have been included for your reference.

We appreciate the opportunity to be of service to you. If you have any questions, or need additional information, please do not hesitate to contact us.

Sincerely,

PETROLEUM TESTING SERVICE, INC.

  
A. Khakoo, Manager  
Reservoir Fluids Lab

PTS:pn

Encl.

PETROLEUM TESTING SERVICE, INC.

File No.: 13518  
Date: May 1990

iii

Well: Unit #208  
Field: Emmons  
County: Ector  
State: Texas  
Sample Type: Separator

Client: Fina Oil & Chemical Co.

## INDEX

Table 1	Sampling Data .....	1
Table 2	Summary of Test Results .....	2
Table 3	Compositional Analysis of Separator Products .....	3
Table 4	Pressure-Volume Relationship at 107 °F, Separator Liquid .....	4
Figure 1	Pressure-Volume Relationship Graph at 107 °F, Separator Liquid .....	5
Table 5	Mettler Paar Density of Separator Liquid.....	6
Table 6	Recombination Data .....	7
Table 7	Calculated Composition of Reservoir Fluid .....	8
Table 8	Compositional Analysis of Reservoir Fluid .....	10
Table 9	Mettler/Paar Density of Recombination .....	12
Table 10	Constant Composition PV Measurements .....	13
Table 11	Pressure-Volume Relationship at 98°F .....	14
Figure 2	Pressure-Volume Relationship Graph at 98°F .....	15
Table 12	Differential Gas Liberation at 98°F .....	16
Table 13	Differential Gas Liberation at 98°F, Compositional Gas Analysis .....	17
Table 14	Combination Bo and Rs.....	18
Figure 3	Oil Formation Volume Factor Graph at 98°F .....	19
Figure 4	Solution Gas-Oil Ratio Graph at 98°F .....	20
Figure 5	Oil Density Graph at 98°F .....	21
Figure 6	Gas Deviation Factor "Z" Graph at 98°F .....	22

PETROLEUM TESTING SERVICE, INC.

File No.: 13518  
Date: May 1990

1v

Well: Unit #208  
Field: Emmons  
County: Ector  
State: Texas  
Sample Type: Separator

Client: Fina Oil & Chemical Co.

#### INDEX, (CONTINUED)

Figure 7	Gas Specific Gravity Graph at 98°F .....	23
Figure 8	Gas Viscosity Graph at 98°F .....	24
Table 15	Reservoir Fluid Viscosity vs. Pressure.....	25
Figure 9	Oil Viscosity Graph at 98°F .....	26
Table 16	Separator Flash Liberation at 51 psig and 107 °F ....	27
Table 17	Separator Flash Liberation at 51 psig and 107 °F, Compositional Gas Analysis .....	28

Client: Fina Oil &amp; Chemical Co.

Well: Unit #208  
Field: Emmons  
County: Ector  
State: Texas  
Sample Type: Separator

Table 1

## SAMPLING DATA

## Reservoir and Well Characteristics

Formation:	San Andres
Tubing Diameter:	
Casing Size:	
Casing Shoe:	ft.
Production Zone Top:	4565 ft.
Production Zone Bottom:	4598 ft.
Initial Static Pressure:	NA psia
Latest Static Pressure:	NA psia
Bottom Hole Temperature:	98 °F

## Sampling Conditions

Type of Sample:	Separator Oil & Gas
Well Status:	Pumping
Date of Sampling:	February 18, 1990
Sampling Duration:	4 hrs, 11.00-15.00
Flowing Bottomhole Pressure:	NA psia
Separator Pressure:	66 psia
Separator Temperature:	107 °F
Tank Temperature:	80 °F
Fluid Fpv Factor:	1.000
Separator Gas Gravity:	0.6
(Air = 1.0000)	
Separator Gas Flow Rate:	63.242 mscf/day
Tank Liquid Flow Rate:	221.09 bbl/day
Gas-Oil Ratio:	286 scf/stb
Water Cut:	Appox. 4%

NR = Not relevant

Client: Fina Oil &amp; Chemical Co.

Well: Unit #208  
Field: Emmons  
County: Ector  
State: Texas  
Sample Type: Separator

Table 2

## SUMMARY OF MAIN RESULTS

## RESERVOIR CONDITIONS

Reservoir Static Pressure:	NA	psia
Reservoir Temperature:	98	°F

## SEPARATION TEST DATA

Gas-Oil Ratio:	202	scf/stb
Stock Tank Gravity:	34.0	°API
Sales Gas Gravity (Air = 1.0000):	1.0495	
Sales Gas Heating Value (Gross, Dry):	1608	BTU/scf

## CONSTANT MASS STUDY AT 98°F

Bubble Point Pressure:	625	psia
Compressibility	$6.658 \times 10^{-6}$	1/psia
From:	3000	psia
To:	1000	psia

## DIFFERENTIAL GAS LIBERATION AT 98°F

At Bubble Point Pressure:	625	Psia
Oil Volume Factor:	1.147	bbl/stb
Solution GOR:	240.0	scf/bbl
Reservoir Fluid Density:	0.7937	gm/cc
Residual Oil Gravity (at 60/60°F):	0.8529	
Residual API Gravity (at 60°F):	34.4	°API

## VISCOSITY DETERMINATION AT 98°F

Viscosity at Bubble Point Pressure:	1.960	cp
-------------------------------------	-------	----

NR = Not relevant

Well: Unit #208  
Field: Emmons  
County: Ector  
State: Texas

Client: Fina Oil &amp; Chemical Company

Sample Type: Separator

Table 3

## COMPOSITIONAL ANALYSES OF SEPARATOR PRODUCTS

Component	Mol. Wt. (gm/gm-mole)	Separator Products		
		Liquid (Mole %)	(Wt %)	Gas (Mole %)
N2	28.01	0.04	0.01	1.66
CO2	44.01	0.12	0.03	2.22
H2S	34.08	1.06	0.20	6.66
C1	16.04	0.13	0.01	41.34
C2	30.07	1.94	0.32	18.78
C3	44.10	4.92	1.20	15.10
i-C4	58.12	1.63	0.52	2.89
n-C4	58.12	4.72	1.51	6.05
i-C5	72.15	3.24	1.29	1.99
n-C5	72.15	3.16	1.25	1.48
C6	86.18	4.95	2.35	1.08
C7	100.20	7.05	3.89	0.61
C8	114.23	8.60	5.41	0.13
C9	128.26	7.06	4.99	0.01
C10	142.29	5.16	4.04	
C11	156.31	4.09	3.52	
C12	170.34	3.24	3.04	
C13	184.37	3.34	3.39	
C14	198.40	2.65	2.89	
C15	212.42	2.52	2.94	
C16	226.45	2.04	2.54	
C17	240.48	1.88	2.49	
C18	254.50	1.76	2.47	
C19	268.53	1.79	2.64	
C20+	373.35	<u>22.91</u>	<u>47.06</u>	
Total		100.00	100.00	100.00

## Separator Liquid C7+ Properties:

Mole %	74.09
Weight %	91.31
Molecular Weight (gm/gm-mole)	223.90
Density (at 60/60°F)	0.8742
API Gravity at 60°F	30.4

Separator Liquid Molecular Weight (gm/gm-mole) ..... 181.63

## Separator Gas Properties:

Gas Gravity (Air = 1.0000)	1.1067
Gross Heating Value (Dry), BTU/scf	1696



PETROLEUM TESTING SERVICE, INC.

File No.: 13518  
Date: December 1990

Page 4

Well: Unit #208  
Field: Emmons  
County: Ector  
State: Texas  
Sample Type: Separator

Client: Fina Oil & Chemical Co.

Table 4

PRESSURE-VOLUME RELATIONSHIP AT 107°F  
(SEPARATOR LIQUID)  
(Constant Composition - Equilibrium Expansion)

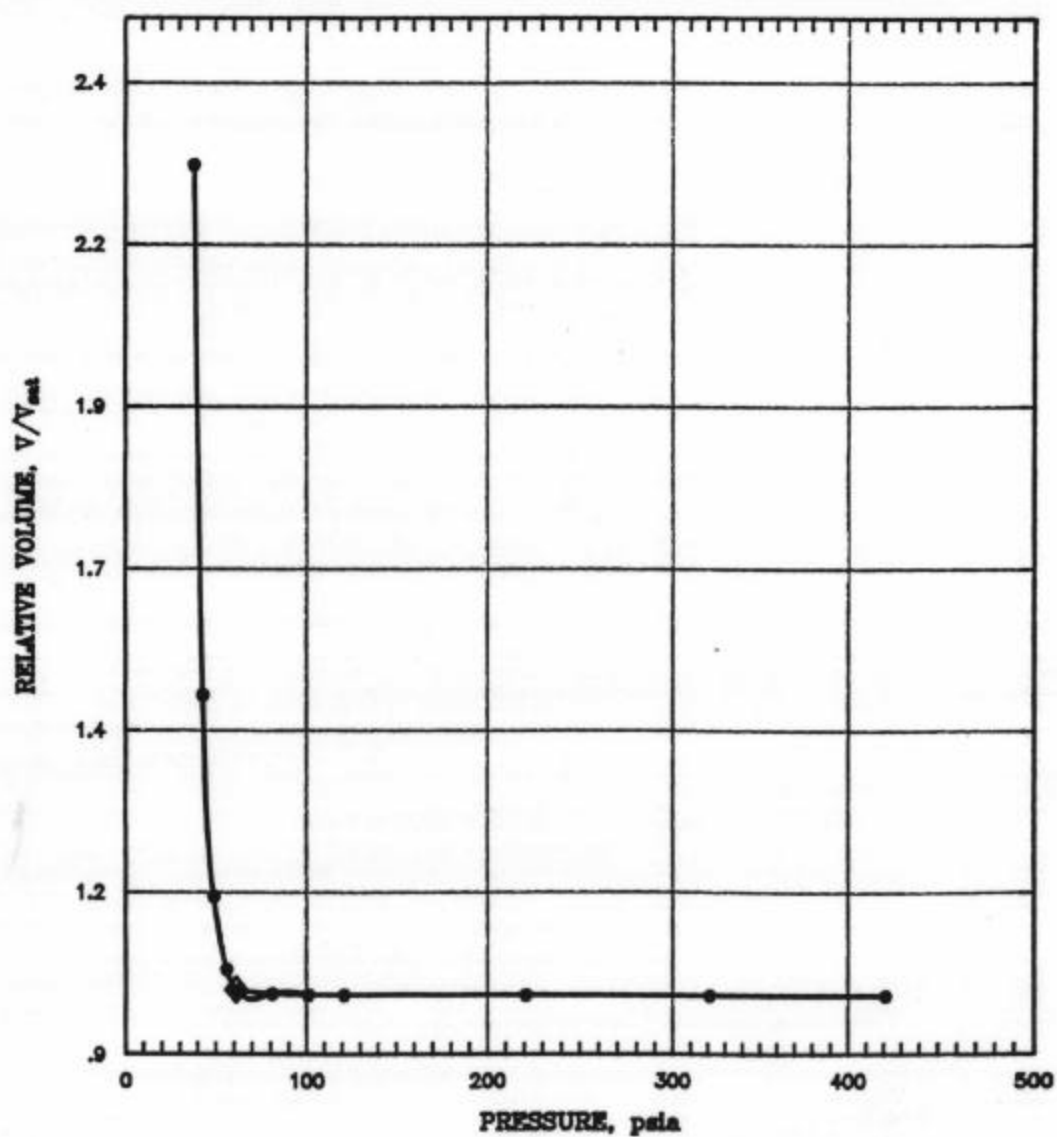
<u>Pressure (psia)</u>	<u>Relative Volume (V/V<sub>sat</sub>)</u>	<u>Y-Function</u>
421	.9915	
321	.9917	
221	.9926	
121	.9928	
101	.9928	
81	.9946	
61	1.0000	
56	1.0321	2.7810
49	1.1447	1.6926
43	1.4563	.9175
38	2.2729	.4755

Field Separator Pressure : 66 psia  
Field Separator Temperature : 107 F

\*Bubble point (saturation) pressure

Figure 1  
Pressure-Volume Relationship at 107°F

◇ Bubble Point Pressure = 61 psia



PETROLEUM TESTING SERVICE, INC.

>

File No.: 13518

Date: May 1990

Well: Unit #208

Field: Emmons

County: Ector

State: Texas

Client: Fina Oil & Chemical Company

Sample Type: Separator

Page 6

Table 5

DENSITY BY METTLER/PAAR DENSITOMETER  
Separator Liquid

Laboratory Conditions

Pressure (psia)	Temperature (°F)	Density (gm/cc)
1000	71.7	0.8471
500	71.7	0.8448

Separator Conditions

Pressure (psia)	Temperature (°F)	Density (gm/cc)
400	98	0.8316
300	98	0.8311
200	98	0.8305
100	98	0.8299
Extrapolated Density at 65 psia*:		0.8297

\* Bubble point pressure

PETROLEUM TESTING SERVICE, INC.

File No.: 13656  
Date: May 1990

Page 7

Well: Unit #208  
Field: Emmons  
County: Ector  
State: Texas  
Sample Type: Separator

Client: Fina Oil & Chemical Co.

Table 6

RECOMBINATION DATA

Correction of Field Gas-Oil Ratio to Laboratory Gas-Oil Ratio<sup>#</sup>

Field Gas-Oil Ratio ..... 288 scf/stb

Laboratory Gas-Oil Ratio:

$$\begin{aligned} [\text{GOR}]_L &= [\text{GOR}]_f \times [(G_f \times Z_f) / (G_L \times Z_L)]^{1/2} \\ &= 288 \times [(.600 \times 1) / (0.9859 \times 1.1067)]^{1/2} \\ &= 213.6 \text{ scf/stb at } 60^\circ\text{F} \end{aligned}$$

Actual GOR = 202.0 scf/stb

$[\text{GOR}]_L$  = Laboratory gas-oil ratio

$[\text{GOR}]_f$  = Field gas-oil ratio

$G_f$  = Field separator gas gravity

$Z_f$  = Field gas deviation "Z" factor

$G_L$  = Laboratory separator gas gravity

$Z_L$  = Laboratory gas deviation "Z" factor

<sup>#</sup> = Laboratory gas-oil ratio needed to be corrected for gas gravity and compressibility factor. Field gas-oil ratio was reported at specific gravity of 0.6, and compressibility factor of 1.0 per Texas Railroad Commission Guideline.

Client: Fina Oil &amp; Chemical Co.

Well: Unit #208  
Field: Emmons  
County: Ector  
State: Texas  
Sample Type: Separator

Table 7

## CALCULATED COMPOSITIONAL ANALYSIS OF RESERVOIR FLUID

Component	Mol. Wt. (gm/gm-mole)	Reservoir Fluid (Mole %) (Wt %)	
N2	28.01	0.43	0.08
CO2	44.01	0.62	0.19
H2S	34.08	2.41	0.56
C1	16.04	10.04	1.11
C2	30.07	5.99	1.24
C3	44.10	7.37	2.23
i-C4	58.12	1.93	0.77
n-C4	58.12	5.04	2.01
i-C5	72.15	2.94	1.46
n-C5	72.15	2.76	1.37
C6	86.18	4.02	2.38
C7	100.20	5.50	3.78
C8	114.23	6.56	5.15
C9	128.26	5.37	4.72
C10	142.29	3.92	3.83
C11	156.31	3.11	3.33
C12	170.34	2.46	2.88
C13	184.37	2.54	3.21
C14	198.40	2.01	2.74
C15	212.42	1.91	2.79
C16	226.45	1.55	2.41
C17	240.48	1.43	2.36
C18	254.50	1.34	2.34
C19	268.53	1.36	2.51
C20+	328.13	<u>17.40</u>	<u>44.57</u>
Total		100.00	100.00

PETROLEUM TESTING SERVICE, INC.

File No.: 13518  
Date: May 1990

Page 9

Well: Unit #208  
Field: Emmons  
County: Ector  
State: Texas

Client: Fina Oil & Chemical Co.

Sample Type: Separator

Table 7 (Continued)

Reservoir Fluid C5+ Properties:

Mole %	66.17
Weight %	91.81
Molecular Weight (gm/gm-mole)	202.14
Density (at 60/60°F)	0.853
API Gravity at 60°F	34.4

Reservoir Fluid C7+ Properties:

Mole %	56.46
Weight %	86.61
Molecular Weight (gm/gm-mole)	223.48
Density (at 60/60°F)	0.874
API Gravity at 60°F	30.4

Reservoir Fluid Molecular Weight (gm/gm-mole) ..... 145.67

PETROLEUM TESTING SERVICE, INC.

File No.: 13518  
Date: May 1990

Page 10

Well: Unit #208  
Field: Emmons  
County: Ector  
State: Texas  
Sample Type: Separator

Client: Fina Oil & Chemical Co.

Table 8

COMPOSITIONAL ANALYSIS OF RECOMBINED FLUID

Component	Mol. Wt. (gm/gm-mole)	Reservoir Fluid	
		(Mole %)	(Wt %)
N2	28.01	1.09	0.21
CO2	44.01	0.80	0.24
H2S	34.08	2.17	0.51
C1	16.04	8.56	0.94
C2	30.07	7.29	1.50
C3	44.10	8.79	2.66
i-C4	58.12	1.92	0.76
n-C4	58.12	5.35	2.13
i-C5	72.15	3.01	1.49
n-C5	72.15	2.83	1.40
C6	86.18	4.08	2.41
C7	100.20	5.44	3.73
C8	114.23	6.31	4.94
C9	128.26	4.93	4.34
C10	142.29	3.60	3.51
C11	156.31	2.88	3.09
C12	170.34	2.35	2.75
C13	184.37	2.35	3.97
C14	198.40	1.99	2.71
C15	212.42	1.50	2.18
C16	226.45	1.45	2.25
C17	240.48	1.34	2.21
C18	254.50	1.23	2.14
C19	268.53	1.16	2.14
C20+	332.90	<u>17.58</u>	<u>46.79</u>
Total		100.00	100.00

PETROLEUM TESTING SERVICE, INC.

File No.: 13518  
Date: May 1990

Page 11

Well: Unit #208  
Field: Emmons  
County: Ector  
State: Texas  
Sample Type: Separator

Client: Fina Oil & Chemical Co.

Table 8 (Continued)

Reservoir Fluid C5+ Properties:

Mole % .....	64.03
Weight % .....	91.05
Molecular Weight (gm/gm-mole) .....	213.17
Density (at 60/60°F) .....	0.853
API Gravity at 60°F .....	34.5

Reservoir Fluid C7+ Properties:

Mole % .....	54.10
Weight % .....	85.75
Molecular Weight (gm/gm-mole) .....	231.19
Density (at 60/60°F) .....	0.8784
API Gravity at 60°F .....	29.7

Reservoir Fluid Molecular Weight (gm/gm-mole) ..... 149.91



PETROLEUM TESTING SERVICE, INC.

File No.: 13518  
Date: May 1990  
Well: Unit #208  
Field: Emmons  
County: Ector  
State: Texas  
Sample Type: Separator

Page 12

Client: Fina Oil & Chemical Co.

Table 9

DENSITY BY METTLER/PAAR DENSITOMETER  
(RECOMBINED FLUID)

Laboratory Conditions

Pressure (psia)	Temperature (°F)	Density (gm/cc)
5000	72.1	0.8335
4000	72.1	0.8294

Reservoir Conditions

Pressure (psia)	Temperature (°F)	Density (gm/cc)
5000	98.0	0.8257
1000	98.0	0.8054
900	98.0	0.8049
800	98.0	0.8043
700	98.0	0.8037

Extrapolated Density at 625 psia\*: 0.8034

\* Bubble point pressure

Well: Unit #208  
Field: Emmons  
County: Ector  
State: Texas  
Client: Fina Oil & Chemical Co. Sample Type: Separator

Table 10

CONSTANT COMPOSITION PRESSURE-VOLUME MEASUREMENTS

- Reservoir Temperature = 98°F
- Bubble Point Pressure = 625 psia
- Coefficient of Thermal Expansion of Reservoir Fluid:  
from 69°F to 98°F @ 5025 psia =  $.5226 \times 10^{-3} / ^\circ\text{F}$

Coefficient of Compressibility

Temperature °F	Pressure Range psia	Coefficient <sup>#</sup> /psi
98	3000 to 1000	$6.658 \times 10^{-6}$
	1000 to 625	$8.040 \times 10^{-6}$

$$^*\text{Coefficient} = \frac{1}{V} \times \frac{V_2 - V_1}{T_2 - T_1}$$

$$^*\text{Coefficient} = \frac{1}{V_{\text{avg}}} \times \frac{V_2 - V_1}{P_1 - P_2}$$

PETROLEUM TESTING SERVICE, INC.

File No.: 13518  
Date: May 1990

Page 14

Client: Fina Oil & Chemical Co.

Well: Unit #208  
Field: Emmons  
County: Ector  
State: Texas  
Sample Type: Separator

Table 11

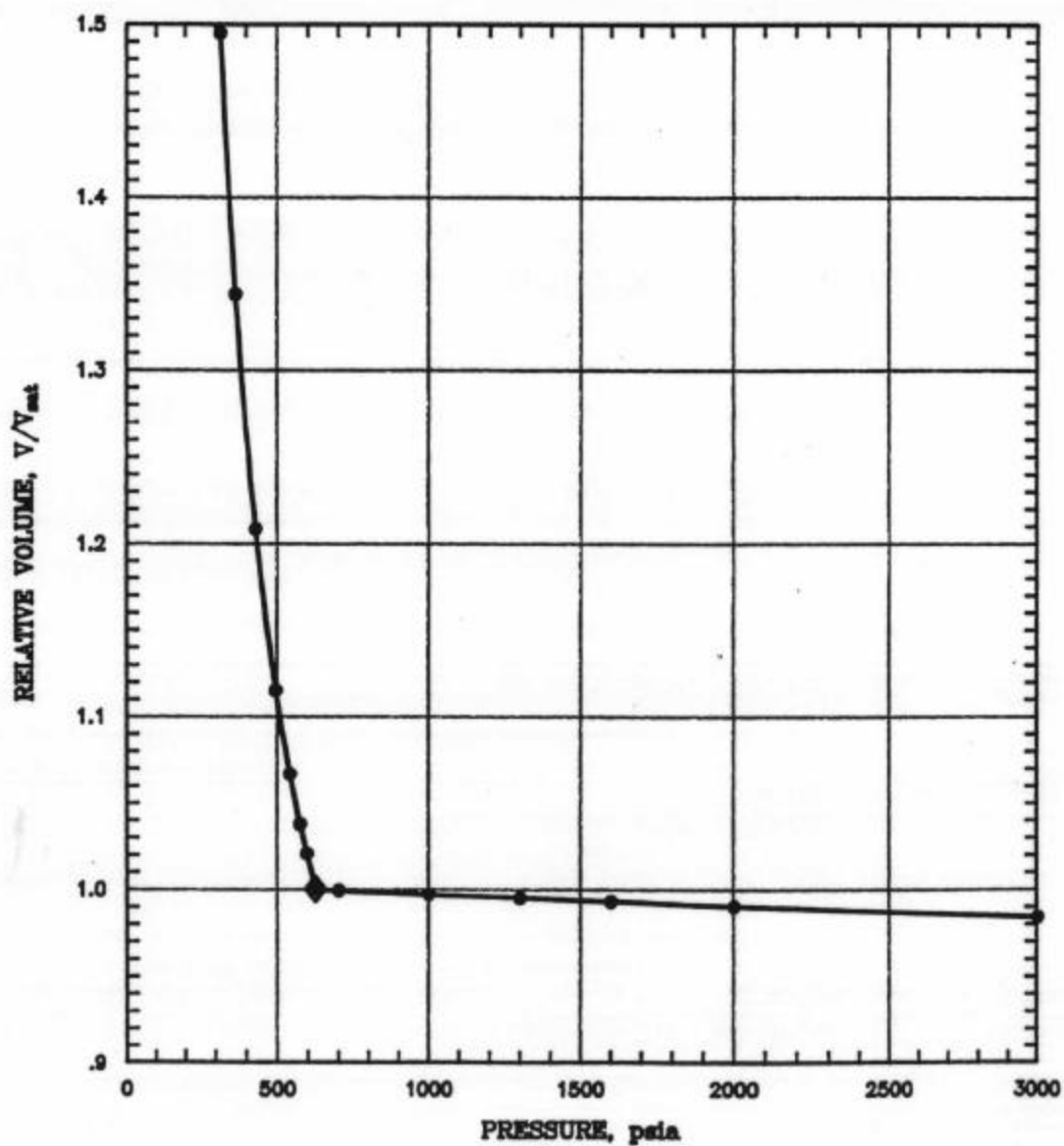
PRESSURE-VOLUME RELATIONSHIP AT 98°F  
(RECOMBINED FLUID)  
(Constant Composition - Equilibrium Expansion)

Pressure (psia)	Relative Volume (V/V <sub>sat</sub> )	Y-Function
5000	.9727	
4000	.9781	
3000	.9838	
2000	.9901	
1600	.9929	
1300	.9950	
1000	.9970	
700	.9992	
625	1.0000	
595	1.0206	2.4451
573	1.0377	2.4092
540	1.0668	2.3558
495	1.1150	2.2827
430	1.2083	2.1768
355	1.3439	2.2115
415	1.4946	1.0230
265	1.7115	1.9094
215	2.0430	1.8283

\* Bubble point (saturation) pressure

Figure 2  
Pressure-Volume Relationship at 98°F

◇ Bubble Point Pressure = 625 psia



File No.: 13518  
Date: May 1990  
Well: Unit #208  
Field: Emmons  
County:  
State:  
Sample Type: Separator

Ector  
Texas

Client: Fina Oil & Chemical Co.

Table 12

DIFFERENTIAL GAS LIBERATION AT 98°F

Pressure (psia)	Oil		Solution Gas-Oil Ratio <sup>1</sup> (R <sub>s</sub> )	Oil Density (gm/cc)	Z Factor	Gas	
	Formation Volume Factor (B <sub>o</sub> ) <sup>2</sup>	Formation Volume Factor (B <sub>g</sub> ) <sup>3</sup>				Specific Gravity <sup>4</sup>	Viscosity (cp) <sup>5</sup>
4000	1.122			0.8115			
3000	1.128			0.8068			
2000	1.136			0.8016			
1600	1.139			0.7994			
1300	1.141			0.7977			
1000	1.144			0.7961			
700	1.146			0.7943			
625	1.147		240	0.7937			
500	1.139		214	0.7956	0.9475	5.321	0.7349
400	1.130		189	0.7984	0.9526	6.691	0.7479
300	1.121		165	0.8012	0.9604	8.988	0.7657
200	1.111		138	0.8036	0.9730	13.667	0.8262
100	1.088		103	0.8138	0.9801	27.528	0.9722
15	1.019		0	0.8336	0.9898	185.340	1.6282

Residual Oil Gravity, °API at 60°F ..... 34.4

<sup>1</sup>Bubble point pressure.

<sup>2</sup>Barrels of reservoir oil at indicated pressure and temperature per barrel of oil at 14.696 psia and 60°F.

<sup>3</sup>Cubic feet of gas at 14.696 psia and 60°F per barrel of oil at 14.696 psia and 60°F.

<sup>4</sup>Barrels of reservoir gas at indicated pressure and temperature per 1000 cubic feet of gas at 14.696 psia and 60°F.

<sup>5</sup>Calculated from gas composition.

Well: Unit #208  
Field: Emmons  
County: Ector  
State: Texas

Client: Fina Oil &amp; Chemical Co.

Sample Type: Separator

Table 13

## DIFFERENTIAL GAS LIBERATION AT 98°F

Pressures: (psia)	Liberated Gas Composition (Mole %)						Residual Liquid (mole%) (wt%)	
	500	400	300	200	100	15	15	
Component								
Mol. Wt. (gm/gm-mole)								
N2	28.01	7.83	5.76	3.42	1.80	0.92	0.18	0.00 0.00
CO2	44.01	2.10	2.24	2.56	3.00	3.78	0.92	0.00 0.00
H2S	34.08	1.99	2.23	2.80	3.84	7.18	9.50	0.00 0.00
C1	16.04	72.74	71.80	70.67	63.74	51.81	0.95	0.00 0.00
C2	30.07	9.38	11.17	12.62	16.46	14.92	20.99	0.00 0.00
C3	44.10	4.21	4.77	5.49	7.72	13.83	31.73	1.97 .41
i-C4	58.12	0.39	0.46	0.57	0.81	1.81	8.17	1.03 .28
n-C4	58.12	0.76	0.92	1.12	1.59	3.52	16.03	3.71 1.02
i-C5	72.15	0.23	0.24	0.28	0.40	0.84	5.02	3.44 1.17
n-C5	72.15	0.17	0.18	0.20	0.29	0.60	3.52	3.47 1.18
C6	86.18	0.11	0.13	0.14	0.21	0.41	1.90	6.65 2.71
C7	100.20	0.07	0.07	0.08	0.11	0.23	0.75	10.31 4.88
C8	114.23	0.02	0.02	0.05	0.03	0.14	0.33	10.31 5.57
C9	128.26	0.00	0.01	0.00	0.00	0.01	0.01	7.77 4.71
C10	142.29							5.65 3.80
C11	156.31							4.47 3.30
C12	170.34							3.58 2.88
C13	184.37							3.50 3.05
C14	198.40							2.71 2.53
C15	212.42							2.50 2.51
C16	226.45							2.06 2.21
C17	240.48							1.85 2.10
C18	254.50							1.66 2.00
C19	268.53							1.66 2.11
C20+	503.60							21.68 51.58
Total		100.00	100.00	100.00	100.00	100.00	100.00	100.00

## Gas Properties:

Gas Gravity 0.7349 0.7479 0.7657 0.8262 0.9722 1.6282  
(Air=1.0000)

Gross Heating Value BTU/scf 1083 1131 1182 1278 1454 2523

Client: Fina Oil &amp; Chemical Co.

Well: Unit #208  
Field: Emmons  
County: Ector  
State: Texas  
Sample: Separator

Table 14

COMBINATION  $B_o$  AND  $R_s$ 

Pressure ( Psia )	Oil Formation Volume Factor ( $B_{of}$ )	Solution Gas-Oil Ratio ( $R_{sf}$ )
4000	1.106	
3000	1.112	
2000	1.120	
1600	1.123	
1300	1.125	
1000	1.128	
700	1.130	
625*	1.131	202.000
500	1.123	176.000
400	1.114	152.000
300	1.105	128.000
200	1.096	101.000
100	1.073	67.000
15	1.005	0.000

$$B_{of} = B_{od} \times ( B_{obf} / B_{obd} )$$

$$R_{sf} = R_{sif} - ( R_{sid} - R_{sd} ) \times ( B_{obf} / B_{obd} )$$

\* Bubble point pressure

 $B_o$  Formation volume factor (res. Bbl/Stb) $R_s$  Solution gas-oil ratio (Scf/Stb)Subscripts

f - Flash gas liberation test

d - Differential gas liberation test

i - initial

b - Bubble point

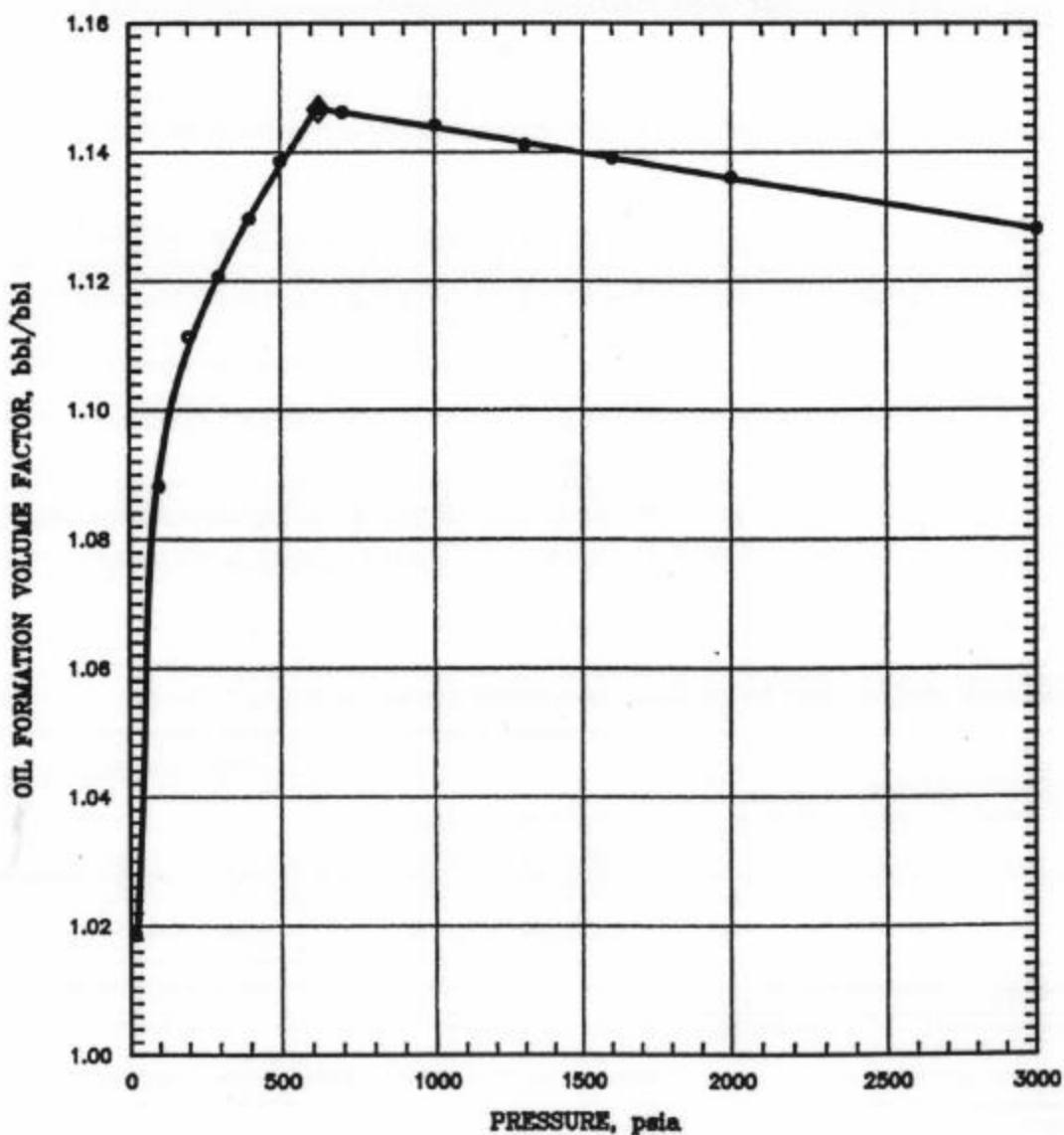
Well: Unit #208  
Field: Emmons  
County: Ector  
State: Texas  
Sample Type: Separator

Client: Fina Oil & Chemical Co.

Figure 3  
Oil Formation Volume Factor vs. Pressure

◇ Bubble Point Pressure = 625 psia

Differential Gas Liberation at 98°F





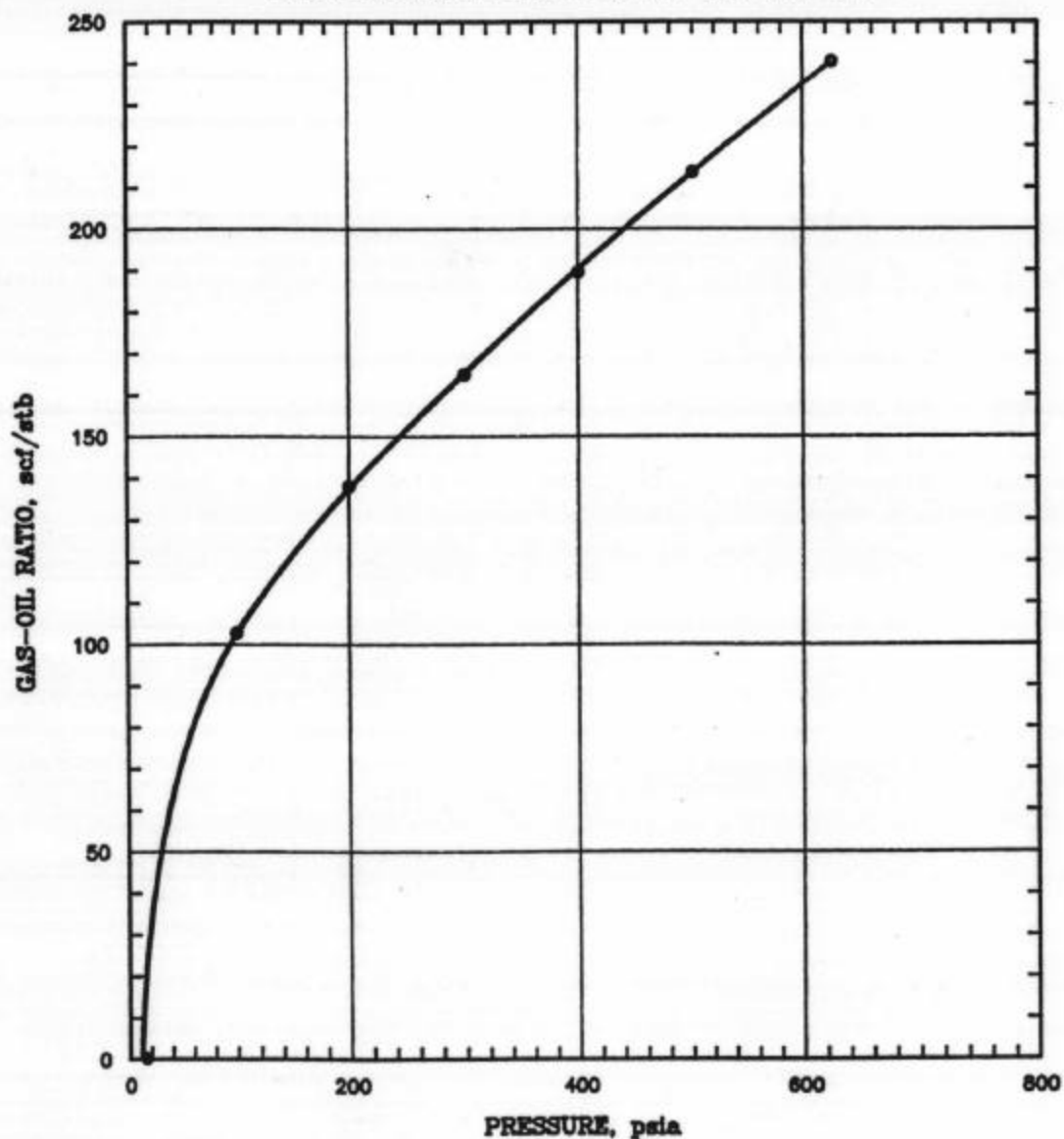
Well: Unit #208  
Field: Emmons  
County: Ector  
State: Texas  
Sample Type: Separator

Client: Fina Oil & Chemical Co.

Figure 4  
Solution Gas-Oil Ratio vs. Pressure

Differential Gas Liberation at 98°F

Basis: Residual Oil Volume at 14.7 psia and 60°F



Well: Unit #208  
Field: Emmons  
County: Ector  
State: Texas  
Sample Type: Separator

Client: Fina Oil & Chemical Co.

Figure 5  
Oil Density vs. Pressure

◇ Bubble Point Pressure = 625 psia

Differential Gas Liberation at 98°F

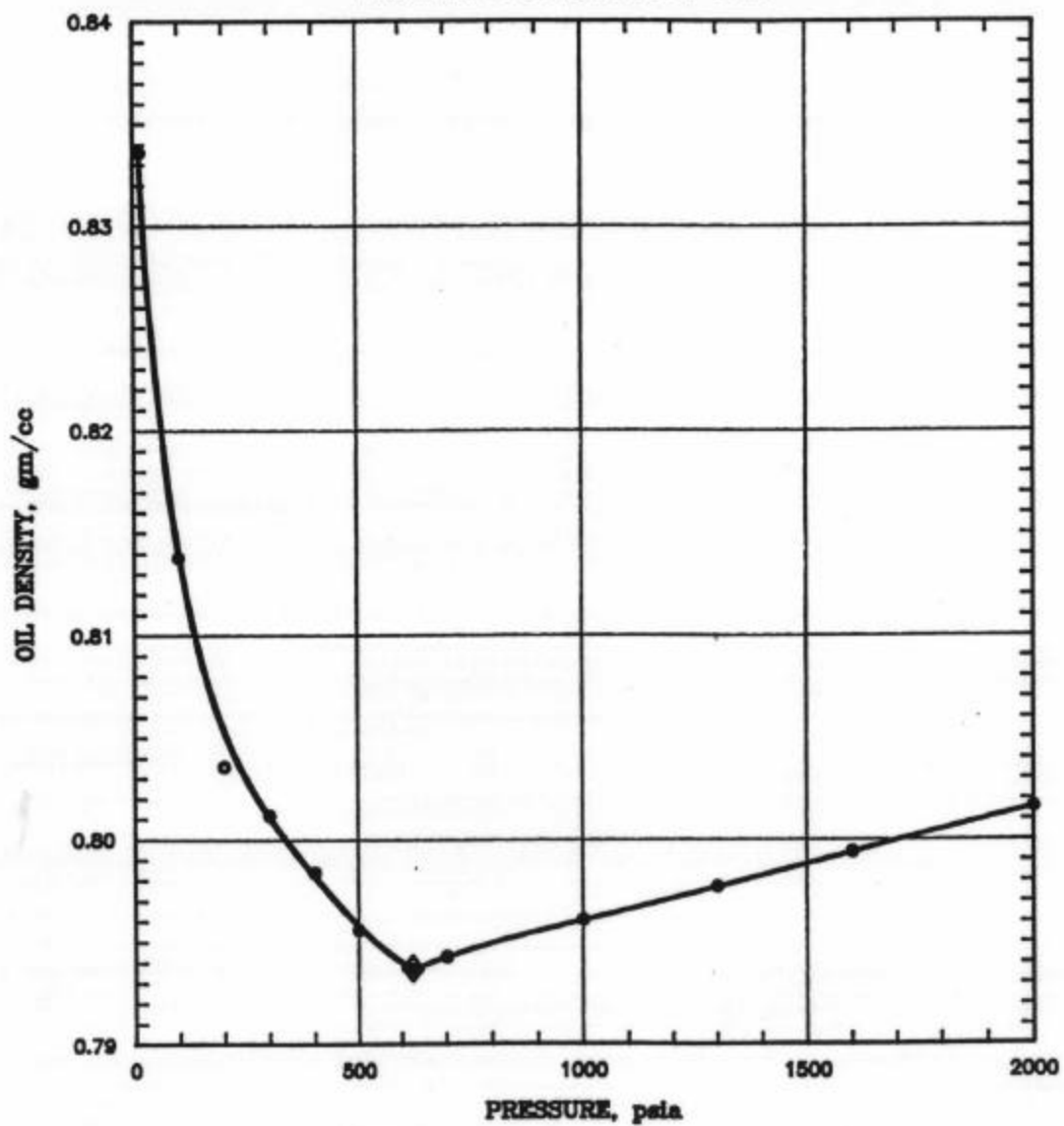


Figure 8  
Z Factor vs. Pressure

Differential Gas Liberation at 98°F

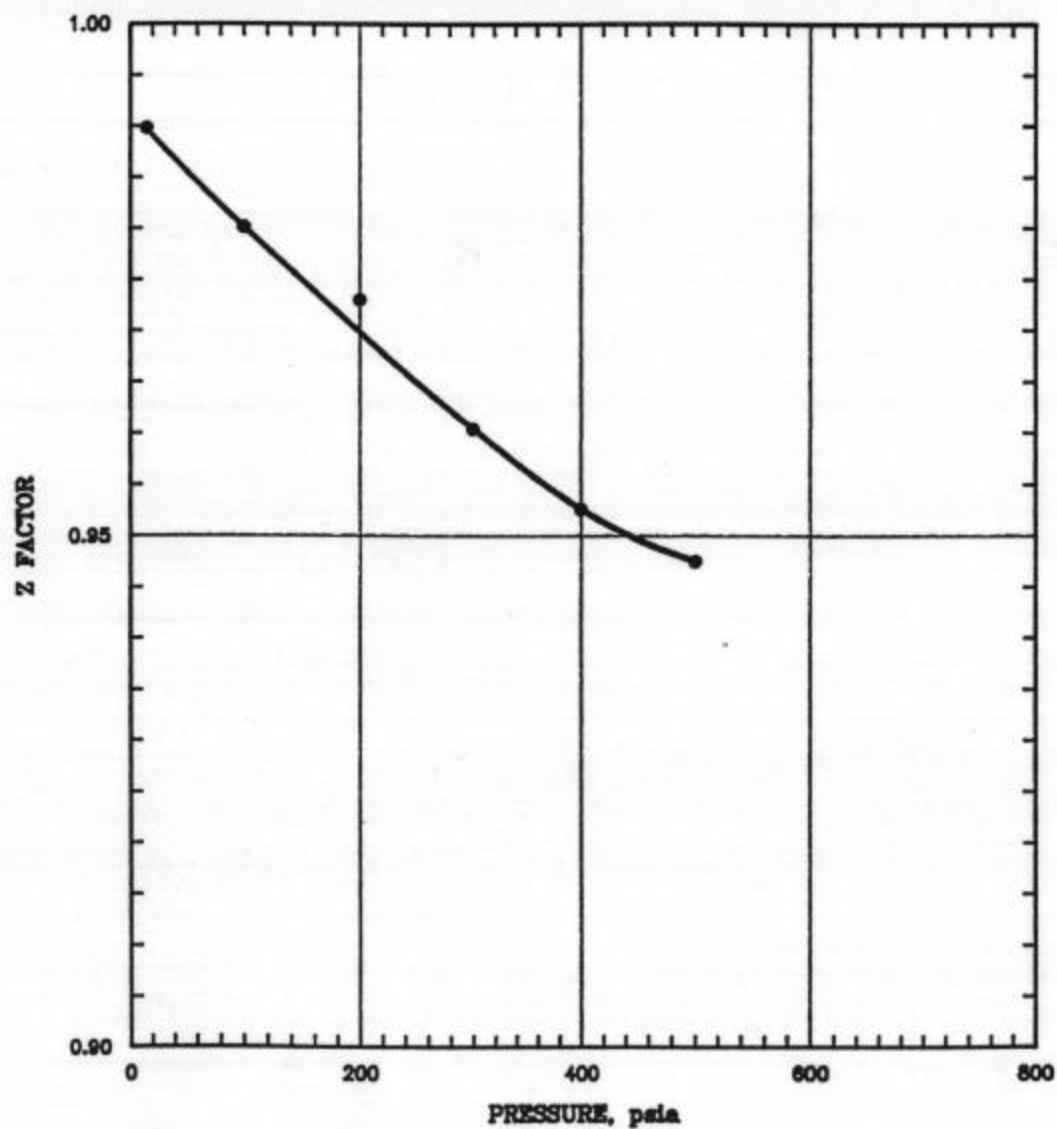


Figure 7  
Gas Specific Gravity vs. Pressure

Differential Gas Liberation at 98°F

Basis: Gas Gravity of Air = 1.0000

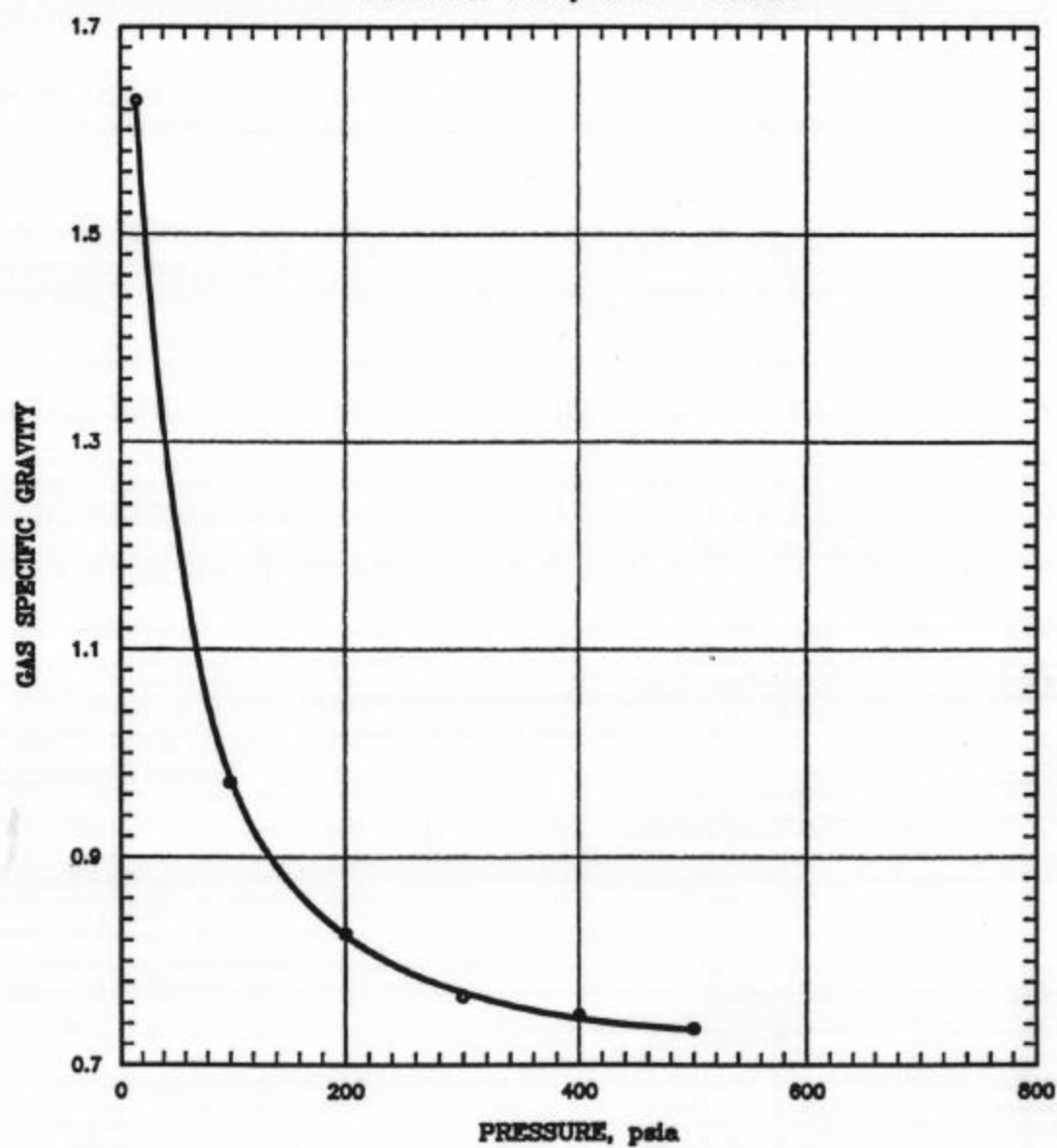
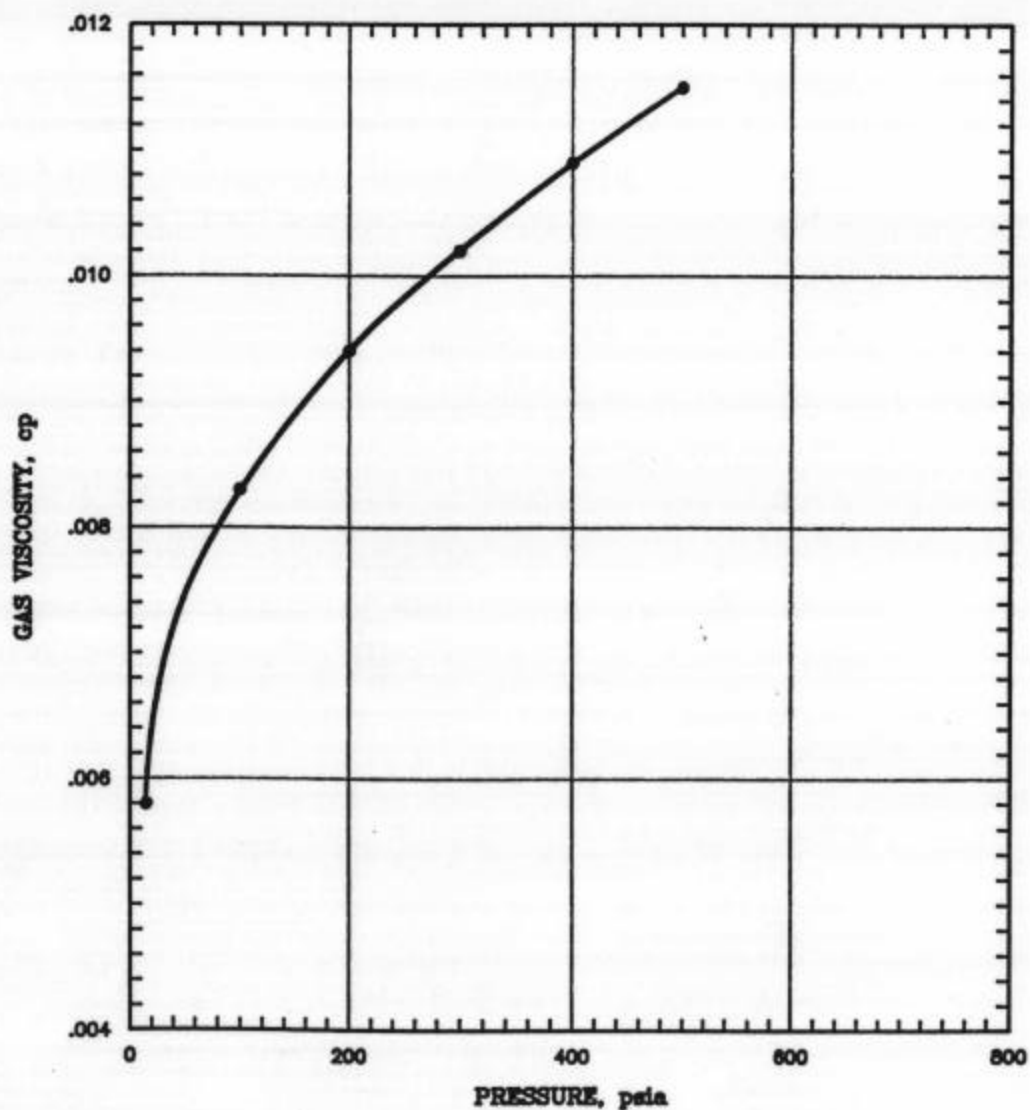


Figure 8  
Gas Viscosity vs. Pressure

Differential Gas Liberation at 98°F



PETROLEUM TESTING SERVICE, INC.

File No.: 13518  
Date: May 1990

Page 25

Client: Fina Oil & Chemical Co.

Well: Unit #208  
Field: Emmons  
County: Ector  
State: Texas  
Sample Type: Separator

Table 15

PRESSURE-OIL VISCOSITY AT 98°F

Pressure (psia)	Oil Viscosity (centipoise)	Oil Viscosity (Centipoise)
	45°Angle	70°Angle
5000	2.69	2.81
4000	2.62	2.72
3000	2.46	2.55
2000	2.19	2.27
1000	1.99	2.06
800	1.98	2.03
625	1.96	2.02
500	1.99	2.05
400	2.10	2.17
300	2.23	2.31
200	2.38	2.48
100	2.63	2.75
15	4.79	5.16

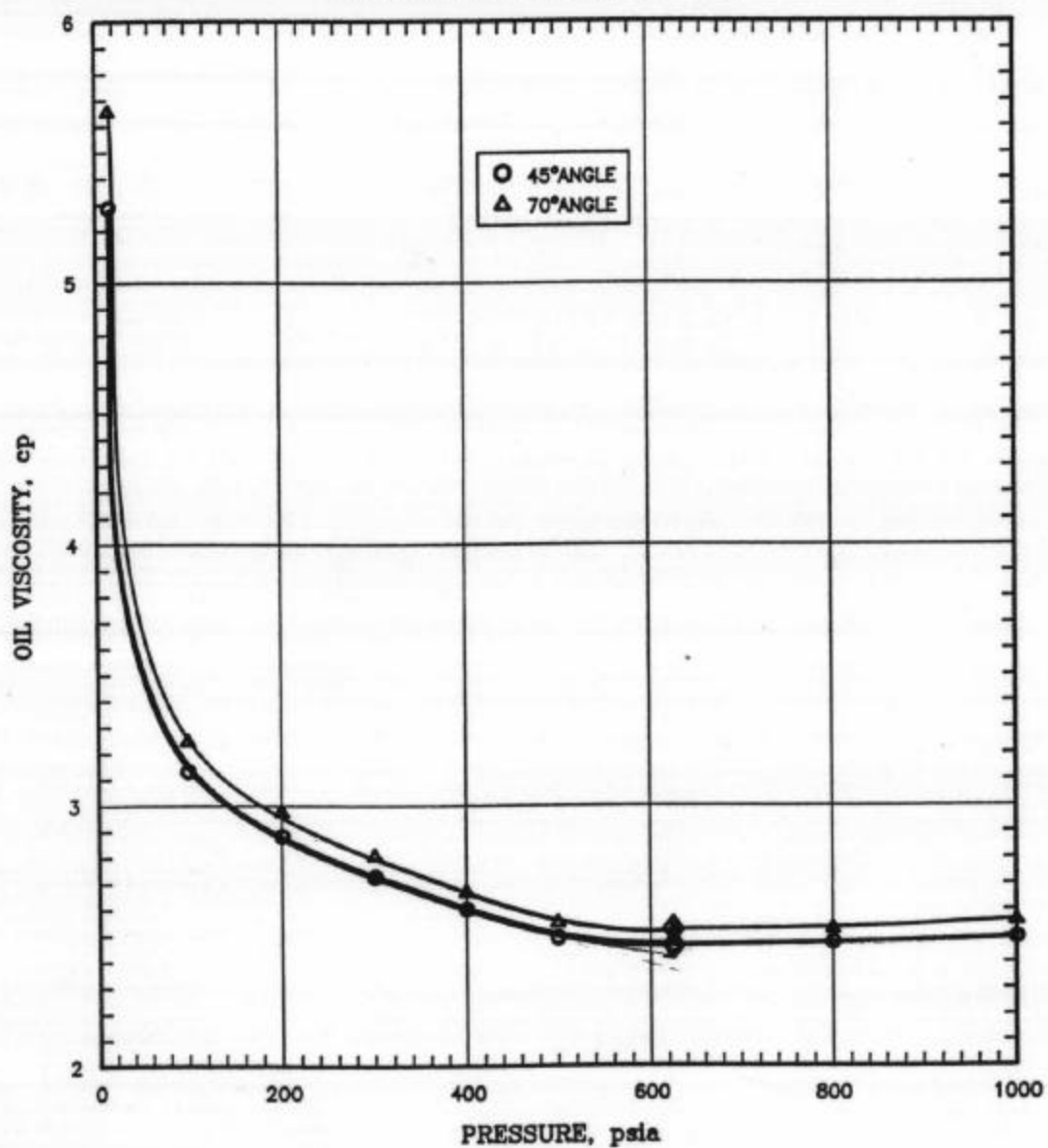
\*Bubble point (saturation) pressure

Figure 9

### Oil Viscosity vs. Pressure

◇Bubble Point Pressure = 625 psia

Differential Gas Liberation at 98°F



Date:

May 1990

Well:

Unit #208

Field:

Emmons

County:

Ector

State:

Texas

Client: Fina Oil &amp; Chemical Co.

Sample Type: Separator

Table 16

## SEPARATOR FLASH LIBERATION TESTS OF RECOMBINED FLUID

Separator Stage:	1	2
Pressure, psig:	51	0
Temperature, °F:	107	80
Gas-Oil ratio, scf/stb <sup>*</sup> :	202	28
Gas Specific Gravity <sup>*</sup> :	1.0495	1.4494
Shrinkage Factor, bbl/bbl <sup>*</sup> :	.952	.993

Stock Tank Oil Gravity, °API ..... 34.0

Total Gas-Oil Ratio, scf/stb<sup>\*</sup> ..... 230Bubble Point Formation Volume Factor, bbl/bbl<sup>2</sup> ..... 1.131

<sup>\*</sup>Cubic feet of gas at 14.696 psia and 60 °F per barrel of oil at 14.696 psia and 60 °F.

<sup>\*</sup>Gas gravity of air = 1.0000.

<sup>\*</sup>Barrels of oil at 14.696 psia and 60 °F per barrel of oil at indicated temperature and pressure.

<sup>2</sup>Barrels of bubble point oil at 5000 psia and 150°F per barrel of oil at 14.696 psia and 60 °F.



Date:

May 1990

Well:

Unit #208

Field:

Emmons

County:

Ector

State:

Texas

Client: Fina Oil &amp; Chemical Co.

Sample Type:

Separator

Table 17

## SEPARATOR FLASH LIBERATION TESTS OF RECOMBINED FLUID

## Liberated Gas Composition

Separator Stage:	1	2			
Pressure, psig:	51	0			
Temperature, °F:	107	80			
Component	Mol. wt (gm/gm-mole)	Flashed Gas (Mole %)		Residual Liquid (Mole%) (wt%)	
N2	28.01	2.13	.64	0.00	0.00
CO2	44.01	2.35	1.85	0.00	0.00
H2S	34.08	5.88	9.70	0.00	0.00
C1	16.04	44.64	9.18	0.00	0.00
C2	30.07	18.78	24.65	0.00	0.00
C3	44.10	14.74	28.79	1.24	.26
i-C4	58.12	2.50	5.70	0.88	.24
n-C4	58.12	5.20	11.65	3.50	.95
i-C5	72.15	1.48	3.38	3.49	1.18
n-C5	72.15	1.07	2.33	3.59	1.21
C6	86.18	.73	1.41	7.10	2.86
C7	100.20	.40	.61	10.84	5.08
C8	114.23	.09	.11	10.09	5.39
C9	128.26	.01	0.00	7.70	4.62
C10	142.29			5.45	3.63
C11	156.31			4.21	3.08
C12	170.34			3.40	2.71
C13	184.37			3.25	2.80
C14	198.40			2.62	2.44
C15	212.42			2.41	2.40
C16	226.45			1.96	2.07
C17	240.48			1.76	1.98
C18	254.50			1.56	1.86
C19	268.53			1.56	1.96
C20+	486.00			23.39	53.28
Total		100.00	100.00	100.00	100.00
Gas Specific Gravity: (Air = 1.0000)		1.0495	1.4514		
Gross Heating Value,		1608	2217		

**EOR STUDY FOR EMMONS #208 RESERVOIR  
FLUID WITH A CO<sub>2</sub>-RICH SOLVENT**

An experimental study carried out by

**DB Robinson Research Ltd.  
Edmonton, Alberta, Canada**

for

**Fina Oil and Chemical Co.  
West Texas Division  
Midland, Texas, USA**

**Project Coordinator: Mr. P.K. Pande**

**DBR File: 200196  
February 13, 1991**

## EOR STUDY FOR EMMONS #208 RESERVOIR FLUID WITH A CO<sub>2</sub>-RICH SOLVENT

### INTRODUCTION

Fina Oil and Chemical Company is interested in carrying out an experimental EOR program for studying the swelling behavior and slim tube displacement of the Emmons #208 reservoir fluid with a CO<sub>2</sub>-rich solvent. It is intended to use the experimental swelling data for appropriately tuning a phase behavior and fluid properties package. The tuned package could then be used for predicting the phase behavior of the reservoir fluid with other similar solvents, or as an aid in selecting suitable solvents for implementing an EOR scheme.

The following scope of work was specified by Fina Oil and Chemical Company for the study.

#### 1. Reservoir Fluid Recombination

Recombining separator oil and gas to a bubble point of 625 psia at 98°F.

#### 2. Swelling Tests

- Conducting a four-point swelling test for the recombined reservoir fluid using a CO<sub>2</sub>-rich mixture as solvent.
- Obtaining all relevant saturation pressure and volumetric data for nominal solvent concentrations of 15, 30, 45 and 70 mole %.
- Obtaining the relative liquid volumes at four pressures between the saturated pressure and the reservoir fluid saturation pressure of 625 psia for each solvent concentration.
- Obtaining two-phase property data for the system containing 45 mole % solvent.
- Measuring all single-phase liquid viscosities at each of five saturation pressures and the equilibrium liquid phase viscosities at the two-phase flash condition.

#### 3. Slim Tube Displacement Tests

- Conducting two slim tube displacement runs at the reservoir temperature of 98°F and two operating pressures of 1600 and 1400 psia with the CO<sub>2</sub>-rich solvent.

4. - Characterization of the Emmons #208 reservoir oil for the EQUI-PHASE phase behavior package using the swelling test data.

The report is organized into three independent parts for the sake of simplicity. Part I contains the fluid preparations, oil recombination and the relevant analyses. Part II includes the swelling test data and the EQUI-PHASE characterization. Part III contains the slim tube displacement runs.

**Part I**  
**Fluids Preparation/Analyses**

## FLUIDS PREPARATION/ANALYSES

### 1.0 RECOMBINATION OF RESERVOIR FLUID

#### 1.1 Separator Samples

Samples of separator oil and gas were supplied by Fina Oil and Gas Company. The separator oil was transferred while in the single phase from the supplied cylinder into a pistoned high pressure cylinder. The floating piston was used to isolate the sour oil from the mercury. The pistoned cylinder and its contents were mounted on a rocking mechanism and mixed in the single phase for several hours before a sample was displaced for compositional analysis.

The analysis was carried out using a flash procedure which involved expanding the sample to atmospheric conditions thereby releasing the gas which was measured and analyzed. The amount of dead oil was weighed and analyzed using an internal standard GC method with a capillary column. The analysis and amounts of oil and gas were then combined to calculate the composition of the original separator oil.

Samples of separator oil from each of the two cylinders were analyzed in this way. The resulting analyses are given in Table 1.1.

Separator gas samples from four different sample cylinders were heated and then analyzed by a GC equipped with a natural gas analyzer. The results of the separator gas analyses are also given in Table 1.1.

In comparing the compositions of separator gas supplied with those analyzed during the field test, it was realized that the H<sub>2</sub>S content of the separator gas in the supplied cylinder had been depleted. This might be due to reaction or adsorption by the steel surface of the cylinder. Hence the supplied separator gas could not be used for reservoir fluid recombination. After consulting with Fina, it was decided to synthetically prepare the separator gas having the same composition as that obtained during the field test. The composition of field test separator gas is given in Table 1.2.

#### 1.2 Separator Gas Preparation

The sour separator gas mixture having the specified composition was prepared synthetically by gravimetric methods. First, the hydrogen sulfide-free mixture was prepared in a stainless steel pressure vessel where the amount of each component successively added was determined by weighing. An appropriate amount of mercury was injected into the vessel. Then the vessel and its contents were mounted on a rocking mechanism and the contents were agitated in the single phase by rocking the cylinder for a period of at least 10 hours.

Following this, the densities of pure hydrogen sulfide and the above prepared hydrogen sulfide-free mixture were determined at a known pressure and temperature using a high pressure pycnometer. A known volume of the hydrogen sulfide-free mixture was then transferred into a one-litre high pressure pistoned storage cylinder using a high pressure displacement pump. Following this, the required amount of hydrogen sulfide was added to the storage cylinder where it was mixed with other components.

The contents in the storage cylinder were mixed by rocking the cylinder and putting it through several heating cycles. Samples of the mixed gas were taken and analyzed as a check on the preparation procedures and on the homogeneity of the resulting mixture. The composition of the prepared separator gas is given in Table 1.2.

### 1.3 Reservoir Fluid Recombination

A sample of prepared separator gas was introduced into a previously evacuated, visual recombination cell. The amount of gas introduced was calculated using the measured recombination cell volume, pressure, temperature and the predicted value of gas compressibility using EQUI-PHASE. Based on the GOR calculated from the EOR program, the appropriate amount of separator oil was added by introducing mercury into the bottom of the high pressure storage cylinder and simultaneously withdrawing oil from the top.

Following this, the temperature of the recombination cell enclosure was brought up to temperature, the pressure was adjusted to a value well above the specified bubble point by introducing mercury into the cell, and the equilibration process was commenced. After reaching equilibrium, the total system volume was measured by reading the scale of the positive displacement pump. The condition of the cell contents was recorded. The procedure was repeated to obtain the required number of points in the single phase region. The pressure was further dropped until a gas phase was just visible in the cell. The contents were equilibrated and the system volume was recorded. This was repeated as required to generate a sufficient number of two-phase points.

The PV curve so obtained, was used to determine the bubble point pressure of the overall fluid mixture in the cell. If this pressure was higher than the desired bubble point pressure, additional oil was added to the cell and the PV determination process was repeated. By this sequence the bubble point pressure of the contents of the cell was adjusted to the desired value.

The specified bubble point pressure was 625 psia. The measured bubble point pressure was 630 psia at 98°F. This value was well within the expected reliability of the experiments for which the oil was required. A sample of the recombined oil was taken from the recombination cell for density measurement and analysis by flash procedure. The analysis is given in Table 1.3. The remaining recombined oil was then transferred into a high pressure pistoned cylinder as stock for the subsequent experimental program.

## 2.0 CO<sub>2</sub>-RICH SOLVENT PREPARATION

The specified CO<sub>2</sub>-rich solvent was prepared in a 316 SS container of 1 litre nominal volume. The procedure was identical to that used for preparing the H<sub>2</sub>S-free gas mixture as described in the previous section. The composition of the prepared solvent is given in Table 1.4.



-7-

## Part II

### Swelling Test and Characterization

## SWELLING TEST AND CHARACTERIZATION

### 1.0 APPARATUS

The experimental swelling test measurements were carried out in a variable volume visual phase behavior cell. The main body of the cell consists of a pyrex glass cylinder 8.0 in (20.3 cm) long with an internal diameter of 1.25 in (3.2 cm) and a 0.5 in (1.26 cm) wall. The effective working volume is about 110 cm<sup>3</sup>. This cylinder is housed inside a sturdy outer steel shell. Vertical opposing tempered flat glass plates mounted in this outer shell permit visual observation over the entire working range of the cell. The volume and hence the pressure of the fluids under investigation are controlled by a positive displacement pump connected through mercury to the cell contents. A second transparent fluid connected through the same hydraulic system and confined between the steel shell and the cylinder is used to balance pressures across the pyrex cylinder. A floating piston is used to separate the sour reservoir fluid and the mercury.

The entire cell assembly is mounted on a rocking mechanism inside a temperature controlled air oven. Temperatures are measured with a resistance temperature device (RTD). The RTD for the cell contents is inserted into the bottom of the cell and protrudes into the mercury. The signals are read out on a digital temperature indicator and are reliable to within  $\pm 0.2^{\circ}\text{F}$ . Pressures are measured using a calibrated Heise pressure gauge.

A specially designed header mounted on top of the cell provides for charging and sampling. The volume of each phase in the cell is determined using a cathetometer readable to the nearest 0.01 mm. A volume vs. height calibration for the cell was obtained by observing the change in elevation of the piston in the cell corresponding to a known change in volume. This calibration is used to transform the height measurements of the vapor-liquid interface to equivalent volumes.

The sampling line from the equilibrium cell was connected to a high pressure capillary viscometer. The viscometer consisted of two high pressure stainless steel reservoirs connected to a 6.1 m long,  $2.54 \times 10^{-4}$  m ID capillary coil. A differential pressure transducer was used to monitor the pressure drop across the capillary coil. A fluid sample was pumped from one reservoir to the next through the capillary coil by an opposed pump. The opposed pump delivered fluid at a preset rate from one side and retrieved fluid from the suction side at the same rate and at constant pressure. This set-up enabled non-destructive viscosity measurements to be made at constant back pressure. Schematic and photographic presentations of the apparatus are shown in Figures 2.1 and 2.2 respectively.

## 2.0 METHOD

### 2.1 Swelling Test

The equilibrium cell and all associated lines were thoroughly cleaned and subsequently evacuated. The piston was moved to the top of the cell by mercury displacement. A sample of recombined oil of known volume was displaced at a known constant pressure and room temperature into a pre-weighed and evacuated, 316 SS sample container. The weight of the oil displaced was determined and thus the oil density was calculated. The same procedure was repeated for determining the density of the swelling test solvent. A known volume of the recombined oil was then displaced into the equilibrium cell through the top valve by the use of a JEFRI positive displacement pump. Mercury was withdrawn from the bottom valve at the same time. The pressure and temperature conditions of transfer were kept the same as the conditions at which the density was measured. Thus the mass and also the number of moles of oil introduced into the cell were calculated. In a similar fashion, a known number of moles of the solvent were introduced into the cell. The overall molar concentration of oil to solvent in the cell was thus known.

The cell was then brought up to temperature and the contents were agitated while maintaining the fluid condition in the single phase. The total system volume was then measured by reading the level of piston in the cell with the cathetometer. The condition of the fluid in the cell was recorded. The pressure was then lowered by withdrawing some mercury. The procedure was repeated to obtain the required number of points in the single phase region. The pressure was further lowered until a gas phase just became visible in the cell. The contents were equilibrated and the system volume was recorded. This was repeated as required to generate a sufficient number of two-phase points. The PV curve so obtained was used to determine the bubble point pressure of the overall fluid mixture in the cell.

The solvent concentration of the mixture in the equilibrium cell was then increased by addition of a known amount of solvent until the next desired concentration was obtained. The saturation pressure of the new mixture was then obtained in the same manner as indicated above. In all, saturation pressures were determined for four solvent concentrations, namely, 15, 30, 41 and 68 mole %. After determination of each saturation pressure, the total hydrocarbon volume of the system was measured. From a knowledge of the masses of oil and solvent added, the total mass and hence the bulk density of the system at the saturation pressure, was calculated.

### 2.2 Relative Volume Determination

After establishing the saturation pressure for each solvent addition, two-phase volumetric data were obtained at four selected pressure points. The system was equilibrated at pressures between 625 psia and the saturation pressure. The total system and liquid phase volume were measured and from this the percent liquid volume at each pressure was calculated.

### 2.3 Viscosity Measurements

After a portion of the single phase fluid resulting from each solvent addition had been transferred at constant pressure into the reservoir of the capillary viscometer, pressure drop measurements were made for a range of flow meters. Using the capillary tube constant, the measured pressure drop and the flowrate data, the viscosity of the sample could then be calculated.

The same procedure was used to determine the viscosity for the equilibrium liquid phase during a VLE study. For each liquid phase viscosity measurement, a back pressure of about 50 psi above the equilibrium pressure or the saturation pressure was maintained in the viscometer in order to keep the fluid in its single phase condition.

### 2.4 Vapor-Liquid-Equilibrium Study

Appropriate amounts of recombined fluid and prepared solvent were charged to the cell to prepare a mixture containing 41% mole solvent. The system was brought to reservoir temperature and was equilibrated at a selected pressure for carrying out two-phase vapor-liquid equilibrium property measurements. After equilibration, relative phase volumes were measured and samples of the vapor and liquid were taken for density determinations and composition analyses. The viscosity of the equilibrium liquid was also determined as described above.

## 3.0 RESULTS

The saturation pressure data measured at each of the first three solvent concentrations is given in Table 2.1. The total hydrocarbon volume, viscosity and the bulk fluid density at the saturation pressure are also given. Figure 2.3 shows the saturation pressures as a function of solvent concentration. The viscosities of the solvent-oil mixtures at the saturation pressure are shown in Figure 2.4. The equilibrium phase compositions of the third solvent addition, 41% solvent concentration, flashed at 634 psia are given in Table 2.2. The analysis of this single phase mixture before it was flashed to 634 psia is also given in Table 2.2. The measured viscosity of the equilibrium liquid phase is also given. A graphical representation of the overall and component molar balance is given in Figure 2.5. This figure shows a 45° line which represents the component or overall mass balance in a typical flash experiment. Any point on the line represents a mass balance closure. Conversely, the extent of the deviation of any point from this line points to a corresponding lack of mass balance. This is a very stringent test of the data and small errors in measurements can often cause a significant deviation from the line.

The relative volume of the vapor and liquid phases for each of the three solvent additions at four selected pressures between saturation and reservoir fluid bubble pressure of 630 psia are given in Table 2.3 and are shown graphically in Figure 2.6.

For the final solvent concentration (68 mole %), retrograde dew point behavior was anticipated. However, at the reservoir temperature of 98°F, a second CO<sub>2</sub>-rich liquid was encountered as the pressure was decreased from the single phase region. It was very difficult to determine visually the initial appearance of the CO<sub>2</sub>-rich liquid phase. This was due to the relatively dark color of both liquid phases in the cell. As the system pressure decreased from 2925 psia, the relative volume of the CO<sub>2</sub>-rich liquid increased to a maximum value of about 28% at about 1300 psia. Upon further pressure reduction the volume of the CO<sub>2</sub>-rich liquid progressively decreased. A gas phase began to appear at about 1290 psia. Three-phase behavior existed for this system at pressures between 1290 and 1130 psia. At pressures less than 1130 psia, no CO<sub>2</sub>-rich liquid phase was observed. Asphaltene precipitation was observed for the system at pressures below 1132 psia.

Table 2.3 also shows the relative volume of the phases as a function of pressure for the 68% solvent-oil mixture. Photographic records of the liquid-liquid and vapor-liquid-liquid behavior are shown in Figure 2.7.

A liquid-liquid equilibrium measurement was made for this mixture at a pressure of 2514 psia. The equilibrium phase compositions of the mixture obtained by flashing at 2514 psia are given in Table 2.4. Viscosities of both liquid phases were also made and these are also given in Table 2.4.

It is important to comment on the behavior of the CO<sub>2</sub>-rich solvent-oil system in the presence of two liquid phases and in the presence of asphaltenes. The presence of a second liquid phase which was rich in CO<sub>2</sub> was observed at pressures between 1270 to 1648 psia for the 68% solvent-oil system. This would indicate that during the slim tube displacement test, three-phase phenomena would occur in the mixing zone.

Precipitation of asphaltene solids was noticed during the tests on the mixture containing 68 mole % solvent. In view of the fact that the single phase 68% solvent-oil system had a black appearance, it was not possible to visually detect the presence of these solids. However, the photographic presentation in Figure 2.5 shows that asphaltene precipitation did occur at pressures lower than 1132 psia. It can be concluded from this that no solid deposition occurred in the presence of the CO<sub>2</sub>-rich liquid phase. This is probably because the CO<sub>2</sub> concentration in the hydrocarbon liquid phase is below that required to initiate asphaltene precipitation. As the system pressure was further reduced, more CO<sub>2</sub> was dissolved in the hydrocarbon liquid and hence asphaltene precipitation occurred.

#### 4.0 EQUI-PHASE CHARACTERIZATION

The data obtained from the swelling test experiment described in the previous section were used to fine-tune the appropriate parameters of the EQUI-PHASE program. The characterized package was then used to predict the data at the conditions where experiments were conducted. In this study, two different sets of groupings for the C6+ fraction were used. In one case, the C6+ fraction was divided into six fractions. They are C6, C7-C9, C10-C14, C15-C19, C20-C29 and C30+. In the second case, the entire C6+ fraction was divided into C6-C9 and C10+ fractions.

Tables 2.5, 2.6 and 2.7 include the comparison of two predicted values and the measured value. It can be seen that the predicted values match the experimental data quite well. This can also be seen from Figure 2.1 which represents a comparison of saturation pressures with respect to solvent concentrations (P-x plot) obtained by experiment and by prediction. The critical properties of the two groupings of C6+ fractions along with molecular weight and acentric factors are given in Table 2.8. The binary interaction parameters of the components in the system with respect to the undefined fractions are given in Table 2.9.

It is recognized that the EQUI-PHASE EOR program does not predict the presence of the CO2-rich liquid phase for this solvent-oil system. Also, in performing the MMP prediction, EQUI-PHASE EOR program does not consider any possible three-phase behavior. In view of these facts, one would question the validity of any MMP predictions using this phase behavior package for CO2-rich solvents.

### Part III

#### Slim Tube Displacements



## SLIM TUBE DISPLACEMENTS

### 1.0 APPARATUS

The slim tube apparatus consisted of a JEFRI motorized positive displacement pump which was used to displace the injection solvent mixture through the slim tube at injection rates comparable to the frontal advance velocities anticipated in the reservoir. The solvent was injected by displacement of mercury which was introduced into a 316 SS solvent reservoir located in an oven maintained at the reservoir temperature. For this study a mercury displacement rate of  $6.94 \text{ cm}^3/\text{hr}$  measured at room temperature and operating pressure was maintained. This was equivalent to a solvent injection rate of  $6.96 \text{ cm}^3/\text{hr}$  at operating pressure and reservoir temperature. The corresponding average frontal advance rate was about  $120.7 \text{ cm/hr}$ . The injection fluid line was connected to a  $6.4 \text{ mm o.d.} \times 12.15 \text{ m}$  long slim tube packed with  $75$  to  $106 \mu\text{m}$  Ottawa Sand to an overall porosity of  $35.3\%$ . The total system volume inclusive of lines and fittings upstream and downstream of the slim tube up to the back pressure regulator was  $69.84 \text{ cm}^3$ . The absolute permeability of the packed slim tube was determined using pure toluene as the displacement fluid and was found to be  $3.5$  darcies. The slim tube was coiled over a short height such that the displacement was essentially horizontal. A high pressure capillary sight glass which allowed observation of the fluids passing through was located downstream of the slim tube. These observations visually revealed the passage of a single phase miscible bank or a gas and liquid phase in slug flow. A precision pressure gauge was connected upstream and a Heise digital gauge downstream of the slim tube. A differential pressure transducer was used to determine the pressure drop across the slim tube during the displacement process. The operating pressure was controlled by a back pressure regulator where the produced oil was flashed to atmospheric conditions. The flashed oil was collected in a calibrated glass receiver and the evolved gas volume was measured using a precision gasometer. A model 5890A Hewlett Packard gas chromatograph was placed in line with the gas flow tubing and was used for gas analyses on a continuous basis. The entire displacement system including the injection and pressure transmission lines, solvent storage cylinder, slim tube and sight glass were housed in a thermostated, forced circulation air oven where the temperature was maintained at the reservoir temperature of  $98^\circ\text{F}$ .

Schematic and photographic presentations of the slim tube apparatus are shown in Figures 3.1 and 3.2 respectively.



## 2.0 METHOD

The slim tube and the downstream production system were saturated with pure toluene from the wash step of the previous run. This was displaced by the recombined oil which was injected into the system for the purpose of saturating the slim tube. As the oil-toluene front passed through the sight glass, appearance of the fluids changed from clear to straw yellow, to dark yellow, to brown and finally to black. The total volume of the oil injected for saturating the system amounted to about 150 cm<sup>3</sup> which was equivalent to about 2.1 times the total system volume. During the saturation step, the back pressuring device was set to the desired operating pressure. The entire system was then brought to 98°F and allowed to stabilize. After this, the desired injection solvent was injected into the slim tube at the appropriate injection rate. The following variables were monitored during the progress of the run:

- (i) System back pressure (slim tube downstream pressure).
- (ii) System injection pressure.
- (iii) Differential pressure across slim tube.
- (iv) Oven temperature.
- (v) Injection solvent temperature.
- (vi) Produced oil level in glass receiver.
- (vii) Produced gas volume at atmospheric conditions.
- (viii) Produced gas composition.
- (ix) Visual observation of sight glass. A photograph of the sight glass was taken approximately once every hour.

The run was terminated generally after three consecutive readings of the produced oil level, each taken at about one hour intervals, remained essentially unchanged, or a plot of produced versus injected volume indicated minimal incremental production, or at about 1.6 pore volume of solvent injected. The 1.6 pore volume figure was selected based on the fact that previous experience using the same slim tube system with similar oils indicated that the ultimate recovery could be attained by the time this volume of solvent had been injected. The objective of the run was therefore to obtain the ultimate recovery. The system was then charged with fresh toluene to clean out all of the oil remaining in the system. The residual oil cleaned out in this manner was collected in a separate collection vessel. When the effluent toluene was completely clear after injection of at least 2.0 pore volumes, the system was assumed to be ready for the next run. The residual oil/toluene/injection solvent solution collected as a result of this toluene flood was transferred to a rotary evaporation apparatus where all of the C7 and lighter components were driven off under vacuum at 86°F. The fluids were trapped, weighed and analyzed by gas chromatography to determine the weight of

C3 to C7 components driven off with the toluene. This weight was added to the residual oil. The oil left behind was also analyzed by gas chromatography to determine the weight of the toluene that had not been driven off. This weight was deducted from the total weight of the residual oil. This allowed the use of an overall mass balance to determine the total oil recovery.

### 3.0 FORMATION VOLUME FACTOR

The reservoir fluid in the slim tube was used to determine the formation volume factor prior to starting the slim tube test. It was obtained by conducting a single stage flash of a known volume of reservoir fluid from the selected operating pressure at 98°F through the back pressure regulator to atmospheric pressure. The resulting dead oil volume was collected and measured in a calibrated glass receiver at 68°F. The formation volume factors determined for two operating pressures of 1600 and 1400 psia were 1.136 and 1.152 respectively. The measured formation volume factors were used to calculate the recovery data of the slim tube run.

### 4.0 RESULTS

It is important to point out that all measurements of injected solvent volumes are initially made at room temperature and the operating pressure. These are then converted to corresponding volumes at the same pressure and 98°F by multiplying the measured values by the ratio of molar volumes of mercury at the above two sets of conditions. The produced fluid volume and the calculated oil volume are all reported at room temperature and the local atmospheric pressure of 13.5 psia and also at the standard conditions of 59°F and 14.7 psia. The conversion from room temperature to 59°F was made by application of a thermal expansion coefficient for oil of 0.00061/°F.

The solvent injection for all the runs is initiated at the operating pressure of the system. Thus, in the initial periods of the run, no oil movement can occur until the injected solvent generates enough pressure at the inlet of the tube to compensate for the differential pressure required to move the oil out of the slim tube. This "compression volume" is eventually expanded back into the slim tube as the differential pressure drops during the progress of the run. Assuming that the "compression volume" can be added back linearly over the complete displacement, the net injected volume may be expressed by the following equation:

$$V_{IN} = \frac{V_T(V_M - V_{ST})(MVR)}{(V_T - V_{ST})(MVR)} \quad (1)$$

- where
- $V_{IN}$  = Corrected Injection Volume of Solvent at Reservoir Temperature and Run Pressure.
  - $V_M$  = Measured Injected Volume (Mercury) at Run Pressure and Room Temperature.
  - $V_{ST}$  = Starting Volume required to produce the differential pressure needed to move the oil. Determined at Run Pressure and Reservoir Temperature.
  - MVR = Molar Volume Ratio of Mercury for conversion from Run Pressure and Room Temperature to Run Pressure and Reservoir Temperature.
  - $V_T$  = Total Injected Volume for the run measured at Run Pressure and Reservoir Temperature.

Equation (1) was used for determining the injected volumes at 98°F reported in the tabular data of the slim tube runs performed for this study. The value of VST and (MVR) are given in the respective table for each run.

The pore volumes reported were determined by the following equation:

$$PV = \frac{V_{IN}}{V_{SYS}} \quad (2)$$

The produced fluid recovery was calculated as:

$$\text{Cumulative Recovery (\%)} = \frac{V_p \times FVF \times 100}{V_{SYS}} \quad (3)$$

where  $V_{SYS}$  = Total System Volume equivalent to 69.84 cm<sup>3</sup>

$V_p$  = Cumulative Produced Volume of fluids at 13.5 psia and room temperature or at 14.7 psia and 59°F

FVF = Oil Formation Volume Factor at run pressure and reservoir temperature relative to oil at 13.5 psia and room temperature or relative to 14.7 psia and 59°F

It is relevant to point out the possible conclusions that can be drawn from the differences in overall recovery as obtained from determination of residual oil by a toluene flood and as obtained directly from fluids collected in the separator. In general, the toluene flood based recovery may be equal to, greater than or less than the separator recovery. As a result of the contact between the injection solvent and the reservoir oil in the slim tube, a transition zone consisting of a growing slug of fluids of variable composition is developed as a function of time. The composition gradient in the transition zone varies from that of the solvent at one end to that of the oil at the other. These fluids have phase behavior characteristics that are different from the characteristics of the oil or the solvent by themselves. Consequently, when these fluids are flashed across the back pressure regulator into the separator, the gas to liquid ratios and also the gas and liquid compositions are different from those of the original oil produced in a similar manner. This results in a situation where the produced separator liquids could either have a surplus volume if the transition zone fluids generate mostly liquids on flashing, or could have a depletion in volume if the transition zone fluids and the dissolved solvent in the oil create a vaporization or extraction mechanism on flashing to the separator. If the condensation and extraction or vaporization mechanisms are competitive, then the separator volume of fluids will be similar to the volume collected if only oil had been flashed to the separator.

The toluene flood based recovery on the other hand considers only the amount of residual oil left in the slim tube and is determined by a volumetric balance of the total original oil in the tube and the amount of oil not produced from it during the run. It is, therefore, more representative of the true recovery and can be either less than or equal to 100% OOIP but never larger. Separator based recoveries on the other hand, can be larger than 100% OOIP if a condensation or swelling mechanism dominates the flashed transition zone fluids. This is often the case for hydrocarbon miscible floods and in some cases for CO<sub>2</sub> miscible floods. Alternately, separator recoveries can be unrealistically low when an extractive type mechanism dominates the displacement. This is often the case with CO<sub>2</sub> floods. For this study, the difference between the two recoveries is linearly distributed over the run, starting from the point where first evidence of the passage of the transition zone through the system is available, to the end of the run. In the tabular data supporting each slim tube run, this prorated fluid volume is termed Sct.

#### 4.1 Slim Tube Run No. 1

This displacement run was conducted at 1600 psia using a CO<sub>2</sub>-rich solvent as the injection fluid. Sight glass observations indicated the black color of the original oil from the start of the experiment until about 0.95 pore volume (PV) solvent was injected. The color of the oil changed to brown at 0.95 PV solvent injected, and then turned progressively lighter through a sequence reddish brown, orange brown, orange, light orange, and yellow. The sight glass became clear at about 1.04 PV solvent injected indicating a short transition zone. No second phase was observed during the entire run. The produced gas analyses did not indicate the presence of a methane bank. Based on these observations, the run was judged to be miscible. The overall recovery based on separator fluid volumes was 97.85% OOIP while the recovery

based on toluene residual determination was found to be equivalent to 96.0% OOIP. This indicates an increase of liquid volume possibly due to residual swelling at the separator.

In view of the fact that miscibility in these displacements is expected to occur through the transfer of intermediate components (C2-C5 hydrocarbons), it is useful to review the intermediate content of the solvent and the oil. For CO<sub>2</sub>-rich solvent displacements, CO<sub>2</sub> is treated as a light component. The oil contains approximately 24 mole % of intermediates which forms the driving force for mass transfer. The direction of transfer of intermediates occurs from the oil to the solvent. This is typical of vaporizing type drives. In such drives it is often not possible to distinguish between multicontact and first miscible drives simply from sight glass observations. This is due to the fact that the transition zone is made up of the enriching gas which leaves the smaller volumes of second phase liquids, if any, behind the front. The sight glass thus reveals a single phase oil transforming to the enriched gas transition zone followed by the injection solvent. First contact or multicontact miscible displacements will both indicate the same observations.

A record of the slim tube run data is given in Table 3.1. The calculated cumulative volumes of Sct are given as a function of time. A summary of the produced gas analyses is given in Table 3.2 which indicates the time of arrival of the leading edge of the transition zone at about 0.95 PV of solvent injected. As indicated earlier, visual observations confirm this arrival at about 0.95 PV solvent displaced. Owing to occasional difficulties in discriminating between fine color changes, visual observations, when compared to produced gas analyses by chromatography, can often be marginally different with respect to time.

A plot of the cumulative produced fluids recovered versus pore volume solvent displaced is given in Figure 3.3. The calculated oil recovery determined by accounting for Sct contribution at each time interval is given on the same plot. The ratio of total produced gas to total fluid produced (GOR) at the separator is given in Figure 3.4. The GOR plot indicated the average solution GOR to be 48 ft<sup>3</sup>/ft<sup>3</sup> at 59°F and 14.7 psia. A photographic record of the run is given in Figure 3.5. In these photographs, the numbers in the lower right corner indicate the elapsed time (in hours and minutes) from the start of the run. As a rule of thumb, every hour of elapsed time corresponds to approximately 0.1 pore volumes of solvent injected.

#### 4.2 Slim Tube Run No. 2

This displacement run was conducted at 1400 psia with the objective of checking to see whether the run would still be miscible. Fina has no intention of lowering the present reservoir pressure, so any slim tube run at pressures below 1400 psia becomes academic issue. Visual observations and production gas analyses for this run were almost identical to those of run No. 1. The fluid produced and observed at the sight glass indicated a change of color at about 0.95 PV. At about 0.99 PV displacement, small bubbles were observed in the sight glass but they only lasted for about 0.01 PV. The produced gas phase composition measurements also indicated a slight increase in methane content at about 0.776 PV displacement.

The overall recovery based on separator fluid volumes was found to be 98.2% OOIP. The overall oil recovery based on toluene residual determination was found to be 95.1% OOIP. This recovery is almost identical to that of run No. 1. On the basis of this observation, it is safe to conclude that this run is also miscible.

A record of the run data is given in Table 3.3 with a summary of the produced gas analyses given in Table 3.4. The cumulative recovery plot versus pore volume of solvent injected is given in Figure 3.6. A photographic record of the run is given in Figure 3.7. In this run, a leak at the produced gas volume measurement device was detected in the middle of the run. An attempt to recover the GOR data for the run was not successful. Hence, no GOR plot is presented.



Table 1.1 Measured Composition of Separator Gas and Separator Liquid Sample

Component	Separator Gas				Separator Liquid
	Cylinder # 438567D	Cylinder # 452596D	Cylinder # 452595D	Cylinder # 438569D	Cylinder #
C02	2.799	2.461	2.383	2.520	0.110
H2S	2.858	3.372	3.763	2.822	0.605
N2	1.780	1.895	1.867	1.822	0.137
C1	46.096	45.858	45.799	46.796	0.876
C2	19.070	18.630	18.532	19.018	2.034
C3	15.921	15.775	15.755	15.731	5.285
iC4	2.269	2.300	2.282	2.227	1.565
nC4	5.117	5.222	5.172	5.014	4.841
iC5	1.492	1.582	1.539	1.456	2.922
nC5	1.140	1.234	1.180	1.112	2.829
C6	0.718	0.789	0.745	0.704	5.010
MCYC-C5	0.132	0.148	0.136	0.131	1.452
Benzene	0.057	0.065	0.057	0.057	0.685
CYC-C6	0.089	0.101	0.092	0.089	1.408
C7	0.236	0.273	0.251	0.238	5.102
MCYC-C6	0.056	0.066	0.061	0.057	1.785
Toluene	0.031	0.039	0.033	0.032	1.400
C8	0.091	0.114	0.131	0.099	5.490
C2-Benzene	-	-	-	-	1.383
M&P Xyl.	0.009	0.013	0.022	0.011	0.736
C9	0.030	0.044	0.098	0.039	0.793
C10	0.009	0.015	0.071	0.016	4.182
C11	0.001	0.003	0.022	0.004	5.698
C12	-	0.001	0.005	0.001	4.498
C13	-	-	0.001	-	3.533
C14					3.074
C15					2.748
C16					2.137
C17					2.019
C18					1.799
C19					1.721
C20					1.446
C21					1.246
C22					1.174
C23					1.013
C24					0.914
C25					0.897
C26					0.490
C27					0.728
C28					0.713
C29					0.541
C30+					9.403

Table 1.2 Specified and Prepared Separator Gas Composition

Component	Concentration, Mole %	
	Prepared	Specified
CO2	2.45	2.45
H2S	6.64	6.66
N2	1.75	1.78
C1	44.46	44.49
C2	18.13	18.14
C3	15.22	15.23
I-C4	2.18	2.19
N-C4	4.95	4.95
I-C5	1.46	1.46
N-C5	1.12	1.12
C6	0.84	0.71
MCYC-C5		0.13
BENZENE	0.06	0.06
CYC-C6	0.09	0.09
C7	0.24	0.24
MCY-C6	0.06	0.06
TOLUENE	0.03	0.03
C8	0.12	0.12
C9	0.05	0.05
C10	0.15	0.04



Table 1.3 Measured Composition of Recombined  
Emmons #208 Reservoir Fluid

Component	Mole %
C02	0.658
H2S	2.094
N2	0.469
C1	11.499
C2	5.748
C3	7.044
I-C4	1.558
N-C4	4.471
I-C5	2.492
N-C5	2.391
C6	4.185
MCYC-C5	1.140
BENZENE	0.546
CYCL-C6	1.119
C7	4.074
MCYCL-C6	1.413
TOLUENE	1.093
C8	4.302
C2-BENZENE	0.878
M&P-XYLENE	0.564
O-XYLENE	0.339
C9	3.651
C10	4.469
C11	3.518
C12	2.736
C13	2.807
C14	2.417
C15	2.095
C16	1.689
C17	1.531
C18	1.466
C19	1.377
C20	1.119
C21	0.951
C22	0.883
C23	0.812
C24	0.737
C25	0.668
C26	0.643
C27	0.635
C28	0.581
C29	0.551
C30+	6.587

**Table 1.4 Specified and Prepared Injection and Swelling Solvent Composition**

Component	Prepared	Specified
CO2	98.48	98.48
N2	1.40	1.40
C1	0.12	0.12

Table 2.1 Swelling Test Data for Emmons #208  
Reservoir Oil at 98°F

Solvent Mole %	Saturation Pressure psia	Viscosity cp	Bulk Density g/cm <sup>3</sup>
0	630	1.82	0.802
15	837	1.44	0.818
30	1069	1.14	0.835
41	1249	0.84	0.836

$$\rho_o = \frac{(m_o)_{c-1} + (m_{cc})_{c-1}}{V_o}$$

Table 2.2 Measured Equilibrium Phase Data and Compositions for Flash at 634 psia & 98°F

Component	Concentration, Mole %		
	Feed	Liquid	Vapor
CO2	40.344	27.707	72.323
H2S	1.020	0.921	0.697
N2	0.975	0.177	2.953
C1	6.685	2.787	15.563
C2	3.395	3.057	4.206
C3	4.290	4.919	2.610
I-C4	0.933	1.175	0.312
N-C4	2.669	3.465	0.675
I-C5	1.468	2.002	0.198
N-C5	1.408	1.938	0.153
C6	2.482	3.463	0.132
MCYC-C5	0.677	0.951	0.024
BENZENE	0.322	0.454	0.011
CYCL-C6	0.668	0.943	0.018
C7	2.464	3.494	0.053
MCYCL-C6	0.850	1.213	0.013
TOLUENE	0.648	0.932	0.008
C8	2.586	3.733	0.025
C2-BENZENE	0.521	0.756	0.000
M&P-XYLENE	0.338	0.487	0.003
O-XYLENE	0.198	0.287	0.000
C9	2.206	3.183	0.005
C10	2.707	3.842	
C11	2.123	3.025	
C12	1.648	2.362	
C13	1.694	2.435	
C14	1.445	2.097	
C15	1.271	1.811	
C16	1.041	1.484	
C17	0.932	1.341	
C18	0.861	1.242	
C19	0.838	1.214	
C20	0.653	0.975	
C21	0.617	0.871	
C22	0.546	0.796	
C23	0.492	0.714	
C24	0.422	0.649	
C25	0.435	0.588	
C26	0.351	0.537	
C27	0.357	0.509	
C28	0.375	0.494	
C29	0.289	0.449	
C30+	3.756	4.525	
Pressure (psia)	1364	634	634
Temperature (°F)	98	98	98
Density (g/cm <sup>3</sup> )	0.819	0.828	0.080
MW	104.2	128.1	38.92
Vol. %	100	47.41	52.59
Viscosity (cp)	0.84	1.41	

Table 2.3 Relative Phase Volumes for  
Four Solvent Oil Mixtures at 98°F

Solvent Mole %	Pressure psia	Vapor	Volume % Liquid Hydrocarbon-rich	Liquid CO2-rich
15	837(B.P.)	0	100	--
	737	4.84	95.16	--
	704	7.71	92.29	--
	679	10.08	89.92	--
	644	13.23	86.77	--
30	1069(B.P.)	0	100	--
	914	7.87	92.13	--
	849	14.06	85.94	--
	744	24.38	75.62	--
	654	33.60	66.40	--
41	1249(B.P.)	0	100	--
	1124	6.92	93.08	--
	959	21.64	78.36	--
	814	37.10	62.90	--
	664	52.74	47.26	--
68	3973**	0	100	0
	3408**	0	100	0
	3078**	0	100	0
	2925	0	88.5	11.5
	2625	0	75.8	24.2
	2350	0	73.9	26.1
	1850	0	72.2	27.8
	1648	0	71.8	28.2
	1485	0	71.6	28.4
	1310	0	71.8	28.2
	1291	4.2	71.3	24.5
	1270	12.1	70.1	17.8
	1132	44.6	55.4	0
	1047*	53.8	46.2	0
	950*	63.7	36.3	0

\* Asphaltene Observed

\*\* No Phase Separation Observed

Table 2.4 Equilibrium CO<sub>2</sub> Rich and Hydrocarbon-Rich Liquid Compositions  
After Flashing 68 Mole % Solvent-Oil Mixture at 2514 psia and  
98°F

Component	Concentration, Mole %	
	CO <sub>2</sub> -Rich	Hydrocarbon-Rich
CO <sub>2</sub>	74.894	64.261
H <sub>2</sub> S	0.513	0.648
N <sub>2</sub>	1.356	1.005
C <sub>1</sub>	3.996	3.587
C <sub>2</sub>	1.766	1.836
C <sub>3</sub>	2.049	2.315
I-C <sub>4</sub>	0.452	0.522
N-C <sub>4</sub>	1.212	1.476
I-C <sub>5</sub>	0.690	0.826
N-C <sub>5</sub>	0.659	0.806
C <sub>6</sub>	1.168	1.483
MCYC-C <sub>5</sub>	0.297	0.411
BENZENE	0.142	0.197
CYCL-C <sub>6</sub>	0.266	0.409
C <sub>7</sub>	1.115	1.460
MCYCL-C <sub>6</sub>	0.352	0.513
TOLUENE	0.272	0.392
C <sub>8</sub>	1.107	1.538
C <sub>2</sub> -BENZENE	0.208	0.319
M&P-XYLENE	0.134	0.206
O-XYLENE	0.078	0.121
C <sub>9</sub>	0.906	1.330
C <sub>10</sub>	1.057	1.643
C <sub>11</sub>	0.778	1.319
C <sub>12</sub>	0.572	1.042
C <sub>13</sub>	0.563	1.047
C <sub>14</sub>	0.470	0.909
C <sub>15</sub>	0.396	0.810
C <sub>16</sub>	0.312	0.668
C <sub>17</sub>	0.266	0.599
C <sub>18</sub>	0.241	0.561
C <sub>19</sub>	0.229	0.527
C <sub>20</sub>	0.175	0.439
C <sub>21</sub>	0.152	0.405
C <sub>22</sub>	0.128	0.361
C <sub>23</sub>	0.119	0.330
C <sub>24</sub>	0.106	0.300
C <sub>25</sub>	0.101	0.278
C <sub>26</sub>	0.071	0.255
C <sub>27</sub>	0.084	0.243
C <sub>28</sub>	0.077	0.232
C <sub>29</sub>	0.065	0.190
C <sub>30</sub> +	0.366	2.183
MW	58.18	81.24
Density (g/cm <sup>3</sup> )	0.797	0.846
Viscosity (cp)	0.175	0.535

Table 2.5 Comparison of EQUI-PHASE Predictions of Swelling Test With Experimental Data

Solvent Concentration Mole %	Saturation Pressure, psia Experimental	Predicted		Saturation Density, g/cm <sup>3</sup> Experimental	Predicted	
		#1	#2		#1*	#2*
0	630	639	619	0.802	0.809	0.819
15	837	839	831	0.818	0.810	0.822
30	1069	1060	1066	0.835	0.815	0.826
41	1249	1241	1260	0.836	0.820	0.829

\* Grouping of C6+ fraction

Table 2.6 Comparison of EQUI-PHASE Predictions of Relative Phase Volumes With Experimental Data

Solvent Conc. Mole %	Pressure Psia	Experiment	Liquid Volume, % Predicted #1*	Predicted #2*
15	737	4.8	7.8	7.6
	704	7.7	10.7	10.7
	679	10.1	13.1	13.2
	644	13.2	16.6	16.8
30	914	7.9	11.0	12.0
	849	14.1	16.9	18.1
	744	24.4	27.5	28.9
	654	33.6	37.4	38.8
41	1124	6.9	8.2	9.8
	959	21.6	22.5	24.5
	814	37.1	36.9	38.8
	664	52.7	52.2	53.6

\* Grouping of C6+ fraction



Table 2.7 Comparison of EQUI-PHASE Predictions With Experimental Data for the Detailed Vapor and Liquid Phase Compositions After Flashing the 41% Mixture at 634 psia and 98°F

Component	Feed	Concentration, Mole %			
		Experimental Vapor	Liquid	Predicted #1 Vapor	Predicted #1 Liquid
H2S	1.020	0.697	0.921	1.21	1.28
CO2	40.344	72.323	27.707	70.85	28.5
N2	0.975	2.953	0.177	2.56	0.16
C1	6.685	15.563	2.787	17.09	2.87
C2	3.395	4.206	3.057	4.31	3.12
C3	4.290	2.610	4.919	2.50	4.93
I-C4	0.933	0.312	1.175	0.30	1.18
N-C4	2.669	0.675	3.465	0.62	3.49
I-C5	1.468	0.198	2.002	0.17	2.00
N-C5	1.408	0.153	1.938	0.13	1.93
C6	4.149	0.185	5.811	0.16	5.69
C7-C9	9.811	0.107	14.085	0.09	13.38
C10-C14	9.617	0.010	13.761	--	13.11
C15-C19	4.943	--	7.098	--	7.63
C20-C29	4.537	--	6.582	--	5.31
C30+	3.756	--	4.525	--	5.42
Volume (%)		52.6	47.4	55.1	44.9
Density (g/cm <sup>3</sup> )		0.080	0.828	0.082	0.828
MW	104.2	38.9	128.1	38.4	129.1

Table 2.7 (Continued) Comparison of EQUI-PHASE Predictions With Experimental Data for the Detailed Vapor and Liquid Phase Compositions After Flashing the 41% Mixture at 634 psia and 98°F

Component	Concentration, Mole %				
	Feed	Experimental Vapor	Liquid	Predicted #2 Vapor	Predicted #2 Liquid
H2S	1.020	0.697	0.921	1.21	1.29
CO2	40.344	72.323	27.707	71.55	27.52
N2	0.975	2.953	0.177	2.47	0.16
C1	6.685	15.563	2.787	1.66	2.87
C2	3.395	4.206	3.057	4.28	3.11
C3	4.290	2.610	4.919	2.51	4.97
I-C4	0.933	0.312	1.175	0.30	1.20
N-C4	2.669	0.675	3.465	0.64	3.53
I-C5	1.468	0.198	2.002	0.17	2.03
N-C5	1.408	0.153	1.938	0.13	1.96
C6-C9	13.960	0.292	19.896	0.20	19.40
C10+	22.853	0.010	31.966	--	31.97
Volume (%)		52.6	47.4	56.4	43.6
Density (g/cm <sup>3</sup> )		0.080	0.828	0.082	0.840
MW	104.2	38.9	128.1	38.6	131.0

Table 2.8 Emmons #208 Reservoir Oil Characterization  
Component Critical Properties

Component	Critical Pressure atm	Critical Temperature K	Acentric Factor	Molecular Weight
Grouping #1				
C6	34.5	528.8	0.190	84.0
C7-C9	30.0	585.8	0.265	110.0
C10-C14	24.46	677.0	0.442	155.0
C15-C19	17.96	741.8	0.619	225.0
C20-C29	13.0	820.0	1.100	340.0
C30+	10.4	870.0	1.600	590.0
Grouping #2				
C6-C9	32.5	570.0	0.250	100.0
C10+	16.6	760.0	0.750	281.0

Table 2.9 Emmons #208 Reservoir Oil Characterization  
Binary Interaction Parameters

Component	Grouping #1					
	C6	C7-C9	C10-C14	C15-C19	C20-C29	C30+
H2S	0.05	0.05	0.05	0.05	0.05	0.05
CO2	0.12	0.12	0.12	0.12	0.10	0.10
N2	0.10	0.11	0.11	0.11	0.11	0.11
C1	0.0	0.02	0.03	0.04	0.06	0.08
C2	0.0	0.0	0.0	0.02	0.03	0.04
C3	0.0	0.0	0.0	0.01	0.02	0.03
I-C4	0.0	0.0	0.0	0.01	0.01	0.02
N-C4	0.0	0.0	0.0	0.0	0.0	0.01
I-C5	0.0	0.0	0.0	0.0	0.0	0.0
C6		0.0	0.0	0.0	0.0	0.0
C7-C9			0.0	0.0	0.0	0.0
C10-C14				0.0	0.0	0.0
C15-C19					0.0	0.0
C20-C29						0.0

Component	Grouping #2	
	C6-C9	C10+
H2S	0.05	0.05
CO2	0.12	0.13
N2	0.11	0.11
C1	0.10	0.06
C2	0.0	0.03
C3	0.0	0.02
I-C4	0.0	0.01
N-C4	0.0	0.01
I-C5	0.0	0.0
C6-C9		0.0

Table 3.1 Slim Tube Displacement Run No. 1 at 1600 psia and 98°F

TIME (min)	VOLUME INJECTED (cc)	VOLUME INJECTED (cc)	PORE VOLUMES <del>PRODUCED</del> INJECTED	CUMULATIVE FLUID PRODUCED (cc)	CUMULATIVE FLUID RECOVERY (cc)	CUMULATIVE FLUID PER. PRODUCED (%)	CUMULATIVE OIL (cc)
Temperature (°F)	69.1	98.1	98.1	69.1	59.0	69.1	
Pressure (psia)	1600.1	1600.1	1600.1	13.5	14.7		
60	7.10	0.81	0.012	0.69	0.68	1.12	0.69
95	11.25	5.27	0.075	2.46	2.44	4.00	2.46
150	17.75	12.26	0.176	6.98	6.94	11.36	6.98
210	24.55	19.57	0.280	12.73	12.65	20.70	12.73
270	31.65	27.21	0.390	20.75	20.62	33.75	20.75
330	38.60	34.68	0.497	26.04	25.88	42.36	26.04
390	45.50	42.10	0.603	33.04	32.83	53.74	33.04
450	52.50	49.63	0.711	39.74	39.49	64.64	39.74
516	60.35	58.07	0.831	47.96	47.67	78.02	47.41
570	66.47	64.65	0.926	53.95	53.62	87.75	52.95
583			0.949				
630	73.46	72.16	1.033	58.64	58.28	95.39	57.57
633			1.040				
690	80.45	79.68	1.141	59.88	59.52	97.41	58.74
750	87.50	87.26	1.249	60.15	59.78	97.85	59.00
780	91.00	91.02	1.303	60.15	59.78	97.85	59.00
810	94.43	94.71	1.356	60.15	59.78	97.85	59.00

VST = 6.35 cc  
VSYS = 69.84 cc

MVR = 1.0030  
FVF = 1.1360

Table 3.1 (Continued) Slim Tube Displacement Run No. 1 at 1600 psia and 98°F

TIME (min)	CUMULATIVE OIL PRODUCED (cc)	CUMULATIVE OIL PERCENT RECOVERY (%)	CUMULATIVE GAS VOLUME PRODUCED (cc)	CUMULATIVE GAS VOLUME PRODUCED (cc)	CUMULATIVE SOLVENT CONDENSABLES (cc)	CUMULATIVE GAS/OIL RATIO	SIGHT GLASS OBSERVATIONS
Temperature (°F)	59.0		69.1	59.0	69.1	59.0	
Pressure (psia)	14.7		13.5	14.7	13.5	14.7	
60	0.68	1.12	19.0	17.1	0.00	25.04	BLACK-S.P.
95	2.44	4.00	127.3	114.8	0.00	46.98	BLACK-S.P.
150	6.94	11.36	367.3	331.1	0.00	47.70	BLACK-S.P.
210	12.65	20.70	669.2	603.3	0.00	47.70	BLACK-S.P.
270	20.62	33.75	1038.0	935.8	0.00	45.39	BLACK-S.P.
330	25.88	42.36	1386.5	1250.0	0.00	48.30	BLACK-S.P.
390	32.83	53.74	1760.5	1587.2	0.00	48.34	BLACK-S.P.
450	39.49	64.64	2125.7	1916.3	0.00	48.52	BLACK-S.P.
516	47.12	77.12	2568.6	2315.7	0.55	48.58	BLACK-S.P.
570	52.62	86.12	2902.0	2616.3	1.00	48.80	BLACK-S.P.
583							BROWN-S.P.
630	57.21	93.65	4037.6	3640.0	1.07	62.45	YELLOW-S.P.
633							CLEAR-S.P.
690	58.37	95.55	6584.7	5936.4	1.14	99.74	CLEAR-S.P.
750	58.63	95.97	9510.5	8574.0	1.16	143.42	CLEAR-S.P.
780	58.63	95.97	11012.7	9928.3	1.16	166.07	CLEAR-S.P.
810	58.63	95.97	12580.5	11341.7	1.16	189.71	CLEAR-S.P.

S.P. = Single Phase

T.P. = Two-Phase

Table 3.2 Produced Gas Analyses for Slim Tube Run No. 1 at 1600 psia and 98°F

H2S	N2	CO2	C1	C2	C3	iC4	nC4	iC5	nC5	C6	C7+	PORE VOL. INJECTED
5.105	6.958	1.515	32.696	15.366	17.882	3.293	8.594	3.375	2.693	2.523	0.000	0.012
6.074	1.924	1.820	33.439	16.086	18.600	3.494	9.011	3.334	2.639	3.579	0.000	0.075
6.570	1.556	2.013	35.846	16.984	18.553	3.263	7.952	2.611	1.991	2.662	0.000	0.176
6.632	1.507	2.044	36.238	17.066	18.445	3.214	7.786	2.538	1.934	2.594	0.000	0.280
6.640	1.480	2.045	36.259	17.067	18.421	3.210	7.786	2.533	1.929	2.629	0.000	0.390
6.643	1.477	2.047	36.257	17.079	18.425	3.209	7.778	2.538	1.932	2.616	0.000	0.497
6.651	1.497	2.049	36.239	17.063	18.415	3.210	7.792	2.537	1.934	2.613	0.000	0.603
6.647	1.495	2.046	36.170	17.038	18.405	3.213	7.802	2.556	1.952	2.677	0.000	0.711
6.658	1.476	2.050	36.171	17.046	18.400	3.210	7.798	2.554	1.948	2.689	0.000	0.831
6.495	1.480	3.855	35.329	16.647	18.075	3.176	7.743	2.552	1.951	2.697	0.000	0.926
5.281	1.560	18.695	29.151	13.459	15.103	2.766	6.960	2.457	1.913	2.655	0.000	0.953
3.204	1.766	45.284	18.789	8.158	9.510	1.847	4.931	2.031	1.676	2.803	0.000	
1.946	1.750	64.307	11.435	4.894	5.789	1.152	3.193	1.483	1.295	2.755	0.000	
1.247	1.455	77.196	5.862	2.951	3.705	0.750	2.141	1.060	0.958	2.674	0.000	1.033
0.712	1.281	86.318	2.117	1.507	2.179	0.465	1.410	0.755	0.715	2.541	0.000	
0.270	1.312	92.589	0.525	0.469	0.870	0.203	0.698	0.418	0.428	2.217	0.000	
0.000	1.402	97.094	0.213	0.000	0.046	0.000	0.050	0.000	0.000	1.195	0.000	1.141
0.000	1.441	98.115	0.199	0.000	0.000	0.000	0.000	0.000	0.000	0.245	0.000	1.249
0.000	1.445	98.215	0.173	0.000	0.000	0.000	0.000	0.000	0.000	0.167	0.000	1.303
0.000	1.559	98.111	0.189	0.000	0.000	0.000	0.000	0.000	0.000	0.141	0.000	1.356

Table 3.3 Slim Tube Displacement Run No. 2 at 1400 psia and 98°F

TIME (min)	VOLUME INJECTED (cc)	VOLUME INJECTED (cc)	PORE VOLUMES INJECTED	CUMULATIVE FLUID PRODUCED (cc)	CUMULATIVE FLUID PRODUCED (cc)	CUMULATIVE FLUID PER. RECOVERY (%)	CUMULATIVE OIL PRODUCED (cc)
Temperature (°F)	68.7	98.1	98.1	68.7	59.0		68.4
Pressure (psia)	1400.0	1400.0	1400.0	13.5	14.7		13.5
60	7.10	2.23	0.032	1.11	1.10	1.83	1.11
120	14.10	9.66	0.138	3.98	3.96	6.57	3.98
180	21.05	17.03	0.244	7.85	7.81	12.95	7.85
240	28.10	24.52	0.351	13.06	12.98	21.54	13.06
300	35.05	31.89	0.457	18.91	18.79	31.19	18.91
360	42.00	39.27	0.562	25.01	24.86	41.26	25.01
420	49.09	46.79	0.670	32.24	32.05	53.18	32.24
480	56.05	54.18	0.776	40.13	39.90	66.20	40.13
540	62.94	61.49	0.880	48.81	48.52	80.51	48.31
578			0.948				
591			0.971				
600	69.92	68.90	0.987	57.44	57.10	94.75	56.44
603			0.992				
609			1.003				
660	76.90	76.31	1.093	59.17	58.82	97.60	57.32
720	83.89	83.73	1.199	59.32	58.97	97.84	57.46
780	90.85	91.11	1.305	59.52	59.17	98.18	57.67
VST =	5.00 cc					MVR =	1.0029
VSYS =	69.84 cc					FVF =	1.1520



Table 3.3 (Continued) Slim Tube Displacement Run No. 2 at 1400 psia and 98°F

TIME (min)	CUMULATIVE OIL PRODUCED (cc)	CUMULATIVE OIL PERCENT RECOVERY (%)	CUMULATIVE GAS VOLUME PRODUCED (cc)	CUMULATIVE GAS VOLUME PRODUCED (cc)	CUMULATIVE SOLVENT CONDENSABLES (cc)	CUMULATIVE GAS/OIL RATIO	SIGHT GLASS OBSERVATIONS
Temperature (°F)	59.0		68.7	59.0	68.7	59.0	
Pressure (psia)	14.7		13.5	14.7	13.5	14.7	
60	1.10	1.83	53.4	48.1	0.00	43.67	BLACK-S.P.
120	3.96	6.57	187.1	168.8	0.00	42.67	BLACK-S.P.
180	7.81	12.95	368.8	332.7	0.00	42.62	BLACK-S.P.
240	12.98	21.54	614.5	554.4	0.00	42.70	BLACK-S.P.
300	18.79	31.19	891.7	804.5	0.00	42.80	BLACK-S.P.
360	24.86	41.26	1181.1	1065.6	0.00	42.86	BLACK-S.P.
420	32.05	53.18	1525.0	1375.7	0.00	42.93	BLACK-S.P.
480	39.90	66.20	1900.5	1714.5	0.00	42.98	BLACK-S.P.
540	48.02	79.69	2300.8	2075.7	0.50	42.78	BLACK-S.P.
578							LT. BROWN-S.P.
591							CLEAR-S.P.
603							SMALL BUBBLE
609							CLEAR-S.P.
600	56.10	93.10	2699.0	2434.9	1.00	42.64	YELLOW-S.P.
660	56.97	94.54	3008.6	2714.2	1.85	46.14	CLEAR-S.P.
720	57.11	94.79	3269.2	2949.3	1.85	50.02	CLEAR-S.P.
780	57.32	95.12	3558.1	3209.9	1.85	54.25	CLEAR-S.P.

S.P. = Single Phase

T.P. = Two-Phase

Table 3.4 Produced Gas Analyses for Slim Tube Run No. 2 at 1400 psia and 98°F

H2S	N2	CO2	C1	C2	C3	iC4	nC4	iC5	nC5	C6	C7+	PORE VOL. INJECTED
5.200	6.979	2.026	32.825	15.923	17.966	3.266	8.126	2.782	2.141	2.766	0.000	0.032
5.726	3.514	2.017	35.304	16.775	18.405	3.255	7.904	2.599	1.973	2.528	0.000	0.138
5.945	2.201	2.046	36.171	17.086	18.517	3.237	7.830	2.550	1.932	2.486	0.000	0.244
6.008	1.844	2.045	36.419	17.174	18.512	3.225	7.800	2.543	1.927	2.502	0.000	0.351
6.043	1.748	2.049	36.464	17.206	18.529	3.221	7.782	2.525	1.925	2.507	0.000	0.457
6.045	1.684	2.053	36.352	17.170	18.528	3.325	7.845	2.563	1.952	2.571	0.000	0.562
6.020	1.989	2.002	36.241	17.106	18.482	3.230	7.823	2.568	1.958	2.579	0.000	0.670
6.108	1.526	2.088	36.884	17.321	18.523	3.180	7.641	2.430	1.841	2.458	0.000	0.776
5.081	1.943	12.865	32.784	14.584	18.953	2.868	7.119	2.420	1.865	2.518	0.000	
1.735	1.322	66.266	9.761	4.874	5.931	1.203	3.304	1.545	1.347	2.711	0.000	0.880
1.061	1.500	79.181	4.914	2.723	3.487	0.709	2.026	1.005	0.912	2.482	0.000	
0.568	1.386	87.571	1.605	1.272	1.949	0.425	1.330	0.730	0.707	2.458	0.000	
0.268	1.523	92.098	0.571	0.475	0.909	0.212	0.763	0.464	0.488	2.231	0.000	
0.000	1.452	95.458	0.339	0.126	0.230	0.055	0.221	0.152	0.182	1.784	0.000	0.987
0.000	1.524	97.012	0.181	0.000	0.043	0.000	0.050	0.000	0.000	1.189	0.000	
0.000	1.567	97.295	0.207	0.000	0.000	0.000	0.000	0.000	0.000	0.930	0.000	
0.000	1.571	97.521	0.192	0.000	0.000	0.000	0.000	0.000	0.000	0.715	0.000	1.093
0.000	1.540	97.958	0.142	0.000	0.000	0.000	0.000	0.000	0.000	0.359	0.000	1.199



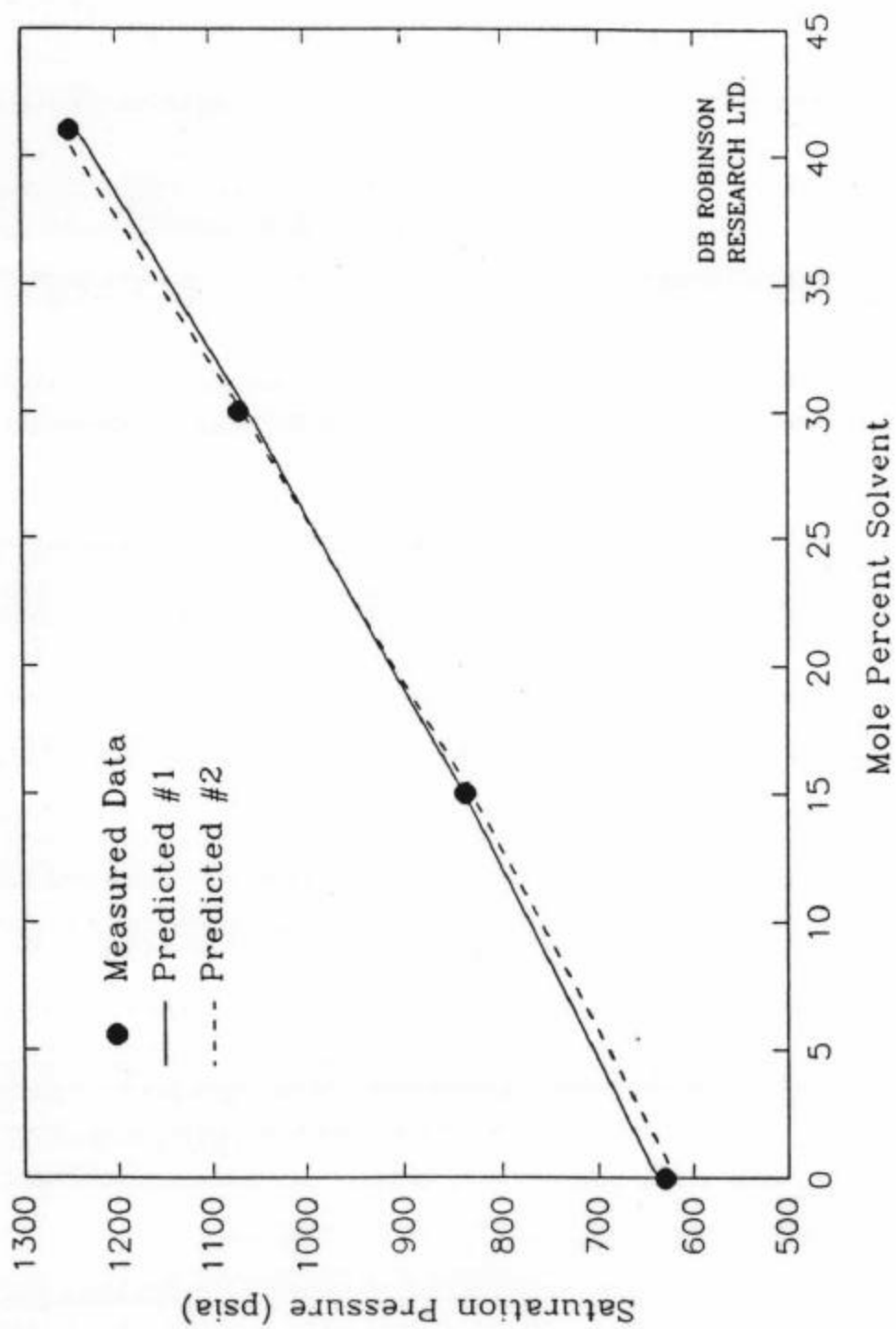


Figure 2.3. Experimental and Predicted Swelling Curve for Solvent-Oil Mixtures at 98°F

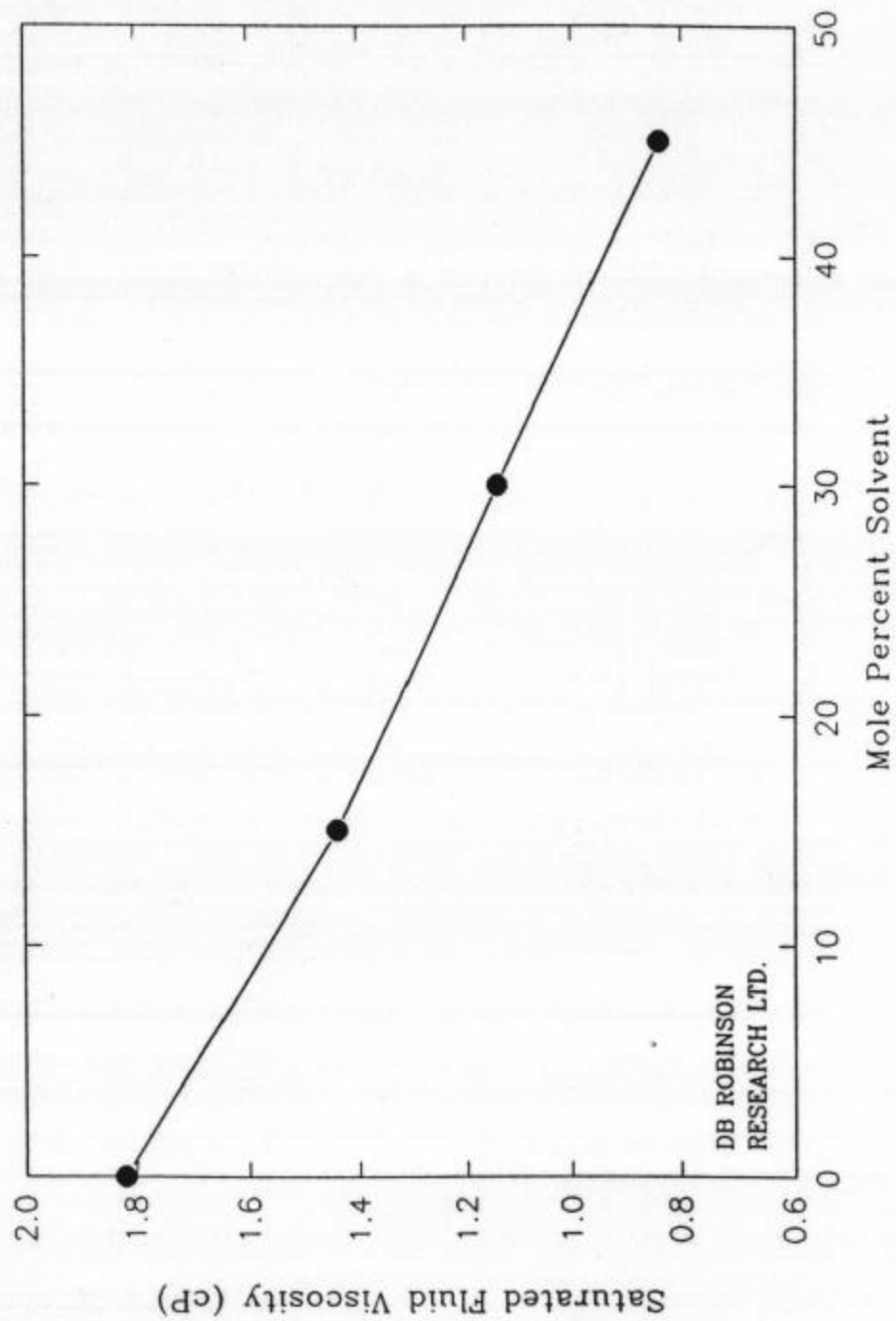


Figure 2.4. Viscosity of solvent--oil mixtures at saturation pressure and 98° F

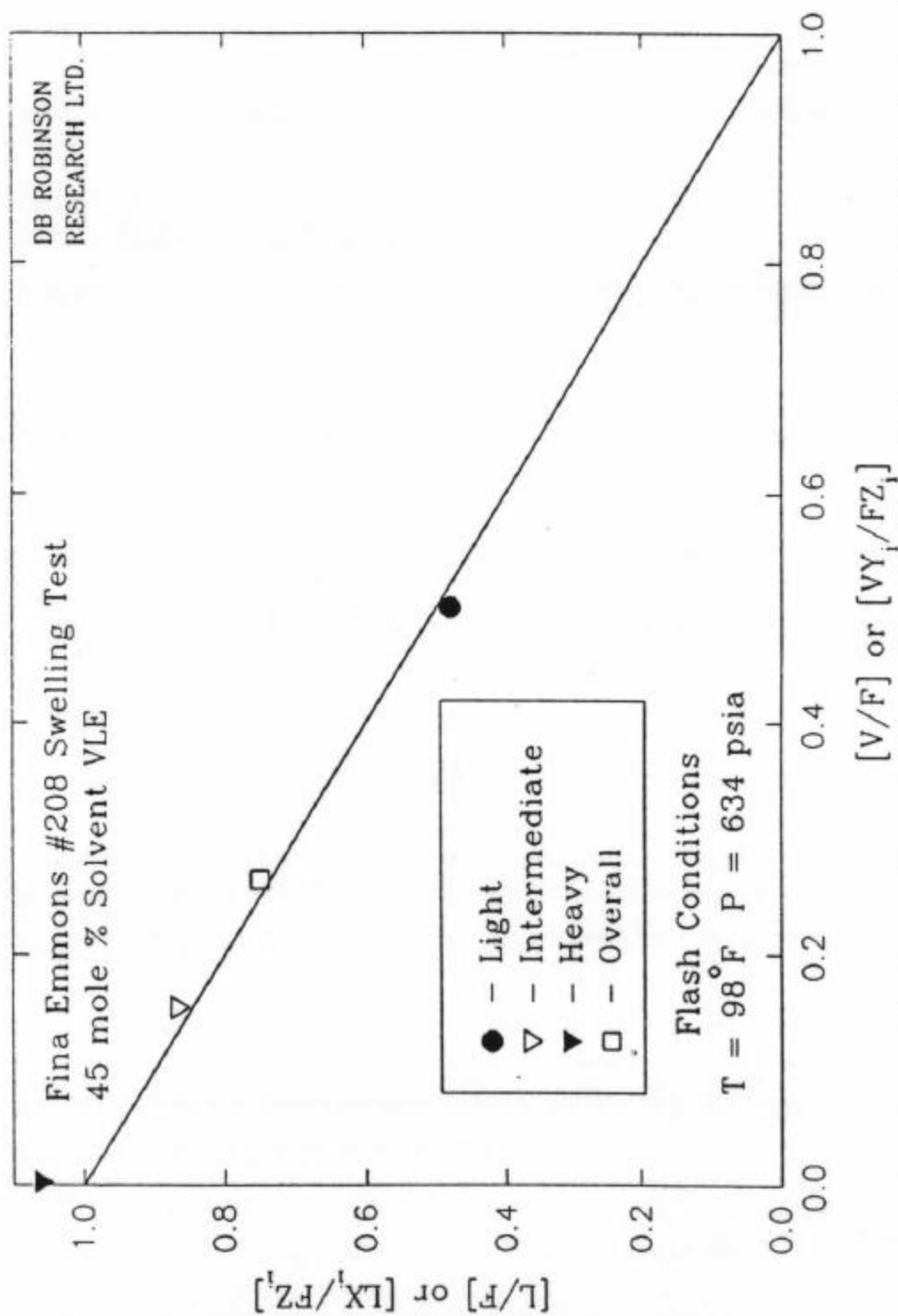


Figure 2.5. Overall and Component Molar Balance of VLE Flash for the 41% Solvent-Oil Mixture at 98°F and 634 psia.

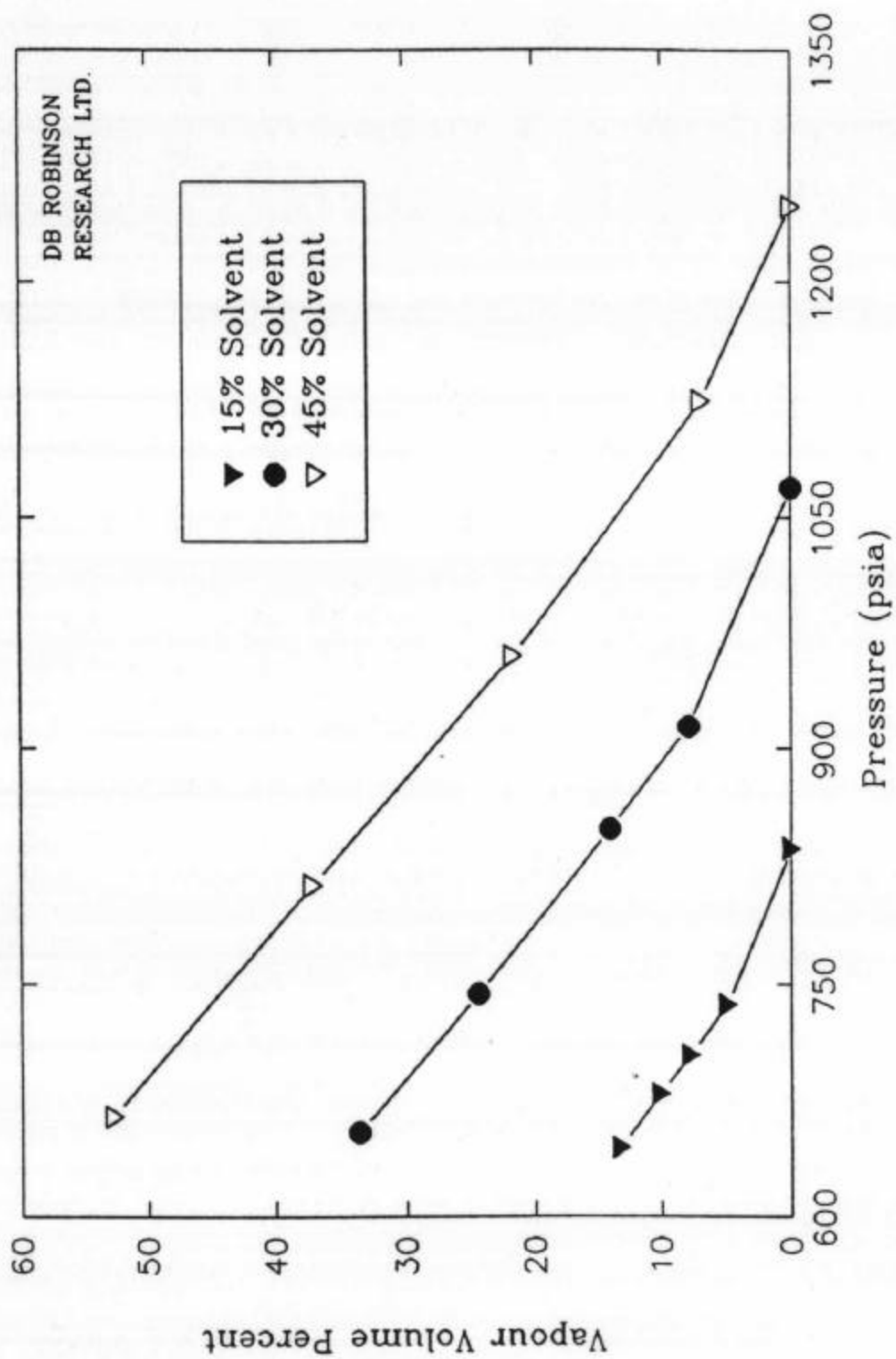


Figure 2.6. Percent Vapour Volume at Selected Pressures for Three Solvent-Oil Mixtures at 98 °F

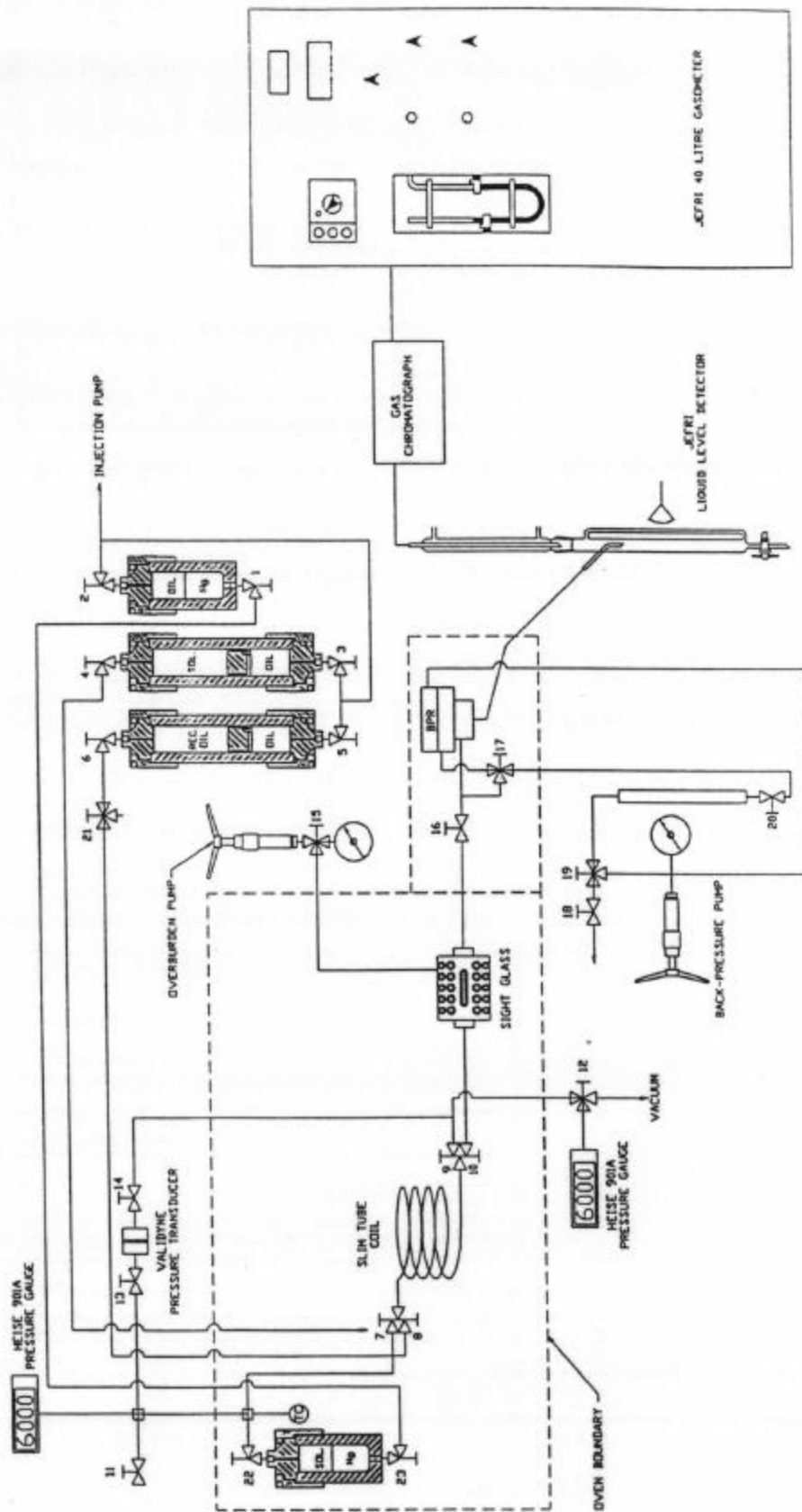


Figure 3.1 Schematic of Slim Tube Apparatus



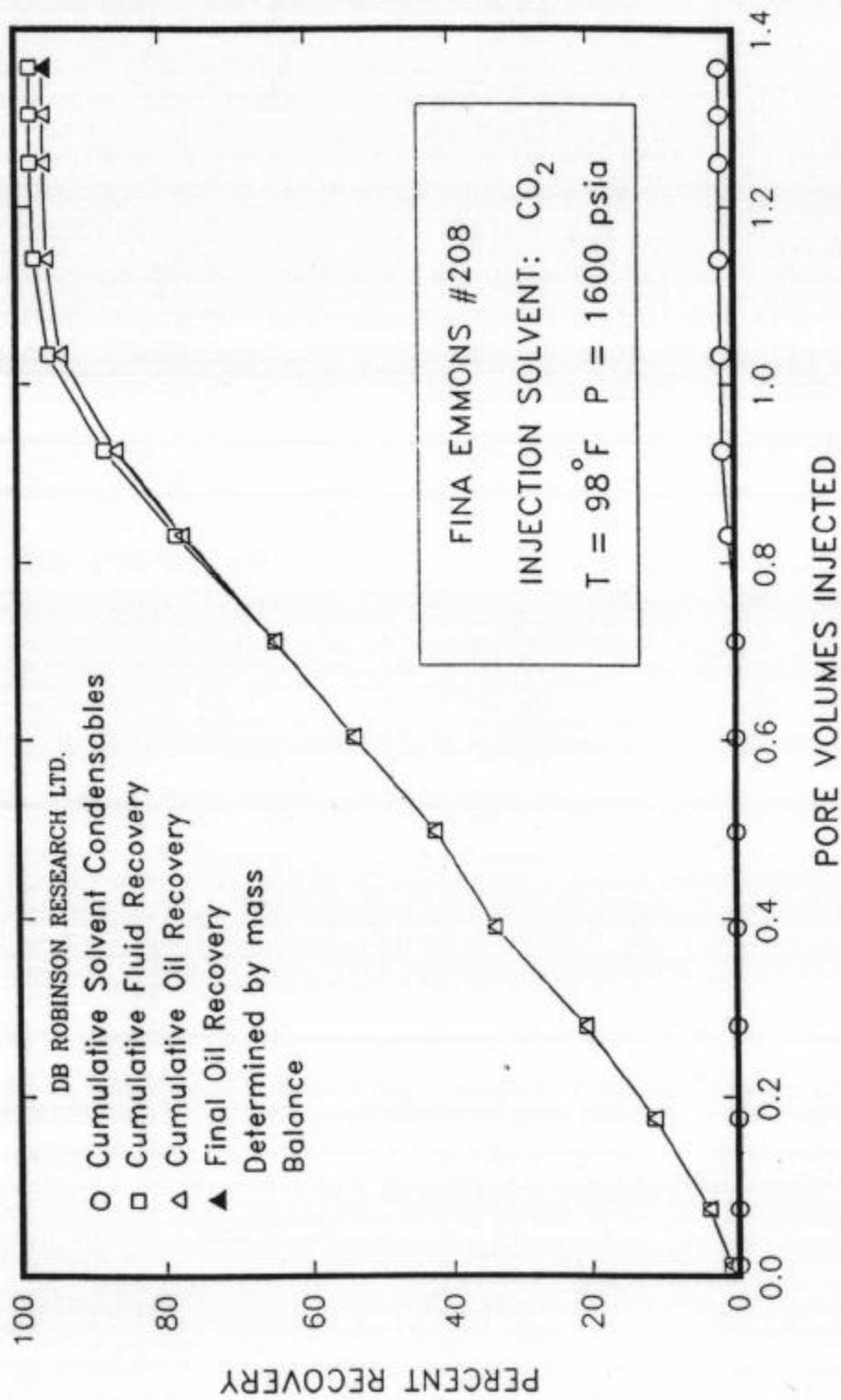


Figure 3.3. Cumulative Fluid Recovery for Slim Tube Run No. 1

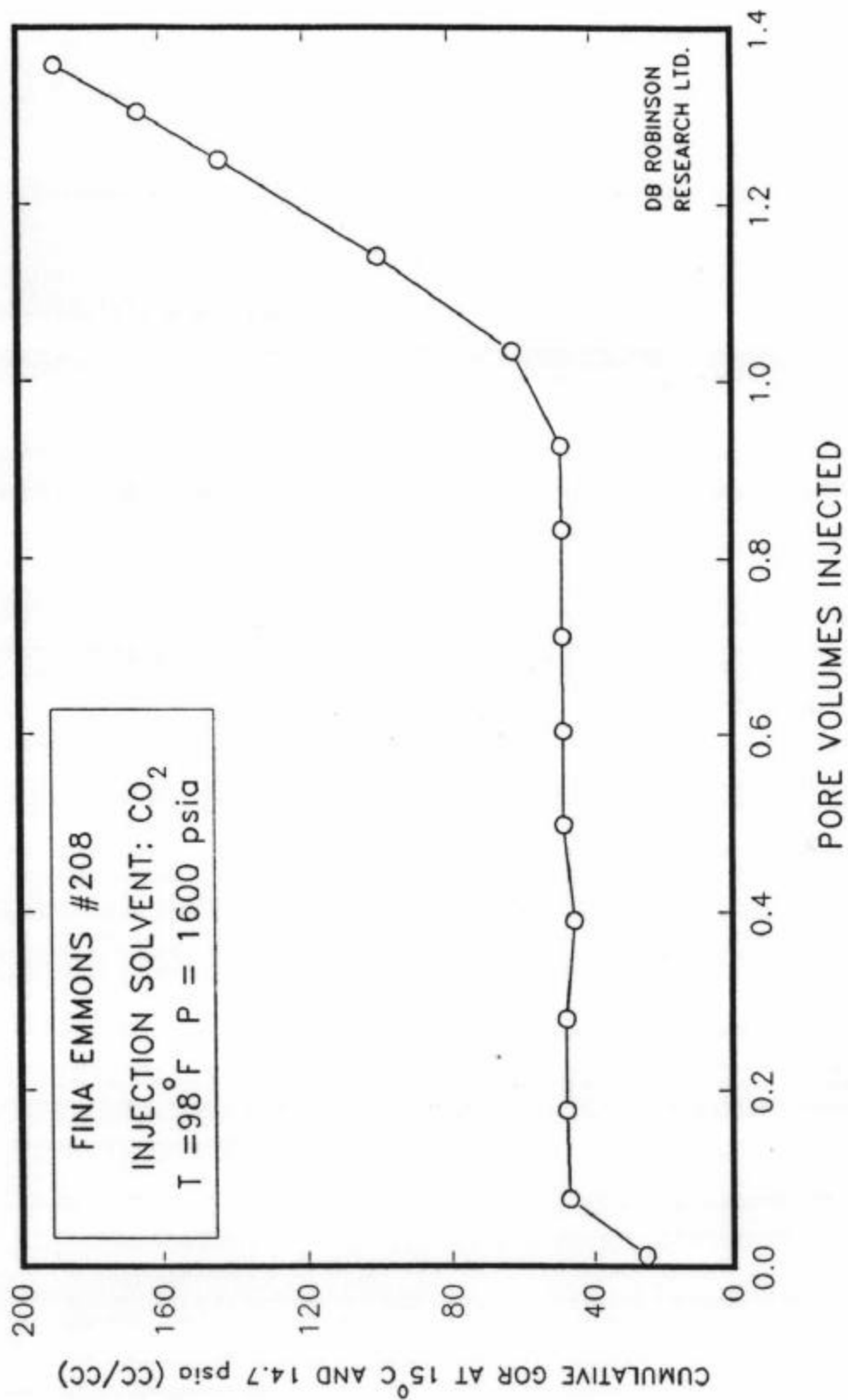


Figure 3.4. Cumulative GOR for Slim Tube Run No. 1

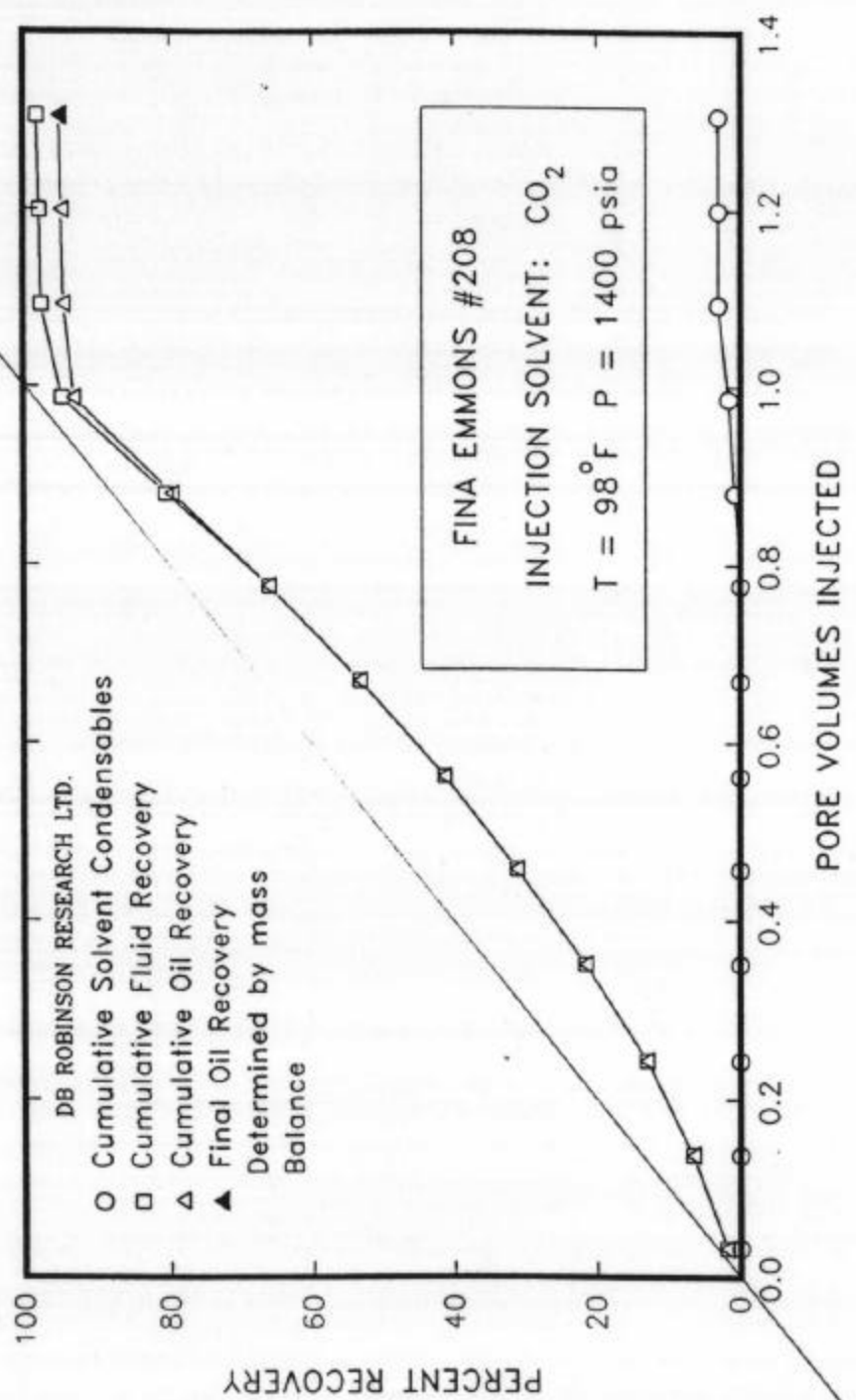


Figure 3.6. Cumulative Fluid Recovery for Slim Tube Run No. 2.

## **CORE ANALYSIS REPORTS**

## SUBTASK 1.6 CORE DESCRIPTION AND PETROGRAPHIC STUDIES

Craig D. Caldwell  
PPCo., Research and Services, Bartlesville, OK

### INTRODUCTION

Subtask 1.6, "Core Description and Petrographic Studies", focuses on the macroscopic and microscopic description of cores from four South Cowden Unit Grayburg wells, the SCU 8-19 (470' of core), 7-10 (249'), 8-11 (170'), and 6-23 (237')(Figs. 1-2). Additionally, a cursory description was made of the Grayburg reservoir interval in the Moss Unit 16-14 (~120' of core). The SCU 8-19 and 6-23 cores include the lower 120 and 35 ft., respectively, of the Queen Formation. The Grayburg and overlying Queen Formation are Upper Permian, Guadalupian age (Fig. 3).

Thin section samples from the SCU 8-19(97 t.s.), 7-10(63 t.s.), 6-23(15 t.s.), and 8-11(12 t.s.) and the Moss Unit 16-14(11 t.s.) were described and point counted. Thin section descriptions and point counting provide mineral and porosity percentages and information about depositional texture, diagenesis, and pore types. Scanning electron microscope studies of pore types and x-ray diffraction (XRD) analyses providing mineralogic data supplement the thin section studies. Twenty-four, twenty, and thirteen samples from the SCU 8-19, 7-10, and 8-11, respectively, were analyzed using XRD. The most complete Grayburg/Queen core (470') was recovered from the SCU 8-19; this well serves as a "type well" for much of the following discussion.

### LITHOFACIES DESCRIPTIONS

Eleven rock types, defined from Grayburg/Queen core studies, are grouped into five dolomite lithofacies (Fig. 4):

1. Fusulinid dolowackestone,
2. Ooid-peloid dolograinstone,
3. Sandy dolopackstone,
4. Burrow-mottled dolopackstone, and
5. Fenestral dolopackstone.

Fusulinid dolowackestones and ooid-peloid dolograinstones comprise the lower Grayburg Formation at South Cowden Unit. The middle part of the Grayburg is interbedded sandy dolopackstone, ooid-peloid dolograinstone, fusulinid

dolowackestone, and burrow-mottled dolopackstone, and the upper Grayburg is dominated by burrow-mottled dolopackstone. Sandy dolopackstones and fenestral dolopackstones make up the lower Queen Formation (Fig. 5).

Anhydrite composes generally less than 1% to 15% of Grayburg Formation samples and as much as 20 to 40% of Queen Formation samples. Siliciclastics are less than 5% in all lithofacies with the exception of the sandy dolopackstone lithofacies. Sandy dolopackstones of the Grayburg Formation and Queen Formation, respectively, are 10 to 20% and 10 to 40% very fine- to fine- grained detrital quartz and feldspar. Gypsum and calcite are generally absent or occur in trace amounts in the Grayburg and lower Queen. Depositional textures are difficult to distinguish in all lithofacies due to diagenesis and in particular dolomitization.

### FUSULINID DOLOWACKESTONE LITHOFACIES

Much of the lower Grayburg Formation at South Cowden Unit is composed of fusulinid dolowackestones and dolopackstones (Fig. 5 and Pl. 1). Fusulinid dolomites are rare in the middle part of the Grayburg Formation and absent in the upper Grayburg and overlying lower Queen Formation. Fusulinids are scarce to common, and echinoderm debris is rare in rocks of this lithofacies; no other bioclasts are distinguishable. Intergranular areas are dolomitized carbonate mud which commonly appears pelleted. Very fine- to fine-sand-size detrital quartz is less than 3%. Carbonaceous/argillaceous stylolitic seams and laminae result in the higher gamma- ray log values of the fusulinid dolowackestones and dolopackstones composing core units 4 and 5 of the SCU 8-19 (Fig. 5 and Pl. 1B). The change in gamma-ray log signature associated with this increase in carbonaceous/argillaceous material is observed at this stratigraphic level throughout the South Cowden Unit.

Fusulinid dolowackestone porosity is mainly biomoldic and intercrystalline (Pl. 2). Biomolds are typically leached fusulinids. Intragranular porosity within fusulinid chambers is very rare. Rare washed dolopackstone beds containing fusulinids, peloidal intraclasts, and ooids(?) display intergranular porosity as well as moldic and intercrystalline. Some burrow-mottled areas also have intergranular porosity. Fusulinid dolomites lacking burrow mottling generally have core analysis porosities of 5 to 17% and Kmax values of 0.4 to 2.5 md. Burrow-mottled, oil-stained fusulinid dolopackstones have core analysis porosities ranging from 15 to 20% and Kmax values from 280 to 880 md. Coarsely to very coarsely crystalline anhydrite varies from 3 to 14% in rocks of this lithofacies and commonly cements biomoldic porosity (Pl. 2 A).

The normal marine biota, bioturbation, including burrow mottled areas and small burrows elliptical in cross section, and generally muddy character of fusulinid dolowackestones and dolopackstones composing this lithofacies suggest deposition in an open-marine outer shelf setting in waters generally below normal wave base

perhaps a few tens of meters deep. Numerous authors have proposed a similar depositional setting for San Andres/Grayburg fusulinid wackestones and packstones in the Permian Basin (e.g., Bebout et al., 1987, Ruppel et al., 1988, Tyler et al., 1991, and Kerans et al., 1994).

### OOID-PELOID DOLOGRAINSTONE LITHOFACIES

Well sorted, medium- to coarse-grained ooid-peloid dolograins and washed dolopackstones occur mainly in the middle part of the Grayburg Formation (Fig. 5). Due to dolomitization ooid nuclei and cortices are difficult to distinguish (Pl. 3). Echinoderm debris, peloidal intraclasts, and grapestone grains are rarely identifiable. Rocks of this lithofacies display small- to medium-scale trough stratification (Pl. 4 A and B) and small relatively rare burrows, elliptical in cross section. Some beds are mottled due to variations in oil staining.

Dolograinstone and washed dolopackstone porosity is intergranular and relatively rare moldic (Pl. 3). Core analysis porosity is typically 6 to 16%, and K<sub>max</sub> varies generally from 3 to 350 md. The ooid dolograins interval at the top of the Grayburg Formation throughout the South Cowden Unit is partially cemented by coarsely to very coarsely crystalline anhydrite (Fig. 5, core unit 18, Pl 3 D). Dolograinstones elsewhere in the Grayburg Formation are generally less than 1% anhydrite. Intergranular porosity in these rocks has been occluded by finely to medium crystalline dolomite cement and trace amounts (<1%) of coarsely crystalline calcite cement.

Cross-bedded and burrowed ooid-peloid dolograins and washed dolopackstones record deposition on moderate to high-energy offshore shoals and in near-shoal areas. Water depths in this setting were a few meters or less. Wave and current energy on shoal crests winnowed mud- size material and produced oolitically coated grains. Carbonate shoals associated with this lithofacies may have formed a discontinuous fringe along the seaward edge of a broad shallow shelf platform.

### SANDY DOLOPACKSTONE LITHOFACIES

Sandy dolopackstones and dolomitic sandstones though relatively scarce in the Grayburg Formation dominate the cored portion of the overlying Queen Formation (Fig. 5). Sandy dolopackstones in the two formations display some noteworthy differences addressed below. Angular to subangular very fine- to fine-grained detrital quartz and feldspar compose typically 10 to 20% of this lithofacies in the Grayburg Formation and 10 to 40% of this lithofacies in the Queen Formation. Siliciclastic material is approximately 85 to 90% quartz and 10 to 15% potassium

feldspar. Carbonaceous/argillaceous stylolitic seams and laminae are common locally, and some beds contain small amounts of sand-size carbonaceous debris (Pl. 4 C and D, Pl. 5 A, and Pl. 6 A). Clay mineral content determined by XRD analyses varies from 1 to 7%. The relatively "hot" gamma-ray log character of sandy dolopackstones and dolomitic sandstones (Fig. 5) is related to the presence of clay minerals, carbonaceous debris, and detrital potassium feldspars. Anhydrite is generally less than 1% in sandy dolopackstones of the Grayburg Formation and less than 1% to 45% in sandy dolomites of the Queen Formation.

Carbonate grains in these rocks are predominantly fine-sand-size peloids of uncertain affinity, most likely fecal pellets and micritized bioclasts (Pls. 6 and 7). Medium- to coarse-sand-size grains, common in sandy dolopackstones of the Queen Formation and rare to common in the Grayburg Formation, include ooids and less numerous peloidal intraclasts (Pl. 6 B and D and Pl. 7 D). Fusulinids and echinoderms are present in some Grayburg sandy dolopackstone beds.

Sandy dolopackstones and washed dolopackstones of the Grayburg Formation are mottled commonly and display small burrows which are elliptical on the slabbed core surfaces. By contrast, sandy dolomites of the Queen Formation display horizontal and low-angle stratification, ripple cross stratification, and burrows (compare Pl. 5 A and B).

Porosity in these rocks is intergranular, intercrystalline, moldic, and leached feldspar (Pl. 6). Core analysis porosity is typically 10 to 13%, and K<sub>max</sub> is 0.1 to 9 md. Some sandy dolopackstone and dolomitic sandstone beds are characterized by permeabilities less than 1 md. The effect of these relatively low-permeability layers on reservoir production is discussed in the Reservoir Character section. Fieldwide sandy dolomite layers in the Grayburg Formation are used to establish the reservoir stratigraphy (see Stratigraphy section).

Low-angle and ripple stratification and common ooids and intraclasts in sandy dolopackstones of the Queen Formation indicate deposition in moderate to relatively high-energy marine waters a few meters or less in depth. The amount of quartz sand, typically greater than 20%, in these dolomites suggests an inner shelf nearshore setting. By contrast, sandy dolopackstones of the Grayburg Formation contain typically less than 20% quartz sand, are burrow mottled, and have relatively scarce ooids, intraclasts, fusulinids, and echinoderms suggesting lower energy, somewhat deeper water deposition in a more basinward setting. Ruppel (1995) suggested that sandy dolomites of the Grayburg Formation at South Cowden field represent the reworking of lowstand eolian deposits during a marine transgression (see Stratigraphy section).



## BURROW-MOTTLED DOLOPACKSTONE LITHOFACIES

South Cowden Unit reservoir rock is a burrow-mottled dolopackstone. These rocks display a distinctive vertically oriented gray/tan mottling reflecting variations in oil staining (Pl. 8). Tan oil-stained areas are commonly 2 to 8 cm in width, up to a few tens of centimeters in length, and are dolograins, dolopackstones, and washed dolopackstones. Tan areas are interpreted to be carbonate-sand-filled burrows. Gray lower porosity interburrow areas lack oil staining, are generally dolopackstones and dolowackstones, and commonly display short anhydrite-cemented fractures. The distinctive gray/tan mottling which characterizes rocks of this lithofacies was observed by the author at Rhodes Cowden field, to the north of South Cowden Unit, and described by numerous other authors working San Andres/Grayburg fields of the Permian Basin (e.g., Longacre, 1980, Bebout et al., 1987, Ruppel and Cander, 1988, and Major et al., 1990). Most of these papers relate this mottling to bioturbation.

Gray areas are a very finely to medium crystalline anhedral-dolomite mosaic (xenotopic fabric). Dolomite crystals are typically 0.01 to 0.1 mm in length with most crystals occurring in the coarser part of this size range i.e., 0.03 to 0.1 mm. Tan dolomite areas are generally finer crystalline and fall into one of three categories based on crystal size. Crystals composing tan dolomites of category I range typically from 0.01 to 0.1 mm (very fine to medium crystalline) with all crystal sizes represented approximately equally. Category II crystals likewise range generally from 0.01 to 0.1 mm, but crystals are predominantly less than 0.03 mm. Tan dolomites of category III are equigranular and very finely to finely crystalline, characterized by crystals less than 0.01 to 0.03 mm. Crystal size in the tan areas can markedly affect reservoir permeability as is discussed in the Reservoir Character section. Crystals composing the tan dolomite areas are typically euhedral to subhedral.

Carbonate grains are difficult to distinguish in burrow-mottled dolopackstones due to diagenesis. Fusulinids and echinoderms are recognizable in some mottled dolopackstone beds in the middle part of the Grayburg Formation, and ooids are distinguishable in some washed dolopackstone and dolograins areas. Bryozoans, green algae, and intraclasts are very rare. Most distinguishable grains are identified only as peloids. Quartz sand is generally absent.

Thin section study indicates that tan dolomite areas have significantly better porosity than the adjacent gray dolomites (Pl. 9). Core plugs were taken specifically from the tan and gray areas to determine the petrophysical properties of these dolomites. Twenty-one plugs were taken from the tan and gray dolomites in the SCU 8-19 core, and seventeen, twenty-seven, and fourteen plugs were taken from tan and gray dolomites in the SCU 7-10, 6-23, and 8-11 cores, respectively.

Gray dolomite plugs generally have 2 to 9% porosity and 0.002 to 2 md permeability. Porosity is moldic and less common intercrystalline (Pl. 9 A and B). Tan dolomite plugs have porosities ranging typically from 10 to 32% and permeabilities ranging from 2 to 400 md. (Figs. 6 and 7). Porosity in the tan areas is intergranular and less common moldic and intercrystalline (Pl. 9 C and D). Dolomite rhombs with leached centers, though common in some finely crystalline tan dolomites, are generally very rare and overall are not a volumetrically significant pore type. Tan carbonate-sand-filled burrows generally contained less intergranular carbonate mud than the adjacent interburrow areas and the resulting intergranular porosity acted as a conduit for the movement of later diagenetic fluids. Core analysis data indicate that burrow-mottled dolopackstone porosity is controlled, at least in part, by the relative amounts of gray and tan dolomite which are a function of bioturbation. Mottled dolopackstone porosity is related also to the amount of intergranular and intercrystalline anhydrite cement. An inverse relationship exists between porosity and anhydrite content. The possible role of anhydrite (or gypsum?) dissolution in porosity development is discussed later in this report.

Leary and Vogt (1986) and Major et al. (1990) studied the isotopic composition of San Andres burrow-mottled dolomites which closely resemble those of South Cowden Unit. Major and his co-workers stated that the "dark-colored unaltered dolomites" of East Penwell Unit, analogous to the gray dolomites of this study, have permeabilities of approximately 1 md or less and oxygen isotopic compositions in the range of 3 to 5.5‰ (PBD). Associated "lighter-colored altered dolomites", analogous to tan dolomites of this study, have permeabilities of approximately 10 md or more and depleted oxygen isotopic compositions of 1 to 4‰ (PDB) (permeabilities from Major's study were determined by minipermeameter). Similar isotopic compositions were published by Leary and Vogt (1986) in their study of San Andres dolomites of the Central Basin Platform. Leary and Vogt suggested that the porous tan dolomites recrystallized at a later time and at either higher temperatures or in isotopically lighter fluids than the associated gray dolomites. By contrast, Major et al. suggested that alteration of the lighter-colored dolomite areas may have resulted from late-stage leaching which increased permeability by widening intercrystalline pore throats and preferentially removing the early isotopically enriched centers of dolomite rhombs. This late-stage leaching resulted in the relatively depleted oxygen isotopic compositions of the tan areas.

Isotopic studies were not conducted for burrow-mottled dolopackstone at South Cowden Unit, but it is speculated that these dolomites are isotopically similar to those discussed in the forementioned studies. It is noteworthy that the dissolution of the central parts of dolomite rhombs is relatively rare in South Cowden Unit burrow-mottled dolopackstones, and in most samples this dissolution had very little effect on porosity and permeability and presumably little effect on isotopic composition of the tan areas.

The average whole-core analysis porosity of mottled dolopackstones composing Zone E of the Grayburg Formation varies from 12.8 to 15.5% for the four South Cowden Unit study wells. The arithmetic average Kmax for the four study wells varies from 4.9 to 30 md (K. Harpole, personal communication).

The variability of carbonate grain types, including fusulinids and ooids, presence of vertical carbonate-sand-filled burrows and muddy intergranular areas, and the general absence of detrital quartz in rocks of this lithofacies suggest deposition generally below normal wave base in open subtidal marine waters on the landward (westward) side of the outer shelf. Ruppel and Cander (1988) proposed an open platform setting for similar burrow-mottled carbonates at Emma San Andres Field, and Major et al. (1990) suggested a subtidal ramp setting for similar mottled pellet grainstones/packstones at East Penwell Unit.

### FENESTRAL DOLOPACKSTONE LITHOFACIES

Rocks of the fenestral dolopackstone lithofacies are restricted to the Queen Formation (Fig. 5). Anhydrite layers and lenses, a few millimeters to several centimeters thick, are associated with fenestral dolopackstones and dolowackestones (Pl. 5 C and D). In most cases these lenses and layers record cementation of dessication cracks by coarsely to very coarsely crystalline, blocky to bladed anhydrite. Finely textured, carbonate internal sediment lines the floor of some dessication structures, and anhydrite-cemented dessication cracks radiate from the upper surface of these structures. Anhydrite layers and associated fenestral dolopackstones and dolowackestones rarely are inclined with dips up to 30 degrees (Pl. 5 D). Inclined beds are interpreted to be teepee structures.

Carbonate grains in rocks of this lithofacies are fine-sand-size peloids, less numerous medium- to coarse-sand-size peloidal intraclasts and coated grains, and rare granule-size broken and coated grains, some resembling vadose pisolites. Thin beds of mollusk dolowackestone and dolopackstone are rare. Anhydrite-cemented fenestral dolopackstones are typically 20 to 25% anhydrite. Quartz sand is less than 1%.

Anhydrite cement occludes most of the porosity in fenestral dolopackstones and dolowackestones. Core analysis porosity and permeability data are not available, but wireline-log porosities are less than 4%.

The fenestral fabric, teepee structures, and anhydrite-cemented dessication cracks which characterize this lithofacies record intermittent subaerial exposure and supratidal deposition. The very small amounts of quartz sand present in fenestral dolopackstones may be indicative of a shelf crest rather than inner shelf setting. Kerans (1995) suggested a shelf crest setting for fenestral carbonates of the Queen Formation which outcrop along the northern shelf of the Delaware Basin.

## DEPOSITIONAL MODEL

During Grayburg and lower Queen deposition South Cowden Unit was part of a broad, gently eastward-dipping shelf or carbonate ramp which faced the Midland Basin. Fusulinid dolowackestones composing most of the lower Grayburg Formation record outer shelf deposition below normal wave base in waters generally a few tens of meters deep. Burrow-mottled dolopackstones composing most of the upper Grayburg reflect shallower water deposition in more landward portions of the outer shelf. The outer shelf passed landward (westward) into a high-energy shelf-crest setting characterized by cross-stratified ooid-peloid dolograins. This shoal-water setting faced prevailing northwesterly winds and open-marine waters of the Midland Basin (see Walker et al., 1995, for a discussion of Late Paleozoic paleogeography of the Permian Basin). Tidal flats may have developed on the landward side of some shoals. Quartz sand is very rare in outer shelf and shelf crest carbonates. The inner shelf was characterized by shallow-water mixed siliciclastic-carbonate deposition. In places wave and current energy in this setting was sufficient to produce oolitically coated grains. Cyclicity of the outer shelf, shelf crest, and inner shelf deposits is discussed below.

## STRATIGRAPHY

Fieldwide sandy dolomite layers characterized by relatively "hot" gamma-ray log signatures are used to divide the Grayburg Formation at South Cowden Unit into seven zones designated A-G in ascending order. These sandy dolopackstones and dolomitic sandstones form the basal units of Zones B, C, D, and F (Fig. 5). The relatively "hot" gamma-ray interval at the base of Zone E is related to the concentration of carbonaceous and argillaceous material along locally common stylolites.

Bebout et al. (1987), likewise, used dolomitic siltstones to establish the Grayburg stratigraphy at Dune field to the south of South Cowden Unit, and Ruppel and Cander (1988) stated that thin siliciclastic units form readily traceable marker beds at Emma San Andres field to the north of South Cowden Unit. Bebout stated that in the area of Dune field dolomitic siltstone beds represent geologic time lines and can be used to establish a time stratigraphic framework. Kerans et al. (1994) wrote that Grayburg dolomites which outcrop along the northwestern shelf of the Delaware Basin contain sandstone beds that record the reworking of eolian lowstand siliciclastics during marine transgression. A similar depositional setting was proposed by Ruppel (1995) for Grayburg dolomitic sandstones at South Cowden field.



Ruppel (1995) stated that the Grayburg Formation at South Cowden field contains four high-frequency sequences (HFS). These HFS are made up of smaller scale high-frequency cycles (HFC). This terminology employed by Ruppel (1995) and Kerans et al. (1995) is based on Mitchum and Van Wagoner's (1991) modification of sequence stratigraphy terminology developed by Vail (1987) and Van Wagoner et al. (1988). Kerans (1995) stated that high-frequency sequences and composite sequences conform to the general definition of depositional sequences, being relatively conformable sets of strata bounded by subaerial unconformities or their correlative conformities. Kerans wrote that composite sequences, made up of two or more HFS, are most similar in scale to seismically resolvable depositional sequences originally discussed by Vail and his co-workers. The term HFC is substituted for Vail and Van Wagoner's parasequence. Kerans estimates that HFS and HFC are 4th and 5th order cycles respectively.

Sandy dolopackstones and dolomitic sandstones comprising core units 10K, 12A, and 15 in the SCU 8-19 (Fig. 5) correlate with the basal transgressive units of three of Ruppel's HFC recognized at South Cowden field (Fig. 8). Application of Kerans and Ruppel's sequence stratigraphy model to Grayburg rocks described in this study suggests that a typical HFC consists of a basal transgressive sandy dolopackstone/dolomitic sandstone, recording reworking of lowstand eolian deposits, overlain by outer shelf fusulinid dolowackestone and/or burrow-mottled dolopackstone and capping the cycle a regressive, shelf-crest ooid-peloid dolograine.

In an alternative model, sandy dolopackstones and dolomitic sandstones of the Grayburg Formation may record deposition in subtidal marine waters landward of the shelf-crest oolite shoals and record the final phase of marine regression. In this model fusulinid dolowackestones and burrow-mottled dolopackstones record the initial phases of marine transgression. These rocks are overlain by regressive ooid-peloid dolograine and capping the sequence sandy dolopackstones. This model lacks the regional insights of Kerans and Ruppel's work, however, and at present is considered the least attractive of the two models.

## RESERVOIR CHARACTER

Grayburg porosity and permeability at South Cowden Unit are a function of original depositional texture and diagenesis. Biomoldic and intercrystalline porosity characterizing rocks of the fusulinid dolowackestone lithofacies, lower Grayburg, is due to secondary dissolution of carbonate grains and intergranular mud. Intergranular porosity in the overlying ooid-peloid dolograine and in some burrow-mottled fusulinid dolopackstones is thought to be mainly primary. These two lithofacies, in places displaying good porosity and permeability, generally occur below the oil/water contact at South Cowden Unit and thus are not hydrocarbon productive. Grayburg sandy dolopackstones above the oil/water contact are

generally finely textured and have relatively poor permeabilities. Porosity in sandy dolopackstones and fenestral dolopackstones composing the Queen Formation is typically occluded by anhydrite cement.

South Cowden Unit reservoir rocks are burrow-mottled dolopackstones. Porosity in these rocks is mainly a function of bioturbation and anhydrite cementation. As discussed in the lithofacies descriptions, tan carbonate-sand-filled burrows have porosities generally ranging from 10 to 32%, and gray interburrow areas have porosities ranging from 2 to 9% (Figs. 6 and 7). Porosity in the tan areas is intergranular, moldic, and intercrystalline. Porosity due to the partial dissolution of dolomite rhombs is rare in most tan dolomites.

A clear mylar sheet with a 1-inch-square grid was used to estimate the relative amounts of gray and tan dolomite and nodular anhydrite for each 1-foot interval of burrow-mottled dolopackstone. The mylar sheet was placed on the slabbed core surface, and the number of squares of gray dolomite, tan dolomite, and nodular anhydrite were counted. Percentages were calculated and plotted on the wireline-log/core graph (Fig. 5). Those intervals dominated by gray dolomite typically have relatively low wireline-log porosities; intervals dominated by tan dolomite typically have relatively good porosities. Comparison of the gray/tan plot and wireline-log porosity for the SCU 8-19 reservoir interval shows that porosity variation is largely a function of the varying amounts of gray and tan dolomite related to the degree of bioturbation. Low-porosity gray-dolomite layers and high-porosity tan-dolomite layers can be correlated in the four SCU study wells in some cases. Laterally continuous gray-dolomite layers may reflect times when depositional conditions were less conducive to bioturbation.

An inverse relationship exists between anhydrite content and porosity in tan dolomites of the burrow-mottled dolopackstone lithofacies i.e., as the amount of poikilotopic anhydrite increases porosity decreases (Fig. 9). Poikilotopic anhydrite cements intergranular, intercrystalline, and moldic pores and replaces dolomite in the tan areas (Pl. 10 C and D). In the lower porosity gray dolomites poikilotopic anhydrite is essentially absent. Though based on limited data, there appears to be a general increase in anhydrite and corresponding decrease in reservoir porosity in wells in the northwestern part of the study area (i.e., compare SCU 8-19 and 6-23 to the more westward SCU 8-11 and Moss Unit 16-14, Fig. 9). This regional variation may be related to a northwestward (paleolandward) source of anhydrite-(or gypsum-?)precipitating fluids.

Ruppel (1995) suggested that sulfate (anhydrite and/or gypsum) dissolution was critical to porosity development in mottled dolomites of the Grayburg Moss Unit immediately to the north of South Cowden Unit. Direct evidence of sulfate dissolution is not readily apparent, however, in most South Cowden Unit burrow-mottled dolopackstones. Partial dissolution of the edges of anhydrite patches is rare in tan dolomites of the burrow-mottled dolopackstone lithofacies. Additionally, pores which would result from poikilotopic anhydrite dissolution in the category II

and III tan dolomites would be significantly larger than the observed pores in these rocks (Pl. 10D). By contrast, the dolomite fabric of some category I anhydrite-cemented areas is very similar to that of immediately adjacent porous areas lacking anhydrite cement suggesting porosity development in these dolomites may have been related in part to sulfate dissolution (Pl. 10 C).

Burrow-mottled dolopackstone permeability is a function of bioturbation, anhydrite content, and pore size; the later is related to crystal size and depositional texture of the tan dolomites. As discussed in the Lithofacies Descriptions section, tan dolomites fall into one of three categories based on crystal size. These categories, designated I, II, and III, are characterized by progressively smaller crystals. Decreases in crystal size are accompanied by decreases in pore size and lower permeabilities. These decreases in permeability are not necessarily related to decreases in porosity. For example, the average porosity of tan dolomite plugs from the SCU 6-23 and 7-10 wells is the same, but the average permeability of plugs from the 7-10 is nearly an order of magnitude less than that of plugs from the 6-23 (Fig. 10). Whole core analysis data of burrow-mottled dolopackstones from these two wells also show this relationship (Fig. 11) and suggest a single porosity/permeability transform may not be adequate to describe the porosity/permeability relationships at South Cowden Unit.

The relatively low permeabilities associated with tan dolomites of the SCU 7-10 are a function of smaller pore-body and pore-throat size (Pl. 10 A and B). Tan dolomites of the SCU 6-23 are predominantly category I, while tan dolomites of the 7-10 are predominantly category III. Burrowing-filling sediments comprising tan dolomite areas in the 7-10 are thought to be finer grained and muddier resulting in smaller dolomite crystal size, decreased intergranular porosity, and smaller pore size. Burrow-filling sediments in the 7-10 appear to be mainly dolopackstones, while those in the 6-23 include dolopackstones, washed dolopackstones, and dolograins. High permeability category I dolomites characterizing the SCU 8-19 likewise appear to be mainly dolograins and washed dolopackstones. Core data is limited, but muddier sediments resulting in category II and III tan dolomites characterizing much of the 7-10 and 8-11 may dominate burrow fillings in the western (paleolandward) part of South Cowden Unit.

Sandy dolopackstone/dolomitic sandstone layers used to establish the reservoir stratigraphy at South Cowden Unit may in some cases partially restrict the vertical movement of fluids and gases within the reservoir. The sandy dolopackstone layer at the base of Zone D, "separating" Zone D from Zone C, has an average Kmax of less than 0.1 to 0.55 md. and an average porosity of approximately 10% in the four study wells (Fig. 5, core unit 12A and Pl. 4 D and 6 D). This low-permeability layer and a thin, low-permeability, anhydrite-cemented fusulinid dolowackstone layer near the middle of Zone D (Kmax values of 0.2 to 2.8 md.) (Fig. 5, core unit 13A and Pl. 1 C) may partially restrict vertical flow between Zone C and reservoir rock composing the upper part of Zone D. RFT data from the SCU 8-19 and 6-23 suggest vertical communication between Zones C and D is partially

restricted. By contrast, the relatively "hot" gamma-ray interval at the base of Zone E is not associated with a sandy dolomite layer, and the average Kmax over this interval for the four study wells varies from 0.37 to 15 md., suggesting Zone E and the upper part of Zone D are in communication.

The average Kmax of the sandy dolomite layer at the base of Zone F, "separating" Zones E and F, varies from 0.23 to 0.6 md in the SCU 8-19, 7-10, and 6-23 but is significantly higher, 6.6 md, in the SCU 8-11. Average core analysis porosity for this layer is 9.5 to 13.5%. While petrographic studies hint that this layer may act as a partial restriction to vertical flow in some wells, RFT data from the SCU 8-19 and 6-23 suggest Zones E and F are in pressure communication.

Low-porosity gray-dolomite-dominated layers in burrow-mottled dolopackstones composing the reservoir interval should not form significant barriers to the vertical movement of reservoir fluids and gases. These layers contain a reduced but still significant amount (25-40%) of tan high-porosity and permeability dolomite typically occurring as vertically oriented structures. RFT data from Zone E in the SCU 8-19 and 6-23 indicate this zone is in vertical communication throughout despite the presence of low-porosity gray-dolomite layers.

## CONCLUSIONS

Fieldwide sandy dolomite layers characterized by relatively "hot" gamma-ray log signatures are used to divide the Grayburg Formation at South Cowden Unit into seven zones designated A-G in ascending order. Zones C-F constitute the reservoir interval. The reservoir interval, approximately 150 ft. (45.8m) thick, is mainly burrow-mottled dolopackstone, recording subtidal open-marine shelf or carbonate ramp deposition. These rocks are characterized by a distinctive vertically oriented gray/tan mottling. Tan dolomite areas are carbonate-sand-filled burrows and have core analysis porosities generally ranging from 10 to 32% and permeabilities ranging from 2 to 400 md. Porosity in the tan dolomite includes intergranular, intercrystalline, and moldic. Gray interburrow areas typically have porosities of 2 to 9% and permeabilities of 0.002 to 2 md.

Reservoir porosity is mainly a function of the degree of bioturbation i.e., the relative amounts of gray and tan dolomite in burrow-mottled dolopackstones, and anhydrite content. An inverse relationship exists between anhydrite content and porosity, and limited core data presented in this study suggest an increase in anhydrite and corresponding decrease in porosity in the northwestern (paleolandward) part of the Unit.

Reservoir permeability is a function of bioturbation, anhydrite content, and pore size; the later is related to depositional texture and crystal size of the tan



dolomites. Smaller pore sizes and lower permeabilities are generally associated with finer crystalline tan dolomites. These lower permeabilities are not necessarily associated with lower porosities. The finer crystalline tan dolomites are most likely muddier sand-filled burrows (i.e., dolopackstones). Limited data from the study wells suggest burrow-fill sediments may be muddier in the western parts of South Cowden Unit resulting in lower permeability reservoir rock and the need for more than one porosity/permeability transform to represent the unit.

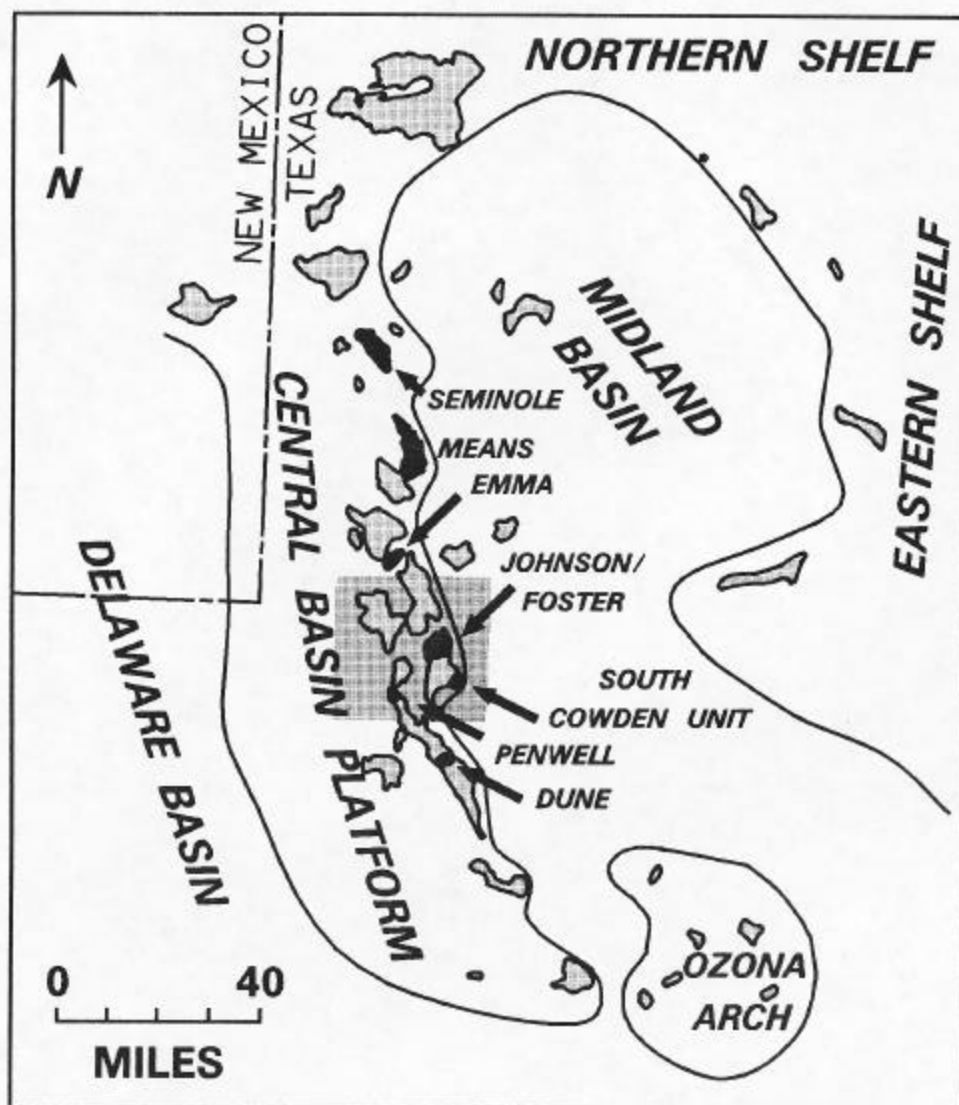
The laterally continuous sandy dolomite layer at the base of Zone D and the low-porosity, anhydrite-cemented fusulinid dolowackestone layer in the middle of Zone D may act as partial restrictions to vertical flow between reservoir rocks of Zone C and burrow-mottled dolopackstones composing the upper part of Zone D. RFT data from the SCU 8-19 and 6-23 suggest vertical communication between Zone C and the upper part of Zone D is limited. Petrographic studies suggest that the sandy dolomite layer at the base of Zone F may partially restrict flow between Zones E and F in some wells; RFT data from the SCU 8-19 and 6-23 do not appear to support this interpretation. Neither petrographic nor RFT data indicate a restriction to flow between Zones D and E. Low-porosity, gray-dolomite-dominated layers in the reservoir interval contain a reduced but still significant amount (25-40%) of porous and permeable tan dolomite and should not act as barriers to the vertical migration of fluids and gases. In general, the vertically oriented, high-permeability tan dolomite areas created by burrowing provide a favorable condition for the application of a CO<sub>2</sub> flood using horizontal injection wells.

## REFERENCES

- Bebout, D. G., F. J. Lucia, C. R. Hocott, G. E. Fogg, and G. W. Vander Stoep, 1987, Characterization of the Grayburg Reservoir, University Lands Dune Field, Crane County, Texas: Univ. Texas, Austin, Bureau of Economic Geology, Report of Investigations No. 168, 98 p.
- Galloway, W. E., T. E. Ewing, C. M. Garrett, N. Tyler, and D. G. Bebout, 1983, Atlas of major Texas oil reservoirs: Univ. Texas, Austin, Bureau of Economic Geology, 139 p.
- Kerans, C., 1995, Use of one- and two-dimensional cycle analysis in establishing high-frequency sequence frameworks, *in* J. F. Read, C. Kerans, and L. J. Weber, eds., Milankovitch sea-level changes, cycles, and reservoirs on carbonate platforms in greenhouse and ice-house worlds: Society of Economic Paleontologists and Mineralogists, Short Course No. 35, part 2, p. 1-20.
- \_\_\_\_\_, F. J. Lucia, R. K. Senger, 1994, Integrated characterization of carbonate ramp reservoirs using Permian San Andres Formation outcrop analogs: American Association of Petroleum Geologists Bulletin, v. 78, no. 2, p. 181-216.
- Leary, D. A. and J. N. Vogt, 1986, Diagenesis of the Permian (Guadalupian) San Andres Formation, Central Basin Platform, West Texas *in* D. G. Bebout and P. M. Harris, eds., Hydrocarbon reservoir studies San Andres/Grayburg Formations, Permian Basin: PBS-SEPM Pub. No. 86-26.
- Longacre, S. A., 1980, Dolomite reservoirs from Permian biomicrites, *in* R. B. Halley and R. G. Loucks, eds., Carbonate reservoir rocks: Society of Economic Paleontologists and Mineralogists, Core Workshop No. 1, p. 105-117.
- Major, R. P., G. W. Vander Stoep, and M. H. Holtz, 1990, Delineation of unrecovered mobile oil in a mature dolomite reservoir: East Penwell San Andres Unit, University Lands, West Texas: Univ. Texas, Austin, Bureau of Economic Geology, Report of Investigations no. 194, 51 p.
- Mitchum, R. M., Jr., and J. C. Van Wagoner, 1991, High-frequency sequences and their stacking patterns: Sequence-stratigraphic evidence of high-frequency eustatic cycles, *in* K. T. Biddle and W. Schlager, eds., The record of sea-level fluctuations: Sedimentary Geology, v. 70, p. 131-160.
- Ramondetta, P. J., 1982, Facies and stratigraphy of the San Andres Formation, northern and northwestern shelves of the Midland Basin, Texas and New Mexico: Univ. Texas, Austin, Bureau of Economic Geology, Report of Investigations No. 116, 56 p.

- Ruppel, S. C. 1995, Effects of stratal architecture and diagenesis on reservoir development in the Grayburg Formation, South Cowden field, Ector County Texas: Univ. Texas, Austin, Bureau of Economic Geology, Technical Report.
- \_\_\_\_\_, and H. S. Cander, 1988, Effects of facies and diagenesis on reservoir heterogeneity: Emma San Andres Field, West Texas: Univ. Texas, Austin, Bureau of Economic Geology, Report of Investigations No. 178, 67 p.
- Tyler, N., D. G. Bebout, C. M. Garrett, Jr., E. H. Guevara, C. R. Hocott, M. H. Holtz, S. D. Hovorka, C. Kerans, F. J. Lucia, R. P. Major, S. C. Ruppel, and G. W. Vander Stoep, 1991, Integrated characterization of Permian Basin reservoirs, University Lands, West Texas: targeting the remaining resource for advanced oil recovery: Univ. Texas, Austin, Bureau of Economic Geology, Report of Investigations No. 203, 136 p.
- Vail, P. R., 1987, Seismic stratigraphy interpretation procedure, *in* A. W. Bally, ed., Atlas of seismic stratigraphy, vol. 1: American Association of Petroleum Geologists studies in Geology, no. 27, p. 1-10.
- Van Wagoner, J. C., H. W. Posamentier, R. M. Mitchum, Jr., P. R. Vail, J. F. Sarg, T. S. Loutit, and J. Hardenbol, 1988, An overview of the fundamentals of sequence stratigraphy and key definitions, *in* C. K. Wilgns, B. S. Hastings, C. G. St. C. Kendall, H. W. Posamentier, C. A. Ross, and J. C. Van Wagoner, eds., Sea-level changes: An integrated approach: Society of Economic Paleontologists and Mineralogists Special Publication No. 42, p. 39-46.
- Walker, D. A., J. Golonka, A. Reid, and S. Reid, 1995, The effects of paleolatitude and paleogeography on Late Paleozoic carbonate sedimentation in West Texas; Part II: Permian: West Texas Geological Society, vol. 34, no. 6, p. 5-15.

FIGURE 1



SYSTEM	SERIES	STRATIGRAPHIC UNIT
UPPER PERMIAN	GUADALUPIAN	TANSILL FM.
		CAPITAN FM.
		YATES FM.
		SEVEN RIVERS FM.
		GOAT SEEP
LOWER PERMIAN	LEONARDIAN	QUEEN FM.
		GRAYBURG FM.
		SAN ANDRES FM.
		GLORIETA FM.
		CLEAR FORK GP.

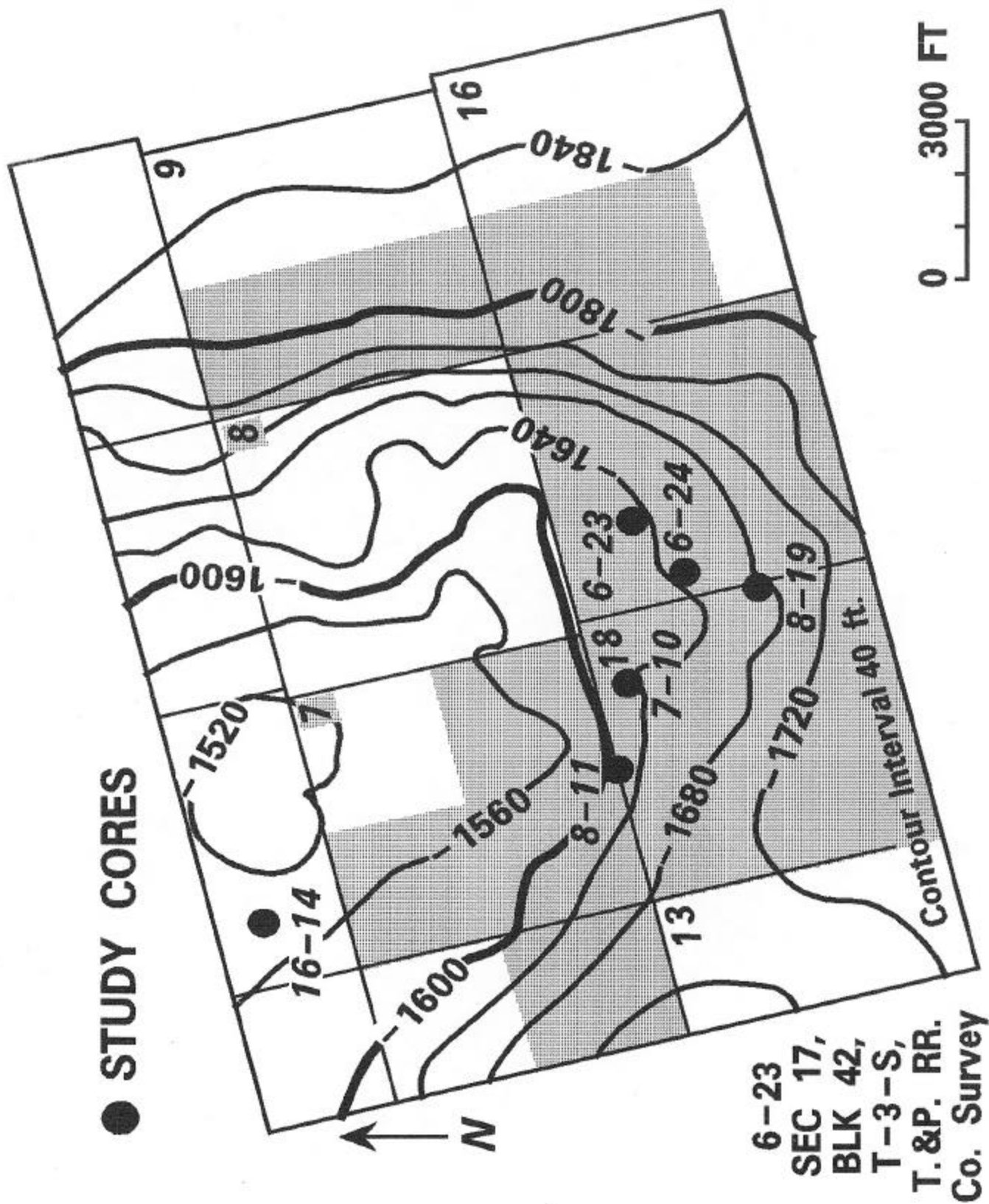
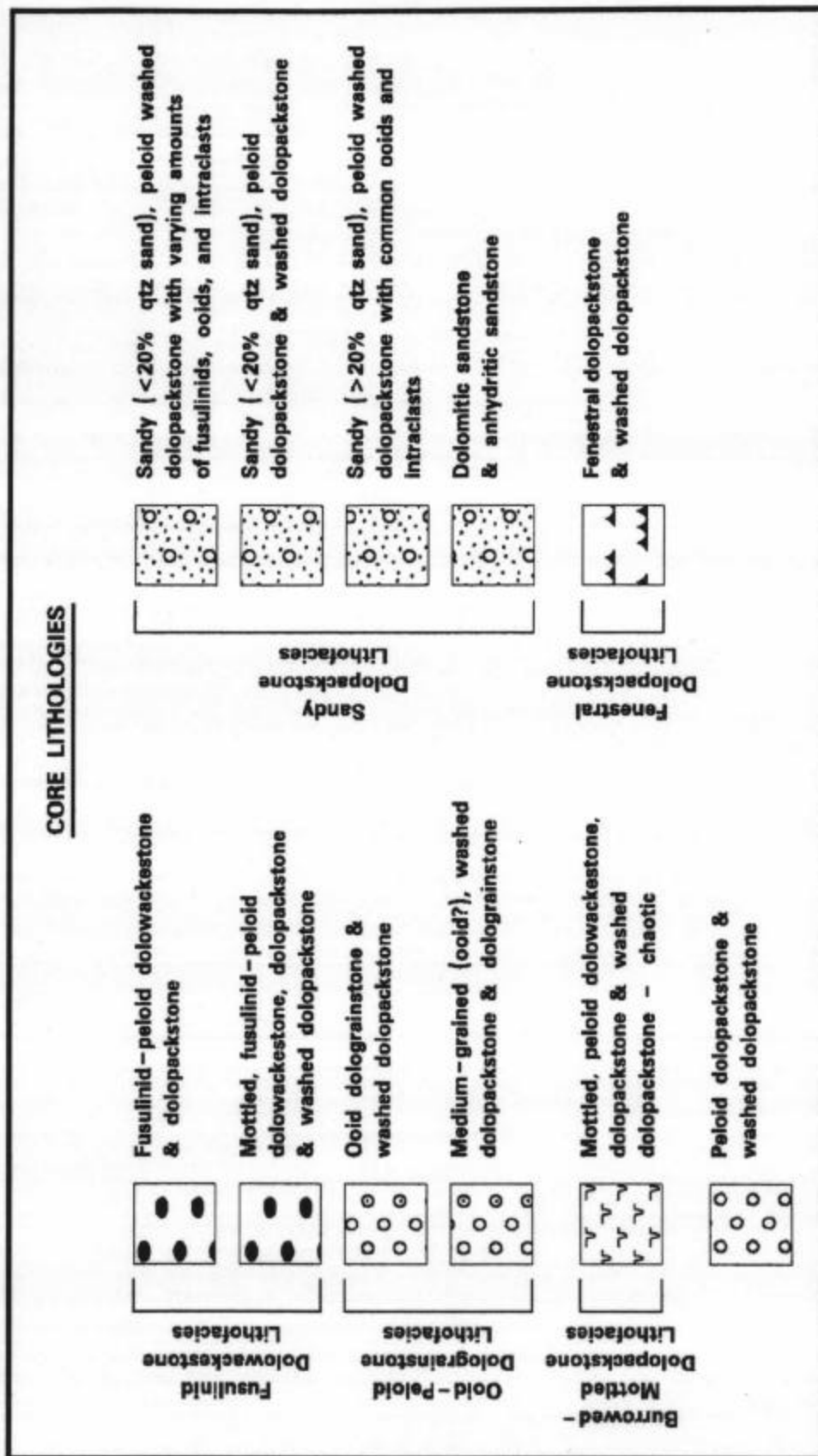


FIGURE 2

<b>SYSTEM</b>	<b>SERIES</b>	<b>STRATIGRAPHIC UNIT</b>
<b>UPPER PERMIAN</b>	<b>OCHOAN</b>	<b>DEWEY LAKE</b>
		<b>RUSTLER</b>
		<b>SALADO</b>
		<b>CASTILE</b>
	<b>GUADALUPIAN</b>	<b>CAPITAN</b> { <b>TANSILL</b>
		<b>YATES</b>
		<b>SEVEN RIVERS</b>
		<b>GOAT SEEP</b> { <b>QUEEN</b>
		<b>GRAYBURG</b>
		<b>SAN ANDRES</b>
<b>LOWER PERMIAN</b>	<b>LEONARDIAN</b>	<b>West Texas Permian Section</b> <b>(Galloway et al., 1983)</b>
	<b>WOLFCAMPIAN</b>	

**FIGURE 3**





AFE/CC092994A. DGM KRC

**FIGURE 4**

FIGURE 5a

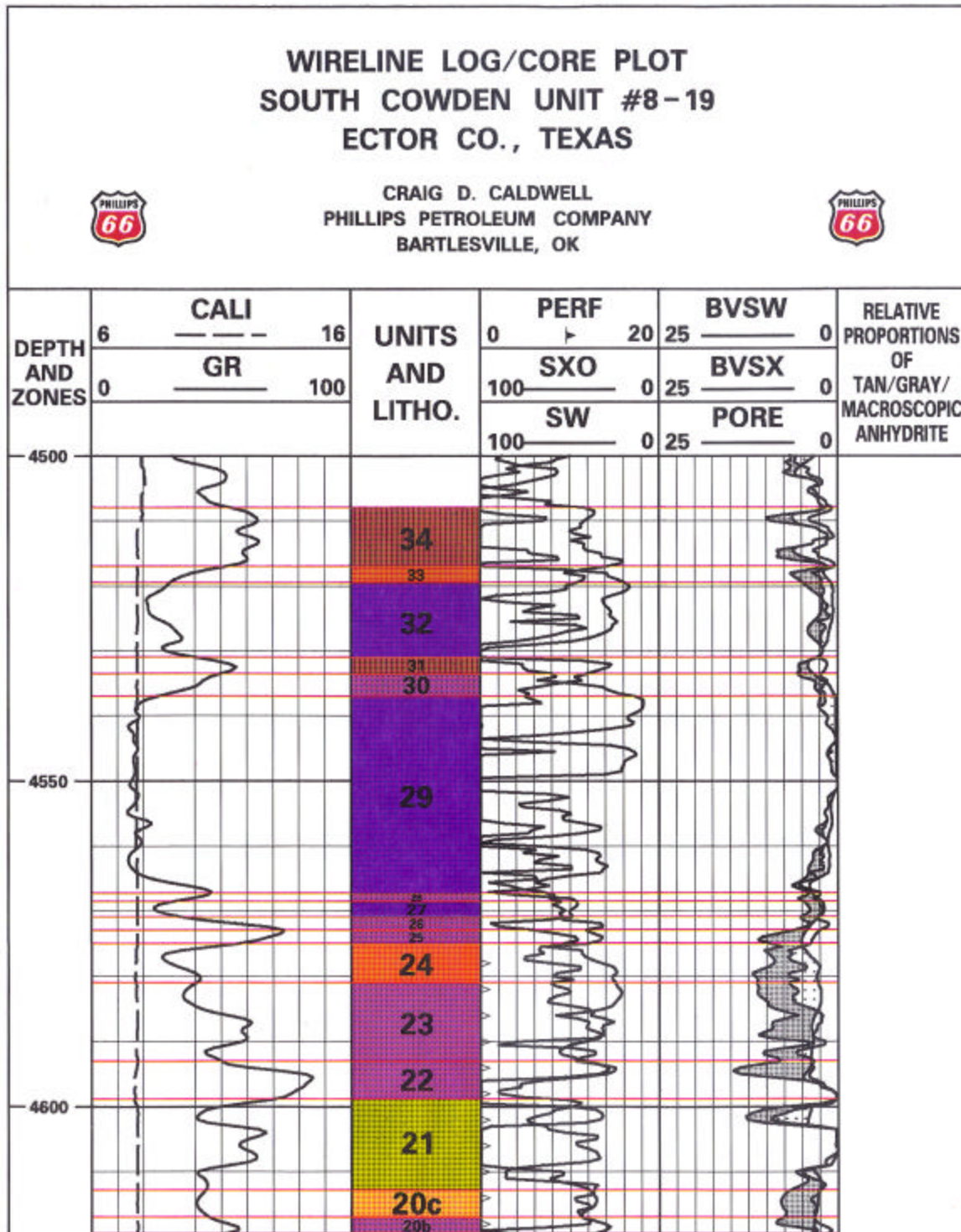




FIGURE 5b

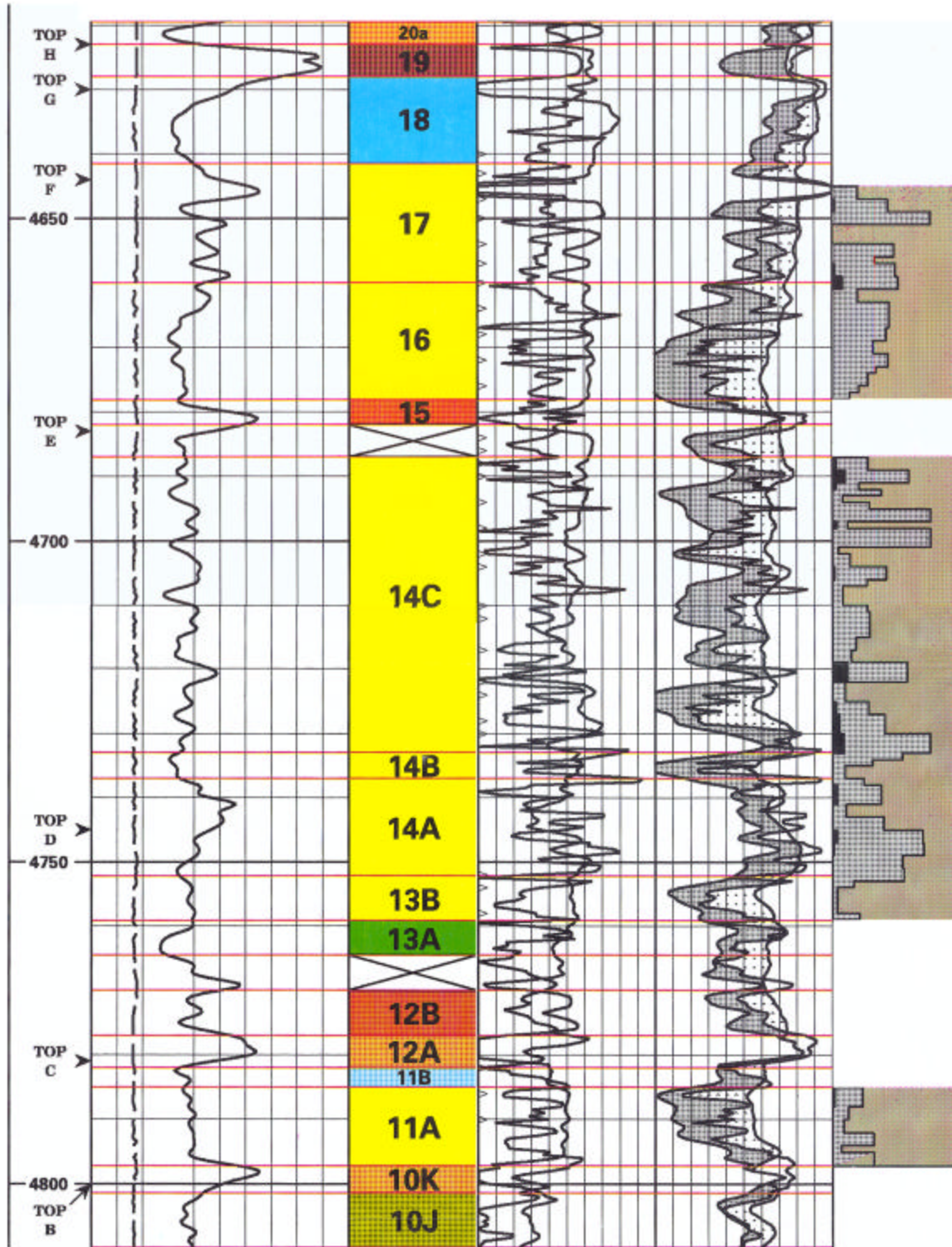


FIGURE 5c

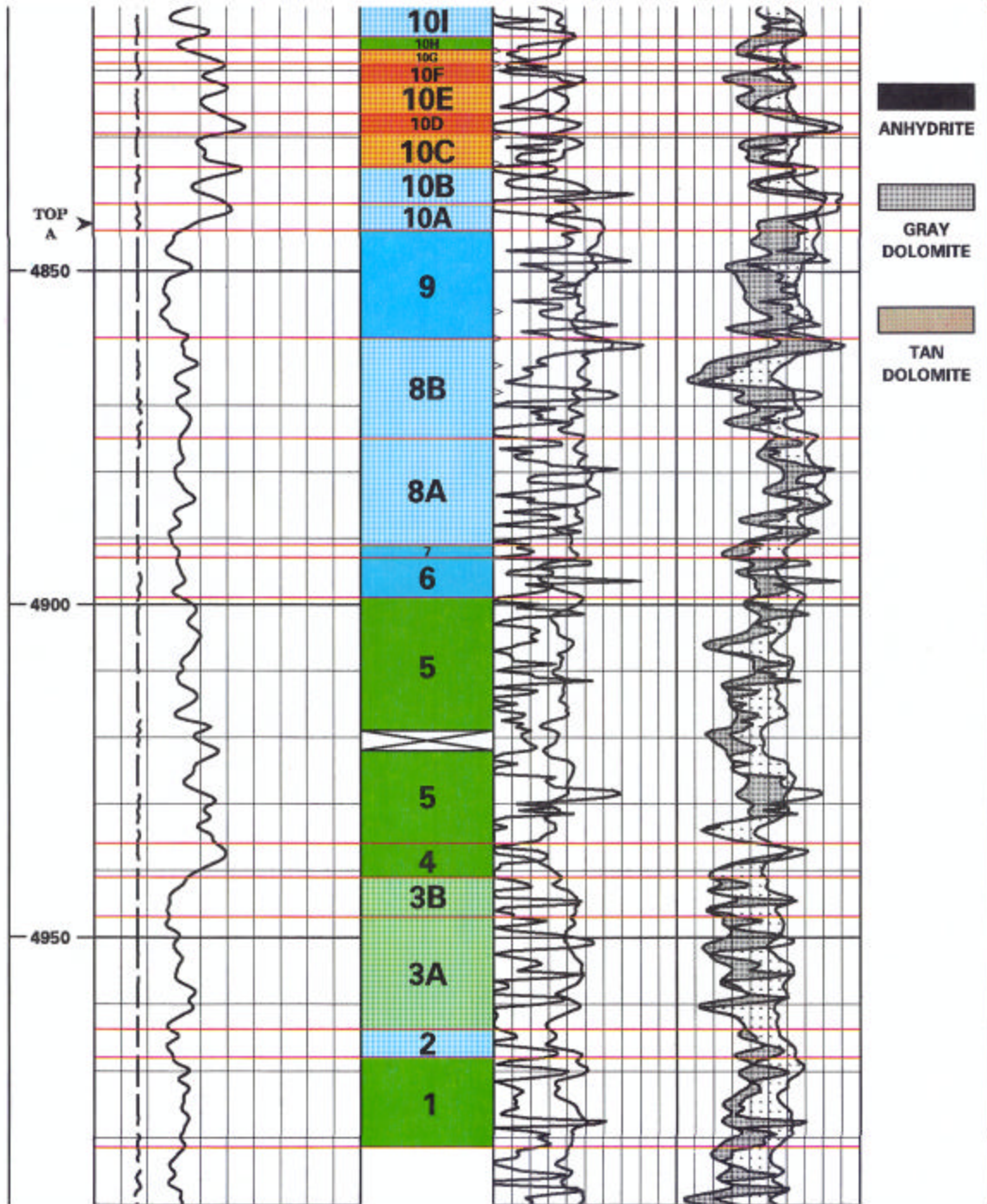
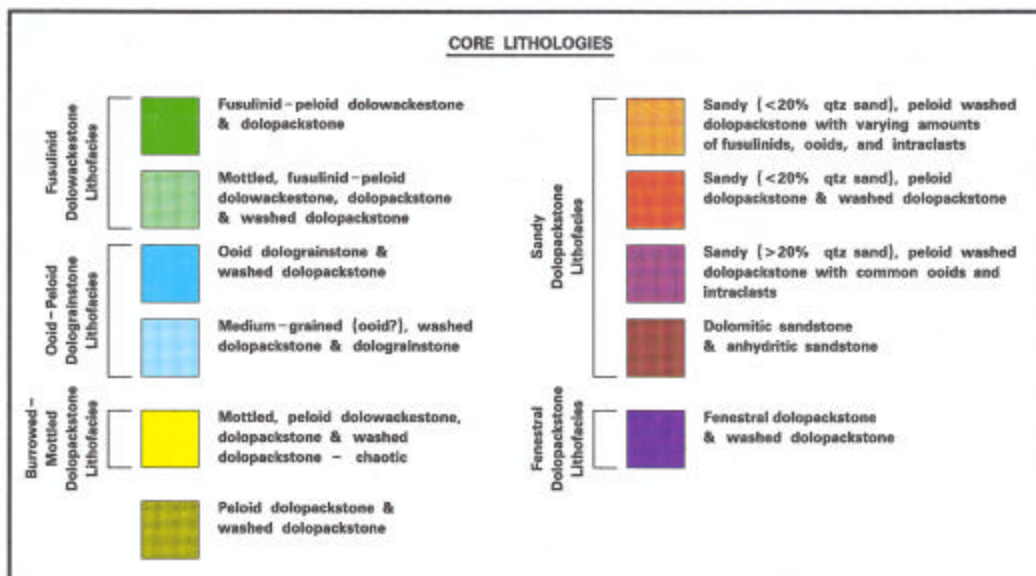
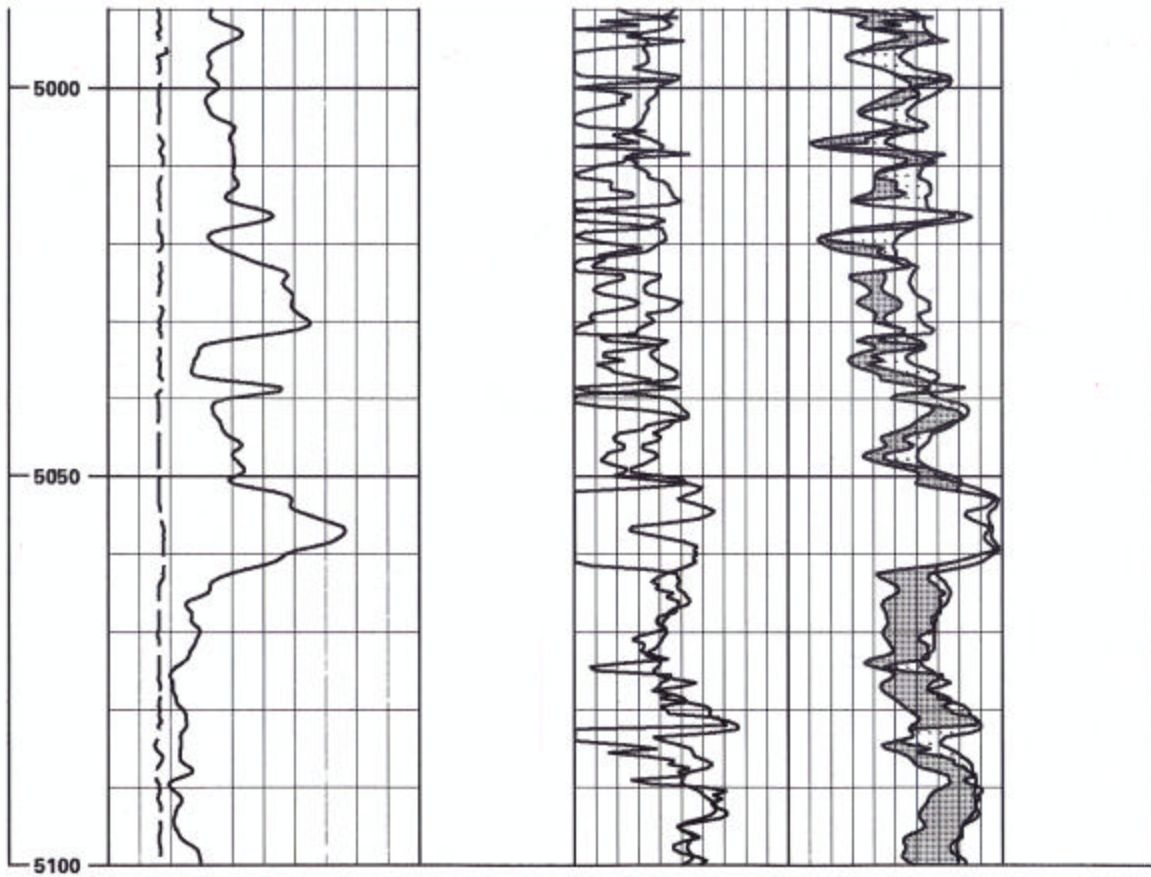




FIGURE 5d



**FIGURE 6**

***CHARACTERISTICS OF TAN AND GRAY DOLOMITES,  
BURROW-MOTTLED DOLOPACKSTONE LITHOFACIES***

**GRAY DOLOMITE**

**2 to 9% Porosity\***

**0.002 to 2 md Permeability**

**Moldic and Intercrystalline Porosity**

**Dolowkst. and Dolopkst.**

**TAN DOLOMITE**

**10 to 32% Porosity\***

**2 to 400 md Permeability**

**Intergranular, Moldic, and Intercrystalline Porosity**

**Dolopkst., Washed Dolopkst., and Dolognst.**

**Oil Stained**

**\* Core Analysis**

***Porosity/Permeability Plot for Tan and Gray Dolomites  
of the Burrow-Mottled Dolopackstone Lithofacies***

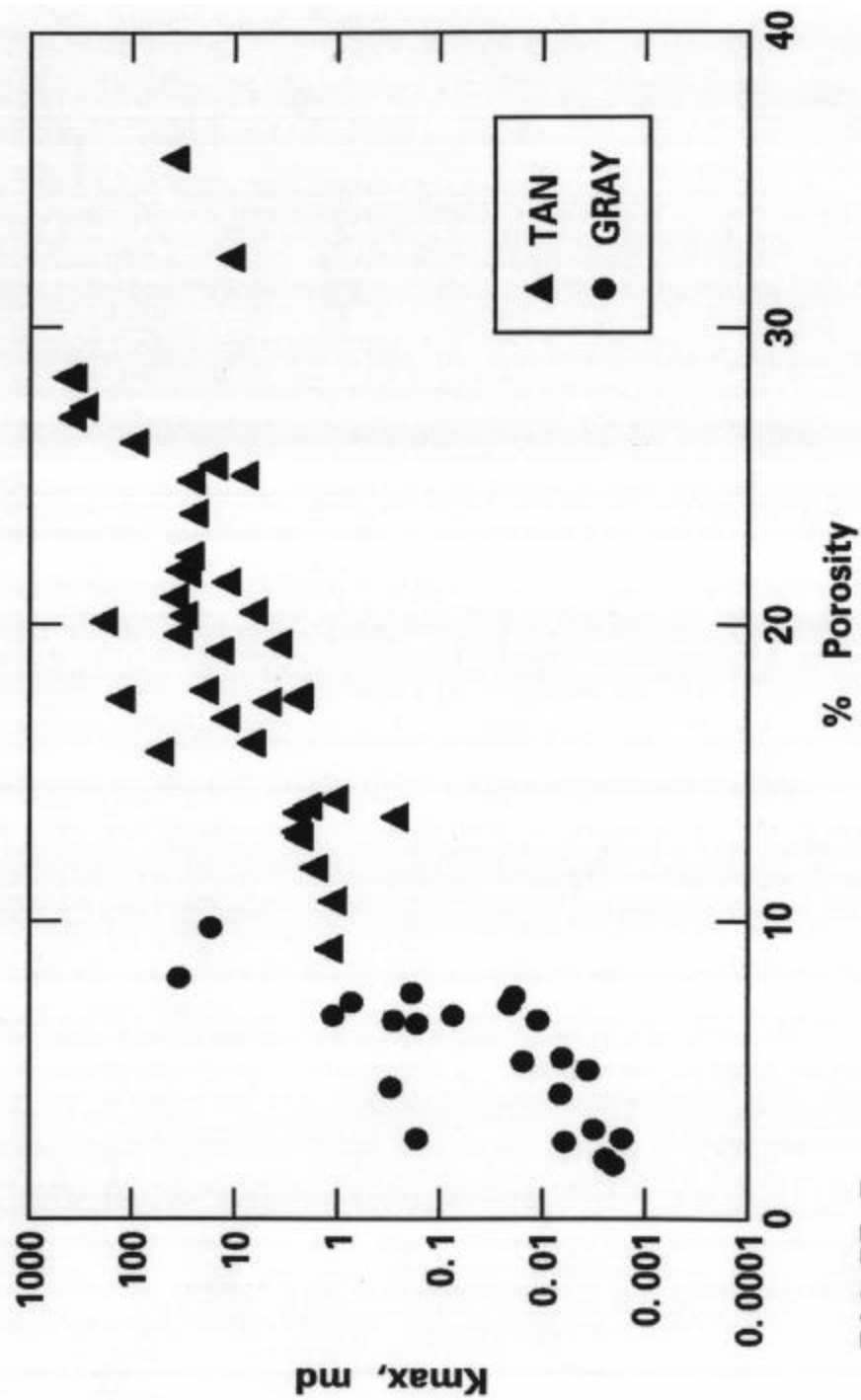


FIGURE 7

**CORRELATION OF RUPPEL'S (1995)  
HFS AND HFC WITH SCU 8-19 CORE UNITS**

<b>GRAYBURG HIGH FREQUENCY SEQUENCES</b>	<b>SELECTED GRAYBURG HIGH FREQUENCY CYCLES</b>
<b>GRAYBURG 4:</b> CORE UNITS 18 A 14A	15 > 18
<b>GRAYBURG 3:</b> CORE UNITS 13B A 10A	14A > 14C
	12A > 13B
	10K > 11B
	10A > 10J
<b>GRAYBURG 2:</b> CORE UNITS 9 A 4	
<b>GRAYBURG 1:</b> CORE UNITS 3B A 1	

**FIGURE 8**

# **RELATIONSHIP OF POROSITY TO ANHYDRITE SOUTH COWDEN UNIT**

<b>WELL</b>	<b>AVERAGE POROSITY TAN DOLO. (Core Analysis)</b>	<b>PERCENT ANHYDRITE TAN DOLO. (Thin Section)</b>
<b>6-23</b>	<b>21.0%</b>	<b>1.0%</b>
<b>7-10</b>	<b>21.0%</b>	<b>5.5%</b>
<b>8-19</b>	<b>24.0%</b>	<b>1.0%</b>
<b>8-11</b>	<b>14.5%</b>	<b>11.5%</b>
<b>16-14 (Moss Unit)</b>	<b>~ 5.5-7%</b>	<b>15.5%</b>

**FIGURE 9**

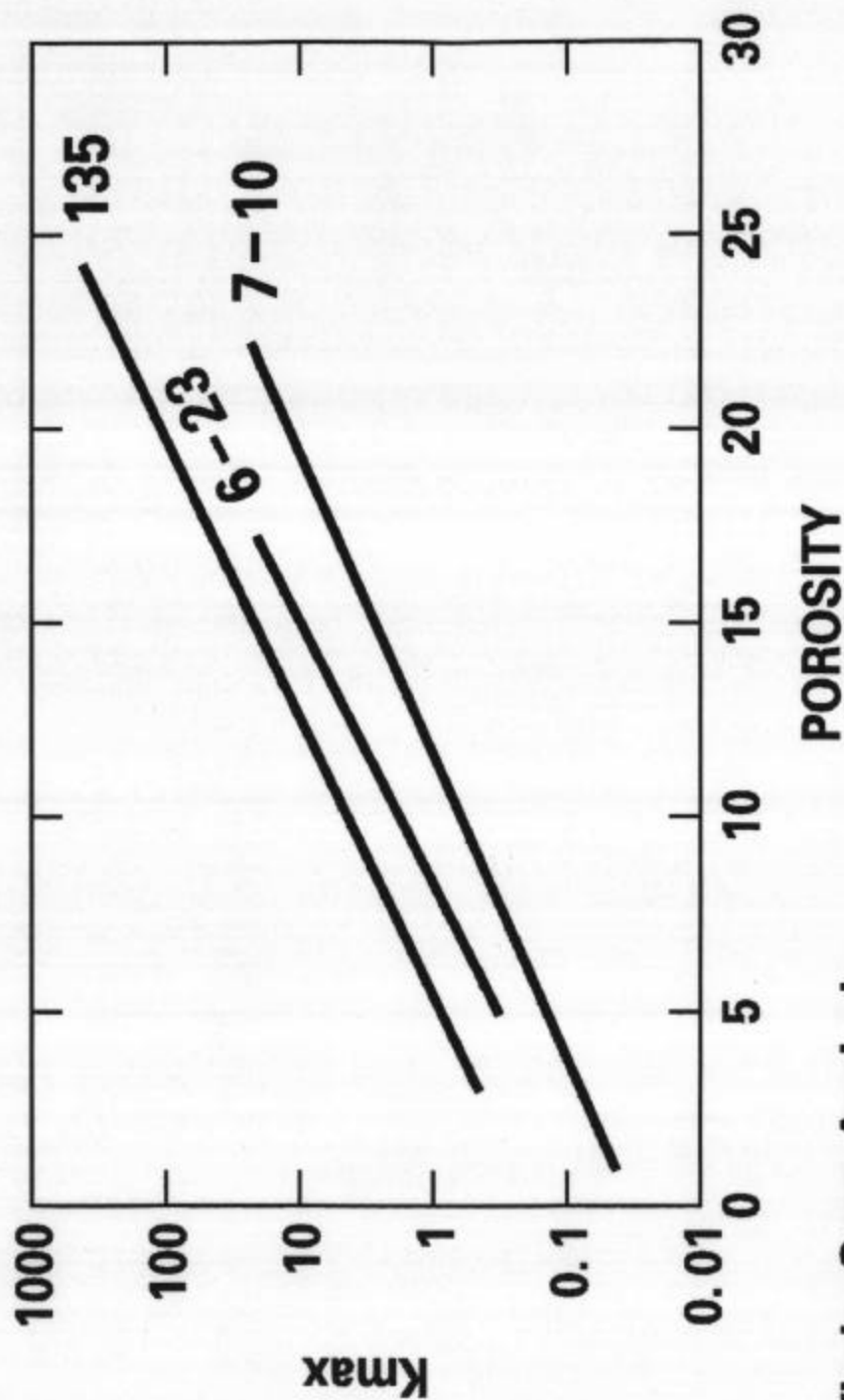
**AVERAGE POROSITY AND PERMEABILITY  
OF TAN DOLOMITE, BURROW-MOTTLED  
DOLOPACKSTONE LITHOFACIES,  
SOUTH COWDEN UNIT**

<u>WELL</u>	<u>AVERAGE POROSITY TAN DOLO.</u>	<u>AVERAGE PERMEABILITY TAN DOLO.</u>
<b>6-23</b>	<b>21.0%</b>	<b>90 md</b>
<b>7-10</b>	<b>21.0%</b>	<b>10 md</b>
<b>8-19</b>	<b>24.0%</b>	<b>175 md</b>
<b>8-11</b>	<b>14.5%</b>	<b>8 md</b>

**FIGURE 10**



**POROSITY/PERMEABILITY PLOTS\* FOR THE  
SCU 7-10 AND 6-23 AND THE EMMONS UNIT 135**



**\* Whole Core Analysis**

**FIGURE 11**

**M.G. Gerard**

## PLATE 1: FUSULINID DOLOWACKESTONE LITHOFACIES

Fusulinid dolowackestones of the lower Grayburg Formation, SCU 8–19. Core samples shown in photos A and B have biomoldic porosity reflecting fusulinid dissolution. Fusulinids in the photo C sample are coarsely crystalline anhydrite. Dark-gray wispy and discontinuous carbonaceous/ argillaceous laminae and stylolitic seams visible in the photo B sample (SCU 8–19, core unit 5) result in slightly higher gamma-ray log values for dolomites of this unit (Fig. 5). Photo A—core unit 3A; photo B—core unit 5; photo C—core unit 13A.

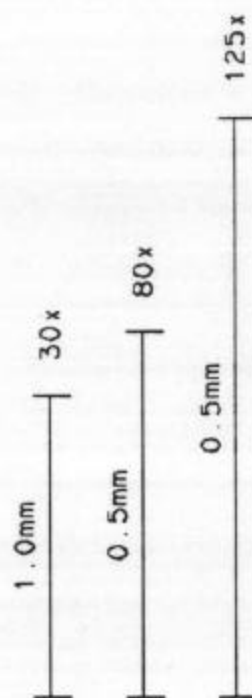


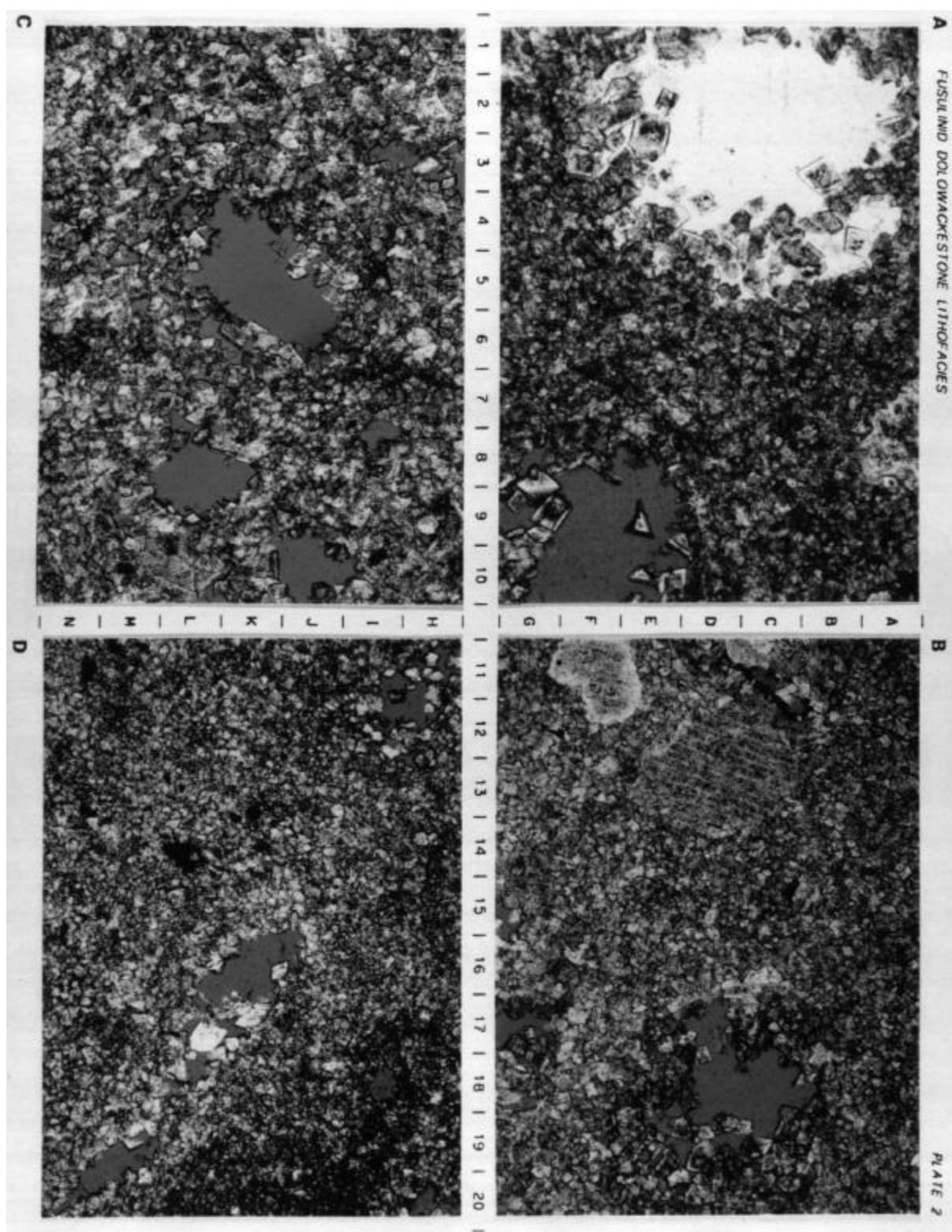
A  
B  
C  
D  
E  
F  
G  
H  
I  
J  
K  
L  
M  
N  
O  
P  
Q  
R  
S  
T  
D

1 2 3 4 5 6 7 8 9 10 11 12 13 14

## PLATE 2: FUSULINID DOLOWACKESTONE LITHOFACIES

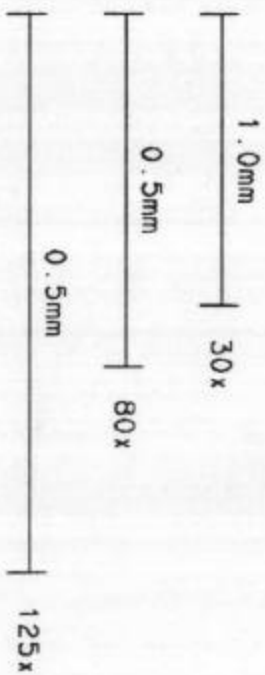
Fusulinid dolowackestones of the lower Grayburg Formation, SCU 8-19. Photomicrographs show leached fusulinid porosity (photo A: 9F; photo B: 18C; and photo D: 16K). The white area at the upper left in photo A is an anhydrite-cemented biomold. Echinoderm debris is visible at left center in photo B. Photo A—core unit 1, 4967', 30X; photos B and C—core unit 3B, 4949', 30X; photo D—core unit 5, 4918.5', 30X. All footages are in core depths.



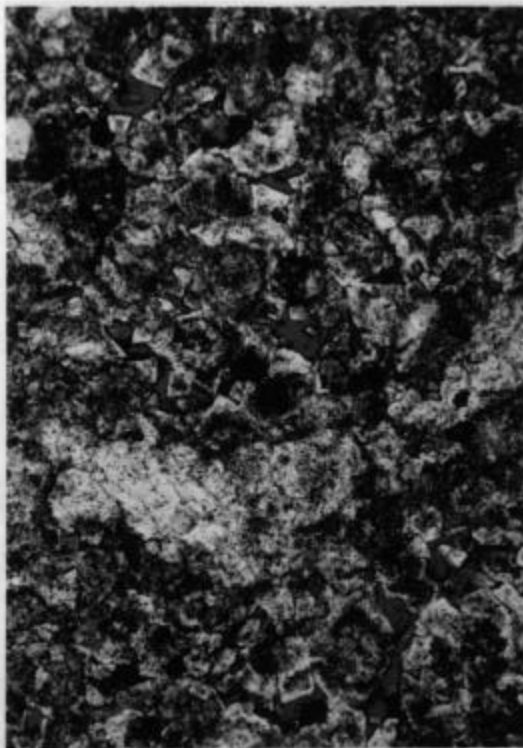


### PLATE 3: OOID-PELOID DOLOGRAINSTONE LITHOFACIES

Ooid-peloid dolograins of the Grayburg Formation, SCU 8-19. Ooid nuclei and cortices are difficult to distinguish due to dolomitization. Intergranular porosity (photo A: 2F, 5D, and 9-10B) is generally occluded by dolomite cement. Ooid dolograins of the uppermost Grayburg Formation (SCU 8-19, core unit 18) is partially anhydrite cemented (photo D). Photo A—core unit 6, 4891', 30X; photo B—core unit 7, 4888', 30X; photo C—core unit 8, 4873', 30X; photo D—core unit 18, 4635', 30X. All footages are in core depth.



**A** COID-PELOID DOLOGRANSTONE LITHOFACIES



**B**

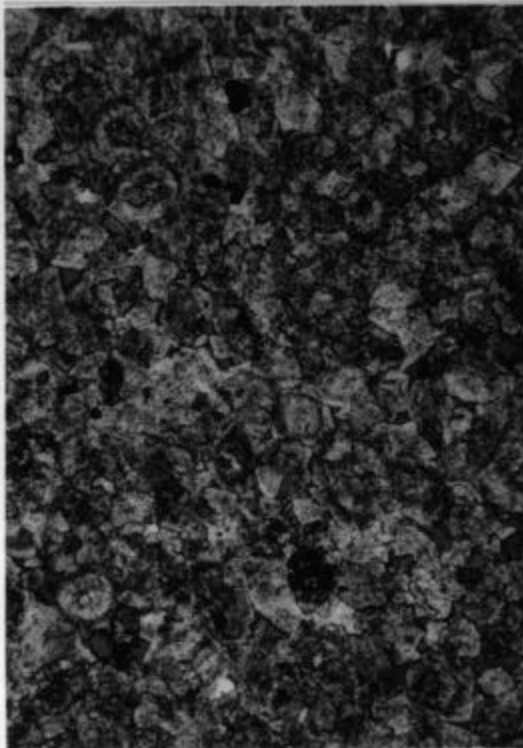
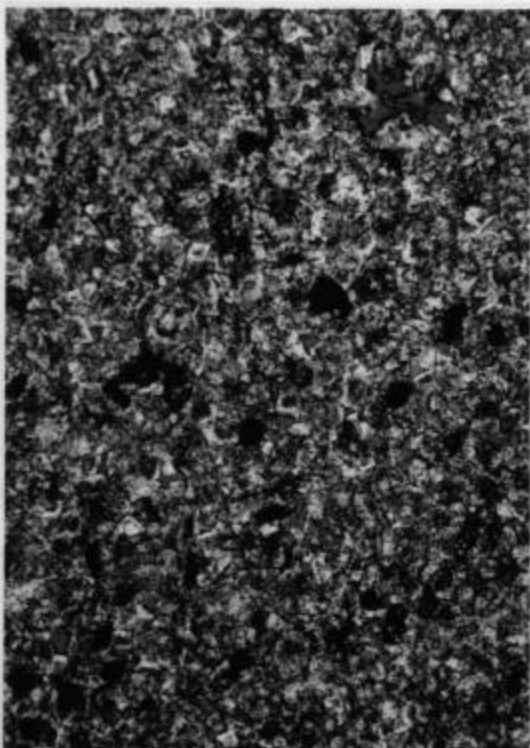
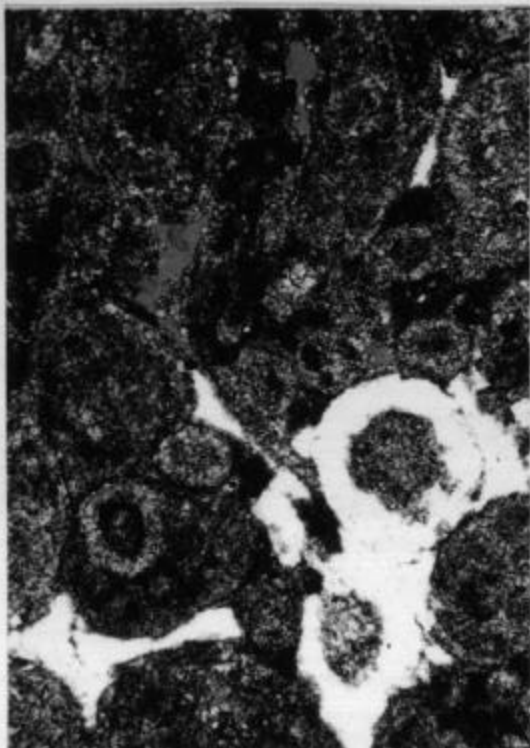


PLATE 3

**C**



**D**

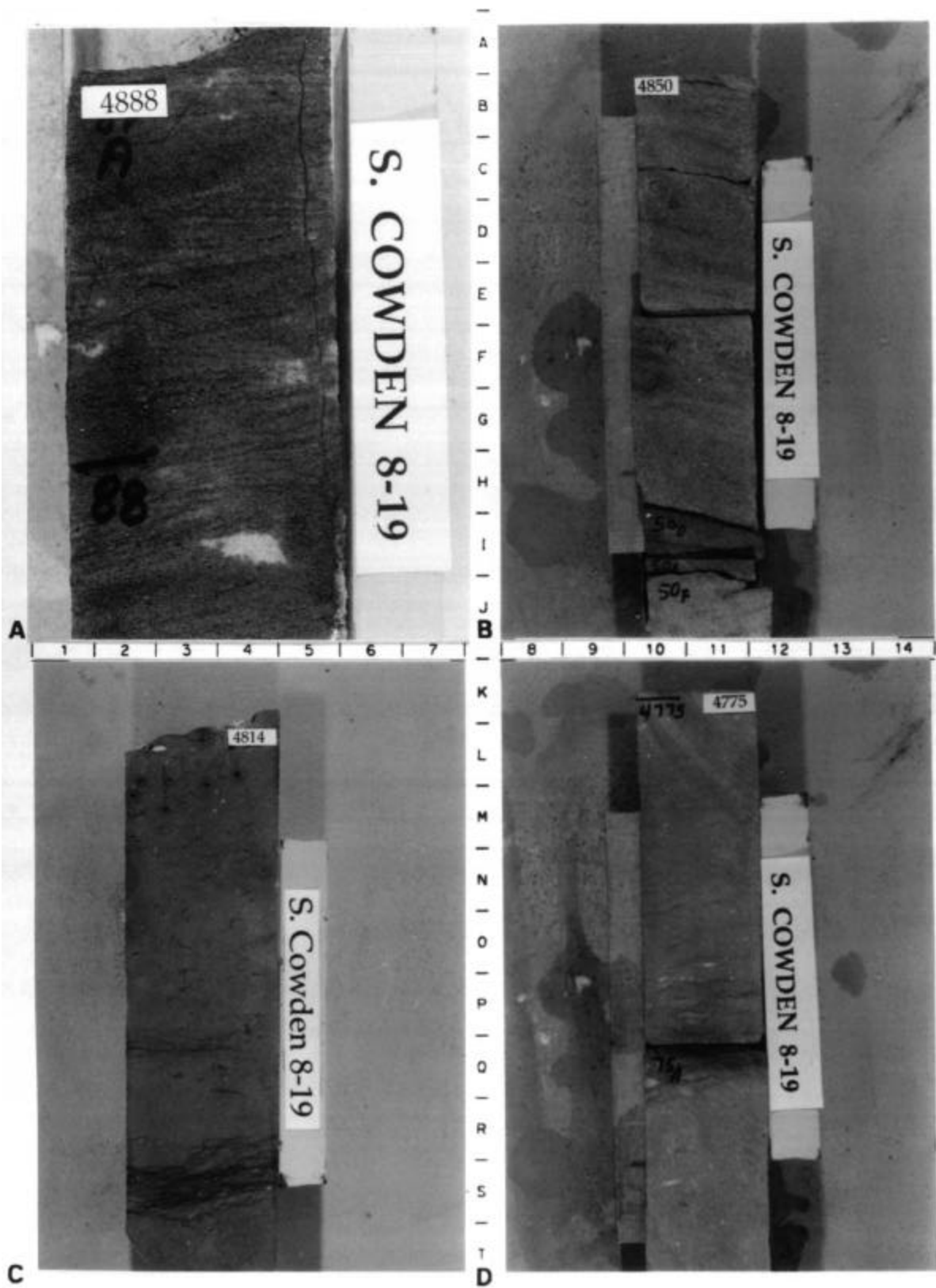




**PLATE 4: OOID-PELOID DOLOGRAINSTONE AND SANDY  
DOLOPACKSTONE LITHOFACIES**

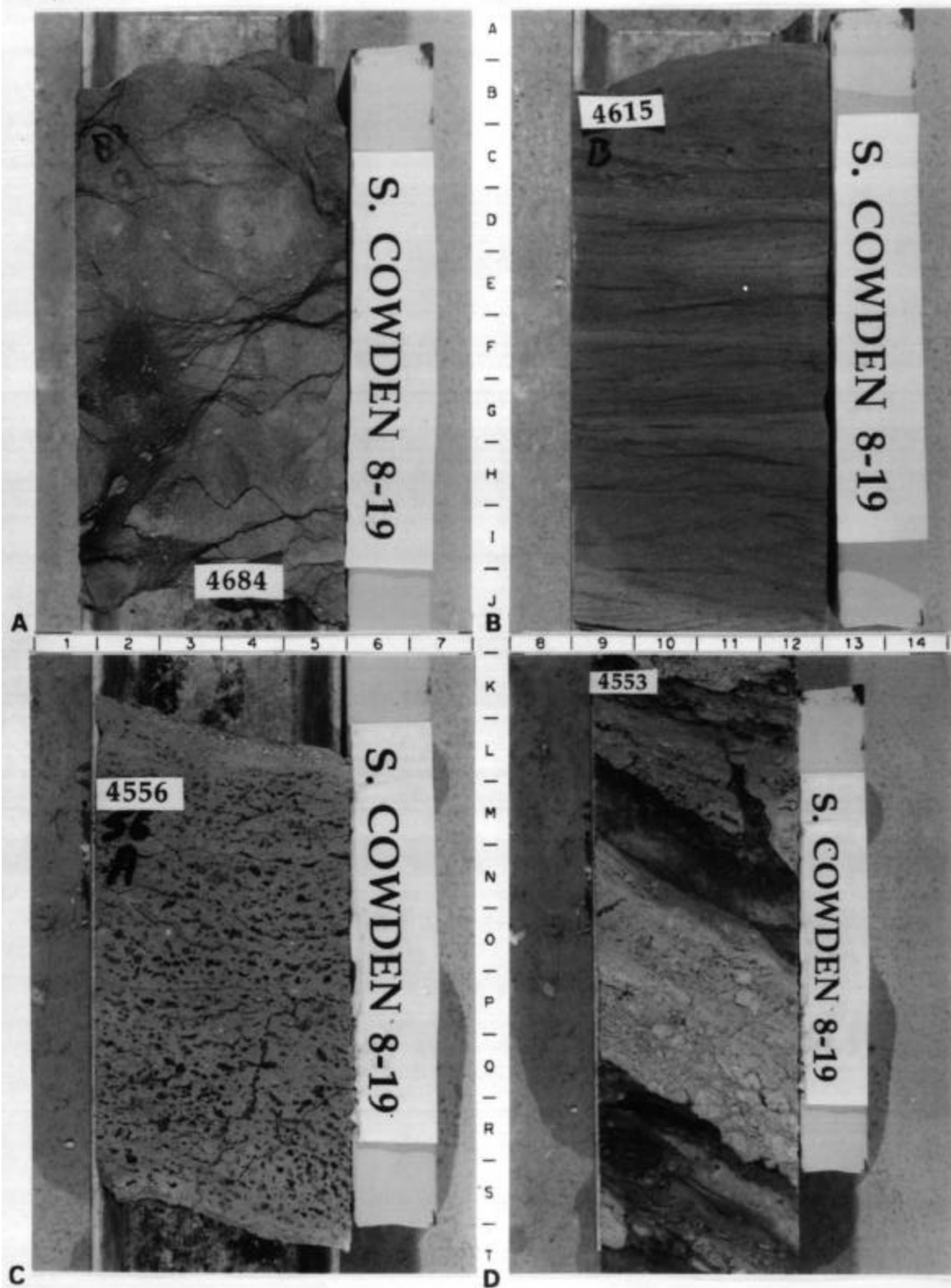
Photos A and B show small- to medium-scale cross-stratified ooid dolograinstones of the Grayburg Formation, SCU 8-19. Sandy dolopackstones of the Grayburg Formation, SCU 8-19, are shown in photos C and D. Sandy dolopackstones display dark-gray carbonaceous/ argillaceous stylolitic laminae. The sandy dolopackstone layer at the base of Zone D in the SCU 8-19 is shown in photo D. Photo A—core unit 7; photo B—core unit 9; photo C—core unit 10F; photo D—core unit 12A.





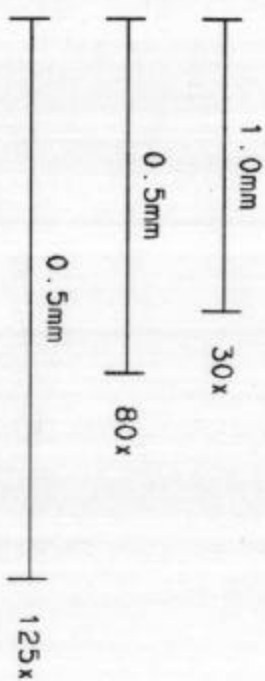
**PLATE 5: SANDY DOLOPACKSTONE AND FENESTRAL  
DOLOPACKSTONE LITHOFACIES**

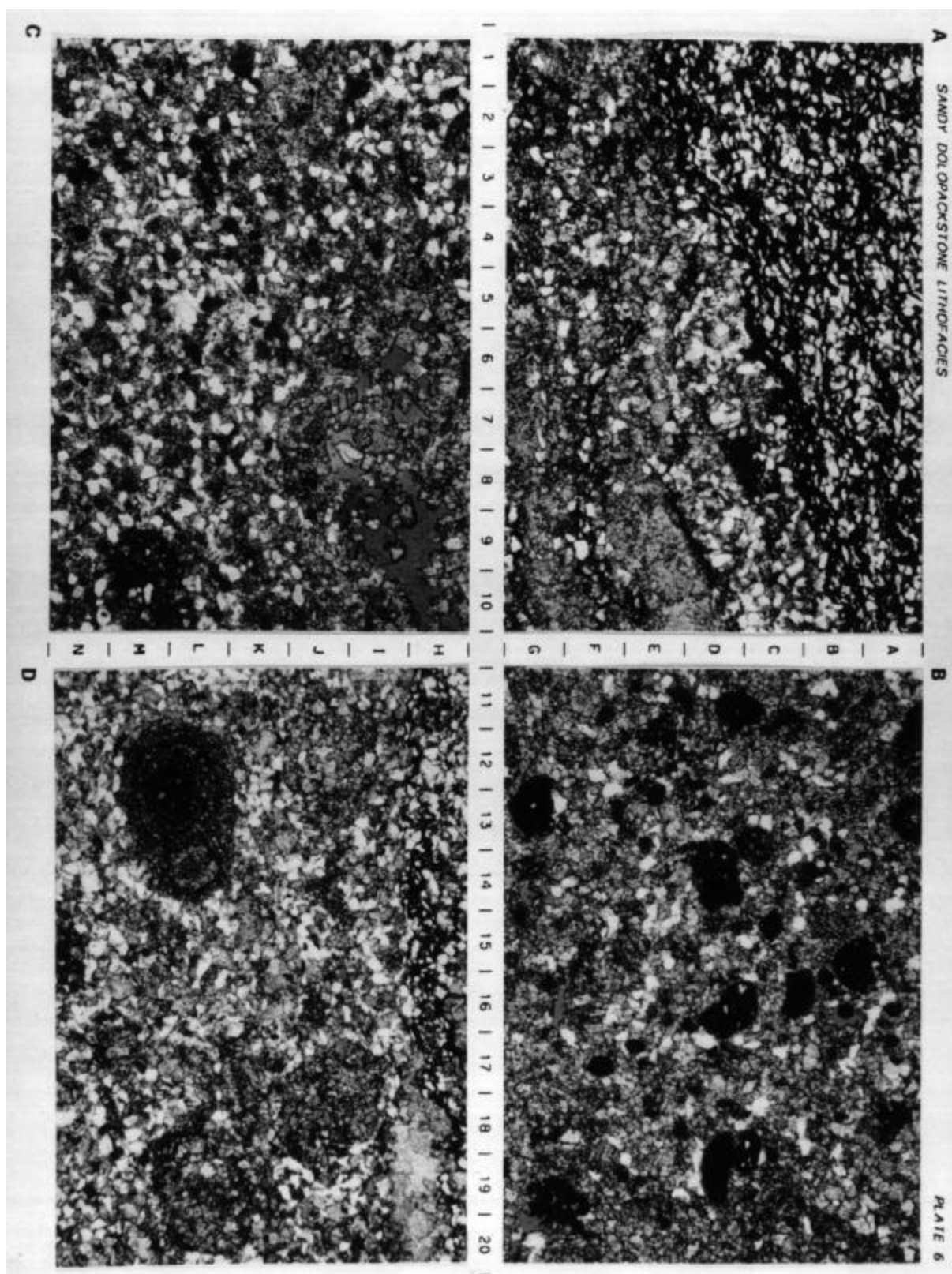
Photos A and B show sandy dolopackstones of the Grayburg and Queen Formations, respectively, SCU 8–19. The sandy dolopackstone shown in photo A displays discontinuous carbonaceous/argillaceous stylolitic seams. This sample is from the sandy dolopackstone/dolomitic sandstone at the base of Zone F (Fig. 5). Sandy dolomite from the Queen Formation, photo B, displays ripple cross stratification. Rocks of the fenestral dolopackstone lithofacies, Queen Formation, are shown in photos C and D. Photo C sample shows an anhydrite–cemented fenestral fabric. Inclined anhydrite–cemented dessication cracks are shown in photo D. Inclined bedding in this sample is indicative of a teepee structure. Photo A—core unit 15; photo B—core unit 20C; photos C and D—core unit 29.



## PLATE 6: SANDY DOLOPACKSTONE LITHOFACIES

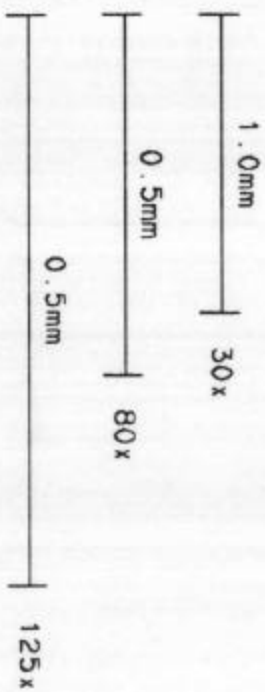
Photomicrographs of sandy dolopackstones of the Grayburg Formation, SCU 8-19. A stylolitic argillaceous/carbonaceous seam is shown in the upper part of photo A. These seams contribute to the relatively hot gamma-ray log signature associated with rocks of this lithofacies. Dark, fine- to medium-sand-size peloids of uncertain affinity are shown in photos B and C, and a coarse-sand-size ooid grapestone grain is shown at the lower left in photo D. The large pore at the upper right in photo C (6-10 H-I) is most likely a leached fusulinid. Photo D is from the sandy dolopackstone layer at the base of Zone D. Photo A—core unit 10D, 4822.4', 30X; photo B—core unit 10E, 4820.2', 30X; photo C—core unit 10G, 4813', 30X; photo D—core unit 12A, 4773.2', 30X. All footages are in core depths.



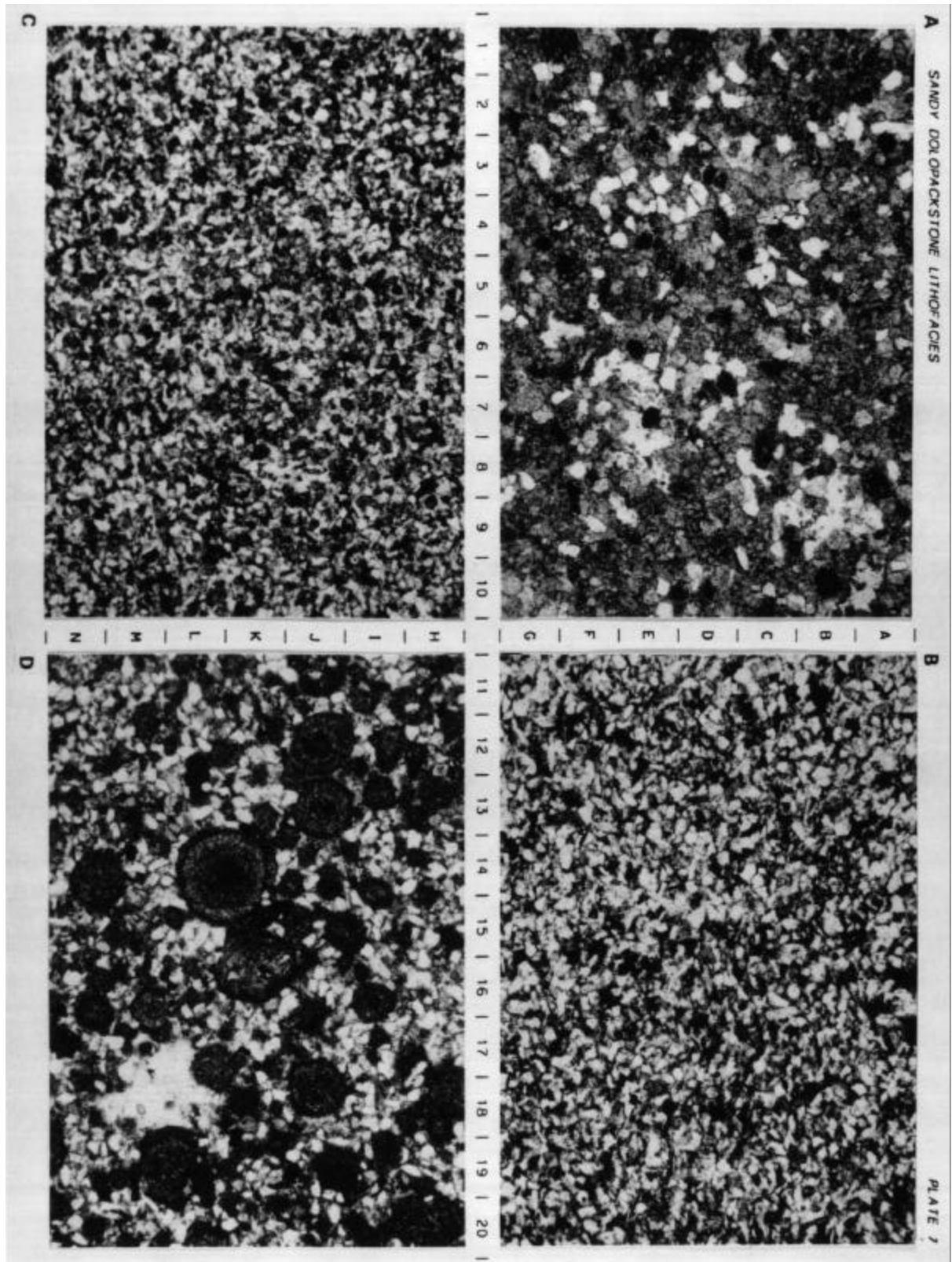


## PLATE 7: SANDY DOLOPACKSTONE LITHOFACIES

Sandy dolopackstones and dolomitic sandstones of the Grayburg (photos A and B) and Queen (photos C and D) Formations, SCU 8-19. The sample shown in photo B is from the dolomitic sandstone/sandy dolopackstone layer at the base of Zone F (Fig. 5). The photo C sample is from the dolomitic sandstone that defines the base of the Queen Formation. Ooids are readily apparent in the photo D sample from the lower Queen Formation. Photo A—core unit 12B, 4766.9', 30X; photo B—core unit 15, 4681.8', 30X; photo C—core unit 19, 4624', 30X; photo D—core unit 26, 4570.6', 30X. All footages are in core depths.



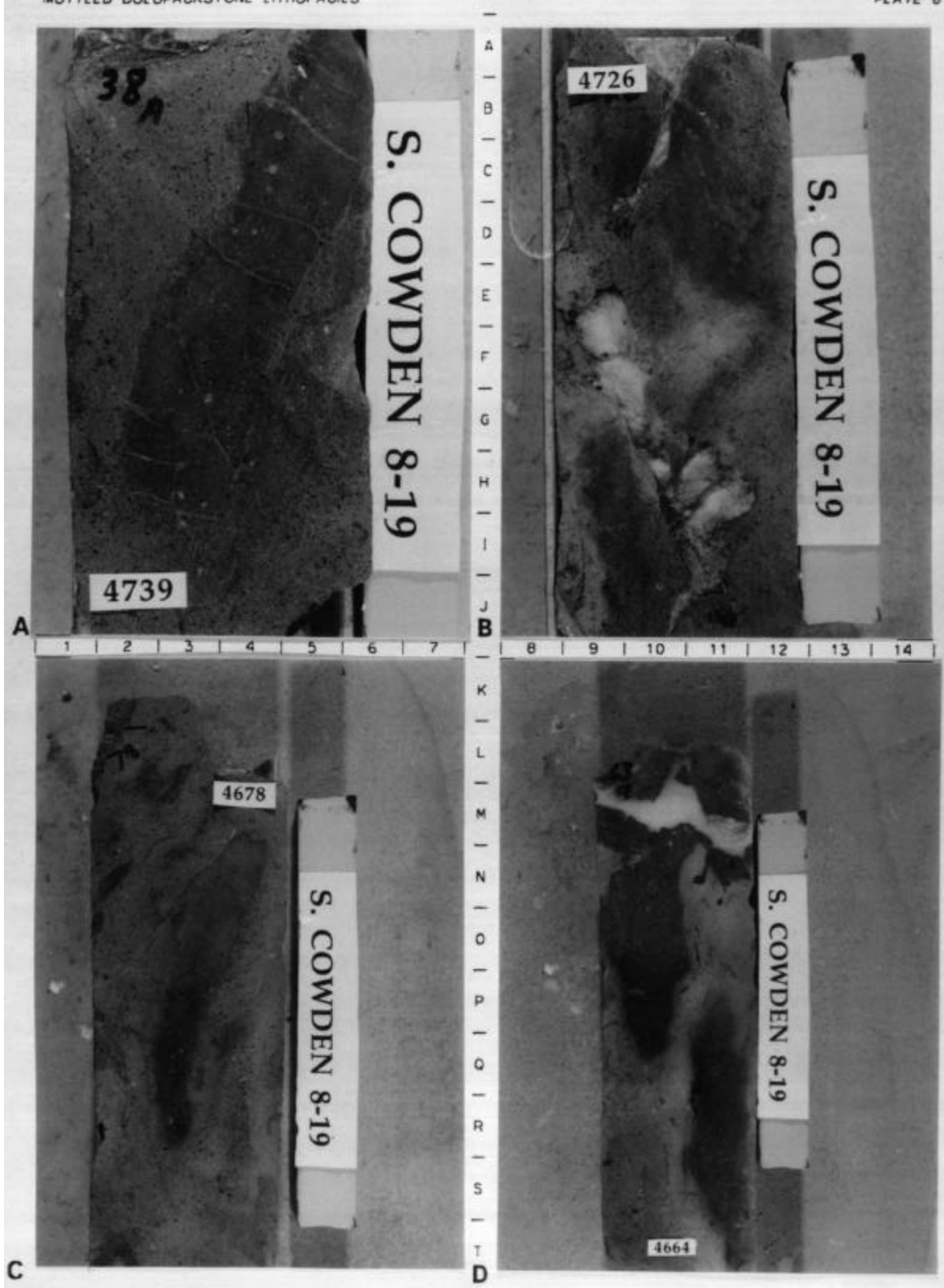




## PLATE 8: BURROW-MOTTLED DOLOPACKSTONE LITHOFACIES

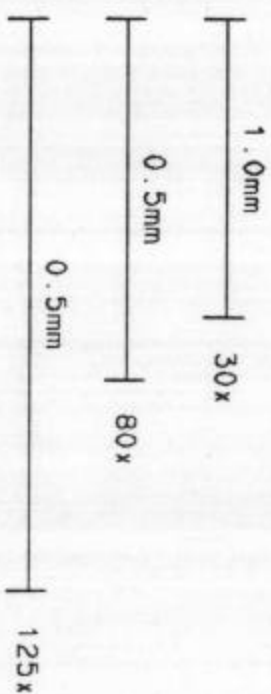
Core photos showing the distinctive gray/tan burrow mottling of the mottled dolopackstone lithofacies, Grayburg Formation, SCU 8-19. Photos show the vertical orientation of gray (dark) and tan (light) areas. Tan areas are interpreted to be carbonate-sand-filled burrows. Interburrow gray dolomite areas typically have porosities of 2 to 9% and permeabilities of 0.002 to 2 md. Tan oil-stained dolomite areas have porosities of 10 to 32% and permeabilities ranging from 2 to 400 md. Anhydrite-cemented fractures are visible in the gray dolomite area shown in the photo A sample. Rocks of this lithofacies compose the reservoir interval at South Cowden Unit. Photo A—core unit 14A; photo B—core unit 14C; photos C and D—core unit 16.



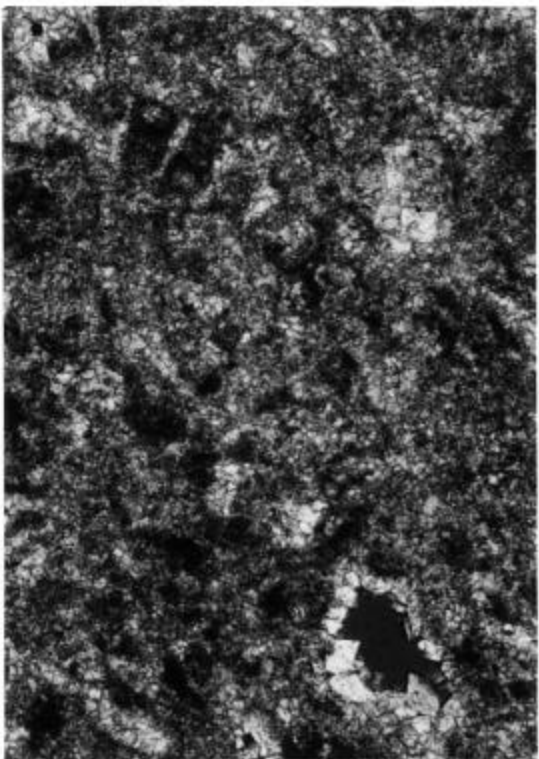


# PLATE 9: BURROW-MOTTLED DOLOPACKSTONE LITHOFACIES

Gray dolomite, photos A and B, and tan dolomite, photos C and D, of the mottled dolopackstone lithofacies, SCU 8-19. Porosity is minor in the gray dolopackstone samples and appears to be mainly biomoldic (photo A: 9B and photo B: 15C). Tan dolomite porosity includes intergranular, intercrystalline, and moldic. Photo A—core unit 14A, 4749', 30X; photo B—core unit 14C, 4728.3', 30X; photo C—core unit 14C, 4703', 80X; photo D—core unit 14C, 4708.7', 80X. All footages are in core depths.



A MOTILED DOL OPAKSTONE LITHOFACIES



A | B | C | D | E | F | G | H | I | J | K | L | M | N

B

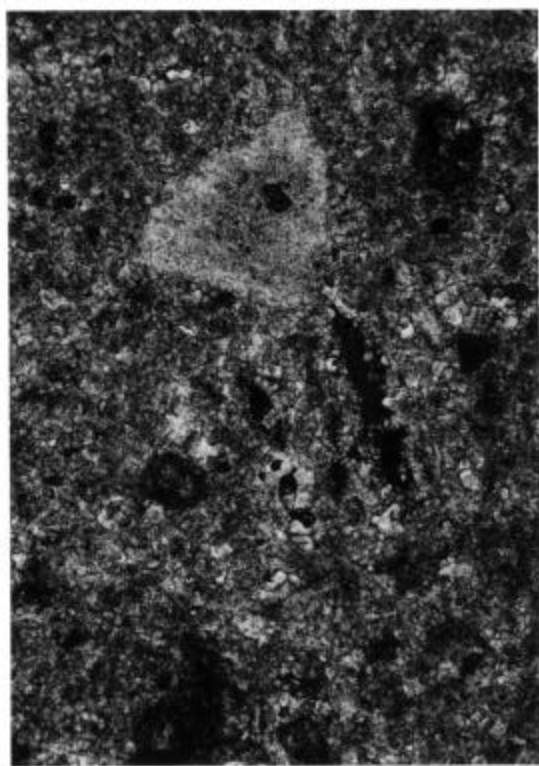
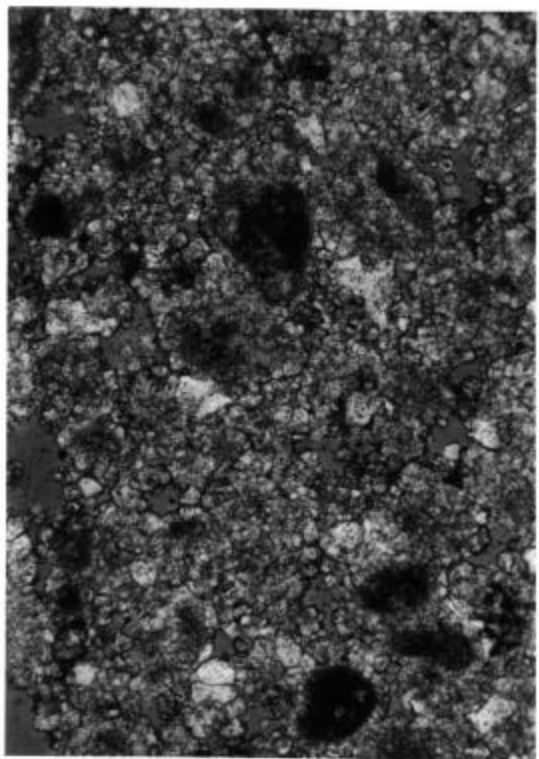


PLATE 9

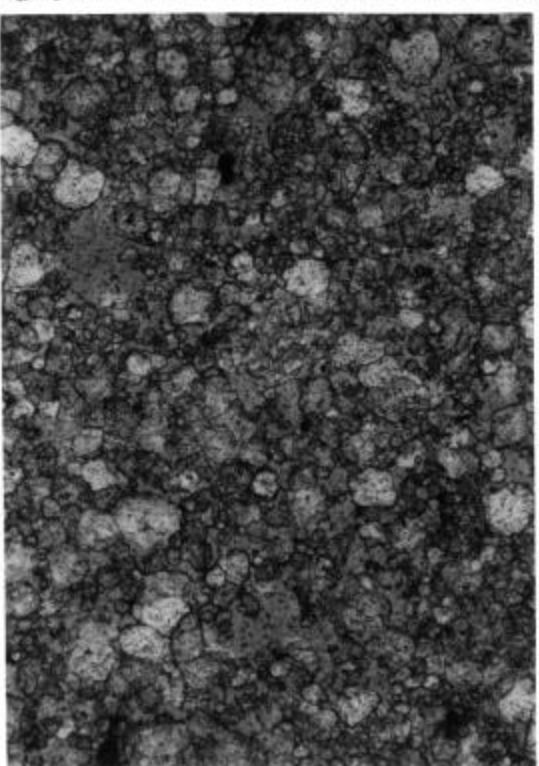
1 | 2 | 3 | 4 | 5 | 6 | 7 | 8 | 9 | 10 | 11 | 12 | 13 | 14 | 15 | 16 | 17 | 18 | 19 | 20 |



O | P | Q | R | S | T | U | V | W | X | Y | Z | AA | BB

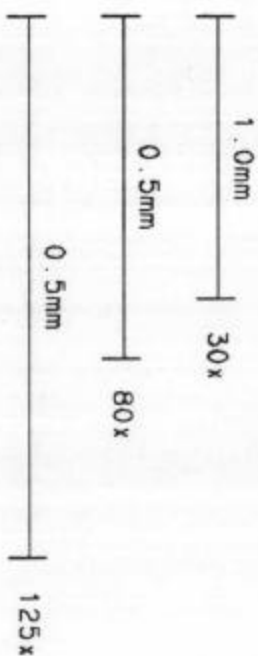
C

D

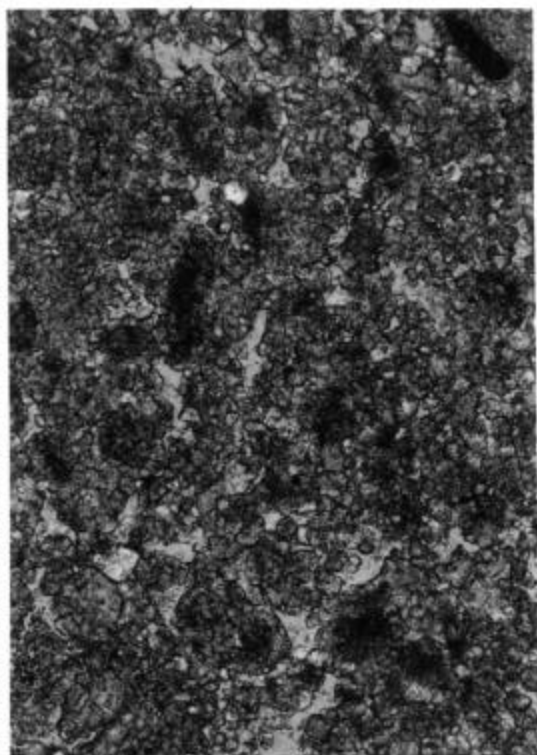


# PLATE 10: BURROW-MOTTLED DOLOPACKSTONE LITHOFACIES

Photos A and B show tan dolomites of the mottled dolopackstone lithofacies. The two samples shown in photos A and B have similar porosities but markedly different permeabilities (photo A sample, SCU 6-23—20% porosity and 190 md permeability; photo B sample, SCU 7-10—20.4% porosity and 6.6 md permeability). The tan dolomite sample shown in photo A is a dolograinstone and has significantly larger pores and larger crystal size than the lower permeability dolopackstone sample shown in photo B. Photos C and D show void-filling and replacement anhydrite in tan dolomites samples. Dissolution of poikilotopic anhydrite in the photo C sample (category I tan dolomite) could result in the porous fabric shown to the left in this photo. By contrast, anhydrite dissolution in the photo D sample (category II tan dolomite) would result in pores significantly larger than those characterizing the sample, suggesting porosity in the photo D sample is not related to anhydrite dissolution. Photo A—SCU 6-23, 4640.7', 80X; photo B—SCU 7-10, 4679', 80X; photo C—SCU 8-19, 4708.7', 80X; photo D—SCU 8-11, 4624.5', 80X. All footages are in core depths.



A MOTTLED DOLOMITIC LITHOCLASTS



B

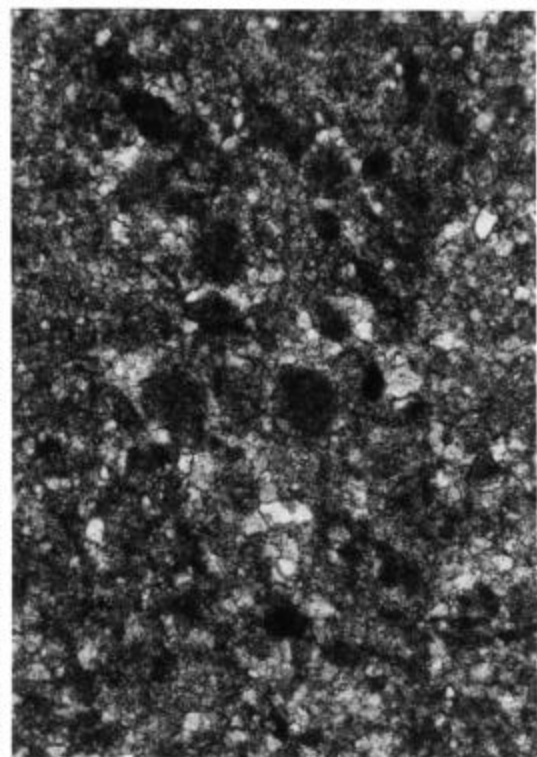
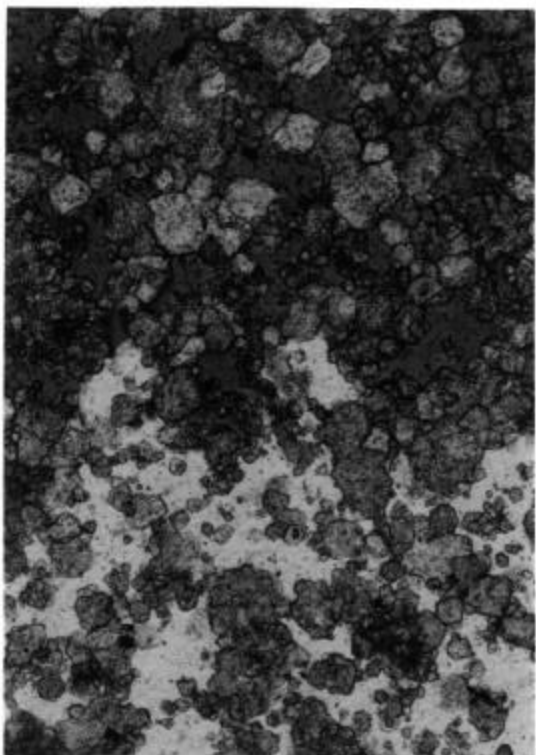
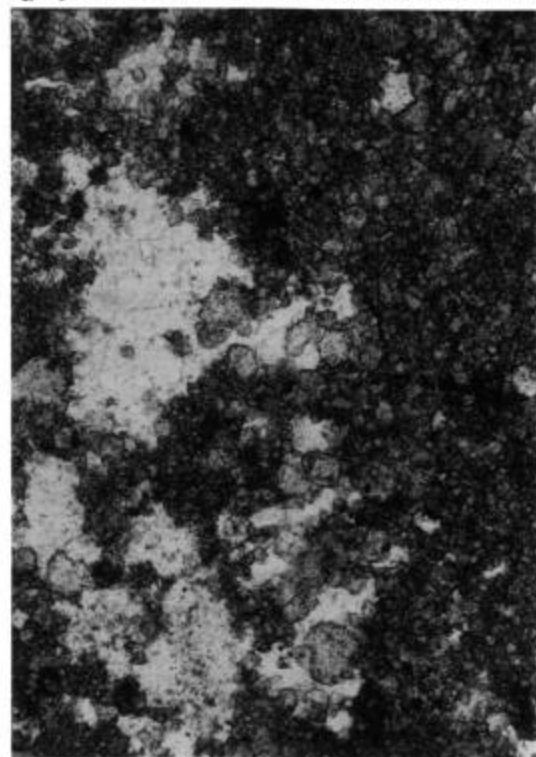


PLATE 10



C



D



**SCAL, Inc.**

SPECIAL CORE ANALYSIS LABORATORIES

## **Phillips Petroleum Company**

### **Special Core Analysis Report**

**Amott Wettability  
Water Oil Relative Permeability**

**South Cowden Unit #8-19  
San Andres  
Ector County, Texas**

The analysis, interpretations or opinions expressed in our reports represent the best judgement of Special Core Analysis Laboratories Inc.. Special Core Analysis Laboratories Inc. assumes no responsibility and makes no warranties of any kind as to the productivity, proper operation or profitability of any oil, gas or any other mineral in connection which such a report is used or relied upon.

P.O. BOX 9730 • MIDLAND, TX 79708-2730 • (915) 561-5406 • FAX (915) 561-5339



## SPECIAL CORE ANALYSIS LABORATORIES, INC

Mr. Larry Hallenbeck  
Reservoir Engineer

Phillips Petroleum Company  
4001 Penbrook  
Odessa, Texas 79762

April 30, 1992

Reference: Special Core Analysis  
South Cowden Unit #8-19  
Ector County, Texas

Dear Mr. Hallenbeck:

Please find enclosed the final special core analysis report. The following analyses and procedures were performed:

- ♦ Amott Wettability and End Point Water-Oil Relative Permeability.
- ♦ Unsteady-State Water-Oil Relative Permeability.

♦ Amott Wettability:

The wettability samples were cut (using synthetic brine as coolant) from the selected preserved core sections.

The selected samples were saturated with produced brine and placed in oil filled individual imbibition tubes at reservoir temperature of 106 °F for 10 days. Most of the imbibition occurred in the first 24 hours. No change in the oil imbibed was noted after 2 days. For consistency reasons the samples were kept under oil for at least 10 days.

The samples were next placed into a core holder and flooded with oil to  $S_{wi}^1$ . The total water produced during this oil flood was recorded and the wettability index to oil was calculated as the oil imbibed divided by oil imbibed plus water produced during the oil flood.

After this oil flood the samples were placed into brine filled individual wettability tubes and allowed to imbibe water at reservoir temperature for 10 days. Most of the imbibition occurred in the first 24 hours.

---

<sup>1</sup> $S_{wi}$  Irreducible Water Saturation



After recording the volume of water imbibed the samples were water flooded. The oil produced was recorded and the wettability index to water was calculated as water imbibed divided by water imbibed plus oil produced during the water flood.

Finally the samples were cleaned using a Dean-Stark carbon dioxide cleaning combination. The Dean-Stark allowed to measure directly the volume of water present in the core after the oil flood. By material balance the oil in the sample after water flooding was determined.

Porosity permeability and grain densities were measured on the cleaned and dried samples. The  $S_{ro}^2$  and  $S_{wi}$  were calculated and the associated end point effective permeabilities were reported.

#### ♦ Unsteady-State Water-Oil Relative Permeability.

The unsteady-state water-oil relative permeability tests were conducted on cleaned restored samples.

The cleaned samples were vacuum saturated with produced brine then flooded with high viscosity mineral oil to  $S_{wi}$ . The permeability to oil was measured ( $K_{eo}^3 @ S_{wi}$ ) and was used as base to calculate the water-oil relative permeabilities.

The samples were next water flooded to  $S_{ro}$ . The water permeability was measured ( $K_{ew}^4 @ S_{ro}$ ). During the constant rate water flood the pressure and oil production were recorded. Using Welge's method the water-oil relative permeability was calculated from the flood data.

It was a pleasure performing these analyses for you. If you have any further questions please feel free to contact us.

Sincerely,

Mihai Vasilache  
Technical Director

---

<sup>2</sup> $S_{ro}$  Residual Oil Saturation  
<sup>3</sup> $K_{eo}$  Effective Oil Permeability  
<sup>4</sup> $K_{ew}$  Effective Water Permeability



# Routine Core Analysis

Company Phillips Petroleum Company

Well : South Cowden Unit #8-19

Formation San Andres

Location : Ector County, Texas

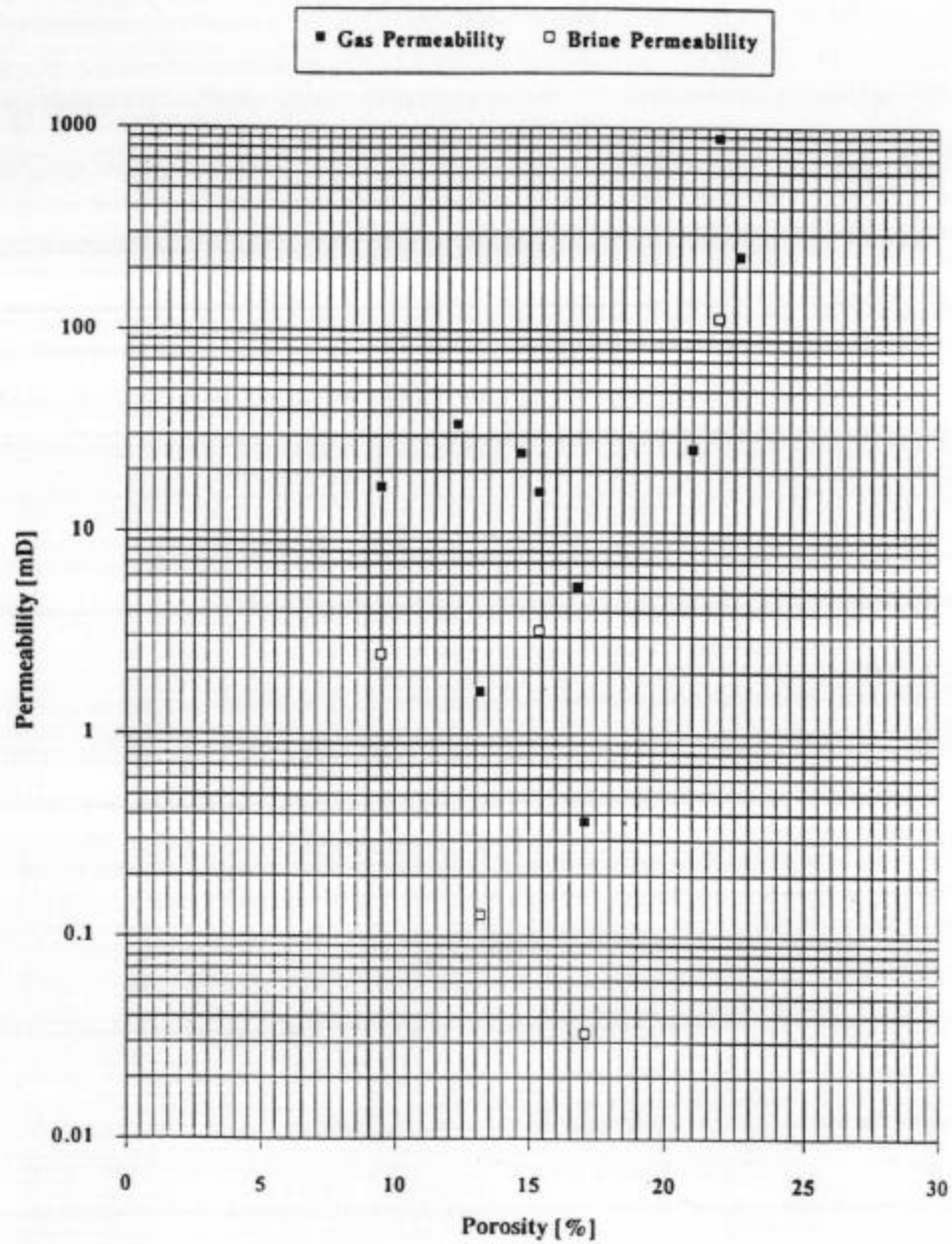
## TEST RESULTS:

Sample No.	Depth ft in	Porosit %	Gas Permeability md	Brine Permeability md	Grain Density g/cc	SCAL Testing **
7	4691 8.0	17.07	0.37	0.033	2.84	WETT, EPWOKR
20	4703 ##	15.38	15.72	3.23	2.83	WETT, EPWOKR
26	4770 4.0	13.18	1.62	0.128	2.78	WETT, EPWOKR
36	4839 4.5	9.49	16.7	2.47	2.83	WETT, EPWOKR
46	4849 6.0	21.91	884	115	2.83	WETT, EPWOKR
48	4665 6.0	21.00	25.67		2.83	USSWOKR
60	4716 6.0	22.66	231.00		2.82	USSWOKR
87	4782 3.5	16.80	5.31		2.83	USSWOKR
111	4830 4.5	14.71	24.59		2.84	USSWOKR
124	4872 ##	12.35	34.01		2.83	USSWOKR

## SCAL Tests \*\*

USSWOKR	Unsteady-State Water-Oil Relative Permeability
WETT	Amott Wettability at Reservoir Temperature
EPWOKR	End Point Water-Oil Relative Permeability at Reservoir Temperature

## South Cowden Unit 8-19



**Amott Wettability  
End Point Water-Oil Relative Permeability**

**South Cowden Unit #8-19  
San Andres  
Ector County, Texas**

The analysis, interpretations or opinions expressed in our reports represent the best judgement of Special Core Analysis Laboratories Inc.. Special Core Analysis Laboratories Inc. assumes no responsibility and makes no warranties of any kind as to the productivity, proper operation or profitability of any oil, gas or any other mineral in connection which such a report is used or relied upon.

# AMOTT WETTABILITY AND END POINT RELATIVE PERMEABILITY

Company : Phillips Petroleum Company

Formation : San Andres

Location : Ector County

Well Name : South Cowden Unit #8-19

Sample : 7

Depth : 4691' 8"

Porosity : 17.07 %

Permeability : 0.37 mD

Grain Density: 2.839 g/cc

## TEST RESULTS :

1) Crude Oil Imbibition at Reservoir Temperature 106 deg. F.

1a) Imbibition Time : 10 days

1b) Oil Imbibed : 0.8 cc

2) Crude Oil Flood at Reservoir Temperature :

2a) Water Recovered : 5.80 cc

2b) Keo @ Swi : 0.04 mD

2c) Swi : 28.70 %

3) OIL WETTABILITY INDEX : 12.12 %

4) Formation Water Imbibition at Reservoir Temperature :

4a) Imbibition Time : 10 days

4b) Water Imbibed : 0.80 cc

5) Water Flood at Reservoir Temperature :

5a) Oil Recovered : 2.50 cc

5b) Kew @ Sro : 0.01 mD

5c) Sro : 33.1 %

6) WATER WETTABILITY INDEX : 24.24 %

# **AMOTT WETTABILITY AND END POINT RELATIVE PERMEABILITY**

**Company :** Phillips Petroleum Company

**Formation :** San Andres

**Location :** Ector County

**Well Name :** South Cowden Unit #8-19

<b>Sample :</b>	<b>20</b>	<b>Porosity :</b>	<b>15.38 %</b>
<b>Depth :</b>	<b>4703' 11"</b>	<b>Permeability :</b>	<b>15.72 mD</b>
		<b>Grain Density:</b>	<b>2.833 g/cc</b>

## **TEST RESULTS :**

**1) Crude Oil Imbibition at Reservoir Temperature** 106 deg. F.

<b>1a) Imbibition Time :</b>	<b>10 days</b>
<b>1b) Oil Imbibed :</b>	<b>1.4 cc</b>

**2) Crude Oil Flood at Reservoir Temperature :**

<b>2a) Water Recovered :</b>	<b>2.20 cc</b>
<b>2b) Keo @ Swi :</b>	<b>4.36 mD</b>
<b>2c) Swi :</b>	<b>25.60 %</b>

**3) OIL WETTABILITY INDEX :** 38.89 %

**4) Formation Water Imbibition at Reservoir Temperature :**

<b>4a) Imbibition Time :</b>	<b>10 days</b>
<b>4b) Water Imbibed :</b>	<b>1.10 cc</b>

**5) Water Flood at Reservoir Temperature :**

<b>5a) Oil Recovered :</b>	<b>0.80 cc</b>
<b>5b) Kew @ Sro :</b>	<b>1.84 mD</b>
<b>5c) Sro :</b>	<b>37.2 %</b>

**6) WATER WETTABILITY INDEX :** 57.89 %

# AMOTT WETTABILITY AND END POINT RELATIVE PERMEABILITY

Company : Phillips Petroleum Company

Formation : San Andres

Location : Ector County

Well Name : South Cowden Unit #8-19

Sample : 26

Depth : 4770' 4"

Porosity : 13.18 %

Permeability : 1.62 mD

Grain Density: 2.78 g/cc

## TEST RESULTS :

1) Crude Oil Imbibition at Reservoir Temperature 106 deg. F.

1a) Imbibition Time : 10 days

1b) Oil Imbided : 1 cc

2) Crude Oil Flood at Reservoir Temperature :

2a) Water Recovered : 3.10 cc

2b)  $K_{eo} @ S_{wi}$  : 0.26 mD

2c)  $S_{wi}$  : 30.60 %

3) OIL WETTABILITY INDEX : 24.39 %

4) Formation Water Imbibition at Reservoir Temperature :

4a) Imbibition Time : 10 days

4b) Water Imbided : 1.40 cc

5) Water Flood at Reservoir Temperature :

5a) Oil Recovered : 1.80 cc

5b)  $K_{ew} @ S_{ro}$  : 0.12 mD

5c)  $S_{ro}$  : 32.15 %

6) WATER WETTABILITY INDEX : 43.75 %

# AMOTT WETTABILITY AND END POINT RELATIVE PERMEABILITY

Company : Phillips Petroleum Company

Formation : San Andres

Location : Ector County

Well Name : South Cowden Unit #8-19

Sample : 36

Depth : 4839' 4.5"

Porosity : 9.49 %

Permeability : 16.7 mD

Grain Density: 2.83 g/cc

## TEST RESULTS :

1) Crude Oil Imbibition at Reservoir Temperature 106 deg. F.

1a) Imbibition Time : 10 days

1b) Oil Imbibed : 0.5 cc

2) Crude Oil Flood at Reservoir Temperature :

2a) Water Recovered : 1.80 cc

2b) Keo @ Swi : 8.41 mD

2c) Swi : 33.80 %

3) OIL WETTABILITY INDEX : 21.74 %

4) Formation Water Imbibition at Reservoir Temperature :

4a) Imbibition Time : 10 days

4b) Water Imbibed : 0.70 cc

5) Water Flood at Reservoir Temperature :

5a) Oil Recovered : 0.50 cc

5b) Kew @ Sro : 3.03 mD

5c) Sro : 27.17 %

6) WATER WETTABILITY INDEX : 58.33 %

# **AMOTT WETTABILITY AND END POINT RELATIVE PERMEABILITY**

**Company :** Phillips Petroleum Company

**Formation :** San Andres

**Location :** Ector County

**Well Name :** South Cowden Unit #8-19

**Sample :** 46

**Porosity :** 21.91 %

**Depth :** 4849'6"

**Permeability :** 884 mD

**Grain Density:** 2.825 g/cc

## **TEST RESULTS :**

**1) Crude Oil Imbibition at Reservoir Temperature** 106 deg. F.

**1a) Imbibition Time :** 10 days

**1b) Oil Imbibed :** 0.1 cc

**2) Crude Oil Flood at Reservoir Temperature :**

**2a) Water Recovered :** 5.40 cc

**2b) Keo @ Swi :** 216.00 mD

**2c) Swi :** 34.90 %

**3) OIL WETTABILITY INDEX :** 1.82 %

**4) Formation Water Imbibition at Reservoir Temperature :**

**4a) Imbibition Time :** 10 days

**4b) Water Imbibed :** 3.70 cc

**5) Water Flood at Reservoir Temperature :**

**5a) Oil Recovered :** 0.60 cc

**5b) Kew @ Sro :** 70.20 mD

**5c) Sro :** 25.9 %

**6) WATER WETTABILITY INDEX :** 86.05 %





SPECIAL CORE ANALYSIS LABORATORIES, INC.

---

## **Unsteady-State Water-Oil Relative Permeability**

**South Cowden Unit #8-19  
San Andres  
Ector County, Texas**

The analysis, interpretations or opinions expressed in our reports represent the best judgement of Special Core Analysis Laboratories Inc.. Special Core Analysis Laboratories Inc. assumes no responsibility and makes no warranties of any kind as to the productivity, proper operation or profitability of any oil, gas or any other mineral in connection with such a report is used or relied upon.

## UNSTEADY-STATE WATER-OIL RELATIVE PERMEABILITY

Company : Phillips Petroleum Company

Formation : San Andres

Location : Ector County, Texas

Well Name : South Cowden #8-19

Sample : 48

Porosity : 21 %

Depth : 4665' 6"

Permeability : 25.67 mD

Temperature : 70 deg. F

Keo @ Siw : 3.15 mD

Oil Viscosity : 22.48 cP

Kew @ Sro : 1.198 mD

Brine Viscosity : 0.96 cP

### TEST RESULTS :

No.	Sw %	* Krw	* Kro	Krw/Kro
—		—	—	—
1	29.00	0.0000	1.0000	0.0000
2	35.88	0.0239	0.5031	0.0474
3	40.88	0.0447	0.3206	0.1395
4	43.31	0.0596	0.2612	0.2282
5	45.06	0.0699	0.2159	0.3237
6	46.00	0.0785	0.2019	0.3887
7	47.88	0.0866	0.1522	0.5692
8	49.59	0.1033	0.1191	0.8676
9	50.33	0.1169	0.1139	1.0268
10	53.38	0.1535	0.0731	2.0982
11	57.55	0.2071	0.0414	5.0000
12	66.44	0.3803	0.0000	n/a

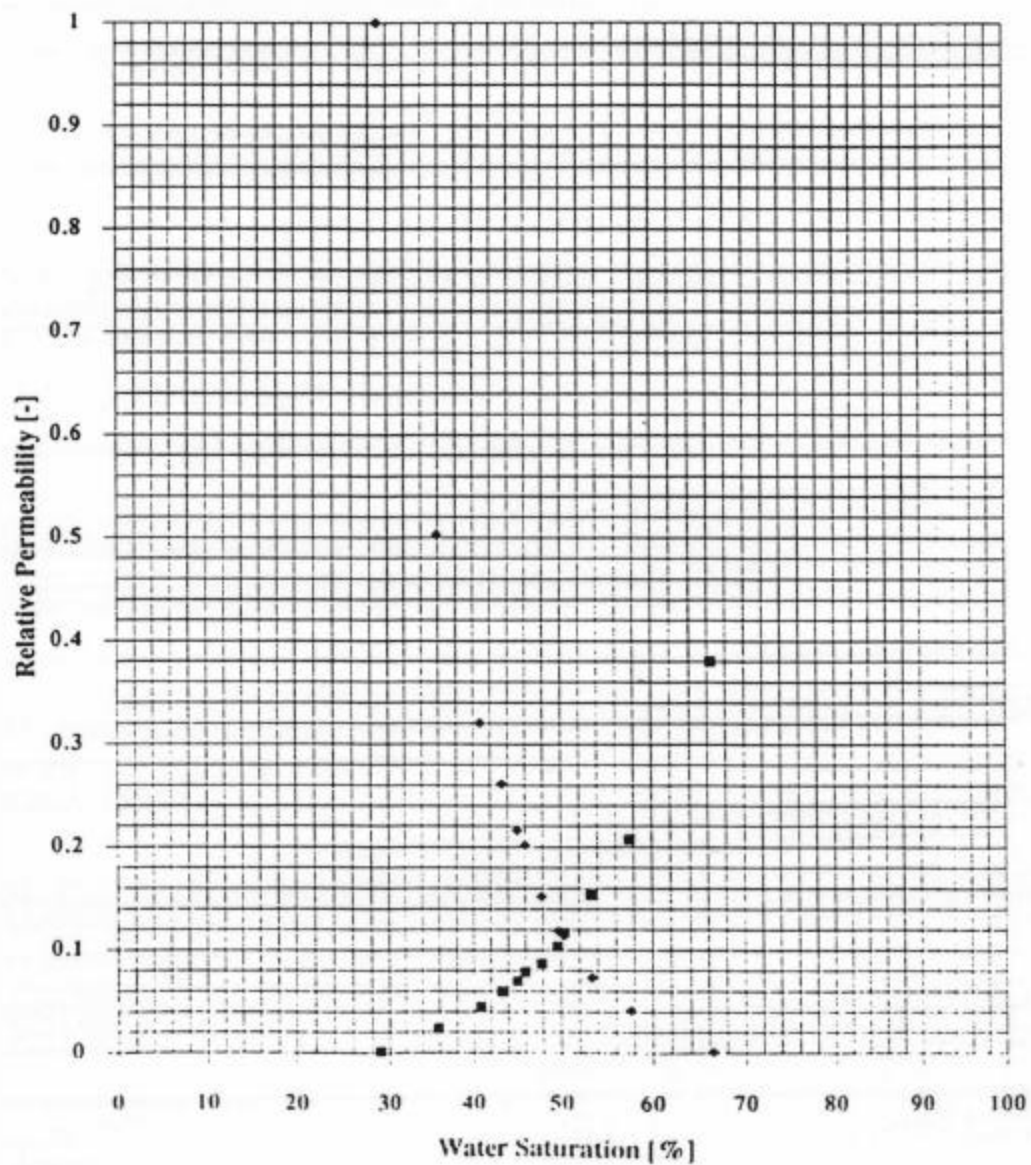
\* Relative to Keo @ Siw

Notations:

Keo Effective Oil Permeability  
 Kew Effective Water Permeability  
 Sro Residual Oil Saturation  
 Siw Irreducible Water Saturation

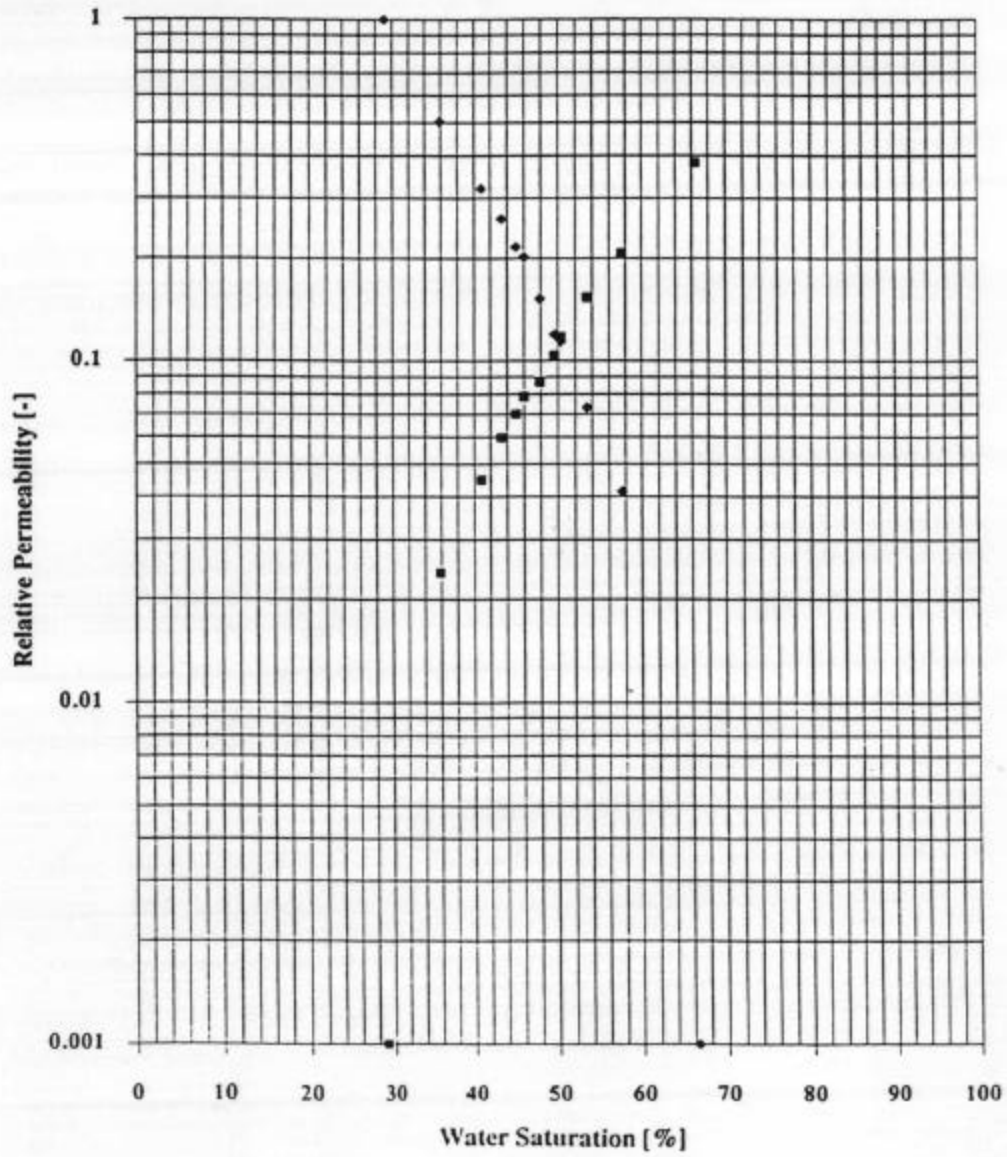
# Unsteady-State Water-Oil Relative Permeability Sample 48

■ Water Relative Permeability    ♦ Oil Relative Permeability

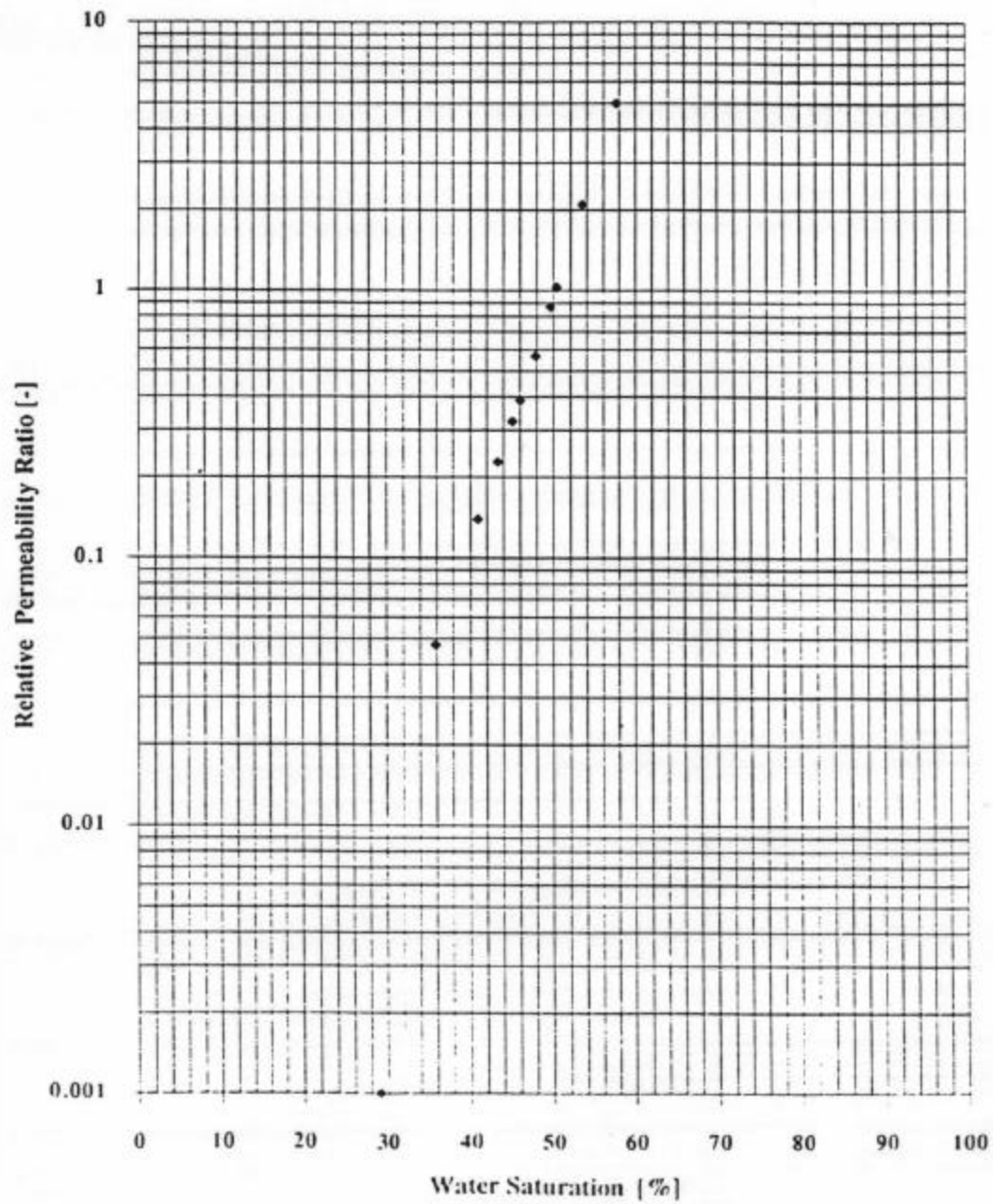


# Unsteady-State Water-Oil Relative Permeability Sample 48

■ Water Relative Permeability ♦ Oil Relative Permeability



Water-Oil Relative Permeability Ratio  
Sample 48



## UNSTEADY-STATE WATER-OIL RELATIVE PERMEABILITY

Company : Phillips Petroleum Company

Formation : San Andres

Location : Ector County, Texas

Well Name : South Cowden #8-19

Sample : 60

Porosity : 22.66 %

Depth : 4716' 6"

Permeability : 231 mD

Temperature : 70 deg. F

Keo @ Siw : 172 mD

Oil Viscosity : 22.48 cP

Kew @ Sro : 46.4 mD

Brine Viscosity : 0.96 cP

### TEST RESULTS :

No.	Sw %	* K <sub>rw</sub>	* K <sub>ro</sub>	K <sub>rw</sub> /K <sub>ro</sub>
—	—	—	—	—
1	19.49	0.0000	1.0000	0.0000
2	26.52	0.0165	0.5692	0.0290
3	33.81	0.0319	0.3578	0.0893
4	37.06	0.0416	0.2981	0.1395
5	39.76	0.0494	0.2459	0.2009
6	41.38	0.0582	0.2329	0.2500
7	44.20	0.0722	0.1925	0.3750
8	48.59	0.0997	0.1489	0.6696
9	52.54	0.1192	0.0980	1.2165
10	58.37	0.1438	0.0433	3.3185
11	68.95	0.2698	0.0000	n/a

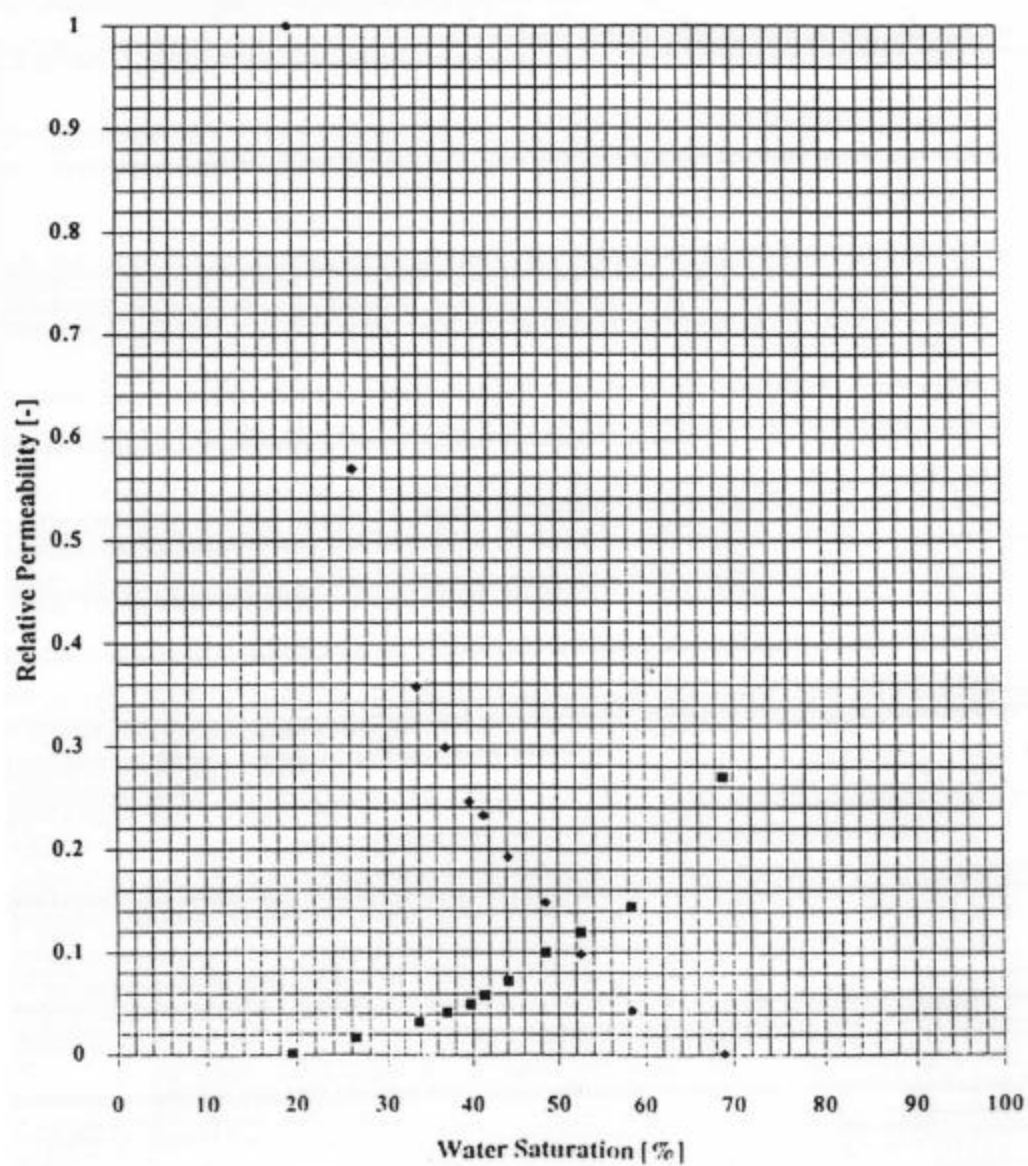
\* Relative to Keo @ Siw

### Notations:

Keo Effective Oil Permeability  
 Kew Effective Water Permeability  
 Sro Residual Oil Saturation  
 Siw Irreducible Water Saturation

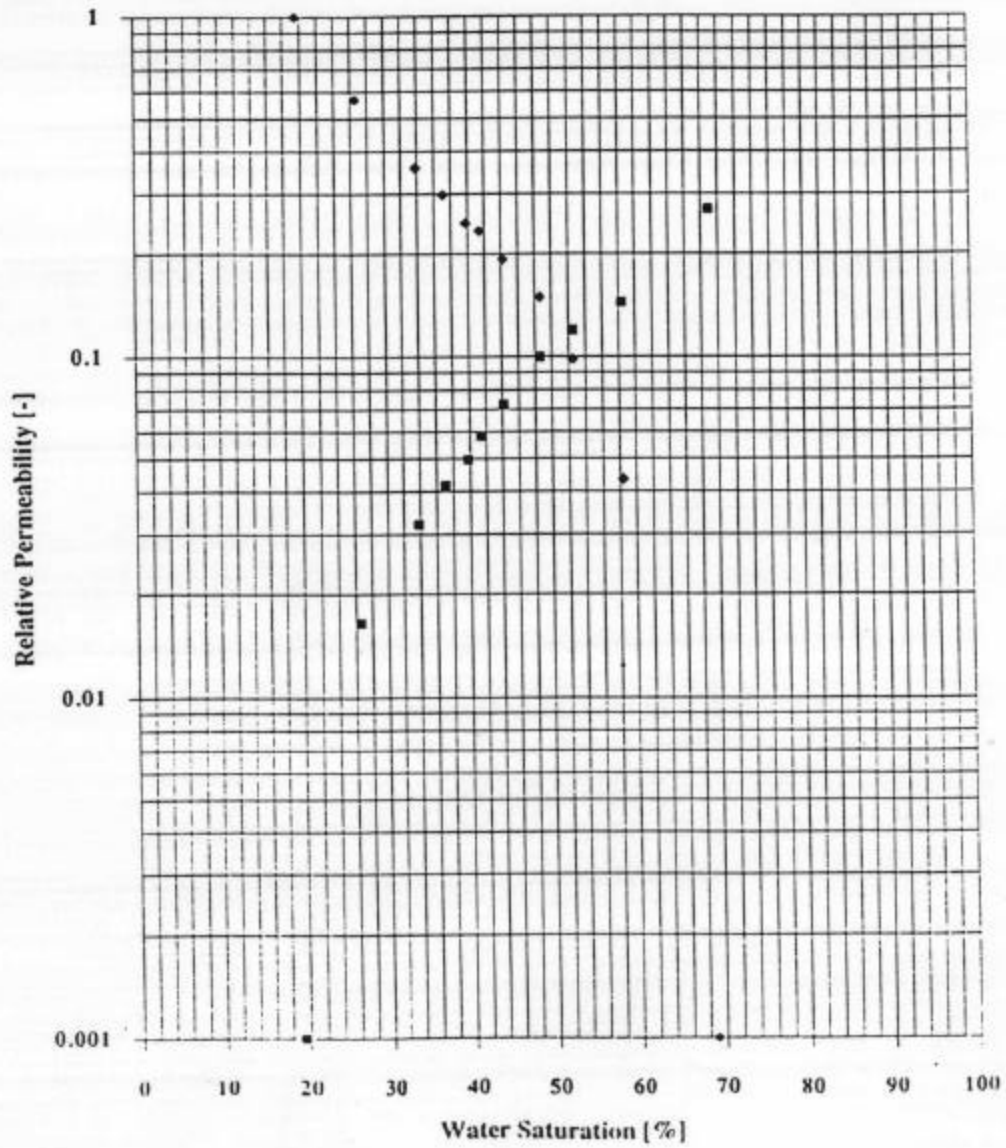
# Unsteady-State Water-Oil Relative Permeability Sample 60

■ Water Relative Permeability ♦ Oil Relative Permeability



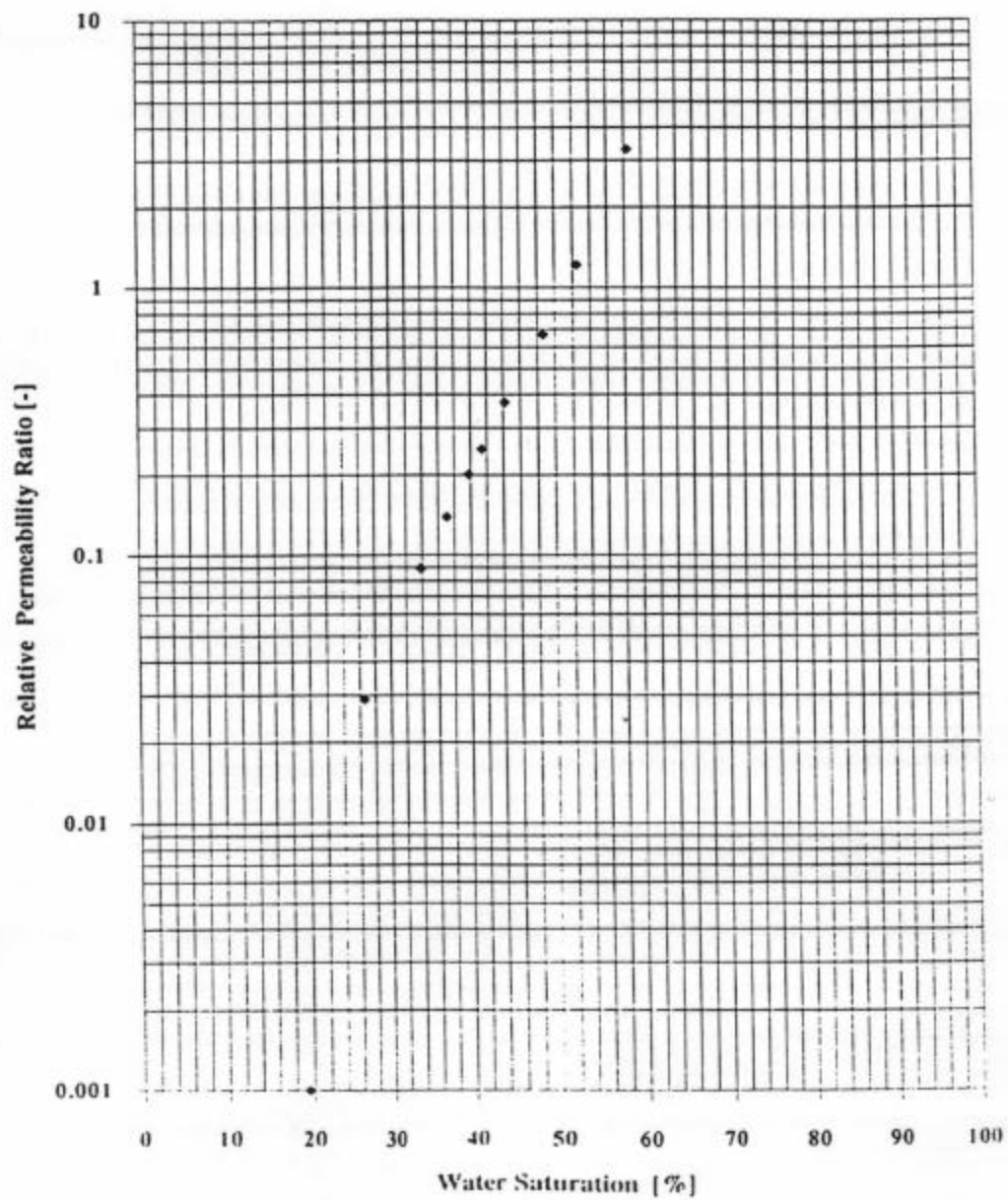
Unsteady-State Water-Oil Relative Permeability  
Sample 60

■ Water Relative Permeability    ♦ Oil Relative Permeability





**Water-Oil Relative Permeability Ratio  
Sample 60**



## UNSTEADY-STATE WATER-OIL RELATIVE PERMEABILITY

Company : Phillips Petroleum Company

Formation : San Andres

Location : Ector County, Texas

Well Name : South Cowden #8-19

Sample : 87

Porosity : 16.8 %

Depth : 4782' 3"

Permeability : 5.31 mD

Temperature : 70 deg. F

Keo @ Siw : 3.2 mD

Oil Viscosity : 22.48 cP

Kew @ Sro : 0.769 mD

Brine Viscosity : 0.96 cP

### TEST RESULTS :

No.	Sw %	* K <sub>rw</sub>	* K <sub>ro</sub>	K <sub>rw</sub> /K <sub>ro</sub>
—	—	—	—	—
1	27.19	0.0000	1.0000	0.0000
2	36.64	0.0586	0.6558	0.0893
3	40.80	0.0849	0.4075	0.2083
4	41.78	0.0982	0.3927	0.2500
5	43.34	0.1080	0.3337	0.3237
6	45.27	0.1187	0.2658	0.4464
7	47.84	0.1298	0.1762	0.7366
8	<del>47.53</del> 48.53(?)	0.1397	0.2019	0.6920
9	49.92	0.1476	0.1438	1.0268
10	51.71	0.1609	0.1138	1.4137
11	53.74	0.1774	0.0828	2.1429
12	55.59	0.1930	0.0660	2.9228
13	58.09	0.2063	0.0413	5.0000
14	67.64	0.2403	0.0000	n/a

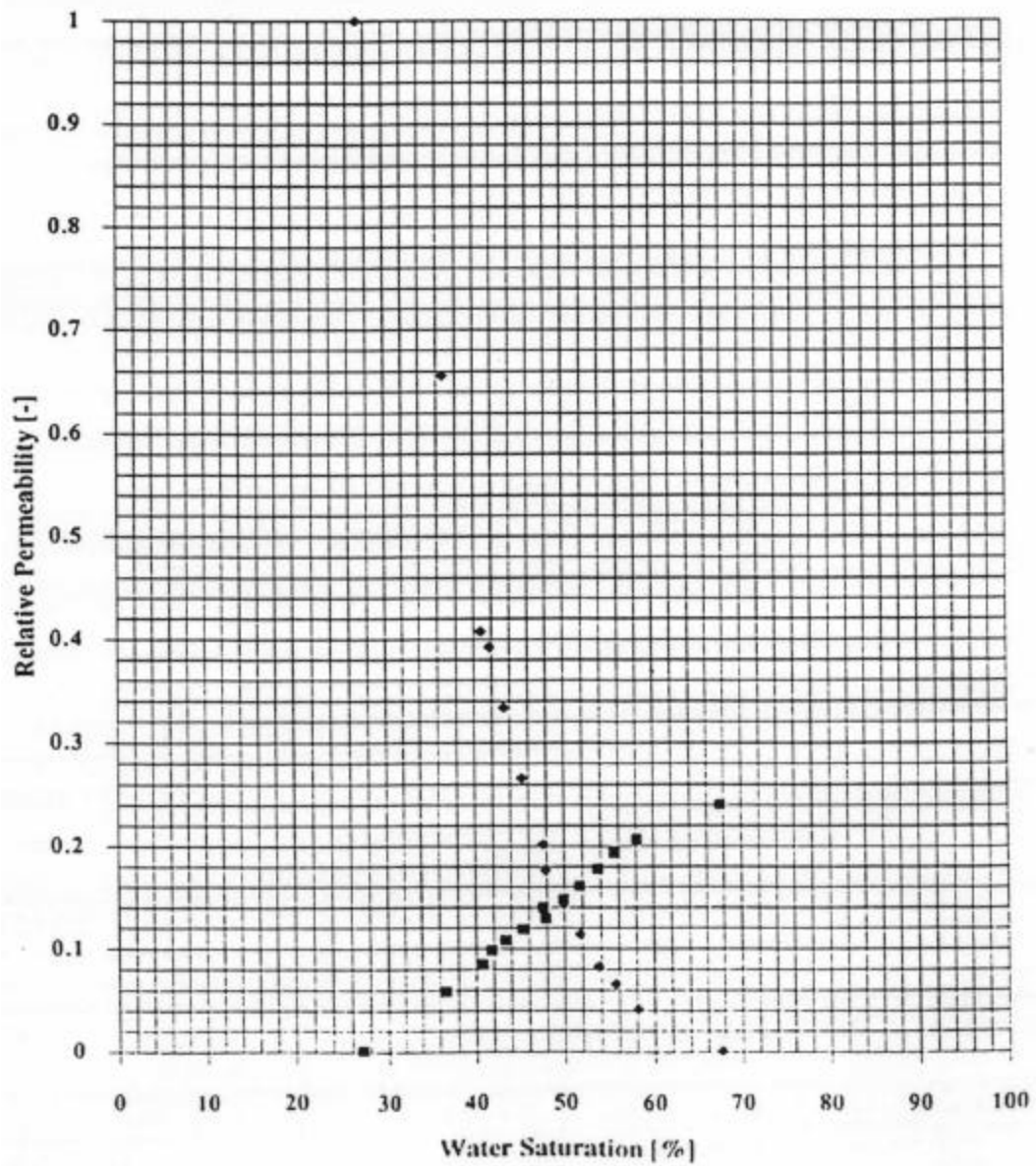
\* Relative to Keo @ Siw

#### Notations:

Keo Effective Oil Permeability  
 Kew Effective Water Permeability  
 Sro Residual Oil Saturation  
 Siw Irreducible Water Saturation

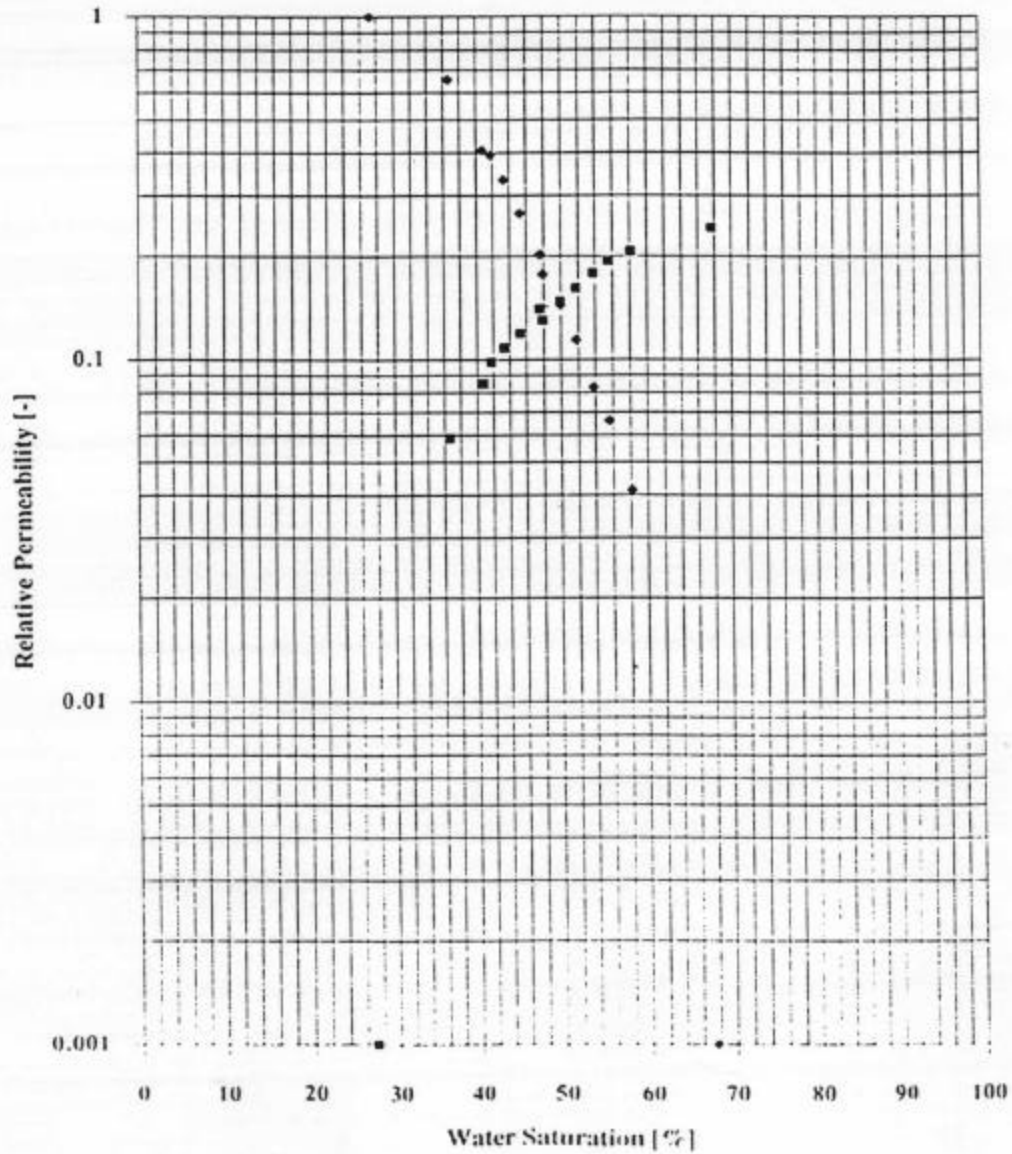
# Unsteady-State Water-Oil Relative Permeability Sample 87

■ Water Relative Permeability ♦ Oil Relative Permeability

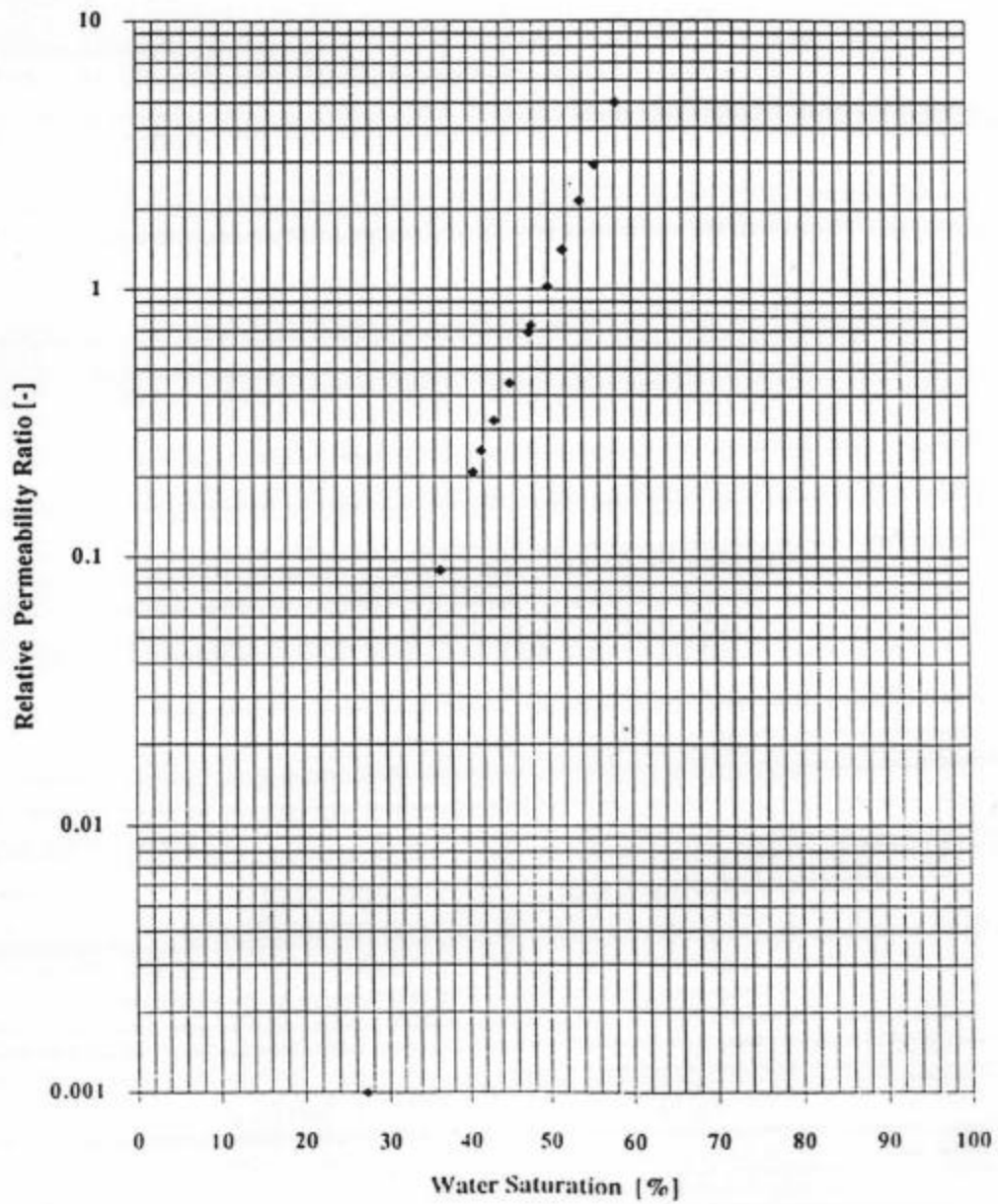


# Unsteady-State Water-Oil Relative Permeability Sample 87

■ Water Relative Permeability    ♦ Oil Relative Permeability



**Water-Oil Relative Permeability Ratio  
Sample 87**



## UNSTEADY-STATE WATER-OIL RELATIVE PERMEABILITY

Company : Phillips Petroleum Company

Formation : San Andres

Location : Ector County, Texas

Well Name : South Cowden #8-19

Sample : 111

Porosity : 14.71 %

Depth : 4830' 4"

Permeability : 24.59 mD

Temperature : 70 deg. F

Keo @ Siw : 14.1 mD

Oil Viscosity : 22.48 cP

Kew @ Sro : 4.7 mD

Brine Viscosity : 0.96 cP

### TEST RESULTS :

No.	Sw %	* Krw	* Kro	Krw/Kro
—		—	—	—
1	26.09	0.0000	1.0000	0.0000
2	33.68	0.0171	0.4062	0.0420
3	43.84	0.0516	0.2476	0.2083
4	46.31	0.0683	0.2110	0.3237
5	48.11	0.0828	0.1854	0.4464
6	50.33	0.0936	0.1353	0.6920
7	53.44	0.1265	0.0914	1.3839
8	55.47	0.1391	0.0649	2.1429
9	58.03	0.1741	0.0525	3.3185
10	61.16	0.2167	0.0342	6.3329
11	71.22	0.3336	0.0000	n/a

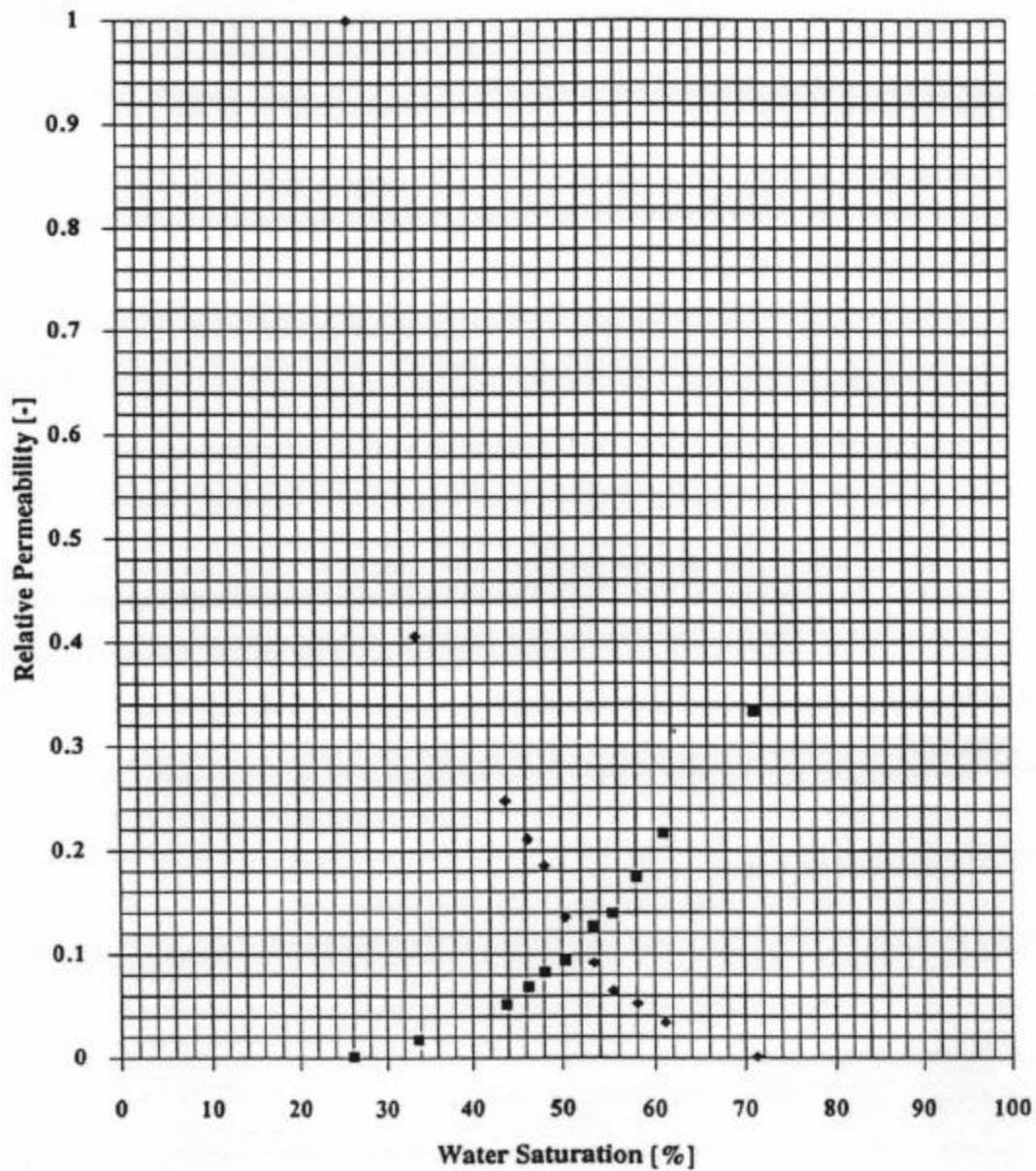
\* Relative to Keo @ Siw

#### Notations:

Keo Effective Oil Premeability  
 Kew Effective Water Permeability  
 Sro Residual Oil Saturation  
 Siw Irreducible Water Saturation

# Unsteady-State Water-Oil Relative Permeability Sample 111

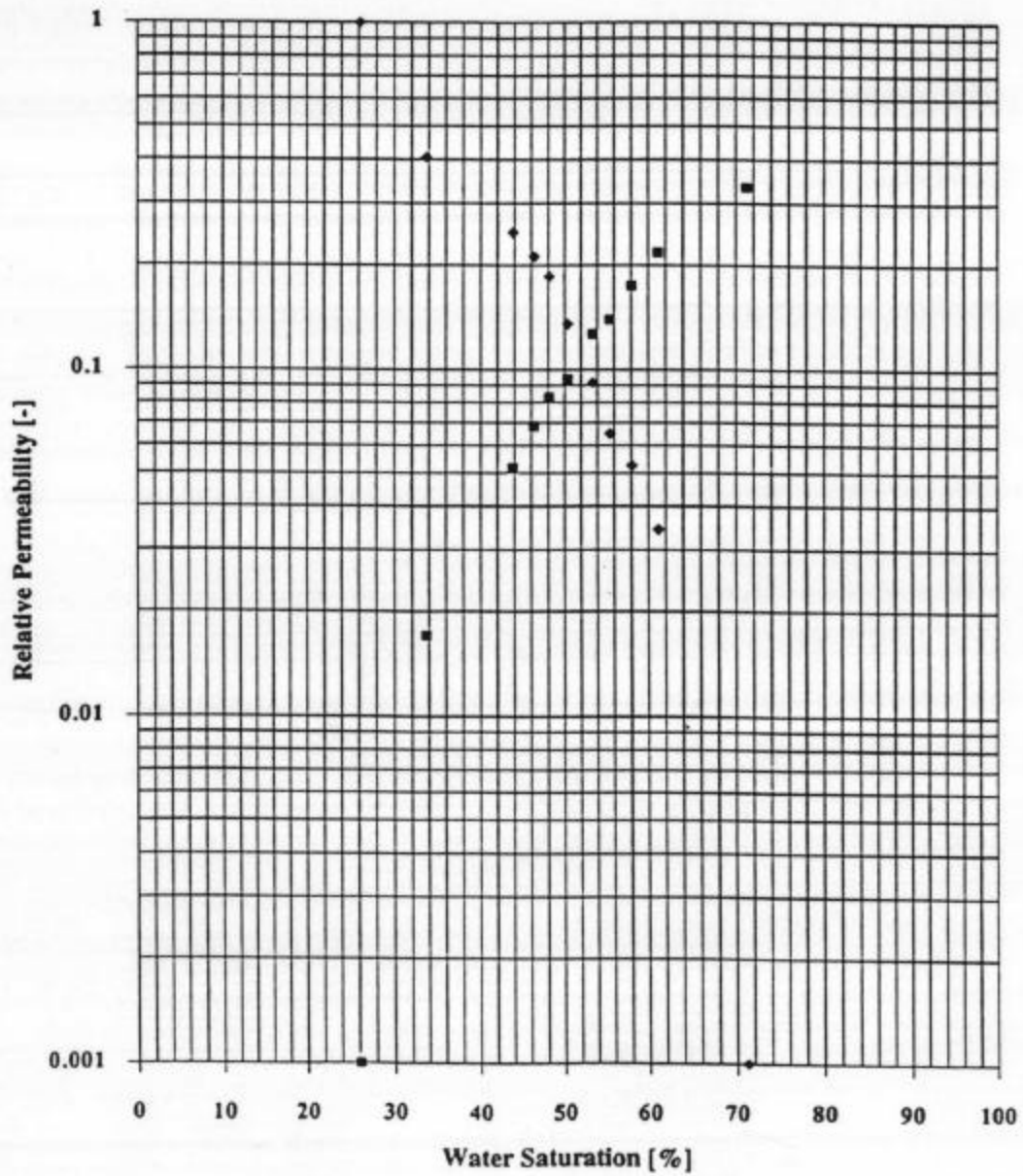
■ Water Relative Permeability   ♦ Oil Relative Permeability





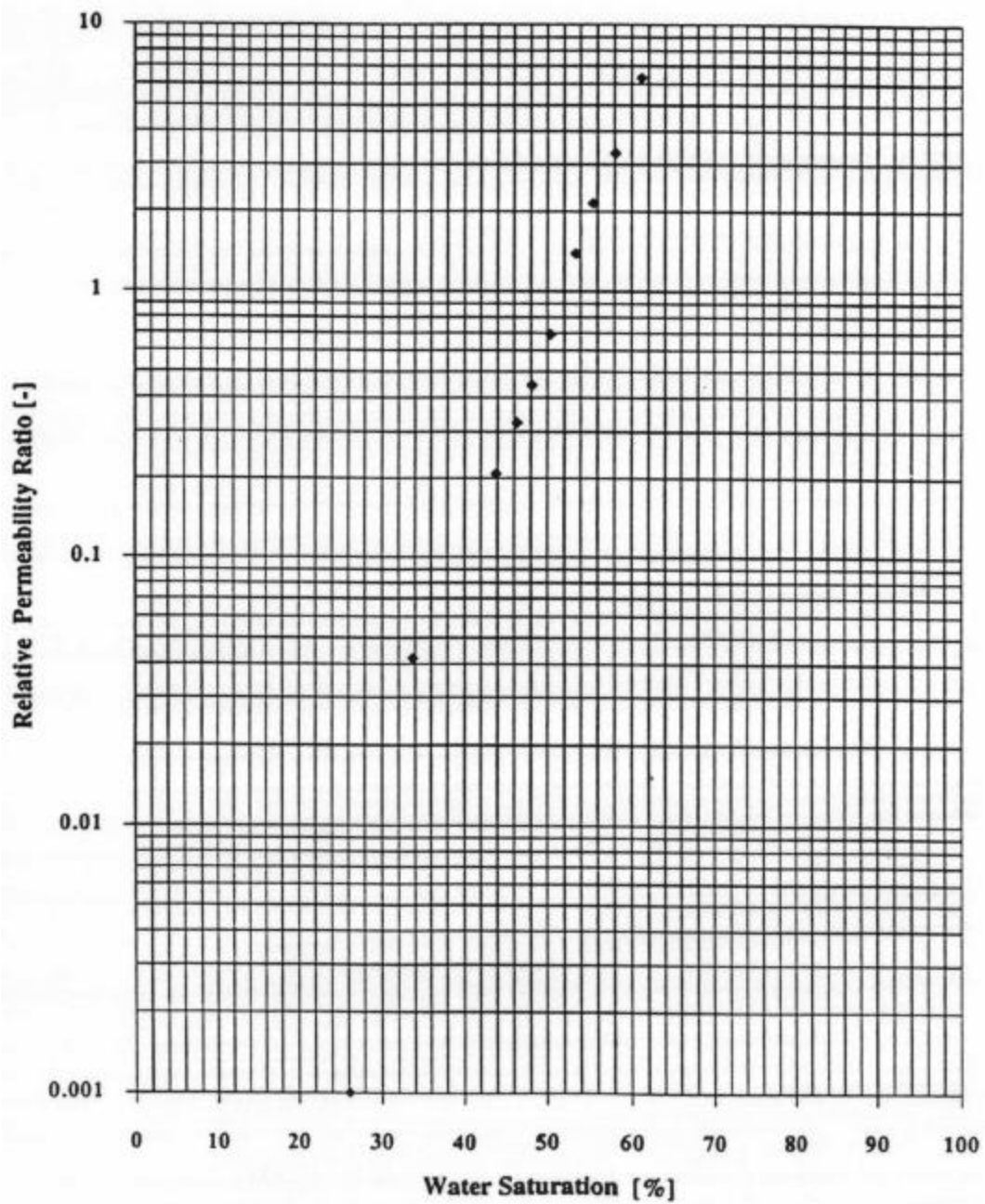
**Unsteady-State Water-Oil Relative Permeability  
Sample 111**

■ Water Relative Permeability ♦ Oil Relative Permeability





**Water-Oil Relative Permeability Ratio  
Sample 111**



## UNSTEADY-STATE WATER-OIL RELATIVE PERMEABILITY

Company : Phillips Petroleum Company

Formation : San Andres

Location : Ector County, Texas

Well Name : South Cowden #8-19

Sample : 124

Porosity : 12.35 %

Depth : 4872' 10"

Permeability : 34.01 mD

Temperature : 70 deg. F

Keo @ Siw : 17.9 mD

Oil Viscosity : 22.48 cP

Kew @ Sro : 5.5 mD

Brine Viscosity : 0.96 cP

### TEST RESULTS :

No.	Sw %	* Krw	* Kro	Krw/Kro
—		—	—	—
1	27.00	0.0000	1.0000	0.0000
2	40.45	0.0432	0.3632	0.1190
3	45.76	0.0767	0.2370	0.3237
4	47.17	0.0926	0.2146	0.4315
5	49.41	0.1055	0.1524	0.6920
6	50.94	0.1168	0.1159	1.0077
7	52.10	0.1346	0.0952	1.4137
8	53.80	0.1436	0.0670	2.1429
9	55.12	0.1556	0.0505	3.0804
10	56.20	0.1691	0.0391	4.3304
11	59.51	0.1958	0.0195	10.0446
12	68.40	0.3073	0.0000	n/a

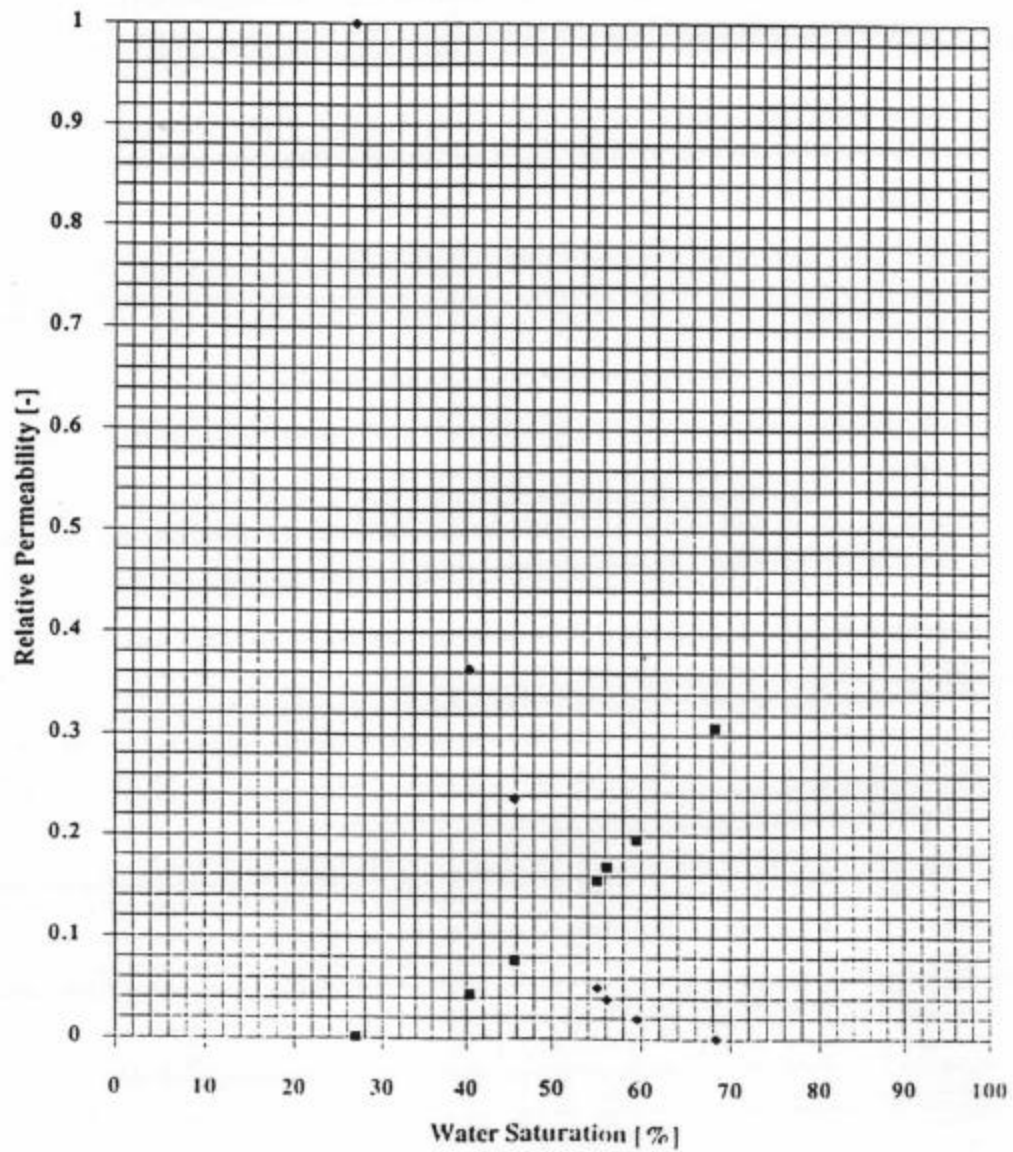
\* Relative to Keo @ Siw

#### Notations:

Keo Effective Oil Permeability  
 Kew Effective Water Permeability  
 Sro Residual Oil Saturation  
 Siw Irreducible Water Saturation

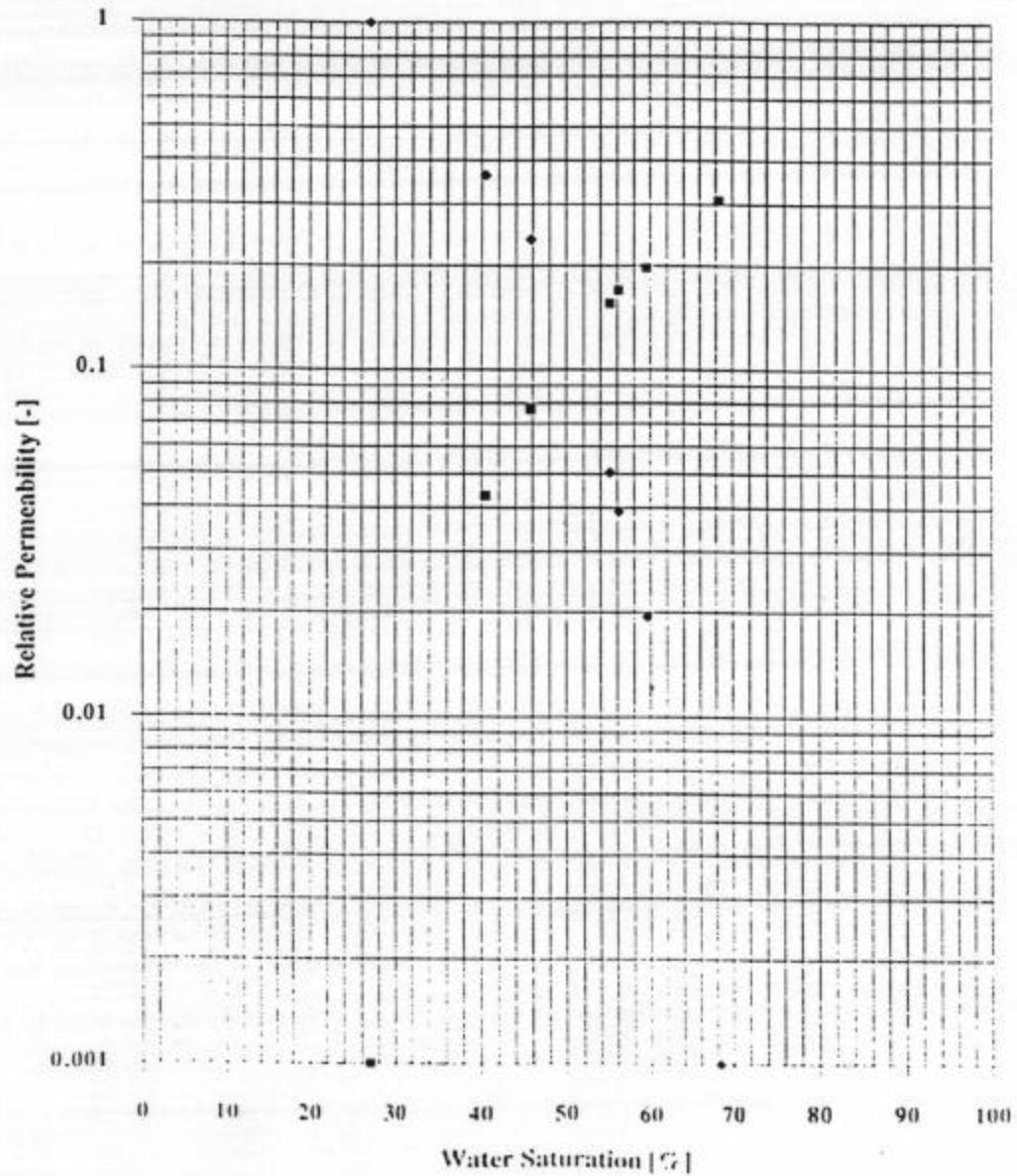
Unsteady-State Water-Oil Relative Permeability  
Sample 124

■ Water Relative Permeability    • Oil Relative Permeability



# Unsteady-State Water-Oil Relative Permeability Sample 124

■ Water Relative Permeability • Oil Relative Permeability



cc: R & D Files (Ex 4 - 7)

Shofner Smith (r)

A. F. Bertuzzi,  
E&P Well Files

R. L. Fayl

T. A. Matthews

F. F. Lovering (r)

R. D. Schropp,

G. W. Edwards (2)

F. F. Lovering (r)

F. W. Forward

S. E. Elliott (r)

B. L. Lawson

R. V. Smith (r) RLC

W. F. Buce

PHILLIPS PETROLEUM COMPANY  
RESEARCH AND DEVELOPMENT DEPARTMENT  
RESERVOIR ENGINEERING LABORATORY  
BARTLESVILLE, OKLAHOMA

LABORATORY REPORT

Report No. RL-239-R-5-73

September 18, 1973

SOUTH COWDEN UNIT WELL NO. 8-11, SOUTH COWDEN FIELD,  
ECTOR COUNTY, TEXAS, CAPILLARY PRESSURE,  
GAS-OIL AND WATER-OIL RELATIVE PERMEABILITY  
TESTS ON SAN ANDRES FORMATION CORE SAMPLES

by

W. F. Buce, C. E. Bailey and B. J. Kellogg

I. SUMMARY

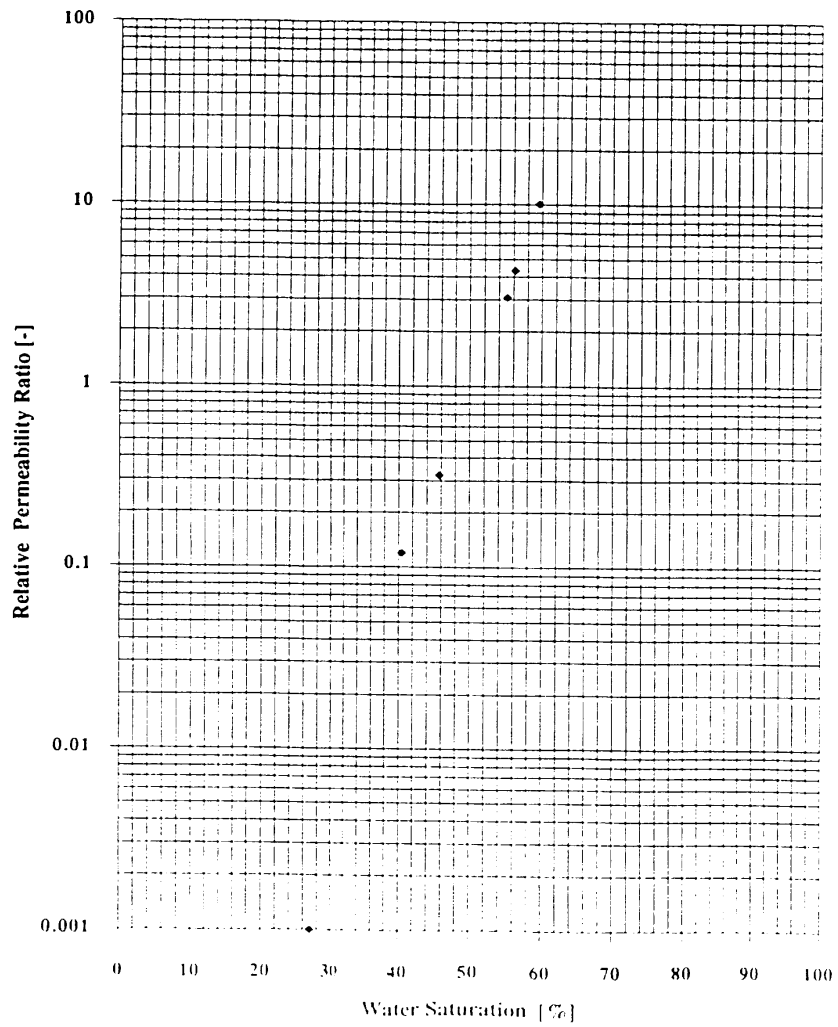
Capillary pressure measurements were made on ten permeability plugs with specific gas permeabilities ranging from 0.113 to 12.8 millidarcys. The residual water saturation at 60 psig varied from 25.0 to 66.7 per cent of the pore volume. Gas-oil relative permeability measurements were made on eight samples with effective permeabilities to oil, with residual water in place, ranging from 0.083 to 40.1 millidarcys, and the displaced oil varied from 23.0 to 55.0 per cent. Water-oil relative permeability measurements were made on seven samples. The effective permeabilities to oil, with residual water in place, ranged from 0.154 to 38.7 millidarcys, and the displaced oil varied from 34.9 to 55.2 per cent of the pore volume.

II. INTRODUCTION

Conventional cores were taken in the San Andres formation from the South Cowden Unit Well No. 8-11, Ector County, Texas, during April, 1973. Core Laboratories, Inc. analyzed the cores by the whole core method, leaving approximately 1/2 foot of every 1 1/2 feet of the core material undamaged for special analysis. All of the core samples were shipped to Bartlesville with 47 feet in a preserved condition.

The special analyses requested by Mr. A. J. Cornelius in his letter of April 10, 1973, (W2-Ed-213-73) to Mr. R. V. Smith consists of capillary pressure tests, gas-oil and water-oil relative permeability tests, and porosity, specific gas permeability, and grain density measurements made on the unused portions of core. This study is to assist in determining the critical gas saturation of the San Andres formation in the South Cowden Field.

Water-Oil Relative Permeability Ratio  
Sample 124



### III. EXPERIMENTAL

Permeability plugs approximately  $3/4$  inch and  $1\frac{1}{2}$  inches in diameter by  $1\frac{1}{2}$  inches to 3 inches in length were cut from the core samples that were not used for whole core analysis. The permeability plug samples were extracted with toluene and tetrahydro-2-methylfuran for approximately two weeks, alternating the two solvents until the effluent was clear. The samples were dried at a temperature below  $140^{\circ}\text{F}$ .

Dry nitrogen gas was used in obtaining the specific gas permeabilities and simulated formation water was used for specific water permeabilities. The composition of the simulated formation water is listed in Table I. The Boyle's law technique using helium gas was employed in obtaining the porosity and grain density measurements of the samples which are listed with the specific gas permeabilities in Table II.

Ten permeability plugs approximately  $3/4$ -inch in diameter by  $1\frac{1}{2}$  inches in length were partially saturated under vacuum with simulated formation water. They were then pressured to 2,500 psi in the same water overnight to attain complete saturation. Capillary pressures were determined by the centrifuge method with air as the displacing fluid. The temperature was maintained at  $77^{\circ}\text{F}$ , at which the density of the simulated water was 1.0605 g/ml. The capillary pressure curves and other pertinent data are presented in Figures 1 through 5. The water saturation at a capillary pressure of 60 psig is shown in Table III along with other pertinent data.

The gas-oil relative permeability measurements were made on eight permeability plugs,  $1\frac{1}{2}$  inches in diameter with lengths varying from 2.02 to 2.92 inches. The samples were saturated with simulated formation water by high vacuum, and to insure complete saturation a pressure of 2,500 psi was applied on the samples while they were in the simulated formation brine. Specific permeabilities to simulated formation water were measured after complete saturation with water. The samples were partly desaturated by centrifugation, and the residual water saturations were determined after measuring the effective gas permeabilities. The samples were then evacuated and saturated with refined oil. A small amount of water was removed and accounted for on each sample during the resaturation of the samples. Effective permeabilities to oil with residual water in place were measured and calculated in accordance with the procedures described by E. T. Guerrero<sup>(1)</sup>. The gas-oil relative permeability curves and relative permeability ratio curves are presented in Figures 6 through 21 along with other information. Table IV presents the amount of oil recovered by gas drive.

Water-oil relative permeability measurements were made on five of the eight samples (representing depths of 4613-14, 4625-26, 4682-83, 4694-95, and 4740-41 feet) on which the gas-oil relative permeability measurements were made. These samples were resaturated after the gas drive, and the small amount of residual water loss was considered.

Two samples representing 4613-14 feet and 4625-26 feet were cleaned and dried after the above water-oil relative permeability tests. The flooding procedures for the second set of water-oil relative permeability tests were the same except to obtain the residual water saturation a displacement pressure of 50 psig was used as compared to 350 psig in the initial tests. The water-oil relative permeability curves and ratio curves are presented on Figures 22 through 30. The amount of oil produced by water drive and other pertinent data are

TABLE I

COMPOSITION OF SIMULATED SOUTH COWDEN UNIT 8-07 WATER  
FROM THE SAN ANDRES FORMATION

Calcium Chloride ( $\text{CaCl}_2$ )	8,736 ppm
Magnesium Chloride ( $\text{MgCl}_2 \cdot 6 \text{H}_2\text{O}$ )	5,837 ppm
Sodium Chloride ( $\text{NaCl}$ )	73,916 ppm
Sodium Bicarbonate ( $\text{NaHCO}_3$ )	1,108 ppm
Sodium Sulfate ( $\text{Na}_2\text{SO}_4$ )	5,037 ppm

(1) Guerrero, E. T., Practical Reservoir Engineering, the Petroleum Publishing Co., Tulsa, Oklahoma, 1968.

IV. DISCUSSION

The capillary pressure curves for the San Andres formation have threshold pressures of 3 to 10 psig which suggest that a water zone of 11 to 36.7 feet in thickness may exist below the oil layer in the formation. The residual water saturations varied from 25 per cent to 66.7 per cent at 60 psig capillary pressure.

None of the gas-oil relative permeability tests were continued to zero production; however, the tests were continued until high gas-oil ratios were attained. The average oil recovery of the gas drive was 34.9 per cent with samples representing depths of 4745-46 feet and 4613-14 feet being the extreme cases, having oil recoveries of 23 and 53 per cent of the pore volume, respectively. The average recovery of oil displaced by water injection was 46.9 per cent of the pore volume, with samples representing depths of 4745-46 feet and 4613-14 feet being the extreme cases, having oil recoveries of 34.9 and 55.2 per cent of the pore volume, respectively. Samples representing depths of 4613-14 feet and 4625-26 feet had displacement pressures of approximately 350 psig and 50 psig applied by centrifugation to obtain the residual water saturations at the prescribed pressures for testing the residual saturation effects on the relative permeability tests. Results were 55.2 and 46.2 per cent at 350 psig pressure, compared to 54.9 and 43.2 per cent at 50 psig, respectively. Although the initial oil saturations before waterflooding were highly dependent upon the capillary pressure used to establish the residual water saturations, the amount of oil recovered by the water flood was only slightly affected as shown in Table V.

V. CONCLUSIONS

1. The capillary pressure curves have threshold pressures of 3 to 10 psig, which suggests that a water zone at least 11 to 37 feet thick may exist below the oil zone. The residual water saturations varied from 25 to 66 per cent at 60 psig capillary displacement pressure.
2. The average oil recovery was 34.9 per cent of the pore volume using gas as the displacement fluid.
3. The average oil recovery was 46.9 per cent of the pore volume using water as the displacement fluid.
4. The residual water saturations had little or no effect on the amount of oil recovered on the samples tested.



**TABLE II**  
**SOUTH COWDEN WELL NO. P-11**  
**POROSITY, SPECIFIC GAS PERMEABILITY AND GRAIN DENSITY MEASUREMENTS**

Depth, Feet From To	Specific Gas, Permeability, Md.		Porosity, Per Cent		Grain Density, g/ml	
	3/4" dia.	1" dia.	3/4" dia.	1" dia.	3/4" dia.	1" dia.
4579 - 4580	0.598	0.392	1.52	5.69	2.86	2.84
4584 - 4585	.037	.075	3.82	2.62	2.80	2.80
4587 - 4588	.318	.30	10.24	3.62	2.89	2.84
4589 - 4590	(a)	.426		4.62		2.85
4590 - 4591		2.64		15.42		2.82
4593 - 4594	.658	1.50	6.01	9.25	2.84	2.84
4595 - 4596	1.39	1.16	17.47	9.86	2.78	2.75
4597 - 4598	3.45	.478	15.27	6.51	2.81	2.81
4598 - 4599	.015		6.54			2.71
4600 - 4601	.006	.022	0.79	0.29	2.80	2.80
4610 - 4611	.167			2.48		2.81
4611 - 4612	.527	.959	11.52	9.17	2.84	2.83
4613 - 4614	9.02	42.2	20.47	22.07	2.83	2.82
4619 - 4620		4.87		18.49		2.84
4621 - 4622	.030	7.83	8.79	15.65	2.80	2.86
4623 - 4624		1.34		17.60		2.83
4625 - 4626	12.8	7.33	16.28	18.63	2.86	2.84
4627 - 4628		50.5		19.28		2.85
4629 - 4630	3.84	11.0	13.54	12.49	2.87	2.88
4630 - 4631		0.087		8.29		2.85
4631 - 4632	5.79	2.71	15.99	12.18	2.82	2.79
4649 - 4650	.844	11.6	12.13	15.78	2.85	2.85
4650 - 4651	3.92	0.328	15.02	11.06	2.86	2.84
4656 - 4657	7.88	10.00	13.32	15.05	2.85	2.83
4661 - 4662	0.022		5.36		2.83	
4670 - 4671	.328		10.80		2.84	
4671 - 4672		0.595		11.48		2.84
4673 - 4674	2.23	6.01	13.27	15.97	2.83	2.83
4674 - 4675	.217		8.26		2.85	
4679 - 4680	0.384	0.805	10.57	9.13	2.85	2.84
4682 - 4683	0.318	0.412	8.25	8.38	2.86	2.85
4684 - 4685	7.23		15.31		2.84	
4689 - 4690	17.5	8.02	15.55	12.59	2.85	2.84
4690 - 4691		.819		10.47		2.84
4692 - 4693	.053		6.92		2.84	
4694 - 4695	0.853	1.16	12.28	10.11	2.83	2.81
4697 - 4698	.033	.315	8.56	6.70	2.85	2.84
4698 - 4699	.112		7.07		2.84	
4702 - 4703		.357		8.77		2.75
4710 - 4711	.122	.687	7.94	10.14	2.82	2.82
4713 - 4714	.052		10.63		2.71	

(a) Samples were too soft to retain identification markings during the cleaning and could not be used.

TABLE II (Cont'd)

Depth, Feet		Specific Gas, Permeability, Md.		Porosity, Per Cent		Grain Density, g/ml	
From	To	3/4" dia.	1 1/2" dia.	3/4" dia.	1 1/2" dia.	3/4" dia.	1 1/2" dia.
4718	- 4719	3.04	5.06	13.66	13.29	2.87	2.83
4723	- 4724	7.18	2.12	18.59	13.88	2.85	2.85
4725	- 4726		.711		11.50		2.85
4728	- 4729		.844		11.75		2.72
4731	- 4732	9.98		9.67		2.85	
4734	- 4735	.609	.803	7.13	9.91	2.84	2.84
4737	- 4738	.245	.413	4.96	6.78	2.85	2.79
4740	- 4741	9.18	6.07	11.03	11.70	2.84	2.84
4743	- 4744	1.65	.655	9.86	8.49	2.84	2.84
4745	- 4746	.361	.378	7.95	8.61	2.86	2.85
4754	- 4755	0.113	0.185	7.12	6.74	2.85	2.85
4756	- 4757	8.84	12.6	13.70	13.21	2.84	2.83
4758	- 4659	0.03	0.21	8.31	8.48	2.84	2.82

TABLE III  
WATER SATURATIONS AT 60 PSIG CAPILLARY PRESSURE  
GAS PERMEABILITIES AND POROSITIES

<u>From</u>	<u>To</u>	<u>Permeability, Millidarcys</u>	<u>Porosity, Per Cent</u>	<u>Water Saturation at 60 psig Capillary Pressure</u>	<u>Grain Density, g/ml</u>
4613	4614	9.02	20.5	33.0	2.83
4625	4626	12.8	16.28	41.5	2.86
4682	4683	0.318	8.25	64.3	2.86
4694	4695	0.853	12.3	51.0	2.83
4718	4719	3.04	13.7	41.5	2.87
4731	4732	9.98	9.67	34.6	2.85
4734	4735	0.609	9.31	55.0	2.84
4740	4741	9.18	11.0	25.0	2.84
4745	4746	0.361	7.95	66.7	2.86
4754	4755	0.113	7.12	59.4	2.85

TABLE IV

SOUTH COWDEN WELL NO. 8-11  
OIL RECOVERY BY LABORATORY NITROGEN GAS DRIVE

Depth, Feet From To	Original Oil Saturation, Per Cent	Final Oil <sup>(c)</sup> Saturation, Per Cent	Oil Recovered, Per Cent Porosity	Porosity, Per Cent	Effective Permeability Md., to Oil
4613 - 4614 (a)	90.5	37.5	53.0	22.07	40.1
4625 - 4626 (a)	82.82	36.82	46.0	18.63	5.95
4682 - 4683 (b)	72.00	45.00	27.0	8.38	0.202
4694 - 4695 (a)	73.62	34.62	39.0	10.11	.23
4718 - 4719 (b)	80.10	45.10	35.0	13.29	3.15
4734 - 4735 (b)	61.00	35.5	25.5	9.91	.438
4745 - 4746 (a)	55.27	32.27	23.0	8.61	.153
4754 - 4755 (b)	65.60	34.90	30.5	6.74	.083

- (a) Capillary displacement pressure was approximately 350 psig.  
(b) Capillary displacement pressure was approximately 918 psig.  
(c) Taken from extrapolation of  $K_{ro}$  curve.

TABLE V  
SOUTH COWDEN WELL NO. 2-11  
OIL RECOVERY BY LABORATORY WATER DRIVE

Depth, Feet From To	Original Oil Saturation, Per Cent	Final(d) Oil Saturation, Per Cent	Oil Recovered, Per Cent Porosity	Porosity, Per Cent	Effective Permeability Md., to Oil
4613 - 4614 (a)	94.2	39.0	55.2	22.07	38.7
4613 - 4614 (b)	74.9	20.0	54.9	22.07	36.1
4625 - 4626 (a)	92.23	46.0	46.23	18.63	6.03
4625 - 4626 (b)	67.3	24.1	43.2	18.63	5.60
4682 - 4683 (c)	77.4	31.4	46.0	8.38	0.150
4694 - 4695 (a)	79.06	26.0	53.06	10.11	0.847
4731 - 4732 (c)	76.20	33.5	42.7	9.65	1.89
4740 - 4741 (-)	81.2	30.0	51.2	1.77	11.70
4740 - 4741 (a)	80.1	25.0	34.9	8.61	0.152

(a) Secondary displacement pressure was approximately 350 psig.  
(b) Tertiary displacement pressure was approximately 50 psig.  
(c) Capillary displacement pressure was approximately 918 psig.  
(d) Taken from extrapolation of  $K_{ro}$  curve.

**Special Core Analysis Study**

**For**

**Phillips Petroleum Company  
South Cowden Unit #6-18 Well  
South Cowden Field  
San Andres Formation  
Ector County, Texas**

CORE LABORATORIES, INC.  
SPECIAL SERVICES



December 15, 1982

Phillips Petroleum Company  
4001 Penbrook  
Odessa, Texas 79762

Attention: Kim Dollins

Subject: Special Core Analysis Study  
South Cowden Unit #6-18 Well  
South Cowden Field  
San Andres Formation  
Ector County, Texas  
File: SCAL-206-82025

Gentlemen:

Presented in this report are the final results of a Special Core Analysis Study performed on selected samples from the subject well. The tests in this study; capillary pressure (mercury injection, drainage and imbibition curves), formation resistivity factor, formation resistivity index, Amott wettability, water-flood susceptibility, and relative permeability (gas-oil and water-oil) were performed in Midland, Texas as directed by Kim Dollins.

Acoustic velocity measurements were performed by Core Laboratories' Special Core Analysis Laboratory located in Dallas, Texas and are presented in this report.

Routine Core Analysis was performed by Core Laboratories' Core Analysis facility located in Midland, Texas and the data reported in final form on March 26, 1982.

The presentation of this report was delayed because it was necessary to re-test several samples to provide reliable data. We wish to apologize for any inconvenience this delay caused.

It has been a pleasure to perform this study for Phillips Petroleum Company and we look forward to working with Phillips in the future. If you should have any questions about the testing procedures, the results obtained, or if we can be of any further assistance, please do not hesitate to contact us.

Very truly yours,  
CORE LABORATORIES, INC.

A handwritten signature in dark ink, appearing to read "James L. Pritchard", is written over the typed name.

James L. Pritchard  
Special Core Analysis  
Laboratory Supervisor

Copies: Seven to Addressee

JLP:clw

## Table of Contents

Laboratory Procedures and Discussion.....	I
Identification and Lithological Description.....	1
Permeability to Air and Porosity.....	2
Formation Resistivity Factor and Resistivity Index	
Tabular.....	3-4
Graphical.....	5-15
Gas-Oil Relative Permeability	
Tabular.....	16-20
Graphical.....	21-30
Water-Oil Relative Permeability	
Summary.....	31
Tabular.....	32-37
Graphical.....	38-47
Waterflood Susceptibility	
Summary.....	48
Tabular.....	49-53
Graphical.....	54-58
Amott Wettability.....	59
Mercury Injection Capillary Pressure	
Tabular.....	60-65
Graphical.....	66-73
Pore Size Distribution	
Tabular.....	74-76
Graphical.....	77-84
Acoustic Velocity	
Tabular.....	85-89
Graphical.....	90
Simulated Brine Composition.....	91



## LABORATORY PROCEDURES AND DISCUSSION

### Initial Activities

Initially, one 1-1/2 inch diameter, horizontal sample was drilled from each preserved sample using a synthetic formation water as a bit coolant and lubricant (see simulated brine composition, page 91). The samples designated for the wettability tests were stored under the synthetic brine until needed for analyses. The remaining samples were cleaned with toluene in a gas-driven-solvents type extraction apparatus, leached with methanol to remove the residual salts, then dried in a vacuum oven at 180°F. Permeability to air and helium (Boyles' Law) porosity were measured for each of the clean, dry samples. The samples used in this study are identified as to depth and lithology on page 1. The permeability and porosity data are presented on page 2.

### Formation Resistivity Factor and Formation Resistivity Index

The samples chosen for the electrical properties tests were placed into a saturation cell and evacuated, then pressure-saturated with the synthetic formation water (0.095 ohm-meters @ 74°F). Each of the brine-saturated cores were placed into a coreholder and its resistance ( $R_o$ ) measured. The formation resistivity factor was calculated from the resistance data from each sample. The formation factor data were plotted as a function of porosity and a best-fit (linear regression) line drawn through the resulting points. The slope of the resulting line defines the "m" (cementation exponent) and the "a" intercept is the point on the line where porosity equals 100 percent. The 100 percent brine-saturated samples were placed into a porous plate capillary pressure cell and allowed to desaturate at a relative high pressure (150 psi). As the samples desaturated, they were removed at 4 lower saturations and their resistance ( $R_t$ ) measured. The  $R_o$  resistivity index ( $R_t/R_o$ ) was calculated for each sample at each brine saturation, then plotted as a function of brine saturation. A best-fit (linear regression) line drawn through the resulting points defines the "n" saturation exponent. The formation factor and resistivity index data are presented in tabular form on pages 3-4 and graphically on pages 5-15. Grouping all the samples tested as one zone gives an "a" of 1.00, an "m" of 1.94, and "n" values ranging from 1.70 to 2.23 with a composite of 2.05. These values compare well to known data from similar reservoirs.

### RELATIVE PERMEABILITY

#### Gas-Oil

The samples selected for the relative permeability tests were placed into a saturation cell and evacuated, then pressure-saturated with the synthetic formation water. Each of the brine-saturated samples were placed into a coreholder and restored by flushing with a refined mineral oil (18 centipoise) until its immobile water saturation was reached. The effective permeability to oil was measured at the immobile water saturation. A gas-drive displacement test was performed on each sample with incremental production data recorded until a gas-oil relative permeability ratio of at least 32 was reached. The gas-oil relative permeability data were calculated from the incremental production data for each sample. The gas-oil relative permeability data are presented in tabular form on pages 16-20 and graphically on pages 21-30.

## II

### Water-Oil

After the gas-oil relative permeability tests, the samples were re-saturated with the mineral oil and the permeability to oil measured. Each sample was flooded with the saturating brine and incremental production data recorded until a water cut of 99.99 percent was reached. The effective permeability to water was measured, then the sample was unloaded and its weight recorded. The sample was re-loaded into the coreholder, flushed with the mineral oil, incremental production data recorded until an oil cut of 99.99 percent oil was reached, then the effective permeability to oil was measured in both flow directions. A "Dean-Stark" type analysis was performed on each sample at the conclusion of the tests to calculate materials balance. The imbibition (water saturation increasing) and drainage (water saturation decreasing) water-oil relative permeability was calculated from the incremental production data. The water-oil relative permeability data are summarized on page 31, and presented in tabular form on pages 32-37 and graphically on pages 38-47.

All of the samples tested for relative permeability exhibited plugging apparently due to the migration of mobile fines. Samples 88 and 134 both exhibited channeling late in the flood which probably indicates erosion or solution of the rock matrix by the flooding brine. Based on the water-oil relative permeability tests, the formation appears to be "oil-wet", however, the wettability index tests tends to indicate the formation is "water-wet". Because of this apparent conflict, both the relative permeability and wettability test were repeated to verify the test results. The same samples were used for the relative permeability tests and new preserved samples were obtained for the wettability tests. On re-testing, the results remained unchanged. The restoration process used for the relative permeability test may alter the wettability of the sample tested. Normally, if the wettability is changed, it is altered to become more "water-wet". Because of the mud program used (some surface active agents were present in the mud filtrate) and the "fresh" condition of the samples used for the wettability tests, the restored state relative permeability tests probably give a better indication of the true formation wettability.

### Waterflood Susceptibility

The samples selected for waterflood susceptibility were saturated with the synthetic brine and flushed with the mineral oil as described earlier. The 18 centipoise mineral oil was dynamically displaced with an oil manufactured to duplicate the estimated reservoir oil-water viscosity ratio of 6.11:1. Each restored sample was flooded with the saturating brine, incremental production data were recorded until a water cut of 99.99 percent was reached, then the permeability to water measured in both flow directions. A "Dean-Stark" type analysis was performed on each sample to calculate materials balance. The waterflood susceptibility was calculated for each sample from its incremental production data. The waterflood susceptibility data are summarized on page 48, presented in tabular form on pages 49-53, and graphically on pages 54-58. The waterflood susceptibility test results also tend to indicate an "oil-wet" formation.

### III

#### Amott Wettability

The samples chosen for the wettability tests were stored under the synthetic formation brine until testing started. Each sample was placed into a coreholder and flushed with the synthetic brine until its residual oil saturation was reached. Each sample was placed under a light refined mineral oil in an imbibition cell. Each sample was allowed to imbibe the oil until the spontaneous imbibition of oil ceased. The amount of oil imbibed was recorded, then each sample was loaded into a coreholder, flushed with the oil, and the oil permeability measured. The water displaced by the oil was recorded, then the sample was placed under water in the imbibition cell and allowed to imbibe water until the spontaneous imbibition of water ceased. The amount of water imbibed was recorded, then the sample was loaded into a coreholder, flooded with the synthetic brine, and the water permeability measured. The amount of oil displaced by the flood was recorded, then a "Dean-Stark" type analysis was performed to clean and determine the fluid saturation for each sample. A wettability index for both oil and water was determined for the imbibition and displacement data.

All of the samples tested tend to indicate a strongly "water-wet" formation with the exception of sample 120, which indicates an intermediate wettability. Because the water-oil relative permeability data indicates "oil-wet", new fresh samples were obtained and tested. The re-test confirmed the initial wettability tests. Because of the mud program used and the "fresh condition" of the wettability tests, the relative permeability data probably gives more reliable wettability characteristics.

#### Mercury Injection Capillary Pressure

Each sample chosen for capillary pressure tests was placed into a mercury pump and evacuated. Mercury, the non-wetting phase, was injected into each sample at 23 pressure increments ranging from 0-2000 psia, then incrementally reduced back to 0 psia. Mercury injection data were recorded for each of the incremental injection pressures. The drainage and imbibition data were calculated from the mercury injection data. The mercury injection capillary pressure data are presented in tabular form on pages 60-65, and in graphical form on pages 66-73.

The pore size distribution was calculated from the mercury injection capillary pressure data for each sample. The pore size distribution data are summarized on pages 74-76, and presented in graphical form on pages 77-84.

#### Acoustic Velocity

The clean, dry core plugs used for acoustic velocity tests were evacuated then pressure-saturated with simulated formation brine. Direct measurements of the transit times for acoustic compression waves were then made on each core plug at effective overburden pressures of 300 psi, 800 psi, 1300 psi, 1800 psi, and 2350 psi. The results of the acoustic velocity tests are presented in tabular form on pages 85-89 and in graphical form on page 90. A trend of increasing transit time with increasing porosity is evident from these data. The test results for sample 138 (depth interval 4707.0-4708.0 feet) appear not to follow closely the trend of the other data, possibly as the result of small vugs which represent a portion of the porosity of this core plug.

**CORE LABORATORIES, INC.**  
2001 COMMERCE DRIVE  
MIDLAND, TEXAS  
(915) 694-7781

Page 1 of 91

File SCAL-206-82025

IDENTIFICATION AND LITHOLOGICAL DESCRIPTION OF SAMPLES

Company: Phillips Petroleum Company Well: South Cowden Unit #6-18  
Formation: San Andres Field: South Cowden  
County (Parish), State: Ector, Texas

<u>Sample Identification</u>	<u>Depth, feet</u>	<u>Lithological Description</u>
26	4595.0-96.0	DOL,gry,slily anhy,styl
34	4603.0-04.0	DOL,gry,slily vug
37	4606.0-07.0	SD,gry,v dolc,slily shy
41	4610.0-11.0	SD,gry,dolc,slily shy
42	4611.0-12.0	SD,gry,dolc,slily shy
52	4621.0-22.0	DOL,gry,slily anhy,slily sdy,p.p. por
55	4624.0-25.0	DOL,gry,slily anhy,slily sdy,p.p. por,fo
57	4626.0-27.0	DOL,gry,sdy,p.p. por,slily shy,foss
59	4628.0-29.0	DOL,gry,sdy,slily shy,p.p. por
62	4631.0-32.0	DOL,gry,slily anhy,slily sd,slily vug,st
70	4639.0-40.0	DOL,gry,slily anhy,p.p. por
78	4647.0-48.0	DOL,gry,slily anhy,slily sd,slily shy,st
84	4653.0-54.0	DOL,gry,slily shy,p.p. por
88	4657.0-58.0	DOL,gry,sdy,p.p. por,slily shy,styl
91	4660.0-61.0	DOL,gry,p.p. por,slily shy,styl
108	4677.0-78.0	DOL,gry,sdy,slily vug
110	4679.0-80.0	DOL,gry,slily anhy,slily sd,p.p. por
113	4682.0-83.0	DOL,gry,slily anhy,slily sd,p.p. por,styl
116	4685.0-86.0	DOL,gry,slily anhy
117	4686.0-87.0	DOL,gry,slily anhy
120	4689.0-90.0	DOL,gry,p.p. por
134	4703.0-04.0	DOL,gry,slily anhy,p.p. por
138	4707.0-08.0	DOL,gry,p.p. por

This report, based on observations and materials supplied by the client, is prepared for the exclusive and confidential use by the client. The analyses, opinions, or interpretations contained herein represent the judgement of Core Laboratories, Inc.; however, Core Laboratories, Inc., and its employees assume no responsibility and make no warranties or representations as to

CORE LABORATORIES, INC.  
2001 COMMERCE DRIVE  
MIDLAND, TEXAS  
(915) 694-7761

Page 2 of 91

File SCAL-206-B2025

PERMEABILITY TO AIR AND POROSITY

Company: Phillips Petroleum Company Well: South Cowden Unit #6-12  
Formation: San Andres Field: South Cowden  
County (Parish), State: Ector, Texas

<u>Sample Identification</u>	<u>Depth, feet</u>	<u>Permeability to Air, Millidarcys</u>	<u>Porosity, Percent</u>
26	4595.0-96.0	0.11	3.1
34	4603.0-04.0	0.004	3.2
37	4606.0-07.0	0.18	9.1
41	4610.0-11.0	0.20	9.1
42	4611.0-12.0	2.3	13.8
52	4621.0-22.0	0.77	5.5
55	4624.0-25.0	0.86	8.5
57	4626.0-27.0	8.2	9.4
59	4628.0-29.0	0.72	7.7
62	4631.0-32.0	0.01	6.4
70	4639.0-40.0	0.53	8.6
78	4647.0-48.0	1.2	9.1
84	4653.0-54.0	1.4	6.6
88	4657.0-58.0	1.4	7.3
91	4660.0-61.0	4.5	6.6
108	4677.0-78.0	0.01	5.9
110	4679.0-80.0	0.34	5.8
113	4682.0-83.0	4.6	9.0
116	4685.0-86.0	0.27	4.6
117	4686.0-87.0	0.04	3.9
120	4689.0-90.0	0.24	4.2
134	4703.0-04.0	1.5	9.1
138	4707.0-08.0	0.55	4.6

**CORE LABORATORIES, Inc.**  
2001 COMMERCE DRIVE  
MIDLAND, TEXAS  
(915) 894-7781

Page 3 of 91

File SCAL-206-82025

FORMATION RESISTIVITY FACTOR AND RESISTIVITY INDEX

Company: Phillips Petroleum Company Well: South Cowden Unit #6-18  
Formation: San Andres Field: South Cowden  
County (Parish), State: Ector, Texas

Saturant: 84,960 mg/l TDS  
Resistivity of Saturant: 0.095 ohm meters at 74 °F

Sample I.D.	Depth, Feet	Permeability to Air millidarcys	Porosity, percent	Formation Resistivity Factor	Brine Saturation, percent pore space	Resist Index
37	4606.0	0.18	9.1	78.93	100.0	1.0
					93.4	1.0
					89.4	1.0
					86.9	1.0
					84.2	1.0
41	4610.0	0.20	9.1	70.40	100.0	1.0
					96.5	1.0
					95.3	1.0
					94.2	1.0
					75.9	1.0
57	4626.0	8.2	9.4	122.41	100.0	1.0
					73.1	1.0
					43.8	4.0
					36.9	5.0
					34.4	6.0
78	4647.0	1.2	9.1	189.36	100.0	1.0
					94.8	1.0
					78.2	1.0
					75.9	1.0
					72.9	1.0
84	4653.0	1.4	6.6	283.41	100.0	1.0
					74.5	1.0
					68.2	2.0
					62.7	2.0
					57.1	3.0

**CORE LABORATORIES, INC.**  
2001 COMMERCE DRIVE  
MIDLAND, TEXAS  
(815) 694-7781

Page 4 of 91

File SCAL-206-82025

FORMATION RESISTIVITY FACTOR AND RESISTIVITY INDEX

Company: Phillips Petroleum Company Well: South Cowden Unit #6-18  
Formation: San Andres Field: South Cowden  
County (Parish), State: Ector, Texas

Saturant: 84,960 mg/l TDS  
Resistivity of Saturant: 0.095 ohm meters at 74 °F

Sample I.D.	Depth, Feet	Permeability to Air millidarcys	Porosity, percent	Formation Resistivity Factor	Brine Saturation, percent pore space	Resist. Inde
113	4682.0	4.6	9.0	192.03	100.0 79.4 63.8 57.6 53.3	1.0 1.7 2.9 3.6 4.3
116	4685.0	0.27	4.6	322.51	100.0 70.9 63.6 55.3 46.2	1.0 1.9 2.3 2.7 3.3
117	4686.0	0.04	3.9	760.13	100.0 96.4 86.3 84.2 82.8	1.0 1.0 1.2 1.3 1.4
134	4703.0	1.5	9.1	217.23	100.0 92.5 89.7 89.3 63.6	1.0 1.2 1.3 1.4 2.8

This report, based on observations and materials supplied by the client, is prepared for the exclusive and confidential use by the client. The analyses, opinions, or interpretations contained herein represent the judgement of Core Laboratories, Inc.; however, Core Laboratories, Inc., and its employees assume no responsibility and make no warranties or representations as to it.

**CORE LABORATORIES, Inc.**  
2001 COMMERCE DRIVE  
MIDLAND, TEXAS  
(915) 694-7761

Page 16 of 91

File SCAL-206-82025

GAS-OIL RELATIVE PERMEABILITY

Company:	<u>Phillips Petroleum Company</u>	Sample Identification:	<u>52</u>
Well:	<u>South Cowden Unit #6-18</u>	Sample Depth:	<u>4621.0-22.0</u> Feet
Formation:	<u>San Andres</u>	Permeability to Air:	<u>0.77</u> mD
Field:	<u>South Cowden</u>	Porosity:	<u>5.5</u> perce
County (Parish):	<u>Ector</u>	Initial Water Saturation:	<u>22.7</u> perce
State:	<u>Texas</u>	Effective Permeability to Oil at $S_{wi}$ :	<u>0.42</u> mD

<u>Gas Saturation, percent pore space</u>	<u>Gas-Oil Relative Permeability Ratio</u>	<u>Relative Permeability to Gas,* fraction</u>	<u>Relative Permeability to Oil,* fraction</u>
0.0	0.000	0.000	1.000
5.2	0.038	0.013	0.344
6.5	0.066	0.019	0.293
7.5	0.099	0.026	0.264
8.4	0.136	0.033	0.247
9.1	0.173	0.041	0.235
9.7	0.214	0.048	0.223
10.4	0.264	0.054	0.206
11.1	0.321	0.061	0.190
12.6	0.478	0.079	0.165
13.7	0.622	0.095	0.152
17.1	1.14	0.142	0.125
20.4	1.86	0.165	0.089
23.4	2.81	0.196	0.070
30.6	11.0	0.234	0.021
34.5	44.2	0.283	0.0064
36.9	299.	0.331	0.0011

\*Relative to the effective permeability to oil at initial water saturation.

These analyses, opinions or interpretations are based on observations and material supplied by the client to whom, and for whose exclusive and confidential use, this report is made. The interpretations or opinions expressed represent the best judgment of Core Laboratories, Inc. All errors and omissions excepted. But Core Laboratories, Inc., will not and does not assume any responsibility and make no warranty or representation as to the production, proper operation, or probabilities of any well.



**CORE LABORATORIES, INC.**  
2001 COMMERCE DRIVE  
MIDLAND, TEXAS  
(915) 694-7761

Page 17 of 91

File SCAL-206-82025

GAS-OIL RELATIVE PERMEABILITY

Company: <u>Phillips Petroleum Company</u>	Sample Identification: <u>57</u>
Well: <u>South Cowden Unit #6-18</u>	Sample Depth: <u>4626.0-27.0</u> Feet
Formation: <u>San Andres</u>	Permeability to Air: <u>8.2</u> mD
Field: <u>South Cowden</u>	Porosity: <u>9.4</u> perce
County (Parish): <u>Ector</u>	Initial Water Saturation: <u>13.7</u> perce
State: <u>Texas</u>	Effective Permeability to Oil at $S_{wi}$ : <u>5.1</u> mD

Gas Saturation, percent pore space	Gas-Oil Relative Permeability Ratio	Relative Permeability to Gas,* fraction	Relative Permeability to Oil,* fraction
0.0	0.000	0.000	1.000
4.2	0.038	0.014	0.365
5.1	0.055	0.018	0.325
5.9	0.076	0.022	0.290
6.8	0.091	0.026	0.286
9.6	0.156	0.039	0.250
13.0	0.270	0.055	0.203
16.6	0.481	0.068	0.142
19.3	0.766	0.087	0.113
22.3	1.26	0.105	0.084
28.1	3.27	0.151	0.046
32.0	6.86	0.177	0.026
34.0	10.0	0.211	0.021
38.6	26.5	0.252	0.0095
42.0	74.7	0.288	0.0039

\*Relative to the effective permeability to oil at initial water saturation.

These analyses, opinions or interpretations are based on observations and material supplied by the client to whom, and for whose exclusive and confidential use, this report is made. The interpretations or opinions expressed represent the best judgment of Core Laboratories, Inc. All errors and omissions excepted, but Core Laboratories, Inc. and its officers and employees, assume no responsibility and make no warranty or representation as to the productivity, proper operation, or profitability of any well.

**CORE LABORATORIES, Inc.**  
2001 COMMERCE DRIVE  
MIDLAND, TEXAS  
(915) 694-7761

Page 18 of 91

File SCAL-206-82025

GAS-OIL RELATIVE PERMEABILITY

Company:	<u>Phillips Petroleum Company</u>	Sample Identification:	<u>78</u>
Well:	<u>South Cowden Unit #6-18</u>	Sample Depth:	<u>4647.0-48.0</u> Feet
Formation:	<u>San Andres</u>	Permeability to Air:	<u>1.2</u> mD
Field:	<u>South Cowden</u>	Porosity:	<u>9.1</u> percer
County (Parish):	<u>Ector</u>	Initial Water Saturation:	<u>21.9</u> percer
State:	<u>Texas</u>	Effective Permeability	
		to Oil at $S_{wi}$ :	<u>0.60</u> mD

<u>Gas Saturation,</u> <u>percent pore space</u>	<u>Gas-Oil Relative</u> <u>Permeability Ratio</u>	<u>Relative Permeability</u> <u>to Gas,* fraction</u>	<u>Relative Permeability</u> <u>to Oil,* fraction</u>
0.0	0.000	0.000	1.000
1.9	0.047	0.013	0.276
3.2	0.087	0.020	0.231
5.0	0.181	0.031	0.171
5.9	0.247	0.042	0.170
7.2	0.347	0.053	0.154
9.5	0.655	0.070	0.107
11.2	1.03	0.086	0.083
14.2	1.97	0.127	0.064
16.8	3.18	0.150	0.047
18.5	4.15	0.166	0.040
20.9	6.27	0.180	0.029
22.2	8.23	0.190	0.023
23.2	10.3	0.198	0.019

\*Relative to the effective permeability to oil at initial water saturation.

These analyses, opinions or interpretations are based on observations and material supplied by the client to whom, and for whose exclusive and confidential use, this report is made. The interpretations or opinions expressed represent the best judgment of Core Laboratories, Inc., all errors and omissions excepted; but Core Laboratories, Inc., and its officers and employees, assume no responsibility and make no warranty or representation as to the productivity, proper operation, or profitability of any well or other operation.

**CORE LABORATORIES, Inc.**  
2001 COMMERCE DRIVE  
MIDLAND, TEXAS  
(915) 694-7761

Page 19 of 91

File SCAL-206-82025

GAS-OIL RELATIVE PERMEABILITY

Company:	<u>Phillips Petroleum Company</u>	Sample Identification:	<u>88</u>
Well:	<u>South Cowden Unit #6-18</u>	Sample Depth:	<u>4657.0-58.0</u> Feet
Formation:	<u>San Andres</u>	Permeability to Air:	<u>1.4</u> mD
Field:	<u>South Cowden</u>	Porosity:	<u>7.3</u> perce
County (Parish):	<u>Ector</u>	Initial Water Saturation:	<u>29.2</u> perce
State:	<u>Texas</u>	Effective Permeability	
		to Oil at $S_{wi}$ :	<u>1.2</u> mD

<u>Gas Saturation,</u> <u>percent pore space</u>	<u>Gas-Oil Relative</u> <u>Permeability Ratio</u>	<u>Relative Permeability</u> <u>to Gas,* fraction</u>	<u>Relative Permeability</u> <u>to Oil,* fraction</u>
0.0	0.000	0.000	1.000
6.0	0.045	0.020	0.436
7.5	0.074	0.027	0.370
8.5	0.104	0.035	0.340
9.4	0.139	0.043	0.313
10.3	0.183	0.051	0.282
11.9	0.300	0.069	0.228
13.6	0.470	0.097	0.207
15.2	0.671	0.120	0.180
16.9	0.926	0.148	0.161
19.9	1.49	0.179	0.120
27.1	6.10	0.237	0.039
29.0	9.70	0.267	0.028
30.0	11.8	0.289	0.025
32.4	21.2	0.305	0.014
34.2	37.8	0.336	0.0089
36.6	103.	0.357	0.0035

\*Relative to the effective permeability to oil at initial water saturation.

These analyses, opinions or interpretations are based on observations and material supplied by the client to whom, and for whose exclusive and confidential use, they are made. The interpretations or opinions expressed represent the best judgment of Core Laboratories, Inc. (all errors and omissions excepted); but Core Laboratories, Inc. and its officers and employees assume no responsibility and make no warranty or representation as to the timeliness, proper operation, or profitability of any well.

**CORE LABORATORIES, Inc.**  
2001 COMMERCE DRIVE  
MIDLAND, TEXAS  
(915) 694-7761

Page 20 of 91

File SCAL-206-82025

GAS-OIL RELATIVE PERMEABILITY

Company:	Phillips Petroleum Company	Sample Identification:	134
Well:	South Cowden Unit #6-18	Sample Depth:	4703.0-04.0 Feet
Formation:	San Andres	Permeability to Air:	1.5 mD
Field:	South Cowden	Porosity:	9.1 perce
County (Parish):	Ector	Initial Water Saturation:	22.0 perce
State:	Texas	Effective Permeability to Oil at $S_{wi}$ :	0.78 mD

Gas Saturation, percent pore space	Gas-Oil Relative Permeability Ratio	Relative Permeability to Gas,* fraction	Relative Permeability to Oil,* fraction
0.0	0.000	0.000	1.000
2.1	0.022	0.026	0.800
3.2	0.055	0.037	0.702
4.6	0.074	0.047	0.634
6.0	0.095	0.057	0.603
7.6	0.121	0.067	0.553
9.4	0.158	0.076	0.479
11.2	0.207	0.085	0.408
12.6	0.258	0.093	0.360
13.5	0.298	0.100	0.337
14.2	0.329	0.107	0.327
17.3	0.484	0.131	0.270
24.4	1.28	0.184	0.144
29.0	2.36	0.215	0.091
32.6	3.92	0.256	0.065
36.9	7.52	0.301	0.040
42.4	17.7	0.351	0.020
47.1	43.9	0.406	0.0092

\*Relative to the effective permeability to oil at initial water saturation.

These analyses, opinions or interpretations are based on observations and material supplied by the client to whom, and for whose exclusive and confidential uses, they are rendered. They are not to be used for any other purpose without the express written consent of Core Laboratories, Inc. (all errors and omissions excepted), but Core Laboratories, Inc.,

**CORE LABORATORIES, INC.**  
2001 COMMERCIAL DRIVE  
MIDLAND, TEXAS 79701  
(915) 694-7761

Page 31 of 91  
File SCAL-206-82025

**SUMMARY OF WATER-OIL RELATIVE PERMEABILITY TEST RESULTS**

Sample Number	Depth, Feet	Permeability To Air, Millidarcys	Porosity, Percent	Initial Conditions		Terminal Conditions		Oil Recovered, Percent
				Water Saturation, Percent	Effective Permeability To Oil, Millidarcys	Oil Saturation, Percent	Effective Permeability To Water, Millidarcys	
52	4621.0-22.0	0.77	5.5	22.7	0.42	53.6	0.24	23.7
57	4626.0-27.0	8.2	9.4	13.7	5.1	49.8	2.20	36.5
78	4647.0-48.0	1.2	9.1	21.9	0.60	56.4	0.20	21.7
88	4657.0-58.0	1.4	7.3	29.2	1.2	46.6	0.21	24.2
134	4703.0-04.0	1.5	9.1	22.0	0.78	58.1	0.12	19.9
								25.5

Sample Number	Depth, Feet	Air Permeability To Air, Millidarcys	Porosity, Percent	Initial Conditions		Terminal Conditions		Oil Recovered, Percent
				Water Saturation, Percent	Effective Permeability To Oil, Millidarcys	Oil Saturation, Percent	Effective Permeability To Water, Millidarcys	
52	4621.0-22.0	0.77	5.5	53.6	0.24	23.5	0.19	(0.22*)
57	4626.0-27.0	8.2	9.4	49.8	2.2	14.1	3.9	(4.7*)
78	4647.0-48.0	1.2	9.1	56.4	0.20	22.7	0.31	(0.39*)
88	4657.0-58.0	1.4	7.3	46.6	0.21	30.7	0.16	(0.31*)
134	4703.0-04.0	1.5	9.1	58.1	0.12	28.7	0.17	(0.34*)

\*Permeability measured in reverse flow direction.

These interpretations are based on observations and materials supplied by the client. Core Laboratories, Inc. and its affiliates and employees, assume no responsibility for the accuracy or completeness of the data or the results of the analysis. The interpretations are based on the best judgment of Core Laboratories, Inc. and its affiliates and employees, assume no responsibility and make no warranty for the accuracy or completeness of the data or the results of the analysis.

**CORE LABORATORIES, INC.**  
2001 COMMERCE DRIVE  
MIDLAND, TEXAS  
(915) 694-7761

Page 32 of 91  
File SCAL-206-82025

WATER-OIL RELATIVE PERMEABILITY

Company: <u>Phillips Petroleum Company</u>	Sample Identification: <u>52</u>
Well: <u>South Cowden Unit #6-18</u>	Sample Depth: <u>4621.0-22.0</u> feet
Formation: <u>San Andres</u>	Permeability to Air: <u>0.77</u> mD
Field: <u>South Cowden</u>	Porosity: <u>5.5</u> percent
County: <u>Ector</u>	Initial Water Saturation: <u>22.7</u> percent
State: <u>Texas</u>	Effective Permeability to Oil at $S_{wi}$ : <u>0.42</u> mD

WATER SATURATION INCREASING

Water Saturation, percent pore space	Water-Oil Relative Permeability Ratio	Relative Permeability to Water,* fraction	Relative Permeability to Oil,* fraction
22.7	0.000	0.000	1.000
39.0	3.09	0.327	0.106
39.6	3.73	0.353	0.095
40.7	6.01	0.377	0.063
41.5	8.66	0.394	0.046
42.0	11.7	0.408	0.035
42.7	18.7	0.426	0.023
43.8	48.8	0.455	0.0093
44.2	85.9	0.471	0.0055
44.6	138.	0.485	0.0035
45.4	495.	0.495	0.00100
45.7	1130.	0.501	0.00044
45.9	1980.	0.508	0.00026
46.4		0.571	

WATER SATURATION DECREASING

46.4		0.571	
31.9	0.0042	0.0018	0.420
31.1	0.0037	0.0016	0.449
29.4	0.0023	0.0011	0.473
28.3	0.0016	0.00078	0.490
27.5	0.0012	0.00060	0.504
26.9	0.00094	0.00049	0.515
26.5	0.00082	0.00043	0.524
26.2	0.00072	0.00039	0.538
25.4	0.00056	0.00031	0.559
23.5			0.585

\*Relative to the effective permeability to oil at initial water saturation.

This report, based on observations and materials supplied by the client, is prepared for the exclusive and confidential use by the client. The analyses, opinions, or interpretations contained herein represent the judgement of Core Laboratories, Inc., however, Core Laboratories, Inc., and its employees assume no responsibility and make no warranties or representations as to the

**CORE LABORATORIES, Inc.**  
 2001 COMMERCE DRIVE  
 MIDLAND, TEXAS  
 (915) 694-7761

Page 33 of 91  
 File SCAL-206-82025

WATER-OIL RELATIVE PERMEABILITY

Company: <u>Phillips Petroleum Company</u>	Sample Identification: <u>57</u>
Well: <u>South Cowden Unit #6-18</u>	Sample Depth: <u>4626 0-27 0</u> feet
Formation: <u>San Andres</u>	Permeability to Air: <u>8.2</u> mD
Field: <u>South Cowden</u>	Porosity: <u>9.4</u> percent
County: <u>Ector</u>	Initial Water Saturation: <u>13.7</u> percent
State: <u>Texas</u>	Effective Permeability to Oil at $S_{wi}$ : <u>5.1</u> mD

WATER SATURATION INCREASING

<u>Water Saturation, percent pore space</u>	<u>Water-Oil Relative Permeability Ratio</u>	<u>Relative Permeability to Water,* fraction</u>	<u>Relative Permeability to Oil,* fraction</u>
13.7	0.000	0.000	1.000
33.5	0.963	0.177	0.184
34.6	1.12	0.196	0.175
36.6	1.56	0.216	0.139
41.5	4.09	0.260	0.064
44.2	9.34	0.286	0.031
45.1	14.4	0.298	0.021
45.9	22.0	0.312	0.014
46.6	33.0	0.333	0.010
47.6	69.2	0.345	0.0050
48.1	110.	0.359	0.0033
48.6	166.	0.376	0.0023
49.8	1610.	0.393	0.00024
49.9	2130.	0.415	0.00019
50.2		0.431	

\*Relative to the effective permeability to oil at initial water saturation.

This report, based on observations and materials supplied by the client, is prepared for the exclusive and confidential use by the client. The analyses, comments, or interpretations contained herein represent the judgement of Core Laboratories, Inc.; however, Core Laboratories, Inc. and its employees assume no responsibility and make no warranties or representations as to the validity of this report to the extent of any third-party's. Printed on 10/15/01. All other reports prepared at 10/15/01. All other reports prepared at 10/15/01.

**CORE LABORATORIES, Inc.**  
2001 COMMERCE DRIVE  
MIDLAND, TEXAS  
(915) 694-7781

Page 34 of 91

File SCAL-206-82025

WATER-OIL RELATIVE PERMEABILITY

Company:	<u>Phillips Petroleum Company</u>	Sample Identification:	<u>57</u>
Well:	<u>South Cowden Unit #6-18</u>	Sample Depth:	<u>4626.0-27.0</u> feet
Formation:	<u>San Andres</u>	Permeability to Air:	<u>8.2</u> mD
Field:	<u>South Cowden</u>	Porosity:	<u>9.4</u> percent
County:	<u>Ector</u>	Initial Water Saturation:	<u>13.7</u> percent
State:	<u>Texas</u>	Effective Permeability	
		to Oil at $S_{wi}$ :	<u>5.1</u> mD

WATER SATURATION DECREASING

<u>Water Saturation,</u> <u>percent pore space</u>	<u>Water-Oil Relative</u> <u>Permeability Ratio</u>	<u>Relative Permeability</u> <u>to Water,* fraction</u>	<u>Relative Permeability</u> <u>to Oil,* fraction</u>
50.2		0.431	
31.3	0.0069	0.0023	0.338
30.7	0.0058	0.0021	0.365
29.7	0.0043	0.0017	0.388
29.0	0.0035	0.0014	0.406
28.5	0.0030	0.0013	0.420
28.0	0.0025	0.0011	0.433
26.2	0.0014	0.00067	0.470
25.2	0.0011	0.00054	0.504
23.4	0.00061	0.00033	0.536
22.1	0.00040	0.00023	0.573
18.9	0.00015	0.000090	0.605
17.1	0.000059	0.000037	0.634
16.9	0.000050	0.000033	0.653
16.2	0.000036	0.000024	0.671
14.2	0.0000017	0.0000012	0.682
14.1			0.765

\*Relative to the effective permeability to oil at initial water saturation.

This report, based on observations and materials supplied by the client, is prepared for the exclusive and confidential use by the client. The analyses, opinions, or interpretations contained herein represent the judgment of Core Laboratories, Inc.; however, Core Laboratories, Inc., and its employees assume no responsibility and make no warranties or representations as to the utility of this report to the client or as to the productivity, proper operation, or profitability of any oil, gas, or other mineral formation or well in connection with which such report may be used.



**CORE LABORATORIES, INC.**  
2001 COMMERCE DRIVE  
MIDLAND, TEXAS  
(915) 694-7761

Page 35 of 91  
File SCAL-206-82025

WATER-OIL RELATIVE PERMEABILITY

Company:	<u>Phillips Petroleum Company</u>	Sample Identification:	<u>78</u>
Well:	<u>South Cowden Unit #6-18</u>	Sample Depth:	<u>4647.0-48.0</u> feet
Formation:	<u>San Andres</u>	Permeability to Air:	<u>1.2</u> mD
Field:	<u>South Cowden</u>	Porosity:	<u>9.1</u> percent
County:	<u>Ector</u>	Initial Water Saturation:	<u>21.9</u> percent
State:	<u>Texas</u>	Effective Permeability	
		to Oil at $S_{wi}$ :	<u>0.60</u> mD

WATER SATURATION INCREASING

<u>Water Saturation,</u> <u>percent pore space</u>	<u>Water-Oil Relative</u> <u>Permeability Ratio</u>	<u>Relative Permeability</u> <u>to Water,* fraction</u>	<u>Relative Permeability</u> <u>to Oil,* fraction</u>
21.9	0.000	0.000	1.000
35.3	1.67	0.183	0.110
36.2	2.08	0.196	0.094
38.0	3.96	0.212	0.053
39.0	6.45	0.222	0.034
39.7	9.66	0.230	0.024
40.1	13.3	0.236	0.018
40.6	19.0	0.245	0.013
41.1	30.5	0.258	0.0085
41.7	58.8	0.270	0.0046
42.1	94.3	0.281	0.0030
42.7	322.	0.298	0.00092
43.1	1550.	0.329	0.00021
43.6		0.333	

WATER SATURATION DECREASING

43.6		0.333	
33.6	0.0048	0.0014	0.283
33.0	0.0041	0.0012	0.295
31.8	0.0021	0.00065	0.307
31.3	0.0015	0.00047	0.317
31.1	0.0013	0.00041	0.325
31.0	0.0012	0.00039	0.332
30.9	0.0011	0.00038	0.339
30.7	0.00098	0.00035	0.355
29.4	0.00051	0.00021	0.400
27.7	0.00025	0.00011	0.440
26.4	0.00014	0.000065	0.468
24.5	0.000040	0.000020	0.485
23.8	0.000019	0.0000094	0.505
22.7			0.515

\*Relative to the effective permeability to oil at initial water saturation.

This report, based on observations and materials supplied by the client, is prepared for the exclusive and confidential use by the client. The analyses, opinions, or interpretations contained herein represent the best estimate of the data and are not to be used for any other purpose. Core Laboratories, Inc. and its employees assume no responsibility and make no warranties or representations as to the accuracy or completeness of the data or the results of the analyses.

**CORE LABORATORIES, Inc.**  
2001 COMMERCE DRIVE  
MIDLAND, TEXAS  
(915) 694-7761

Page 36 of 91  
File SCAL-206-R2025

WATER-OIL RELATIVE PERMEABILITY

Company: <u>Phillips Petroleum Company</u>	Sample Identification: <u>88</u>
Well: <u>South Cowden Unit #6-18</u>	Sample Depth: <u>4657.0-58.0</u> feet
Formation: <u>San Andres</u>	Permeability to Air: <u>1.4</u> mD
Field: <u>South Cowden</u>	Porosity: <u>7.3</u> percent
County: <u>Ector</u>	Initial Water Saturation: <u>29.2</u> percent
State: <u>Texas</u>	Effective Permeability to Oil at $S_{wi}$ : <u>1.2</u> mD

WATER SATURATION INCREASING

<u>Water Saturation, percent pore space</u>	<u>Water-Oil Relative Permeability Ratio</u>	<u>Relative Permeability to Water,* fraction</u>	<u>Relative Permeability to Oil,* fraction</u>
29.2	0.000	0.000	1.000
45.4	2.60	0.085	0.033
47.4	5.17	0.083	0.016
48.1	7.09	0.081	0.011
48.6	9.10	0.079	0.0087
50.4	28.3	0.075	0.0026
51.7	167.	0.073	0.00044
52.0	360.	0.076	0.00021
52.2	614.	0.085	0.00014
52.5	951.	0.103	0.00011
53.1	3020.	0.117	0.000039
53.4		0.175	

WATER SATURATION DECREASING

53.4		0.175	
35.2	0.0046	0.00053	0.115
34.4	0.0038	0.00046	0.121
32.6	0.0020	0.00026	0.126
31.8	0.0013	0.00017	0.129
31.3	0.0010	0.00014	0.131
30.9	0.00086	0.00011	0.132
30.7			0.133

\*Relative to the effective permeability to oil at initial water saturation.

This report, based on observations and materials supplied by the client, is prepared for the exclusive and confidential use by the client. The analyses, opinions, or interpretations contained herein are the property of Core Laboratories, Inc. and its employees assume no responsibility and make no warranties or representations as to the accuracy or completeness of the information contained herein.

**CORE LABORATORIES, Inc.**  
2001 COMMERCE DRIVE  
MIDLAND, TEXAS  
(915) 694-7761

Page 37 of 91  
File SCAL-206-82025

WATER-OIL RELATIVE PERMEABILITY

Company:	<u>Phillips Petroleum Company</u>	Sample Identification:	<u>134</u>
Well:	<u>South Cowden Unit #6-18</u>	Sample Depth:	<u>4703.0-04.0</u> feet
Formation:	<u>San Andres</u>	Permeability to Air:	<u>1.5</u> mD
Field:	<u>South Cowden</u>	Porosity:	<u>9.1</u> percent
County:	<u>Ector</u>	Initial Water Saturation:	<u>22.0</u> percent
State:	<u>Texas</u>	Effective Permeability to Oil at $S_{wi}$ :	<u>0.78</u> mD

WATER SATURATION INCREASING

<u>Water Saturation, percent pore space</u>	<u>Water-Oil Relative Permeability Ratio</u>	<u>Relative Permeability to Water,* fraction</u>	<u>Relative Permeability to Oil,* fraction</u>
22.0	0.000	0.000	1.000
29.1	1.63	0.101	0.062
29.9	1.92	0.094	0.049
31.8	3.00	0.092	0.031
33.2	4.34	0.091	0.021
35.6	9.40	0.089	0.0094
37.4	19.0	0.089	0.0047
39.2	55.4	0.091	0.0016
40.3	213.	0.094	0.00044
40.6	482.	0.105	0.00022
41.0	1060.	0.119	0.00011
41.4	2310.	0.138	0.000060
41.9		0.154	

WATER SATURATION DECREASING

41.9		0.154	
32.6	0.0036	0.00060	0.164
32.2	0.0033	0.00051	0.155
31.2	0.0021	0.00032	0.153
30.5	0.0015	0.00023	0.152
29.6	0.00097	0.00015	0.154
28.5	0.00059	0.000097	0.165
27.1	0.00035	0.000066	0.187
24.7			0.212

\*Relative to the effective permeability to oil at initial water saturation.

This report, based on observations and materials supplied by the client, is prepared for the exclusive and confidential use by the client. The analyses, opinions, or interpretations contained herein represent the judgment of Core Laboratories, Inc.; however, Core Laboratories, Inc., and its employees assume no responsibility and make no warranties or representations as to the accuracy or completeness of the information supplied by the client.

CORE LABORATORIES, INC.  
2001 COMM DRIVE  
MIDLAND AS  
(915) 694-1161

Page 48 of 91

File SCAL-206-82025

SUMMARY OF WATERFLOOD TEST RESULTS

Sample Number	Depth, Feet	Permeability To Air, Millidarcys	Porosity, Percent	Initial Conditions		Terminal Conditions		
				Water Saturation, Percent	Effective Permeability To Oil, Millidarcys	Oil Saturation, Percent	Effective Permeability To Water, Millidarcys	Oil Recovered, Percent
42	4611.0-12.0	2.3	13.8	11.9	1.6	43.0	0.54 (0.63*)	45.1
59	4628.0-29.0	0.72	7.7	25.3	0.49	48.4	1.4 (1.7*)	26.3
70	4639.0-40.0	0.53	8.6	24.7	0.36	50.8	0.19 (0.20*)	24.7
84	4653.0-54.0	1.4	6.6	29.6	0.49	47.5	0.37 (0.58*)	22.9
113	4682.0-83.0	4.6	9.0	20.0	1.4	57.1	1.9 (2.1*)	22.9
								51.2
								35.2
								32.5
								32.5
								28.6

\* Permeability measured in reverse flow direction.

These are estimates or interpretations based on observations and materials supplied by the client. They are not intended to represent the best judgment of Core Laboratories, Inc. (all errors and omissions excepted). Core Laboratories, Inc. and its officers and employees, assume no responsibility and make no warranty or representation as to the productivity, proper operation, or profitability of any oil, gas or other mineral well or used in connection with which such report is used or relied upon.

**CORE LABORATORIES, INC.**  
2001 COMMERCE DRIVE  
MIDLAND, TEXAS  
(915) 694-7781

Page 49 of 91  
File SCAL-206-82025

WATERFLOOD SUSCEPTIBILITY

Company:	<u>Phillips Petroleum Company</u>	Sample Identification:	<u>42</u>	
Well:	<u>South Cowden Unit #6-18</u>	Sample Depth:	<u>4611.0-12.0</u>	fe
Formation:	<u>San Andres</u>	Permeability to Air:	<u>2.3</u>	mD
Field:	<u>South Cowden</u>	Porosity:	<u>13.8</u>	pe
County (Parish):	<u>Ector</u>	Initial Water Saturation:	<u>11.9</u>	pe
State:	<u>Texas</u>	Effective Permeability to Oil at $S_{wi}$ :	<u>1.6</u>	mD

<u>Water Input, pore volumes</u>	<u>Cummulative Oil Recovery, percent pore space</u>	<u>Average Oil Recovery,* percent pore space</u>	<u>Average Water Cut,** percent</u>
0.135	13.5***	--	--
0.219	20.0	16.7	21.6
0.301	24.4	22.2	45.8
0.434	29.1	26.8	64.7
0.589	32.1	30.6	80.9
0.803	34.2	33.2	89.8
1.21	36.4	35.3	94.7
1.71	37.9	37.1	97.0
2.36	39.2	38.5	98.1
3.28	40.1	39.6	99.0
4.33	41.0	40.5	99.1
7.18	42.4	41.7	99.5
10.2	43.0	42.7	99.8
15.9	44.1	43.5	99.8
21.6	44.4	44.2	99.94
32.9	44.7	44.6	99.97
44.2	45.0	44.8	99.98
55.6	45.1	45.0	99.99

- \* Calculated for mid-point of incremental throughput  
\*\* Calculated from incremental throughput volumes  
\*\*\* Breakthrough recovery

This report, based on observations and materials supplied by the client, is prepared for the exclusive and confidential use by the client. The analyses, opinions, or interpretations contained herein represent the judgement of Core Laboratories, Inc. However, Core Laboratories, Inc. and its employees assume no responsibility and make no warranties or representations as to the accuracy or reliability of the data or the results of the analyses, opinions, or interpretations. No part of this report may be reproduced or transmitted in any form or by any means electronic or mechanical, including photocopying, recording, or by any information storage or retrieval system, without permission in writing from Core Laboratories, Inc.

WATERFLOOD SUSCEPTIBILITY

Company:	<u>Phillips Petroleum Company</u>	Sample Identification:	<u>59</u>
Well:	<u>South Cowden Unit #6-18</u>	Sample Depth:	<u>4628.0-29.0</u> fe
Formation:	<u>San Andres</u>	Permeability to Air:	<u>0.72</u> mD
Field:	<u>South Cowden</u>	Porosity:	<u>7.7</u> pe
County (Parish):	<u>Ector</u>	Initial Water Saturation:	<u>25.3</u> pe
State:	<u>Texas</u>	Effective Permeability to Oil at $S_{wi}$ :	<u>0.49</u> mD

<u>Water Input, pore volumes</u>	<u>Cumulative Oil Recovery, percent pore space</u>	<u>Average Oil Recovery,* percent pore space</u>	<u>Average Water Cut,** percent</u>
0.059	5.9***	--	--
0.109	8.4	7.2	22.9
0.375	14.7	11.6	76.5
0.866	18.8	16.8	91.7
2.13	23.1	22.0	96.6
3.92	24.1	23.6	99.5
5.73	24.4	24.3	99.8
9.27	25.0	24.7	99.8
17.5	25.3	25.2	99.96
33.1	25.6	25.4	99.98
63.6	25.9	25.8	99.99
94.2	26.3	26.1	99.99

\* Calculated for mid-point of incremental throughput

\*\* Calculated from incremental throughput volumes

\*\*\* Breakthrough recovery

This report, based on observations and materials supplied by the client, is prepared for the exclusive and confidential use by the client. The analysis, opinions, or interpretations contained herein represent the judgement of Core Laboratories, Inc.; however, Core Laboratories, Inc., and its employees assume no responsibility and make no warranties or representations as to the utility of this report to the client or as to the productivity, proper operation, or productivity of any oil, gas, or other mineral formation or well in connection with which such report may be used or relied upon.

CORE LABORATORIES, Inc.  
2001 COMMERCE DRIVE  
MIDLAND, TEXAS  
(915) 694-7761

Page 51 of 91

File SCAL-206-82025

WATERFLOOD SUSCEPTIBILITY

Company:	<u>Phillips Petroleum Company</u>	Sample Identification:	<u>70</u>
Well:	<u>South Cowden Unit #6-18</u>	Sample Depth:	<u>4639.0-40.0</u> f.
Formation:	<u>San Andres</u>	Permeability to Air:	<u>0.53</u> m.
Field:	<u>South Cowden</u>	Porosity:	<u>8.6</u> p.
County (Parish):	<u>Ector</u>	Initial Water Saturation:	<u>24.7</u> p.
State:	<u>Texas</u>	Effective Permeability to Oil at $S_{wi}$ :	<u>0.36</u> m.

Water Input, pore volumes	Cumulative Oil Recovery, percent pore space	Average Oil Recovery,* percent pore space	Average Water Cut,** percent
0.154	15.4***	--	--
0.245	18.3	16.8	34.6
0.503	21.3	19.8	88.2
0.836	22.5	21.9	96.5
1.18	23.0	22.8	98.5
1.17	23.4	23.2	99.4
2.45	23.7	23.6	99.5
3.39	23.9	23.8	99.8
5.14	24.0	24.0	99.90
9.76	24.2	24.1	99.96
18.3	24.4	24.3	99.98
34.9	24.5	24.5	99.99

\* Calculated for mid-point of incremental throughput

\*\* Calculated from incremental throughput volumes

\*\*\* Breakthrough recovery

This report, based on observations and materials supplied by the client, is prepared for the exclusive and confidential use by the client. The analysis, opinions, or interpretations contained herein represent the judgment of Core Laboratories, Inc. However, Core Laboratories, Inc. and its employees assume no responsibility and make no warranties or representations as to the accuracy or completeness of the information provided.

WATERFLOOD SUSCEPTIBILITY

Company:	<u>Phillips Petroleum Company</u>	Sample Identification:	<u>84</u>
Well:	<u>South Cowden Unit #6-18</u>	Sample Depth:	<u>4653.0-54.0</u> f
Formation:	<u>San Andres</u>	Permeability to Air:	<u>1.4</u> m
Field:	<u>South Cowden</u>	Porosity:	<u>6.6</u> p
County (Parish):	<u>Ector</u>	Initial Water Saturation:	<u>29.6</u> p
State:	<u>Texas</u>	Effective Permeability to Oil at $S_{wi}$ :	<u>0.49</u> m

<u>Water Input, pore volumes</u>	<u>Cumulative Oil Recovery, percent pore space</u>	<u>Average Oil Recovery,* percent pore space</u>	<u>Average Water Cut,* percent</u>
0.103	10.3***	--	--
0.229	15.3	12.8	59.3
0.447	18.7	17.0	84.6
0.765	19.5	19.1	97.4
2.02	20.6	20.0	99.2
3.28	21.4	20.9	99.3
5.41	22.1	21.8	99.7
10.9	22.3	22.2	99.96
21.4	22.5	22.4	99.98
41.8	22.7	22.6	99.99
62.6	22.9	22.8	99.99

- \* Calculated for mid-point of incremental throughput
- \*\* Calculated from incremental throughput volumes
- \*\*\* Breakthrough recovery

This report, based on observations and materials supplied by the client, is prepared for the exclusive and confidential use by the client. The analyses, opinions, or interpretations contained herein represent the judgement of Core Laboratories, Inc. However, Core Laboratories, Inc. and its employees assume no responsibility and make no warranties or representations as to the accuracy or completeness of the information provided by the client.



**CORE LABORATORIES, Inc.**  
 2001 COMMERCE DRIVE  
 MIDLAND, TEXAS  
 (915) 694-7761

Page 53 of 91  
 File SCAL-206-82025

WATERFLOOD SUSCEPTIBILITY

Company:	<u>Phillips Petroleum Company</u>	Sample Identification:	<u>113</u>
Well:	<u>South Cowden Unit #6-18</u>	Sample Depth:	<u>4682.0-83.0</u> ft
Formation:	<u>San Andres</u>	Permeability to Air:	<u>4.6</u> mD
Field:	<u>South Cowden</u>	Porosity:	<u>9.0</u> pe
County (Parish):	<u>Ector</u>	Initial Water Saturation:	<u>20.0</u> pe
State:	<u>Texas</u>	Effective Permeability to Oil at $S_{wi}$ :	<u>1.40</u> mD

<u>Water Input, pore volumes</u>	<u>Cumulative Oil Recovery, percent pore space</u>	<u>Average Oil Recovery,* percent pore space</u>	<u>Average Water Cut,** percent</u>
0.111	11.1***	--	--
0.33	15.1	13.1	53.9
0.84	16.9	16.0	96.7
1.66	18.9	17.9	97.5
2.79	19.7	19.3	99.2
4.35	20.3	20.0	99.6
5.85	20.6	20.4	99.0
8.23	20.9	20.7	99.90
11.6	21.1	21.0	99.92
26.5	21.7	21.4	99.96
55.5	22.3	22.0	99.98
83.3	22.6	22.4	99.99
111.	22.9	22.7	99.99

\* Calculated for mid-point of incremental throughput

\*\* Calculated from incremental throughput volumes

\*\*\* Breakthrough recovery

This report, based on observations and materials supplied by the client, is prepared for the exclusive and confidential use by the client. The analyses, opinions, or interpretations contained herein represent the judgement of Core Laboratories, Inc.; however, Core Laboratories, Inc. and its employees assume no responsibility and make no warranties or representations as to the utility of this report to the client or as to the productivity, proper operation, or profitability of any oil, gas, or other mineral formation or well in connection with which such report may be used.

**CORE LABORATORIES, Inc.**  
2001 COMMERCE DRIVE  
MIDLAND, TEXAS  
(915) 694-7761

Page 59 of 91

File SCAL-206-82025

SUMMARY OF WETTABILITY TEST RESULTS

Company: Phillips Petroleum Company Well: South Cowden Unit #6-18  
Formation: San Andres Field: South Cowden  
County (Parish), State: Ector, Texas

Sample Condition:	Fresh-State				Initial Fluid Imbibed is Oil			
Sample Identification	26	55	91	120				
Depth, feet	4595.0	4624.0	4660.0	4689.0				
Permeability to Air, md	0.11	0.86	4.5	0.24				
Porosity, percent	3.1	8.5	6.6	4.2				
Immobile Oil Saturation,* percent pore space	87.0	24.4	18.6	16.5				
Permeability to Water at Immobile Oil Saturation, md	0.01	0.20	2.5	0.11				
Oil Imbibed, percent pore space	0.0	0.3	0.4	1.2				
Water Displaced Dynamically, percent pore space	3.8	41.7	52.5	49.1				
Total Water Recovered, percent pore space	3.8	42.0	52.9	50.3				
Immobile Water Saturation,** percent pore space	83.2	33.6	28.5	33.2				
Permeability to Oil at Immobile Water Saturation, md	0.006	0.22	2.7	0.085				
Water Imbibed, percent pore space	1.3	3.1	10.2	0.9				
Oil Displaced Dynamically, percent pore space	0.0	13.6	17.1	13.2				
Total Oil Recovered, percent pore space	1.3	16.7	27.3	14.1				
Wettability Index to Oil	0.0	0.007	0.007	0.027				
Wettability Index to Water	1.0	0.18	0.37	0.062				

\* Oil present just prior to oil imbibition  
\*\* Water present just prior to water imbibition

$$\text{Wettability Index} = \frac{\text{Fluid Imbibed}}{\text{Total Fluid Displaced}}$$

These analyses, opinions or interpretations are based on observations and material supplied by the client to whom, and for whose exclusive and confidential uses, they apply.

SUMMARY OF MERCURY INJECTION TEST RESULTS  
DRAINAGE

Company: Phillips Petroleum Company Well: South Cowden Unit #6-18  
 Formation: San Andres Field: South Cowden  
 County (Parish), State: Ector, Texas

Sample Identification:	37	41	57
Depth, Feet:	4606.0	4610.0	4626.0
Permeability to Air, md:	0.18	0.20	8.2
Porosity, percent:	9.1	9.1	9.4

<u>Injection Pressure, psia</u>	<u>Mercury Saturation, percent pore space</u>		
3	0.0	0.0	0.0
6	0.0	0.0	0.0
9	0.0	0.0	0.0
12	0.0	0.0	0.0
15	0.0	0.0	0.0
18	0.0	0.0	0.5
21	0.0	0.0	4.7
24	0.0	0.0	12.6
27	0.0	0.0	28.3
30	0.0	0.0	38.5
40	0.0	0.0	55.9
60	0.0	0.0	65.6
80	0.0	0.0	69.8
100	0.0	0.0	70.4
200	24.8	24.4	74.9
300	31.9	42.6	76.7
500	40.2	57.2	78.2
750	47.5	65.0	80.0
1000	52.9	69.3	80.3
1250	56.4	72.3	81.0
1500	58.2	74.2	81.1
1750	59.3	76.1	81.4
2000	61.3	77.3	82.3

**CORE LABORATORIES, Inc.**  
 2001 COMMERCE DRIVE  
 MIDLAND, TEXAS  
 (915) 694-7761

Page 61 Of 91

File SCAL-206-82025

SUMMARY OF MERCURY INJECTION TEST RESULTS  
IMBIBITION

Company: Phillips Petroleum Company Well: South Cowden Unit #6-18  
 Formation: San Andres Field: South Cowden  
 County (Parish), State: Ector, Texas

Sample Identification:	37	41	57
Depth, Feet:	4606.0	4610.0	4626.0
Permeability to Air, md:	0.18	0.20	8.2
Porosity, percent:	9.1	9.1	9.4
<u>Injection Pressure, psia</u>	<u>Mercury Saturation, percent pore space</u>		
2000	61.3	77.3	82.3
1500	60.6	76.5	81.8
1250	59.5	76.4	81.6
1000	59.1	76.3	81.4
750	58.8	75.6	81.2
500	58.3	74.4	81.0
300	56.9	72.4	80.7
200	54.6	70.7	80.6
100	52.1	67.0	80.5
80	51.2	66.2	80.4
60	32.9	64.1	80.3
40	32.2	60.6	77.6
30	30.3	58.7	74.1
15	29.8	57.1	62.8
0	29.7	56.1	60.2

This report, based on observations and materials supplied by the client, is prepared for the exclusive and confidential use by the client. The analyses, opinions, or interpretations contained herein represent the judgement of Core Laboratories, Inc.; however, Core Laboratories, Inc., and its employees assume no responsibility and make no warranties or representations as to the

**CORE LABORATORIES, Inc.**  
 2001 COMMERCE DRIVE  
 MIDLAND, TEXAS  
 (915) 694-7761

Page 62 Of 91

File SCAL-206-82025

SUMMARY OF MERCURY INJECTION TEST RESULTS  
DRAINAGE

Company: Phillips Petroleum Company Well: South Cowden Unit #6-18  
 Formation: San Andres Field: South Cowden  
 County (Parish), State: Ector, Texas

Sample Identification:	78	84	113
Depth, Feet:	4647.0	4653.0	4682.0
Permeability to Air, md:	1.2	1.4	4.6
Porosity, percent:	9.1	6.6	9.0

<u>Injection Pressure, psia</u>	<u>Mercury Saturation, percent pore space</u>		
3	0.0	0.0	0.0
6	0.0	0.0	0.0
9	0.0	0.0	0.0
12	0.0	0.0	0.0
15	0.0	0.0	1.7
18	0.0	0.0	7.1
21	0.0	0.0	12.5
24	0.0	1.7	17.7
27	0.0	7.1	22.8
30	0.0	20.7	27.2
40	0.4	38.4	36.6
60	4.3	56.0	46.3
80	12.5	63.9	51.2
100	18.5	67.5	54.7
200	31.8	75.7	68.8
300	37.1	78.6	71.0
500	41.6	82.4	80.9
750	43.7	83.5	86.9
1000	44.7	84.2	90.7
1250	45.5	84.9	96.7
1500	45.7	85.6	94.0
1750	45.8	85.8	94.3
2000	45.9	86.1	95.6

SUMMARY OF MERCURY INJECTION TEST RESULTS  
IMBIBITION

Company: Phillips Petroleum Company Well: South Cowden Unit #6-18  
 Formation: San Andres Field: South Cowden  
 County (Parish), State: Ector, Texas

Sample Identification:	78	84	113
Depth, Feet:	4647.0	4653.0	4682.0
Permeability to Air, md:	1.2	1.4	4.6
Porosity, percent:	9.1	6.6	9.0

<u>Injection Pressure, psia</u>	<u>Mercury Saturation, percent pore space</u>		
2000	45.9	86.1	95.6
1500	45.6	85.9	94.9
1250	45.5	85.9	94.7
1000	45.2	85.9	93.5
750	44.6	85.9	90.8
500	44.0	85.8	86.4
300	42.7	85.6	83.2
200	42.5	85.3	79.1
100	42.4	85.1	72.3
80	42.2	84.9	71.5
60	41.9	84.6	68.3
40	41.6	84.0	62.0
30	41.0	82.9	48.2
15	38.6	77.6	32.4
0	33.5	71.1	30.1

SUMMARY OF MERCURY INJECTION TEST RESULTS  
DRAINAGE

Company: Phillips Petroleum Company Well: South Cowden Unit #6-18  
Formation: San Andres Field: South Cowden  
County (Parish), State: Ector, Texas

Sample Identification:	116	117
Depth, Feet:	4685.0	4686.0
Permeability to Air, md:	0.27	0.04
Porosity, percent:	4.6	3.9

<u>Injection Pressure, psia</u>	<u>Mercury Saturation, percent pore space</u>	
3	0.0	0.0
6	0.0	0.0
9	0.0	0.0
12	0.0	0.0
15	0.0	0.0
18	0.0	0.0
21	0.0	0.0
24	0.0	0.0
27	2.1	0.0
30	4.1	0.0
40	15.5	0.0
60	31.0	4.8
80	40.5	7.6
100	45.7	9.3
200	58.0	20.0
300	64.1	26.3
500	68.8	39.3
750	72.2	51.4
1000	73.6	62.1
1250	75.2	58.1
1500	76.1	71.3
1750	77.6	72.2
2000	78.9	73.1

**CORE LABORATORIES, Inc.**  
 2001 COMMERCE DRIVE  
 MIDLAND, TEXAS  
 (915) 694-7761

Page 65 Of 91  
 File SCAL-206-82025

SUMMARY OF MERCURY INJECTION TEST RESULTS  
IMBIBITION

Company: Phillips Petroleum Company Well: South Cowden Unit #6-18  
 Formation: San Andres Field: South Cowden  
 County (Parish), State: Ector, Texas

Sample Identification:	116	117
Depth, Feet:	4685.0	4686.0
Permeability to Air, md:	0.27	0.04
Porosity, percent:	4.6	3.9

<u>Injection Pressure, psia</u>	<u>Mercury Saturation, percent pore space</u>	
2000	78.9	73.1
1500	78.1	72.4
1250	77.8	71.4
1000	77.5	66.7
750	77.3	61.1
500	77.2	55.0
300	77.1	49.0
200	76.5	45.7
100	75.4	41.6
80	75.0	41.0
60	74.5	40.2
40	73.0	39.8
30	71.3	39.4
15	66.4	39.1
0	63.8	38.8



**CORE LABORATORIES, Inc.**  
2001 COMMERCE DRIVE  
MIDLAND, TEXAS  
(915) 694-7761

Page 74 of 91

File SCAL-206-82025

SUMMARY OF PORE SIZE DISTRIBUTION

Company: Phillips Petroleum Company Well: South Cowden Unit #6-18  
Formation: San Andres Field: South Cowden  
County (Parish), State: Ector, Texas

Sample Identification:	37	41	57
Depth, feet	4606.0	4610.0	4626.0
Permeability to Air, mD:	0.18	0.20	8.2
Porosity, percent:	9.1	9.1	9.4

Pore Aperture Radius, Microns	Cumulative Percent Pore Space		
	37	41	57
35.	100.0	100.0	100.0
30.	100.0	100.0	100.0
25.	100.0	100.0	100.0
20.	100.0	100.0	100.0
15.	100.0	100.0	100.0
10.	100.0	100.0	100.0
8.	100.0	100.0	100.0
6.	100.0	100.0	99.6
4.	100.0	100.0	73.3
3.	100.0	100.0	49.4
2.	100.0	100.0	36.8
1.	100.0	100.0	29.1
0.8	100.0	100.0	27.6
0.6	77.0	82.4	25.8
0.4	70.1	62.0	23.7
0.3	65.3	51.8	22.7
0.2	58.8	41.4	21.6
0.10	46.0	29.8	19.5
0.09	44.3	28.4	19.2
0.08	42.9	27.0	19.0
0.07	41.7	25.6	18.8
0.06	40.6	23.7	18.5
0.055	39.3	22.9	18.0

**CORE LABORATORIES, Inc.**  
2001 COMMERCE DRIVE  
MIDLAND, TEXAS  
(915) 694-7761

Page 75 of 91

File SCAL-206-82025

SUMMARY OF PORE SIZE DISTRIBUTION

Company: Phillips Petroleum Company Well: South Cowden Unit #6-18  
Formation: San Andres Field: South Cowden  
County (Parish), State: Ector, Texas

Sample Identification:	78	84	113
Depth, feet	4647.0	4653.0	4682.0
Permeability to Air, mD:	1.2	1.4	4.6
Porosity, percent:	9.1	6.6	9.0

Pore Aperture Radius, Microns	Cumulative Percent Pore Space		
35.	100.0	100.0	100.0
30.	100.0	100.0	100.0
25.	100.0	100.0	100.0
20.	100.0	100.0	100.0
15.	100.0	100.0	100.0
10.	100.0	100.0	100.0
8.	100.0	100.0	100.0
6.	100.0	100.0	93.4
4.	100.0	94.2	77.8
3.	100.0	68.3	67.0
2.	98.4	48.5	56.1
1.	80.0	31.5	44.5
0.8	75.2	28.4	41.3
0.6	70.1	25.3	37.6
0.4	64.3	22.2	31.4
0.3	61.2	20.0	25.5
0.2	58.0	17.4	18.1
0.10	55.1	15.6	8.7
0.09	54.7	15.3	7.8
0.08	54.4	14.9	6.8
0.07	54.3	14.4	5.9
0.06	54.2	14.1	5.6
0.055	54.2	14.0	4.8

**CORE LABORATORIES, INC.**  
2001 COMMERCE DRIVE  
MIDLAND, TEXAS  
(915) 694-7761

Page 76 of 91

File SCAL-206-82025

SUMMARY OF PORE SIZE DISTRIBUTION

Company: Phillips Petroleum Company Well: South Cowden Unit #6-18  
Formation: San Andres Field: South Cowden  
County (Parish), State: Ector, Texas

Sample Identification:	116	117
Depth, feet	4685.0	4686.0
Permeability to Air, mD:	0.27	0.04
Porosity, percent:	4.6	3.9

Pore Aperture Radius, Microns	Cumulative Percent Pore Space	
35.	100.0	100.0
30.	100.0	100.0
25.	100.0	100.0
20.	100.0	100.0
15.	100.0	100.0
10.	100.0	100.0
8.	100.0	100.0
6.	100.0	100.0
4.	98.0	100.0
3.	89.4	100.0
2.	73.4	96.5
1.	53.1	90.0
0.8	49.0	86.4
0.6	44.0	81.6
0.4	37.5	75.6
0.3	34.1	69.9
0.2	30.7	59.1
0.10	26.0	36.0
0.09	25.2	33.2
0.08	24.5	30.6
0.07	23.8	28.5
0.06	22.8	27.0
0.055	21.4	26.9

**CORE LABORATORIES, INC.**  
2001 COMMERCE DRIVE  
MIDLAND, TEXAS  
(915) 694-7761

Page 85 Of 91

File SCAL-206-82025

SUMMARY OF ACOUSTIC VELOCITY TEST RESULTS

Company: Phillips Petroleum Company Well: South Cowden Unit #6-1A  
Formation: San Andres Field: South Cowden  
County (Parish), State: Ector, Texas

Sample Identification:	26A	34A
Depth, Feet:	4595.0-96.0	4603.0-04.0
Porosity, percent:	8.4	2.7

<u>Effective Overburden</u> <u>Pressure, psi</u>	<u>Transit Time, microseconds/ft</u>	
300	57.43	48.41
800	56.98	47.47
1300	56.75	46.84
1800	56.75	46.53
2350	56.53	46.22

CORE LABORATORIES, INC.  
2001 COMMERCE DRIVE  
MIDLAND, TEXAS  
(915) 694-7761

Page 86 Of 91

File SCAL-206-82025

SUMMARY OF ACOUSTIC VELOCITY TEST RESULTS

Company: Phillips Petroleum Company Well: South Cowden Unit #6-18  
Formation: San Andres Field: South Cowden  
County (Parish), State: Ector, Texas

Sample Identification: 42A 57A  
Depth, Feet: 4611.0-12.0 4626.0-27.0  
Porosity, percent: 8.3 7.1

Effective Overburden Pressure, psi	Transit Time, microseconds/ft	
300	65.76	55.08
800	65.34	52.94
1300	64.72	52.02
1800	62.42	51.41
2350	61.17	51.11

is based on observations and materials supplied by the client. It is prepared for the exclusive and confidential use by the client. The analyses, opinions, or interpretations contained herein are not to be used for any other purpose. Core Laboratories, Inc. and its employees assume no responsibility and make no warranties or representations as to the accuracy or completeness of the information provided.

**CORE LABORATORIES, INC.**  
 2001 COMMERCE DRIVE  
 MIDLAND, TEXAS  
 (915) 694-7761

Page 87 Of 91  
 File SCAL-206-B2025

SUMMARY OF ACOUSTIC VELOCITY TEST RESULTS

Company: Phillips Petroleum Company Well: South Cowden Unit #6-18  
 Formation: San Andres Field: South Cowden  
 County (Parish), State: Ector, Texas

Sample Identification:	59A	78A
Depth, Feet:	4628.0-29.0	4647.0-48.0
Porosity, percent:	6.2	6.6

Effective Overburden Pressure, psi	Transit Time, microseconds/ft	
300	51.08	51.41
800	49.40	51.21
1300	48.99	51.00
1800	48.57	50.80
2350	48.15	50.60

This report, based on observations and materials supplied by the client, is prepared for the exclusive and confidential use by the client. The analyses, opinions, or interpretations contained herein represent the judgment of Core Laboratories, Inc., and its employees assume no responsibility and make no warranties or representations as to its utility or its value to the client or as to the results of any other work or as to the results of any other work or as to the results of any other work.

**CORE LABORATORIES, INC.**  
 2001 COMMERCE DRIVE  
 MIDLAND, TEXAS  
 (915) 694-7761

Page 88 Of 91  
 File SCAL-206-82025

SUMMARY OF ACOUSTIC VELOCITY TEST RESULTS

Company: Phillips Petroleum Company Well: South Cowden Unit #6-18  
 Formation: San Andres Field: South Cowden  
 County (Parish), State: Ector, Texas

Sample Identification:	108A	116A
Depth, Feet:	4677.0-78.0	4685.0-86.0
Porosity, percent:	5.7	5.7

Effective Overburden Pressure, psi	Transit Time, microseconds/ft	
300	53.96	55.54
800	53.56	54.17
1300	53.23	52.79
1800	53.23	52.33
2350	53.23	51.87

its report, based on observations and materials supplied by the client, is prepared for the exclusive and confidential use by the client. The analyses, opinions, or interpretations contained herein represent the information of Core Laboratories, Inc. However, Core Laboratories, Inc. and its employees assume no responsibility and make no warranties or representations as to the

SUMMARY OF ACOUSTIC VELOCITY TEST RESULTS

Company: Phillips Petroleum Company Well: South Cowden Unit #6-18  
Formation: San Andres Field: South Cowden  
County (Parish), State: Ector, Texas

Sample Identification:	134A	138A
Depth, Feet:	4703.0-04.0	4707.0-08.0
Porosity, percent:	11.0	15.2

Effective Overburden Pressure, psi	Transit Time, microseconds/ft	
300	64.30	60.73
800	63.54	58.79
1300	63.29	58.41
1800	62.78	58.02
2350	62.28	57.25

This report, based on observations and materials supplied by the client, is prepared for the exclusive and confidential use by the client. The analyses, opinions, or interpretations contained herein represent the judgement of Core Laboratories, Inc.; however, Core Laboratories, Inc., and its employees assume no responsibility and make no warranties or representations as to the accuracy or completeness of the data or information upon which this report was prepared.





**CORE LABORATORIES**

**SPECIAL CORE ANALYSIS PROGRAM**

**EMMONS UNIT**

**FINAL REPORT**

Performed for:  
**FINA OIL AND CHEMICAL COMPANY**  
P.O. Box 2990  
Midland, Texas 79702

Fina Project Coordinators:  
**P.K. Pande (Special Core Quality Assurance)**  
**Bertrand Meyer (Emmons Unit Reservoir Engineer)**

**March 5, 1993**

Performed by:  
**Core Laboratories**  
Dallas Advanced Technology Center  
Reservoir Flow Studies Laboratory  
1875 Monetary Lane  
Carrollton, Texas 75006

**File: DRP-91200**

This report contains information that is confidential and proprietary to Core Laboratories, Inc. and its subsidiaries. It is not to be distributed outside the company without the written consent of Core Laboratories, Inc. The information contained herein is for the use of the client only and is not to be used for any other purpose. Core Laboratories, Inc. assumes no responsibility for the accuracy or completeness of the information contained herein. The information contained herein is for the use of the client only and is not to be used for any other purpose. Core Laboratories, Inc. assumes no responsibility for the accuracy or completeness of the information contained herein. The information contained herein is for the use of the client only and is not to be used for any other purpose. Core Laboratories, Inc. assumes no responsibility for the accuracy or completeness of the information contained herein.



## CORE LABORATORIES

March 5, 1993

Fina Oil and Chemical Company  
Post Office Box 2990  
Midland, Texas 79702

Attention: Mr. P.K. Pande

Subject: Interim Final Report  
Special Core Analysis Program  
Emmons Unit  
File: DRP-91200

Dear Mr. Pande:

A special core analysis program on core material from the Emmons Unit has been completed for Fina Oil and Chemical Company (Fina). Final results of two steady-state gas-oil and four steady-state water-oil relative permeability tests as well as four tertiary oil recovery tests are presented herein. Mercury injection capillary pressure and pore volume compressibility test results will be presented in a separate addendum report. This testing program was authorized by Mr. P.K. Pande of Fina. Test procedures were discussed in a series of meetings between representatives of Fina and Core Laboratories in March 1992. Preliminary data have been provided to Fina throughout the course of the project.

### Fluid Preparation

One five gallon container of degassed crude oil was received on February 24, 1992. The crude oil was dewatered and prefiltered through a 0.2 micron Cuno™ filter before use. A crude oil blend was prepared to match the reservoir oil viscosity by diluting the filtered oil with petroleum ether. One two liter cylinder of two-phase reservoir fluid was received on May 11, 1992. The two-phase fluid was reconditioned as described on Page 1-2 and crude oil properties measured as described in Section 1.

Synthetic formation brine was prepared from the Central Battery water analysis (see Section 1) using reagent grade chemicals and deionized water. Synthetic formation brine was equilibrated with crushed core material, degassed, and prefiltered through a 0.22 micron Millipore™ filter prior to use. Waterflood brines (undoped and tritium doped) were equilibrated with methane and crushed core material at reservoir conditions.

A synthetic injection gas was prepared to match the supplied gas analysis by Core Laboratories' Reservoir Fluids Laboratory. Injection gas composition is presented in Section 2.

### **Sample Preparation**

Twenty-two 1-1/2 inch diameter core plugs in individual jars under crude oil were provided by Fina to Core Laboratories on February 24, 1992. Effective permeability to the crude oil blend for sample selection was determined using the procedures outlined on Page 1-1. A summary of effective permeability to oil measurements and sample selection appears in Section 2 on Page 2-1.

### **Experimental Procedures and Results**

#### **Steady-State Gas-Oil and Water-Oil Relative Permeability**

Steady-State imbibition and drainage gas-oil and water-oil relative permeability tests were performed on samples E1-10 and E1-15 as outlined on Pages 1-3 and 1-4. Steady-state imbibition and drainage water-oil relative permeability tests were performed on samples E1-3 and E1-7 as described on Pages 1-6 and 1-7. In-place water saturation values were determined on the trimmed ends of the samples; however, these values were much lower than those from the x-ray method, due to heterogeneities in the samples. Unsteady-state gas-oil relative permeability tests were performed on cleaned samples E1-10 and E1-15 for comparison as described on Page 1-5. Test results are presented in summary, tabular and graphic format in Section 3.

#### **Tertiary Oil Recovery**

Unsteady-state tertiary oil recovery tests were performed on companion samples to the steady-state samples; E1-1, E1-6, E1-11, and E1-14 using the procedures outlined on Pages 1-8 and 1-9. Waterflood oil recoveries ranged from 39.1 to 51.4 percent pore space (43.9 to 56.1 percent oil in place) yielding waterflood residual oil saturations ranging from 37.9 to 49.9 percent pore space.

Gasflooding recovered an additional 22.1 to 42.1 percent pore space oil (61.0 to 84.3 percent oil in place) resulting in gasflood residual oil saturations ranging from 7.1 to 16.7 percent pore space.

Unsteady-state water-oil relative permeability relationships were determined for all samples. The dimensionless groups for these displacements were calculated as requested. Tertiary oil recovery test results are presented in summary, tabular and graphic format in Section 4.

#### **Data Reduction and Error Analysis**

A summary of data reduction methods and an error analysis for all tests is presented in Section 5.

#### **Pore Volume Compressibility**

Pore volume compressibility tests were performed on one sample from each well using the protocol described on pages 1-11 and 1-12. To calculate hydrostatic pore volume compressibility in the range of interest, the measurements were performed over a range of stress conditions expected in the reservoir and beyond abandonment pressure. The pore volume reduction between 800 psi and 5000 psi net stress amounted to a loss of 2.1 percent of the initial pore volume for sample E1-4 (Well 143) and 1.5 percent for sample E1-19 (Well 142) over the intervals of pressure and time tested.

Based on an approximate current reservoir pressure of 2000 psi and an average depth of 4600 feet, the net stress currently in the reservoir is approximately 2600 psi which is equivalent to a hydrostatic stress of 1500 psi at approximately equivalent hydrostatic stress (1600 psi), the average measured hydrostatic pore volume compressibility is  $6.85/\text{psi} \cdot \text{E6}$  and the average  $C_u$  which is generally considered equal to  $C_f$  (formation compressibility) was  $4.245/\text{psi} \cdot \text{E6}$ . Pore volume compressibility test results appear in Section 6.

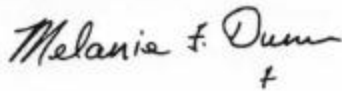
#### **Mercury Injection**

Mercury injection capillary pressure tests were performed on the ten selected samples, including end trims from the eight relative permeability test samples, using the procedures outlined on Pages 1-13 and 1-14. The total percent pore space invaded by mercury at the maximum injection pressure of 50,000 psia ranges from 83.8 to 84.8 for these samples. No trend with permeability or porosity was apparent. The median pore throat radius ranged from sub-nano to super-nano. Mercury injection test results are presented in Section 7.

Fina Oil and Chemical Company  
File: DRP-91200  
Page Four

Thank you for this opportunity to be of service to Fina Oil and Chemical Company. If you have any questions concerning the enclosed information, or if we can be of any additional service, please contact me at 214-323-3991. It has been a pleasure to work with Fina on this interesting project and I look forward to our continuing relationship.

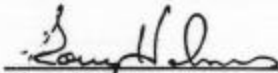
Very truly yours,

A handwritten signature in cursive script that reads "Melanie F. Dunn". The signature is written in dark ink and is positioned above the printed name.

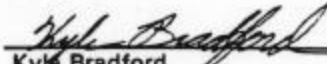
Melanie F. Dunn  
Supervisor, Reservoir Flow Studies  
Dallas Advanced Technology Center

## PROJECT PARTICIPANTS

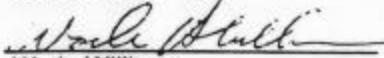
Sample Preparation

  
Kory Holmes

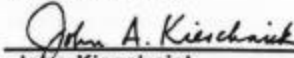
Steady-State Relative Permeability

  
Kyle Bradford

Tertiary Oil Recovery

  
Wade Williams

Pore Volume Compressibility

  
John Kieschnick

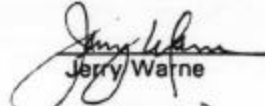

Mercury Injection

  
Tommy Wallace

Reservoir Fluids Preparation

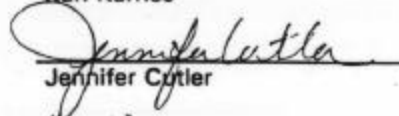
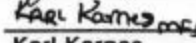
  
Henry Cole

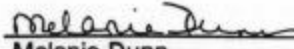
Data Evaluation

  
Jerry Warne  
  
Melanie Dunn

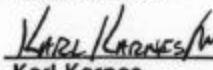
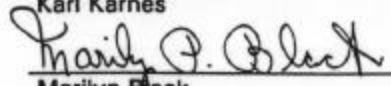
  
Karl Karnes

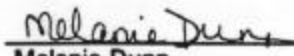
Report Preparation

  
Jennifer Cutler  
  
Karl Karnes

  
Melanie Dunn

Final Review

  
Karl Karnes  
  
Marilyn Black

  
Melanie Dunn

## **TABLE OF CONTENTS**

<b>Section 1:</b>	<b>Experimental Procedures</b>
<b>Section 2:</b>	<b>Sample and Fluid Preparation</b>
<b>Section 3:</b>	<b>Steady-State Relative Permeability Test Results</b>
<b>Section 4:</b>	<b>Tertiary Oil Recovery Test Results</b>
<b>Section 5:</b>	<b>Data Reduction and Error Analysis</b>
<b>Section 6:</b>	<b>Pore Volume Compressibility Test Results</b>
<b>Section 7:</b>	<b>Mercury Injection Results</b>

## **SECTION 1**

### **Experimental Procedures**



## **EXPERIMENTAL PROCEDURES**

### **Sample Preparation and Selection**

1. Load preserved-state sample in a hydrostatic coreholder located in an air bath oven. Apply 1500 psi net overburden pressure, and establish 500 psi backpressure. Elevate temperature to 98°F and inject degassed crude oil, which has been diluted to match the reservoir viscosity of 2.1 cp and prefiltered through a 0.2 micron Cuno<sup>TM</sup> filter, at a constant rate until a stable differential pressure is achieved. Determine effective permeability to oil at initial water saturation. Report data to Fina for sample selection.
2. Cool sample to room temperature, unload, and place in a glass jar under crude oil.

## **EXPERIMENTAL PROCEDURES**

### **Crude Oil Reconditioning**

1. The two-phase reservoir fluid sample is recombined by injecting mercury until the cylinder pressure equals 5000 psi and shaken vigorously.
2. A reservoir condition bubble-point is measured and compared to the previous results to confirm sample suitability.

## EXPERIMENTAL PROCEDURES

### Steady-State Gas-Oil and Water-Oil Relative Permeability Test

1. Trim a 1/4" inch long wafer from the upstream end of the sample using crude oil as the lubricant and submit to Dean Stark extraction to determine water saturation.
2. Load cleaned sample (sacrificial core for tertiary oil recovery tests) in the specially designed Hassler-type coreholder which is constructed of a special alloy that allows penetration by the x-rays used to monitor saturation changes during steady-state testing and apply 1500 psi net confining pressure.
3. A dry scan of the sample is performed. The sample is then saturated with crude oil, reloaded in the core holder, reservoir conditions established, and dead crude oil injected until equilibrium. Specific permeability to oil is determined while scanning the sample.
4. The sample is recleaned, saturated with brine, reloaded in the X-ray core holder, and synthetic brine, which has been equilibrated with crushed core material, is injected until equilibrium. Specific permeability to brine is determined while scanning the sample. These scans will be used for determination of approximate saturations while running the steady-state tests.
5. Load selected sample in the specially designed Hassler-type coreholder which is constructed of a special alloy that allows penetration by the x-rays used to monitor saturation changes during steady-state testing and apply 1500 psi confining pressure.
6. Degassed crude oil, which has been diluted to the reservoir viscosity of 2.1 cp with iododecane and prefiltered through a 0.2 micron Cuno<sup>TM</sup> filter (dead crude oil), is injected at a slow rate to establish a backpressure of 200 psi. Elevate temperature to 98°F and inject dead crude oil at a constant rate, until a stable differential pressure is achieved and the effective permeability to oil at initial water saturation is determined while the sample is scanned with x-rays to determine saturation.
7. Humidified nitrogen and dead crude oil next are injected simultaneously at several increasing gas-oil injection ratios to allow the gas saturation within the sample to increase. Saturation changes are monitored by x-ray scan.
8. Injection is continued at each ratio until an equilibrium, steady-state condition within the core plug is established, based on the consistency of the saturation

profile and differential pressure. (Flow rates and differential pressures are monitored throughout the test process.) Finally, gas alone is injected and an effective permeability to gas at residual oil saturation is determined.

9. For the oil-gas (gas saturation decreasing) portion of the test, oil and humidified nitrogen are injected simultaneously at several increasing oil-gas injection ratios to allow the oil saturations in the sample to increase. Injection is continued at each ratio until an equilibrium, steady-state condition within the core plug is established, based on the consistency of the saturation profile and differential pressure. Finally, dead crude oil alone is injected and an effective permeability to oil in the presence of the residual gas saturation is determined.
10. The backpressure was removed to allow the residual gas to be expelled, the backpressure reestablished, and dead crude oil injected to displace any remaining gas until equilibrium. Effective permeability to oil at initial water saturation is determined while scanning the sample and those values compared to the previous results. If the values are acceptable, the test will continue.
11. Steps 7, 8, and 9 are repeated substituting synthetic formation brine, which has been equilibrated with crushed core material, as the displacing phase.
12. The sample is cooled, unloaded, and cleaned by injection of alternating volumes of toluene and methanol. Dry sample by injecting nitrogen at ambient conditions. Determine Klinkenberg permeability and Boyle's law helium porosity at net confining stress. The effluents are analyzed for water content by Karl Fisher.
13. The clean sample is then loaded into the X-ray core holder and a dry scan of the sample is performed. The sample is then saturated with crude oil, reloaded in the core holder, reservoir conditions reestablished, and dead crude oil injected until equilibrium. Specific permeability to oil is determined while scanning the sample.
14. The sample is recleaned, saturated with brine, reloaded in the X-ray core holder, and synthetic brine, which has been equilibrated with crushed core material, is injected until equilibrium. Specific permeability to brine is determined while scanning the sample.
15. Reservoir condition flow rates and differential pressures at equilibrium conditions for each gas-oil and water-oil injection ratio are used to calculate the relative permeability data for each sample. Saturation values are calculated from the x-ray scan data and confirmed by material balance.

## EXPERIMENTAL PROCEDURES

### Unsteady-State Room Condition Gas-Oil Relative Permeability Test

1. The sample is extracted of hydrocarbons with toluene and leached of salts with methanol. The sample is air dried to a constant weight at 72°F. Permeability to air and Boyles' Law helium porosity are determined at 1500 psi confining pressure.
2. The core plug is then evacuated of air and saturated with a laboratory oil, which has a viscosity of approximately 20 cp at ambient conditions.
3. The sample is loaded in a hydrostatic coreholder, reservoir net confining stress applied, 500 psi back pressure established, and the laboratory oil injected at an appropriate constant pressure until a stable production rate is obtained. The backpressure is relieved, and specific permeability to oil is determined at two injection pressures. The sample is unloaded and weighed.
4. The sample is reloaded, reservoir net confining stress applied, and humidified nitrogen is injected at a suitable constant pressure, while collecting produced oil and gas volumes and monitoring differential pressure and cumulative time, until a gas-oil permeability ratio of approximately 30 is achieved. Effective permeability to gas at residual oil saturation is determined at two injection pressures. The sample is unloaded and weighed.
5. Gas-oil relative permeability relationships are calculated using the theory of Welge as expanded by Johnson, Bossler, and Naumann.

## EXPERIMENTAL PROCEDURES

### Steady-State Water-Oil Relative Permeability Test

1. Trim a 1/4" inch long wafer from the upstream end of the sample using crude oil as the lubricant and submit to Dean Stark extraction to determine water saturation.
2. Load cleaned sample (sacrificial core for tertiary oil recovery tests) in the specially designed Hassler-type coreholder which is constructed of a special alloy that allows penetration by the x-rays used to monitor saturation changes during steady-state testing and apply 1500 psi net confining pressure.
3. A dry scan of the sample is performed. The sample is then saturated with crude oil, reloaded in the core holder, reservoir conditions established, and dead crude oil injected until equilibrium. Specific permeability to oil is determined while scanning the sample.
4. The sample is recleaned, saturated with brine, reloaded in the X-ray core holder, and synthetic brine, which has been equilibrated with crushed core material, is injected until equilibrium. Specific permeability to brine is determined while scanning the sample. These scans will be used for determination of approximate saturations while running the steady-state tests.
5. Load selected sample in the specially designed Hassler-type coreholder which is constructed of a special alloy that allows penetration by the x-rays used to monitor saturation changes during steady-state testing and apply 1500 psi confining pressure.
6. Degassed crude oil, which has been diluted to the reservoir viscosity of 2.1 cp with iododecane and prefiltered through a 0.2 micron Cuno<sup>TM</sup> filter (dead crude oil), is injected at a slow rate to establish a backpressure of 200 psi. Elevate temperature to 98°F and inject dead crude oil at a constant rate, until a stable differential pressure is achieved and the effective permeability to oil at initial water saturation is determined while the sample is scanned with x-rays to determine saturation.
7. Synthetic formation brine, which has been equilibrated with crushed core material, and dead crude oil next are injected simultaneously at several increasing water-oil injection ratios to allow the water saturation within the sample to increase. Saturation changes are monitored by x-ray scan.

8. Injection is continued at each ratio until an equilibrium, steady-state condition within the core plug is established, based on the consistency of the saturation profile and differential pressure. (Flow rates and differential pressures are monitored throughout the test process.) Finally, water alone is injected and an effective permeability to water at residual oil saturation is determined.
9. For the oil-water (water saturation decreasing) portion of the test, oil and water are injected simultaneously at several increasing oil-water injection ratios to allow the oil saturation in the sample to increase. Injection is continued at each ratio until an equilibrium, steady-state condition within the core plug is established, based on the consistency of the saturation profile and differential pressure. Finally, dead crude oil alone is injected and an effective permeability to oil at irreducible water saturation is determined.
10. The sample is cooled, unloaded, and cleaned by injection of alternating volumes of toluene and methanol. Dry sample by injecting nitrogen at ambient conditions. Determine Klinkenberg permeability and Boyles' law helium porosity at net confining stress. The effluents are analyzed for water content by Karl Fisher.
11. The clean sample is then loaded into the X-ray core holder and a dry scan of the sample is performed. The sample is then saturated with crude oil, reloaded in the core holder, reservoir conditions reestablished, and dead crude oil injected until equilibrium. Specific permeability to oil is determined while scanning the sample.
12. The sample is recleaned, saturated with brine, reloaded in the X-ray core holder, and synthetic brine, which has been equilibrated with crushed core material, is injected until equilibrium. Specific permeability to brine is determined while scanning the sample.
13. Reservoir condition flow rates and differential pressures at equilibrium conditions for each water-oil injection ratio are used to calculate the relative permeability data for each sample. Saturation values are calculated from the x-ray scan data and confirmed by material balance.

## EXPERIMENTAL PROCEDURES

### Tertiary Oil Recovery Test

1. Trim a 1/4" inch long wafer from the upstream end of the sample using crude oil as the lubricant and submit to Dean Stark extraction to determine water saturation.
2. Load selected preserved-state sample in a hydrostatic coreholder located in an air bath oven. Apply 1500 psi net overburden pressure. Install a crude oil saturated sand-packed slim tube upstream of the core sample and establish 2000 psi backpressure by injecting degassed crude oil, which has been diluted to match the reservoir viscosity of 2.1 cp and prefiltered through a 0.2 micron Cuno<sup>TM</sup> filter (dead crude oil), at a slow rate. Elevate temperature to 98°F and inject dead crude oil at a constant rate, until a stable differential pressure is achieved. Determine effective permeability to oil at initial water saturation. Compare to previous results.
3. Displace dead crude oil by injecting a minimum of two pore volumes of recombined reservoir crude oil at a constant rate, while monitoring differential pressure and produced volumes, until a stable differential pressure is achieved.
4. Allow the sample to sit overnight. Repeat Step 3.
5. Record differential pressure at two injection rates and determine effective permeability to oil at initial water saturation. Compare to previous results. Measure gas-oil ratio and compare to reported value.
6. Close in the slim tube. Install a sacrificial core sample, which has been miscibly cleaned, saturated with brine, and loaded in a hydrostatic coreholder, upstream of the test core.
7. Inject synthetic brine, which has been pre-equilibrated with crushed core and saturated with methane at the bubble-point of the crude oil, at constant rate of approximately 3 cc/min (to minimize end effects), while monitoring produced volumes, differential pressure, and backpressure until the producing gas-water ratio is stabilized and a water-cut of 99.95 percent is achieved. Record differential pressure at two injection rates and determine effective permeability to water at waterflood residual oil saturation.



8. Inject 5 pore volumes of synthetic brine, which has been saturated with methane and doped with tritium tracer, and collect produced effluent in a batch. Inject 1 additional pore volume and collect it separately. Analyze effluents by scintillation counter for tritium content.
9. Repeat Step 8 using undoped brine displacing the in-place doped brine.
10. Close in the sacrificial core and reconnect the slim tube. Inject injection gas (98.48 mole percent carbon dioxide, 1.4 mole percent nitrogen, and 0.12 mole percent methane) at a constant rate of approximately one foot per day (calculated for the core plug) through the crude oil saturated slim tube into the core while monitoring produced volumes, and differential pressure.
11. When the produced hydrocarbon effluent is amber in color, the slim tube is closed off from the system and injection gas is injected directly into the core. The injection is continued until a producing gas-oil ratio of 561,400 scf/stb (100,000 cc/cc) is achieved. Record differential pressure at two injection rates and determine effective permeability to gas at residual oil saturation.
12. Depressure the sample to room conditions while measuring produced fluids. Measure void volume by helium expansion.
13. Clean sample by injection of alternating volumes of toluene and methanol. Dry sample by injecting nitrogen at ambient conditions. Determine Klinkenberg permeability and Boyles' law helium porosity at net confining stress.
14. Determine residual water saturation by Karl Fisher analysis. The gas saturation is determined from the void volume measurement, corrected for blow down fluid volumes. The residual oil saturation is determined by material balance. The waterflood residual oil saturation is determined from the tritium tracer analysis, and the initial water saturation calculated by material balance.

**15. Report data as follows:**

Klinkenberg Permeability  
Boyles' Law Helium Porosity  
Initial Water Saturation  
Effective Permeability to Oil at Initial Water Saturation  
Waterflood Oil Recovery  
Waterflood Susceptibility Data  
Unsteady-State Water-Oil Relative Permeability (if possible)  
Waterflood Residual Oil Saturation  
Effective Permeability to Water at  
Waterflood Residual Oil Saturation  
Gasflood Recovery  
Gasflood Residual Oil Saturation  
Effective Permeability to Gas at Gasflood Residual Oil Saturation

## **EXPERIMENTAL PROCEDURES**

### **Pore Volume Compressibility Test**

1. The selected sample was endface ground to provide parallel endfaces, a calipered bulk volume determined, and installed in a hydrostatic coreholder. A minimum confining pressure was applied, then the sample was evacuated until a minimum vacuum of -29 in/Hg was attained and held for approximately thirty minutes.
2. The sample was pressure saturated in place with simulated formation brine. A constant pore pressure of 1000 psia and a constant confining pressure of 1800 psi were applied and maintained for approximately four hours.
3. Both ends of the sample were connected by a pressure line to a positive displacement pump. The pump maintained a constant pore pressure of 1000 psi (to ensure any gas not removed from the system remains in solution) throughout the entire test to eliminate fluid compressibility as a test variable.
4. Confining pressures were increased incrementally over a full-cycle of increasing and decreasing net stresses, ranging from 800 psi to 5000 psi. The fluid volume changes, necessary to maintain the constant pore pressure, which occurred after each increase in confining pressure were monitored using optical linear encoders.
5. The initial pressure-point at 1800 psi confining pressure (net stress of 800 psi) was maintained for 4 hours to establish complete pressure equilibrium before increasing to the next pressure point. The first pressure point at 800 psi net stress was used to normalize the data to the measured CMS-300 data.
6. Confining pressure was increased at a rate of 200 psi/hour to a maximum confining pressure of 6000 psi, or net hydrostatic stress of 5000 psi, then decreased incrementally at the same rate to a final net stress of 1800 psi.
7. The sample was unloaded from the coreholder, extracted of hydrocarbons with toluene, leached of salts with methanol, and air dried to a constant weight. Basic properties measurements were performed to acquire stressed vertical Klinkenberg permeabilities and porosities on the CMS-300 at a normalizing nominal confining stress of 900 psi (actual net stress calculated at 800 psi).

8. Pore volumes were normalized to the final direct pore volume measured on the CMS-300 at an equivalent net stress of 800 psi. The calculation of hydrostatic pore volume compressibility was performed by first modeling the actual expressed pore volume data on the increasing half cycle using the TABLECURVE™ Software. The following model was used to express the half-cycle of data points at increasing net stress:

$$V_p = (a + b + c \ln(x) + d \sqrt{x})$$

where:  $V_p$  = stressed pore volume  
 $x$  = net stress  
 $a, b, c$  &  $d$  are parameters of fit for each sample

9. Compressibility was determined by applying a log natural (slope) equation to the normalized pore volume and net stress data. Compressibility was calculated at each net stress point using:

$$C_f = \ln((NPV1/NPV2)/(NS2-NS1)) \cdot 1E6$$

10. An approximate of the uniaxial pore volume compressibility (generally considered to represent reservoir stress conditions) was determined from the measured hydrostatic pore volume compressibility by multiplying the hydrostatic pore volume compressibility by a translation factor.
11. The translation factor was determined using Teeuw's equation which uses an assumed Poisson's ratio which relates the amount of axial to lateral strain. Assuming Poisson's ratio to be 0.30, the translation factor, 0.619, was calculated using the following equation and used to determine  $C_u$  values for the data.

$$T_f = (1 + 0.30)/3 \cdot (1 - 0.30)$$

## EXPERIMENTAL PROCEDURES

### Mercury Injection Test

1. Eight 1-inch diameter plug samples representing depth intervals of 4532.8 to 4644.6 feet were drilled from 1-1/2 inch diameter core plugs using synthetic formation brine as the bit coolant and lubricant.
2. The samples were extracted of hydrocarbons with toluene and leached of inorganic salts with methanol in a solvent reflux apparatus using cool solvents, then air dried to a constant weight. Permeability to air and Boyle's law helium porosity were determined at 400 psi net confining stress.
3. Mercury injection tests were performed using the Micromeritics Autopore II 9220, an automated, high-pressure mercury injection device which operates at injection pressures of 0 to 50,000 psia.
4. The selected sample was loaded into a glass penetrometer consisting of a sample chamber attached to a capillary stem with a Cylindrical Coaxial Capacitor.
5. The sample/penetrometer assembly was weighed, then placed into a low pressure system of the apparatus. The sample chamber was evaluated and filled with mercury, then the pressure was increased incrementally to atmospheric pressure with time allowed at each pressure for saturation equilibrium.
6. After achieving saturation equilibrium at atmospheric pressure the assembly was removed, reweighed, then installed in the high-pressure system of the apparatus. The pressure was increased incrementally to a maximum of approximately 50,000 psia. The volume of mercury injected at each pressure was determined by the change in capacitance of the capillary stem.
7. Pore-size distribution for each sample was calculated from the mercury injection test results. Pore radii were calculated by the formula:

$$R_i = \frac{2T \cdot \cos\theta \cdot c}{P_c}$$

where:  $R_i$  = pore radius, microns  
 $T$  = air-mercury interfacial tension = 485 dynes, cm  
 $\Theta$  = air-mercury contact angle =  $140^\circ$   
 $C$  = unit conversion constant = 0.145  
 $P_c$  = mercury injection pressure, psia

8. Leverett J-Function values were calculated from the basic sample properties using the following equation:

$$J\text{-Function} = \frac{P_c}{(T \cdot \cos \theta)} \cdot (k/\phi)^{1/2} \cdot 0.2166$$

where:  $P_c$  = injection pressure, psi  
 $T$  = interfacial tension (a/Hg = 485) dynes/cm  
 $\Theta$  = contact angle (a/Hg =  $140^\circ$ )  
 $K$  = permeability to air, millidarcies  
 $\phi$  = porosity, fraction

9. Conversions to air/brine, air/oil and water/oil capillary pressure systems were calculated using the following formulas:

$$\text{Air/brine} = \frac{(T \cdot \cos \theta)_{a/b}}{(T \cdot \cos \theta)_{a/Hg}}$$

$$\text{Air/oil} = \frac{(T \cdot \cos \theta)_{a/o}}{(T \cdot \cos \theta)_{a/Hg}}$$

$$\text{Oil/brine} = \frac{(T \cdot \cos \theta)_{o/b}}{(T \cdot \cos \theta)_{a/Hg}}$$

where:  $T$  = interfacial tension (a/b = 72, a/o = 24, o/b = 48), and  
 $a/Hg = 140^\circ$ .  
= contact angle (a/b and a/o =  $0^\circ$ , 1/b =  $30^\circ$ , and a/hg =  $140^\circ$ )

## **SECTION 2**

### **Sample and Fluid Preparation**

SUMMARY OF INITIAL EFFECTIVE PERMEABILITY TO OIL MEASUREMENTS

Fina Oil and Chemical Company  
Emmons Unit

<u>Sample</u>	<u>Depth, ft</u>	<u>Well</u>	<u>Effective to Oil, md</u>	<u>Permeability Test Performed</u>
E1-1	4532.8	E-143	1.94	CO <sub>2</sub>
E1-2	4532.9	E-143	6.63	
E1-3	4533.6	E-143	3.76	SS W/O
E1-4	4565.8	E-143	3.42	
E1-5	4572.8	E-143	0.173	
E1-6	4590.6	E-143	16.0	CO <sub>2</sub>
E1-7	4593.8	E-143	55.0	SS <sup>2</sup> W/O
E1-8	4595.6	E-143	39.3	
E1-9	4635.8	E-142	0.00053	
E1-10	4638.8	E-142	9.44	SS G/O, W/O
E1-11	4638.9	E-142	6.76	CO <sub>2</sub>
E1-12	4641.8	E-143	0.182	
E1-13	4643.9	E-142	9.77	
E1-14	4644.5	E-143	21.9	CO <sub>2</sub>
E1-15	4644.6	E-143	24.7	SS <sup>2</sup> G/O, W/O
E1-16	4645.8	E-143	18.3	
E1-17	4655.9	E-142	4.49	
E1-18	4664.8	E-142	0.256	
E1-19	4666.8	E-142	2.89	
E1-20	4691.8	E-142	0.0027	
E1-21	4691.9	E-142	0.0039	
E1-22	4692.9	E-142	105	



SYNTHETIC BRINEFina Oil and Chemical Company  
Emmons Unit

Central Battery

<u>Constituent</u>	<u>Concentration, g/l</u>
Sodium Chloride	60.420
Calcium Chloride	6.928
Magnesium Chloride Hexahydrate	4.390
Sodium Bicarbonate	1.436
Sodium Sulfate	4.532

Brine Analysis

<u>Cations</u>	<u>Concentration, mg/l</u>	<u>Anions</u>	<u>Concentration, mg/l</u>
Sodium	25616	Chloride	42600
Calcium	2502	Sulfate	3065
Magnesium	525	Bicarbonate	1043



## CORE LABORATORIES

Page 1 of 1

File RFL 920134

Well DRS-91200

### SYNTHETIC GAS COMPOSITION

<u>Component</u>	<u>Mole Percent</u>		<u>Molecular Weight(1)</u>	<u>Density,gm/cc at 60°F(1)</u>
	<u>Desired</u>	<u>Actual</u>		
Carbon Dioxide	98.48	98.50	44.010	0.81720
Nitrogen	1.40	1.39	28.013	0.80860
Methane	0.12	0.11	16.043	0.29970
	100.00	100.00		

### Calculated Properties of Synthetic Gas

Molecular weight	43.76
Gas gravity (air = 1.000)	1.511
Gross Btu/scf dry gas	1

Standard conditions = 14.65 psia and 60°F

(1) Assigned properties taken from literature.

This report contains information that may be used by others in the industry and is not to be distributed outside the company. The information is confidential and its use is restricted to the company. The information is not to be used for any other purpose without the written consent of the company. The information is not to be used for any other purpose without the written consent of the company.

## **Laboratory Procedures**

Finna Oil & Chemical Company  
Reservoir Fluid Study  
Emmons 208 Well  
Emmons Field  
Ector County, Texas

RFL 920144

On May 9, 1992, a sample of recombined separator products was received in our Carrollton, Texas laboratory. As a quality check, a bubblepoint determination was measured at ambient temperature. This value was determined to be 547 psig at 68°F.

The composition of the reservoir fluid sample was measured through an eicosanes plus residual fraction by flash-chromatographic technique. The composition of the fluid can be found on page one.

A portion of the reservoir fluid was charged to a high pressure, windowed cell heated to the reported reservoir temperature (98°F). During the constant composition expansion at this temperature, a bubblepoint was observed at 607 psig. The results of the pressure-volume relations are presented on pages two and three.

**Fina Oil & Chemical Company**  
**Emmons 208**  
RFL 820144

**Composition of Reservoir Fluid**  
( From Chromatographic Technique )

Component	Mol %	Wt %	Density (gm/cc)	MW	Vol %
Hydrogen Sulfide	3.46	.81	.801	34.1	0.81
Carbon Dioxide	1.82	.55	.817	44.0	0.54
Nitrogen	.52	.10	.809	28.0	0.10
Methane	10.90	1.20	.300	16.0	3.21
Ethane	5.81	1.20	.356	30.1	2.70
Propane	6.80	2.06	.506	44.1	3.26
iso-Butane	1.63	.65	.562	58.1	0.93
n-Butane	4.33	1.73	.583	58.1	2.38
iso-Pentane	2.38	1.18	.624	72.2	1.52
n-Pentane	2.42	1.20	.630	72.2	1.52
Hexanes	4.16	2.40	.685	84.0	2.81
Heptanes	6.46	4.26	.722	96.0	4.73
Octanes	6.44	4.73	.745	107.0	5.09
Nonanes	5.14	4.27	.764	121.0	4.48
Decanes	3.90	3.59	.778	134.0	3.70
Undecanes	3.09	3.12	.789	147.0	3.17
Dodecanes	2.44	2.70	.800	161.0	2.71
Tridecanes	2.51	3.02	.811	175.0	2.98
Tetradecanes	2.12	2.77	.822	190.0	2.70
Pentadecanes	1.97	2.79	.832	206.0	2.69
Hexadecanes	1.54	2.35	.839	222.0	2.25
Heptadecanes	1.40	2.28	.847	237.0	2.16
Octadecanes	1.37	2.36	.852	251.0	2.22
Nonadecanes	1.23	2.22	.857	263.0	2.08
Eicosanes plus	16.16	46.46	.949	418.0	39.26
<b>Totals</b>	<b>100.00</b>	<b>100.00</b>			<b>100.00</b>

**Sample Characteristics**

Total Liquid Molecular Weight ..... 145.6  
Total Liquid Density (gm/cc) ..... 0.8020  
Total Liquid API Gravity ..... 44.9

**Properties of Heavy Fractions**

Plus Fractions	Mol %	Wt %	Density (gm/cc)	*API	MW
Heptanes plus	55.77	86.92	0.869	31.3	226.7
Undecanes plus	33.83	70.07	0.903	25.1	301.2
Pentadecanes plus	23.67	58.46	0.926	21.4	359.2
Eicosanes plus	16.16	46.46	0.949	17.6	418.0

## Fina Oil & Chemical Company

Emmons 208

RFL 920144

### VOLUMETRIC DATA

(at 98 °F)

Saturation Pressure (Psat)	607	psig
Density at Psat	--	gm/cc
Thermal Exp @ 5000 psig	1.01308	V at 98 °F / V at 68 °F

### AVERAGE SINGLE-PHASE COMPRESSIBILITIES

Pressure Range psig			Single-Phase Compressibility v/v/psi
5000	to	4000	5.57 E -6
4000	to	3000	6.00 E -6
3000	to	2000	6.47 E -6
2000	to	607	7.03 E -6

# Fina Oil & Chemical Company

Emmons 208

RFL 920144

## PRESSURE-VOLUME RELATIONS

(at 98 °F)

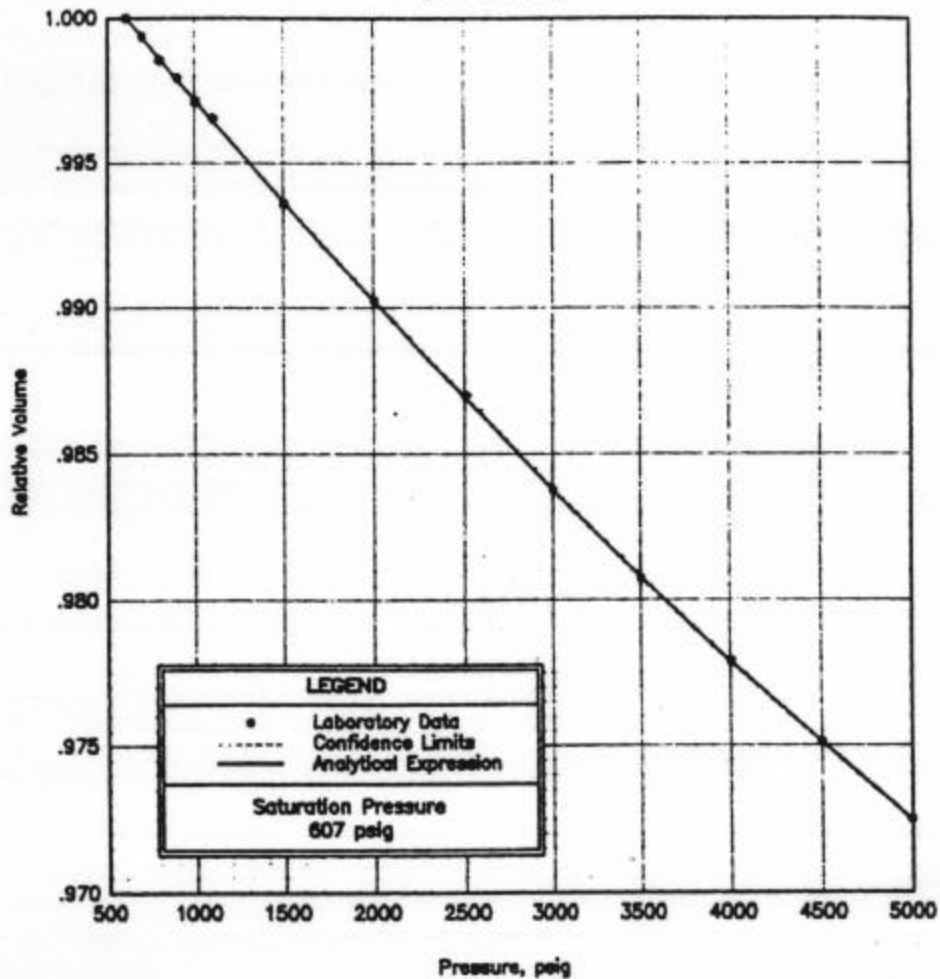
Pressure psig	Relative Volume (A)	Y-Function (B)	Density gm/cc
5000	0.9725		
4500	0.9751		
4000	0.9779		
3500	0.9808		
3000	0.9838		
2500	0.9869		
2000	0.9902		
1500	0.9936		
1100	0.9964		
1000	0.9972		
900	0.9979		
800	0.9986		
700	0.9993		
b-607	1.0000		

(A) Relative Volume:  $V/V_{sat}$  or volume at indicated pressure per volume at saturation pressure.

(B) Where: Y-Function = 
$$\frac{(P_{sat} - P)}{(P_{abs}) * (V/V_{sat} - 1)}$$

Fina Oil & Chemical Company  
Emmons 208  
RFL 920144

RELATIVE VOLUME  
( at 98 °F )



<b>Analytical Expression</b> $1 - 10^{-5} [ -5.174E00 + 1.015E00 (\log(dP)) + -2.652E-06 (\log(dP))^2 ]$ <p><small>Note: dP is defined as   P1 - P2  , psig</small></p>	
<b>Statistical Summary</b> r squared: 0.999984 Confidence Interval (+/-): 0.0000 Confidence: 99 %	<b>Pressure-Volume Relations</b> Figure A-1

### **SECTION 3**

#### **Steady-State Relative Permeability**



## SUMMARY OF GAS-OIL AND WATER-OIL RELATIVE PERMEABILITY TEST RESULTS

Fina Oil and Chemical Company

Sample I.D.	Depth, feet	Klinkenberg Permeability, millidarcies	Porosity, percent	Initial Conditions			Terminal Conditions			Oil Recovered	
				Water Saturation, percent pore space	Effective Permeability to Oil, millidarcies	Oil Saturation, percent pore space	Effective Permeability to Liquid, millidarcies	Relative Permeability to Liquid, fraction	percent pore space	percent oil in place	
Well 142 / Rock Type: Chaotic / Facies: M3/M34											
E1-10	4638.8	12.5 (17.1)+	16.4								
				11.4	12.4	Gas Saturation Increasing 49.6	3.40*	0.274*	39.0	44.0	
				11.4	-	Gas Saturation Decreasing 98.2	13.5**	1.09**	-	-	
				1.8	12.4	Water Saturation Increasing 26.8	3.26***	0.263***	71.4	72.7	
				73.2	-	Water Saturation Decreasing 72.2	3.70**	0.298**	45.4	-	
Well 142 / Rock Type: Moldic / Facies: M37/M4											
E1-15	4644.6	25.9 (30.6)+	16.0								
				11.2	24.9	Gas Saturation Increasing 42.9	3.19*	0.128*	45.9	51.7	
				11.2	-	Gas Saturation Decreasing	9.46**	0.380**	42.5	99.1	
				11.2	9.0	Water Saturation Increasing 46.7	2.37***	0.263***	42.1	47.4	
				53.3	-	Water Saturation Decreasing 64.5	4.90**	0.545**	17.8	36.1	

## SUMMARY OF WATER-OIL RELATIVE PERMEABILITY TEST RESULTS

Well ID	Depth (ft)	Permeability (md)	Porosity (%)	Well 143 / Rock Type: Top / Facies: M2/M25				Well 143 / Rock Type: Chaotic / Facies: M3/M34			
				Water Saturation (%)	Oil Saturation (%)	Relative Permeability (fraction)	Oil Recovered (%)	Water Saturation (%)	Oil Saturation (%)	Relative Permeability (fraction)	Oil Recovered (%)
E1-3	4533.6	1.44 (2.5)*	10.2	10.2	3.0	Water Saturation Increasing	0.747**	0.249**	52.7	58.7	
				62.9	-	Water Saturation Decreasing	1.13*	0.378*	17.9	-	
Well 143 / Rock Type: Chaotic / Facies: M3/M34											
E1-7	4593.8	51.3 (63.3)*	18.4	10.9	54.7	Water Saturation Increasing	10.8**	0.197**	47.5	53.3	
				58.4	-	Water Saturation Decreasing	13.3*	0.244*	29.0	-	

\*Specific permeability to brine

\*\*To oil

\*\*\*To water

SUMMARY OF GAS-OIL AND WATER-OIL RELATIVE PERMEABILITY TEST RESULTSFina Oil and Chemical Company  
Well 142Rock Type: Chaotic  
Facies: M3/M34

Sample Depth, _I.D._ feet	Klinkenberg Permeability, _millidarcies_	Porosity, _percent_	Initial Conditions		Terminal Conditions		
			Water Saturation, percent pore space	Effective Permeability to Oil, _millidarcies_	Oil Saturation, percent pore space	Effective Permeability to Liquid, _fraction_	Oil Recovered, percent pore space _in place_
E1-10 4638.8	12.5 (17.1)+	16.4					
			Gas Saturation Increasing				
			11.4	12.4	49.6	3.40*	0.274* 39.0 44.0
			Gas Saturation Decreasing				
			11.4	-	98.2	13.5**	1.09** - -
			Water Saturation Increasing				
			1.8	12.4	26.8	3.26***	0.263*** 71.4 72.7
			Water Saturation Decreasing				
			73.2	-	72.2	3.70**	0.298** 45.4 -

+Specific permeability to brine

\*To gas

\*\*To oil

\*\*\*To water

GAS-OIL RELATIVE PERMEABILITY TEST RESULTS

Temperature: 98°F

Fina Oil and Chemical Company  
Emmons Unit  
Well 142  
M3/M34 Facies  
Chaotic Rock Type

Sample I.D.: E1-10  
Depth: 4638.8 feet  
Permeability to Air: 14.4 md  
Porosity: 16.4 percent  
Effective Permeability to Oil  
at Initial Water Saturation: 12.4 md

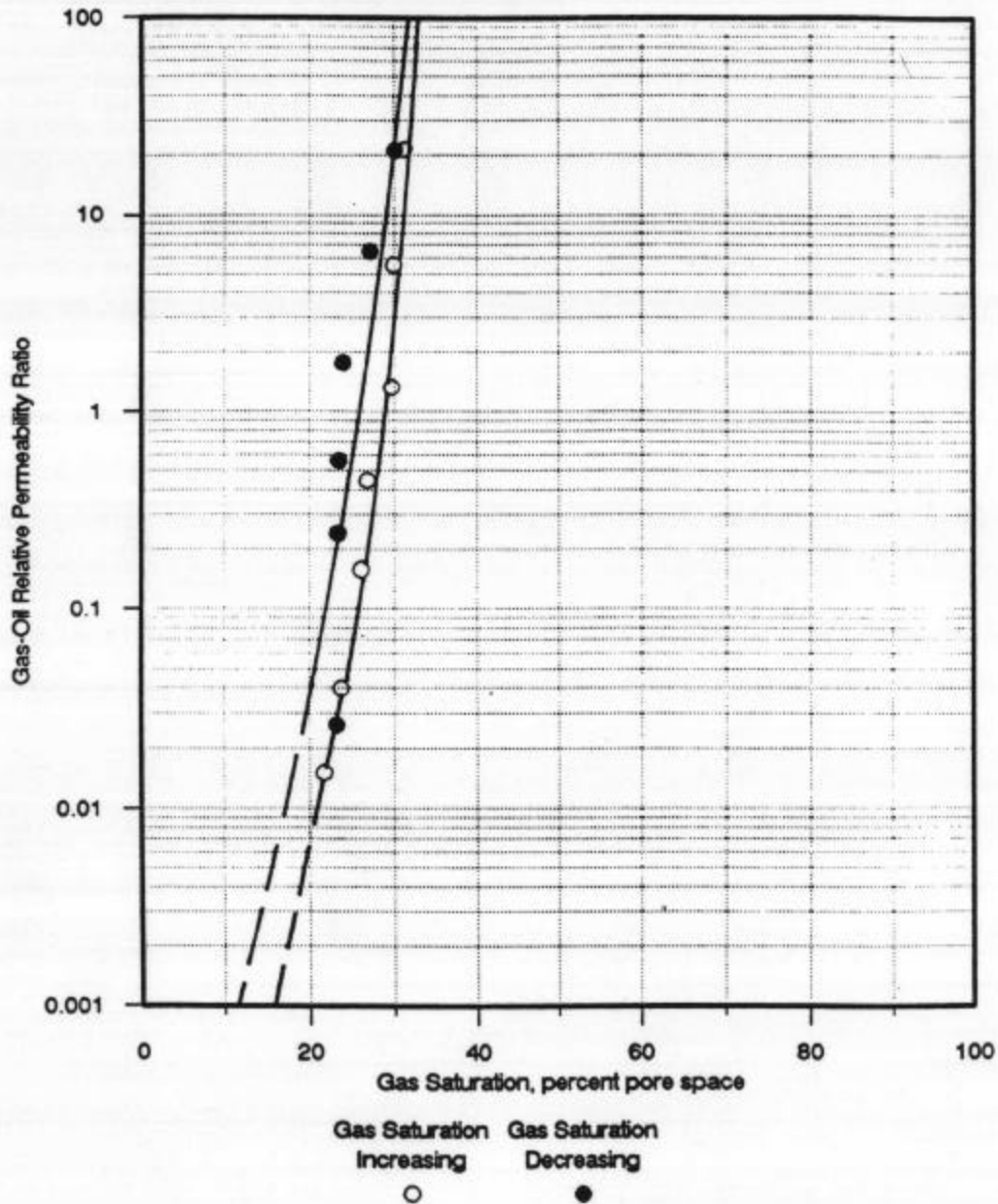
<u>Gas Saturation, percent pore space</u>	<u>Gas-Oil Relative Permeability Ratio</u>	<u>Relative Permeability to Gas,* fraction</u>	<u>Relative Permeability to Oil,* fraction</u>
0.0	0.000	0.000	1.000
21.7	0.015	0.0052	0.355
23.7	0.040	0.0095	0.236
26.1	0.158	0.020	0.124
26.8	0.446	0.039	0.088
29.7	1.32	0.071	0.054
29.9	5.56	0.190	0.034
31.2	21.5	0.204	0.010
32.8	106	0.223	0.0021
39.0	-	0.274	-
33.3	106	0.234	0.0022
30.1	21.1	0.186	0.0088
27.2	6.53	0.141	0.022
24.0	1.75	0.094	0.054
23.5	0.562	0.050	0.089
23.4	0.242	0.036	0.149
23.2	0.026	0.0062	0.238
-7.3			1.09

\* Relative to the Effective Permeability to Oil at Initial Water Saturation

**STEADY - STATE GAS - OIL RELATIVE PERMEABILITY**

Sample I.D.: E1-10

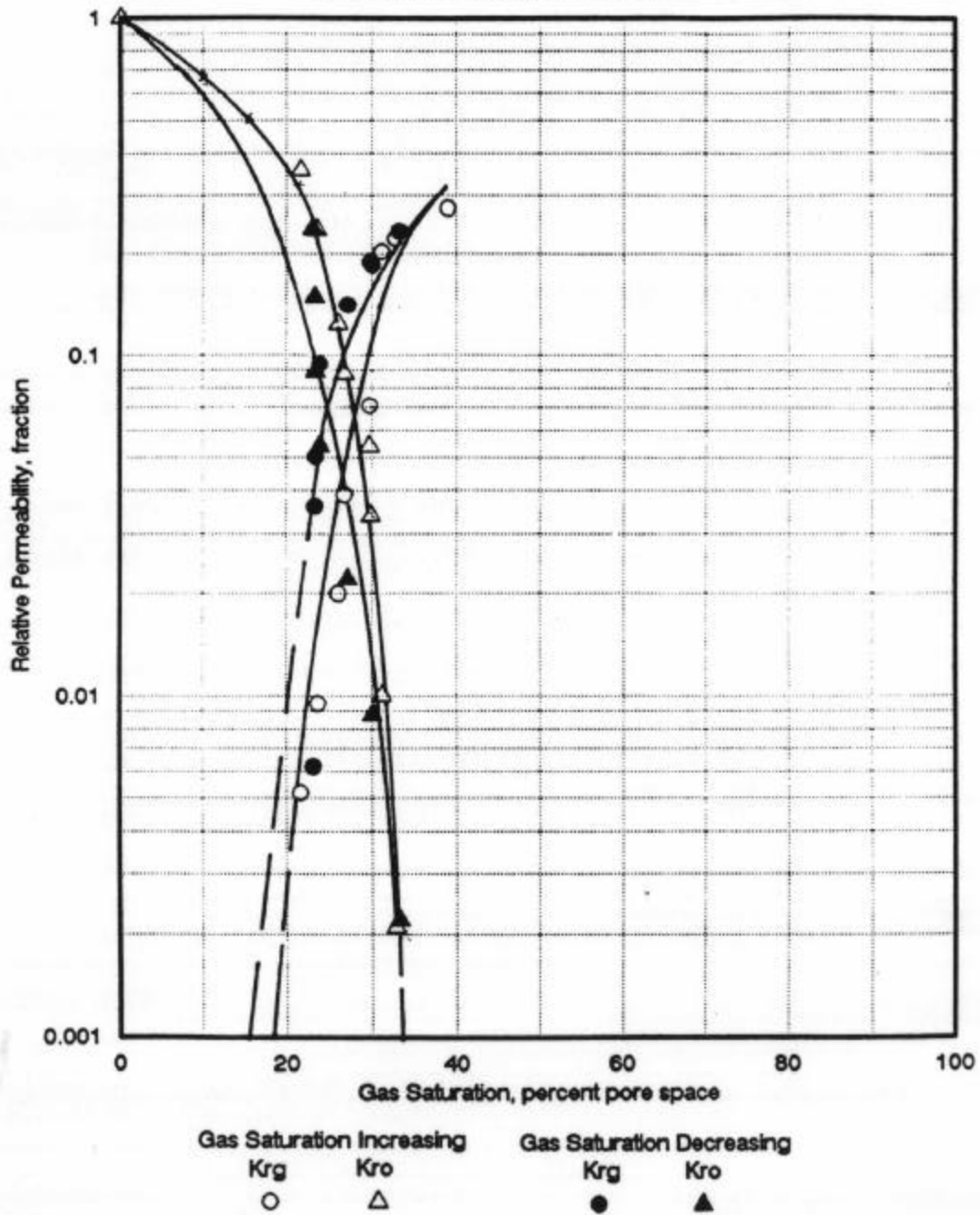
Klinkenberg Permeability: 12.5 md



**STEADY-STATE GAS - OIL RELATIVE PERMEABILITY**

Sample I.D.: E1-10

Kirkenberg Permeability: 12.5 md



GAS-OIL RELATIVE PERMEABILITY TEST RESULTS

Temperature: 72°F

Fina Oil and Chemical Company  
Emmons Unit  
Well 142  
M3/M34 Facies  
Chaotic Rock Type

Sample I.D.: El-10  
Depth: 4638.8 feet  
Permeability to Air: 14.4 md  
Porosity: 16.4 percent  
Specific Permeability to Oil: 10.6 md

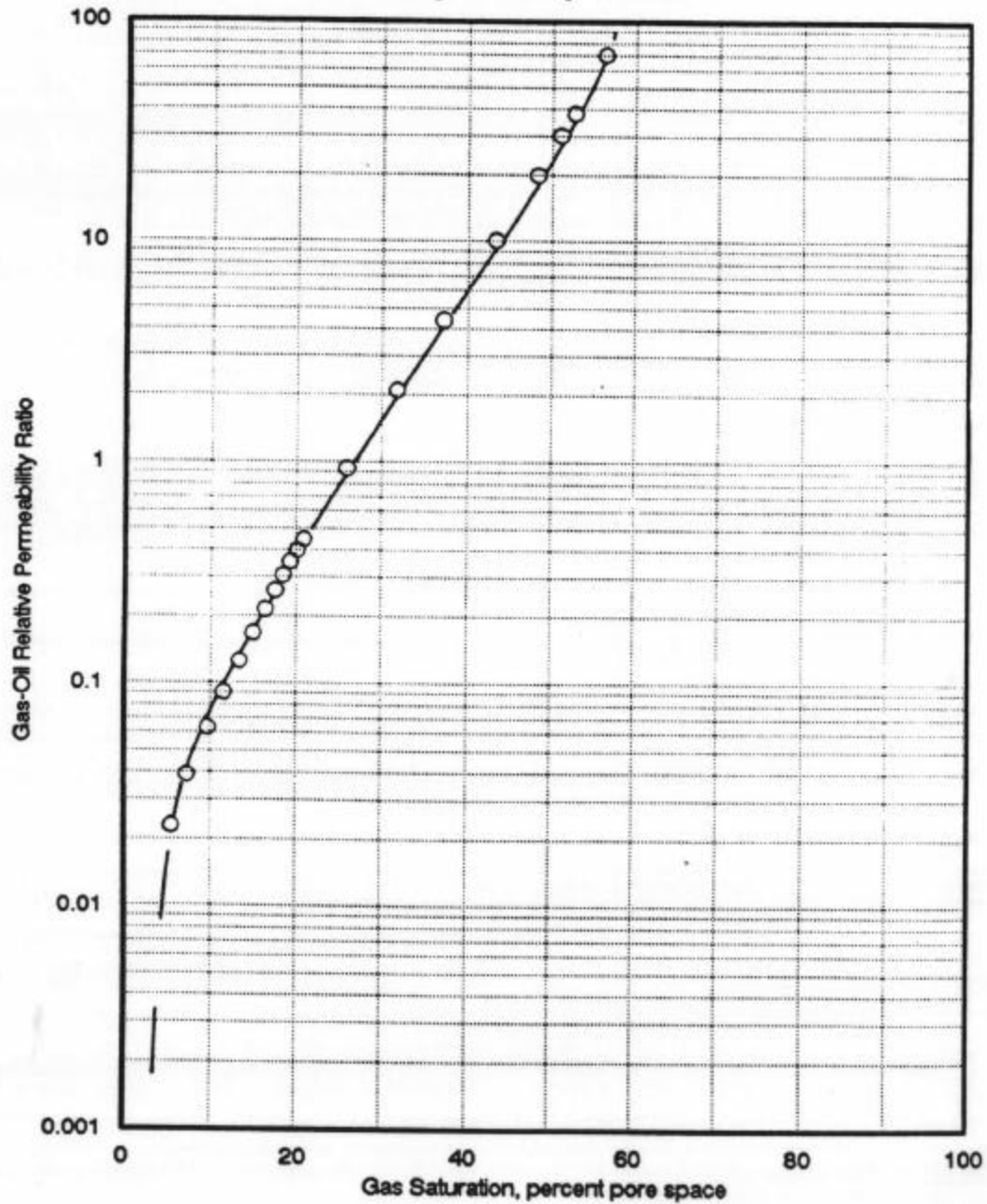
<u>Gas Saturation, percent pore space</u>	<u>Gas-Oil Relative Permeability Ratio</u>	<u>Relative Permeability to Gas,* fraction</u>	<u>Relative Permeability to Oil,* fraction</u>
0.0	0.000	0.0000	1.000
5.5	0.023	0.0150	0.660
7.3	0.039	0.0230	0.590
9.7	0.063	0.031	0.492
11.6	0.091	0.039	0.429
13.4	0.126	0.046	0.365
15.0	0.168	0.054	0.321
16.4	0.215	0.061	0.284
17.6	0.262	0.068	0.260
18.5	0.307	0.075	0.244
19.4	0.353	0.081	0.229
20.2	0.399	0.088	0.221
21.0	0.447	0.093	0.208
26.0	0.936	0.130	0.139
31.8	2.10	0.175	0.083
37.2	4.390	0.224	0.051
43.3	10.100	0.287	0.028
48.3	20.000	0.349	0.017
51.1	30.400	0.388	0.013
52.7	38.00	0.408	0.011
56.4	70.50	0.445	0.0063
61.8		0.533	

\* Relative to the Effective Permeability to Oil at Initial Water Saturation

**UNSTEADY - STATE GAS - OIL RELATIVE PERMEABILITY**

Sample I.D.: E1-10

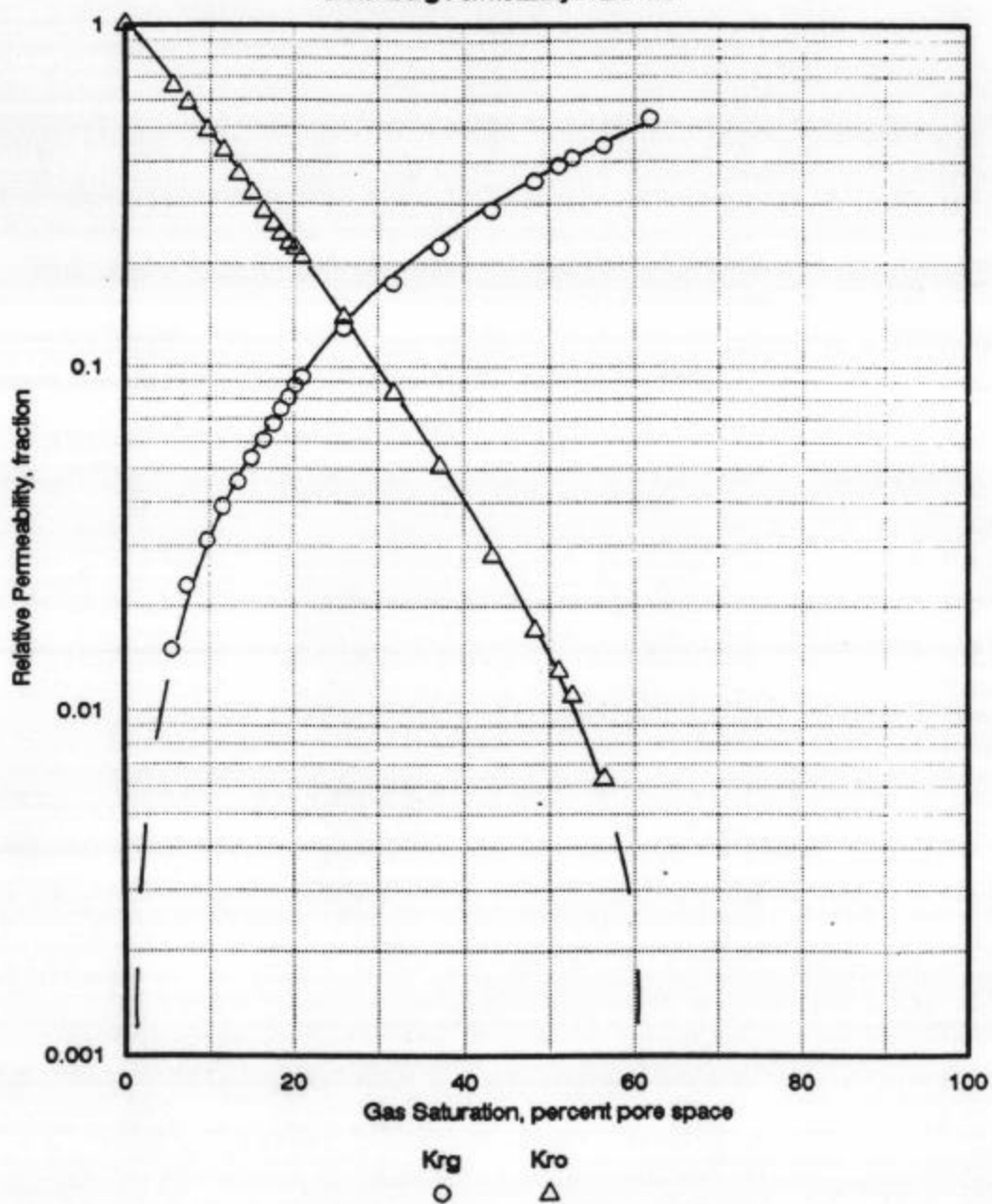
Kinkenberg Permeability: 12.5 md



**UNSTEADY-STATE GAS - OIL RELATIVE PERMEABILITY**

Sample I.D.: E1-10

Klinkenberg Permeability: 12.5 md





WATER-OIL RELATIVE PERMEABILITY TEST RESULTS

Temperature: 98°F

Fina Oil and Chemical Company  
Emmons Unit  
Well 142  
M3/M34 Facies  
percent  
Chaotic Rock Type

Sample I.D.: E1-10  
Depth: 4638.8 feet  
Permeability to Air: 14.4 md  
Porosity: 16.4

Effective Permeability to Oil  
at Initial Water Saturation: 12.4 md

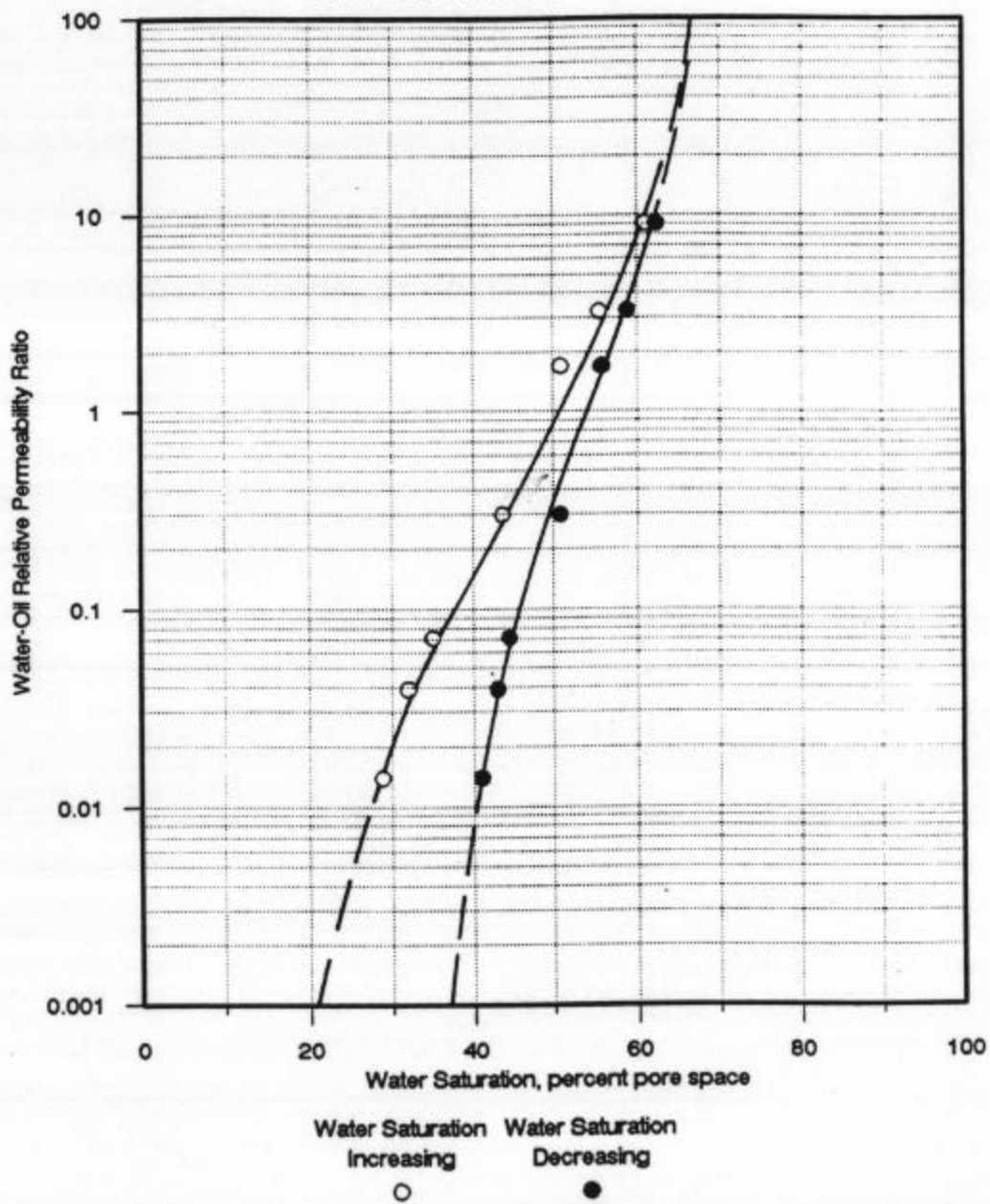
<u>Water Saturation, percent pore space</u>	<u>Water-Oil Relative Permeability Ratio</u>	<u>Relative Permeability to Water,* fraction</u>	<u>Relative Permeability to Oil,* fraction</u>
1.8	0.000	0.0000	1.000
28.8	0.014	0.0077	0.534
32.0	0.039	0.020	0.510
34.9	0.071	0.025	0.354
43.6	0.299	0.073	0.244
50.9	1.69	0.147	0.087
55.5	3.23	0.155	0.048
61.0	9.05	0.181	0.020
73.2	-	0.263	-
62.4	9.08	0.108	0.012
58.9	3.26	0.075	0.023
55.8	1.69	0.061	0.036
50.8	0.299	0.029	0.097
44.5	0.071	0.0097	0.137
43.0	0.039	0.0059	0.150
41.0	0.014	0.0025	0.175
27.8	-	-	0.298

\* Relative to the Effective Permeability to Oil at Initial Water Saturation

**STEADY - STATE WATER - OIL RELATIVE PERMEABILITY**

Sample I.D.: E1-10

Kinkenberg Permeability: 12.5 md

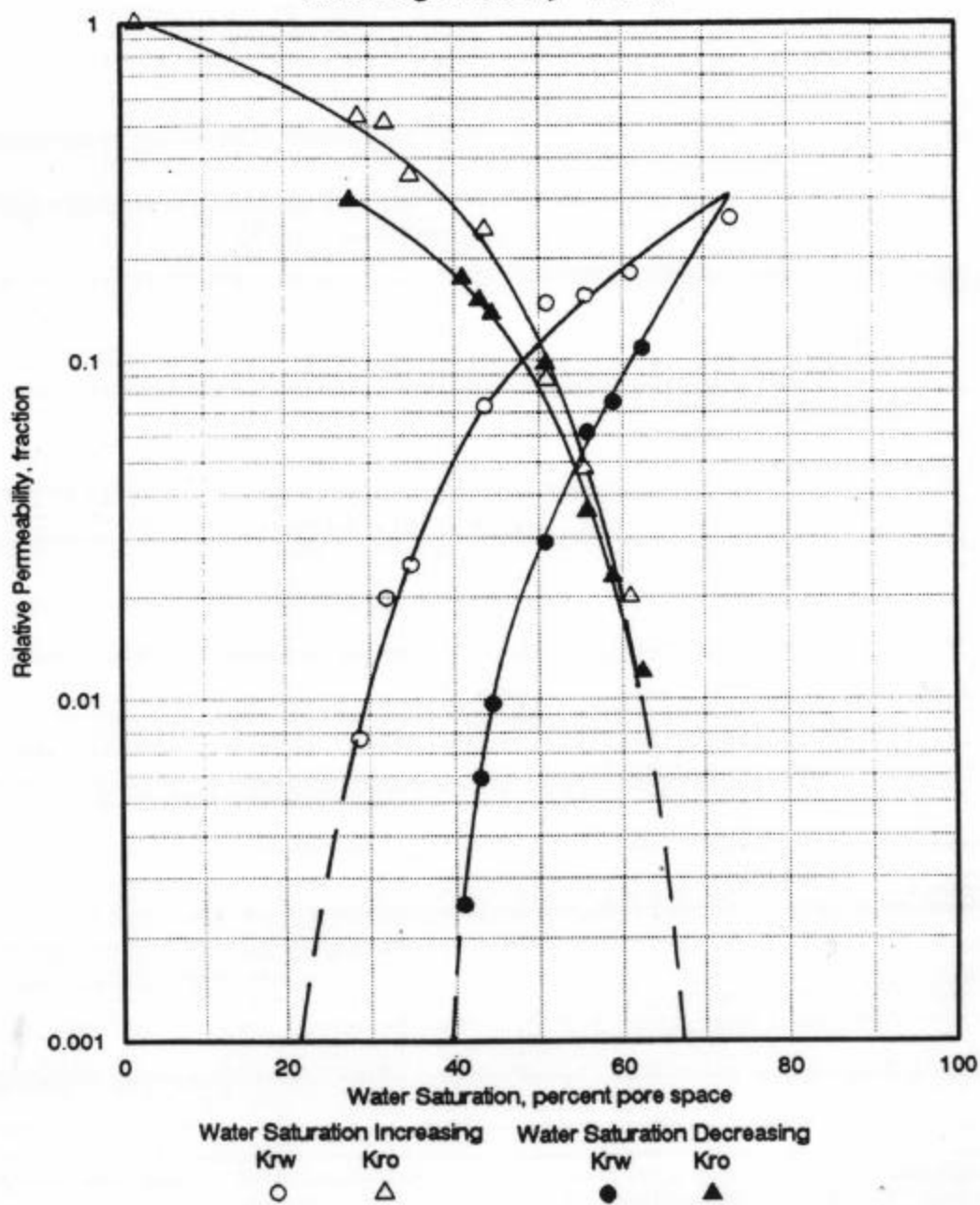


3-10

**STEADY-STATE WATER - OIL RELATIVE PERMEABILITY**

Sample I.D.: E1-10

Klinkenberg Permeability: 12.5 md



SUMMARY OF GAS-OIL AND WATER-OIL RELATIVE PERMEABILITY TEST RESULTSFina Oil and Chemical Company  
Well 142Rock Type: Moldic  
Facies: M37/M4

Sample Depth, I.D. feet	Klinkenberg Permeability, millidarcies	Porosity, percent	Initial Conditions		Terminal Conditions			Oil Recovered, percent oil pore space in place
			Water Saturation, percent pore space	Effective Permeability to Oil, millidarcies	Oil Saturation, percent pore space	Effective Permeability to Liquid, millidarcies	Relative Permeability to Liquid, fraction	
E1-15	4644.6	25.9 (30.6)+	16.0					
					Gas Saturation Increasing			
			11.2	24.9	42.9	3.19*	0.128*	45.9
					Gas Saturation Decreasing			51.7
			11.2	-	-	9.46**	0.380**	42.5
					Water Saturation Increasing			99.1
			11.2	9.0	46.7	2.37***	0.263***	42.1
					Water Saturation Decreasing			47.4
			53.3	-	64.5	4.90**	0.545**	17.8
								38.1

+Specific permeability to brine

\*To gas

\*\*To oil

\*\*\*To water

GAS-OIL RELATIVE PERMEABILITY TEST RESULTS

Temperature: 98°F

Fina Oil and Chemical Company  
Emmons Unit  
Well 142  
M37/M4 Facies  
Moldic Rock Type

Sample I.D.: E1-15  
Depth: 4644.6 feet  
Permeability to Air: 27.9 md  
Porosity: 16.0 percent  
Effective Permeability to Oil  
at Initial Water Saturation: 24.9 md

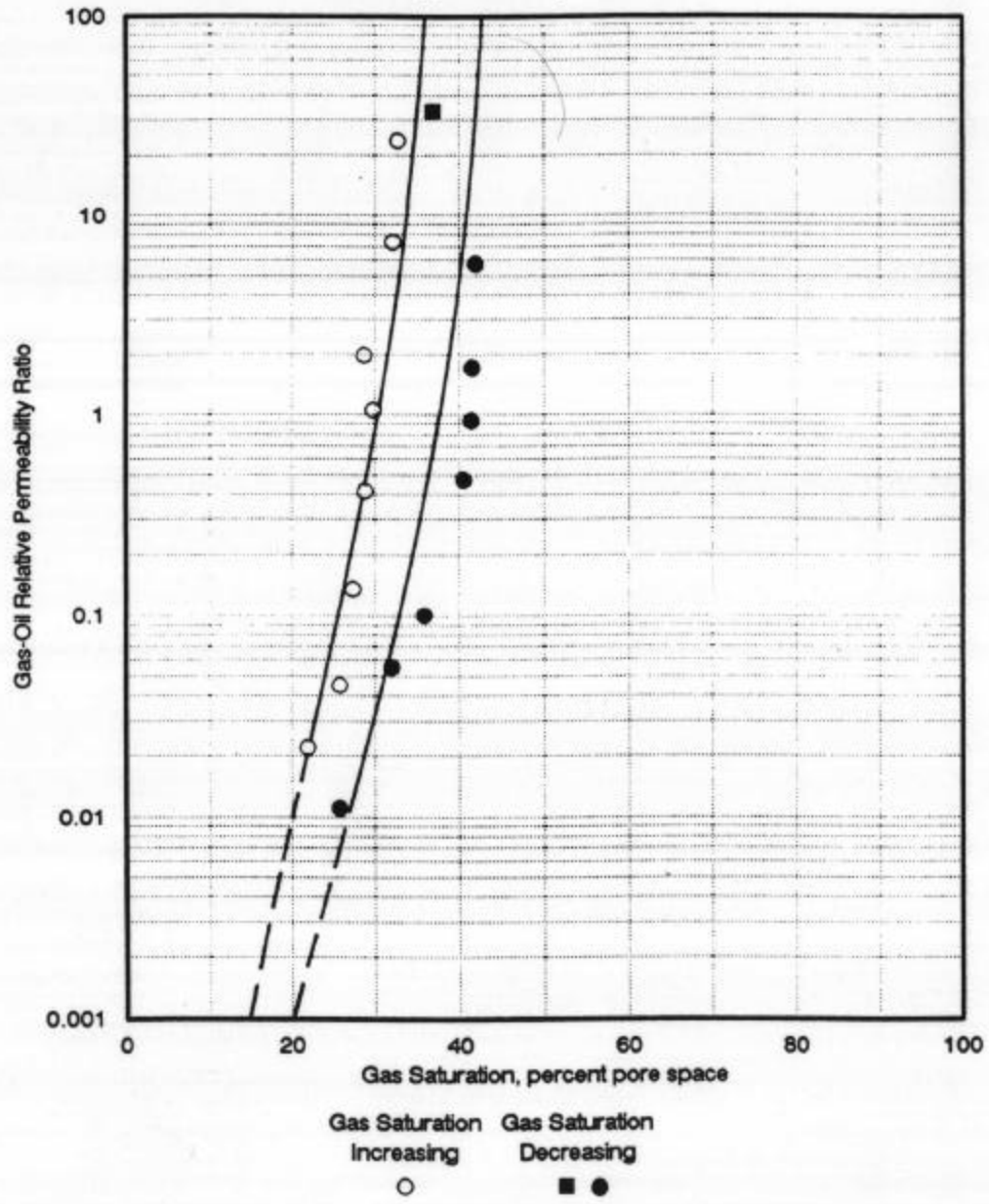
<u>Gas Saturation, percent pore space</u>	<u>Gas-Oil Relative Permeability Ratio</u>	<u>Relative Permeability to Gas,* fraction</u>	<u>Relative Permeability to Oil,* fraction</u>
0.0	0.000	0.0000	1.000
21.9	0.022	0.0091	0.407
25.8	0.045	0.013	0.285
27.4	0.135	0.025	0.182
28.8	0.414	0.042	0.101
29.8	1.06	0.070	0.066
28.7	1.98	0.055	0.028
32.1	7.38	0.066	0.0090
32.7	23.7	0.090	0.0038
36.4	115	0.115	0.0010
45.9		0.128	
38.9	163	0.070	0.00043
36.9	33.2	0.063	0.0019
Restart After Power Failure			
48.2	-	0.090	-
41.9	5.71	0.036	0.0063
41.5	1.72	0.031	0.018
41.4	0.935	0.029	0.031
40.5	0.471	0.024	0.051
35.9	0.100	0.011	0.110
32.0	0.055	0.0088	0.160
25.8	0.011	0.0033	0.290
3.4			0.380

\* Relative to the Effective Permeability to Oil at Initial Water Saturation

**STEADY - STATE GAS - OIL RELATIVE PERMEABILITY**

Sample I.D.: E1-15

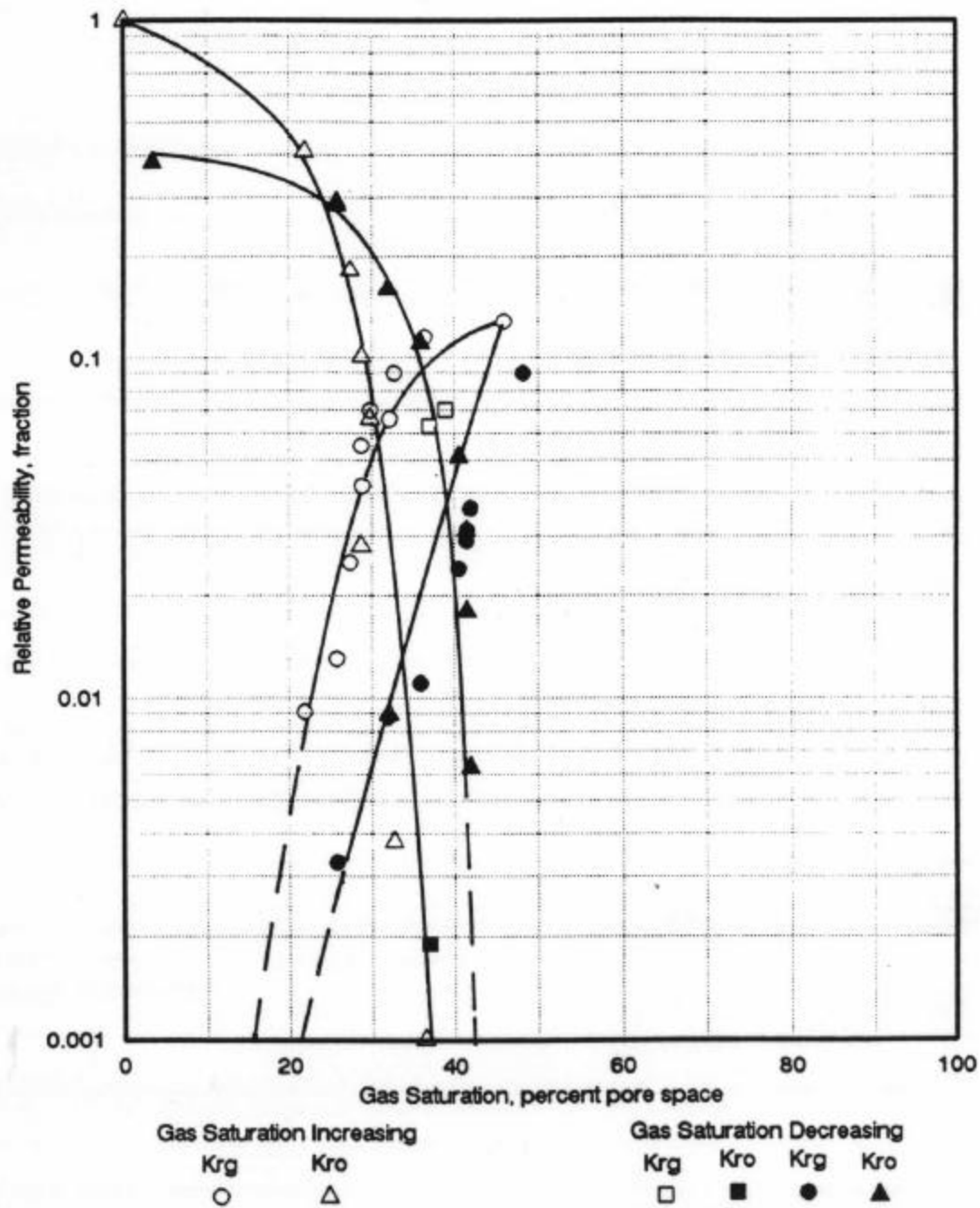
Klinkenberg Permeability: 25.9 md



# STEADY-STATE GAS - OIL RELATIVE PERMEABILITY

Sample I.D.: E1-15

Klinkenberg Permeability: 25.9 md



GAS-OIL RELATIVE PERMEABILITY TEST RESULTS

Temperature: 72°F

Fina Oil and Chemical Company  
Emmons Unit  
Well 142  
M37/M4 Facies  
Moldic Rock Type

Sample I.D.: E1-15  
Depth: 4644.6 feet  
Permeability to Air: 27.7 md  
Porosity: 15.9 percent  
Specific Permeability to Oil: 23.2 md

<u>Gas Saturation, percent pore space</u>	<u>Gas-Oil Relative Permeability Ratio</u>	<u>Relative Permeability to Gas,* fraction</u>	<u>Relative Permeability to Oil,* fraction</u>
0.0	0.000	0.0000	1.000
4.2	0.007	0.0048	0.690
5.5	0.013	0.0077	0.608
7.2	0.023	0.012	0.524
8.8	0.039	0.018	0.461
10.3	0.060	0.024	0.403
11.5	0.082	0.030	0.364
12.6	0.110	0.037	0.335
13.5	0.137	0.042	0.307
14.5	0.177	0.050	0.283
16.6	0.280	0.068	0.243
19.2	0.449	0.088	0.196
22.2	0.747	0.112	0.150
26.2	1.37	0.150	0.109
31.8	2.87	0.199	0.069
36.9	5.63	0.260	0.046
40.7	9.30	0.305	0.033
42.5	12.2	0.329	0.027
44.4	15.6	0.357	0.023
48.2	26.6	0.402	0.015
50.2	38.3	0.437	0.011
51.4	46.7	0.448	0.0096
58.9		0.547	

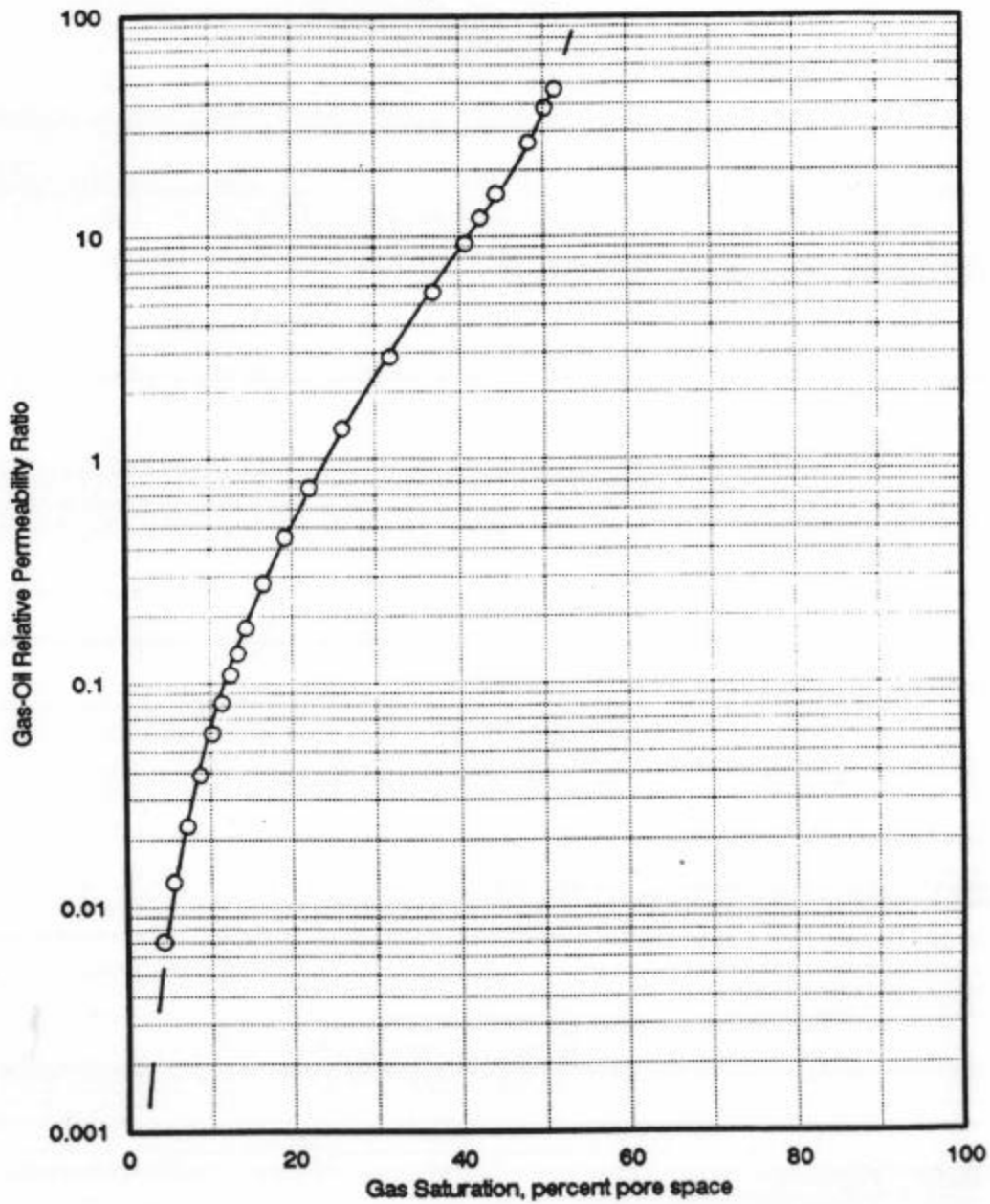
\* Relative to the Effective Permeability to Oil at Initial Water Saturation



**UNSTEADY - STATE GAS - OIL RELATIVE PERMEABILITY**

Sample I.D.: E1-15

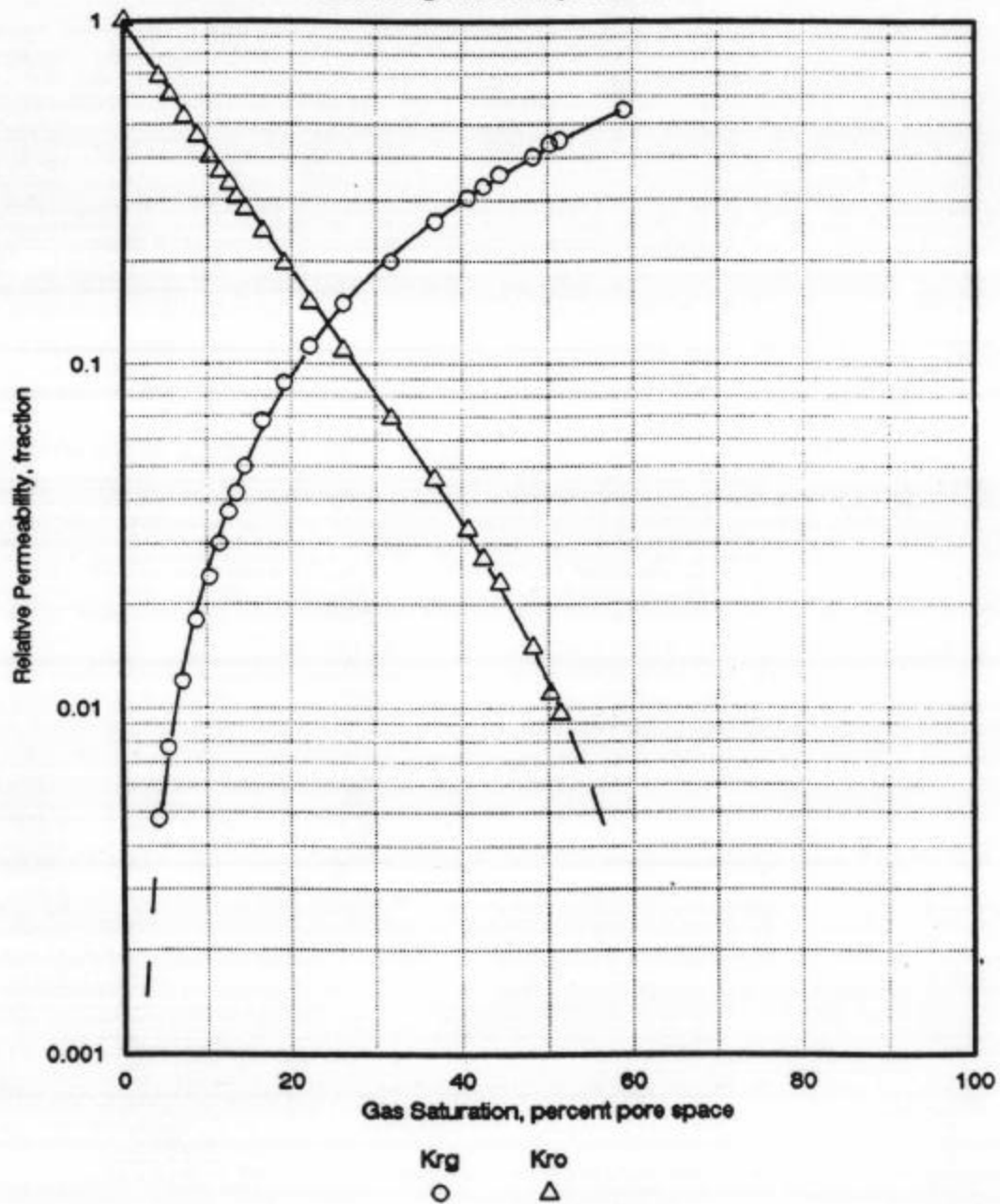
Klinkenberg Permeability: 25.9 md



**UNSTEADY-STATE GAS - OIL RELATIVE PERMEABILITY**

Sample I.D.: E1-15

Klinkenberg Permeability: 25.9 md



WATER-OIL RELATIVE PERMEABILITY TEST RESULTS

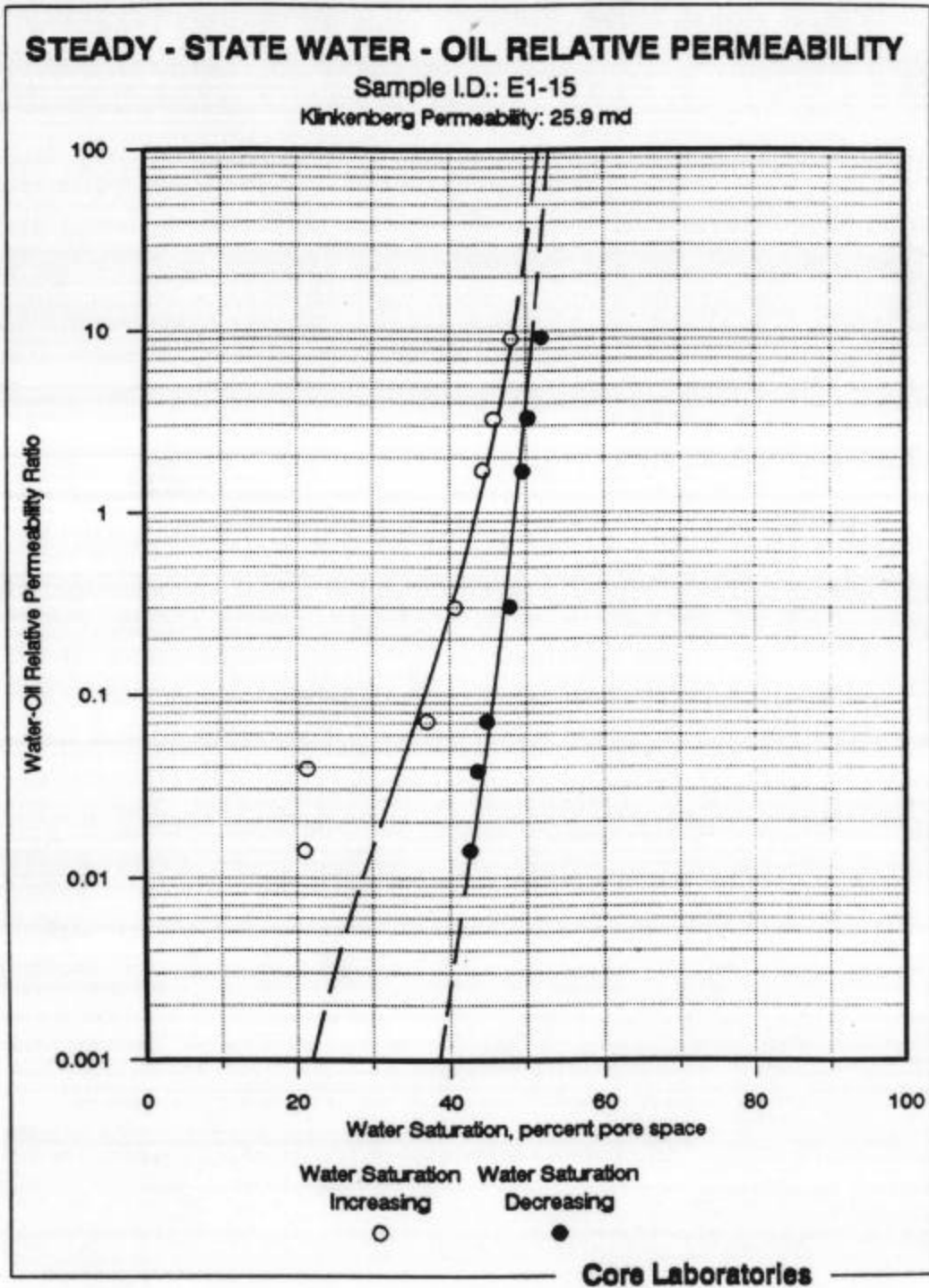
Temperature: 98°F

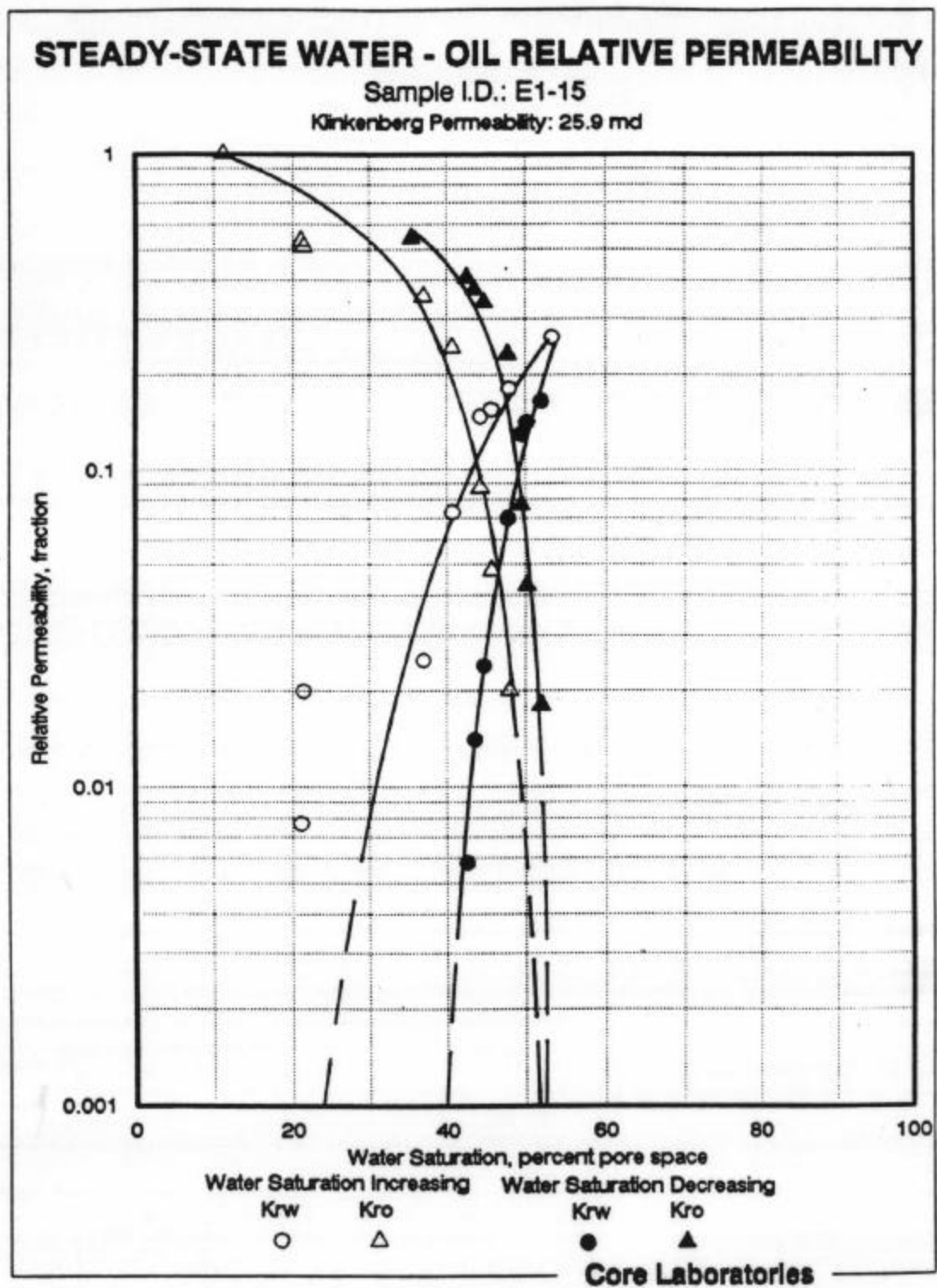
Fina Oil and Chemical Company  
Emmons Unit  
Well 142  
M37/M4 Facies  
Moldic Rock Type

Sample I.D.: E1-15  
Depth: 4644.6 feet  
Permeability to Air: 27.9 md  
Porosity: 16.0 percent  
Effective Permeability to Oil  
at Initial Water Saturation: 9.0 md

<u>Water Saturation, percent pore space</u>	<u>Water-Oil Relative Permeability Ratio</u>	<u>Relative Permeability to Water,* fraction</u>	<u>Relative Permeability to Oil,* fraction</u>
11.2	0.000	0.0000	1.000
21.1	0.014	0.0077	0.534
21.4	0.039	0.020	0.510
37.0	0.071	0.025	0.354
40.7	0.299	0.073	0.244
44.3	1.69	0.147	0.087
45.7	3.23	0.155	0.048
48.0	9.05	0.181	0.020
53.3	-	0.263	-
52.0	9.17	0.165	0.018
50.2	3.28	0.141	0.043
49.5	1.68	0.129	0.077
47.8	0.302	0.070	0.232
44.8	0.071	0.024	0.339
43.6	0.038	0.014	0.371

\* Relative to the Effective Permeability to Oil at Initial Water Saturation





SUMMARY OF WATER-OIL RELATIVE PERMEABILITY TEST RESULTS

Fina Oil and Chemical Company  
Well 143

Rock Type: Top  
Facies: M2/M25

Sample I.D.	Depth, feet	Klinkenberg Permeability, millidarcies	Porosity, percent	Initial Conditions		Terminal Conditions			Oil Recovered, percent pore space in place
				Water Saturation, percent pore space	Effective Permeability to Oil, millidarcies	Oil Saturation, percent pore space	Effective Permeability to Liquid, millidarcies	Relative Permeability to Liquid, fraction	
E1-3	4533.6	1.44	(2.5) + 10.2						
Water Saturation Increasing									
				10.2	3.0	37.1	0.747**	0.249**	52.7
									58.7
Water Saturation Decreasing									
				62.9	-	55.0	1.13*	0.378*	17.9
									-

+Specific permeability to brine  
\*To oil  
\*\*To water

WATER-OIL RELATIVE PERMEABILITY TEST RESULTS

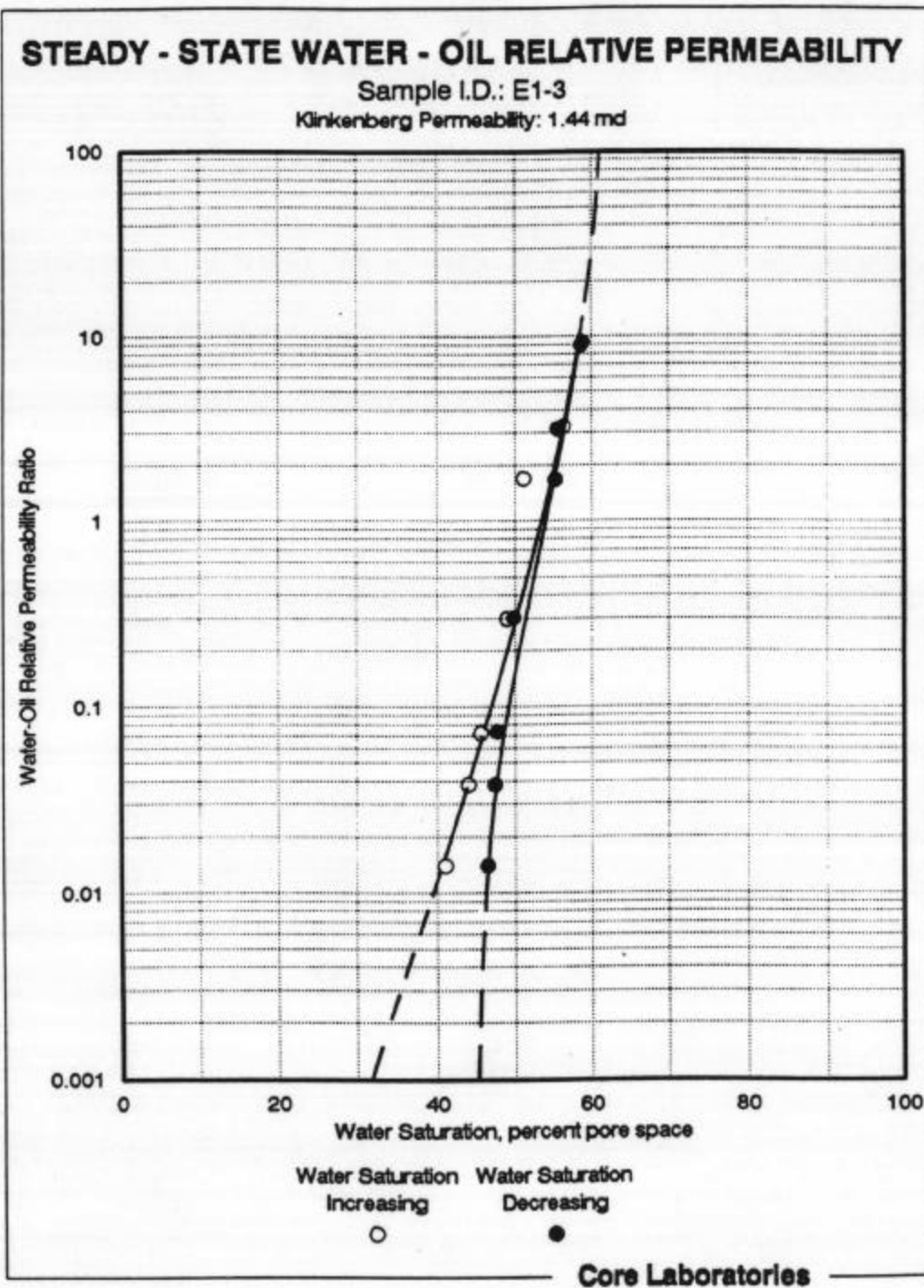
Temperature: 98°F

Fina Oil and Chemical Company  
Emmons Unit  
Well 143  
M2/M25 Facies  
Top Rock Type

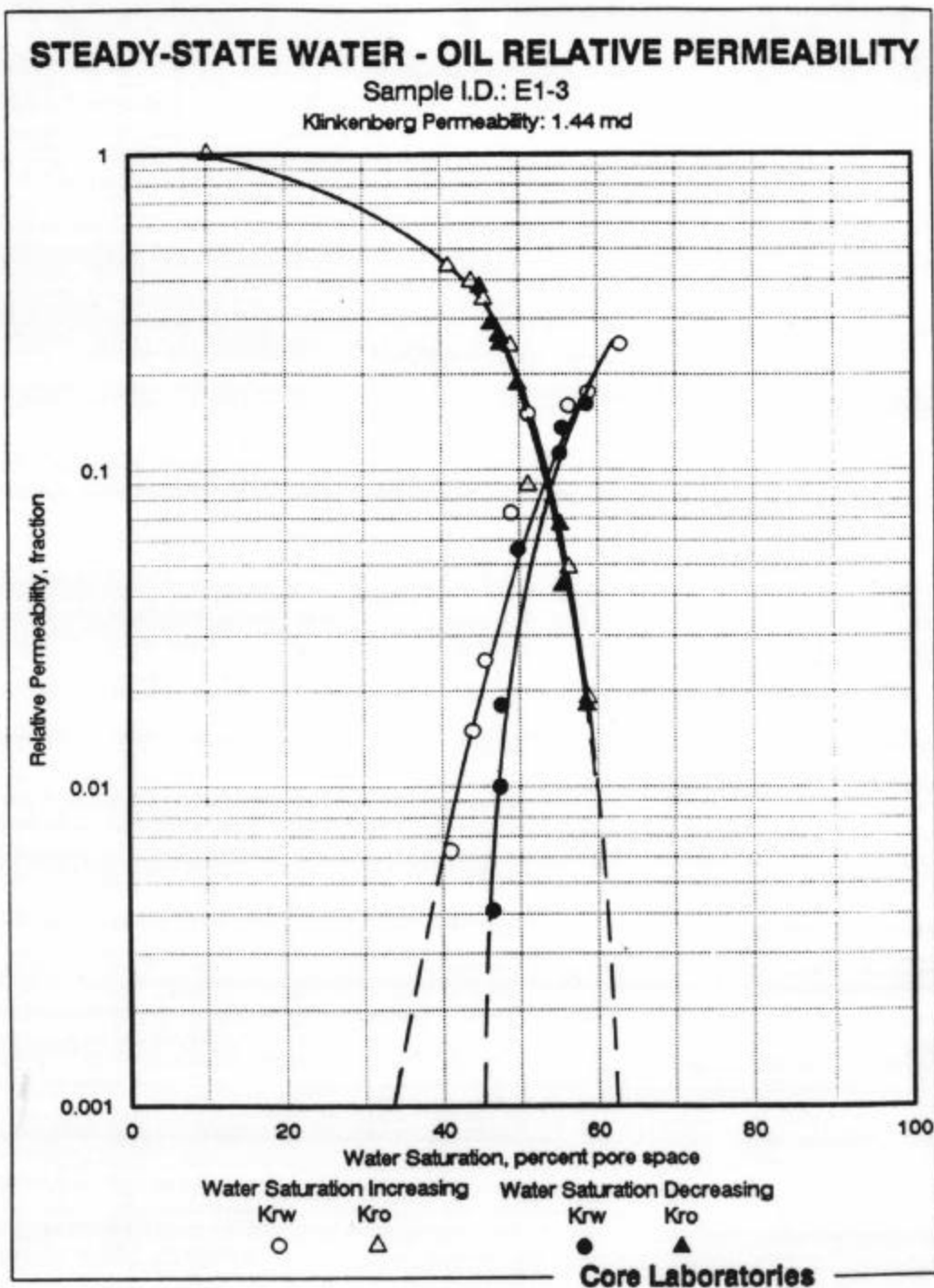
Sample I.D.: E1-3  
Depth: 4533.6 feet  
Permeability to Air: 1.66 md  
Porosity: 10.2 percent  
Effective Permeability to Oil  
at Initial Water Saturation: 3.0 md

<u>Water Saturation, percent pore space</u>	<u>Water-Oil Relative Permeability Ratio</u>	<u>Relative Permeability to Water,* fraction</u>	<u>Relative Permeability to Oil,* fraction</u>
10.2	0.000	0.0000	1.000
41.0	0.014	0.0063	0.442
43.9	0.038	0.015	0.394
45.5	0.072	0.025	0.347
48.9	0.298	0.073	0.245
51.1	1.69	0.150	0.089
56.3	3.24	0.159	0.049
58.8	9.21	0.175	0.019
62.9	-	0.249	-
58.6	8.94	0.161	0.018
55.5	3.14	0.135	0.043
55.2	1.67	0.112	0.067
49.8	0.301	0.056	0.186
47.6	0.073	0.018	0.248
47.4	0.038	0.010	0.264
46.4	0.014	0.0041	0.288
45.0	-	-	0.378

\* Relative to the Effective Permeability to Oil at Initial Water Saturation







3-25

SUMMARY OF WATER-OIL RELATIVE PERMEABILITY TEST RESULTSFina Oil and Chemical Company  
Well 143Rock Type: Chaotic  
Facies: M3/M34

Sample Depth, I.D. feet	Klinkenberg Permeability, millidarcies	Porosity, percent	Initial Conditions		Terminal Conditions		
			Water Saturation, percent	Effective Permeability to Oil, millidarcies	Oil Saturation, percent	Effective Permeability to Liquid, millidarcies	Relative Permeability to Liquid, fraction
E1-7	4593.8	51.3 (63.3)+	18.4				
Water Saturation Increasing							
			10.9	54.7	41.6	10.8**	0.197**
							47.5
							53.3
Water Saturation Decreasing							
			58.4	-	70.6	13.3*	0.244*
							29.0
							-

+Specific permeability to brine

\*To oil

\*\*To water

WATER-OIL RELATIVE PERMEABILITY TEST RESULTS

Temperature: 98°F

Fina Oil and Chemical Company  
Emmons Unit  
Well 143  
M3/M34 Facies  
Chaotic Rock Type

Sample I.D.: E1-7  
Depth: 4593.8 feet  
Permeability to Air: 55.6 md  
Porosity: 18.4 percent  
Effective Permeability to Oil  
at Initial Water Saturation: 54.7 md

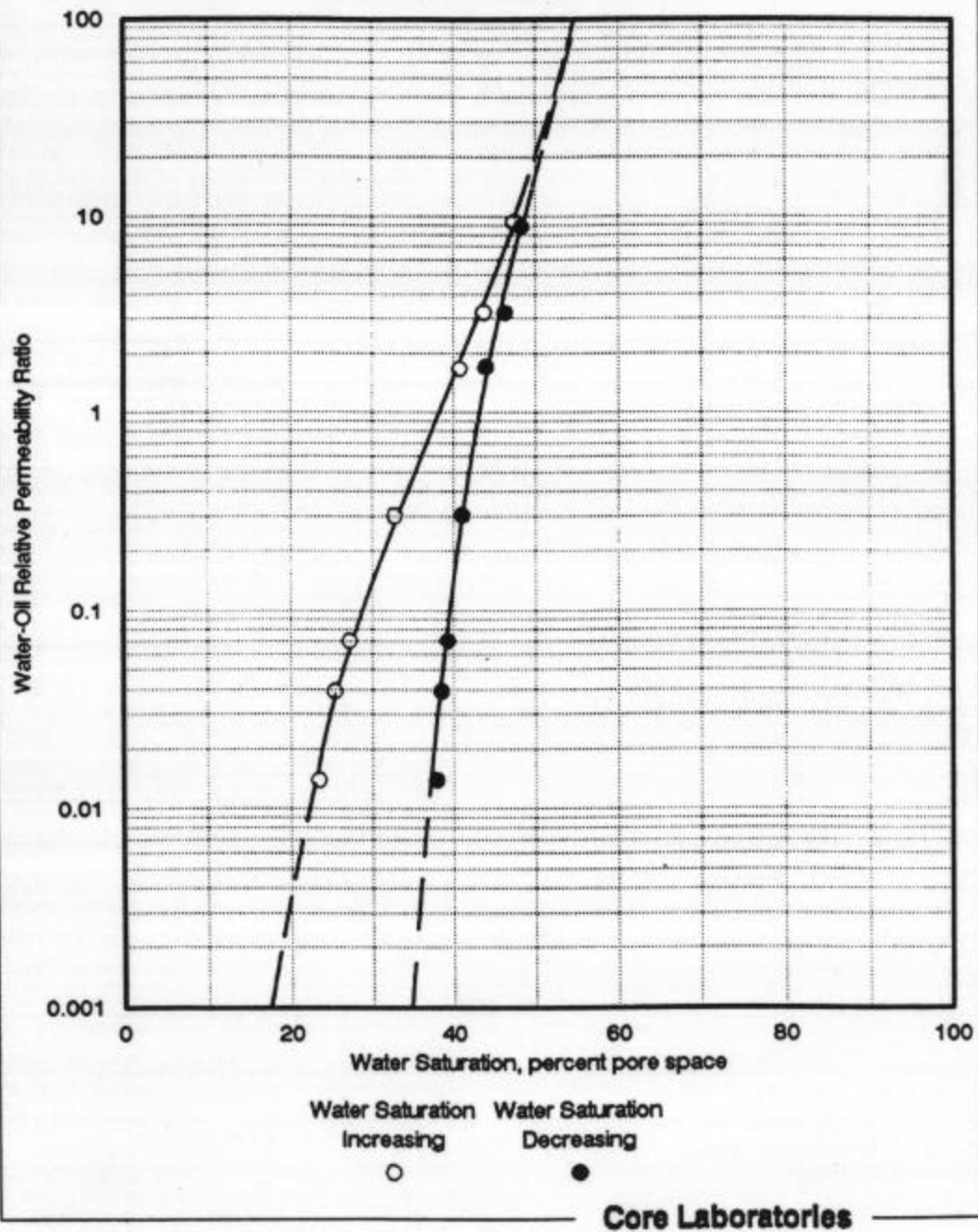
<u>Water Saturation, percent pore space</u>	<u>Water-Oil Relative Permeability Ratio</u>	<u>Relative Permeability to Water,* fraction</u>	<u>Relative Permeability to Oil,* fraction</u>
10.9	0.000	0.0000	1.000
23.4	0.014	0.0046	0.323
25.3	0.039	0.011	0.271
27.1	0.070	0.016	0.227
32.7	0.302	0.039	0.129
40.8	1.67	0.085	0.051
43.7	3.22	0.103	0.032
47.4	9.38	0.122	0.013
58.4	-	0.197	-
48.3	8.82	0.097	0.011
46.3	3.20	0.080	0.025
44.0	1.70	0.063	0.037
41.1	0.303	0.030	0.099
39.3	0.070	0.0093	0.132
38.5	0.039	0.0055	0.140
37.9	0.014	0.0022	0.153
29.4	-	-	0.244

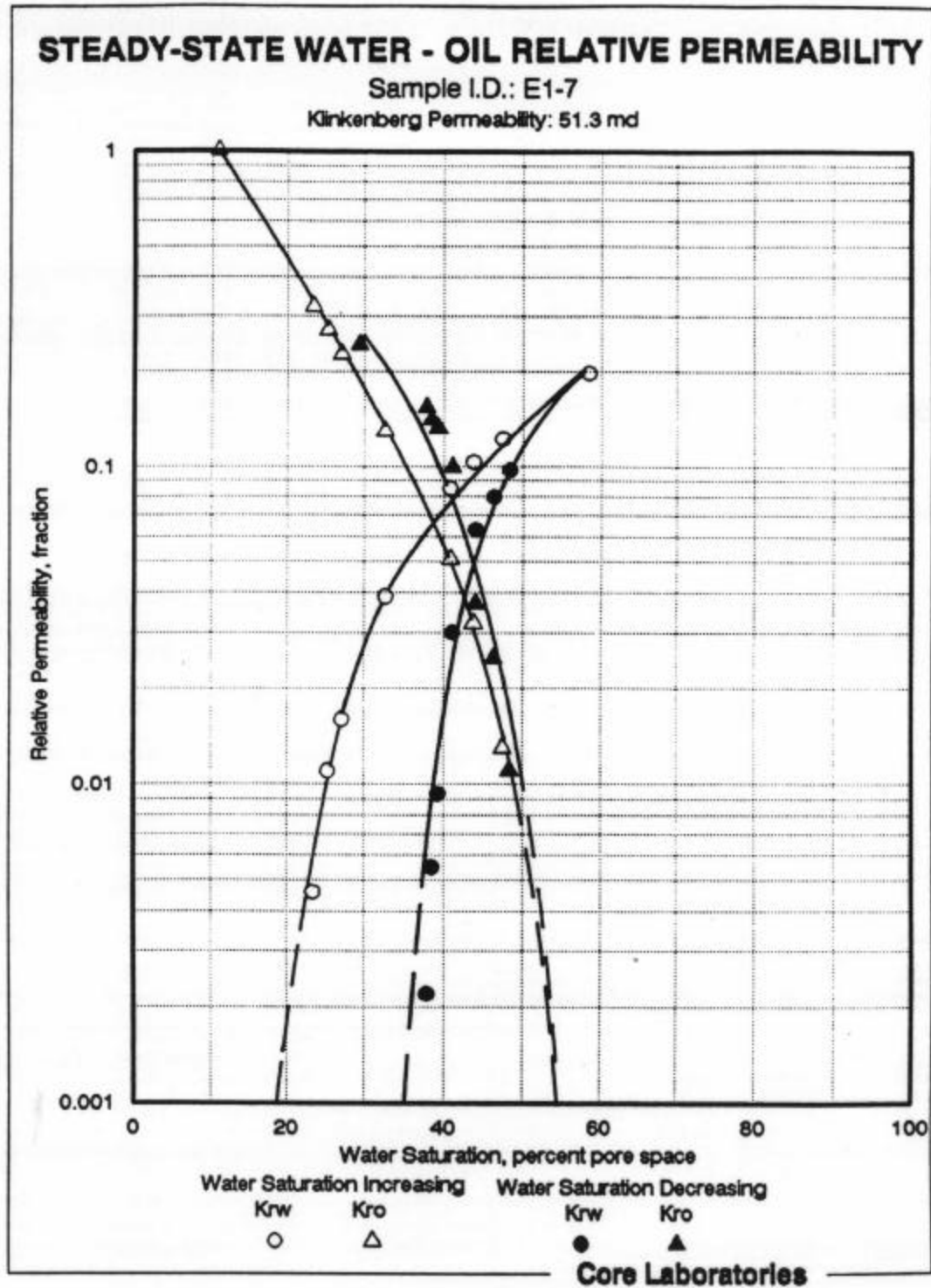
\* Relative to the Effective Permeability to Oil at Initial Water Saturation

**STEADY - STATE WATER - OIL RELATIVE PERMEABILITY**

Sample I.D.: E1-7

Klinkenberg Permeability: 51.3 md





## **SECTION 4**

### **Tertiary Oil Recovery Test Results**

## SUMMARY OF TERTIARY OIL RECOVERY TEST RESULTS

Fina Oil and Chemical Company

Sample I.D.	Depth, feet	Klinkenberg Permeability, millidarcies	Porosity, percent	Initial Conditions			Terminal Conditions			Oil Recovered, percent pore space in place				
				Saturation, percent pore space	Effective Permeability to Oil, millidarcies	Relative Permeability to Liquid, fraction	Saturation, percent pore space	Effective Permeability to Liquid, millidarcies						
									Gas		Water	Oil	Gas	Water
Well 143 / Rock Type: Top / Facies: M3/M25														
E1-1	4532.8	1.76	8.9	0.0	8.3	91.7	1.15	Waterflood 0.0	57.9	40.3	0.736**	0.639**	51.4	56.1
				0.0	59.7	40.3	-	Gasflood 52.1	40.8	7.1	0.106*	0.092*	33.2	82.4
Well 143 / Rock Type: Chaotic / Facies: M3/M34														
E1-6	4590.6	21.8	24.1	0.0	17.7	82.3	18.5	Waterflood 0.0	62.1	37.9	6.83**	0.369**	44.4	54.0
				0.0	62.1	37.9	-	Gasflood 52.3	31.8	15.8	2.45*	0.132*	22.1	58.3
Well 142 / Rock Type: Chaotic / Facies: M3/M34														
E1-11	4638.9	13.9	15.8	0.0	7.6	92.4	8.05	Waterflood 0.0	57.2	42.8	3.02**	0.427**	49.6	53.7
				0.0	57.2	42.8	-	Gasflood 48.2	35.1	16.7	1.37*	0.170*	26.1	61.0
Well 143 / Rock Type: Moldic / Facies: M37/M4														
E1-14	4644.5	56.2	17.8	0.0	11.0	89.0	20.8	Waterflood 0.0	50.1	49.9	3.90**	0.188**	39.1	43.9
				0.0	50.1	49.9	-	Gasflood 72.5	19.7	7.8	1.87*	0.090*	42.1	84.3

\* Relative to the Effective Permeability to Oil at Initial Water Saturation

\* to gas

\*\* to water

Rock Type: Top  
Facies: M3/M25

Sample I.D.	Depth, feet	Klinkenberg Permeability, millidarcies	Porosity, percent	Initial Conditions			Terminal Conditions					Oil Recovered, percent pore space in place		
				Saturation, percent pore space		Effective Permeability to Oil, millidarcies	Saturation, percent pore space		Effective Permeability to Liquid, millidarcies	Relative Permeability to Liquid, + fraction				
				Gas	Water		Gas	Water						
				Oil	Oil		Oil	Oil						
E1-1	4532.8	1.76	8.9	Waterflood										
				0.0	8.3	91.7	1.15	0.0	57.9	40.3	0.736**	0.639**	51.4	56.1
				Gasflood										
				0.0	59.7	40.3	-	52.1	40.8	7.1	0.106*	0.092*	33.2	82.4

+ Relative to the Effective Permeability to Oil at Initial Water Saturation

★ To gas

\*\*\* To water



SUMMARY OF PERMEABILITY TO LIQUID MEASUREMENTS

Fina Oil and Chemical Company  
Emmons Unit  
Well 143  
M2/M25 Facies  
Top Rock Type

Sample I.D.: E1-1  
Depth: 4532.8 feet  
Length: 4.91 cm  
Area: 11.45 cm<sup>2</sup>  
Klinkenberg Permeability: 1.76 md  
Permeability to Air: 2.05 md  
Porosity: 8.9 percent

Produced Volume, cc	Corrected Volume, cc	Time, sec	Read Differential Pressure, psi	Differential Pressure Zero, psi	Corrected Differential Pressure, psi	Permeability to Liquid, millidarcies
---------------------------	----------------------------	--------------	--	--	---	--

Effective Permeability to Crude Oil at  $S_{wi}$ 

0.82	0.93	65.5	183	20	163	1.15
0.38	0.43	61.4	100	20	80.0	1.16

Effective Permeability to Brine at  $S_{or}$ 

2.90	2.90	60.9	344	18	326	0.736
1.47	1.47	62.2	180	18	162	0.735

Effective Permeability to CO<sub>2</sub> at  $S_{or}$ 

450	0.97	756	12.5	7.80	4.70	0.101
800	1.72	421	22.0	7.80	14.2	0.107
400	0.86	531	13.5	7.80	5.70	0.106

SUMMARY OF SATURATION CALCULATIONS

Fina Oil and Chemical Company  
Emmons Unit  
Well 143  
M2/M25 Facies  
Top Rock Type

Sample I.D.: E1-1

Vb/Vw	1.025 cc/cc 72°F	Overburden Pressure:	1500 psi
Oil Density	0.803 cc/cc 72°F	Back Pressure:	2000 psi
WTM Correction	0.9380	Temperature:	98 °F
Brine VCF	1.009 cc 98°F + 2000 psi / cc 72°F + 14.7 psi		
Oil VCF	1.136 cc 98°F + 2000 psi / cc 72°F + 14.7 psi		
Gas Factor	0.0022 cc 98°F + 2000 psi / cc 72°F + 14.7 psi		
GWR	0.6 cc/72°F +14.7 psi		

Sample Number	E1-1	Endtrim
Depth	4532.8	
Dry Weight	143.72	53.45
Length	4.91	1.86
Area	11.45	11.45
Ka - RESV OB	2.05	
Porosity, RESV OB	8.9	8.9
PV-Direct RESV OB	4.97	2.28
Swi, cc	0.41	0.20
Swi, %	8.3	8.8

Waterflood

OIP	4.56
Recovery, Room	3.36
Recovery, Res Con	3.82
Dead Volume	1.26
Adj. Recovery, cc	2.56
Recovery, % PS	51.4
Recovery, % OIP	56.1
Sor, cc Tritium	2.00
Sor, % Tritium	40.3

Gasflood

Recovery, %PS CO <sub>2</sub>	33.2
Recovery, %OIP CO <sub>2</sub>	82.4

SUMMARY OF SATURATION CALCULATIONS

Fina Oil and Chemical Company  
 Emmons Unit  
 Well 143  
 M2/M25 Facies  
 Top Rock Type

Sample I.D.: E1-1

**Gasflood Residual Saturations**

Weight After Test	146.79	55.36
Weight Before D/S		55.36
Weight plus tare		55.36
H2O Evaporation		0.00
Blowdown H2O ***	0.38	
KF Water, cc	1.58	0.18
Total Brine (Live)	2.03	0.18
Sw, %	40.8	8.1
-----	-----	-----
Weight After D/S		53.45
Weight Loss D/S		1.91
Wgt. Residual Oil		1.73
Vol. Residual Oil		2.15
Blowdown Oil ***		
Corr. Residual Oil		2.15
Sor, %	7.1	94.5
-----	-----	-----
Blowdown Gas, cc	2000	
Dead Volume, cc	1.26	
Corrected Gas, cc	2.79	
Sg, % BD	56.1	
Void Volume	2.97	
Sg, % VV	52.1	
D/S Pore Volume		2.34
He Pore Volume	4.97	2.28

SUMMARY OF X-RAY ANALYSIS VALUES

Fina Oil and Chemical Company  
 Emmons Unit  
 Well 143  
 M2/M25 Facies  
 Top Rock Type

Sample I.D.: E1-1

<u>I.D.</u>	<u>Volume, cc</u>	<u>Analysis, picocuries/l</u>	
1.	17.18	650	Pore Volume: 4.97 cc
2.	24.92	4700000	Dead Volume: 6.60 cc
3.	47.96	4000000	
4.	20.25	4800000	
4a.	24.39	4800000	
5.	22.10	20800	
6.	45.38	994000	
7.	20.92	29900	
7a.	18.36	13400	

61.50 cc doped brine in Effluent Sample  
 6.71 cc undoped brine in Effluent Sample (from core)

Sw, cc = 0.05 cc brine in sample  
 Sw, percent = 1.1 percent  
 Sor, percent = 100 - Sw  
               = 98.9 percent

For Undoped Brine Displacing Doped Brine  
 9.57 cc doped brine in Effluent Sample (from core)

Sw, cc = 2.97 cc brine in sample  
 Sw, percent = 59.7 percent  
 Sor, percent = 100 - Sw  
               = 40.3 percent

WATERFLOOD SUSCEPTIBILITY TEST RESULTS

Temperature: 98°F

Fina Oil and Chemical Company  
Emmons Unit  
Well No. 143  
Top Rock Type  
M2/M25 Facies

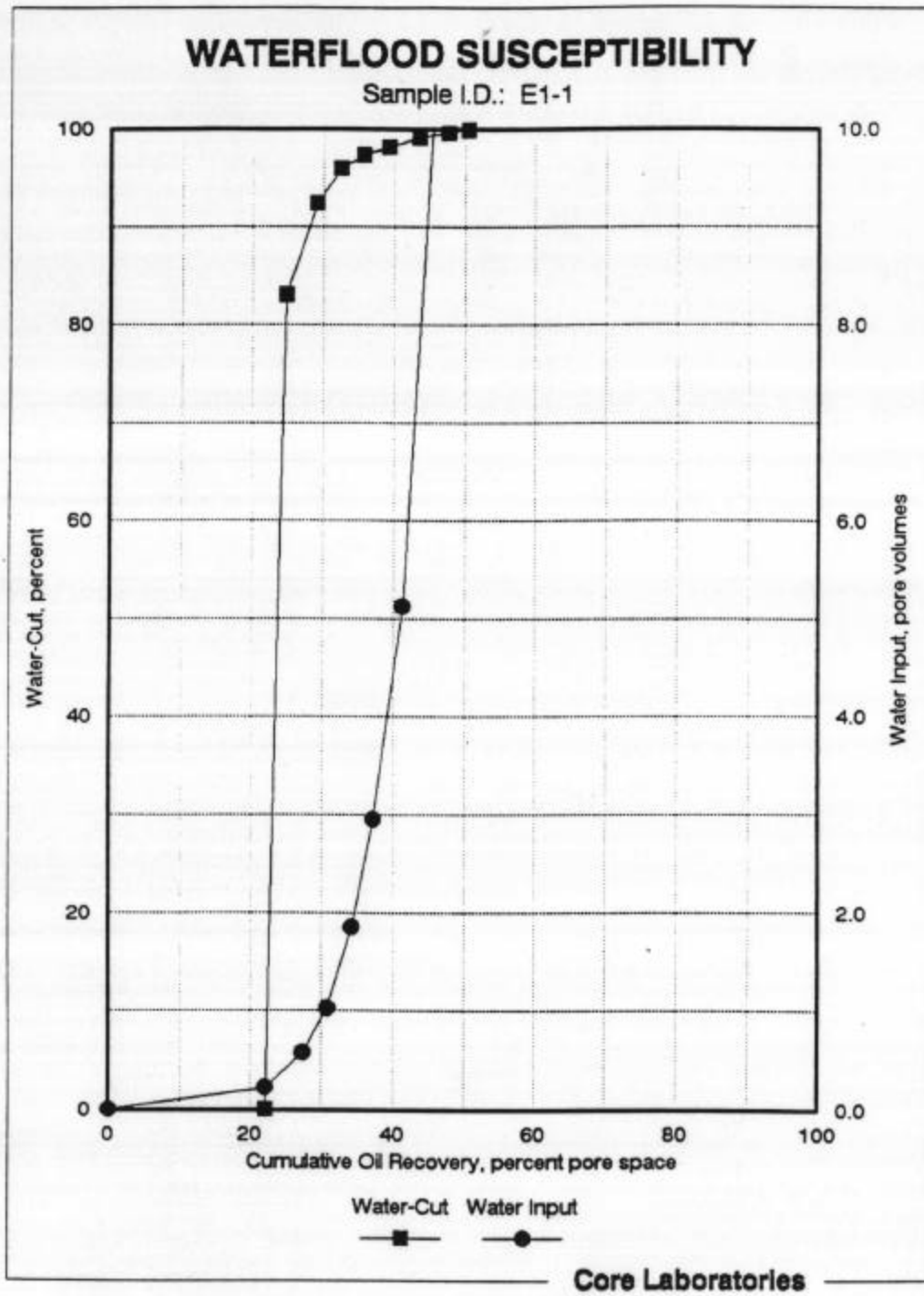
Sample Identification: E1-1  
Sample Depth: 4532.8 feet  
Permeability to Air: 1.76 md  
Porosity: 15.8 percent  
Initial Water Saturation: 8.3 percent  
Effective Permeability  
to Oil at  $S_{wi}$ : 1.15 md

<u>Water Input,</u> <u>pore volumes</u>	<u>Cumulative Oil</u> <u>Recovery,</u> <u>percent pore space</u>	<u>Average Oil</u> <u>Recovery*,</u> <u>percent pore space</u>	<u>Average</u> <u>Water Cut,**</u> <u>percent</u>
0.221	22.1***	-	-
0.575	27.4	24.8	83.1
1.03	30.8	29.1	92.4
1.86	34.2	32.5	95.9
2.96	37.2	35.7	97.3
5.13	41.3	39.3	98.1
10.4	45.9	43.6	99.1
20.5	49.6	47.7	99.6
39.7	51.4	50.5	99.9

\*Calculated for mid-point of incremental throughput

\*\*Calculated from incremental throughput volumes

\*\*\*Breakthrough recovery



WATER-OIL RELATIVE PERMEABILITY TEST RESULTS

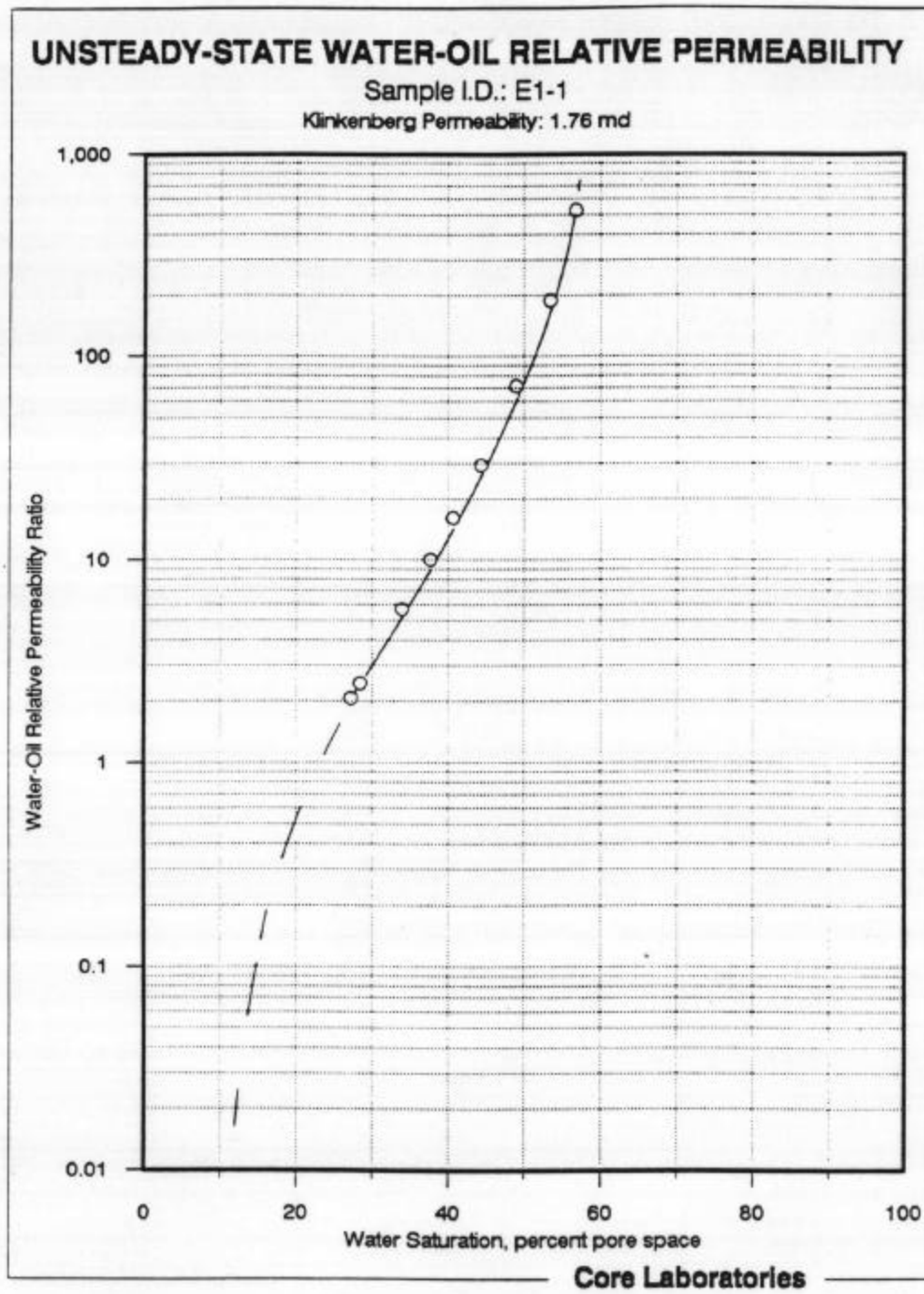
Temperature: 98°F

Fina Oil and Chemical Company  
Emmons Unit  
Well 143  
M2/M25 Facies  
Top Rock Type

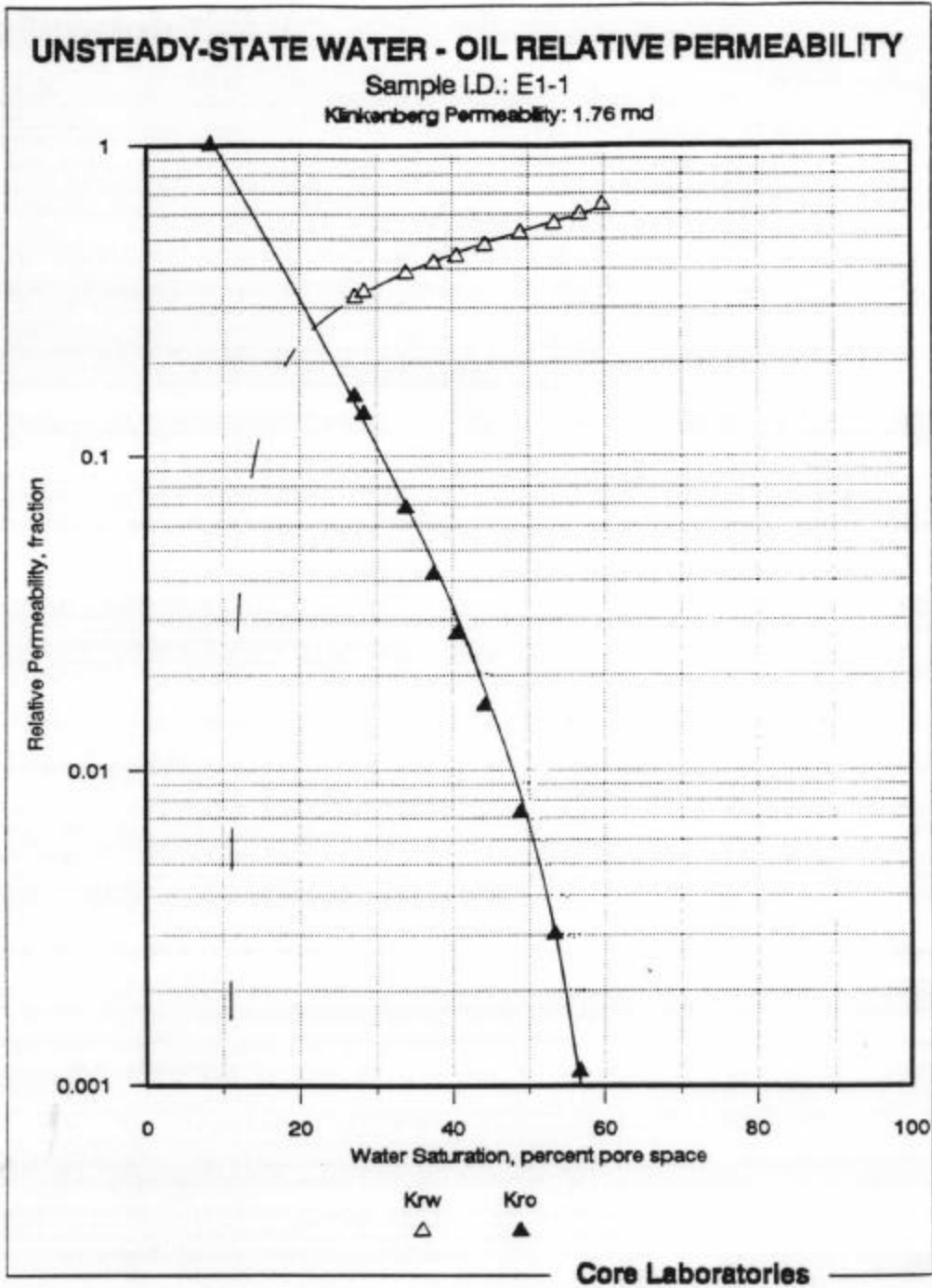
Sample I.D.: E1-1  
Depth: 4532.8 feet  
Permeability to Air: 1.76 md  
Porosity: 8.9 percent  
Effective Permeability to Oil  
at Initial Water Saturation: 1.15 md

<u>Water Saturation, percent pore space</u>	<u>Water-Oil Relative Permeability Ratio</u>	<u>Relative Permeability to Water,* fraction</u>	<u>Relative Permeability to Oil,* fraction</u>
8.3	0.00	0.000	1.000
27.2	2.07	0.323	0.156
28.4	2.46	0.337	0.137
33.9	5.69	0.386	0.068
37.6	10.0	0.417	0.042
40.6	16.1	0.438	0.027
44.3	29.3	0.475	0.016
48.9	71.2	0.520	0.0073
53.4	189	0.558	0.0030
56.8	527	0.598	0.0011
59.7		0.639	

\* Relative to the Effective Permeability to Oil at Initial Water Saturation







SUMMARY OF DIMENSIONLESS GROUPS

Fina Oil and Chemical Company

Sample I.D.: E1-1

## Input Information

Interfacial Tension, dynes/cm (IFT)	30.2
Porosity, fraction ( $\phi$ )	0.158
Effective Permeability to Oil at Swi, md ( $K_o$ )	1.15
Viscosity of Oil, cp ( $\mu_o$ )	2.100
Viscosity of Brine, cp ( $\mu_w$ )	0.800
Flow Rate, cc/min	3.00
Length, cm (L)	4.91
Diameter, cm (D)	3.82
Area, cm <sup>2</sup>	11.45
Velocity, cm/sec (v)	2.76E-02
Relative Permeability to Oil, fraction ( $k_{ro}$ )	0.011
Relative Permeability to Water, fraction ( $k_{rw}$ )	0.598
Density of Oil, grams/cc ( $\rho_o$ )	0.803
Density of Water, grams/cc ( $\rho_w$ )	1.043
Gravity, cm/sec <sup>2</sup> (g)	978

## Capillary End-Effect Number

$$N_c, \text{ end} = [\text{IFT} * \text{SQRT}(\phi * K_o)] / (\mu_w * v * L)$$

$$= 119$$

## Microscopic Capillary Number

$$N_c = (\mu_w * v) / \text{IFT}$$

$$= 7.32\text{E-}04$$

## Mobility Ratio

$$M = (k_{rw} * \mu_o) / (k_{ro} * \mu_w)$$

$$= 143$$

## Effective Aspect Ratio

$$R_1 = \text{SQRT}(L/D * K_o/K_o) \quad R_1 = \text{SQRT}(L/D * K_w/K_o)$$

$$= 2.22 \quad = 0.877$$

## Buoyancy to Viscous Ratio

$$N_g = (K_o * k_{rw} * (\rho_w - \rho_o) * g) / (\mu_o * v) * (L/D)$$

$$= 3570$$

## Density Number

$$N_p = (\rho_w - \rho_o) / \rho_o \quad N_p = (\rho_w - \rho_o) / \rho_w$$

$$= 0.298 \quad = 0.230$$

SUMMARY OF TERTIARY OIL RECOVERY TEST RESULTSFina Oil and Chemical Company  
Well 143Rock Type: Chaotic  
Facies: M3/M34

Sample I.D.	Depth, feet	Klinkenberg Permeability, millidarcies	Porosity, percent	Initial Conditions			Terminal Conditions				Oil Recovered	
				Saturation, percent	pore space	Effective Permeability to Oil, millidarcies	Saturation, percent	pore space	Effective Permeability to Liquid, millidarcies	Relative Permeability to Liquid, + fraction	percent pore space	percent oil in place
							Gas	Water	Oil			
E1-6	4590.6	21.8	24.1									
Waterflood												
				0.0	17.7	82.3	18.5	0.0	62.1	37.9	6.83**	54.0
											0.369**	44.4
Gasflood												
				0.0	62.1	37.9	-	52.3	31.8	15.8	2.45*	58.3
											0.132*	22.1

+ Relative to the Effective Permeability to Oil at Initial Water Saturation

\* To gas

\*\* To water

SUMMARY OF PERMEABILITY TO LIQUID MEASUREMENTS

Fina Oil and Chemical Company  
Emmons Unit  
Well 143  
M3/M34 Facies  
Chaotic Rock Type

Sample I.D.: E1-6  
Depth: 4590.6 feet  
Length: 5.74 cm  
Area: 11.12 cm<sup>2</sup>  
Klinkenberg Permeability: 21.8 md  
Permeability to Air: 25.7 md  
Porosity: 24.1 percent

Produced Volume, cc	Corrected Volume, cc	Time, sec	Read Differential Pressure, psi	Differential Pressure Zero, psi	Corrected Differential Pressure, psi	Permeability to Liquid, millidarcies
---------------------------	----------------------------	--------------	--	--	---	--

Effective Permeability to Crude Oil at  $S_{wi}$ 

0.80	0.91	60.6	15.5	2.60	12.9	18.5
0.40	0.45	61.0	9.0	2.60	6.4	18.5

Effective Permeability to Brine at  $S_{or}$ 

2.86	2.86	61.0	43.7	1.97	41.7	6.82
1.33	1.33	61.5	21.0	1.97	19.0	6.90

Effective Permeability to CO<sub>2</sub> at  $S_{or}$ 

300	0.65	369	1.37	1.05	0.32	2.45
300	0.65	138	1.90	1.05	0.85	2.47
650	1.40	723	1.40	1.05	0.35	2.48

SUMMARY OF SATURATION CALCULATIONS

Fina Oil and Chemical Company  
 Emmons Unit  
 Well 143  
 M3/M34 Facies  
 Chaotic Rock Type

Sample I.D.: E1-6

Vb/Vw:	1.025 cc/cc 72°F	Overburden Pressure:	1500 psi
Oil Density:	0.803 cc/cc 72°F	Back Pressure:	2000 psi
WTM Correction:	0.9380	Temperature:	98 °F
Brine VCF:	1.009 cc 98°F + 2000 psi / cc 72°F + 14.7 psi		
Oil VCF:	1.136 cc 98°F + 2000 psi / cc 72°F + 14.7 psi		
Gas Factor:	0.0022 cc 98°F + 2000 psi / cc 72°F + 14.7 psi		
GWR:	0.6 cc/cc 98F		

Sample Number:	E1-6	Endtrim
Length:	5.74	1.49
Area:	11.12	11.12
Ka - RESV OB:	25.7	
Porosity, RESV OB	24.1	14.8
PV-Direct RESV OB:	15.57	3.34
Swi, cc:	2.76	0.43
Swi, % MB:	17.7	12.9

Waterflood

OIP:	12.81
Recovery, Room:	7.18
Recovery, Res Con:	8.16
Dead Volume:	1.26
Adj. Recovery, cc:	6.90
Recovery, % PS:	44.4
Recovery, % OIP:	54.0

Sor, cc Tritium:	5.91
Sor, % Tritium:	37.9

Gasflood

Recovery, %PS CO <sub>2</sub> :	22.1
Recovery, %OIP CO <sub>2</sub> :	58.3

SUMMARY OF SATURATION CALCULATIONS

Fina Oil and Chemical Company  
 Emmons Unit  
 Well 143  
 M3/M34 Facies  
 Chaotic Rock Type

Sample I.D.: E1-6

Gasflood Residual Saturations

Weight After Test:	147.64	39.41
Weight Before D/S:		39.41
Weight plus tare:		39.41
H2O Evaporation:		0.00
Blowdown H2O:	0.33	
KF Water, cc:	4.79	0.42
Total Brine (Live):	4.95	0.43
Sw, %:	31.8	12.9
-----		
Weight After D/S:		36.26
Weight Loss D/S:		3.15
Wgt. Residual Oil:		2.73
Vol. Residual Oil:		3.40
Blowdown Oil:		
Corr. Residual Oil:		3.40
Sor, % :	15.8	101.8
-----		
Blowdown Gas, cc:*	3940	
Dead Volume, cc:	1.26	
Corrected Gas, cc:	6.65	
Sg, % BD:	42.7	
Void Volume:	8.48	
Sg, % VV:	52.3	
D/S Pore Volume:		3.83
He Pore Volume:	15.57	3.34

\*(Tube Blew Off, lost estimated 1000 cc gas)

SUMMARY OF X-RAY ANALYSIS VALUES

Fina Oil and Chemical Company  
 Emmons Unit  
 Well 143  
 M3/M34 Facies  
 Chaotic Rock Type

Sample I.D.: E1-6

<u>I.D.</u>	<u>Volume, cc</u>	<u>Analysis, picocuries/l</u>		
1.	22.12	6710	Pore Volume	15.57 cc
2.	20.77	47700000	Dead Volume	6.60 cc
3.	74.43	48100000		
4.	30.14	47900000		
4a.	22.64	47800000		
5.	22.21	225000		
6.	60.71	12600000		
7.	23.26	459000		
7a.	29.12	176000		

105.32 cc doped brine in Effluent Sample  
 -0.75 cc undoped brine in Effluent Sample (from core)

Sw, cc = -7.41 cc brine in sample  
 Sw, percent = -47.6 percent  
 Sor, percent = 100 - Sw  
 = 147.6 percent

For Undoped Brine Displacing Doped Brine  
 16.32 cc doped brine in Effluent Sample (from core)

Sw, cc = 9.66 cc brine in sample  
 Sw, percent = 62.1 percent  
 Sor, percent = 100 - Sw  
 = 37.9 percent

WATERFLOOD SUSCEPTIBILITY TEST RESULTS

Temperature: 98°F

Fina Oil and Chemical Company  
Emmons Unit  
Well No. 143  
Chaotic Rock Type  
M3/M34 Facies

Sample Identification: E1-6  
Sample Depth: 4590.6 feet  
Permeability to Air: 25.7 md  
Porosity: 24.1 percent  
Initial Water Saturation: 17.1 percent  
Effective Permeability  
to Oil at  $S_{wi}$ : 18.5 md

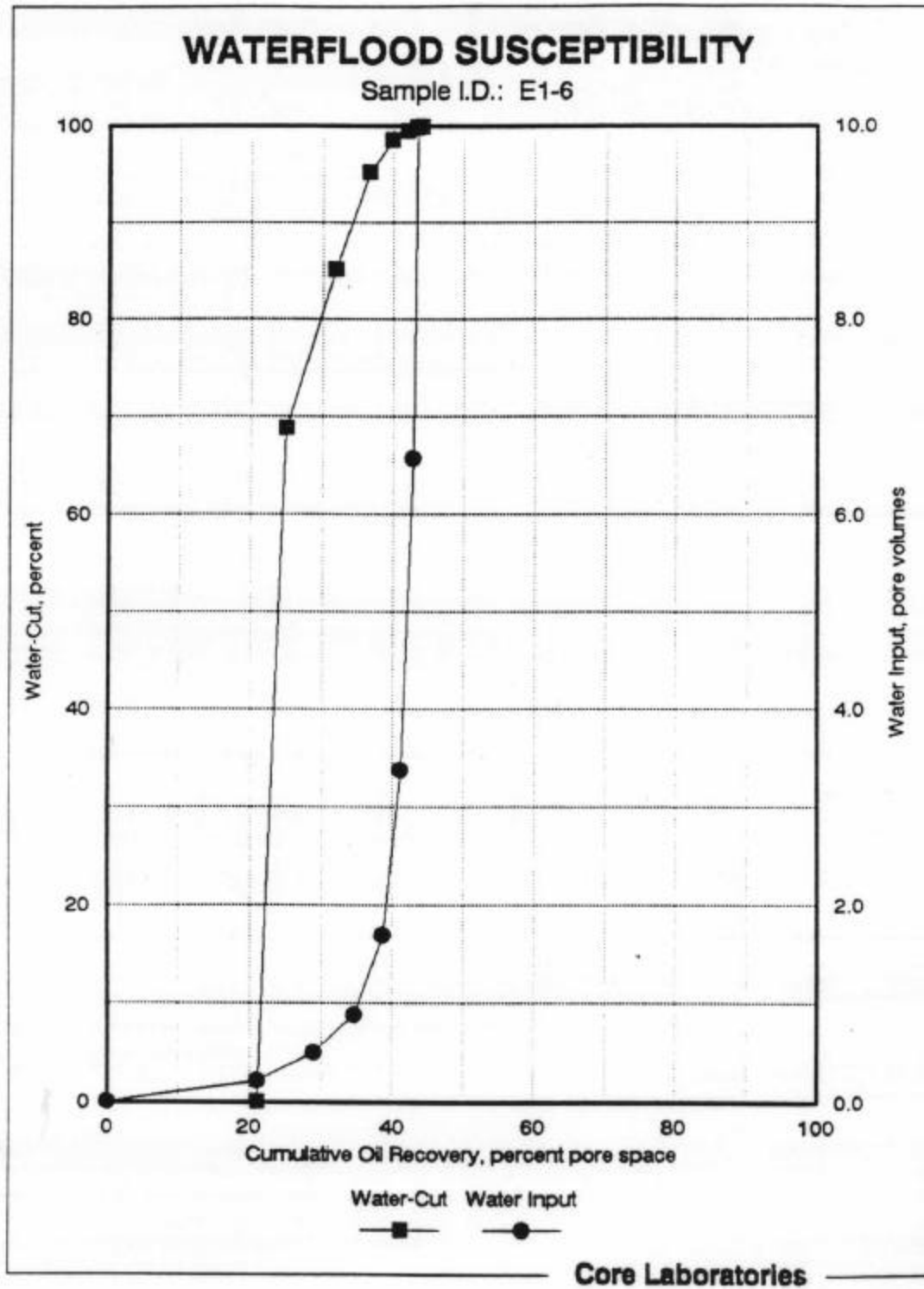
<u>Water Input,</u> <u>pore volumes</u>	<u>Cumulative Oil</u> <u>Recovery,</u> <u>percent pore space</u>	<u>Average Oil</u> <u>Recovery*,</u> <u>percent pore space</u>	<u>Average</u> <u>Water Cut,**</u> <u>percent</u>
0.210	21.1***	-	-
0.494	29.0	25.0	68.8
0.884	34.7	31.9	85.2
1.70	38.7	36.7	95.2
3.38	41.1	39.9	98.5
6.57	42.8	42.0	99.5
13.1	43.9	43.3	99.8
19.5	44.4	44.1	99.9

\*Calculated for mid-point of incremental throughput

\*\*Calculated from incremental throughput volumes

\*\*\*Breakthrough recovery





WATER-OIL RELATIVE PERMEABILITY TEST RESULTS

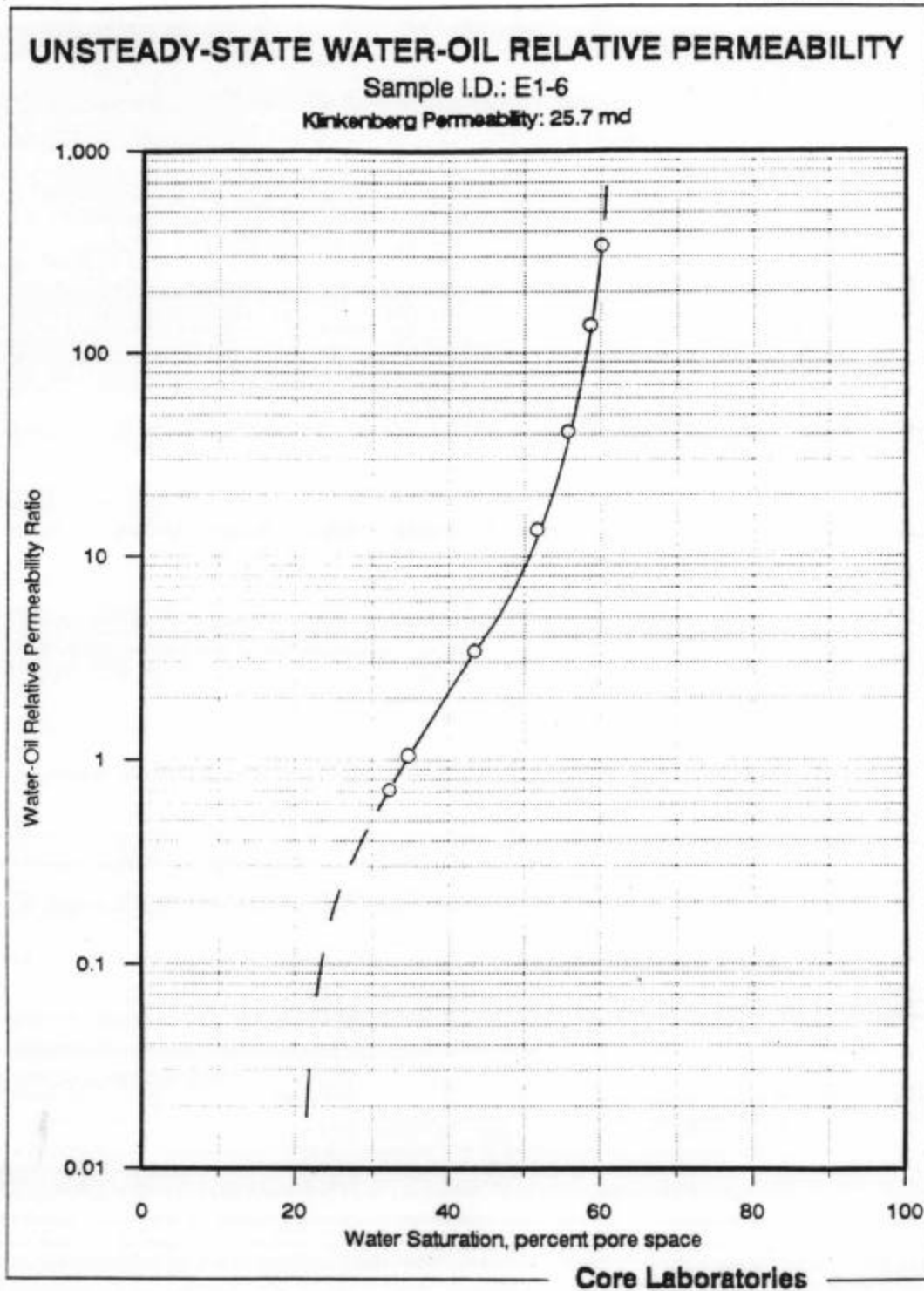
Temperature: 98°F

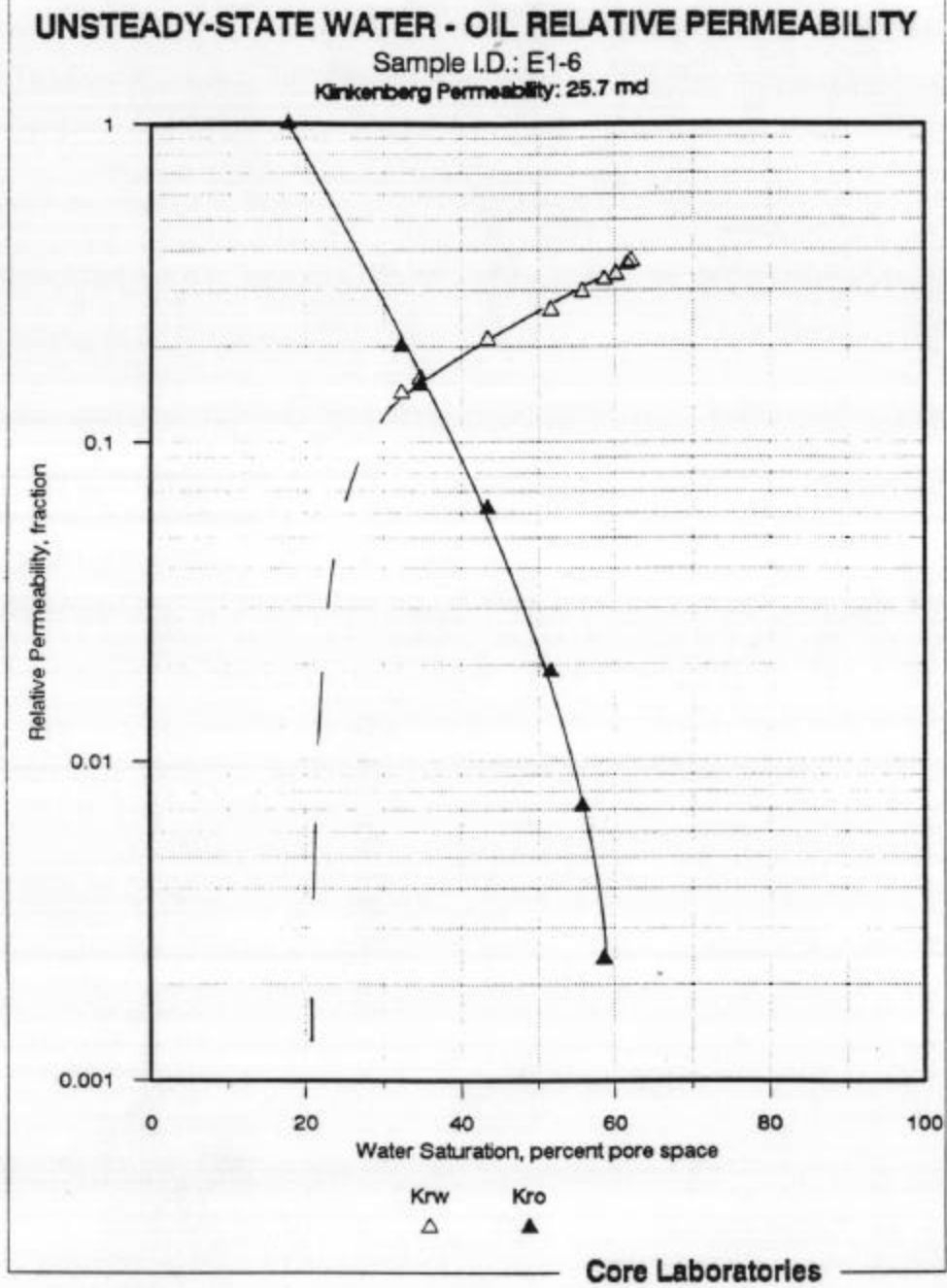
Fina Oil and Chemical Company  
Emmons Unit  
Well 143  
M3/M34 Facies  
Chaotic Rock Type

Sample I.D.: E1-6  
Depth: 4590.6 feet  
Permeability to Air: 25.7 md  
Porosity: 24.1 percent  
Effective Permeability to Oil  
at Initial Water Saturation: 18.5 md

<u>Water Saturation, percent pore space</u>	<u>Water-Oil Relative Permeability Ratio</u>	<u>Relative Permeability to Water,* fraction</u>	<u>Relative Permeability to Oil,* fraction</u>
17.7	0.000	0.000	1.000
32.3	0.710	0.142	0.200
34.7	1.05	0.158	0.150
43.4	3.39	0.210	0.062
51.6	13.4	0.260	0.019
55.7	41.1	0.295	0.0072
58.6	137	0.322	0.0024
60.1	342	0.335	0.00098
61.6	2100	0.360	0.00017
62.1		0.369	

\* Relative to the Effective Permeability to Oil at Initial Water Saturation





SUMMARY OF DIMENSIONLESS GROUPS

Fina Oil and Chemical Company

Sample I.D.: E1-6

## Input Information

Interfacial Tension, dynes/cm (IFT)	30.2
Porosity, fraction ( $\phi$ )	0.241
Effective Permeability to Oil at Swi, md ( $K_o$ )	18.5
Viscosity of Oil, cp ( $\mu_o$ )	2.100
Viscosity of Brine, cp ( $\mu_w$ )	0.800
Flow Rate, cc/min	3.00
Length, cm (L)	5.74
Diameter, cm (D)	3.76
Area, cm <sup>2</sup>	11.12
Velocity, cm/sec (v)	1.87E-02
Relative Permeability to Oil, fraction ( $k_{ro}$ )	1.70E-04
Relative Permeability to Water, fraction ( $k_{rw}$ )	0.360
Density of Oil, grams/cc ( $\rho_o$ )	0.803
Density of Water, grams/cc ( $\rho_w$ )	1.043
Gravity, cm/sec <sup>2</sup> (g)	978

## Capillary End-Effect Number

$$N_c, \text{ end} = [\text{IFT} * \text{SQRT}(\phi * K_o)] / (\mu_w * v * L)$$

$$= 744$$

## Microscopic Capillary Number

$$N_c = (\mu_w * v) / \text{IFT}$$

$$= 4.94\text{E-}04$$

## Mobility Ratio

$$M = (k_{rw} * \mu_o) / (k_{ro} * \mu_w)$$

$$= 5559$$

## Effective Aspect Ratio

$$R_1 = \text{SQRT}(L/D * K_o/K_o) \quad R_1 = \text{SQRT}(L/D * K_w/K_o)$$

$$= 2.40 \quad = 0.741$$

## Buoyancy to Viscous Ratio

$$N_g = (K_o * k_{rw} * (\rho_w - \rho_o) * g) / (\mu_o * v) * (L/D)$$

$$= 60763$$

## Density Number

$$N_p = (\rho_w - \rho_o) / \rho_o \quad N_p = (\rho_w - \rho_o) / \rho_w$$

$$= 0.298 \quad = 0.230$$

SUMMARY OF TERTIARY OIL RECOVERY TEST RESULTSFina Oil and Chemical Company  
Well 142Rock Type: Chaotic  
Facies: M3/M34

Sample I.D.	Depth, feet	Klinkenberg Permeability, millidarcies	Porosity, percent	Initial Conditions			Terminal Conditions				Oil Recovered,	
				Saturation, percent	pore space	Effective Permeability to Oil, millidarcies	Saturation, percent	pore space	Effective Permeability to Liquid, + millidarcies	Relative Permeability to Liquid, + fraction	percent pore space	percent oil in place
							Gas	Water	Oil			

E1-11 4638.9 13.9 15.8

## Waterflood

0.0 7.6 92.4 8.05 0.0 57.2 42.8 3.02\*\* 0.427\*\* 49.6 53.7

## Gasflood

0.0 57.2 42.8 - 48.2 35.1 16.7 1.37\* 0.170\* 26.1 61.0

+ Relative to the Effective Permeability to Oil at Initial Water Saturation

\* To gas

\*\* To water

SUMMARY OF PERMEABILITY TO LIQUID MEASUREMENTS

Fina Oil and Chemical Company  
Emmons Unit  
Well 142  
M3/M34 Facies  
Chaotic Rock Type

Sample I.D.: E1-11  
Depth: 4638.9 feet  
Length: 5.68 cm  
Area: 11.73 cm<sup>2</sup>  
Klinkenberg Permeability: 13.9 md  
Permeability to Air: 16.1 md  
Porosity: 15.8 percent

Produced Volume, cc	Corrected Volume, cc	Time, sec	Read Differential Pressure, psi	Differential Pressure Zero, psi	Corrected Differential Pressure, psi	Permeability to Liquid, millidarcies
---------------------------	----------------------------	--------------	--	--	---	--

Effective Permeability to Crude Oil at  $S_{wi}$ 

0.72	0.82	60.3	23.7	-1.50	25.2	8.05
0.46	0.52	61.5	14.3	-1.50	15.8	8.04

Effective Permeability to Brine at  $S_{or}$ 

2.90	2.90	60.7	91.0	1.00	90.0	3.02
1.37	1.37	61.0	43.50	1.00	42.5	3.01

Effective Permeability to CO<sub>2</sub> at  $S_{or}$ 

780	1.62	4140	1.10	0.98	0.12	1.37
600	1.25	523	1.75	0.98	0.77	1.30
200	0.42	409	1.30	0.98	0.32	1.34

SUMMARY OF SATURATION CALCULATIONS

Fina Oil and Chemical Company  
 Emmons Unit  
 Well 142  
 M3/M34 Facies  
 Chaotic Rock Type

Sample I.D.: E1-11

Vb/Vw:	1.025 cc/cc 72°F	Overburden Pressure:	1500 psi
Oil Density:	0.803 cc/cc 72°F	Back Pressure:	2000 psi
WTM Correction:	0.9380	Temperature:	98 °F
Brine VCF:	1.009 cc 98°F + 2000 psi / cc 72°F + 14.7 psi		
Oil VCF:	1.136 cc 98°F + 2000 psi / cc 72°F + 14.7 psi		
Gas Factor:	0.0022 cc 98°F + 2000 psi / cc 72°F + 14.7 psi		
GWR:	0.6 cc/cc 98°F		

Sample Number	E1-11	Endtrim
Depth:	4638.9	
Length:	5.68	1.21
Area:	11.73	11.73
Ka - RESV OB:	13.9	
Porosity, RESV OB:	15.8	14.8
PV-Direct RESV OB:	10.43	2.03
Swi, cc :	0.80	0.31
Swi, % MB:	7.6	15.3

Waterflood

OIP:	9.63
Recovery, Room:	5.66
Recovery, Res Con:	6.43
Dead Volume:	1.26
Adj. Recovery, cc:	5.17
Recovery, % PS:	49.6
Recovery, % OIP:	53.7

Sor, cc Tritium:	4.46
Sor, % Tritium:	42.8

Gasflood

Recovery, %PS CO <sub>2</sub> :	26.1
Recovery, %OIP:	61.0



SUMMARY OF SATURATION CALCULATIONS

Fina Oil and Chemical Company  
 Emmons Unit  
 Well 143  
 M2/M25 Facies  
 Top Rock Type

Sample I.D.: E1-11

Gasflood Residual Saturations

Weight After Test:	161.78	35.27
Weight Before D/S:		35.27
Weight plus tare:		35.27
H2O Evaporation:		0.00
Blowdown H2O: ***	1.17	
KF Water, cc:	2.37	0.31
Total Brine (Live):	3.66	0.32
Sw, %:	35.1	15.7
-----		-----
Weight After D/S:		33.46
Weight Loss D/S:		1.81
Wgt. Residual Oil:		1.50
Vol. Residual Oil:		1.87
Blowdown Oil: ***		
Corr. Residual Oil:		1.87
Sor, % :	16.7	92.2
-----		-----
Blowdown Gas, cc:	3215	
Dead Volume, cc:	1.26	
Corrected Gas, cc:	5.42	
Sg, % BD:	51.9	
Void Volume:	6.20	
Sg, % VV:	48.2	
D/S Pore Volume:		2.19
He Pore Volume:	10.43	2.03

SUMMARY OF X-RAY ANALYSIS VALUES

Fina Oil and Chemical Company  
 Emmons Unit  
 Well 142  
 M3/M34 Facies  
 Chaotic Rock Type

Sample I.D.: E1-11

<u>I.D.</u>	<u>Volume,</u> <u>cc</u>	<u>Analysis,</u> <u>picocuries/l</u>
1.	19.78	7920
2.	21.06	47800000
3.	56.21	37100000
4.	28.71	48000000
4a.	28.16	47400000
5.	21.37	90900
6.	54.04	10900000
7.	24.13	198000
7a.	24.13	247000

Pore Volume: 10.46 cc  
 Dead Volume: 6.60 cc

72.46 cc doped brine in Effluent Sample  
 12.46 cc undoped brine in Effluent Sample (from core)

Sw, cc = 5.80 cc brine in sample  
 Sw, percent = 55.5 percent  
 Sor, percent = 100 - Sw  
               = 44.5 percent

For Undoped Brine Displacing Doped Brine  
 12.64 cc doped brine in Effluent Sample (from core)

Sw, cc = 5.98 cc brine in sample  
 Sw, percent = 57.2 percent  
 Sor, percent = 100 - Sw  
               = 42.8 percent

WATERFLOOD SUSCEPTIBILITY TEST RESULTS

Temperature: 98°F

Fina Oil and Chemical Company  
Emmons Unit  
Well No. 142  
Chaotic Rock Type  
M3/M34 Facies

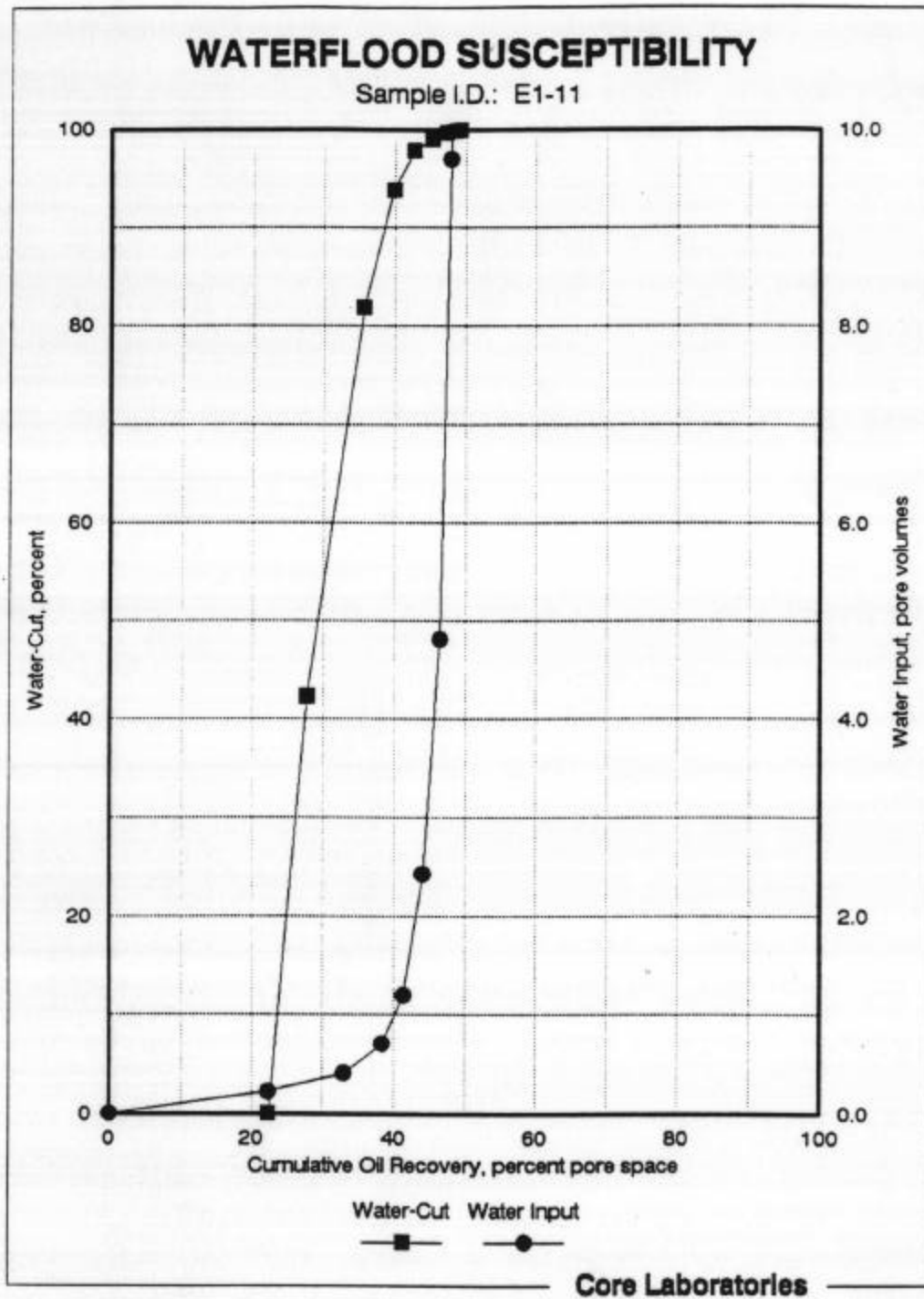
Sample Identification: E1-11  
Sample Depth: 4638.9 feet  
Permeability to Air: 16.1 md  
Porosity: 15.8 percent  
Initial Water Saturation: 7.7 percent  
Effective Permeability  
to Oil at  $S_{wi}$ : 8.05 md

<u>Water Input,</u> <u>pore volumes</u>	<u>Cumulative Oil</u> <u>Recovery,</u> <u>percent pore space</u>	<u>Average Oil</u> <u>Recovery*,</u> <u>percent pore space</u>	<u>Average</u> <u>Water Cut,**</u> <u>percent</u>
0.223	22.3***	-	-
0.411	33.0	27.7	42.3
0.706	38.4	35.7	81.9
1.20	41.4	39.9	93.8
2.43	44.1	42.8	97.8
4.81	46.5	45.3	99.0
9.70	48.0	47.3	99.7
18.7	49.1	48.6	99.88
28.4	49.6	49.3	99.96

\*Calculated for mid-point of incremental throughput

\*\*Calculated from incremental throughput volumes

\*\*\*Breakthrough recovery



WATER-OIL RELATIVE PERMEABILITY TEST RESULTS

Temperature: 98°F

Fina Oil and Chemical Company  
Emmons Unit  
Well 142  
M3/M34 Facies  
Chaotic Rock Type

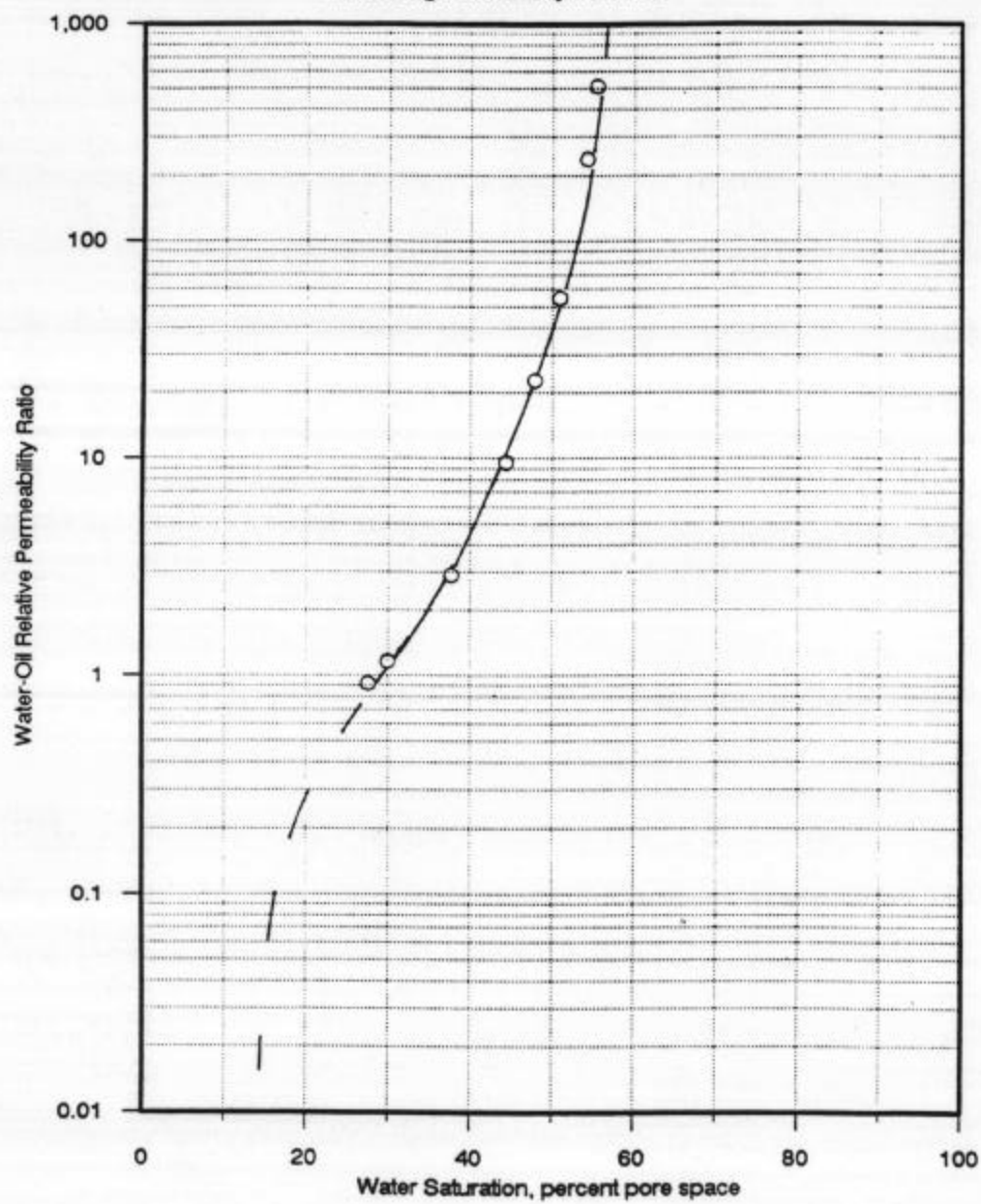
Sample I.D.: E1-11  
Depth: 4638.9 feet  
Permeability to Air: 16.1 md  
Porosity: 15.8 percent  
Effective Permeability to Oil  
at Initial Water Saturation: 8.05 md

<u>Water Saturation, percent pore space</u>	<u>Water-Oil Relative Permeability Ratio</u>	<u>Relative Permeability to Water,* fraction</u>	<u>Relative Permeability to Oil,* fraction</u>
7.6	0.000	0.000	1.000
27.6	0.918	0.284	0.309
30.0	1.16	0.302	0.260
37.7	2.90	0.353	0.122
44.4	9.54	0.387	0.041
47.8	22.7	0.401	0.018
50.9	54.5	0.411	0.0075
54.2	237	0.420	0.0018
55.4	511	0.424	0.00083
56.8	2570	0.427	0.00017
57.2		0.427	

\* Relative to the Effective Permeability to Oil at Initial Water Saturation

**UNSTEADY-STATE WATER-OIL RELATIVE PERMEABILITY**

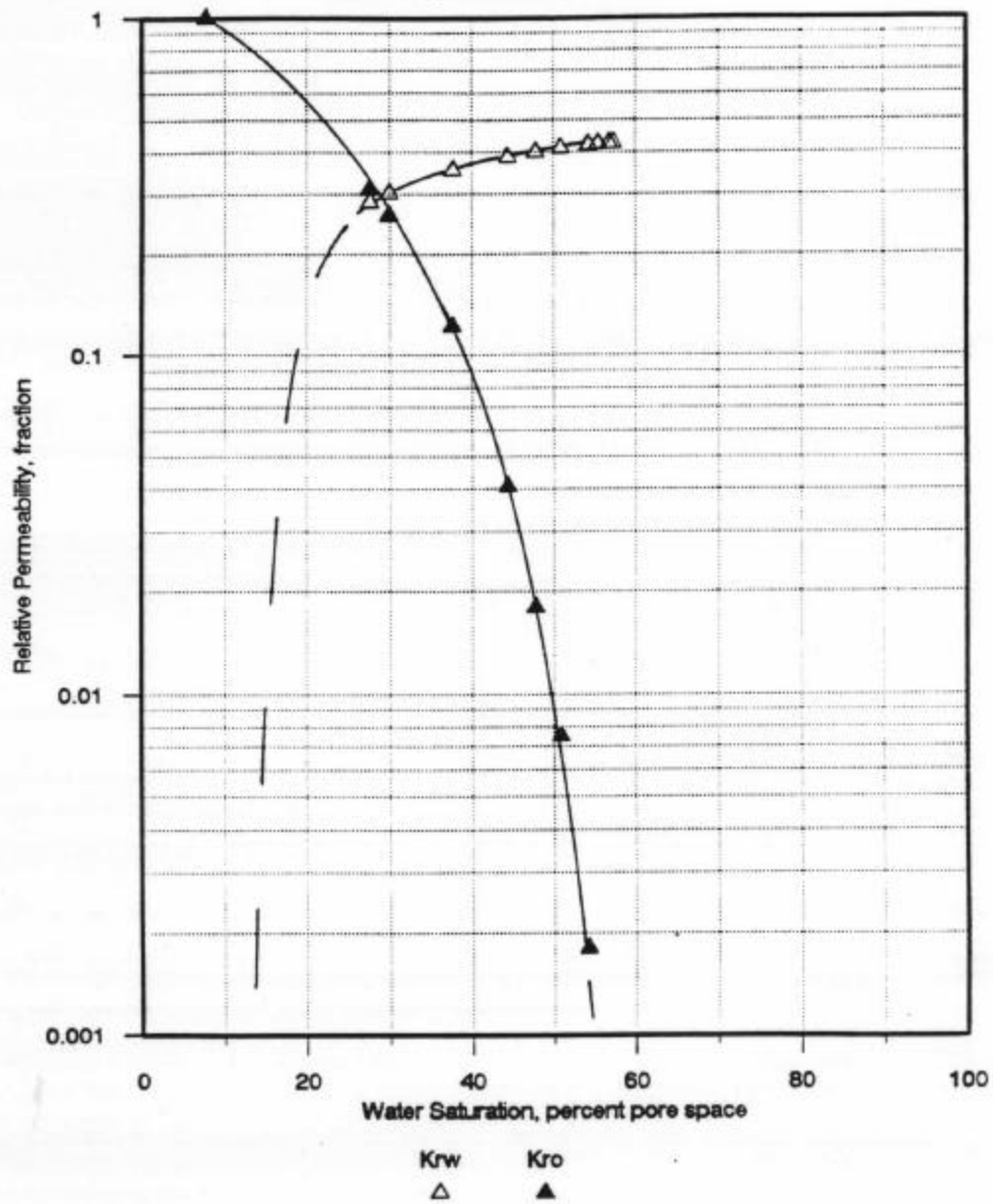
Sample I.D.: E1-11  
Klinkenberg Permeability: 13.9 md



**UNSTEADY-STATE WATER - OIL RELATIVE PERMEABILITY**

Sample I.D.: E1-11

Klinkenberg Permeability: 13.9 mD



SUMMARY OF DIMENSIONLESS GROUPS

Fina Oil and Chemical Company

Sample I.D.: E1-11

## Input Information

Interfacial Tension, dynes/cm (IFT)	30.2
Porosity, fraction ( $\phi$ )	0.158
Effective Permeability to Oil at $S_{wi}$ , md ( $K_o$ )	8.05
Viscosity of Oil, cp ( $\mu_o$ )	2.100
Viscosity of Brine, cp ( $\mu_w$ )	0.800
Flow Rate, cc/min	3.00
Length, cm (L)	5.68
Diameter, cm (D)	3.86
Area, cm <sup>2</sup>	11.73
Velocity, cm/sec (v)	2.70E-02
Relative Permeability to Oil, fraction ( $k_{ro}$ )	1.70E-04
Relative Permeability to Water, fraction ( $k_{rw}$ )	0.427
Density of Oil, grams/cc ( $\rho_o$ )	0.803
Density of Water, grams/cc ( $\rho_w$ )	1.043
Gravity, cm/sec <sup>2</sup> (g)	978

## Capillary End-Effect Number

$$N_c, \text{ end} = [IFT * \text{SQRT}(\phi * K_o)] / (\mu_w * v * L)$$

$$= 278$$

## Microscopic Capillary Number

$$N_c = (\mu_w * v) / IFT$$

$$= 7.15E-04$$

## Mobility Ratio

$$M = (k_{rw} * \mu_o) / (k_{ro} * \mu_w)$$

$$= 6593$$

## Effective Aspect Ratio

$$R_1 = \text{SQRT}(L/D * K_o/K_o) \quad R_1 = \text{SQRT}(L/D * K_w/K_o)$$

$$= 2.38 \quad = 0.792$$

## Buoyancy to Viscous Ratio

$$N_g = (K_o * k_{rw} * (\rho_w - \rho_o) * g) / (\mu_o * v) * (L/D)$$

$$= 20896$$

## Density Number

$$N_p = (\rho_w - \rho_o) / \rho_o \quad N_p = (\rho_w - \rho_o) / \rho_w$$

$$= 0.298 \quad = 0.230$$





SUMMARY OF PERMEABILITY TO LIQUID MEASUREMENTS

Fina Oil and Chemical Company  
Emmons Unit  
Well 143  
M37/M4 Facies  
Moldic Rock Type

Sample I.D.: E1-14  
Depth: 4644.5 feet  
Length: 6.45 cm  
Area: 11.39 cm<sup>2</sup>  
Klinkenberg Permeability: 56.2 md  
Permeability to Air: 60.2 md  
Porosity: 8.9 percent

Produced Volume, cc	Corrected Volume, cc	Time, sec	Read Differential Pressure, psi	Differential Pressure Zero, psi	Corrected Differential Pressure, psi	Permeability to Liquid, millidarcies
---------------------------	----------------------------	--------------	--	--	---	--

Effective Permeability to Crude Oil at  $S_{wi}$ 

1.05	1.19	83.5	15.3	3.70	11.6	21.5
0.80	0.91	66.7	15.3	3.70	11.6	20.5
0.53	0.60	71.2	10.8	3.70	7.1	20.8

Effective Permeability to Brine at  $S_{or}$ 

2.95	2.95	62.6	82.0	1.50	80.5	3.90
1.45	1.45	61.5	41.0	1.50	39.5	3.97

Effective Permeability to CO<sub>2</sub> at  $S_{or}$ 

250	0.52	426	0.9	0.58	0.32	1.87
2000	4.16	1219	1.46	0.58	0.88	1.90
900	1.87	595	1.450	0.58	0.87	1.77

SUMMARY OF SATURATION CALCULATIONS

Fina Oil and Chemical Company  
Emmons Unit  
Well 143  
M37/M4 Facies  
Moldic Rock Type

Sample I.D.: E1-14

Vb/Vw:	1.025 cc/cc 72°F	Overburden Pressure:	1500 psi
Oil Density:	0.803 cc/cc 72°F	Back Pressure:	2000 psi
WTM Correction:	0.9380	Temperature:	98 °F
Brine VCF:	1.009 cc 98°F + 2000 psi / cc 72°F + 14.7 psi		
Oil VCF:	1.136 cc 98°F + 2000 psi / cc 72°F + 14.7 psi		
Gas Factor:	0.0022 cc 98°F + 2000 psi / cc 72°F + 14.7 psi		
GWR:	0.6 cc/cc 98°F		

Sample Number	E1-14	Endtrim
Depth:	4644.5	
Length:	6.45	0.69
Area:	11.39	11.44
Ka - RESV OB:	56.2	
Porosity, RESV OB:	17.8	13.2
PV-Direct RESV OB:	12.99	1.02
Swi, cc:	1.43	0.21
Swi, % MB:	11.0	20.6

Waterflood

OIP:	11.56
Recovery, Room:	5.58
Recovery, Res Con:	6.34
Dead Volume:	1.26
Adj. Recovery, cc:	5.08
Recovery, % PS:	39.1
Recovery, % OIP:	43.9

Sor, cc Tritium:	6.48
Sor, % Tritium:	49.9

Gasflood

Recovery, %PS CO <sub>2</sub> :	42.1
Recovery, %OIP CO <sub>2</sub> :	84.3

SUMMARY OF SATURATION CALCULATIONS

Fina Oil and Chemical Company  
 Emmons Unit  
 Well 143  
 M37/M4 Facies  
 Moldic Rock Type

Sample I.D.: E1-14

## Gasflood Residual Saturations

Weight After Test:		19.62
Weight Before D/S:		19.62
Weight plus tare:		19.62
H2O Evaporation:		0.00
Blowdown H2O:		
KF Water, cc:	2.47	0.20
Total Brine (Live):	2.55	0.21
Sw, %:	19.7	20.1
-----	-----	-----
Weight After D/S:		18.75
Weight Loss D/S:		0.87
Wgt. Residual Oil:		0.67
Vol. Residual Oil:		0.83
Blowdown Oil:		
Corr. Residual Oil:		0.83
Sor, %:	7.8	81.9
-----	-----	-----
Blowdown Gas, cc:	5085	
Dead Volume, cc:	1.26	
Corrected Gas, cc:	9.31	
Sg, % BD:	71.6	
Void Volume:	9.42	
Sg, % VV:	72.5	
D/S Pore Volume:		1.04
He Pore Volume:	12.99	1.02

SUMMARY OF X-RAY ANALYSIS VALUES

Fina Oil and Chemical Company  
 Emmons Unit  
 Well 143  
 M37/M4 Facies  
 Moldic Rock Type

Sample I.D.: E1-14

<u>I.D.</u>	<u>Volume, cc</u>	<u>Analysis, millicuries/l</u>
1.	40.51	0.007
2.	16.81	48.4
3.	57.51	36.7
4.	13.42	47.5
4a.	11.79	48.4
5.	25.00	0.1
6.	56.03	11.2
7.	13.30	0.5
7a.	13.13	0.3

Pore Volume: 12.99 cc  
 Dead Volume: 6.60 cc

56.78 cc doped brine in Effluent Sample  
 14.15 cc undoped brine in Effluent Sample (from core)

Sw, cc = 7.50 cc brine in sample  
 Sw, percent = 57.7 percent  
 Sor, percent = 100 - Sw  
 = 42.3 percent

For Undoped Brine Displacing Doped Brine  
 13.17 cc doped brine in Effluent Sample (from core)

Sw, cc = 6.51 cc brine in sample  
 Sw, percent = 50.1 percent  
 Sor, percent = 100 - Sw  
 = 49.9 percent

WATERFLOOD SUSCEPTIBILITY TEST RESULTS

Temperature: 98°F

Fina Oil and Chemical Company  
Emmons Unit  
Well No. 143  
Moldic Rock Type  
M37/M4 Facies

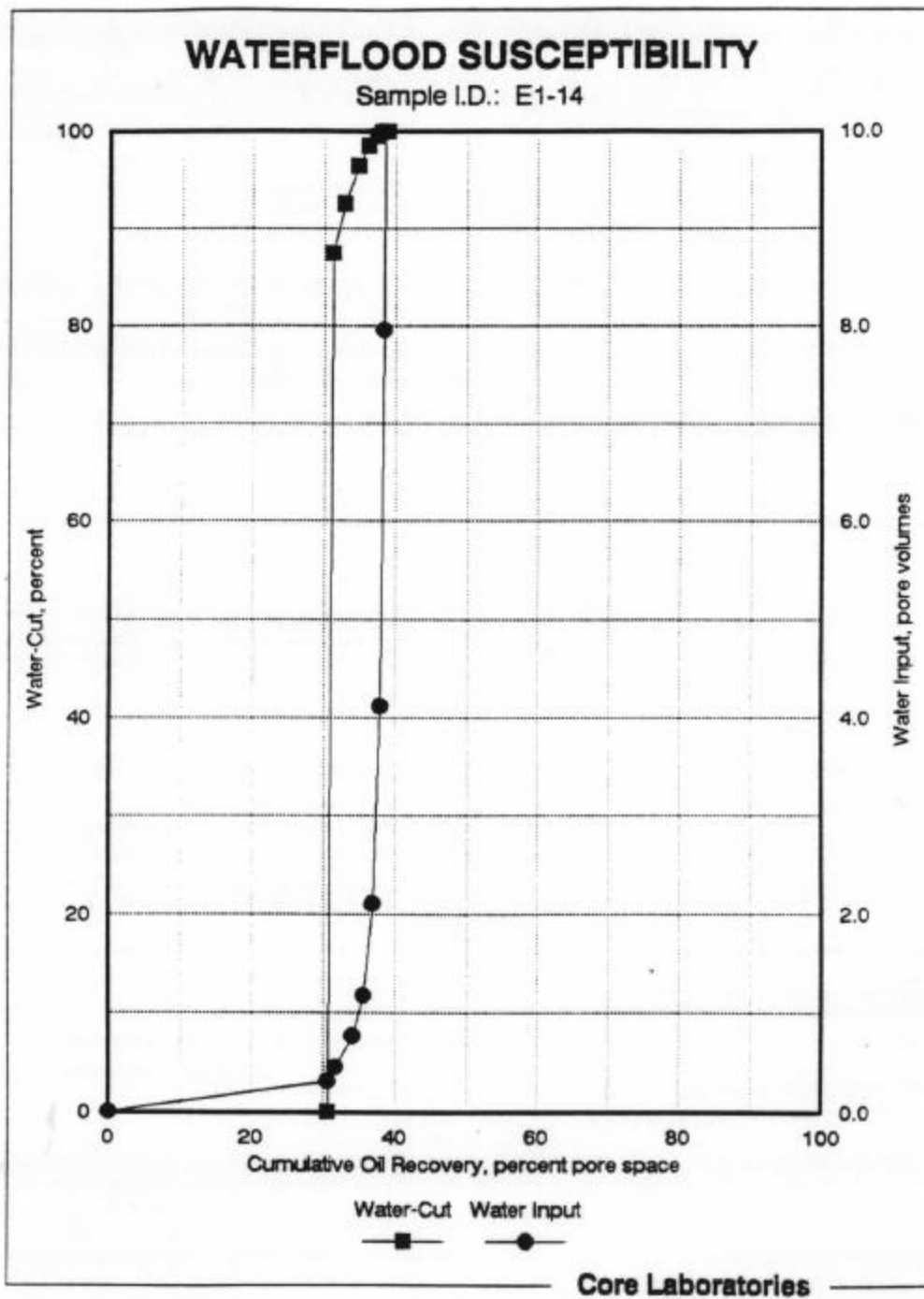
Sample Identification: E1-14  
Sample Depth: 4644.5 feet  
Permeability to Air: 60.2 md  
Porosity: 17.8 percent  
Initial Water Saturation: 11.0 percent  
Effective Permeability  
to Oil at  $S_{wi}$ : 20.8 md

<u>Water Input,</u> <u>pore volumes</u>	<u>Cumulative Oil</u> <u>Recovery,</u> <u>percent pore space</u>	<u>Average Oil</u> <u>Recovery*,</u> <u>percent pore space</u>	<u>Average</u> <u>Water Cut,**</u> <u>percent</u>
0.306	30.6***	-	-
0.447	31.7	31.2	87.5
0.769	34.1	32.9	92.6
1.18	35.6	34.8	96.5
2.11	36.9	36.2	98.5
4.12	37.9	37.4	99.5
7.96	38.4	38.1	99.86
15.6	38.9	38.6	99.94
23.3	39.1	39.0	99.97

\*Calculated for mid-point of incremental throughput

\*\*Calculated from incremental throughput volumes

\*\*\*Breakthrough recovery



WATER-OIL RELATIVE PERMEABILITY TEST RESULTS

Temperature: 98°F

Fina Oil and Chemical Company  
Emmons Unit  
Well 143  
M37/M4 Facies  
Moldic Rock Type

Sample I.D.: E1-14  
Depth: 4644.5 feet  
Permeability to Air: 60.2 md  
Porosity: 17.8 percent  
Effective Permeability to Oil  
at Initial Water Saturation: 20.8 md

<u>Water Saturation, percent pore space</u>	<u>Water-Oil Relative Permeability Ratio</u>	<u>Relative Permeability to Water,* fraction</u>	<u>Relative Permeability to Oil,* fraction</u>
11.0	0.00	0.000	1.000
39.1	4.41	0.144	0.033
39.4	4.67	0.147	0.031
40.7	6.36	0.153	0.024
43.7	15.4	0.161	0.010
45.8	37.7	0.167	0.0044
47.8	151	0.172	0.0011
48.7	458	0.177	0.00039
49.2	845	0.182	0.00022
49.8	2830	0.185	0.000065
50.1		0.188	

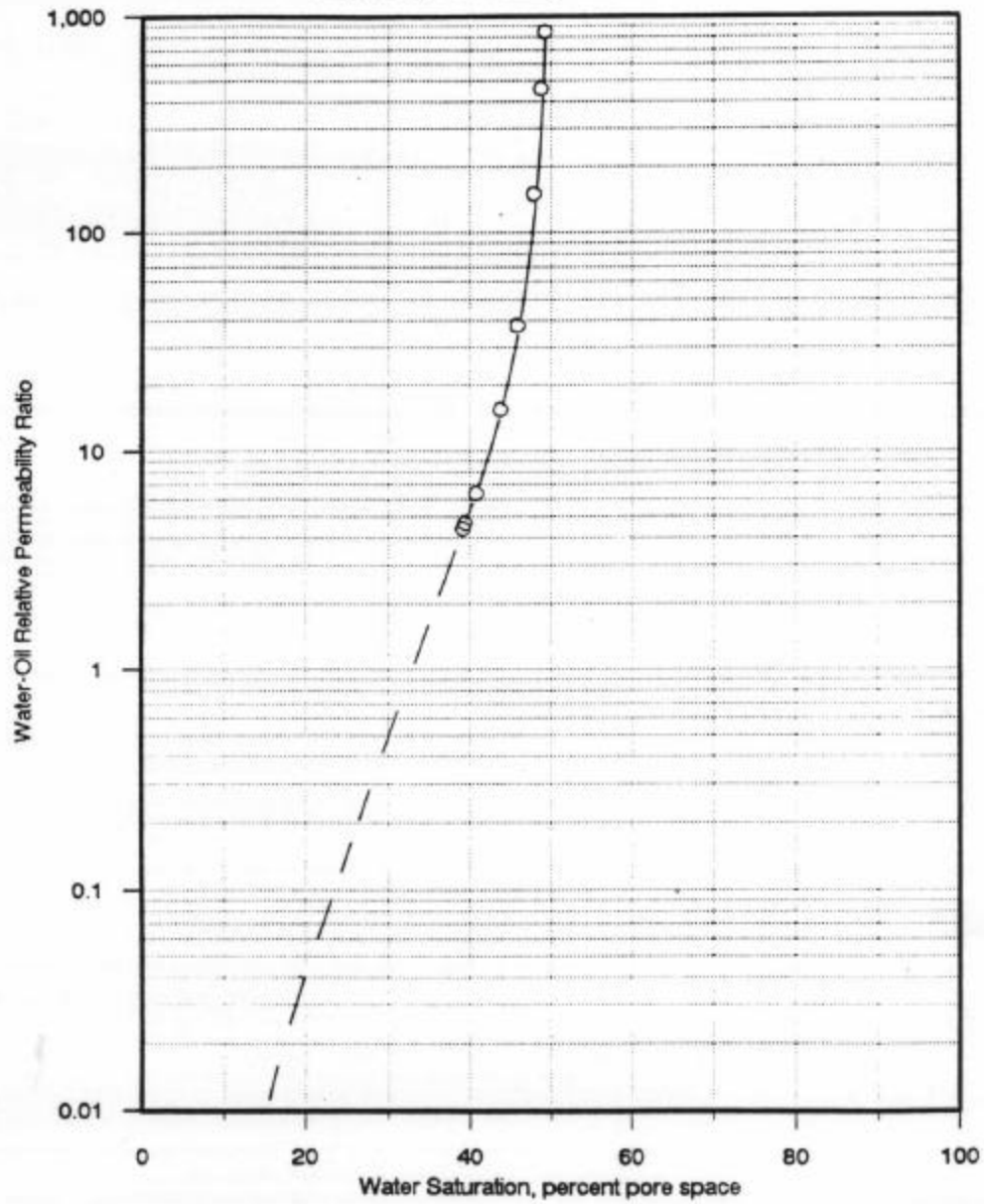
\* Relative to the Effective Permeability to Oil at Initial Water Saturation



**UNSTEADY-STATE WATER-OIL RELATIVE PERMEABILITY**

Sample I.D.: E1-14

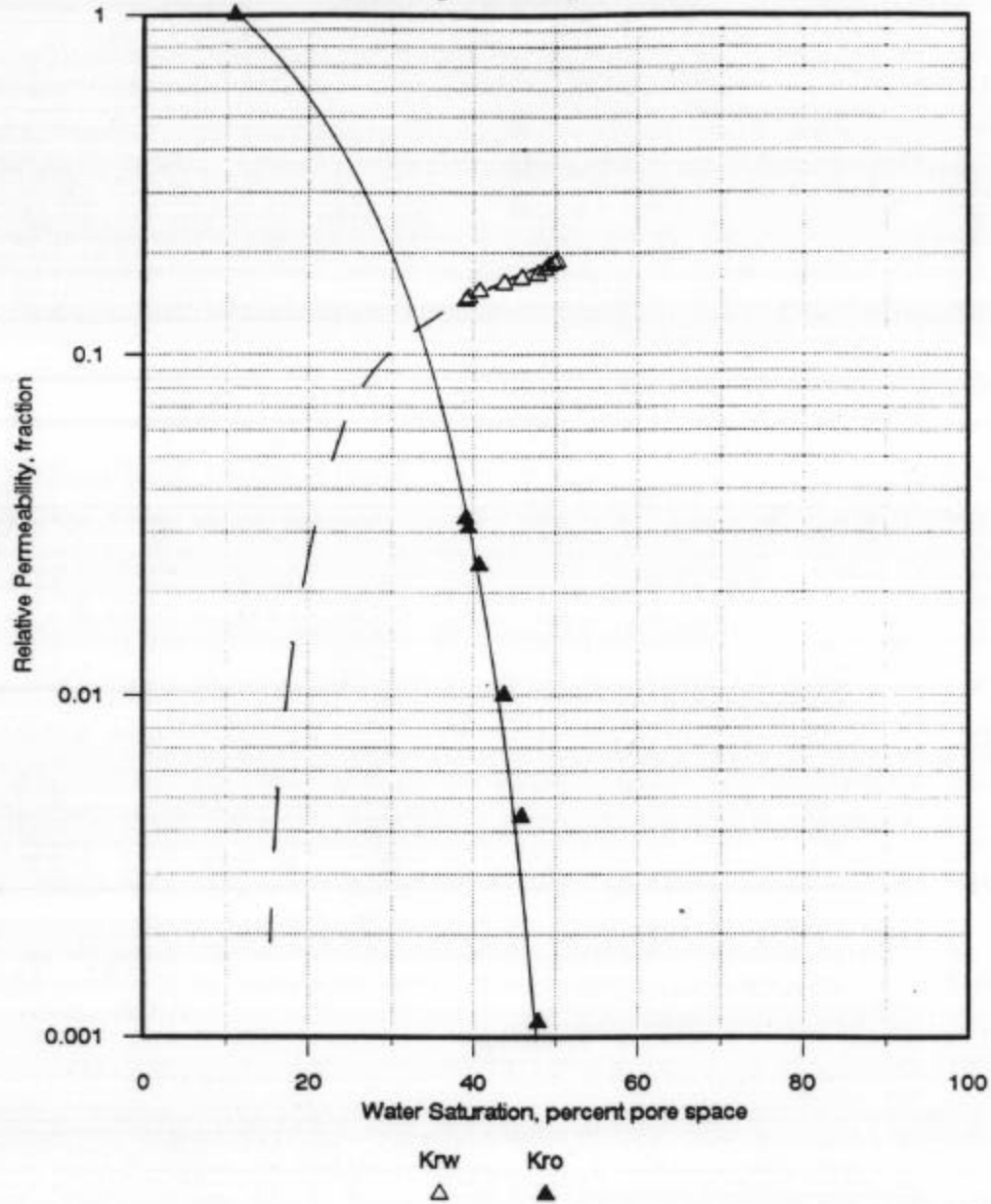
Klinkenberg Permeability: 56.2 md



**UNSTEADY-STATE WATER - OIL RELATIVE PERMEABILITY**

Sample I.D.: E1-14

Kirkenberg Permeability: 56.2 md



SUMMARY OF DIMENSIONLESS GROUPS

Fina Oil and Chemical Company

Sample I.D.: E1-14

## Input Information

Interfacial Tension, dynes/cm (IFT)	30.2
Porosity, fraction ( $\phi$ )	0.178
Effective Permeability to Oil at $S_{wi}$ , md ( $K_o$ )	20.8
Viscosity of Oil, cp ( $\mu_o$ )	2.100
Viscosity of Brine, cp ( $\mu_w$ )	0.800
Flow Rate, cc/min	3.00
Length, cm (L)	6.45
Diameter, cm (D)	3.81
Area, cm <sup>2</sup>	11.39
Velocity, cm/sec (v)	2.47E-02
Relative Permeability to Oil, fraction ( $k_{ro}$ )	6.50E-05
Relative Permeability to Water, fraction ( $k_{rw}$ )	0.185
Density of Oil, grams/cc ( $\rho_o$ )	0.803
Density of Water, grams/cc ( $\rho_w$ )	1.043
Gravity, cm/sec <sup>2</sup> (g)	978

## Capillary End-Effect Number

$$N_c, \text{ end} = [\text{IFT} * \text{SQRT}(\phi * K_o)] / (\mu_w * v * L)$$

$$= 457$$

## Microscopic Capillary Number

$$N_c = (\mu_w * v) / \text{IFT}$$

$$= 6.53\text{E-}04$$

## Mobility Ratio

$$M = (k_{rw} * \mu_o) / (k_{ro} * \mu_w)$$

$$= 7471$$

## Effective Aspect Ratio

$$R1 = \text{SQRT}(L/D * K_o/K_o) \quad R1 = \text{SQRT}(L/D * K_w/K_o)$$

$$= 2.54 \quad = 0.560$$

## Buoyancy to Viscous Ratio

$$N_g = (K_o * k_{rw} * (\rho_w - \rho_o) * g) / (\mu_o * v) * (L/D)$$

$$= 29489$$

## Density Number

$$N_p = (\rho_w - \rho_o) / \rho_o \quad N_p = (\rho_w - \rho_o) / \rho_w$$

$$= 0.298 \quad = 0.230$$

SUMMARY OF DIMENSIONLESS GROUPS

Fina Oil and Chemical Company

Sample I.D.: E1-14

## Input Information

Interfacial Tension, dynes/cm (IFT)	30.2
Porosity, fraction ( $\phi$ )	0.178
Effective Permeability to Oil at $S_{wi}$ , md ( $K_o$ )	20.8
Viscosity of Oil, cp ( $\mu_o$ )	2.100
Viscosity of Brine, cp ( $\mu_w$ )	0.800
Flow Rate, cc/min	3.00
Length, cm (L)	6.45
Diameter, cm (D)	3.81
Area, cm <sup>2</sup>	11.39
Velocity, cm/sec (v)	2.47E-02
Relative Permeability to Oil, fraction ( $k_{ro}$ )	6.50E-05
Relative Permeability to Water, fraction ( $k_{rw}$ )	0.185
Density of Oil, grams/cc ( $\rho_o$ )	0.803
Density of Water, grams/cc ( $\rho_w$ )	1.043
Gravity, cm/sec <sup>2</sup> (g)	978

## Capillary End-Effect Number

$$N_c, \text{ end} = \frac{IFT * \text{SQRT}(\phi * K_o)}{\mu_w * v * L}$$

$$= 457$$

## Microscopic Capillary Number

$$N_c = (\mu_w * v) / IFT$$

$$= 6.53E-04$$

## Mobility Ratio

$$M = (k_{rw} * \mu_o) / (k_{ro} * \mu_w)$$

$$= 7471$$

## Effective Aspect Ratio

$$R_1 = \text{SQRT}(L/D * K_o/K_o) \quad R_1 = \text{SQRT}(L/D * K_w/K_o)$$

$$= 2.54 \quad = 0.560$$

## Buoyancy to Viscous Ratio

$$N_g = (K_o * k_{rw} * (\rho_w - \rho_o) * g) / (\mu_o * v) * (L/D)$$

$$= 29489$$

## Density Number

$$N_p = (\rho_w - \rho_o) / \rho_o \quad N_p = (\rho_w - \rho_o) / \rho_w$$

$$= 0.298 \quad = 0.230$$

## **SECTION 5**

### **Data Reduction and Error Analyses for Steady-State Relative Permeability and Tertiary Oil Recovery Tests**

## DATA REDUCTION SUMMARY

## Steady-State Gas-Oil and Water-Oil Displacement

## Permeability to Liquid Calculations

Permeabilities to liquid are calculated from observed flow rate and differential pressure data using Darcy's law as follows:

$$K_l = (C_1 * C_2 * L * u_l * Q) / (P * C_3 * A)$$

where:

- $K_l$  = Permeability to liquid, millidarcies
- $C_1$  = Constant, psi/atm
- $C_2$  = Constant, millidarcies/darcy
- $L$  = Length, cm
- $u_l$  = Viscosity of liquid, cp
- $Q$  = Flow rate, cc/min
- $P$  = Differential pressure, psi
- $C_3$  = Constant, sec/min
- $A$  = Area, cm<sup>2</sup>

## Saturation Determinations

Saturations are determined by the X-ray attenuation method where X-ray scans measured at each saturation are combined with base scans at 100% saturations by the following equations:

$$Sg_x = 100 - Sw_i - (100 - Sw_i) * \frac{\log(scan_x) - \log(scan_w)}{\log(scan_o) - \log(scan_w)}$$

$$Sw_x = \frac{\log(scan_x) - \log(scan_w)}{\log(scan_o) - \log(scan_w)}$$

where:

- $Sg_x$  = Gas Saturation at event x, percent pore space
- $Sw_x$  = Water Saturation at event x, percent pore space
- $Sw_i$  = Initial Water Saturation, percent pore space
- $scan_x$  = X-ray scan at event x, counts
- $scan_o$  = X-ray scan at 100% gas saturation, counts
- $scan_o$  = X-ray scan at 100% oil saturation, counts
- $scan_w$  = X-ray scan at 100% water saturation, counts

## DATA REDUCTION SUMMARY

## Unsteady-State Tertiary Oil Recovery Test

## Permeability to Liquid Calculations

Permeabilities to liquid are calculated from observed flow rate and differential pressure data using Darcy's law as follows:

$$K_l = (C_1 * C_2 * L * u_l * Q) / (P * C_3 * A)$$

where:

- $K_l$  = Permeability to liquid, millidarcies
- $C_1$  = Constant, psi/atm
- $C_2$  = Constant, millidarcies/darcy
- $L$  = Length, cm
- $u_l$  = Viscosity of liquid, cp
- $Q$  = Flow rate, cc/min
- $P$  = Differential pressure, psi
- $C_3$  = Constant, sec/min
- $A$  = Area,  $\text{cm}^2$

## Residual Fluid Saturations after Gasflood

Residual Water Saturation

The residual water saturation is determined using a Karl Fischer titration of the toluene and methanol effluent mixture from the sample cleaning. The water content of a check solution is measured for quality control purposes. Then the baseline water content values of the toluene and methanol are determined, and followed by duplicate measurements of the water content of the effluent. Finally, the check solution is measured again. The average of the effluent measurements is used in the calculation as follows:

$$\text{Wgt}_x = \text{Wgt}_{\text{eff}} * \text{WC}_{\text{eff}} - \text{Wgt}_{\text{tol}} * \text{WC}_{\text{tol}} - \text{Wgt}_{\text{met}} * \text{WC}_{\text{met}}$$

$$\text{SW}_r = [(\text{Wgt}_x + \text{BD}) * \text{VCF} * V_b/V_w] * 100 / \text{PV}$$

where:

- $\text{Wgt}_x$  = Weight of water from sample, grams
- $\text{Wgt}_{\text{eff}}$  = Weight of total effluent, grams
- $\text{Wgt}_{\text{tol}}$  = Weight of toluene in effluent, grams
- $\text{Wgt}_{\text{met}}$  = Weight of methanol in effluent, grams
- $\text{WC}_{\text{eff}}$  = Water content of effluent, percent
- $\text{WC}_{\text{tol}}$  = Water content of toluene, percent
- $\text{WC}_{\text{met}}$  = Water content of methanol, percent
- $\text{SW}_r$  = Residual water saturation, percent pore space
- $\text{BD}$  = Blowdown water, grams
- $\text{VCF}$  = Volume correction factor,  $\text{cc}^{2000 \text{ psi} + 98^\circ\text{F}} / \text{cc}^{14.7 \text{ psi} + 72^\circ\text{F}}$
- $V_b/V_w$  = Volume brine/volume water, cc/cc
- $\text{PV}$  = Pore volume, cc

## DATA REDUCTION SUMMARY (continued)

## Unsteady-State Tertiary Oil Recovery Test

Residual Gas Saturation

The residual gas saturation is determined by measuring the void volume of the sample following post-test blowdown and cooling using a helium porosimeter and subtracting any blowdown fluid volumes as follows:

$$S_{g_r} = [(VV - BD) * 100]/PV$$

where:  $S_{g_r}$  = Residual gas saturation, percent pore space  
 $VV$  = Void volume, cc  
 $BD$  = Blowdown volume water and oil, cc  
 $PV$  = Pore volume of sample x, cc

Residual Oil Saturation

The residual oil saturation is determined by material balance as follows:

$$S_{o_r} = 100 - S_{w_r} - S_{g_r}$$

where:  $S_{o_r}$  = Residual oil saturation sample x, percent pore space  
 $S_{w_r}$  = Residual water saturation sample x, percent pore space  
 $S_{g_r}$  = Residual gas saturation sample x, percent pore space

Residual Fluid Saturations after Waterflood

The residual fluid saturations after waterflood are determined by displacing the in place undoped brine at the end of the waterflood with tritium doped brine and then the tritium doped brine with undoped brine. Effluent samples are collected and analyzed for tritium content as outlined below.

1. Undoped blank (taken from produced effluent immediately prior to displacement)
2. Doped blank (taken from bypassed effluent immediately prior to displacement)
3. 5 pore volumes of effluent from doped brine displacing undoped
4. 1 additional pore volume of effluent from doped brine displacing undoped
- 4a. 1 additional pore volume of effluent from doped brine displacing undoped
5. Second undoped blank (taken from bypassed effluent immediately prior to displacement)
6. 5 pore volumes of effluent from undoped brine displacing doped
7. 1 additional pore volume of effluent from undoped brine displacing doped.
- 7a. 1 additional pore volume of effluent from undoped brine displacing doped.



## DATA REDUCTION SUMMARY (continued)

## Unsteady-State Tertiary Oil Recovery Test

The brine content from the sample is first determined using the doped brine displacing undoped brine values as follows:

$$X = [V * (A - U)] / (D - U)$$

where: A = Analysis in counts/cc (Sample 3)  
 X = cc Doped Brine in Effluent Sample  
 U = Counts/cc of Undoped blank (Sample 1)  
 D = Counts/cc of Doped blank (Sample 2)  
 V = Volume of Effluent Sample, cc

The reported brine content from the sample is determined using the undoped brine displacing doped brine values as follows:

$$F = [V * (B - U)] / (D - U) + [V * (C - U)] / (D - U) + [V * (E - U)] / (D - U)$$

where: B = Counts/cc (Sample 6)  
 F = cc Undoped Brine in Effluent Sample  
 U = Counts/cc of Undoped blank (Sample 1)  
 D = Counts/cc of Doped blank (Sample 4a)  
 C = Counts/cc (Sample 7)  
 E = Counts/cc (Sample 7a)  
 V = Volume of Effluent Sample, cc

The determined volume of brine is corrected to reservoir conditions and the waterflood residual saturations determined as follows:

$$Sw_r = (B * VCF * V_b/V_w) * 100/PV$$

$$So_r = 100 - Sw_r$$

where:  $Sw_r$  = Residual water saturation, percent pore space  
 $So_r$  = Residual oil saturation, percent pore space  
 B = Volume of brine from tritium analysis, cc  
 VCF = Volume correction factor,  $cc^{2000 \text{ psi} + 98^\circ F} / cc^{14.7 \text{ psi} + 72^\circ F}$   
 $V_b/V_w$  = Volume brine/volume water, cc/cc  
 PV = Pore volume of sample x, cc

## Gasflood Oil Recovery

Gasflood oil recovery is determined by material balance as follows:

$$Ro_{gf} = So_{rwf} - So_{rgf}$$

where:  $Ro_{gf}$  = Gasflood oil recovery, percent pore space  
 $So_{rwf}$  = Waterflood residual oil saturation, percent pore space  
 $So_{rgf}$  = Gasflood residual oil saturation, percent pore space

**DATA REDUCTION SUMMARY (continued)**  
**Unsteady-State Tertiary Oil Recovery Test**

**Unsteady-State Water-Oil Relative Permeability**

During the waterflood, the incremental produced oil and water volumes, differential pressure drop, and cumulative time values are recorded. The produced volumes are corrected to reservoir conditions and all data are entered into Core Laboratories' Johnson-Bossler-Naumann based relative permeability calculation program. The calculated oil recovery is added to the waterflood residual oil saturation determined by tritium analysis to calculate the original oil in place and initial water saturation as follows:

$$S_{w_i} = 100 - R_{o_{wf}} - S_{o_{rwf}}$$

where:

$S_{w_i}$	= Initial water saturation, percent pore space
$R_{o_{wf}}$	= Waterflood oil recovery, percent pore space
$S_{o_{rwf}}$	= Waterflood residual oil saturation, percent pore space

SUMMARY OF X-RAY ANALYSIS VALUES - DEAD VOLUME

Fina Oil and Chemical Company  
Emmons Unit

Dead Volume Measurement

<u>I.D.</u>	<u>Volume, cc</u>	<u>Analysis picocuries/l</u>
1	19.67	12900
2	19.89	48500000
3	47.28	41000000
4	18.91	84200000
4a	18.70	47800000
5	19.59	27600
6	47.09	6660000
7	20.98	4900
7a	20.40	96300

58.76 cc doped brine in Effluent Sample  
7.43 cc undoped brine in Effluent Samples

DV, cc = 7.43 brine in sample

For undoped Brine displacing Doped Brine

6.60 cc doped brine in Effluent Sample (from core)  
DV, cc = 6.60 brine in sample

PERMEABILITY TO LIQUID MEASUREMENT ERROR ANALYSIS

Fina Oil and Chemical Company

Sample I.D.: E1-6

<u>Input Parameter</u>	<u>Accuracy (+/-)</u>	<u>units</u>	<u>Example Values</u>	<u>(E1-1 Ko) Maximum</u>	<u>Minimum</u>
Constant, psi/atm	0.100 psi/atm		14.7	14.8	14.6
Length, cm	0.010 cm		4.91	4.92	4.90
Vicosity, cp	0.002 cp		0.800	0.802	0.798
Flow Rate, cc/min	0.010 cc/min		0.85	0.86	0.84
Constant, sec/min	0.000 sec/min		60.000	60.000	60.000
Delta Pressure, psi	1.0 % full scale		163	173	153
Area, cm <sup>2</sup>	0.003 cm <sup>2</sup>		11.45	11.45	11.45
Permeability, md			0.439	0.423	0.457
Percentage Difference				3.6	-4.1

STEADY-STATE SATURATION ERROR ANALYSIS

Fina Oil and Chemical Company

Sample I.D.: E1-6

<u>Reported Values</u>	<u>Minimum Values</u>	<u>Maximum Values</u>	<u>Absolute Value of Difference</u>
10.2%	12.6%	9.7%	2.9
41.0%	42.7%	43.0%	0.4
43.9%	45.4%	46.0%	0.5
45.6%	47.1%	47.7%	0.7
48.9%	50.3%	52.0%	1.7
51.1%	49.7%	51.6%	1.9
56.3%	54.2%	57.6%	3.4
58.8%	54.7%	59.6%	5.0
62.9%	63.9%	63.9%	0.1
100.0%	100.0%	100.0%	0.0
0.0%	0.0%	0.0%	0.0
58.6%	58.2%	61.0%	2.8
55.5%	52.9%	56.2%	3.3
55.2%	56.4%	57.2%	0.7
49.8%	51.2%	51.6%	0.3
47.6%	49.5%	48.1%	1.5
47.4%	46.7%	46.8%	0.2
46.4%	44.2%	45.3%	1.1
45.0%	46.5%	45.4%	1.1

Sample I.D.: EI-6 Emmons

5-9

UNSTEADY-STATE TRITIUM SATURATION ERROR ANALYSIS

Fina Oil and Chemical Company

Sample I.D.: E1-1

I.D.	Volume, cc	Volume Error (+/-)	Analysis, picocuries/l	Tritium Error (+/-)	Maximum Value	Minimum Value	
1.	17.18	0.02	650	148	798	502	Pore Volume: 4.97 cc
2.	24.92	0.02	4700000	9530	4709530	4690470	Dead Volume: 6.60 cc
3.	47.96	0.02	4000000	8830	4008830	3991170	
4.	20.25	0.02	4800000	9620	4809620	4790380	
4a.	24.39	0.02	4800000	9660	4809660	4790340	
5.	22.10	0.02	20800	644	21444	20156	
6.	45.38	0.02	994000	4030	998030	989970	
7.	20.92	0.02	29900	765	30665	29135	
7a.	18.36	0.02	13400	518	13918	12882	
			<u>Reported</u>	<u>Maximum</u>	<u>Minimum</u>		
			61.50	61.54	61.45 cc doped brine in Effluent Sample		
			6.71	6.67	6.76 cc undoped brine in Effluent Sample (from Core)		
			0.05	0.01	0.10 cc brine in sample		
			1.1	0.2	2.0 percent		
			100 - Sw		98.0 percent		
			98.9	99.8			

For Undoped Brine Displacing Doped Brine

Sw, cc =	9.57	9.59	9.54 cc doped brine in Effluent Sample (from Core)
Sw, percent =	2.97	2.99	2.94 cc brine in sample
Sor, percent =	59.7	60.2	59.2 percent
	100 - Sw		
	40.3	39.8	40.8 percent

KARL FISCHER WATER CONTENT MEASUREMENT ERROR ANALYSIS

Fina Oil and Chemical Company

## Karl Fischer Analyses

Repeat Analyses	(1)	(2)	Error, +/- %
Check Solution	0.1175	0.1193	1.5
Effluent	1.192	1.179	1.1

Weight Acceptance Criteria are +/- 0.1 grams in this range.

	<u>Reported</u>	<u>Maximum</u>	<u>Minimum</u>
Weight of Toluene, grams	98	98	98
Weight of Methanol, grams	113	113	113
Total Effluent Weight, grams	211	211	211

Weight Acceptance Criteria are +/- 0.0001 grams in this range.

Check Solution Weight, grams	0.5582	0.5583	0.5582
Analysis, % H2O	0.1175		
Toluene Solution Weight, grams	0.3828	0.3829	0.3828
Analysis, % H2O	0.0243	0.0248	0.0238
Calculated H2O Content, grams	0.0238	0.0243	0.0233
Methanol Solution Weight, grams	0.4849	0.4850	0.4849
Analysis, % H2O	0.0905	0.0923	0.0887
Calculated H2O Content, grams	0.1023	0.1044	0.1002
Effluent Solution Weight, grams	0.4196	0.4197	0.4196
Analysis, % H2O	1.184	1.208	1.160
Calculated H2O Content, grams	2.498	2.549	2.448
Plug Sample Water Content, grams (Effluent - Toluene - Methanol)	2.37	2.42	2.32



CO<sub>2</sub> FLOOD RESIDUAL SATURATION CALCULATION ERROR ANALYSIS

Fina Oil and Chemical Company

Sample I.D.: E11-1

Helium Pore Volume and Void Volume Measurements

Acceptance Criteria for these measurements is +/- 0.3 percent.

	<u>Reported</u>	<u>Maximum</u>	<u>Minimum</u>
Pore Volume, cc	10.43	10.46	10.40
Void Volume, cc	6.20	6.22	6.18
Blowdown Water	1.17	1.19	1.15
Sample Residual Gas Saturation, % PS 100 * (Void Volume - Blowdown Water) / Pore Volume	48.2	48.1	48.4
KF Plug Sample Water Content, grams (Effluent - Toluene - Methanol)	2.37	2.42	2.32
Water Volume Correction Factor (VCF), cc/cc	1.009	1.019	0.999
Volume Brine/Volume Water (Vb/Vw), cc/cc	1.025	1.035	1.015
Sample Residual Water Saturation, % PS 100 * ((KF Water + Blowdown Water) * VCF * Vb/Vw) / (Pore Volume)	35.1	36.4	33.9
Sample Residual Oil Saturation, % PS (100 - Water Saturation - Gas Saturation)	16.7	15.5	17.7

FLUID PROPERTIES**Synthetic Brine**

Viscosity, cp: 0.8  
 Density, g/cc: @ 72°F 1.050  
 Resistivity, ohm-meters @ 98°F: 0.081

<u>Measured Resistance, ohms</u>	<u>Measured Temp. °F</u>	<u>Temp. °C</u>	<u>Resistance, ohms @ 25°C</u>
54.049	74.1	23.39	52.18
53.953	74.2	23.44	52.15

Average Resistance @ 25°C: 52.16

Correct to 98°F using ARP's equation

Where: R1 = Resistance at Temperature T1  
 R2 = Resistance at Temperature T2  
 T1 = Temperature T1  
 T2 = Temperature T2

$$R2 = R1 \times (T1 - 21.5) / (T2 - 21.5)$$

Resistance (98F, 36.67C) =

$$52.16 \times (23.42 + 21.5) / (36.67 + 21.5) = 40.28 \text{ ohms}$$

Resistivity, ohm-meters @ 98F = Resistance X Cell Constant

$$40.28 \times 0.002 = 0.081 \text{ ohm-meters @ 98°F}$$

**Dead Crude Oil**

Viscosity, cp at 98°F: 2.13

**Live Crude Oil**

Viscosity, cp at 98°F: 2.10  
 Gas-Oil Ratio, scf/STB: 240  
 Volume Correction Factor, cc/cc: 1.136

**SECTION 6**

**PORE VOLUME COMPRESSIBILITY TEST RESULTS**

HYDROSTATIC VOLUMETRIC REDUCTION

Parameters to Fit  
(Increasing Stress)

Fina Oil and Chemical Company  
Emmons Unit  
143 and 142 Wells

San Andres Formation  
Midland County, Texas

Sample E1-4:    a = -6.04586    b = 0.0004134    c = 1.258147    d = -0.097311

Sample E1-19:    a = -3.29035    b = 0.0001872    c = 0.674532    d = -0.049565

COMPRESSIBILITY DATA SUMMARY

Fina Oil and Chemical Company  
Emmons Unit Well E-143  
San Andres Formation  
Midland County, Texas

Sample Identification: E1-4  
Sample Depth: 4565.8 feet  
Klinkenberg Permeability: 2.86 md  
Porosity: 9.8 percent  
Sample Condition: 100 percent  $S_w$   
Saturant: SIMFORM Brine

Net Stress, psi	Raw VPO cm <sup>2</sup>	Modeled VPO, cm	<u>HYDROSTATIC</u>		Porosity, percent	Ch 1/PSI*E6	Cu 1/PSI*E6
			PV cm <sup>2</sup>	NPV Vp/Vpi			
800		6.5800	1.0000	9.80	5.93	3.67	
1000	-0.0071	-0.0078	6.5722	0.9988	9.79	7.46	4.62
1200	-0.018	-0.0176	6.5624	0.9973	9.78	8.24	5.10
1400	-0.0258	-0.0284	6.5516	0.9957	9.76	8.63	5.34
1600	-0.0335	-0.0397	6.5403	0.9940	9.75	8.72	5.40
1800	-0.0374	-0.0511	6.5289	0.9922	9.73	8.58	5.31
2000	-0.0413	-0.0623	6.5177	0.9905	9.72	8.37	5.18
2200	-0.0433	-0.0732	6.5068	0.9889	9.70	8.07	5.00
2400	-0.0459	-0.0837	6.4963	0.9873	9.69	7.63	4.72
2600	-0.053	-0.0936	6.4864	0.9858	9.68	7.10	4.39
2800	-0.0601	-0.1028	6.4772	0.9844	9.66	6.64	4.11
3000	-0.0711	-0.1114	6.4686	0.9831	9.65	6.19	3.83
3200	-0.0844	-0.1194	6.4606	0.9819	9.64	5.50	3.40
3400	-0.0936	-0.1265	6.4535	0.9808	9.63	5.04	3.12
3600	-0.0964	-0.133	6.4470	0.9798	9.62	4.42	2.74
3800	-0.1012	-0.1387	6.4413	0.9789	9.62	3.88	2.40
4000	-0.1065	-0.1437	6.4363	0.9782	9.61	3.26	2.02
4200	-0.1187	-0.1479	6.4321	0.9775	9.60	2.72	1.68
4400	-0.1303	-0.1514	6.4286	0.9770	9.60	2.18	1.35
4600	-0.1432	-0.1542	6.4258	0.9766	9.60	1.56	0.96
4800	-0.1561	-0.1562	6.4238	0.9763	9.59	1.09	0.67
5000	-0.1577	-0.1576	6.4224	0.9760	9.59		
4800	-0.1544	-0.1571	6.4229	0.9761	9.59		
4600	-0.1563	-0.1558	6.4242	0.9763	9.59		
4400	-0.159	-0.1542	6.4258	0.9766	9.60		
4200	-0.1517	-0.1524	6.4276	0.9768	9.60		
4000	-0.1449	-0.1502	6.4298	0.9772	9.60		
3800	-0.1375	-0.1479	6.4321	0.9775	9.60		
3600	-0.1359	-0.1452	6.4348	0.9779	9.61		
3400	-0.131	-0.1423	6.4377	0.9784	9.61		
3200	-0.1267	-0.1392	6.4408	0.9788	9.62		
3000	-0.1246	-0.1359	6.4441	0.9793	9.62		
2800	-0.1238	-0.1323	6.4477	0.9799	9.62		
2600	-0.1243	-0.1286	6.4514	0.9805	9.63		
2400	-0.1248	-0.1248	6.4552	0.9810	9.63		
2200	-0.1107	-0.1208	6.4592	0.9816	9.64		

COMPRESSIBILITY DATA SUMMARY

Fina Oil and Chemical Company  
Emmons Unit Well E-143  
San Andres Formation  
Midland County, Texas

Sample Identification: E1-4 (cont'd)  
Sample Depth: 4565.8 feet  
Klinkenberg Permeability: 2.86 md  
Porosity: 9.8 percent  
Sample Condition: 100 percent  $S_w$   
Saturant: SIMFORM Brine

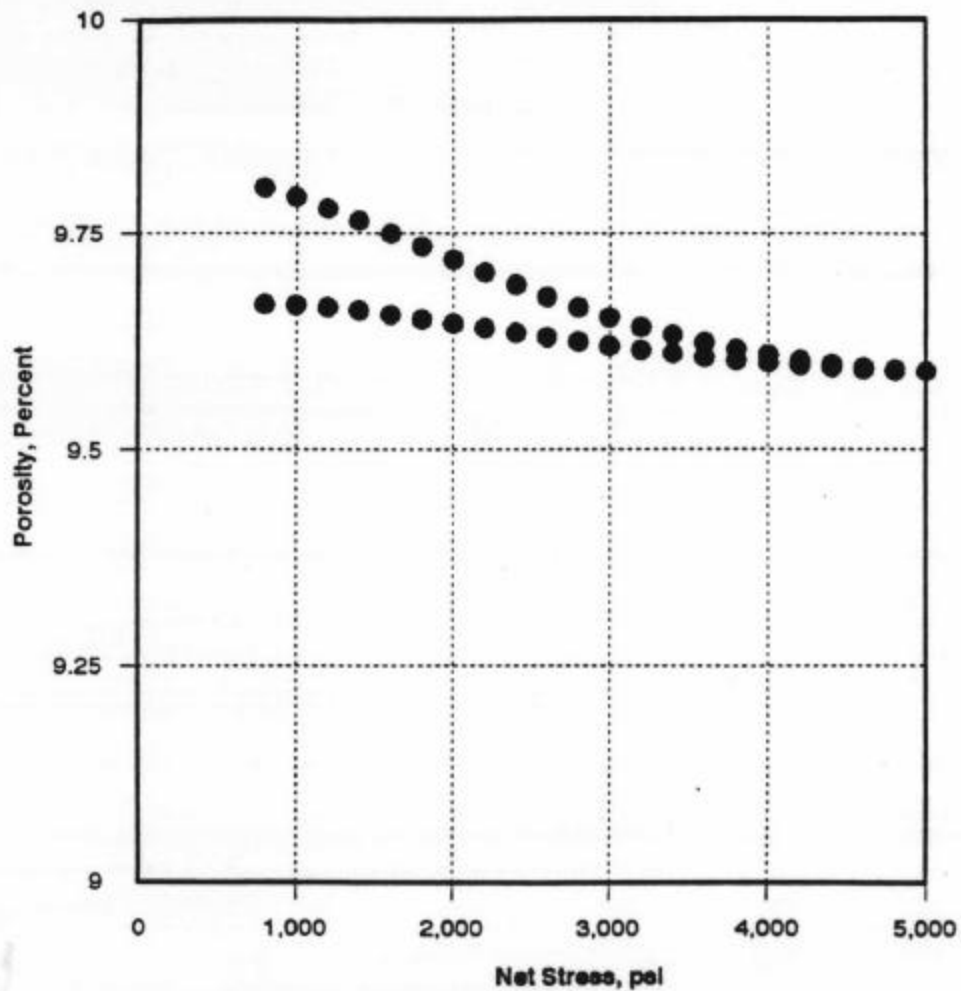
Net Stress, psi	Raw VPO, cm <sup>2</sup>	Modeled VPO, cm	HYDROSTATIC		Porosity, percent	Ch 1/PSI*E6	Cu 1/PSI*E6
			PV cm <sup>2</sup>	NPV Vp/Vpi			
2000	-0.1072	-0.1168	6.4632	0.9822	9.65		
1800	-0.1139	-0.1129	6.4671	0.9828	9.65		
1600	-0.1097	-0.1092	6.4708	0.9834	9.66		
1400	-0.1111	-0.1058	6.4742	0.9839	9.66		
1200	-0.1101	-0.1030	6.4770	0.9843	9.66		
1000	-0.1078	-0.1010	6.4790	0.9847	9.67		
800	-0.1003	-0.1003	6.4797	0.9848	9.67		

## Porosity vs Net Stress

Constant Pore Pressure - Changing Confining Pressure

FINA OIL AND CHEMICAL COMPANY  
WELL E-143  
SAN ANDRES FORMATION  
EMMONS UNIT  
MIDLAND COUNTY, TEXAS

SAMPLE ID: E1-4  
SAMPLE DEPTH, feet: 4565.8  
KLINKENBERG PERM., md: 2.86  
POROSITY, percent: 9.8  
SAMPLE CONDITION: 100% Sw  
SATURANT: SIMFORM



STRESS: Hydrostatic

Core Laboratories

COMPRESSIBILITY DATA SUMMARY

Fina Oil and Chemical Company  
Emmons Unit Well E-142  
San Andres Formation  
Midland County, Texas

Sample Identification: E1-19  
Sample Depth: 4666.8 feet  
Klinkenberg Permeability: 1.99 md  
Porosity: 9.6 percent  
Sample Condition: 100 percent  $S_w$   
Saturant: SIMFORM Brine

Net Stress, psi	Raw VPO cm <sup>2</sup>	Modeled VPO, cm	HYDROSTATIC		Porosity, percent	Ch	Cu
			PV cm <sup>2</sup>	NPV Vp/Vpi		1/PSI*E6	1/PSI*E6
800	0.0000	7.9550	1.0000	9.62	3.40	2.10	
1000	-0.0056	-0.0054	7.9496	0.9993	9.62	4.03	2.49
1200	-0.0109	-0.0118	7.9432	0.9985	9.61	4.60	2.85
1400	-0.0218	-0.0191	7.9359	0.9976	9.60	4.85	3.00
1600	-0.0314	-0.0268	7.9282	0.9966	9.59	4.98	3.09
1800	-0.0404	-0.0347	7.9203	0.9956	9.59	5.12	3.17
2000	-0.0493	-0.0428	7.9122	0.9946	9.58	5.12	3.17
2200	-0.0596	-0.0509	7.9041	0.9936	9.57	5.00	3.09
2400	-0.0692	-0.0588	7.8962	0.9926	9.56	4.94	3.06
2600	-0.0788	-0.0666	7.8884	0.9916	9.55	4.82	2.98
2800	-0.0859	-0.0742	7.8808	0.9907	9.54	4.63	2.87
3000	-0.0929	-0.0815	7.8735	0.9898	9.53	4.45	2.75
3200	-0.1000	-0.0885	7.8665	0.9889	9.53	4.32	2.68
3400	-0.1013	-0.0953	7.8597	0.9880	9.52	4.07	2.52
3600	-0.1045	-0.1017	7.8533	0.9872	9.51	3.95	2.44
3800	-0.1077	-0.1079	7.8471	0.9864	9.51	3.70	2.29
4000	-0.1128	-0.1137	7.8413	0.9857	9.50	3.51	2.17
4200	-0.1192	-0.1192	7.8358	0.9850	9.49	3.32	2.05
4400	-0.1256	-0.1244	7.8306	0.9844	9.49	3.07	1.90
4600	-0.1301	-0.1292	7.8258	0.9838	9.48	2.94	1.82
4800	-0.1327	-0.1338	7.8212	0.9832	9.48	2.69	1.66
5000	-0.1378	-0.1380	7.8170	0.9827	9.47		
4800	-0.1378	-0.1370	7.8180	0.9828	9.47		
4600	-0.1385	-0.1356	7.8194	0.9830	9.48		
4400	-0.1385	-0.1341	7.8209	0.9831	9.48		
4200	-0.1378	-0.1324	7.8226	0.9834	9.48		
4000	-0.1340	-0.1305	7.8245	0.9836	9.48		
3800	-0.1301	-0.1284	7.8266	0.9839	9.48		
3600	-0.1269	-0.1261	7.8289	0.9841	9.49		
3400	-0.1224	-0.1236	7.8314	0.9845	9.49		
3200	-0.1199	-0.1210	7.8340	0.9848	9.49		
3000	-0.1173	-0.1181	7.8369	0.9852	9.49		
2800	-0.1154	-0.1151	7.8399	0.9855	9.50		
2600	-0.1122	-0.1120	7.8430	0.9859	9.50		
2400	-0.1090	-0.1087	7.8463	0.9863	9.51		
2200	-0.1045	-0.1052	7.8498	0.9868	9.51		



COMPRESSIBILITY DATA SUMMARY

Fina Oil and Chemical Company  
Emmons Unit Well E-142  
San Andres Formation  
Midland County, Texas

Sample Identification: E1-19 (cont'd)  
Sample Depth: 4666.8 feet  
Klinkenberg Permeability: 1.99 md  
Porosity: 9.6 percent  
Sample Condition: 100 percent  $S_w$   
Saturant: SIMFORM Brine

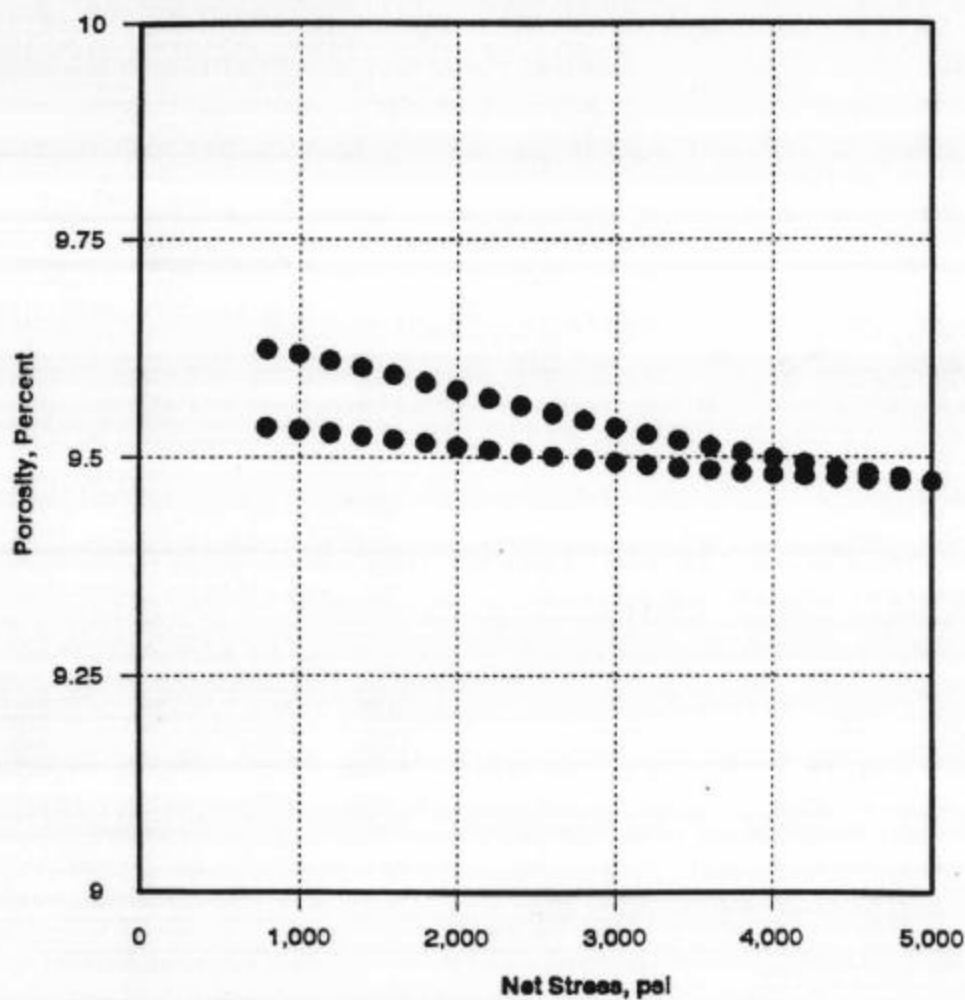
Net Stress, psi	Raw VPO cm <sup>2</sup>	Modeled VPO, cm	HYDROSTATIC		Porosity, percent	Ch 1/PSI*E6	Cu 1/PSI*E6
			PV cm <sup>2</sup>	NPV Vp/Vpi			
2000	-0.1025	-0.1017	7.8533	0.9872	9.51		
1800	-0.1013	-0.0980	7.8570	0.9877	9.52		
1600	-0.1013	-0.0944	7.8606	0.9881	9.52		
1400	-0.1038	-0.0908	7.8642	0.9886	9.52		
1200	-0.1058	-0.0874	7.8676	0.9890	9.53		
1000	-0.1058	-0.0842	7.8708	0.9894	9.53		
800	-0.0814	-0.0815	7.8735	0.9898	9.53		

## Porosity vs Net Stress

Constant Pore Pressure - Changing Confining Pressure

FINA OIL AND CHEMICAL COMPANY  
WELL E-142  
SAN ANDRES FORMATION  
EMMONS UNIT  
MIDLAND COUNTY, TEXAS

SAMPLE ID: E1-19  
SAMPLE DEPTH, feet: 4666.8  
KLINKENBERG PERM., md: 1.99  
POROSITY, percent: 9.6  
SAMPLE CONDITION: 100% Sw  
SATURANT: SIMFORM



STRESS: Hydrostatic

Core Laboratories

## **SECTION 7**

### **Mercury Injection Test Results**

PERMEABILITY, POROSITY AND GRAIN DENSITY

Fina Oil and Gas Company  
Emmons Unit  
E-142 and E-143 Wells

San Andres Formation  
Midland County, Texas

<u>Sample I.D.</u>	<u>Depth, feet</u>	<u>Permeability to Air, millidarcies</u>	<u>Porosity, percent</u>	<u>Grain Density, g/cm<sup>3</sup></u>
E1-1	4532.8	1.05	7.0	2.85
E1-3	4533.6	3.6	9.1	2.85
E1-4	4565.8	3.06	9.8	2.80
E1-6	4590.6	88	18.9	2.85
E1-7	4593.8	222	21.9	2.87
E1-10	4638.8	17	17.4	2.85
E1-11	4638.9	N/A	14.8	2.86
E1-14	4644.5	127	21.3	2.86
E1-15	4644.6	14.9	12.2	2.82
E1-19	4666.8	26.8	9.6	2.83

MERCURY INJECTION TEST RESULTS

## Pore Throat Distribution by Classification

Fina Oil and Gas Company  
Emmons Unit  
E-142 and E-143 Wells

San Andres Formation  
Midland County, Texas

Sample Number	Classification						
	<u>1</u>	<u>2</u>	<u>3</u>	<u>4</u>	<u>5</u>	<u>6</u>	<u>7</u>
	Controlled Pore Space, percent pore volume						
E1-1	12	10	27	12	27	12	-
E1-3	14	10	11	4	27	33	1
E1-6	13	4	15	10	26	32	-
E1-7	13	4	4	3	13	50	13
E1-10	18	1	4	5	32	39.5	0.50
E1-11	14	4	5	6.5	46	21.5	3
E1-14	12	2	2	2	12	68	2
E1-15	18	5	5	4	28	39	1

Classification Number	Pore Radius Classification	Pore Radius, microns	
		Minimum	Maximum
1	sub-nano	-	0.01
2	nano	0.01	0.05
3	sub-micro	0.05	0.25
4	micro	0.25	0.50
5	meso	0.50	2.5
6	macro	2.5	10
7	super-macro	10	-

SUMMARY OF MERCURY INJECTION DATA

Fina Oil and Gas Company  
Emmons Unit  
E-143 Well  
San Andres Formation  
Midland County, Texas

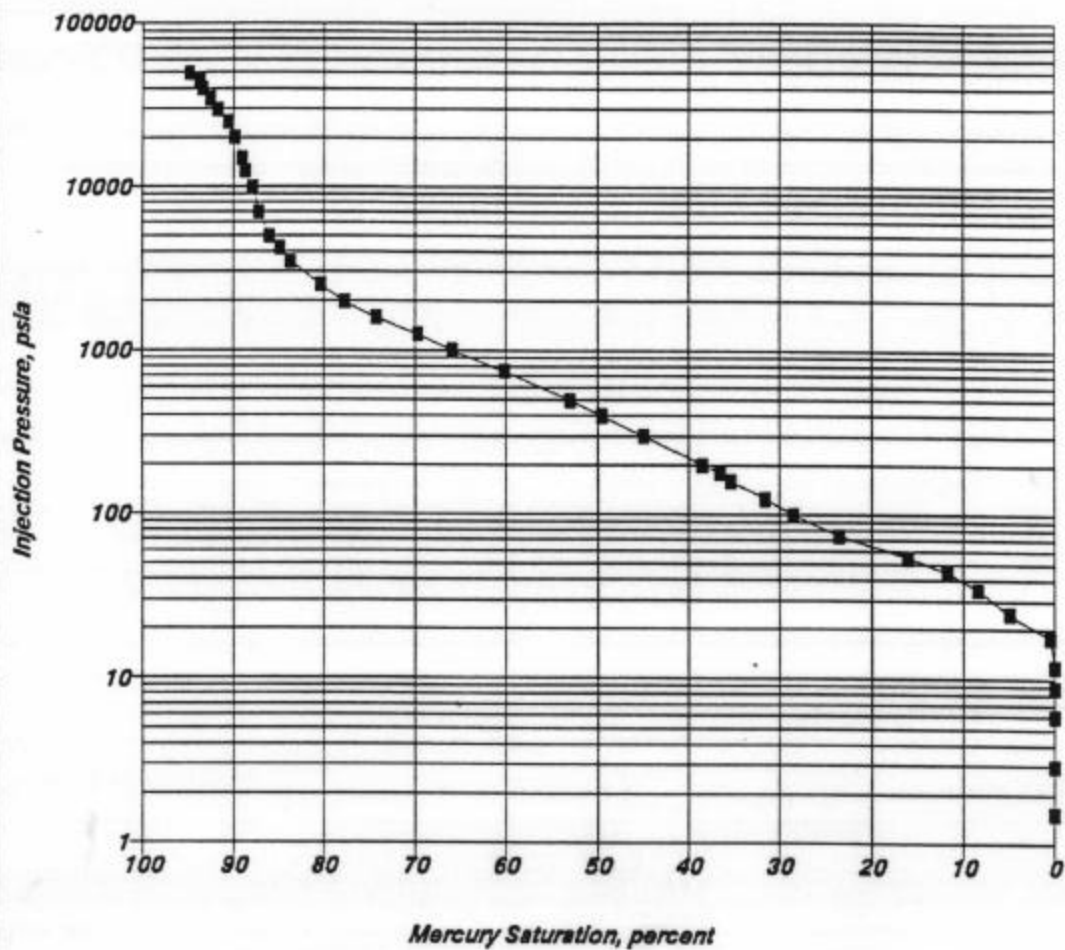
Sample I.D.: E1-1  
Porosity: 7.0 percent  
Permeability to Air: 105 md

Injection Pressure psia	Mercury Saturation percent	100-Mercury Saturation percent	Pore Radius microns	J Function dimensionless	Air/Brine System psia	Air/Oil System psia	Oil/Brine System psia
1.5	0.0	100.0	71.862	0.000	0.3	0.1	0.2
3.0	0.0	100.0	36.410	0.001	0.6	0.2	0.3
6.0	0.0	100.0	18.297	0.001	1.2	0.4	0.7
9.0	0.0	100.0	12.177	0.002	1.7	0.6	1.0
12.0	0.0	100.0	9.125	0.003	2.3	0.8	1.3
17.9	0.4	99.6	6.089	0.004	3.5	1.2	2.0
24.9	4.9	95.1	4.383	0.006	4.8	1.6	2.8
35.0	8.4	91.6	3.119	0.008	6.8	2.3	3.9
45.0	11.8	88.2	2.429	0.010	8.7	2.9	5.0
55.0	16.0	84.0	1.988	0.012	10.6	3.5	6.1
74.9	23.6	76.4	1.458	0.017	14.5	4.8	8.4
99.9	28.6	71.4	1.094	0.023	19.4	6.5	11.2
124.8	31.6	68.4	0.875	0.028	24.2	8.1	14.0
159.7	35.4	64.6	0.684	0.036	30.9	10.3	17.9
180.4	36.6	63.4	0.605	0.041	35.0	11.7	20.2
200.1	38.5	61.5	0.546	0.045	38.8	12.9	22.4
299.9	44.9	55.1	0.364	0.068	58.1	19.4	33.6
401.7	49.5	50.5	0.272	0.091	77.9	26.0	44.9
498.7	52.9	47.1	0.219	0.113	96.7	32.2	55.8
747.3	60.2	39.8	0.146	0.169	144.8	48.3	83.6
997.1	65.9	34.1	0.110	0.226	193.2	64.4	111.6
1254.4	69.7	30.3	0.087	0.284	243.1	81.0	140.3
1592.6	74.3	25.7	0.069	0.360	308.6	102.9	178.2
1990.5	77.7	22.3	0.055	0.450	385.8	128.6	222.7
2497.9	80.3	19.7	0.044	0.565	484.1	161.4	279.5
3489.4	83.8	16.2	0.031	0.789	676.2	225.4	390.4
4238.8	84.9	15.1	0.026	0.959	821.5	273.8	474.3
4979.4	86.1	13.9	0.022	1.126	965.0	321.7	557.1
6974.3	87.2	12.8	0.016	1.578	1351.6	450.5	780.3
9956.8	88.0	12.0	0.011	2.252	1929.6	643.2	1114.0
12438.0	88.7	11.3	0.009	2.814	2410.4	803.5	1391.6
14940.4	89.1	10.9	0.007	3.380	2895.3	965.1	1671.6
19968.4	89.9	10.1	0.005	4.517	3869.7	1289.9	2234.2
24901.8	90.6	9.4	0.004	5.633	4825.8	1608.6	2786.2
29862.3	91.8	8.2	0.004	6.755	5787.1	1929.0	3341.2
34888.4	92.5	7.5	0.003	7.892	6761.1	2253.7	3903.5
39852.7	93.3	6.7	0.003	9.015	7723.1	2574.4	4459.0
44809.3	93.7	6.3	0.002	10.136	8683.7	2894.6	5013.5
49767.9	94.8	5.2	0.002	11.258	9644.6	3214.9	5568.3

### *Injection Pressure vs Mercury Saturation*

**Company :** Fina Oil and Chemical Company  
**Well :** E-143  
**Formation :** San Andres  
**Field :** N/A  
**County, State :** Midland County, Texas

**Sample No :** E1-1  
**Sample Depth, feet :** 4532.8  
**Permeability to Air, mD :** 1.05  
**Porosity, percent :** 7.0

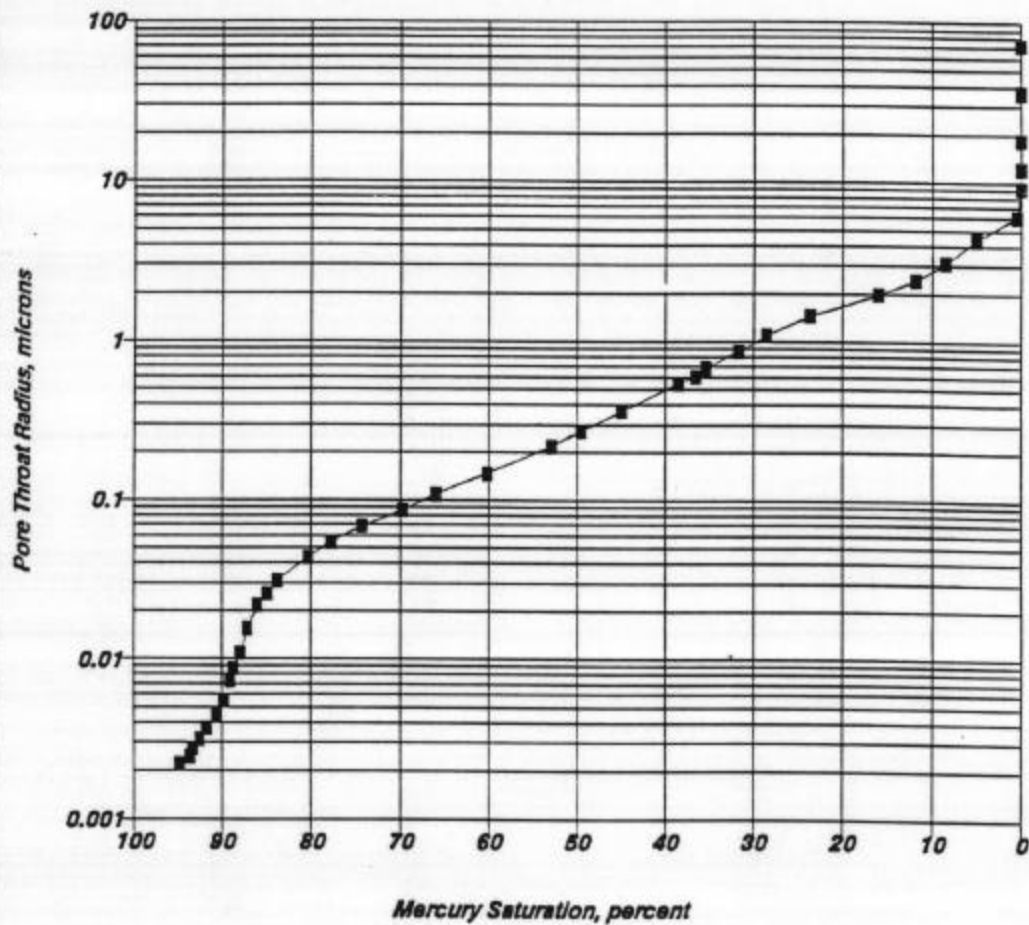


Core Laboratories

### *Pore Aperture Radius vs Mercury Saturation*

**Company:** Fina Oil and Chemical Company  
**Well:** E-143  
**Formation:** San Andres  
**Field:** N/A  
**County, State:** Midland County, Texas

**Sample No:** E1-1  
**Sample Depth, feet:** 4532.8  
**Permeability To Air, mD:** 1.05  
**Porosity, percent:** 7.0

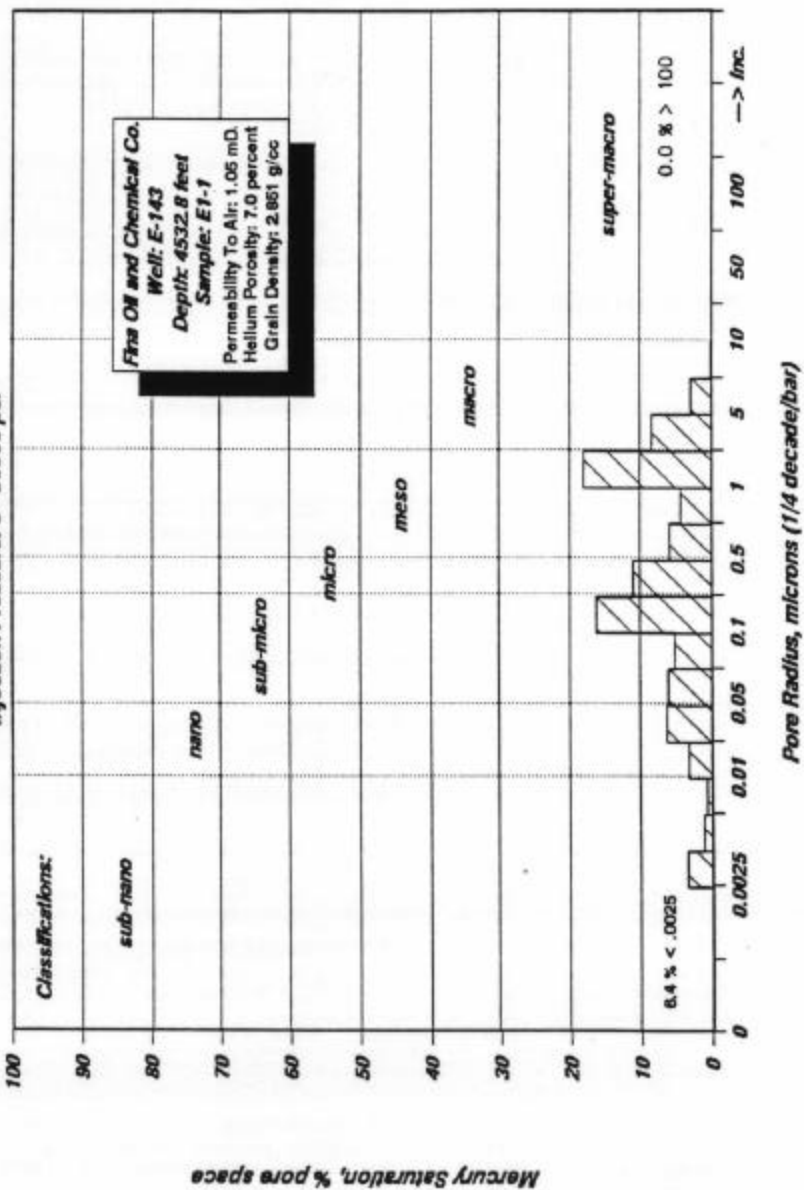


Core Laboratories



# **PORE SIZE DISTRIBUTION MERCURY INJECTION DATA**

Injection Pressure: 0 - 50000 psi



SUMMARY OF MERCURY INJECTION DATA

Fina Oil and Gas Company  
Emmons Unit  
E-143 Well  
San Andres Formation  
Midland County, Texas

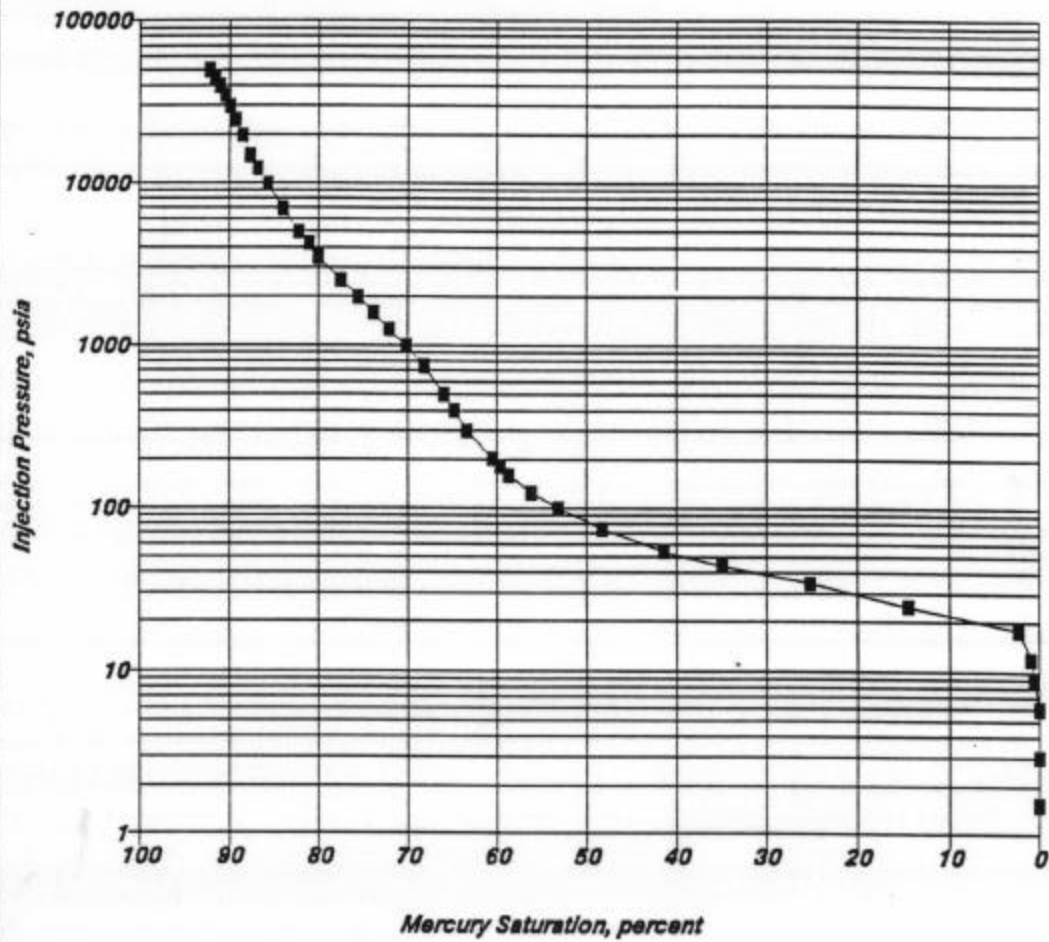
Sample I.D.: E1-3  
Porosity: 9.1 percent  
Permeability to Air: 3.6 md

Injection Pressure psia	Mercury Saturation percent	100-Mercury Saturation percent	Pore Radius microns	J Function dimensionless	Air/Brine System psia	Air/Oil System psia	Oil/Brine System psia
1.5	0.0	100.0	71.862	0.001	0.3	0.1	0.2
3.0	0.0	100.0	36.410	0.001	0.6	0.2	0.3
6.0	0.0	100.0	18.297	0.002	1.2	0.4	0.7
9.0	0.6	99.4	12.177	0.003	1.7	0.6	1.0
12.0	0.9	99.1	9.125	0.004	2.3	0.8	1.3
17.9	2.3	97.7	6.089	0.007	3.5	1.2	2.0
24.9	14.5	85.5	4.383	0.009	4.8	1.6	2.8
34.6	25.3	74.7	3.157	0.013	6.7	2.2	3.9
44.4	34.9	65.1	2.462	0.016	8.6	2.9	5.0
54.3	41.4	58.6	2.013	0.020	10.5	3.5	6.1
74.3	48.2	51.8	1.471	0.027	14.4	4.8	8.3
99.2	53.1	46.9	1.102	0.036	19.2	6.4	11.1
124.1	56.2	43.8	0.880	0.046	24.1	8.0	13.9
157.9	58.7	41.3	0.692	0.058	30.6	10.2	17.7
179.7	59.6	40.4	0.608	0.066	34.8	11.6	20.1
200.0	60.5	39.5	0.546	0.073	38.8	12.9	22.4
299.3	63.3	36.7	0.365	0.110	58.0	19.3	33.5
401.2	64.7	35.3	0.272	0.147	77.7	25.9	44.9
498.2	65.8	34.2	0.219	0.183	96.5	32.2	55.7
747.0	68.1	31.9	0.146	0.274	144.8	48.3	83.6
996.6	70.1	29.9	0.110	0.366	193.1	64.4	111.5
1253.8	72.1	27.9	0.087	0.461	243.0	81.0	140.3
1592.2	73.8	26.2	0.069	0.585	308.6	102.9	178.1
1990.2	75.5	24.5	0.055	0.731	385.7	128.6	222.7
2497.5	77.5	22.5	0.044	0.917	484.0	161.3	279.4
3489.0	80.0	20.0	0.031	1.282	676.1	225.4	390.4
4238.4	81.2	18.8	0.026	1.557	821.4	273.8	474.2
4979.2	82.3	17.7	0.022	1.829	964.9	321.6	557.1
6972.0	84.0	16.0	0.016	2.561	1351.1	450.4	780.1
9956.4	85.7	14.3	0.011	3.658	1929.5	643.2	1114.0
12439.5	86.8	13.2	0.009	4.570	2410.7	803.6	1391.8
14941.9	87.7	12.3	0.007	5.489	2895.6	965.2	1671.8
19971.8	88.5	11.5	0.005	7.337	3870.4	1290.1	2234.6
24901.4	89.4	10.6	0.004	9.148	4825.7	1608.6	2786.1
29861.9	90.0	10.0	0.004	10.970	5787.0	1929.0	3341.1
34887.9	90.5	9.5	0.003	12.816	6761.0	2253.7	3903.5
39852.2	91.1	8.9	0.003	14.640	7723.1	2574.4	4458.9
44812.7	91.7	8.3	0.002	16.463	8684.4	2894.8	5013.9
49769.4	92.2	7.8	0.002	18.283	9644.9	3215.0	5568.5

### *Injection Pressure vs Mercury Saturation*

**Company :** Fina Oil and Chemical Company  
**Well :** E-143  
**Formation :** San Andres  
**Field :** N/A  
**County, State :** Midland County, Texas

**Sample No :** E1-3  
**Sample Depth, feet :** 4533.6  
**Permeability to Air, mD :** 3.6  
**Porosity, percent :** 9.1

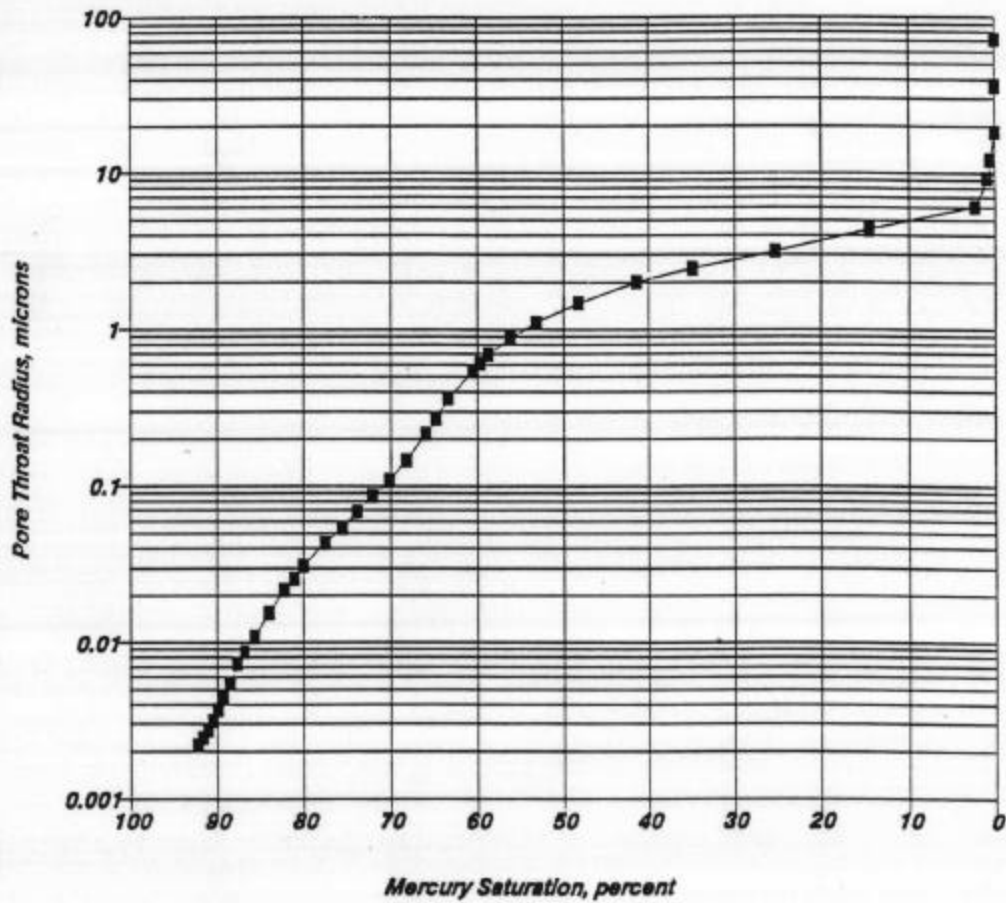


Core Laboratories

### *Pore Aperture Radius vs Mercury Saturation*

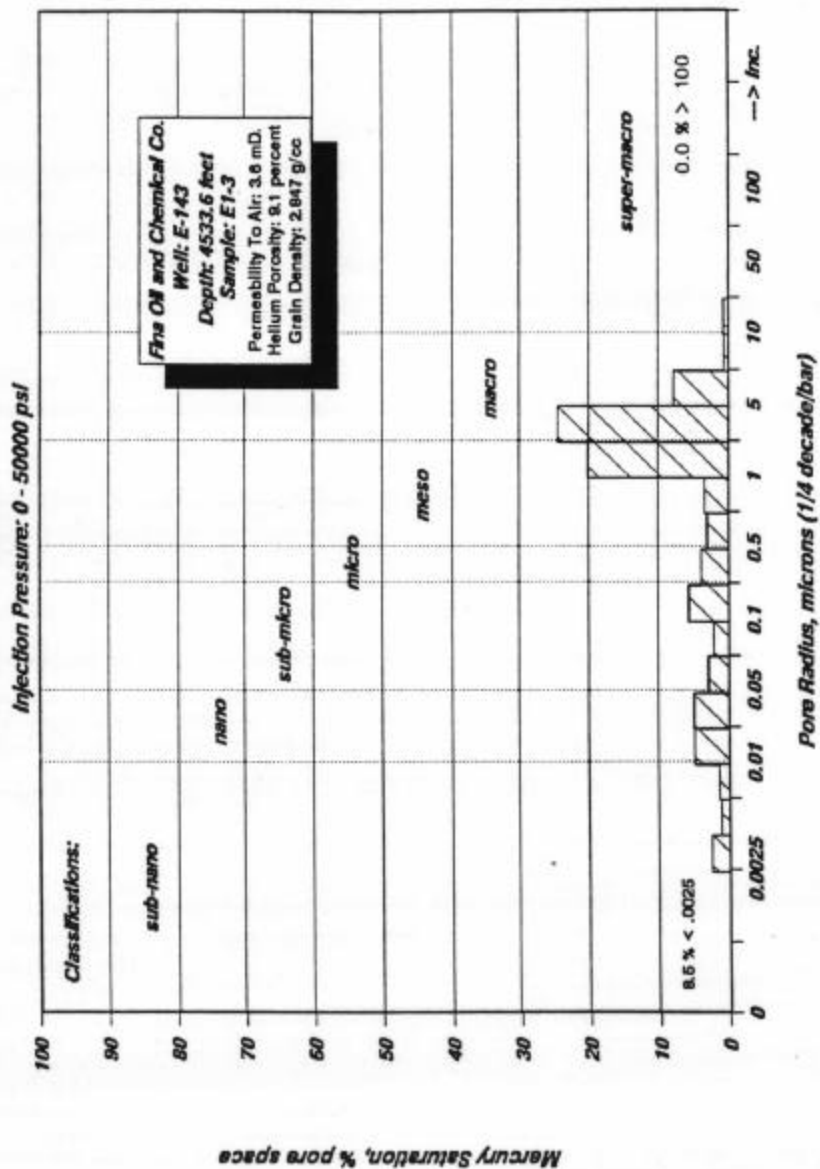
**Company:** Fina Oil and Chemical Company  
**Well:** E-143  
**Formation:** San Andres  
**Field:** N/A  
**County, State:** Midland County, Texas

**Sample No:** E1-3  
**Sample Depth, feet:** 4533.6  
**Permeability To Air, mD:** 3.6  
**Porosity, percent:** 9.1



Core Laboratories

# **PORE SIZE DISTRIBUTION MERCURY INJECTION DATA**



SUMMARY OF MERCURY INJECTION DATA

Fina Oil and Gas Company  
Emmons Unit  
E-143 Well  
San Andres Formation  
Midland County, Texas

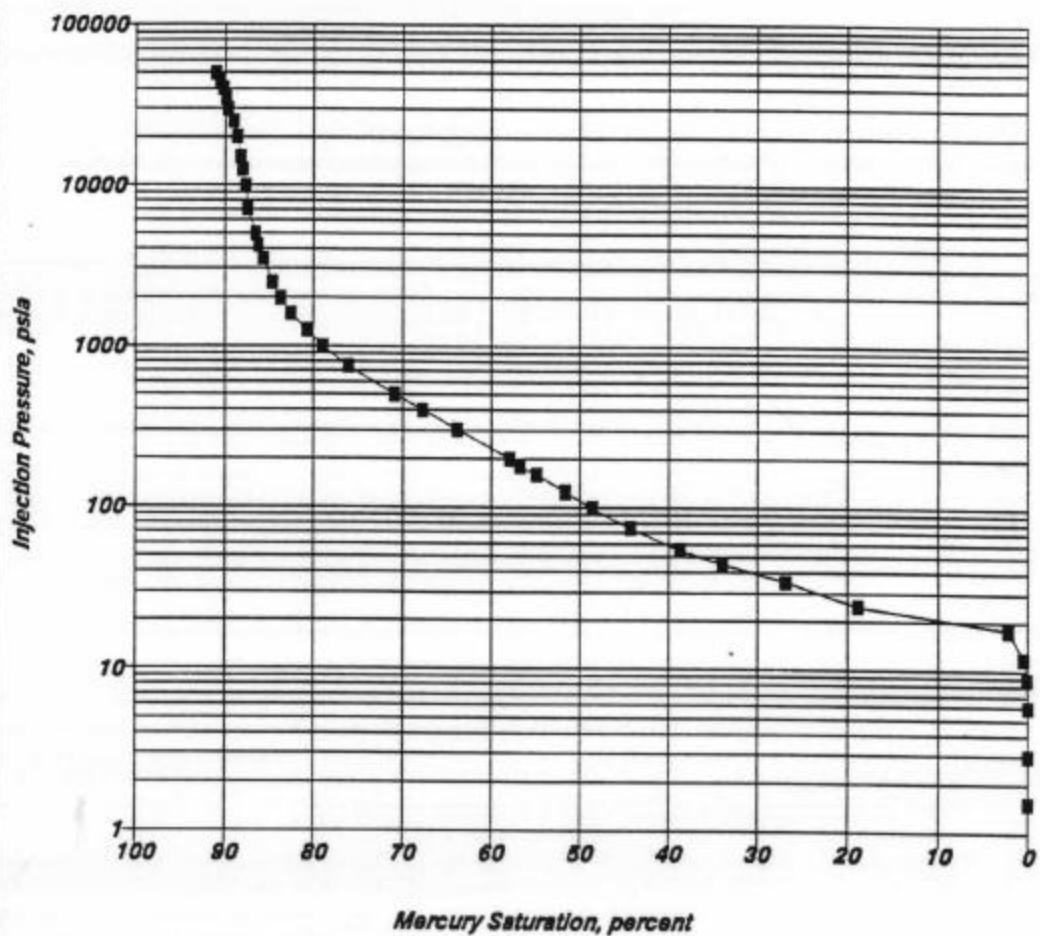
Sample I.D.: E1-6  
Porosity: 18.9 percent  
Permeability to Air: 88 md

Injection Pressure psia	Mercury Saturation percent	100-Mercury Saturation percent	Pore Radius microns	J Function dimensionless	Air/Brine System psia	Air/Oil System psia	Oil/Brine System psia
1.5	0.0	100.0	71.862	0.002	0.3	0.1	0.2
3.0	0.0	100.0	36.410	0.004	0.6	0.2	0.3
6.0	0.0	100.0	18.266	0.008	1.2	0.4	0.7
9.0	0.1	99.9	12.177	0.011	1.7	0.6	1.0
12.0	0.4	99.6	9.133	0.015	2.3	0.8	1.3
17.9	2.2	97.8	6.089	0.023	3.5	1.2	2.0
24.9	18.9	81.1	4.383	0.031	4.8	1.6	2.8
35.1	26.9	73.1	3.111	0.044	6.8	2.3	3.9
45.0	34.0	66.0	2.426	0.057	8.7	2.9	5.0
55.2	38.7	61.3	1.980	0.070	10.7	3.6	6.2
75.4	44.4	55.6	1.448	0.095	14.6	4.9	8.4
99.6	48.6	51.4	1.097	0.125	19.3	6.4	11.1
125.2	51.6	48.4	0.873	0.158	24.3	8.1	14.0
159.7	54.9	45.1	0.684	0.201	30.9	10.3	17.9
179.5	56.7	43.3	0.609	0.226	34.8	11.6	20.1
199.4	57.9	42.1	0.548	0.251	38.6	12.9	22.3
302.1	63.8	36.2	0.362	0.381	58.6	19.5	33.8
399.8	67.7	32.3	0.273	0.504	77.5	25.8	44.7
499.1	70.9	29.1	0.219	0.629	96.7	32.2	55.8
746.0	76.1	23.9	0.146	0.940	144.6	48.2	83.5
996.7	79.1	20.9	0.110	1.256	193.2	64.4	111.5
1253.4	80.8	19.2	0.087	1.580	242.9	81.0	140.2
1592.9	82.6	17.4	0.069	2.008	308.7	102.9	178.2
1996.8	83.8	16.2	0.055	2.517	387.0	129.0	223.4
2488.5	84.7	15.3	0.044	3.136	482.3	160.8	278.4
3488.5	85.8	14.2	0.031	4.397	676.0	225.3	390.3
4234.3	86.3	13.7	0.026	5.337	820.6	273.5	473.8
4984.2	86.6	13.4	0.022	6.282	965.9	322.0	557.7
6988.2	87.5	12.5	0.016	8.807	1354.3	451.4	781.9
9955.2	87.7	12.3	0.011	12.547	1929.2	643.1	1113.8
12461.5	88.1	11.9	0.009	15.705	2414.9	805.0	1394.3
14927.2	88.3	11.7	0.007	18.813	2892.8	964.3	1670.1
19930.1	88.7	11.3	0.005	25.118	3862.3	1287.4	2229.9
24888.7	89.1	10.9	0.004	31.367	4823.2	1607.7	2784.7
29856.9	89.7	10.3	0.004	37.629	5786.0	1928.7	3340.6
34911.8	89.9	10.1	0.003	43.999	6765.6	2255.2	3906.1
39831.8	90.3	9.7	0.003	50.200	7719.1	2573.0	4456.6
44774.9	90.7	9.3	0.002	56.430	8677.0	2892.3	5009.7
49883.9	91.0	9.0	0.002	62.869	9667.1	3222.4	5581.3

### *Injection Pressure vs Mercury Saturation*

**Company :** Fina Oil and Chemical Company  
**Well :** E-143  
**Formation :** San Andree  
**Field :** N/A  
**County, State :** Midland County, Texas

**Sample No :** E1-6  
**Sample Depth, feet :** 4590.6  
**Permeability to Air, mD :** 88  
**Porosity, percent :** 18.9

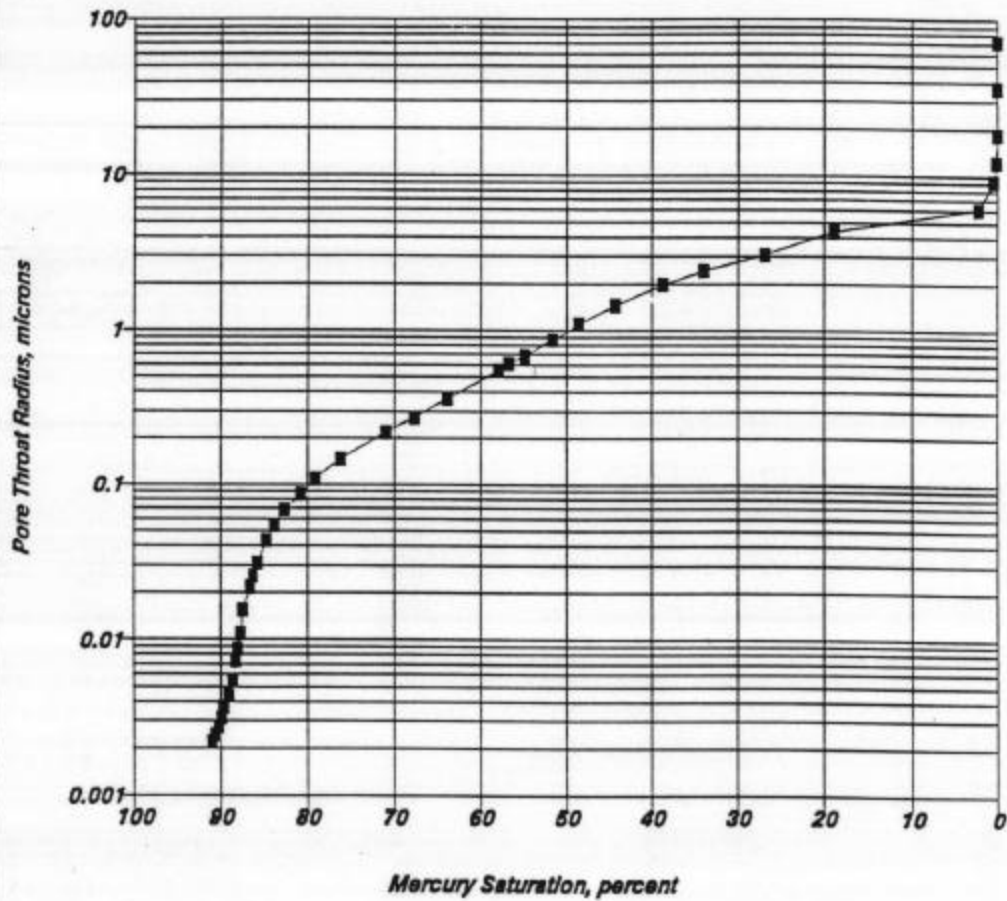


Core Laboratories

### *Pore Aperture Radius vs Mercury Saturation*

**Company:** Fina Oil and Chemical Company  
**Well:** E-143  
**Formation:** San Andres  
**Field:** N/A  
**County, State:** Midland County, Texas

**Sample No:** E1-6  
**Sample Depth, feet:** 4590.6  
**Permeability To Air, mD:** 88  
**Porosity, percent:** 18.9

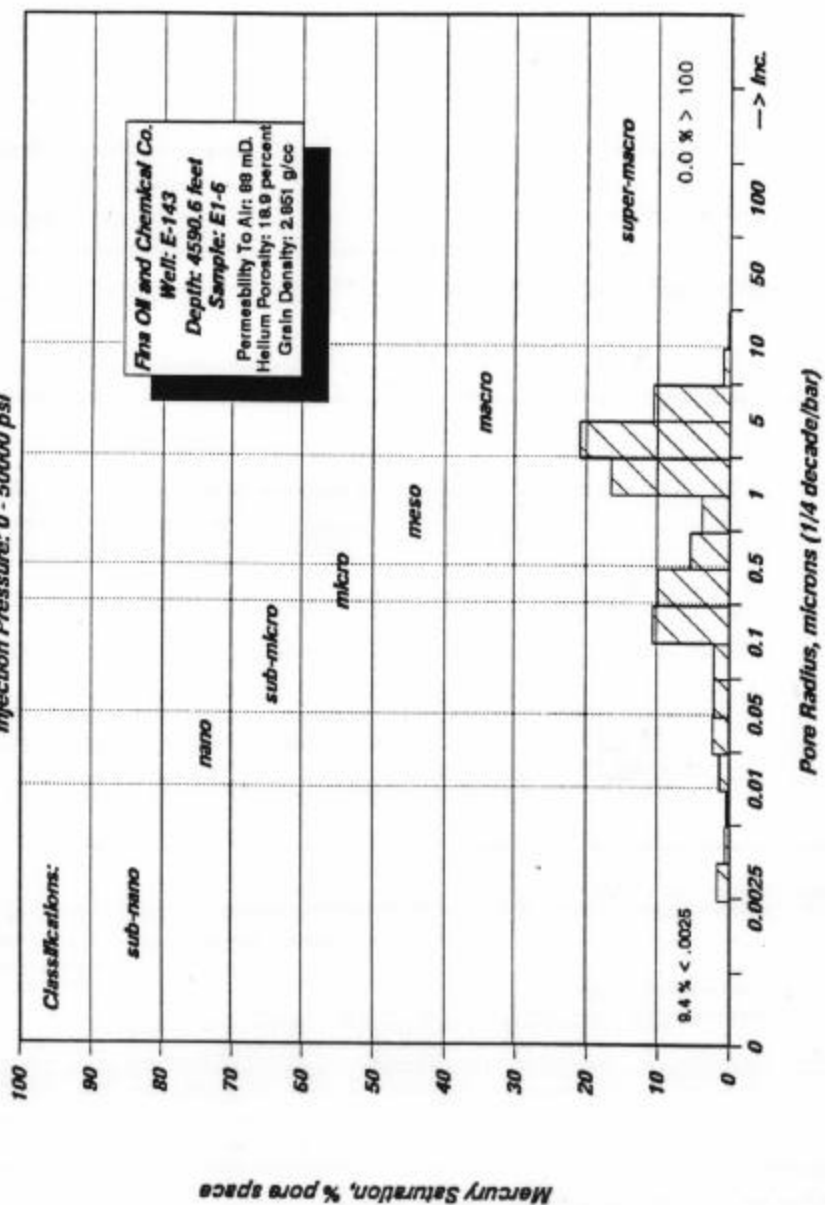


Core Laboratories



# **PORE SIZE DISTRIBUTION MERCURY INJECTION DATA**

Injection Pressure: 0 - 50000 psi



SUMMARY OF MERCURY INJECTION DATA

Fina Oil and Gas Company  
Emmons Unit  
E-143 Well  
San Andres Formation  
Midland County, Texas

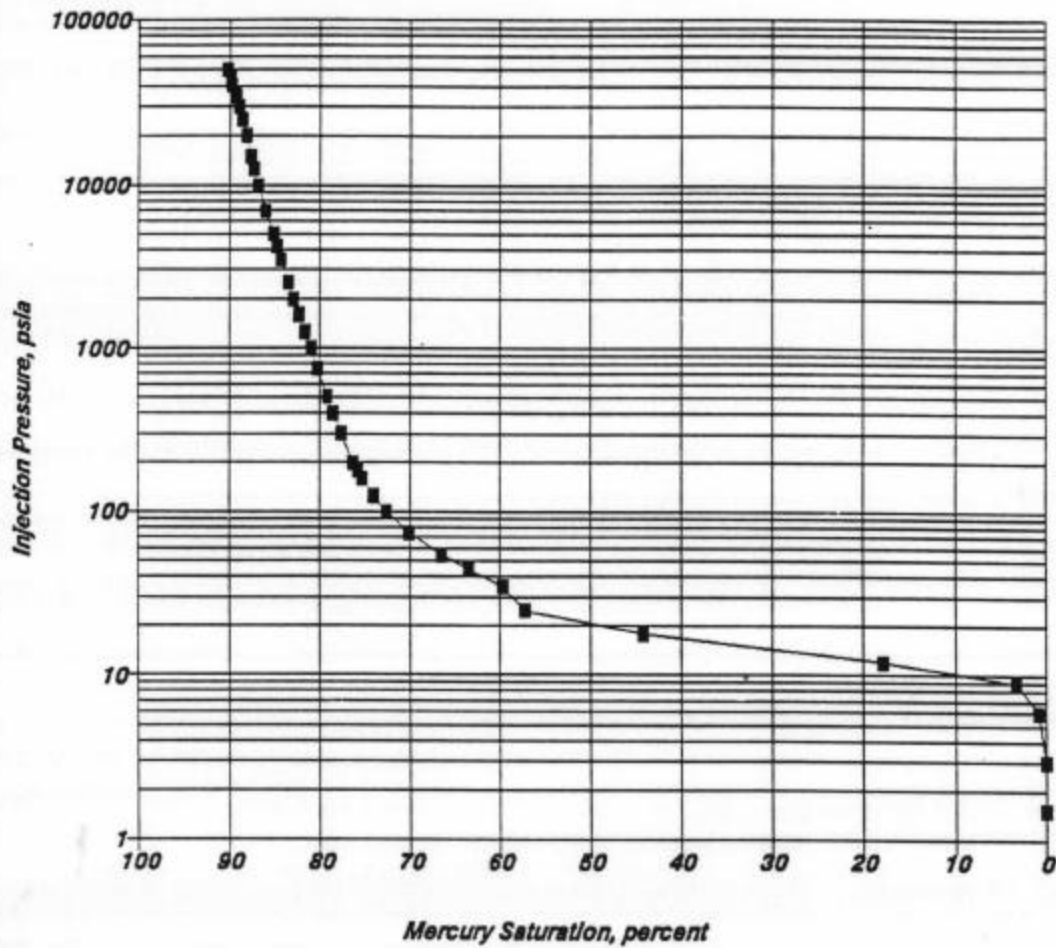
Sample I.D.: E1-7  
Porosity: 21.9 percent  
Permeability to Air: 222 md

Injection Pressure psia	Mercury Saturation percent	100-Mercury Saturation percent	Pore Radius microns	J Function dimensionless	Air/Brine System psia	Air/Oil System psia	Oil/Brine System psia
1.5	0.0	100.0	71.862	0.003	0.3	0.1	0.2
3.0	0.0	100.0	36.289	0.006	0.6	0.2	0.3
6.0	0.8	99.2	18.266	0.011	1.2	0.4	0.7
9.0	3.3	96.7	12.177	0.017	1.7	0.6	1.0
12.0	17.8	82.2	9.141	0.022	2.3	0.8	1.3
17.9	44.2	55.8	6.089	0.033	3.5	1.2	2.0
24.9	57.2	42.8	4.383	0.046	4.8	1.6	2.8
34.9	59.6	40.4	3.131	0.065	6.8	2.3	3.9
44.9	63.4	36.6	2.433	0.083	8.7	2.9	5.0
54.8	66.5	33.5	1.993	0.102	10.6	3.5	6.1
74.6	70.1	29.9	1.464	0.139	14.5	4.8	8.4
99.9	72.6	27.4	1.093	0.186	19.4	6.5	11.2
125.1	74.0	26.0	0.873	0.233	24.2	8.1	14.0
159.4	75.3	24.7	0.685	0.296	30.9	10.3	17.8
179.6	75.8	24.2	0.608	0.334	34.8	11.6	20.1
199.4	76.3	23.7	0.548	0.371	38.6	12.9	22.3
299.8	77.7	22.3	0.364	0.558	58.1	19.4	33.5
398.4	78.6	21.4	0.274	0.741	77.2	25.7	44.6
504.3	79.2	20.8	0.217	0.938	97.7	32.6	56.4
748.4	80.3	19.7	0.146	1.392	145.0	48.3	83.7
997.6	81.0	19.0	0.109	1.855	193.3	64.4	111.6
1251.9	81.7	18.3	0.087	2.328	242.6	80.9	140.1
1599.2	82.3	17.7	0.068	2.974	309.9	103.3	178.9
2000.2	82.9	17.1	0.055	3.720	387.6	129.2	223.8
2497.9	83.6	16.4	0.044	4.645	484.1	161.4	279.5
3491.6	84.4	15.6	0.031	6.493	676.6	225.5	390.7
4232.3	84.8	15.2	0.026	7.870	820.2	273.4	473.5
4996.5	85.2	14.8	0.022	9.291	968.3	322.8	559.0
6976.6	86.1	13.9	0.016	12.974	1352.0	450.7	780.6
9961.0	86.9	13.1	0.011	18.523	1930.4	643.5	1114.5
12471.1	87.4	12.6	0.009	23.191	2416.8	805.6	1395.3
14929.2	87.7	12.3	0.007	27.762	2893.2	964.4	1670.4
19935.9	88.2	11.8	0.005	37.073	3863.4	1287.8	2230.6
24900.2	88.6	11.4	0.004	46.304	4825.5	1608.5	2786.0
29878.1	89.1	10.9	0.004	55.561	5790.1	1930.0	3342.9
34950.7	89.4	10.6	0.003	64.994	6773.2	2257.7	3910.5
39876.1	89.8	10.2	0.003	74.153	7727.7	2575.9	4461.6
44907.9	90.0	10.0	0.002	83.511	8702.8	2900.9	5024.6
49775.9	90.3	9.7	0.002	92.563	9646.2	3215.4	5569.2

### *Injection Pressure vs Mercury Saturation*

**Company :** Fina Oil and Chemical Company  
**Well :** E-143  
**Formation :** San Andres  
**Field :** N/A  
**County, State :** Midland County, Texas

**Sample No :** E1-7  
**Sample Depth, feet :** 4593.8  
**Permeability to Air, mD :** 222  
**Porosity, percent :** 21.9

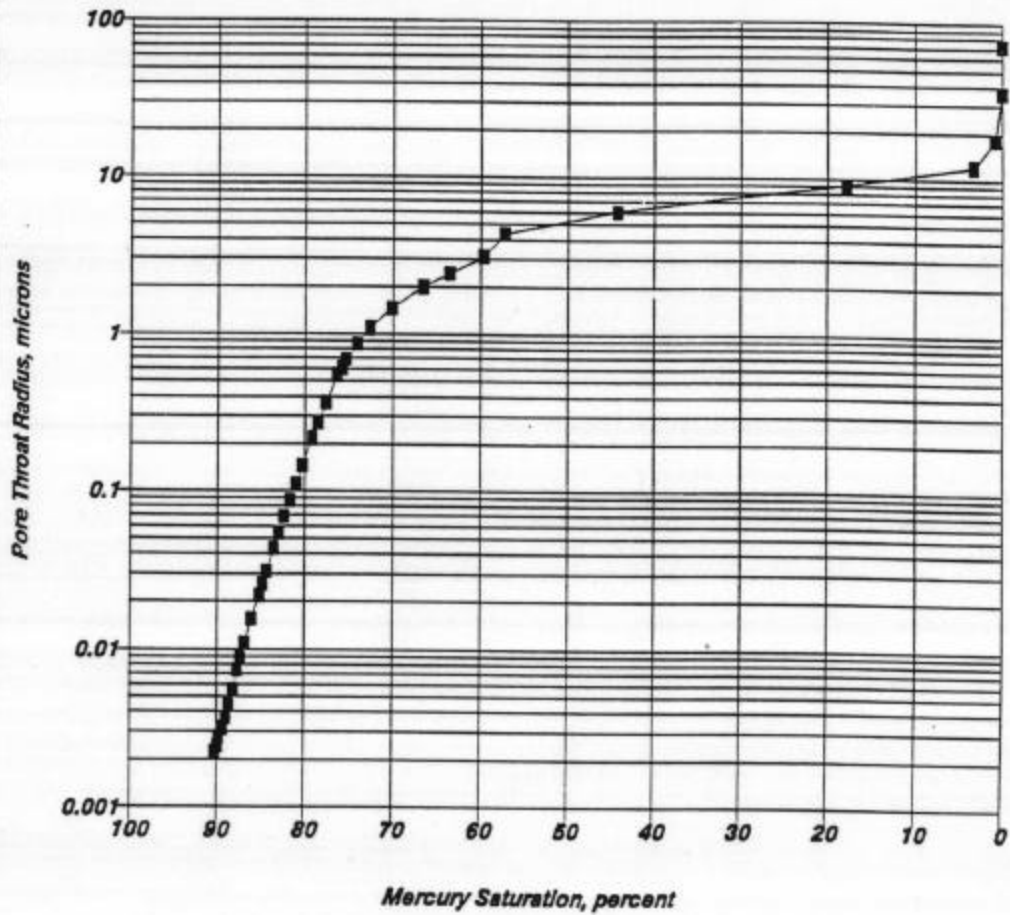


Core Laboratories

### *Pore Aperture Radius vs Mercury Saturation*

**Company:** Fina Oil and Chemical Company  
**Well:** E-143  
**Formation:** San Andres  
**Field:** N/A  
**County, State:** Midland County, Texas

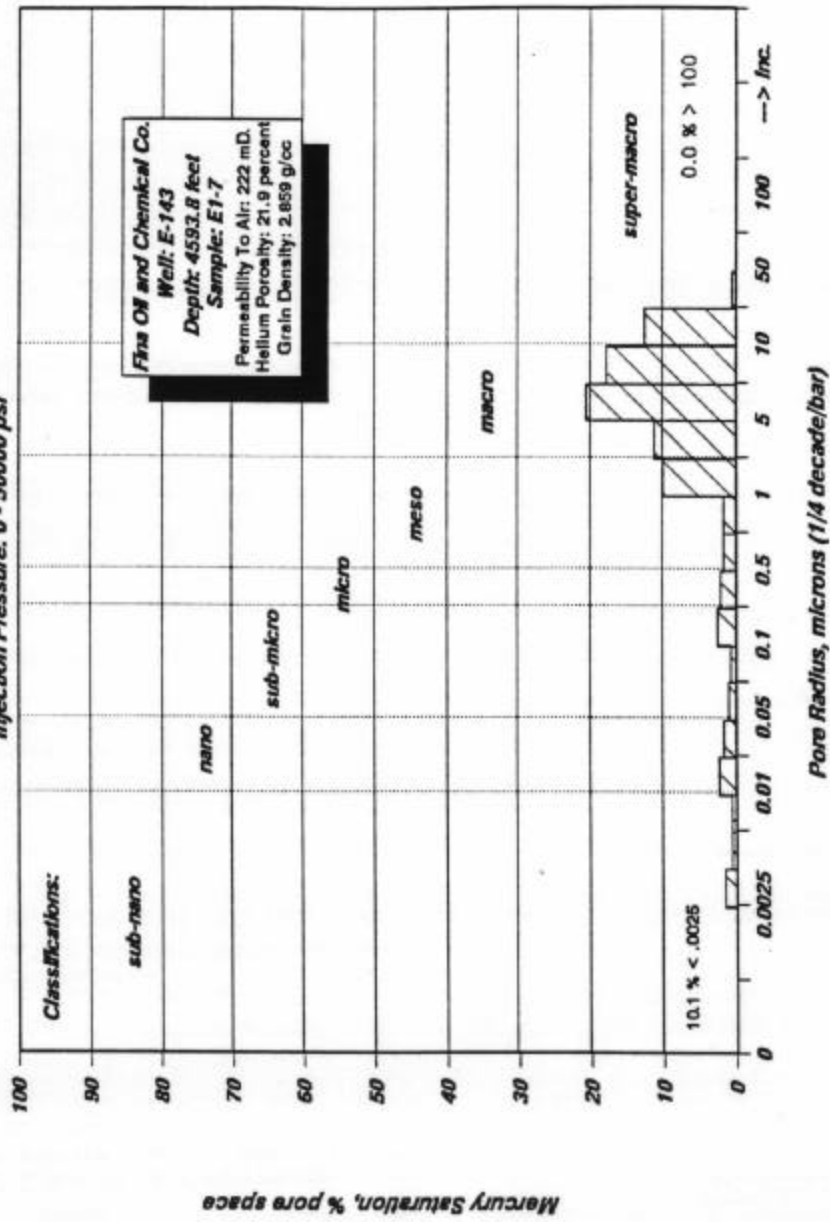
**Sample No:** E1-7  
**Sample Depth, feet:** 4593.8  
**Permeability To Air, mD:** 222  
**Porosity, percent:** 21.9



Core Laboratories

# **PORE SIZE DISTRIBUTION MERCURY INJECTION DATA**

Injection Pressure: 0 - 50000 psi



SUMMARY OF MERCURY INJECTION DATA

Fina Oil and Gas Company  
Emmons Unit  
E-142 Well  
San Andres Formation  
Midland County, Texas

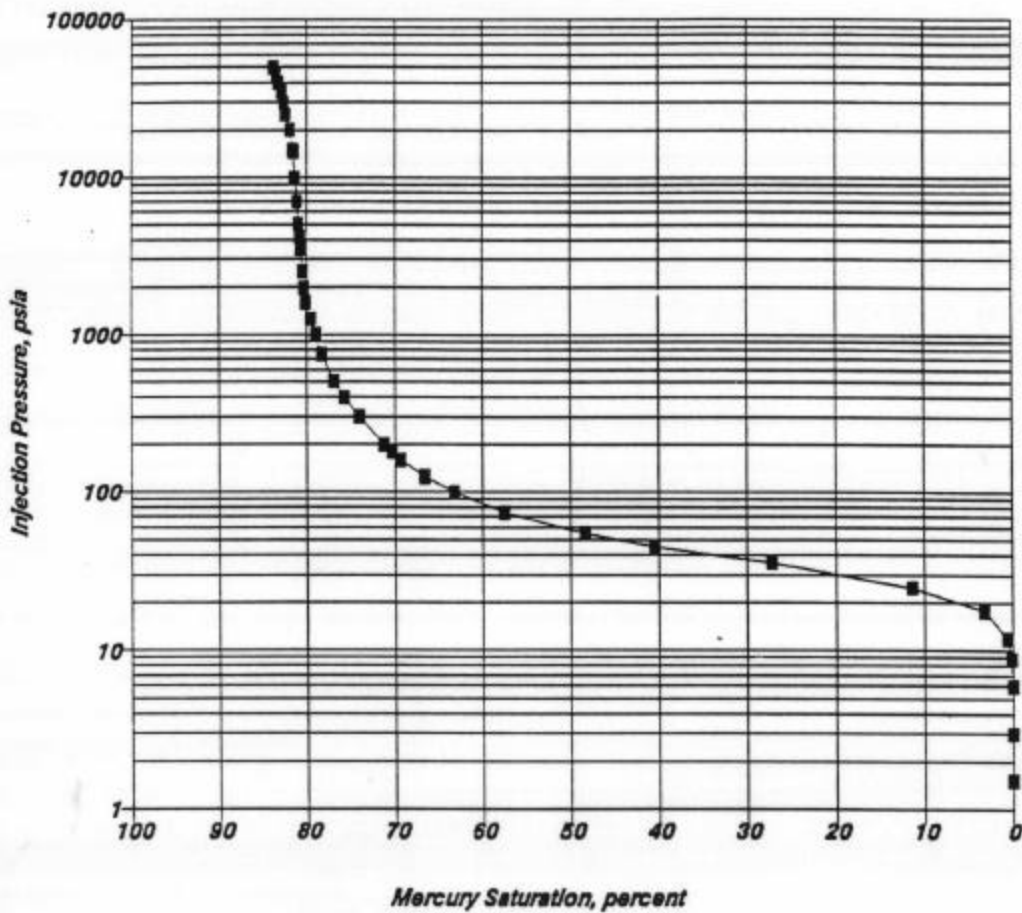
Sample I.D.: E1-10  
Porosity: 17.4 percent  
Permeability to Air: 17 md

Injection Pressure psia	Mercury Saturation percent	100-Mercury Saturation percent	Pore Radius microns	J Function dimensionless	Air/Brine System psia	Air/Oil System psia	Oil/Brine System psia
1.5	0.0	100.0	71.862	0.001	0.3	0.1	0.2
3.0	0.0	100.0	36.289	0.002	0.6	0.2	0.3
6.0	0.0	100.0	18.266	0.003	1.2	0.4	0.7
9.0	0.1	99.9	12.177	0.005	1.7	0.6	1.0
12.0	0.5	99.5	9.141	0.007	2.3	0.8	1.3
17.9	3.2	96.8	6.089	0.010	3.5	1.2	2.0
24.9	11.4	88.6	4.383	0.014	4.8	1.6	2.8
35.9	27.3	72.7	3.041	0.021	7.0	2.3	4.0
45.6	40.5	59.5	2.398	0.026	8.8	2.9	5.1
55.3	48.4	51.6	1.975	0.032	10.7	3.6	6.2
74.9	57.5	42.5	1.458	0.043	14.5	4.8	8.4
100.1	63.2	36.8	1.091	0.058	19.4	6.5	11.2
125.2	66.6	33.4	0.872	0.072	24.3	8.1	14.0
159.5	69.4	30.6	0.685	0.092	30.9	10.3	17.8
179.6	70.3	29.7	0.608	0.104	34.8	11.6	20.1
199.4	71.3	28.7	0.548	0.115	38.6	12.9	22.3
299.8	74.1	25.9	0.364	0.173	58.1	19.4	33.5
398.2	75.8	24.2	0.274	0.230	77.2	25.7	44.5
504.2	76.9	23.1	0.217	0.291	97.7	32.6	56.4
748.3	78.4	21.6	0.146	0.432	145.0	48.3	83.7
997.6	79.0	21.0	0.109	0.576	193.3	64.4	111.6
1251.6	79.6	20.4	0.087	0.723	242.6	80.9	140.0
1599.1	80.1	19.9	0.068	0.923	309.9	103.3	178.9
2000.1	80.4	19.6	0.055	1.155	387.6	129.2	223.8
2497.6	80.5	19.5	0.044	1.442	484.0	161.3	279.5
3491.3	80.8	19.2	0.031	2.016	676.6	225.5	390.6
4232.2	80.9	19.1	0.026	2.443	820.2	273.4	473.5
4995.5	81.0	19.0	0.022	2.884	968.1	322.7	558.9
6976.7	81.2	18.8	0.016	4.028	1352.0	450.7	780.6
9961.0	81.4	18.6	0.011	5.751	1930.4	643.5	1114.5
14473.0	81.6	18.4	0.008	8.356	2804.8	934.9	1619.3
14931.1	81.7	18.3	0.007	8.620	2893.5	964.5	1670.6
19937.9	82.0	18.0	0.005	11.510	3863.8	1287.9	2230.8
24900.3	82.5	17.5	0.004	14.375	4825.5	1608.5	2786.0
29878.1	82.6	17.4	0.004	17.249	5790.1	1930.0	3342.9
34938.8	82.9	17.1	0.003	20.171	6770.9	2257.0	3909.2
39878.1	83.3	16.7	0.003	23.022	7728.1	2576.0	4461.8
44911.9	83.6	16.4	0.002	25.928	8703.6	2901.2	5025.0
49776.0	83.8	16.2	0.002	28.736	9646.2	3215.4	5569.2

### Injection Pressure vs Mercury Saturation

**Company :** Fina Oil and Chemical Company  
**Well :** E-142  
**Formation :** San Andres  
**Field :** N/A  
**County, State :** Midland County, Texas

**Sample No.:** E1-10  
**Sample Depth, feet :** 4638.8  
**Permeability to Air, mD :** 17  
**Porosity, percent :** 17.4

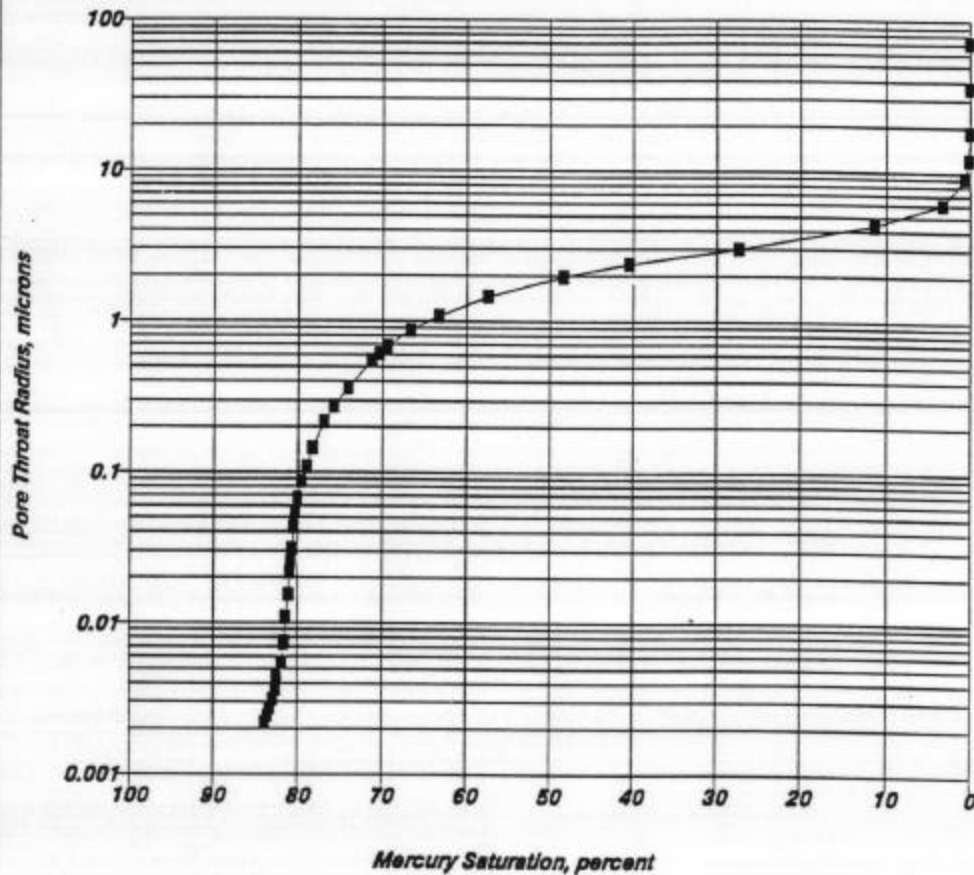


Core Laboratories

### *Pore Aperture Radius vs Mercury Saturation*

**Company:** Fina Oil and Chemical Company  
**Well:** E-142  
**Formation:** San Andres  
**Field:** N/A  
**County, State:** Midland County, Texas

**Sample No:** E1-10  
**Sample Depth, feet:** 4638.8  
**Permeability To Air, mD:** 17  
**Porosity, percent:** 17.4

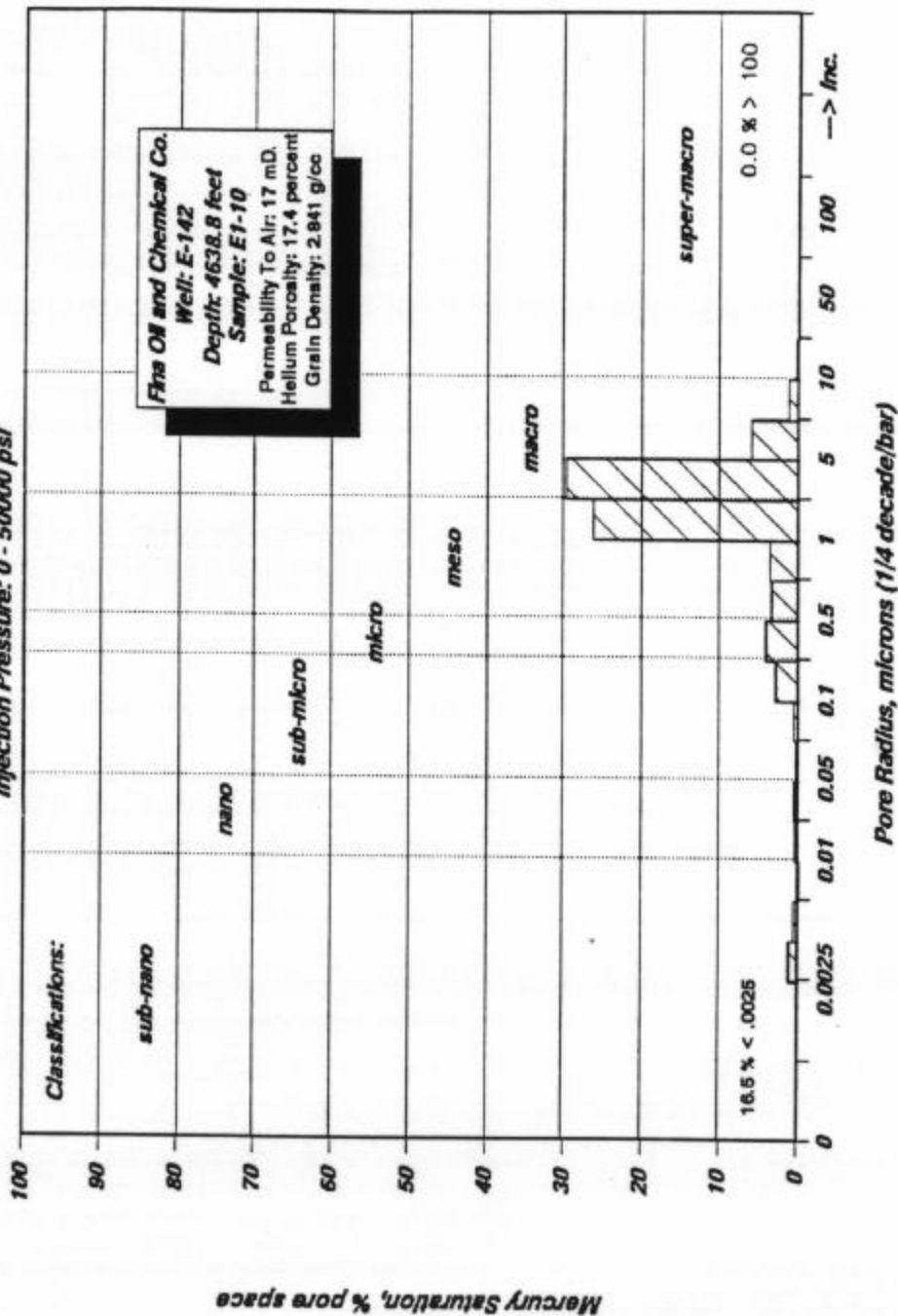


Core Laboratories



# **PORE SIZE DISTRIBUTION** **MERCURY INJECTION DATA**

Injection Pressure: 0 - 50000 psi



SUMMARY OF MERCURY INJECTION DATA

Fina Oil and Gas Company  
Emmons Unit  
E-142 Well  
San Andres Formation  
Midland County, Texas

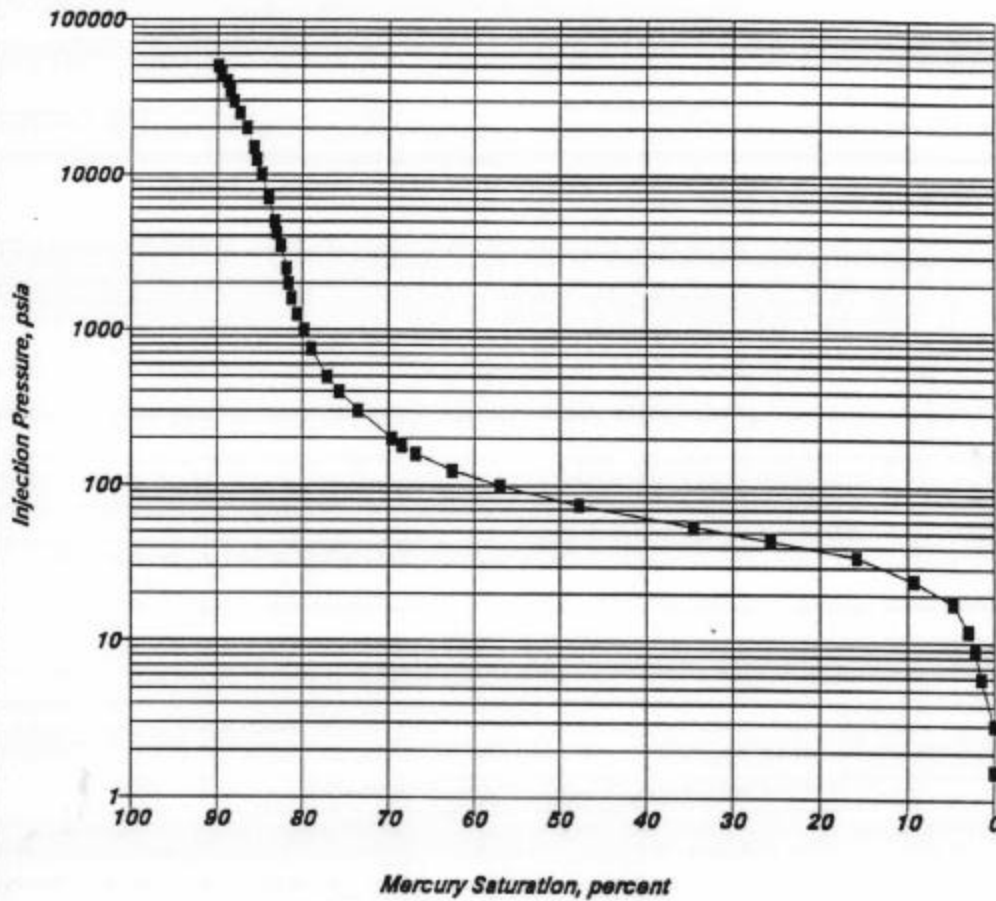
Sample I.D.: E1-11  
Porosity: 14.8 percent  
Permeability to Air: N/A md

Injection Pressure psia	Mercury Saturation percent	100-Mercury Saturation percent	Pore Radius microns	J Function dimensionless	Air/Brine System psia	Air/Oil System psia	Oil/Brine System psia
1.5	0.0	100.0	72.338	0.000	0.3	0.1	0.2
3.0	0.0	100.0	36.532	0.000	0.6	0.2	0.3
6.0	1.5	98.5	18.297	0.000	1.2	0.4	0.7
9.0	2.1	97.9	12.177	0.000	1.7	0.6	1.0
12.0	3.0	97.0	9.141	0.000	2.3	0.8	1.3
17.9	4.8	95.2	6.089	0.000	3.5	1.2	2.0
24.9	9.2	90.8	4.383	0.000	4.8	1.6	2.8
35.0	15.8	84.2	3.120	0.000	6.8	2.3	3.9
44.9	25.7	74.3	2.435	0.000	8.7	2.9	5.0
54.8	34.6	65.4	1.992	0.000	10.6	3.5	6.1
75.0	47.7	52.3	1.456	0.000	14.5	4.8	8.4
99.9	57.0	43.0	1.094	0.000	19.4	6.5	11.2
124.6	62.6	37.4	0.877	0.000	24.1	8.0	13.9
160.0	66.8	33.2	0.683	0.000	31.0	10.3	17.9
179.8	68.5	31.5	0.607	0.000	34.8	11.6	20.1
200.0	69.6	30.4	0.546	0.000	38.8	12.9	22.4
301.9	73.6	26.4	0.362	0.000	58.5	19.5	33.8
400.3	75.7	24.3	0.273	0.000	77.6	25.9	44.8
498.3	77.2	22.8	0.219	0.000	96.6	32.2	55.7
747.1	79.0	21.0	0.146	0.000	144.8	48.3	83.6
995.0	79.8	20.2	0.110	0.000	192.8	64.3	111.3
1255.1	80.7	19.3	0.087	0.000	243.2	81.1	140.4
1596.9	81.3	18.7	0.068	0.000	309.5	103.2	178.7
1992.5	81.6	18.4	0.055	0.000	386.1	128.7	222.9
2491.5	82.0	18.0	0.044	0.000	482.8	160.9	278.8
3488.0	82.6	17.4	0.031	0.000	676.0	225.3	390.3
4236.5	83.1	16.9	0.026	0.000	821.0	273.7	474.0
4981.3	83.3	16.7	0.022	0.000	965.3	321.8	557.3
6085.7	84.0	16.0	0.016	0.000	1353.8	451.3	781.6
9970.0	84.8	15.2	0.011	0.000	1932.1	644.0	1115.5
12447.4	85.4	14.6	0.009	0.000	2412.2	804.1	1392.7
14944.0	85.8	14.2	0.007	0.000	2896.0	965.3	1672.0
19964.2	86.6	13.4	0.005	0.000	3868.9	1289.6	2233.7
24917.0	87.4	12.6	0.004	0.000	4828.7	1609.6	2787.9
29877.5	88.1	11.9	0.004	0.000	5790.0	1930.0	3342.9
34899.6	88.6	11.4	0.003	0.000	6763.3	2254.4	3904.8
39871.7	88.9	11.1	0.003	0.000	7726.8	2575.6	4461.1
44922.8	89.5	10.5	0.002	0.000	8705.7	2901.9	5026.2
49769.5	89.9	10.1	0.002	0.000	9645.0	3215.0	5568.5

### Injection Pressure vs Mercury Saturation

**Company :** Fina Oil and Chemical Company  
**Well :** E-142  
**Formation :** San Andres  
**Field :** N/A  
**County, State :** Midland County, Texas

**Sample No. :** E1-11  
**Sample Depth, feet :** 4638.9  
**Permeability to Air, mD :** N/A  
**Porosity, percent :** 14.8

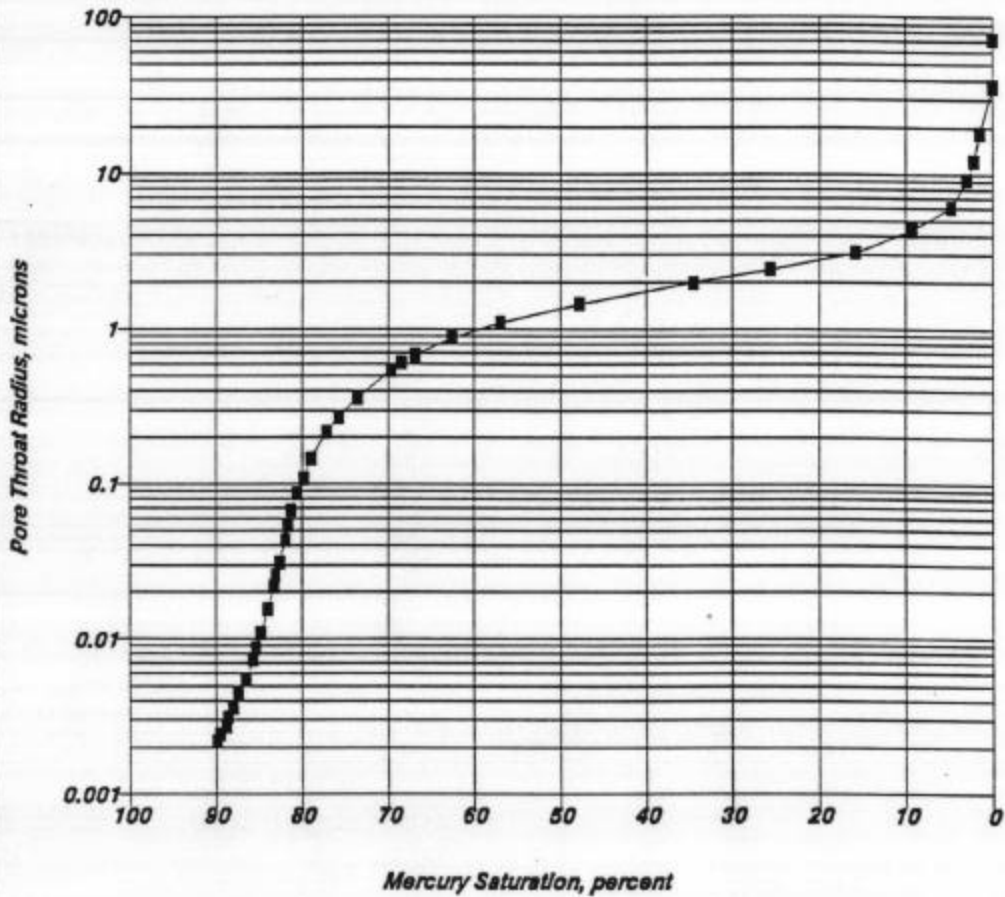


Core Laboratories

### *Pore Aperture Radius vs Mercury Saturation*

**Company:** Fina Oil and Chemical Company  
**Well:** E-142  
**Formation:** San Andres  
**Field:** N/A  
**County, State:** Midland County, Texas

**Sample No:** E1-11  
**Sample Depth, feet:** 4638.9  
**Permeability To Air, mD:** N/A  
**Porosity, percent:** 14.8

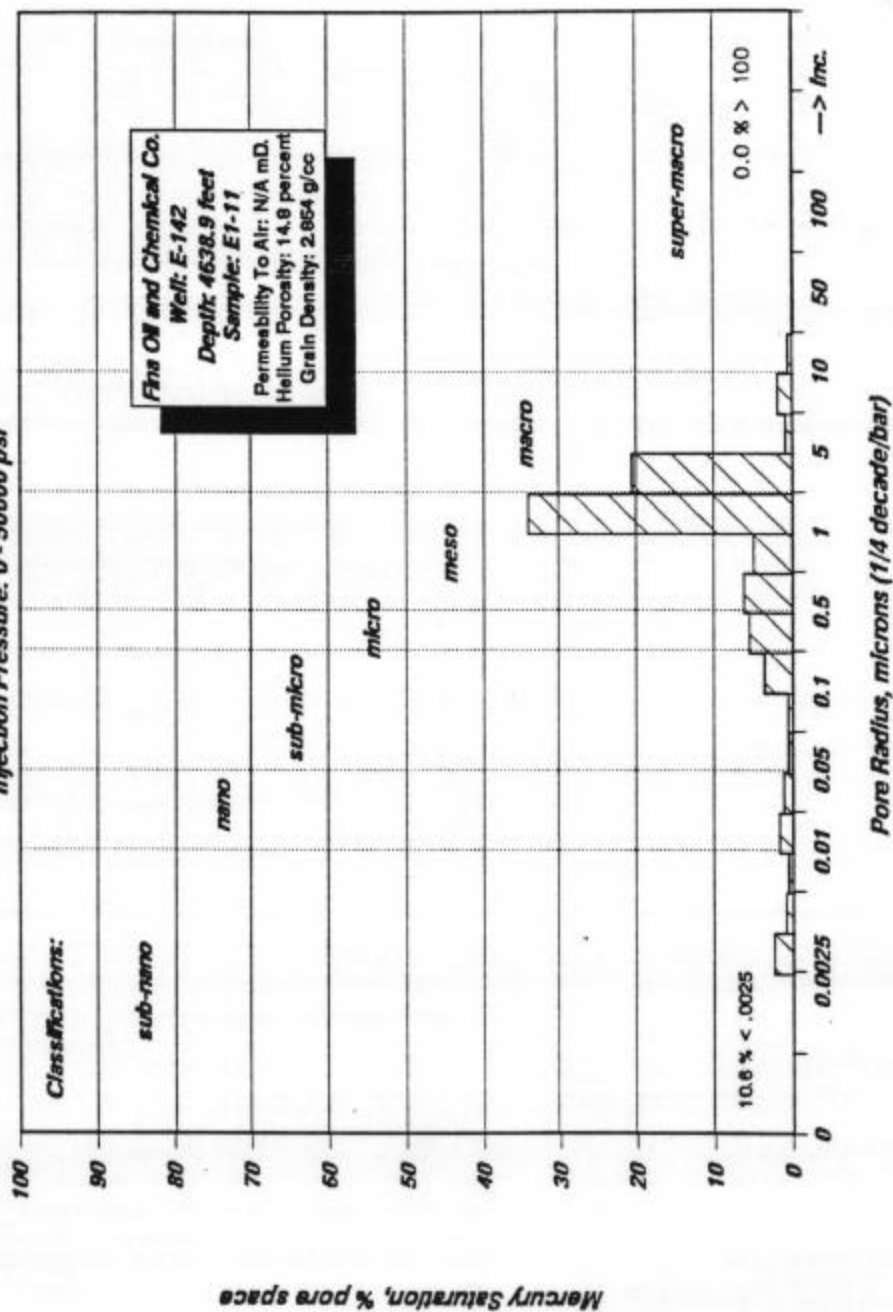


Core Laboratories

7-25

# **PORE SIZE DISTRIBUTION** **MERCURY INJECTION DATA**

Injection Pressure: 0 - 50000 psi



SUMMARY OF MERCURY INJECTION DATA

Fina Oil and Gas Company  
Emmons Unit  
E-143 Well  
San Andres Formation  
Midland County, Texas

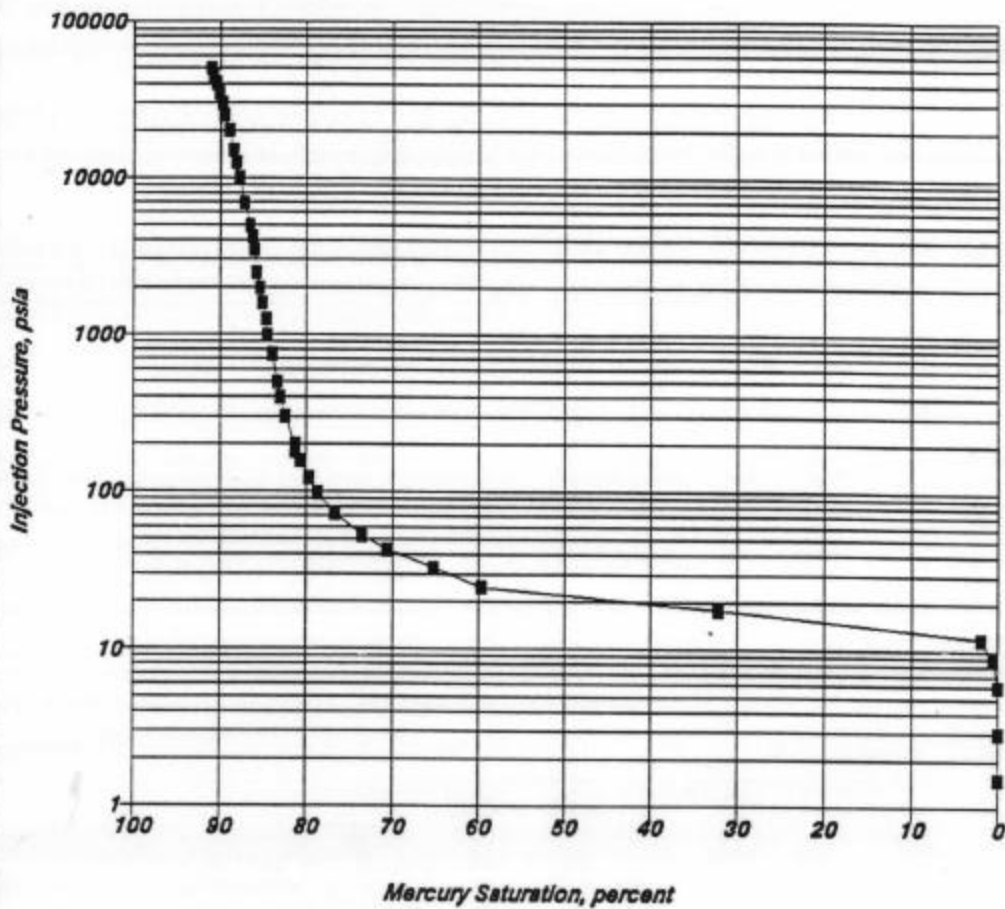
Sample I.D.: E1-14  
Porosity: 21.3 percent  
Permeability to Air: 121 md

Injection Pressure psia	Mercury Saturation percent	100-Mercury Saturation percent	Pore Radius microns	J Function dimensionless	Air/Brine System psia	Air/Oil System psia	Oil/Brine System psia
1.5	0.0	100.0	72.338	0.002	0.3	0.1	0.2
3.0	0.0	100.0	36.532	0.004	0.6	0.2	0.3
6.0	0.0	100.0	18.297	0.008	1.2	0.4	0.7
9.0	0.5	99.5	12.177	0.012	1.7	0.6	1.0
12.0	1.9	98.1	9.141	0.017	2.3	0.8	1.3
17.9	32.2	67.8	6.089	0.025	3.5	1.2	2.0
24.9	59.6	40.4	4.383	0.035	4.8	1.6	2.8
33.2	65.2	34.8	3.294	0.046	6.4	2.1	3.7
43.0	70.6	29.4	2.538	0.060	8.3	2.8	4.8
53.1	73.6	26.4	2.058	0.074	10.3	3.4	5.9
73.4	76.7	23.3	1.488	0.102	14.2	4.7	8.2
98.4	78.7	21.3	1.110	0.137	19.1	6.4	11.0
123.2	79.7	20.3	0.887	0.172	23.9	8.0	13.8
158.7	80.8	19.2	0.688	0.221	30.7	10.2	17.8
178.5	81.3	18.7	0.612	0.248	34.6	11.5	20.0
198.7	81.4	18.6	0.550	0.277	38.5	12.8	22.2
300.6	82.5	17.5	0.363	0.418	58.3	19.4	33.6
399.0	83.1	16.9	0.274	0.555	77.3	25.8	44.6
496.8	83.4	16.6	0.220	0.692	96.3	32.1	55.6
745.7	84.0	16.0	0.146	1.038	144.5	48.2	83.4
993.9	84.5	15.5	0.110	1.384	192.6	64.2	111.2
1253.8	84.7	15.3	0.087	1.745	243.0	81.0	140.3
1596.0	85.2	14.8	0.068	2.222	309.3	103.1	178.6
1991.0	85.5	14.5	0.055	2.772	385.8	128.6	222.8
2490.0	85.9	14.1	0.044	3.466	482.5	160.8	278.6
3486.9	86.1	13.9	0.031	4.854	675.7	225.2	390.1
4235.5	86.3	13.7	0.026	5.896	820.8	273.6	473.9
4979.9	86.6	13.4	0.022	6.932	965.1	321.7	557.2
6982.5	87.3	12.7	0.016	9.720	1353.1	451.0	781.2
9968.8	87.9	12.1	0.011	13.877	1931.9	644.0	1115.4
12446.1	88.2	11.8	0.009	17.326	2412.0	804.0	1392.5
14940.8	88.5	11.5	0.007	20.799	2895.4	965.1	1671.7
19961.0	89.0	11.0	0.005	27.788	3868.3	1289.4	2233.4
24913.8	89.6	10.4	0.004	34.682	4828.1	1609.4	2787.5
29876.2	89.8	10.2	0.004	41.590	5789.8	1929.9	3342.7
34898.4	90.2	9.8	0.003	48.582	6763.0	2254.3	3904.6
39868.5	90.5	9.5	0.003	55.500	7726.2	2575.4	4460.7
44923.4	90.8	9.2	0.002	62.537	8705.8	2901.9	5026.3
49772.1	91.0	9.0	0.002	69.287	9645.5	3215.2	5568.8

### Injection Pressure vs Mercury Saturation

**Company :** Fina Oil and Chemical Company  
**Well :** E-143  
**Formation :** San Andres  
**Field :** N/A  
**County, State :** Midland County, Texas

**Sample No :** E1-14  
**Sample Depth, feet :** 4644.5  
**Permeability to Air, mD :** 121  
**Porosity, percent :** 21.3

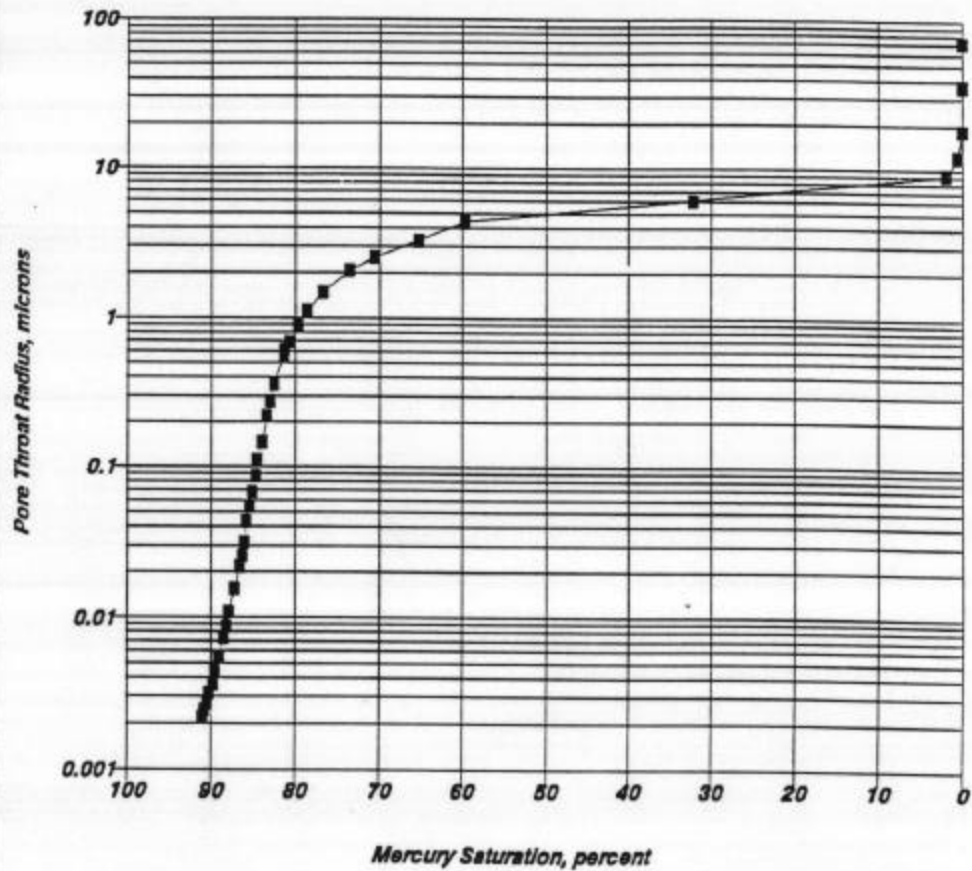


Core Laboratories

### *Pore Aperture Radius vs Mercury Saturation*

**Company:** Fina Oil and Chemical Company  
**Well:** E-143  
**Formation:** San Andres  
**Field:** N/A  
**County, State:** Midland County, Texas

**Sample No:** E1-14  
**Sample Depth, feet:** 4644.5  
**Permeability To Air, mD:** 121  
**Porosity, percent:** 21.3

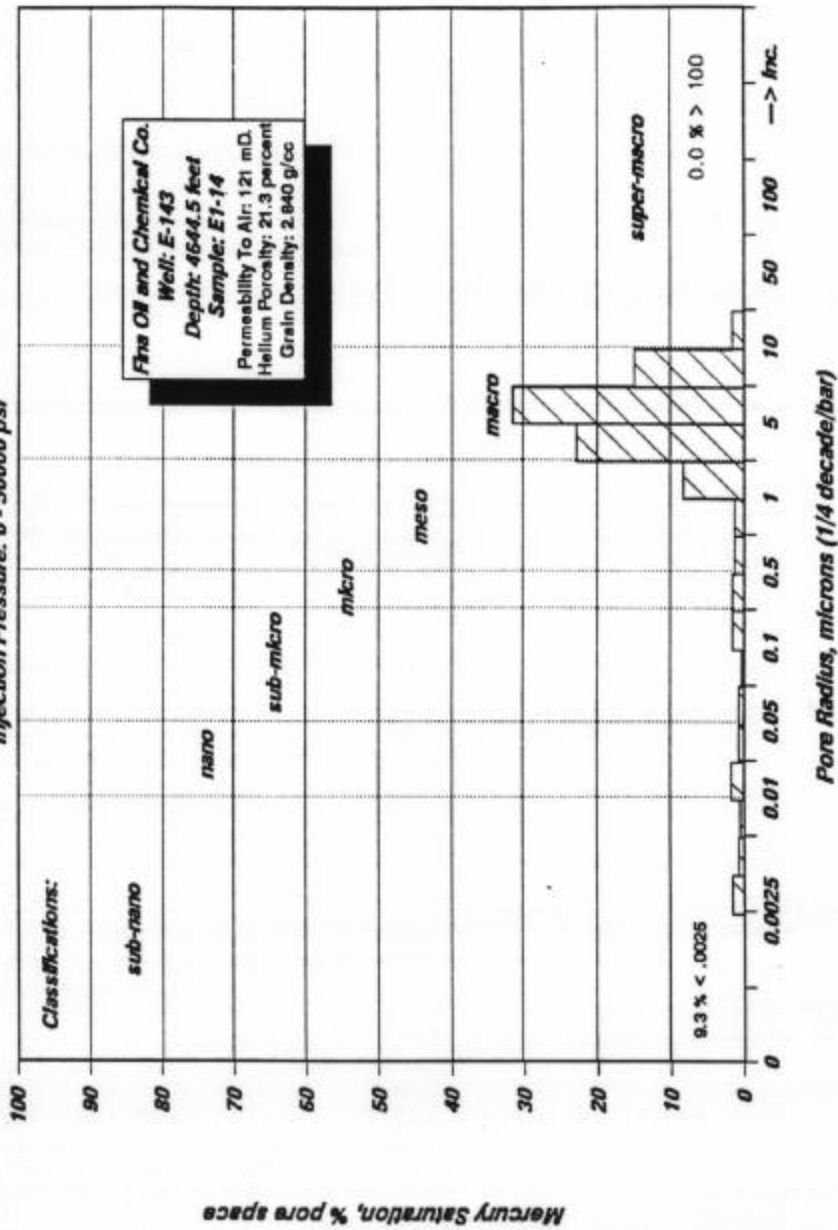


Core Laboratories



# **PORE SIZE DISTRIBUTION** **MERCURY INJECTION DATA**

Injection Pressure: 0 - 50000 psi



SUMMARY OF MERCURY INJECTION DATA

Fina Oil and Gas Company  
Emmons Unit  
E-143 Well  
San Andres Formation  
Midland County, Texas

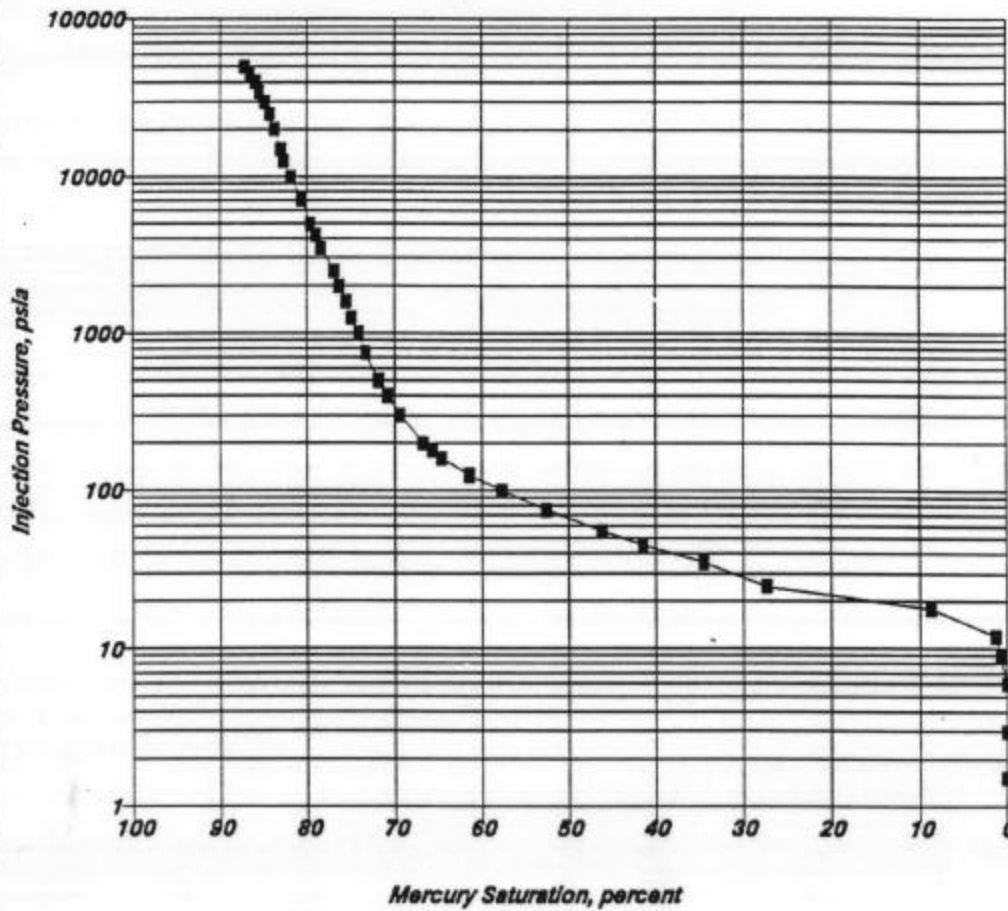
Sample I.D.: E1-15  
Porosity: 12.2 percent  
Permeability to Air: 14.9 md

<u>Injection Pressure psia</u>	<u>Mercury Saturation percent</u>	<u>100-Mercury Saturation percent</u>	<u>Pore Radius microns</u>	<u>J Function dimensionless</u>	<u>Air/Brine System psia</u>	<u>Air/Oil System psia</u>	<u>Oil/Brine System psia</u>
1.5	0.0	100.0	71.862	0.001	0.3	0.1	0.2
3.0	0.0	100.0	36.410	0.002	0.6	0.2	0.3
6.0	0.0	100.0	18.266	0.004	1.2	0.4	0.7
9.0	0.6	99.4	12.177	0.006	1.7	0.6	1.0
12.0	1.2	98.8	9.133	0.008	2.3	0.8	1.3
17.9	8.6	91.4	6.089	0.012	3.5	1.2	2.0
24.9	27.3	72.7	4.383	0.016	4.8	1.6	2.8
35.2	34.5	65.5	3.100	0.023	6.8	2.3	3.9
45.2	41.5	58.5	2.417	0.029	8.8	2.9	5.1
55.4	46.2	53.8	1.971	0.036	10.7	3.6	6.2
75.7	52.5	47.5	1.443	0.049	14.7	4.9	8.5
99.9	57.7	42.3	1.094	0.064	19.4	6.5	11.2
125.5	61.4	38.6	0.870	0.081	24.3	8.1	14.0
160.0	64.7	35.3	0.683	0.103	31.0	10.3	17.9
179.9	65.7	34.3	0.607	0.116	34.9	11.6	20.1
199.8	66.7	33.3	0.547	0.129	38.7	12.9	22.4
302.7	69.4	30.6	0.361	0.195	58.7	19.6	33.9
400.6	70.8	29.2	0.273	0.259	77.6	25.9	44.8
500.0	71.8	28.2	0.218	0.323	96.9	32.3	55.9
746.9	73.3	26.7	0.146	0.482	144.7	48.2	83.6
997.8	74.1	25.9	0.109	0.644	193.4	64.5	111.6
1254.4	74.9	25.1	0.087	0.810	243.1	81.0	140.3
1594.1	75.5	24.5	0.069	1.029	308.9	103.0	178.4
1997.5	76.4	23.6	0.055	1.289	387.1	129.0	223.5
2489.6	77.0	23.0	0.044	1.607	482.5	160.8	278.6
3489.7	78.4	21.6	0.031	2.253	676.3	225.4	390.5
4235.5	79.0	21.0	0.026	2.734	820.8	273.6	473.9
4985.3	79.6	20.4	0.022	3.218	966.1	322.0	557.8
6989.3	80.7	19.3	0.016	4.511	1354.5	451.5	782.0
9954.3	81.9	18.1	0.011	6.425	1929.1	643.0	1113.8
12462.5	82.7	17.3	0.009	8.044	2415.1	805.0	1394.4
14928.8	83.1	16.9	0.007	9.636	2893.1	964.4	1670.3
19931.2	83.7	16.3	0.005	12.865	3862.5	1287.5	2230.0
24889.7	84.4	15.6	0.004	16.066	4823.4	1607.8	2784.8
29857.9	85.0	15.0	0.004	19.272	5786.2	1928.7	3340.7
34914.8	85.6	14.4	0.003	22.537	6766.2	2255.4	3906.5
39832.9	86.0	14.0	0.003	25.711	7719.3	2573.1	4456.7
44777.9	86.6	13.4	0.002	28.903	8677.6	2892.5	5010.0
49884.9	87.2	12.8	0.002	32.199	9667.3	3222.4	5581.4

### *Injection Pressure vs Mercury Saturation*

**Company :** Fina Oil and Chemical Company  
**Well :** E-143  
**Formation :** San Andres  
**Field :** N/A  
**County, State :** Midland County, Texas

**Sample No :** E1-15  
**Sample Depth, feet :** 4644.6  
**Permeability to Air, mD :** 14.9  
**Porosity, percent :** 12.2

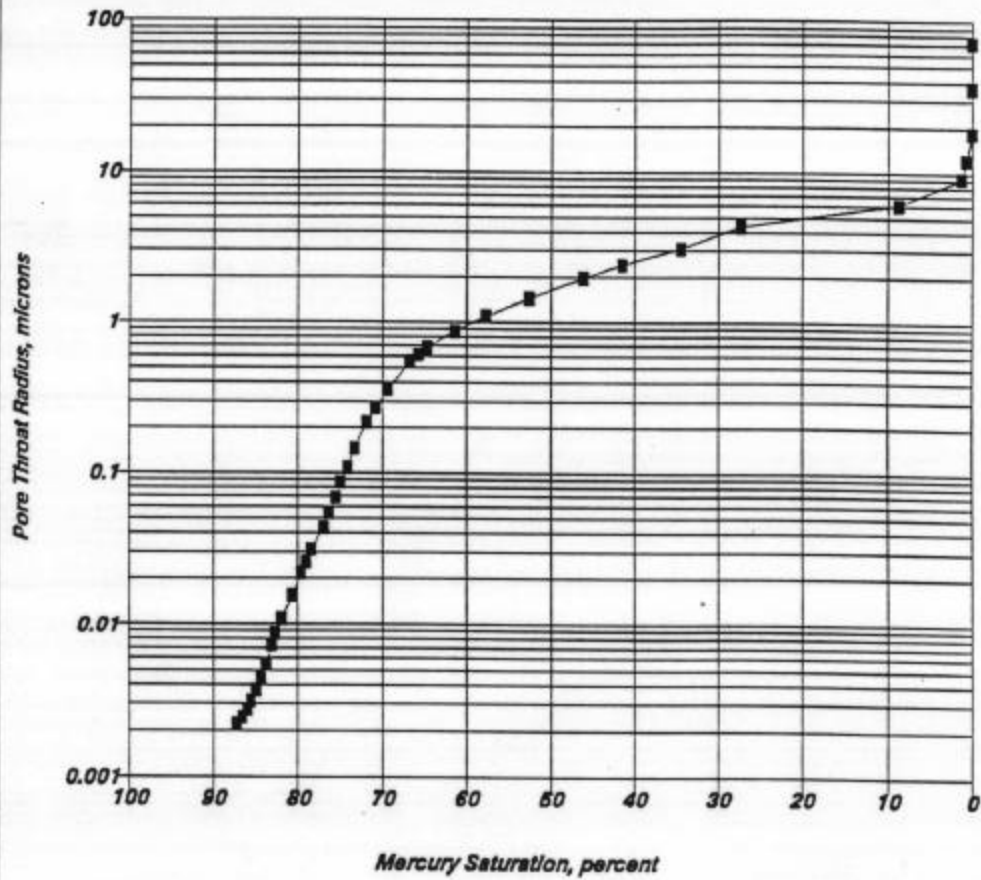


Core Laboratories

### *Pore Aperture Radius vs Mercury Saturation*

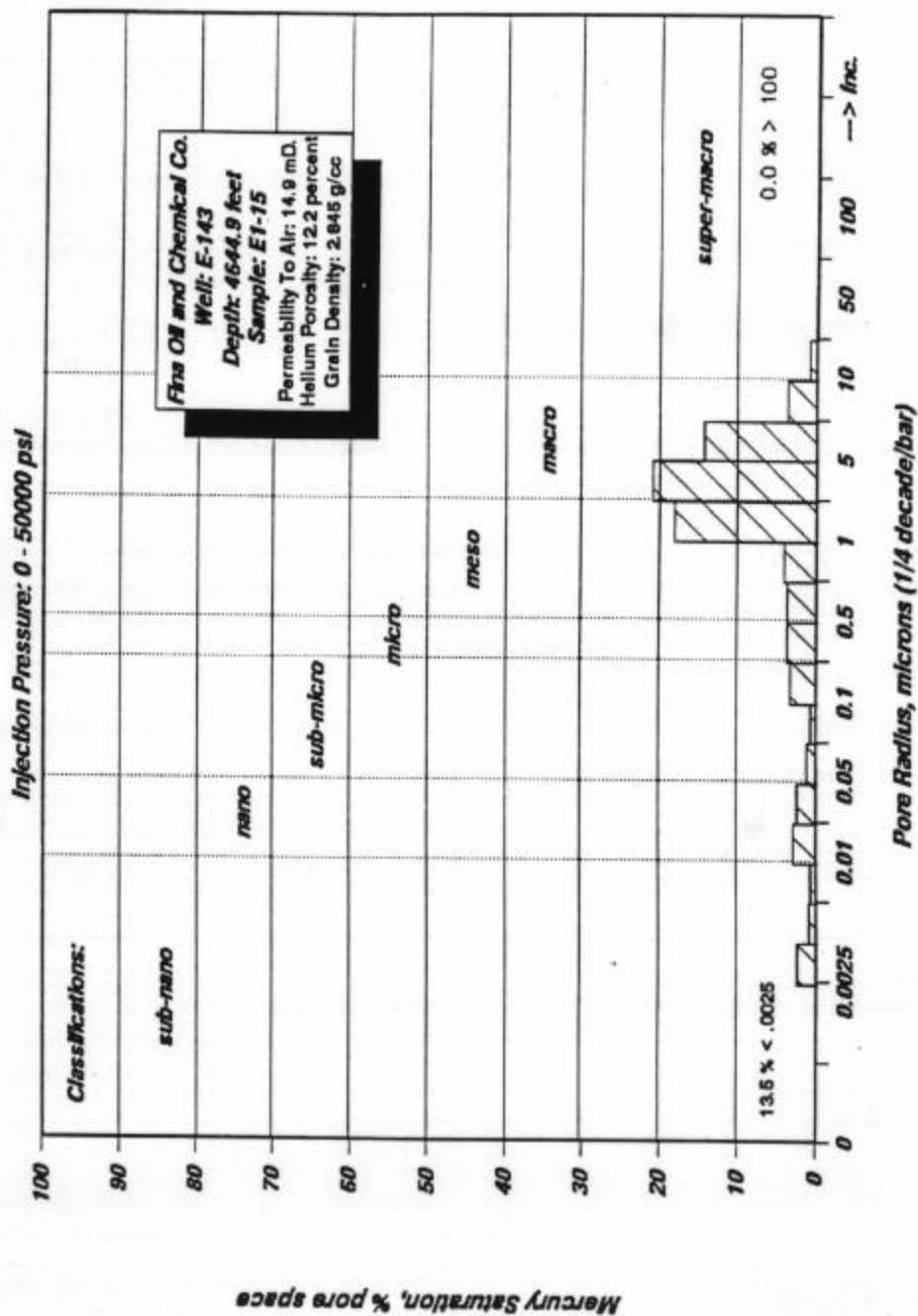
**Company:** Fina Oil and Chemical Company  
**Well:** E-143  
**Formation:** San Andres  
**Field:** N/A  
**County, State:** Midland County, Texas

**Sample No:** E1-15  
**Sample Depth, feet:** 4644.9  
**Permeability To Air, mD:** 14.9  
**Porosity, percent:** 12.2



Core Laboratories

# **PORE SIZE DISTRIBUTION** **MERCURY INJECTION DATA**



## **DIRECTIONAL SURVEYS**

SCIENTIFIC DRILLING INTERNATIONAL

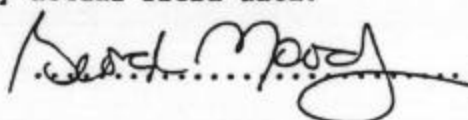
MIDLAND, TEXAS

PHILLIPS PETROLEUM CORP.

Well Name : PHILLIPS/SOUTH COWDEN #7-10  
Location : ECTOR COUNTY, TEXAS  
:  
:  
Date Surveyed : 12/28/92  
Job Number : 32G1292233/32D1292232  
Surveyor : RICK EATON/GEORGY MOODY

Surf Long -102.38457  
Lat 31.75954

This survey is correct to the best of my knowledge  
and is supported by actual field data.

 COMPANY REPRESENTATIVE

RECORD COPY  
DOSSA CENTRAL FILE

## SCIENTIFIC DRILLING INTERNATIONAL

Company : PHILLIPS PETROLEUM CORP.  
 Well Name : PHILLIPS/SOUTH COWDEN #7-10  
 Location : ECTOR COUNTY, TEXAS

Page 1 of 2  
 Date 12/28/92  
 Filename : SCU7-10

o Interpolation

MD	INC	DIR	TVD	LAT	DEP	VS	D'LEG
ft	deg	deg	ft	ft	ft	ft	°/100
0.0	0.00	N 0.00°E	0.00	0.00	0.00	0.00	0.0
100.0	0.64	S42.77°E	100.00	-0.41	0.38	-0.55	0.6
200.0	1.24	S53.25°E	199.98	-1.47	1.63	-2.17	0.6
300.0	1.07	S45.00°E	299.96	-2.78	3.15	-4.17	0.2
400.0	0.96	S29.23°E	399.95	-4.17	4.22	-5.84	0.3
500.0	0.86	S44.39°E	499.94	-5.43	5.16	-7.33	0.3
600.0	1.58	S29.40°E	599.91	-7.17	6.36	-9.31	0.8
700.0	1.13	S14.27°E	699.88	-9.33	7.28	-11.30	0.6
800.0	1.27	S11.05°W	799.86	-11.37	7.31	-12.48	0.5
900.0	0.96	S27.01°W	899.84	-13.21	6.72	-13.04	0.4
1000.0	1.95	S29.18°W	999.81	-15.44	5.51	-13.32	1.0
1100.0	1.08	S70.34°W	1099.78	-17.24	3.79	-12.93	1.3
1200.0	0.98	S46.91°W	1199.76	-18.14	2.28	-12.21	0.4
1300.0	0.71	S66.04°W	1299.75	-18.98	1.09	-11.70	0.4
1400.0	1.29	S59.14°W	1399.74	-19.81	-0.45	-10.92	0.6
1500.0	0.63	S51.07°W	1499.72	-20.73	-1.84	-10.30	0.7
1600.0	0.71	S65.86°W	1599.71	-21.33	-2.83	-9.82	0.2
1700.0	0.29	S89.08°W	1699.71	-21.58	-3.65	-9.30	0.5
1800.0	0.41	N52.68°W	1799.71	-21.37	-4.19	-8.73	0.3
1900.0	0.70	N75.23°W	1899.70	-21.00	-5.07	-7.80	0.4
2000.0	0.66	S40.91°W	1999.70	-21.28	-6.03	-7.16	0.7
2100.0	0.61	S18.50°W	2099.69	-22.22	-6.58	-7.25	0.3
2200.0	0.11	S53.25°E	2199.69	-22.78	-6.67	-7.50	0.6
2300.0	0.18	N61.68°W	2299.69	-22.76	-6.73	-7.44	0.3
2400.0	0.79	S13.65°W	2399.69	-23.36	-7.03	-7.53	0.9
2475.0	0.80	S29.99°W	2474.68	-24.32	-7.42	-7.76	0.3
2533.0	1.00	S81.00°W	2532.67	-24.75	-8.12	-7.42	1.4
2564.0	2.00	N81.00°W	2563.66	-24.70	-8.92	-6.74	3.5
2627.0	4.75	N70.00°W	2626.55	-23.64	-12.46	-3.23	4.5
2659.0	6.00	N63.00°W	2658.41	-22.43	-15.19	-0.29	4.4
2768.0	9.00	N50.00°W	2766.47	-14.36	-26.80	13.85	3.1
2881.0	10.00	N50.00°W	2877.92	-2.37	-41.09	32.42	0.9
3004.0	10.00	N50.00°W	2999.05	11.36	-57.45	53.69	0.0
3129.0	9.75	N48.00°W	3122.20	25.42	-73.63	75.00	0.3
3254.0	10.00	N46.00°W	3245.35	40.04	-89.31	96.21	0.3
3441.0	9.50	N47.00°W	3429.65	61.84	-112.27	127.50	0.3
3597.0	9.25	N46.00°W	3583.56	79.33	-130.71	152.62	0.2
3784.0	9.00	N41.00°W	3768.20	100.81	-151.11	181.63	0.4
3910.0	8.50	N39.00°W	3892.73	115.49	-163.44	200.12	0.5
4034.0	8.00	N37.00°W	4015.45	129.50	-174.40	217.11	0.5



# SCIENTIFIC DRILLING INTERNATIONAL


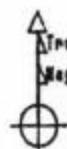
Company : PHILLIPS PETROLEUM CORP.  
Well Name : PHILLIPS/SOUTH COWDEN #7-10  
Location : ECTOR COUNTY, TEXAS

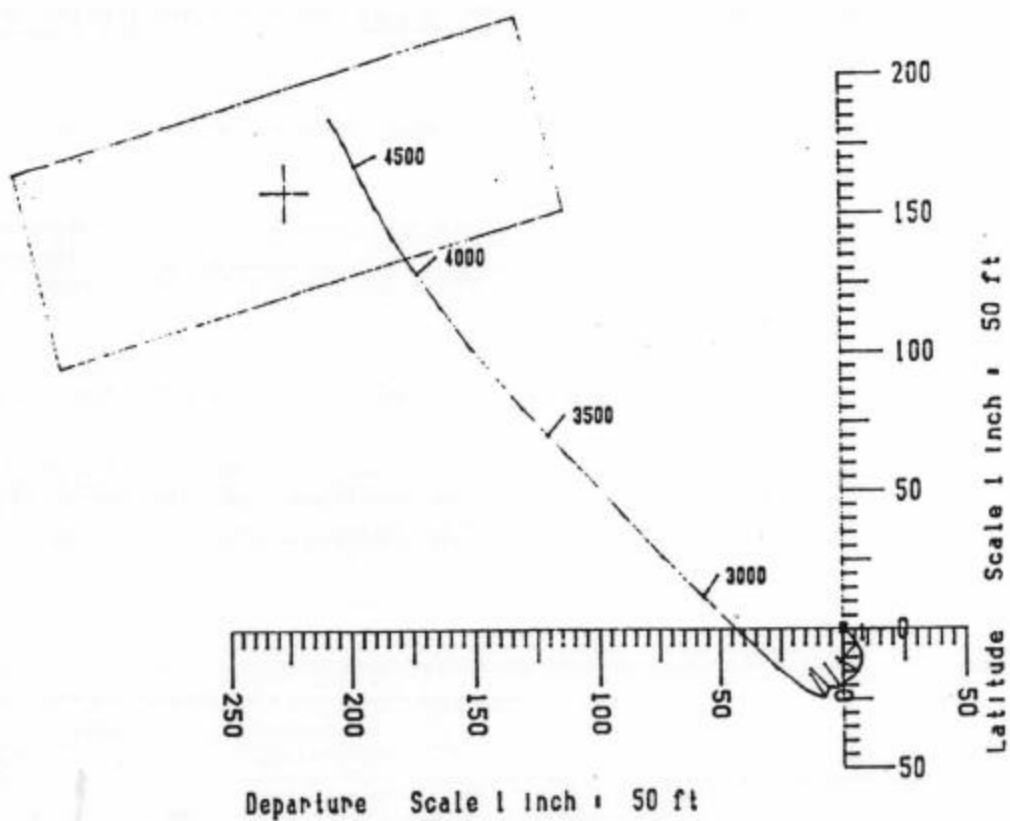
Page 2 of 2  
Date 12/28/92  
Filename : SCU7-10

No Interpolation

MD	INC	DIR	TVD	<sup>NS</sup> Del Y LAT	<sup>EW</sup> Del X DEP	VS	D'LEG
ft	deg	deg	ft	ft	ft	ft	°/100
4137.0	6.75	N35.00°W	4117.59	140.18	-182.18	229.59	1.2
4263.0	5.25	N28.00°W	4242.90	151.34	-189.14	241.66	1.3
4389.0	3.75	N35.00°W	4368.51	159.81	-194.21	250.65	1.3
4514.0	3.00	N23.00°W	4493.29	166.17	-197.83	257.25	0.8
4699.0	2.50	N30.00°W	4678.08	174.12	-201.74	265.00	0.3
4836.0	3.00	N35.00°W	4814.92	179.64	-205.29	271.06	0.4
4921.0	3.00	N35.00°W	4899.81	183.28	-207.84	275.23	0.0

Origin of Bottom Hole Closure PLATFORM CENTRE  
Bottom Hole Closure 277 ft N48.59°W

	<p>SCIENTIFIC DRILLING INTERNATIONAL FOR PHILLIPS PETROLEUM CORP. SOUTH COCKER UNIT 87-10 IN ECTOR COUNTY, TEXAS</p>	<p>True (° S) Mag (° S)</p> 
---	--	---



PLANE OF VERT SECTn N55 16W



SCIENTIFIC DRILLING INTERNATIONAL

MIDLAND, TEXAS

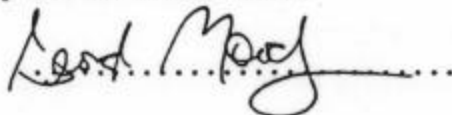
PHILLIPS PETROLEUM COMPANY

Well Name : PHILLIPS/SOUTH COWDEN #8-19  
Location : ECTOR COUNTY, TEXAS  
:  
:  
Date Surveyed : 12/12/91  
Job Number : 32G1291226/32D1291227  
Survey Performed By : RICK EATON/CHARLES WOOLFOLK

State Plane Coord

Long - 102.37833  
Lat 31.75411

This survey is correct to the best of my knowledge  
and is supported by actual field data.

 COMPANY REPRESENTATIVE

## SCIENTIFIC DRILLING INTERNATIONAL

Well Name : PHILLIPS PETROLEUM COMPANY  
 Location : PHILLIPS/SOUTH COWDEN #8-19  
 : ECTOR COUNTY, TEXAS

Page 1 of 2  
 Date 12/12/91  
 Filename : SCDEM819

No Interpolation

MD	INC	DIR	TVD	LAT	DEP	VS	D'LEO
ft	deg	deg	ft	ft	ft	ft	*/100
0.0	0.00	N 0.00°E	0.00	0.00	0.00	0.00	0.0
100.0	0.44	S 1.36°W	100.00	-0.38	-0.01	0.21	0.4
200.0	0.34	S57.62°W	200.00	-0.93	-0.27	0.71	0.4
300.0	0.32	S45.68°W	300.00	-1.28	-0.72	1.28	0.1
400.0	0.58	N74.03°W	399.99	-1.34	-1.41	1.90	0.5
500.0	0.10	N70.98°W	499.99	-1.17	-1.97	2.29	0.5
600.0	0.54	S13.32°E	599.99	-1.60	-1.95	2.50	0.4
700.0	0.74	S34.59°E	699.98	-2.59	-1.47	2.61	0.1
800.0	0.91	S50.72°E	799.97	-3.62	-0.49	2.31	0.1
900.0	0.93	S45.94°E	899.96	-4.69	0.71	1.84	0.1
1000.0	1.05	S52.27°E	999.95	-5.82	2.01	1.31	0.1
1100.0	0.34	S16.54°E	1099.94	-6.66	2.82	1.06	0.1
1200.0	0.98	S 8.80°E	1199.93	-7.79	3.04	1.47	0.1
1300.0	0.54	S16.62°W	1299.92	-9.09	3.03	2.15	0.1
1400.0	0.78	S26.54°E	1399.92	-10.15	3.20	2.56	0.1
1500.0	0.77	S70.19°E	1499.91	-10.98	4.14	2.20	0.1
1600.0	0.56	N63.43°E	1599.90	-10.99	5.21	1.29	0.1
1700.0	0.27	S73.94°W	1699.90	-10.84	5.42	1.03	0.1
1800.0	0.44	S50.84°E	1799.90	-11.15	5.49	1.13	0.1
1900.0	0.37	N86.65°W	1899.90	-11.37	5.47	1.27	0.1
2000.0	0.24	N76.79°E	1999.90	-11.30	5.35	1.33	0.1
2100.0	0.92	S15.64°E	2099.89	-12.03	5.77	1.35	0.1
2200.0	0.79	S 2.17°E	2199.88	-13.49	6.01	1.91	0.1
2300.0	0.89	S57.52°E	2299.87	-14.60	6.69	1.90	0.1
2400.0	1.46	S45.83°E	2399.85	-15.90	8.26	1.24	0.1
2500.0	1.20	S13.23°E	2499.82	-17.81	9.41	1.25	0.1
2600.0	0.87	S53.64°E	2599.81	-19.28	10.27	1.29	0.1
2700.0	1.39	S51.51°E	2699.79	-20.48	11.83	0.59	0.1
2800.0	1.14	S21.09°E	2799.77	-22.17	13.13	0.35	0.1
2900.0	0.65	S46.18°E	2899.75	-23.49	13.90	0.39	0.1
3000.0	0.84	S67.94°E	2999.75	-24.16	14.99	-0.19	0.1
3100.0	0.64	S29.51°E	3099.74	-24.92	15.94	-0.61	0.1
3200.0	0.29	N 2.44°E	3199.74	-25.15	16.23	-0.73	0.1
3270.0	0.58	N73.63°E	3269.74	-24.87	16.58	-1.17	0.1
3333.0	1.75	S27.00°W	3332.73	-25.64	16.45	-0.66	3.1
3392.0	4.00	S59.00°W	3391.65	-27.50	14.27	2.16	4.1
3506.0	7.50	S73.00°W	3505.07	-31.73	3.75	13.35	3.1
3537.0	8.75	S74.00°W	3535.75	-32.97	-0.46	17.58	4.1
3632.0	9.75	S75.00°W	3629.52	-37.04	-15.17	32.26	1.1
3786.0	9.50	S72.00°W	3781.35	-44.35	-39.85	57.13	0.1

SCIENTIFIC DRILLING INTER. 'IONAL

Well Name : PHILLIPS PETROLEUM COMPANY  
 Location : PHILLIPS/SOUTH COWDEN #8-19  
 : ECTOR COUNTY, TEXAS

Page 2 of 2  
 Date 12/12/91  
 Filename : SCDEM815

No Interpolation

MD ft	INC deg	DIR deg	TVD ft	<i>NS</i> LAT ft	<i>EW</i> DEF ft	VS ft	D'LEC */100
3942.0	9.00	S72.00*W	3935.32	-52.09	-63.70	81.52	0.2
4129.0	9.00	S73.00*W	4120.02	-60.89	-91.60	109.91	0.1
4315.0	8.00	S75.00*W	4303.97	-68.49	-118.02	136.42	0.6
4471.0	9.00	S81.00*W	4458.26	-73.21	-140.55	158.11	0.5
4574.0	8.00	S80.00*W	4560.13	-75.72	-155.57	172.23	1.0
4760.0	8.00	S80.00*W	4744.32	-80.21	-181.06	196.33	0.0
4946.0	7.75	S80.00*W	4928.56	-84.64	-206.16	220.05	0.1
5132.0	7.00	S81.00*W	5113.02	-88.59	-229.71	242.20	0.6
5172.0	7.00	S81.00*W	5152.73	-89.35	-234.52	246.70	0.6

- 90                      - 235

Origin of Bottom Hole Closure PLATFORM CENTRE  
 Bottom Hole Closure 251 ft S69.14\*W

## **INJECTIVITY TESTS**

# South Cowden Unit Injection Surveys

Well No.	ID	Perf/IDH	Layer	Date	Intensity	1 Velocity	Date	Intensity	2 Velocity	Date	Intensity	3 Velocity	Date	Intensity	4 Velocity
1W04	4725	OH 4615-4725	Above	5/2/85	6.2	25	5/30/84	12.5	-	5/13/83	55	53	3/30/83	10/23/72	41.5
		G 4645-4664			38.1	21		39.7	-		20	23.6		-	4.6
		F 4664-4701			55.7	54		47.8	-		21.9	18		32.7	36.7
		E 4701-4767									3.1	5.4		38.3	17.2
2W06	4685	OH 4480-4685	Above	11/2/84			6/2/84	27	51	8/29/81	32.8	32	10/23/72	-	9/2/67
		G 4508-4522			0	0		0	0		7.2	18		0	3.4
		F 4522-4564			21	0		3.9	0		24.6	17		5	1.6
		E 4564-4631			79	100		32.5	23.1		29.4	1.2		33.4	58.4
		D 4631-4662			0	0		28.7	21.4		6	31.8		27	36.6
		C 4662						7.9	4.5						
2W13	4712	OH 4455-4712	Above	12/12/83	41	84	3/12/83		26	10/24/72	-	12.6	9/3/67		
		G 4608-4619			0	0			74		-	8.2			
		F 4619-4669			7.5	0		9			-	6.4		32	
		E 4669-4738			23.5	6		91			-	35.8		28	
		D 4738			28	10					-	37		40	
2W14	4732	P 4535-4708	Above	8/29/81			10/27/72			6/12/69					
		G 4476-4486													
		F 4486-4529			51.2	32									
		E 4529-4595			34.8	35					15.7	40			
		D 4595-4624			10.7	2.5		-	22.9		48.3	18			
		C 4624-4643			3.3	27.8		-	13.8		3	4			
		B 4643-4671				2.7		-	13.3		20.1	38			
		A 4671						-	50		12.9	-			
2W15	4700	P 4531-4659	Above	9/2/82			2/18/82			10/26/72					
		G 4480-4500													
		F 4500-4538			43	57		55	54						
		E 4538-4605			18.6	11.8		19	46		-	56			
		D 4605-4637			11.4	10.3		26	-		-	35.5			
		C 4637-4654			18	17.9					-	8			
		B 4654			9	3					-	0.5			



**South Cowden Unit  
Injection Surveys**

Well No.	ID	Part/Off	Layer	Date	Intensity	Velocity	Date	Intensity	Velocity	Date	Intensity	Velocity	Date	Intensity	Velocity	Date	Intensity	Velocity
2V16	4700	P 4524-4666	Above G 4511-4532 F 4532-4563 E 4563-4629 D 4629-4657 C 4657-4669 B 4669	11/14/84			3/30/83											
2V19	4700	P 4546-4660	Above G 4533-4552 F 4552-4587 E 4587-4652 D 4652	2/3/84			12/12/83			3/23/83								
3V05	4747	OH 4604-4747	Above		NO LAYERS													
4V01	4737	OH 4604-4737	Above G 4685-4715 F 4715	2/3/84	73	-	3/30/83	57.9	-									
4V03	4715	P 4695-4699 OH 4700-4715	Above G 4678															
5V01	4780	OH 4486-4780	Above G 4588-4606 F 4606-4641 E 4641-4703 D 4703	7/7/92	95.5	84.2	5/13/84	76	85	4/8/83	78.6	89	9/16/71	73.5	82	10/5/67	-	86.7
5V04	4738	OH 4501-4738	Above G 4659-4680 F 4680-4724 E 4724-4784	8/8/84	84	76	3/12/83	73	78	10/27/72	-	63						

South Cowden Unit																			
Injection Surveys																			
Well No.	ID	Partion	Layer	Date	Intensity	Intensity	Intensity	Intensity	Intensity	Intensity	Intensity	Intensity	Intensity	Intensity	Intensity	Intensity	Intensity	Intensity	Intensity
5W06	4736	OH 4633-4736	Above	8/7/85															
		G 4657-4672		3/29/83	41.6	-	10/29/72												
		F 4672			3.9	-		13											
					100	100													
6W03	4699	OH 4496-4699	Above	7/7/92	84.6	80	3/15/84	18.5	46	8/11/83	26.4	56.4	9/2/87						
		G 4587-4602			2	0		10	0		4	6							
		F 4602-4640			2.3	5		11.3	24		15.6	11.6							
		E 4640			11.1	15		60.2	30		54	26							
6W07	4759	OH 4464-4759	Above																
		G 4575-4592																	
		F 4592-4631																	
		E 4631-4694																	
		D 4694-4720																	
		C 4720-4739																	
		B 4739																	
6W11	4768	OH 4530-4749	Above	11/7/83			8/28/81			9/26/71	22	36.6	5/25/66	-	31.6				
		G 4658-4671																	
		F 4671-4713			100	100		100	100		12.2	18.5		-	0.9				
		E 4713-4773									17.8	10.9		-	6.5				
		D 4773									20	26		-	30				
											28	8		-	31				
6W12	4767	OH 4550-4746	Above	5/30/84	100	100	3/16/84	100	-	3/11/83	100	100							
		G 4690-4702																	
		F 4702-4745																	
		E 4745																	

South Cowden Unit Injection Surveys																			
Well No.	ID	Partion	Layer	Date	Intensity	Δ Velocity	Date	Intensity	Δ Velocity	Date	Intensity	Δ Velocity	Date	Intensity	Δ Velocity	Date	Intensity	Δ Velocity	Date
6W15	4851	P 4560-4718	Above	12/14/83			9/17/82	8.8											
			G 4547-4560		4.6	0		4.2	0										
			F 4560-4609		30.4	43.5		12.1	17.6										
			E 4609-4679		7	8.7		10.9	4.4										
			D 4679-4707		18.2	32.8		19.7	28.8										
			C 4707-4725		24	5.3		44.3	49.2										
			B 4725-4751		6.3	9.7													
			A 4751		9.5														
6W16	4825	P 4630-4724	Above	7/11/84			7/12/83			3/30/83									
			G 4555-4571		0	0		0	0		0	0							
			F 4571-4612		0	0		0	0		0	0							
			E 4612-4665		78	44.8		37.6	47.4		39.5	62							
			D 4665-4715		22	55.2		30.4	40.6		34.6	28.3							
			C 4715-4732					32	12		25.9	9.7							
			B 4732																
7W03	4690	OH 4532-4677	Above	9/22/97	2														
			G 4573-4591																
			F 4591-4639																
			E 4639-4705		98														
			D 4705																
7W04	4695	OH 4536-4695	Above	11/2/84	30.1	15	10/27/83	22	22	10/28/72	-	25	5/27/66						
			G 4605-4619		4.1	7.7		0.3	0		-	0							
			F 4619-4667		12.8	26.3		21.6	21		-	29.4							
			E 4667-4737		53	51		56.1	57		-	45.6							
			D 4737																

[illegible]

South Cowden Unit																			
Injection Surveys																			
Well No.	ID	Part/OH	Layer	Date	Σ Intensity	Σ Velocity	Date	Σ Intensity	Σ Velocity	Date	Σ Intensity	Σ Velocity	Date	Σ Intensity	Σ Velocity	Date	Σ Intensity	Σ Velocity	Σ Velocity
8V11	4760	P 4568-4690	Above	5/13/83															
			G 4559-4574		9.2	26													
			F 4574-4616		26.8	23.8													
			E 4616-4683		64	50.2													
			D 4683-4712																
			C 4712-4726																
			B 4726																
8V15	4800	P 4695-4791	Above	7/9/85	48.4	35	7/18/74			7/18/74	2.6								
			G 4698-4717		14.6	54.2		5.9	6.8		8	2.7							
			F 4717-4766			4.8		21.7	38.5		16.8	21							
			E 4766		37	6		36.4	25.7		34.6	34.3							
								36	29		38	42							
9V02	4822	OH 4636-4725	Above	7/9/85		NO LAYERS													

## **SIMULATION MODEL PROPERTIES**

- 1) Historical production and injection data by well is provided in digital format as an Oil Field Manager database.
- 2) Simulation model data is provided in digital form in an ASCII file “SCUMODEL.DAT”. This file contains model input data for:-

Grid dimensions and structural configuration:

Delta X  
Delta Y  
Delta Z  
Subsea depth

Grid cell properties:

Porosity  
Permeability  
Initial Water Saturation

PVT properties

Relative Permeability Data by Rock Type

Initial Reservoir Pressure Distribution

Volumetric Calculations of Fluid - in –Place

## **SPECIAL LABORATORY STUDIES**

## **SLIM TUBE DISPLACEMENTS TO MEASURE MINIMUM MISCIBILITY PRESSURE AT THE SOUTH COWDEN UNIT**

### **Evaluate Effects of Changing Recycle Gas Composition on MMP**

Laboratory slim tube displacement data were obtained for pipeline-quality CO<sub>2</sub> at 1400 psia and 1600 psia. The experimental apparatus, methods, and results for these laboratory displacements are included with the supporting data in this report. Compositional simulations were run to match the laboratory slim tube displacements and verify the equation-of-state (EOS) fluid characterizations. The simulation predictions matched laboratory slim tube displacements very closely using both 16-component and 8-component EOS fluid characterizations. The simulation work indicated that minimum miscibility pressure (MMP) for the South Cowden crude is approximately 1200 psia. Current reservoir pressure at South Cowden is approximately 2200 psi - substantially above the minimum required for effective multi-contact miscible displacement by pipeline-quality CO<sub>2</sub>.

Compositional simulation model predictions of CO<sub>2</sub> project performance include forecasts of changes in the volume and composition of produced gas vs. time. The project development plan calls for the produced gas to be mixed with pipeline CO<sub>2</sub> and reinjected. This will result in a changing injection gas composition over the project life and could raise the MMP required to achieve adequate oil recovery efficiency. Additional laboratory slim tube displacements, were considered necessary to evaluate the impact of changes in injection gas composition on MMP during the CO<sub>2</sub> flood project.

The forecast of average injection gas composition vs. time for the Base Case development plan is presented in Table II.1.3.1. The changes in injection gas composition over the life of the project are not large because the South Cowden crude has a relatively small solution gas content. The impact of these small composition changes on MMP was initially evaluated by simulating additional slim tube displacements with the compositional model using the varying injection gas compositions. This work showed that recycling produced gas resulted in negligible changes in oil recovery efficiency and MMP (Figure II.1.3.1) compared with that obtained using pipeline-quality CO<sub>2</sub>. Because the average flooding pressure during the project life was so far above the predicted MMP, it was judged unnecessary to conduct further laboratory slim tube displacements.



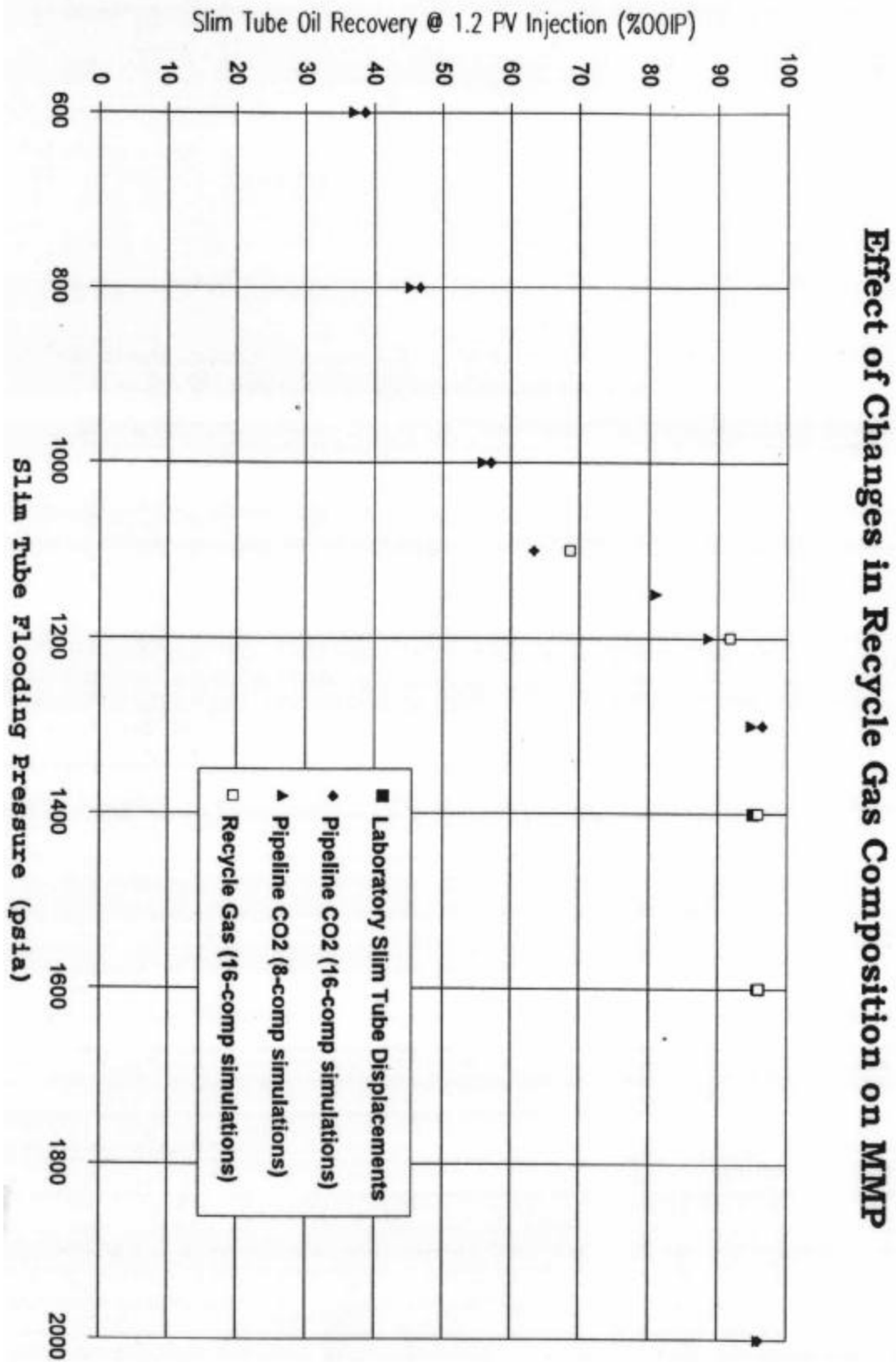
**Table II.1.3.1**  
**Average Injection Gas Composition vs. Time (mol%)**  
**South Cowden CO2 Project Base Case Forecast**

	1996	1997	1998	1999	2000	2001	2002	2003	2004	2005
N2	0.03%	0.04%	0.12%	0.12%	0.12%	0.12%	0.13%	0.13%	0.12%	0.13%
CO2	98.16%	97.58%	92.63%	92.41%	92.48%	92.16%	91.59%	91.15%	91.98%	91.18%
H2S	0.12%	0.16%	0.47%	0.48%	0.47%	0.49%	0.52%	0.55%	0.50%	0.54%
C1	0.81%	1.03%	2.84%	2.82%	2.75%	2.84%	3.03%	3.15%	2.87%	3.13%
C2	0.37%	0.48%	1.36%	1.36%	1.33%	1.38%	1.47%	1.54%	1.40%	1.53%
C3	0.32%	0.44%	1.41%	1.47%	1.47%	1.53%	1.64%	1.72%	1.56%	1.72%
iC4	0.04%	0.06%	0.24%	0.26%	0.26%	0.28%	0.30%	0.32%	0.29%	0.32%
nC4	0.08%	0.13%	0.52%	0.58%	0.60%	0.64%	0.69%	0.74%	0.67%	0.75%
iC5	0.02%	0.03%	0.14%	0.17%	0.18%	0.19%	0.21%	0.23%	0.21%	0.24%
nC5	0.01%	0.02%	0.11%	0.13%	0.14%	0.15%	0.16%	0.18%	0.16%	0.19%
C6	0.01%	0.02%	0.11%	0.14%	0.15%	0.16%	0.18%	0.20%	0.18%	0.21%
C7+	0.00%	0.01%	0.04%	0.05%	0.06%	0.06%	0.07%	0.08%	0.07%	0.09%

	2006	2007	2008	2009	2010	2011	2012	2013	2014	2015
N2	0.13%	0.13%	0.12%	0.13%	0.12%	0.12%	0.12%	0.11%	0.10%	0.09%
CO2	91.12%	90.87%	91.83%	91.08%	91.19%	91.52%	91.50%	91.87%	92.30%	92.64%
H2S	0.55%	0.56%	0.50%	0.54%	0.53%	0.51%	0.51%	0.48%	0.45%	0.42%
C1	3.12%	3.18%	2.86%	3.09%	3.00%	2.85%	2.85%	2.67%	2.50%	2.35%
C2	1.53%	1.56%	1.40%	1.51%	1.48%	1.41%	1.41%	1.32%	1.24%	1.17%
C3	1.72%	1.77%	1.58%	1.73%	1.70%	1.63%	1.63%	1.55%	1.46%	1.39%
iC4	0.32%	0.33%	0.29%	0.32%	0.32%	0.31%	0.31%	0.30%	0.29%	0.28%
nC4	0.76%	0.79%	0.71%	0.79%	0.79%	0.78%	0.78%	0.77%	0.74%	0.72%
iC5	0.24%	0.26%	0.23%	0.26%	0.27%	0.27%	0.27%	0.28%	0.28%	0.28%
nC5	0.19%	0.21%	0.18%	0.21%	0.22%	0.22%	0.22%	0.23%	0.23%	0.23%
C6	0.22%	0.24%	0.21%	0.25%	0.26%	0.27%	0.27%	0.29%	0.29%	0.30%
C7+	0.09%	0.10%	0.09%	0.10%	0.11%	0.11%	0.12%	0.13%	0.13%	0.13%

Figure II.1.3.1



## **SPECIAL CORE FLOOD TESTS**

### **MAGNETIC RESONANCE IMAGING OF SOUTH COWDEN CORE PLUGS**

R.L. King and B.A. Baldwin  
Phillips Petroleum Co.  
Bartlesville, OK

#### **Summary**

Magnetic Resonance Images were made of 123 core plugs from three locations in the South Cowden reservoir. These images assisted in the selection of the most representative plugs for use in further core analysis. Dramatic variations in porosity occurred within fractions of a millimeter in some of the plugs. Without the imaging it would have been easy to select plugs which would have given misleading information for reservoir simulation.

This report summarizes the experimental procedures for obtaining MRI images and gives examples of the information obtained.

#### **Introduction**

Magnetic Resonance Imaging, MRI, produces images, or pictures, of oil and water inside porous rocks. Sometimes the information generated is sufficient to solve specific concerns, other times it is combined with other geophysical measurements to solve problems.

MRI technology was leveraged from medical science, where it was developed to examine the internal organs and tissue of humans, without surgery. We have slightly modified the hardware and data acquisition parameters to similarly image oil and water inside cores. MRI uses the resonance absorption and emission of energy from the interaction between the magnetic spin of a nucleus with an unpaired electron, hydrogen in our case, and Radio Frequency pulses to determine number of nuclei in a sample and their interaction with the pore surface. MRI is complimentary to X-ray CAT Scanning. MRI measures only the fluid inside the pores. CAT measures the density of the sample, and by subtraction can determine doped fluids in the pores.

In the past, reservoir engineers and petroleum researchers were forced to assume that core samples were of uniform porosity and permeability because they did not have non-destructive methods which examined the interior of cores. MRI images show the spatial distribution of fluids inside porous rocks which allows the determination of porosity distribution and heterogeneity (1,2). Because MRI is both non-invasive and non-destructive it does not interfere with flow processes and leaves the core available for additional tests. Converting from animal tissue to rocks required only minor modifications in hardware and software. By collecting the images as a function of time and displaying them sequentially animated movies are made of fluid movement. A spatial distribution of pore sizes can be determined by

a T1 mapping technique. Sometimes the core is treated in another laboratory and measured at selected times. Other times the process is allowed to take place inside the MRI and the process monitored continuously. The output can be an image of fluid or porosity distribution, a chart depicting changes, an average number or an animated movie of fluid movement with time.

For the present study the MRI was used to determine the individual porosity distributions of several groups of South Cowden plugs. This screening helped in the selection of the most homogeneous plugs for additional testing. Heterogeneities greatly increase the complexity of fluid flow and it's interpretation. In this report we will show representative images, describe how they were taken and discuss what they indicate.

## Experimental

Images were made with a Sisco 85/310 CSI which operates at 85.55 Mhz for hydrogen nuclei. The 2 Telsa (20,000 Gauss) magnet, Fig. 1, has a 31 cm bore with 22 cm free diameter inside the standard gradient coil set. However, for this study the high performance gradient coil set, with a 13 cm bore, was used. This HPAG has a gradient strength of 10 Gauss/cm which provides better resolution and greater signal to noise compared to the standard gradient set with 3 gauss/cm. The core plugs were centered in a 9 cm I.D. saddle coil which acted as both RF transmitter and receiver, right center in Fig. 2. The core was contained in a sealed glass container, left center in Fig. 2, to minimize evaporation during the measurement. During imaging the core plug and container were inserted into the saddle coil and both were placed into the center of the magnet. The electronics, Fig. 3, consist of a magnetic gradient power supply, far right, the electric distribution center and RF transmitters, center right, the acquisition computer and pulse shapers, center left and the I/O computer in the foreground.

Listed in Table 1 are the typical parameters used to screen these cores. On some occasions the cores were too long to image at one time. These cores were moved inside the MRI coil and images collected separately for the top and bottom.

**Table 1**

**Typical MRI Parameters used to Image South Cowden Core Plugs**

<b>Frequency</b>	<b>85.55 Mhz</b>	<b>Acquisition Time</b>	<b>2.7 ms</b>
<b>Number of points</b>	<b>512</b>	<b>Signal width</b>	<b>94.246 kHz</b>
<b>90 deg. Pulse</b>	<b>500 us</b>	<b>180 deg. Pulse</b>	<b>500 us</b>
<b>Recovery Time</b>	<b>0.5 sec</b>	<b>Echo Time</b>	<b>4.0 ms</b>

<b>90 deg. Power</b>	<b>102</b>	<b>180 deg. Power</b>	<b>114</b>
<b>Averages</b>	<b>4</b>	<b>Pulse Shape</b>	<b>Gauss</b>
<b>Read Out Grad.</b>	<b>400</b>	<b>Phase Encode Grad.</b>	<b>-8</b>
<b>Slice Select. Grad.</b>	<b>300</b>	<b>Bandwidth Sw1</b>	<b>1028 Hz</b>
<b># Phase encode step</b>	<b>128</b>	<b># Pixels Read Out</b>	<b>512</b>
<b># Pixels Phase Enc</b>	<b>512</b>	<b># slices</b>	<b>5</b>
<b>Vertical Size</b>	<b>11 cm</b>	<b>Horizontal Size</b>	<b>6 cm</b>
<b>Orientation</b>	<b>Zxy</b>	<b>Douple Precision</b>	<b>Yes</b>
<b>Pilot</b>	<b>Yes</b>	<b>Inversion Recovery</b>	<b>no</b>

With these parameters the pixel size in these images is 0.43 mm x 0.43 mm. Slice thickness is about 4 mm.

Two imaging orientations were used, one along the length of the core (coronal) and the other across the core (transverse). Fig. 4 shows the appearance of each image for the two orientations. Using two orientations improves the chance of detecting heterogeneities because they are often more visible in one orientation than another. Multiple slices, each approximately 4 mm thick, provide 3-D information about the location of the heterogeneities inside each plug. Most of these cores were very easy to image and gave sharp pictures. The few plugs which were difficult to image produced a very grainy appearance. This latter is due to a weaker signal producing a lower signal to noise ratio.

Three sets of South Cowden core were imaged. The first set of 17 plugs were obtained from Emmons Field and imaged as received, in a preserved state. These plugs were imaged primarily to demonstrate what could be learned from MRI characterization and to optimize the MRI parameters for imaging South Cowden core. The second set of 54 plugs, from Well #6-23, Ector Co., were imaged as received in a preserved state from being stored under produced oil. A few of the third set, Well # 8-19 South Cowden Unit, were imaged as received, in an unpreserved state. These tended to produce weak images due to the loss of fluids, primarily water. The remainder of this third set, 52 plugs, were imaged after being saturated with water which produced strong signals.

For a few plugs in the third set, particularly one after CO<sub>2</sub> flooding, T1 relaxation maps were made. These maps show relative pore size distribution and are useful to differentiate between the effects on image intensity due to pore sizes and the absolute saturation of fluid at a specific location. The T1 relaxation maps are made by collecting several images, typically 9 to 12, at different inversion recovery times then fitting each pixel to an exponential equation. The inverse of the relaxation rate is the T1 relaxation time. The intensity of each pixel in these T1 relaxation maps is proportional to the relaxation time in that pixel, the brighter the intensity the longer the relaxation time. For a given surface interaction,

wettability, the relaxation time is controlled by diffusion to a pore wall. Thus a longer relaxation time indicates larger pores and a shorter relaxation times indicates smaller pores. When the intensity of each pixel is extrapolated to zero inversion recovery time the rate contribution is eliminated and an absolute hydrogen nuclei density, or porosity, map is produced.

## Results and Discussion

Figs. 5-7 show examples of the three major lithologies represented in these South Cowden core plugs. The first, Fig. 5, shows a homogenous distribution of porosity in a zone identified as chaotic. There is a slight indication of bedding planes in the transverse image, but it is not very significant. Fig. 6 shows a plug from the chaotic zone where significant differences in porosity are observed in fractions of a mm. These changes appear to be randomly, but not uniformly distributed. Fig. 7 shows moldic rock. The bright streaks are the voids left behind when the shells of the deposited forams dissolved. The matrix also contains fluid, the background intensity, but this is largely swamped by the intensity from the vugs. These images help identify the lithology of the core plugs without requiring cutting or slabbing of the core. It is extremely important to help to select those zones are more homogeneous, or at least where the heterogeneities are uniformly distributed. The information collected from such plugs is easier to interpret than plugs where the porosity is grossly heterogeneous.

An example of a difficult to interpret core plug is shown in Fig. 8. From routine core analysis this plug an average porosity of 20.6% was determined. However, analysis of the image showed the porosity to range from about 8% near the top to 45% near the bottom. This particular plug was part of a set being imaged to determine which would be best for CO<sub>2</sub> flooding experiments. In a flow experiment the flow rate would be determined by the tightest portion, typically in the 8% porosity section. Thus on a flow basis this plug would act like an 8% porosity plug, but the results would be plotted as, or attributed to, a porosity of 20.6%. Such a discrepancy would skew or bias further interpretation and prediction of flood parameters.

The last image, Fig. 9, shows a South Cowden plug after several CO<sub>2</sub> flooding experiments. The concave shape at the top of the images shows where core had been completely dissolved away. The bright spot just below the surface indicates the presence of additional fluid. The bright spot in the T1 relaxation map shows that this additional porosity was obtained by enlargement of the individual pores near the initial contact of the flood brine and the core. The darker region in the middle of the porosity map suggests, but does not prove, that part of the dissolved material may have been redeposited as it moved through the core. The slight darkening in the same area of the T1 map corroborates this suggestion. However, for proof it would be necessary to follow these changes at several times during the flood.

## Conclusions

From these imaging studies of South Cowden core it can be concluded that:

1. South Cowden core is often heterogeneous
2. To obtain easily interpreted results, each core plug should be examined for porosity heterogeneities and anomalies
3. Magnetic Resonance Imaging is an effective method for determining porosity distribution in South Cowden carbonate cores.

## **References**

1. B.A. Baldwin and W.S. Yamanashi, "NMR Imaging of Fluid Saturation Distributions in Cores" The Log Analyst, pp 536-49 (Sept.-Oct., 1991).
2. "Special Issue - Proceedings of the Second International Meeting on Recent Advances in MR Applications to Porous Media" Mag. Resonance Imaging, Vol. 12, No. 2 (1994).

## TABLE OF FIGURES

- Fig. 1 MRI 2 Tesla superconducting magnet. Sample/coil bore in the center of the magnet
- Fig. 2 Core plug container and RF coil
- Fig. 3 MRI electronics cabinets - magnetic Gradient Power Supply, far right; electrical distribution and RF amplifiers, center right; data acquisition computer and pulse shapers, center left; I/O computer in foreground
- Fig. 4 Two slice orientations used to collect images, upper along the plug's major axis and lower across the plug's major axis
- Fig. 5 Example of homogeneous porosity distribution in a chaotic zone
- Fig. 6 Example of inhomogeneous porosity distribution in a chaotic zone
- Fig. 7 Example of moldic porosity, a mixture of vugs and matrix porosity
- Fig. 8 Example of a plug with porosity change along the major axis
- Fig. 9 T1 relaxation time and porosity maps of a plug after CO<sub>2</sub> flooding



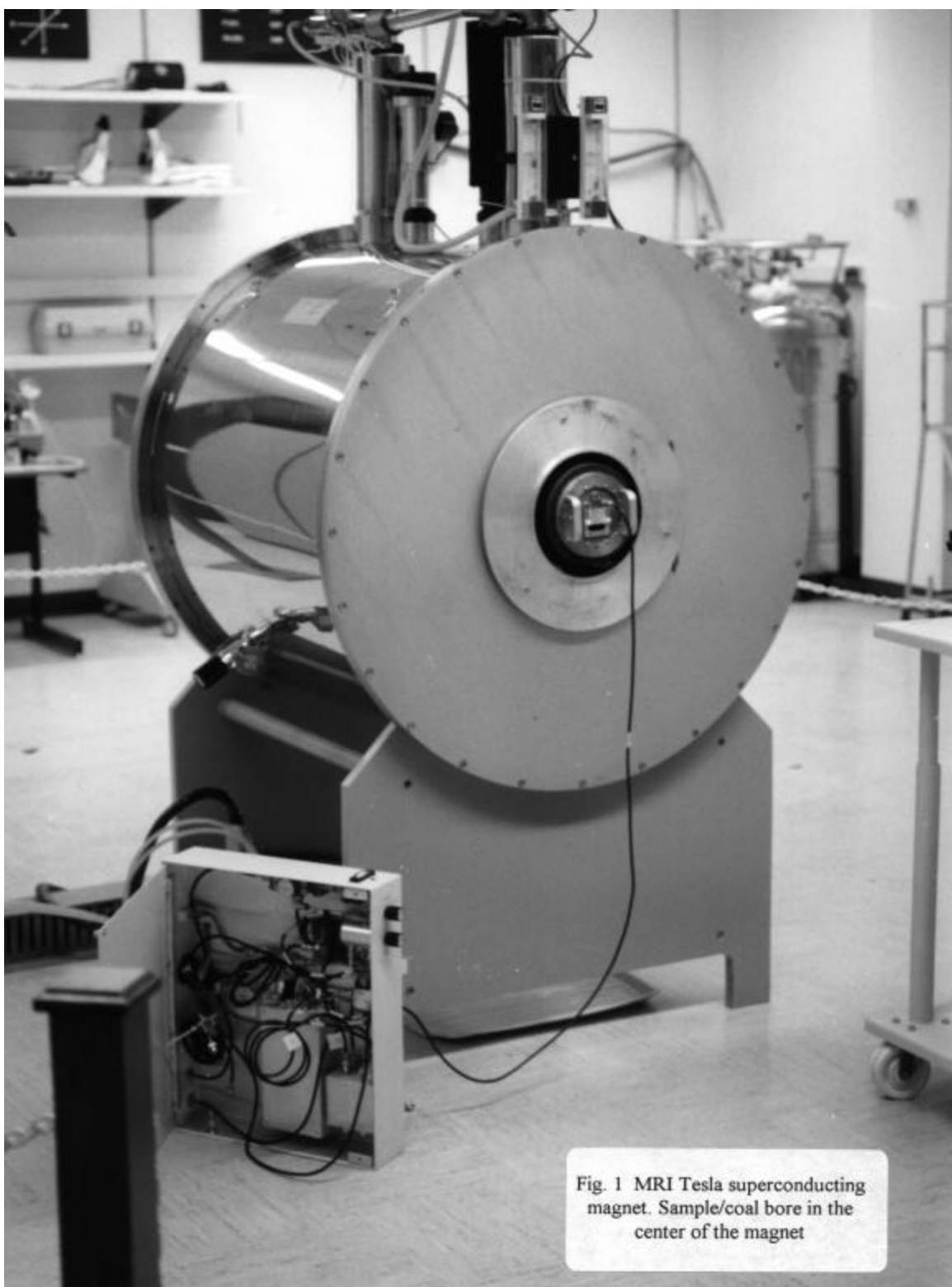


Fig. 1 MRI Tesla superconducting magnet. Sample/coil bore in the center of the magnet

Figure 1. MRI 2 Tesla superconducting magnet. Sample/coil bore in the center of the magnet



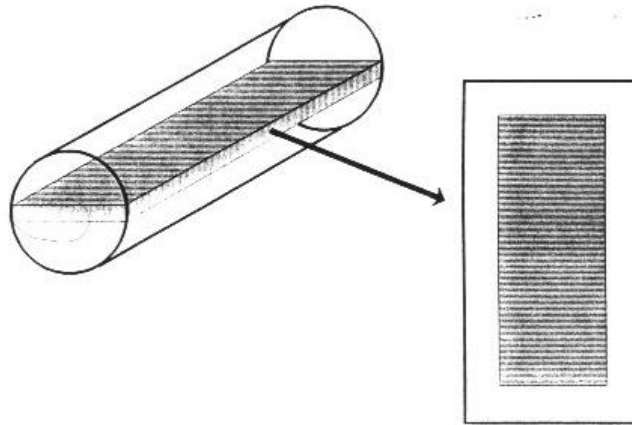
Figure 2. Core plug container and RF coil



Fig. 3 MRI electronics cabinets-magnetic Gradient Power Supply, far right; electrical distribution and RF amplifiers, center right; data acquisition computer and pulse shapers, center left; I/O computer in foreground

Figure 3. MRI electronics cabinets - magnetic Gradient Power Supply, far right; electrical distribution and RF amplifiers, center right; data acquisition computer and pulse shapers, center left; I/O computer in foreground.

### MRI Imaging - Coronal View



### MRI Imaging - Transverse View

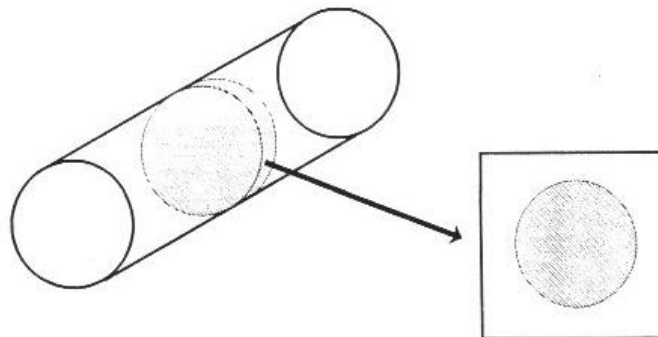


Fig. 4 Two slice orientations used to collect images, upper along the plug's major axis and lower across the plug's major axis

Figure 4. Two slice orientations used to collect images, upper along the plug's major axis and lower across the plug's major axis.

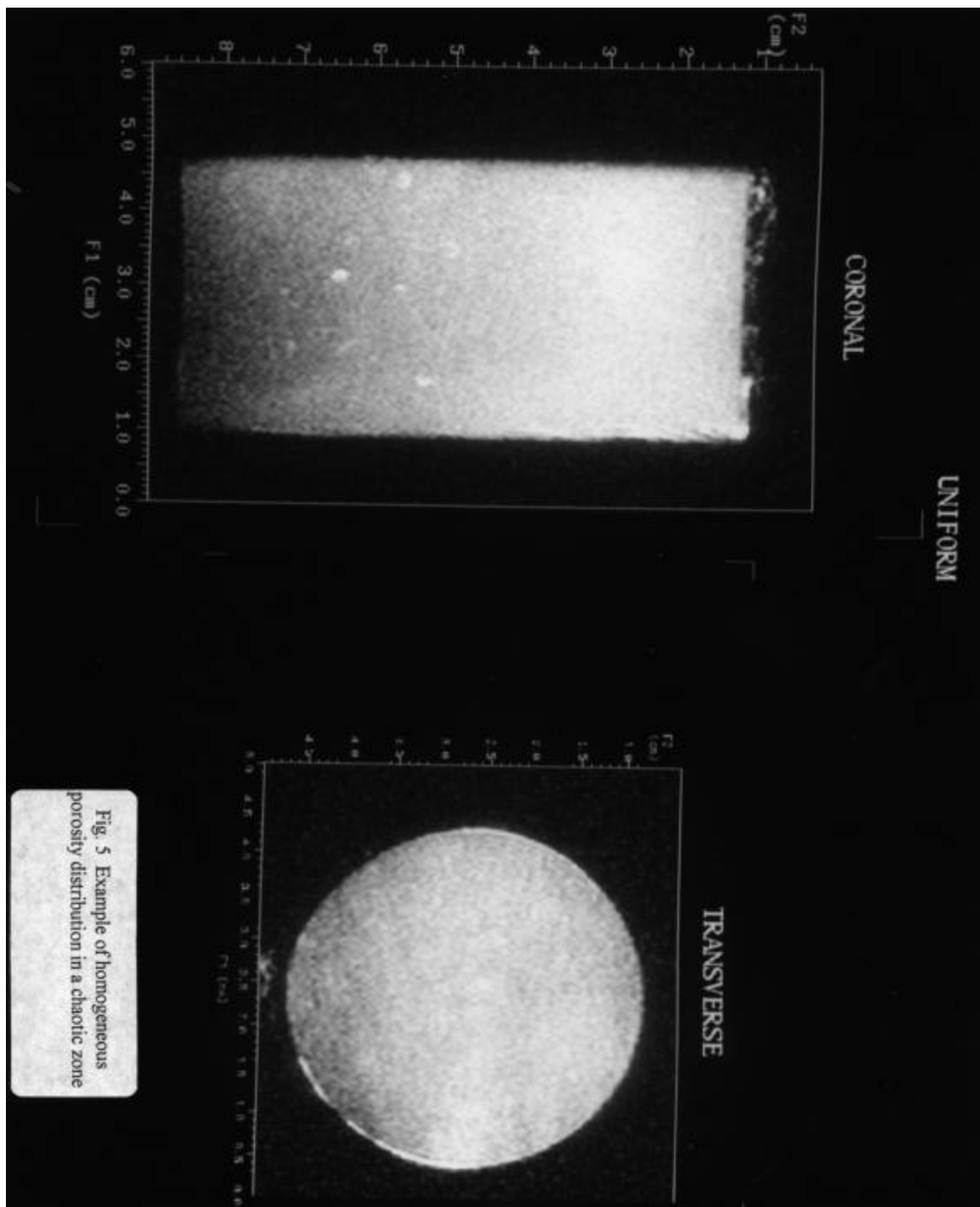


Fig. 5 Example of homogeneous porosity distribution in a chaotic zone

Figure 5. Example of homogeneous porosity distribution in a chaotic zone.

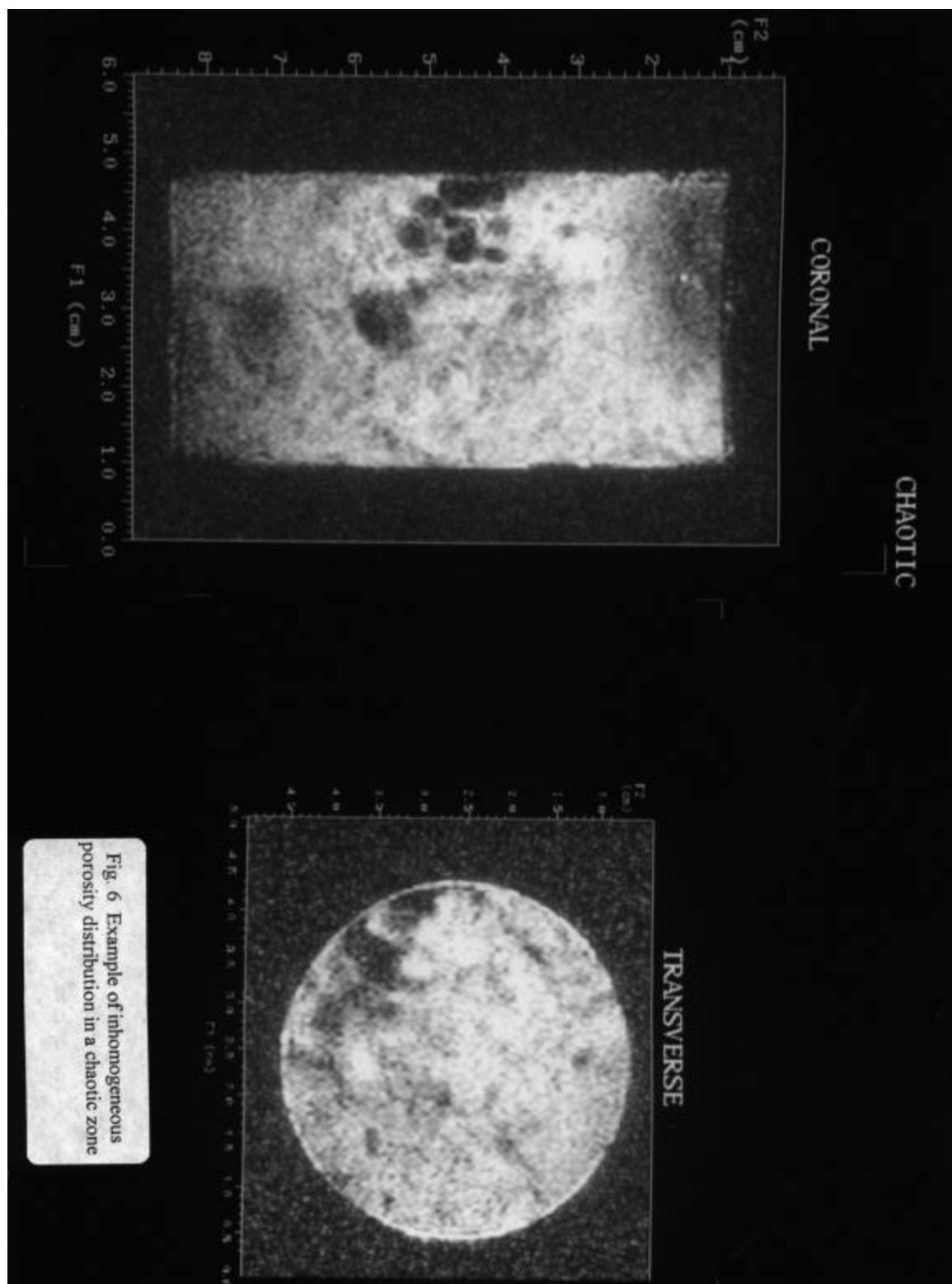


Fig. 6 Example of inhomogeneous porosity distribution in a chaotic zone

Figure 6. Example of inhomogeneous porosity distribution in a chaotic zone.

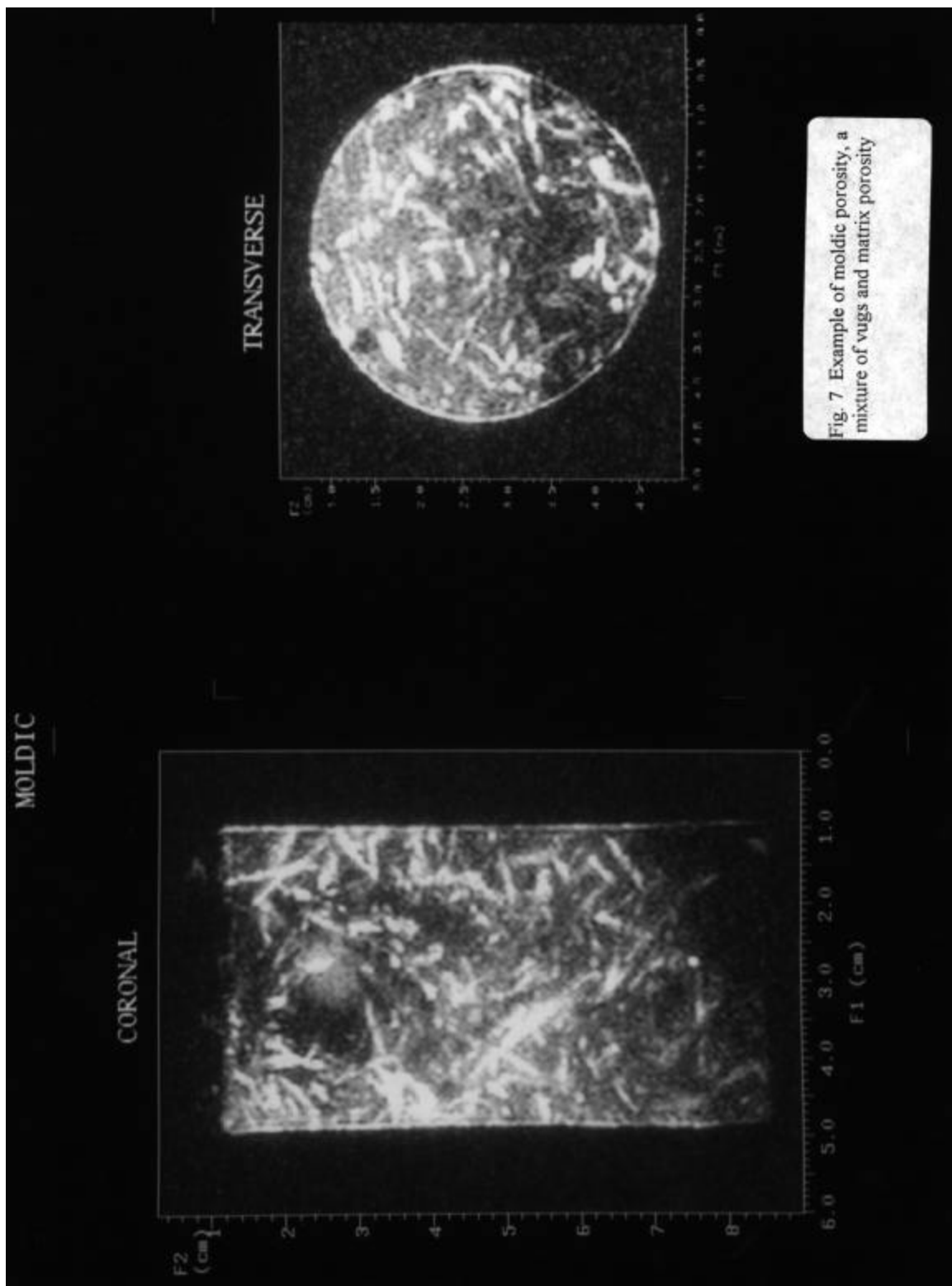


Figure 7. Example of moldic porosity, a mixture of vugs and matrix porosity.

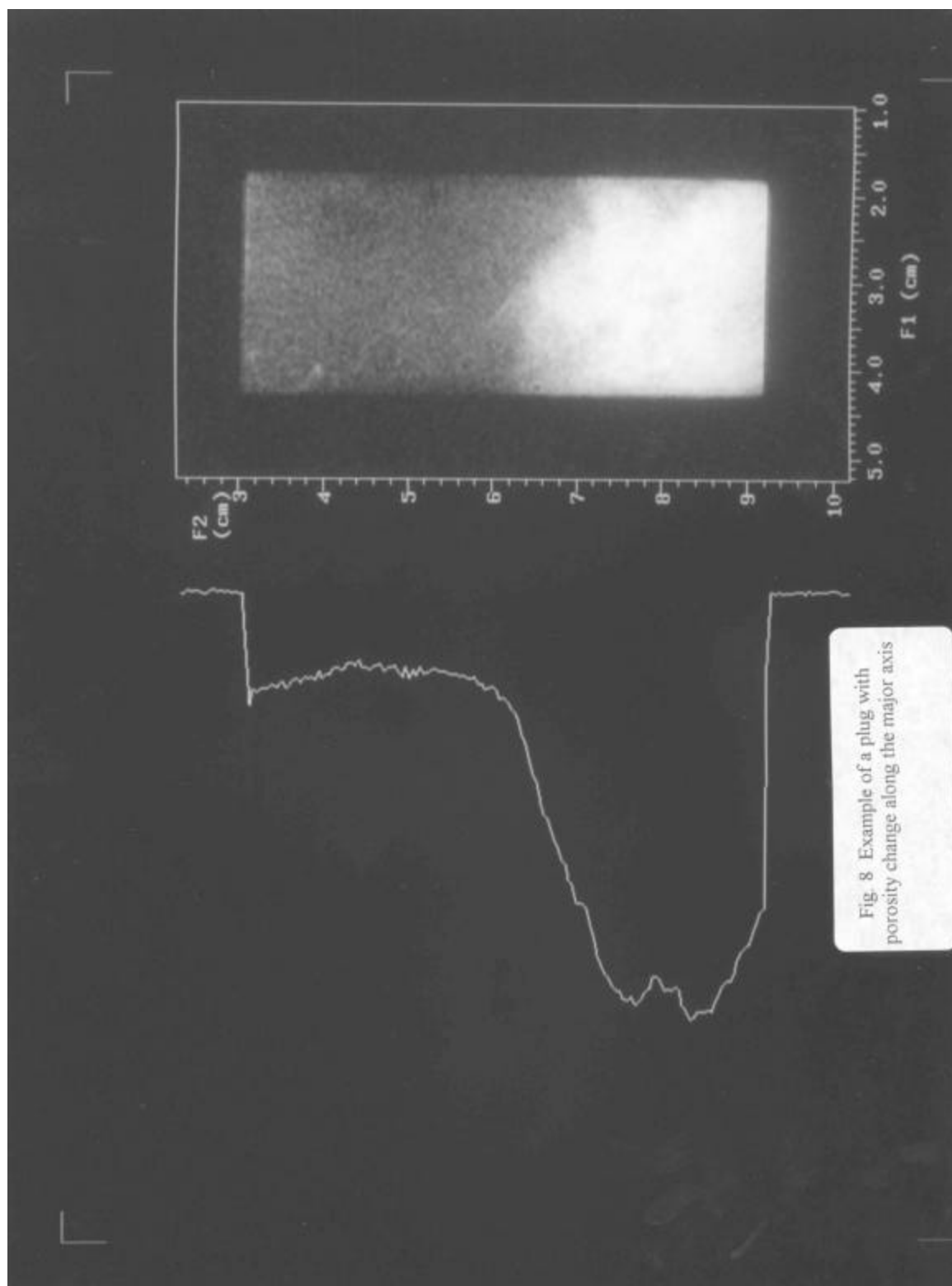


Figure 8. Example of a plug with porosity change along the major axis.



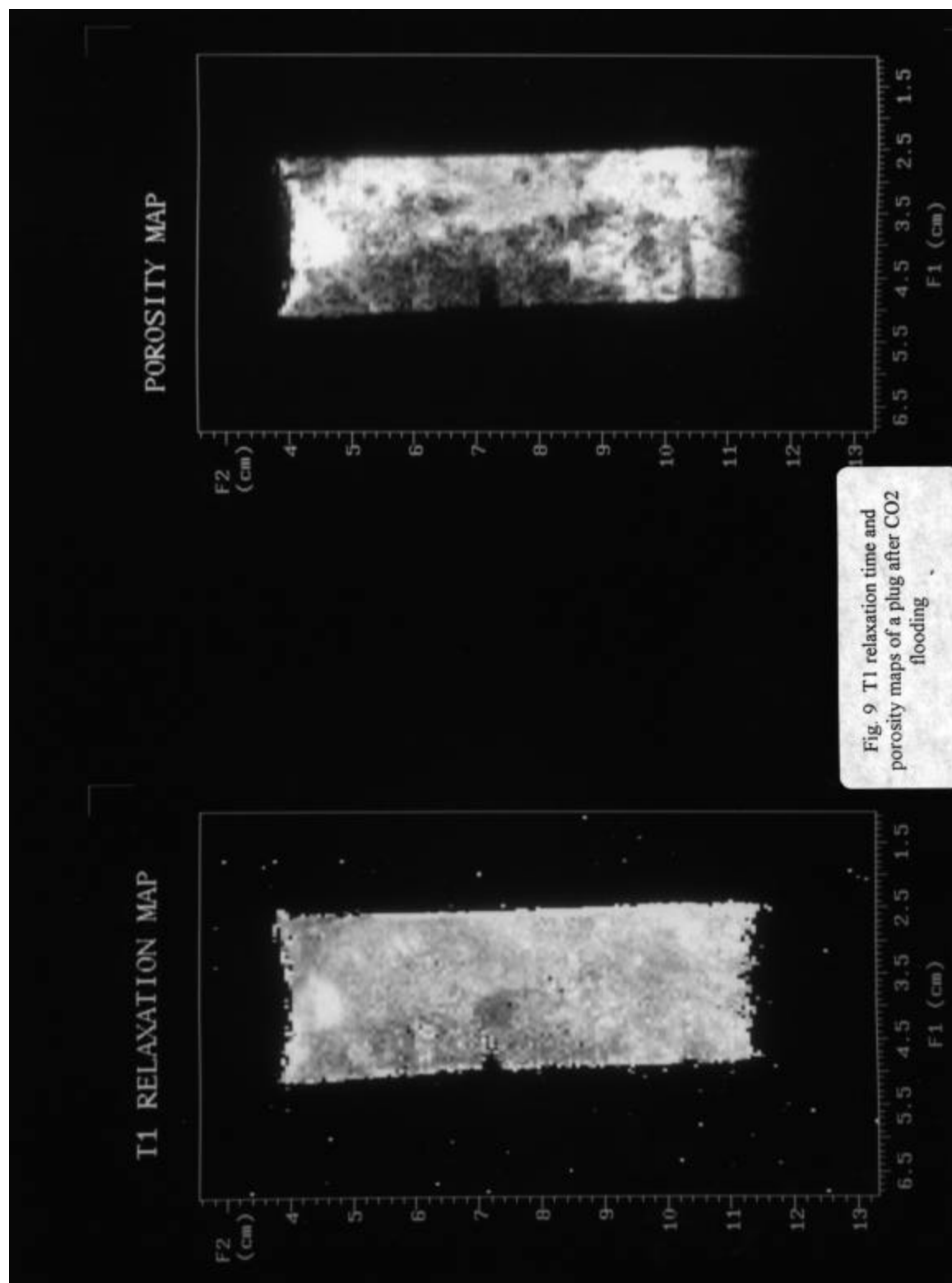


Figure 9. T1 relaxation time and porosity maps of a plug after CO<sub>2</sub> flooding.

## **SPECIAL LABORATORY STUDIES**

### **SOUTH COWDEN CO<sub>2</sub> MISCIBLE WAG TRAPPED GAS & RESIDUAL OIL EXPERIMENTS**

#### **OBJECTIVE**

The objective of this task was to determine, for the South Cowden Reservoir, representative CO<sub>2</sub> trapped gas saturations and residual oil saturations after CO<sub>2</sub> flooding under miscible displacement conditions.

#### **INTRODUCTION**

CO<sub>2</sub> relative permeability, trapped gas saturation, Sorm, and hysteresis effects are key parameters in determining injectivity and displacement in a miscible CO<sub>2</sub> WAG injection project. In an effort to measure these parameters to provide data for use in making predictions of WAG performance in the South Cowden Reservoir, a series of six coreflood experiments were conducted. South Cowden live oil, synthetic live brines, along with Magnetic Resonance Imaging (MRI) screened native state carbonate cores from the subject reservoir were used in conducting the corefloods, which were performed at South Cowden reservoir conditions of 98 F and 1800 psig. In this report, a review is presented of the four coreflood experiments considered most representative and/or informative (Corefloods 1, 2, 3, and 6).

#### **EXPERIMENTAL**

**Materials:** The study was conducted in two segments. Corefloods 1, 2, and 3 were conducted during the first segment with Coreflood 6 being conducted in the second segment. Segments one and two were primarily differentiated by the source of materials used. The cores, oil, and brine recipe used in segment one were obtained from the Emmons Unit of the South Cowden Reservoir; whereas, the same materials for segment two were obtained from the South Cowden Unit (SCU) of the South Cowden Reservoir.

Materials for Corefloods 1, 2, and 3: The live oil used for Corefloods 1, 2, and 3 was prepared from filtered (0.45 microns) Emmons Unit stock tank oil. The filtered oil was enriched with C5's and C6's and recombined with a C4- gas to a bubble point of 621 psia at 98 F (this closely approximated bubble points of Emmons Unit live oils studied by Petroleum Testing Service and D.B. Robinson Ltd.).

The cores used in conducting these first three corefloods were selected from sixty-six “native state” core plugs from the Emmons Unit. These 1.5 inch diameter by 2.5 - 3.0 inch long core plugs were obtained

from Emmons Unit Wells Nos. 146, 135, and 213. The uncleaned core plugs were received in individual glass jars which, in addition to the cores, had been filled with sand and crude oil.

Preliminary screening of the plugs was based upon the routine core analysis data of nearby plugs and supplemental geological descriptions about the plugs. The twenty-two cores which passed the pre-screening phase were subjected to subsequent screening by Magnetic Resonance Imagery (MRI) and/or STO permeability tests at 98 F. Six of these plugs were eventually selected and used in making the composite cores (two core plugs) used in conducting Corefloods 1, 2, and 3.

The composite cores were made up of two core plugs from the same facies with approximately equal oil permeabilities. A listing of the six plugs used in Corefloods 1, 2, and 3 is provided in Table I. Example MRI images of South Cowden core plugs can be found in the Magnetic Resonance Imaging section of this report. Somewhat more emphasis was placed upon the cores from the chaotic facies than that those from the moldic facies. One reason for this was that few cores with adequately high permeabilities were identified from the moldic facies. Another factor was the tendency of the moldic cores to plug-off during testing.

The composition of the synthetic brine was patterned after a water analysis of the Emmons Unit brine dated March, 1992. The total dissolved solids content of the brine used in the experiments was approximately 78,000 ppm. The synthetic brine used during the initial water injection step was saturated with methane at 98 F and 1800 psig so that no significant gas would be taken from that which was soluble in the live oil. The synthetic brine used during the second water injection step was saturated with CO<sub>2</sub> at 98 F and 1800 psig so that no significant CO<sub>2</sub> would be taken from that which was otherwise trapped in the core.

Materials for Coreflood 6: The live oil used for Coreflood 6 was prepared from filtered (0.45 micron) SCU stock tank oil. The filtered oil was enriched with C5's and C6's and recombined with a C4- gas to a bubble point of approximately 625 psia at 98 F. The STO was compositionally similar to the Emmons Unit oil used in Corefloods 1-5.

“Native state” core plugs were received from SCU Well 6-23. The plugs were shipped in groups in one gallon cans containing Isopar (a light refined oil). Fifteen core plugs were selected from a group of seventy-six which were subjected to MRI. These plugs were further screened by measuring their permeability to brine. Based upon both MRI and permeability screening, two plugs were selected for subsequent use in a CO<sub>2</sub> miscible WAG trapped gas experiment. The selected cores were used as set in forming a composite core.

The composition of the synthetic brine was patterned after an analysis of SCU formation water dated February, 1995. The total dissolved solids content of the brine was approximately 72,000 ppm. As described above, the synthetic brine was saturated at test conditions with methane used during the initial water injection step and CO<sub>2</sub> during the second water injection step.

**Apparatus:** Schematics of the apparatus used in this experimental program are provided in Figures 1a and 1b. In Figure 1a, the oven containing the core holder along with some of the more important external pieces of equipment are shown. One of the more notable of the external pieces of equipment is the Boyle's Law apparatus which was used in determining the trapped gas saturation. Due to the minimal success achieved in attempting to measure relative permeabilities during earlier corefloods, the rel-perm visual cell was removed prior to conducting Coreflood 6.

The oven in Figure 1b was largely devoted to containment of the pressurized supply fluids which included brine, stock tank oil, live oil, and CO<sub>2</sub>. One vessel permitted CO<sub>2</sub> to be bubbled into live oil and thus allowed a gradient live oil/CO<sub>2</sub> front to be passed through the core to simulate a miscible front. The brine vessel could be rocked which assisted in equilibration of the brine/CH<sub>4</sub> and brine/CO<sub>2</sub> solutions.

**Procedures:** The initial plan for all the coreflood experiments was to follow a WAG injection process in which restored composite cores would be sequentially subjected to an initial water injection step, a CO<sub>2</sub> injection step, and a secondary water injection step. This procedure worked reasonably well with cores taken from the chaotic facies but not with cores taken from the moldic facies. The moldic cores generally exhibited low permeabilities and the tendency to plug during water injection. Coreflood 3, in which a moldic composite core was used, was prematurely terminated during the initial water injection step due to plugging of the composite core.

Core Restoration: As mentioned above, the cores used in Corefloods 1, 2, and 3 had been oil flooded as part of the selection process; whereas, the cores used in Coreflood 6 had been brine flooded. In either case, restoration was initiated by first flooding the core with filtered STO. This was followed by live oil floods to displace the dead oil. The live oil floods were conducted on consecutive days. After displacing the STO, the composite core was shut-in overnight and allowed to equilibrate with the brine in the core. Additional live oil was injected on the following day to better insure that the GOR of the live oil was similar to that in the live oil supply vessel. This second live oil flood essentially completed the restoration process.

During the latter stages of the second live oil flood, data was obtained from which  $K_o$  at  $S_{wi}$  could be calculated. This permeability measurement served as the reference permeability in the subsequent relative permeability calculations ( $K_{rw}$  at  $S_{orw}$ ,  $K_{rco2}$  at  $S_{orm}$ , and  $K_{rw}$  at  $S_{gtrap}$ ).

Initial Waterfloods: For reasons mentioned above, methane saturated brine, at 98 F and 1800 psig, was injected during the initial water injection step. A high water-oil ratio was the primary criteria used in deciding when to terminate the initial waterflood.

Attempts were made during the initial waterfloods of Corefloods 1, 2, and 3 to obtain unsteady-state water/oil relative permeability data. A Beckman HPLC pump was used to inject the water during the initial waterfloods of these corefloods to fulfill the requirement of maintaining the pressures at the injection and production ends of the composite cores relatively constant. Due to the above mentioned plugging, the relative permeability data collected for Coreflood 3 was obviously of no value. Since the

fluids produced during the initial water injections of Corefloods 1 and 2 tended to go from oil to a high water cut, with very short transition periods during which there were significant fractional flows of both oil and water, the relative permeability data for these corefloods were also determined to be of little if any value. No attempt was made to collect unsteady-state relative permeability data during the initial waterflood of Coreflood 6. With constant upstream pressure no longer being a requirement, a Ruska positive displacement pump was used during the initial waterflood of Coreflood 6. In addition, the Ruska sight glass, used to measure oil production during the initial waterfloods of Corefloods 1, 2, and 3 was removed prior to conducting Coreflood 6.

CO<sub>2</sub> Floods: The CO<sub>2</sub> flood step was somewhat more involved than simply injecting dry CO<sub>2</sub> after the initial brine flood. To initiate the CO<sub>2</sub> flood step, the lines were first flushed up to the core inlet (at the top of the core) with live reservoir fluid. CO<sub>2</sub> was then injected into the bottom of a mixing accumulator (containing live oil) at a rate of 10 cc/hr. The CO<sub>2</sub> mixed with and dissolved in the live oil, swelling it. Effluent from the accumulator, after passing through a filter, was the injectant for the core flood. Initially the core would see reservoir fluid. The displacing phase “graduated” to CO<sub>2</sub> as the CO<sub>2</sub> content of the mixing cylinder increased. In this manner the CO<sub>2</sub> coreflood was stabilized. This process created a CO<sub>2</sub>/oil viscosity-graduated zone that presumably played some role in reducing viscous fingering.

Second Waterflood: CO<sub>2</sub> saturated brine was injected during the post-CO<sub>2</sub> waterflood. The total water volume input during this step of the WAG injection process was not to exceed 1.2 pore volumes.

Post WAG Analyses: The post WAG analyses was comprised of several steps. The primary focus of these steps was to determine the trapped gas saturation in the composite core which existed after the second brine flood.

Subsequent to the second brine flood, the core was shut-in and allowed to cool to room temperature while maintaining a constant confining pressure. The core was then de-pressurized through a multi-stage separator. Produced liquid weights (later converted to volumes) were recorded. The void volume created in the core during the de-pressurization process was then measured via using a Boyle’s Law of Expansion process. These produced liquid volumes and the measured void volume were the primary input from which the trapped gas volume was determined.

After the de-pressurization (or blow down) of a composite core, a two step cleaning method, vacuum distillation followed by solvent injection, was implemented with the composite core still mounted in the core holder with a confining pressure still applied. The vacuum distillation step was conducted at approximately 180 F. The primary purpose of this step was to remove the water from the core(s). Effluent from the vacuum distillation, primarily water, was captured in a cold trap and gravimetrically measured. Any residual oil produced during this step was volumetrically estimated. An adjustment was made to convert water volume produced to brine volume. At the end of the vacuum distillation step, the core was again allowed to cool to room temperature and the void volume was again measured via Boyle’s Law of Expansion. At this point in the cleaning process, the salt that had been in the brine and residual oil was still remaining in the pore structure of the cores. This “in-situ” cleaning was conducted

such that the remaining fluid volumes and the total pore volume of a composite core could be determined while the cores were in-place and relatively undisturbed. After completing of the solvent cleaning step, the core(s) were removed and subjected to Dean Stark Cleaning/Analysis.

After the vacuum distillation step, solvent cleaning of the composite cores with toluene and methanol was conducted at 150 F to remove most of the salt and residual oil which remained in the pores after the preceding vacuum distillation step. These solvents were sequentially pumped through the composite cores until the effluent was colorless. The core was then vacuum dried to remove the solvents. After drying, the composite cores were allowed to cool and the total pore volumes were measured via Boyle's Law of Expansion. A Dean Stark cleaning/analysis was subsequently conducted after the cores were removed from the trapped gas experimental apparatus.

After completing the Dean Stark cleaning and analysis steps, grain, bulk, and pore volumes along with grain density and N<sub>2</sub> permeabilities were subsequently measured via routine core analysis procedures.

Calculation of CO<sub>2</sub> Trapped Gas Saturation: The CO<sub>2</sub> trapped gas saturations were determined using data obtained from conducting certain of the above procedures. (The trapped gas should be envisioned to be a gas which is rich in CO<sub>2</sub> and not pure CO<sub>2</sub>.) In verbal form, the equation to calculate the trapped gas volume can be simplistically written as follows:

Volume of CO<sub>2</sub>-Rich Phase Trapped at 98 F and 1800 psig =

Void Volume from Boyle's Law Measurement at Lab Conditions -

Volume of Water Expelled during Blow Down Adjusted for Shrinkage -

Shrinkage of Water Left in Core after Blow Down -

Shrinkage of Residual Oil Volume Left after Blow Down.

In symbolic form, the equation can be expressed as:

$$V_{CO_2} = V_{BL} - (V_{WBD} * FVF_W) - (V_{WR} * FVF_W - V_{WR}) - (V_{OR} * FVF_O - V_{OR}). \quad (1)$$

## **RESULTS AND DISCUSSION**

A summary of the results of the South Cowden CO<sub>2</sub> Miscible WAG Trapped Gas Experiments is provided in Table II. In addition to the trapped gas data, key data of interest include Krw @ Sorw, Krco<sub>2</sub> @ Sorm, Sorm, and Krw @ Sgtrap.

The Krw @ Sorw values might more accurately be described as Krw at an oil saturation which is approaching Sorw. The initial waterfloods were terminated when the oil production had lined out at a

low level that was approaching the detection limits. (The actual endpoint of each coreflood may have taken multiple pore volumes of water injection to achieve which would not have been compatible with the WAG injection scheme.) As mentioned above, the initial water injection of Coreflood 3 was terminated early due to plugging. The initial water injections of Corefloods 1, 2, and 6 were respectively terminated after 1.04, 1.44 and 0.79 pore volumes of methane-saturated brine injection. Confirmation that the  $K_w$ 's were reasonably stabilized near the end of the initial water injections of Corefloods 1, 2, and 6 is apparent from the associated injectivity (cc/hr/psi) versus pore volumes throughput data presented in Figures 2, 3, and 5. This injectivity data represents the ease with which each fluid could be injected into the associated composite core at the prevailing conditions.

The Sorm values of 16.92 and 14.14% PV for Corefloods 1 and 2 are reported on a dead oil basis. Conversion to a live oil basis would add approximately 1.5 - 2.0% PV to each of these values. These Sorm's are both considered to fall within a reasonable range. The Sorm for Coreflood 6 is reported as 4.26% PV on a dead oil basis which is considered questionably low. Different ways of assessing the Coreflood 6 Sorm data are still being considered.

The  $K_{rw}$  @  $S_{orw}$ ,  $K_{rco_2}$  @ Sorm, and  $K_{rw}$  @  $S_{gtrap}$  data for Corefloods 1, 2, and 6 all exhibit similar trends and demonstrate the hysteresis behavior associated with a  $CO_2$  miscible WAG injection process. In each case, the trapped gas is shown to reduce the water injectivity. This is apparent from both the relative permeability data of Table II and the injectivity data of the sequential floods shown in Figures 2, 3, and 5. The injectivity behavior for Coreflood 3, which was terminated early due to plugging, is shown in Figure 4.

High, low, and average estimates (where the average is simply the average of the high and low determinations) of the trapped gas saturations are also provided in Table II. The following error analysis data were applied to equation (1) in determining the high and low estimates of the trapped gas saturation.

Boyle's Low Volume after Blow Down (cc)	$\pm 0.1$
Calculated Volume Water Collected (cc)	$\pm 0.25$
Brine FVF w/ $CO_2$ at 98 F and 1800 psig	$\pm 0.0065$
Total Water Collected during Vacuum Dist. (cc)	$\pm 0.5$
Estimated Sorm (cc)	$\pm 0.026$
Residual Oil FVF w/ $CO_2$ prior to Blow Down (rb/stb)	$\pm 0.05$
Total Pore Volume of Individual Core Plugs (%)	$\pm 1.0$

## **CONCLUSIONS**

- 1) Cores from the South Cowden Reservoir “moldic” facies tended to plug when subjected to brine injection. Thus, this facies may not be amendable to water injection.
- 2) Significant gas is “trapped” in the pores of cores from the South Cowden Reservoir “chaotic” facies when gas is injected as part of a CO<sub>2</sub> miscible WAG injection process.
- 3) Trapped gas saturations in the range of 17-25% pore volumes are considered representative of what will occur when chaotic facies cores from the South Cowden Reservoir are subjected to a CO<sub>2</sub> miscible WAG injection process.
- 4) Trapped gas results in a significant reduction in water injectivity.
- 5) Sorm values of in the range of 15-20% pore volumes are considered representative of what will occur when chaotic facies cores from the South Cowden Reservoir are subjected to a CO<sub>2</sub> miscible WAG injection process.



## SPECIAL LABORATORY STUDIES

### CONDUCT LABORATORY COREFLOODS TO IDENTIFY POTENTIAL FOAMING SURFACTANTS FOR CO<sub>2</sub> MOBILITY CONTROL

#### OBJECTIVE

The primary objective of this subtask was aimed at identifying specific foaming surfactants through a five part laboratory program for possible use in CO<sub>2</sub> mobility control in the South Cowden project CO<sub>2</sub> foam systems developed under this subtask will be considered for use in the planned horizontal injection wells to improve injection conformance as/if needed. This report summarizes the results and details procedures of laboratory work completed through the Phase I time period.

**Surfactant Adsorption in South Cowden Unit Field Cores:** We began this subtask with the determination of surfactant adsorption in South Cowden Unit Field cores. Figure 1 shows a schematic diagram of the adsorption test setup. A Waters Model 410 refractometer set at a sensitivity level of 32, was used to monitor the surfactant concentration in the core effluents. About one liter of synthetic Free Water Knock Out (FWKO) brine (TDS=7.84%) was circulated through the core while monitoring the effluents on the refractometer. This was done to obtain an equilibrated brine to avoid changes in refractive index due to dissolution of core material during surfactant adsorption testing. An overnight circulation at 60 cc/hr was sufficient to achieve equilibration of the brine. A portion of this brine was used to prepare the surfactant solutions used in adsorption tests. The “Calibration Sample Loop” shown in Figure 1 was filled with about a 9 ml aliquot of the surfactant solution at a given concentration. This solution was then pushed through the sample side of the refractometer while recording its response. This process was repeated for at least four surfactant concentrations. A linear plot of the refractometer’s response vs. known surfactant concentration was used to calculate the surfactant concentration in core effluents during the adsorption tests for that surfactant. This calibration procedure was repeated for each surfactant studied.

Seven adsorption experiments in cleaned South Cowden Unit field cores were performed. Cores were selected for use after evaluation by MRI to avoid severe fractures, obstructions, etc. before they were epoxy coated and equipped with end plates. Each core was then placed in a core holder and pressurized to a confining pressure of 2000 psi. An aliquot of the equilibrated brine was used to prepare a 0.5 wt % surfactant solution. About 0.3 to 1.2 PV of 0.5% surfactant solution was injected into the core at a flow rate of 9 cc/hr (~6-12 ft/day) using the “Injection Sample Loop” shown in Figure 1. The core was then flushed with several pore volumes (PV) of equilibrated brine while monitoring the effluent concentration on the refractometer. Figure 2 shows a plot of surfactant concentration in the core effluents for Chaser™ CD-1045 in a clean South Cowden Unit field core at 98° F. Each tick mark on the x axis represents one pore volume of effluent. In this particular coreflood experiment we injected

60.0 mg of surfactant into the core, recovering 18.4 mg of surfactant in 5 PV of the effluents which translates to a surfactant adsorption of 2127 lbs/acre-ft. While refractive index data indicate a slow surfactant desorption even after 10 PV of core effluents, we chose to calculate surfactant adsorption at 5 and 10 PV of effluents. A value of 1593 lbs/acre-ft was calculated for 10 PV of the effluents. These kind of high surfactant adsorption represent the surfactant adsorption values for the flow near the injection well. The results can be used in models to estimate volume of surfactant necessary for a given depth of penetration.

Figure 3 shows a plot of adsorption versus rock porosity for Chaser™ CD-1045, Chaser™ CD-1050, Rhodapex CD-128 and Foamer NES-25 calculated from seven tests performed in South Cowden cores. While the data points at 15.1% porosity (Foamer NES-25) might be anomalies, the adsorption data for the 5- and 10-PV effluents appear to have a maximum around 20% porosity. It is evident from this Figure that the adsorption values measured at 10-PV core effluents are smaller than those measured at 5-PV, indicating the surfactant can be moved deeper into the reservoir with following brine injection. Figure 3 also indicates that surfactant adsorption has a higher dependency on core porosity (surface area) than surfactant type.

**Evaluation of Resistance Effect for Foaming Surfactants in SCU Field Cores:** A coreflooding apparatus was set up to evaluate the resistance generating performance of various CO<sub>2</sub> - foaming surfactants for application in the South Cowden Unit. Figure 4 shows a schematic diagram for this core flooding setup. A South Cowden Unit core fitted with three pressure taps and epoxy coated was placed in a vessel and pressurized to about 2100 psi with water. Transducers were used to monitor the flowing pressure in the four sections of the core. A capillary tube was used to monitor the viscosity of the fluids leaving the core. After measuring the permeability of the four sections of the core (18 to 170 md) to brine, various mixtures of a 500 ppm Chaser™ CD-1045 surfactant solution and CO<sub>2</sub> (2000 psi) were injected in the core at 98° F. A data acquisition system was used to monitor the performance of the produced foam in the core.

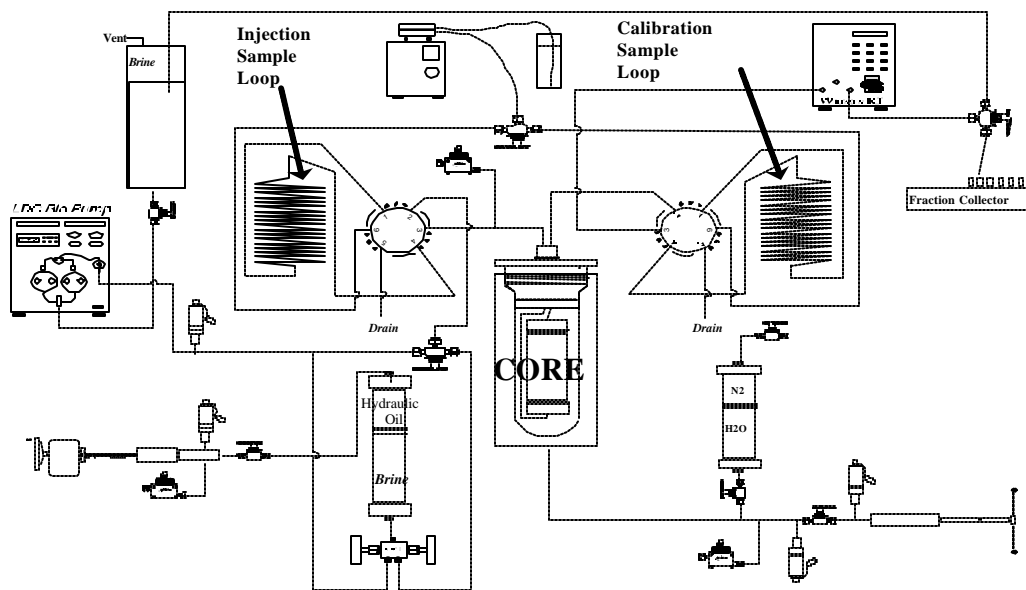
We then performed two foam tests with 1000 ppm Chaser™ CD-1045 at 50-100% foam quality using the same core. However, due to the dissolution of core material, the front end of this core collapsed at completion of the third CO<sub>2</sub>-foam experiment. We repeated the same experiments in a different core using 20-100% foam quality. However, the second core also collapsed at the face due to dissolution of core material and weakening of the core inlet. To avoid this problem, we placed a short South Cowden field core designated as the “Pre-Foamer” core ahead of our “Test Core”. This modification improved the longevity of the test core allowing us to evaluate the performance of four surfactants at three concentrations with foams of 20-100% quality. Figures 5- 8 show the average Resistance Factor (RF) for the four sections of the core as a function of foam quality for the four surfactants tested.

Figure 5 shows that the foams produced with 500 ppm Rhodapex CD-128 and CO<sub>2</sub> has a maximum RF around 50% foam quality. This maximum is shifted to about 70% foam quality for solutions of 1000 ppm and 2000 ppm Rhodapex CD-128. A similar behavior was observed for Foamer NES-25 (Figure

6), Chaser™ CD-1050 (Figure 7) and Chaser™ CD-1045 (Figure 8). Results summarized in Figures 5-8 also indicate that Rhodapex CD-128 and Chaser™ CD-1050 produced the best foams followed by Chaser™ CD-1045 and Foamer NES-25.

Figure 9 shows the effect of foam quality on RF for the four sections of the core when mixtures of 500 ppm Rhodapex CD-128 and CO<sub>2</sub> were co-injected into the core. The permeability for sections 1, 2, 3 and 4 of this core were 486 md, 216 md, 46 md and 41 md, respectively. It is evident from this plot that RF increases with permeability of that section. A similar behavior was observed for all four surfactants tested in this core. This effect which might occur at a given rock permeability is desirable and would improve the efficiency of foam to block the higher permeability zones to a larger extent. This “smart foam” effect was first observed by J. P. Heller and his group at New Mexico Petroleum Recovery Research Center.

In an effort to evaluate the effect of frontal velocity on foam performance, we modified the core setup shown in Figure 4 by installing a second ISCO pump. This pump coupled with a Ruska motorized pump set on withdrawal mode and another ISCO pump control the frontal velocity of the foam. Figure 10 shows a schematic diagram of this setup. Preliminary results obtained with the foam produced with 500 ppm Chaser CD-1045 at 70% foam quality shown in Figure 11 indicate a shear thinning effect on frontal velocity.



**Figure 1 - Schematic Diagram for Adsorption Setup**

C:\BGSWS-Correl\TOPICREP\FIG-1, 10/17/95

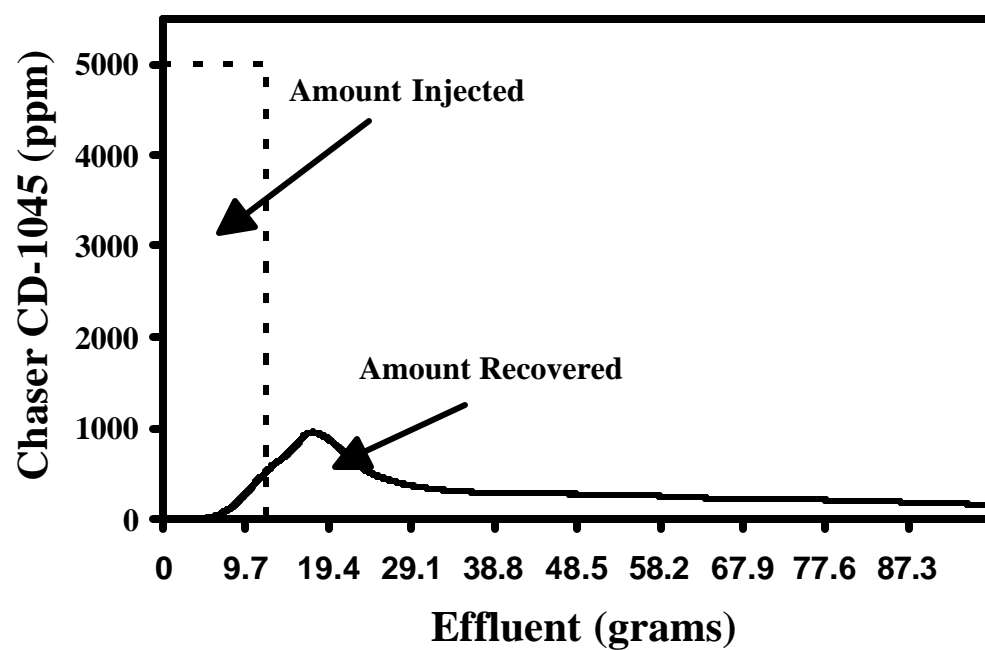


Figure 2 Adsorption of Chaser CD-1045 in South Cowden Field Core at 98

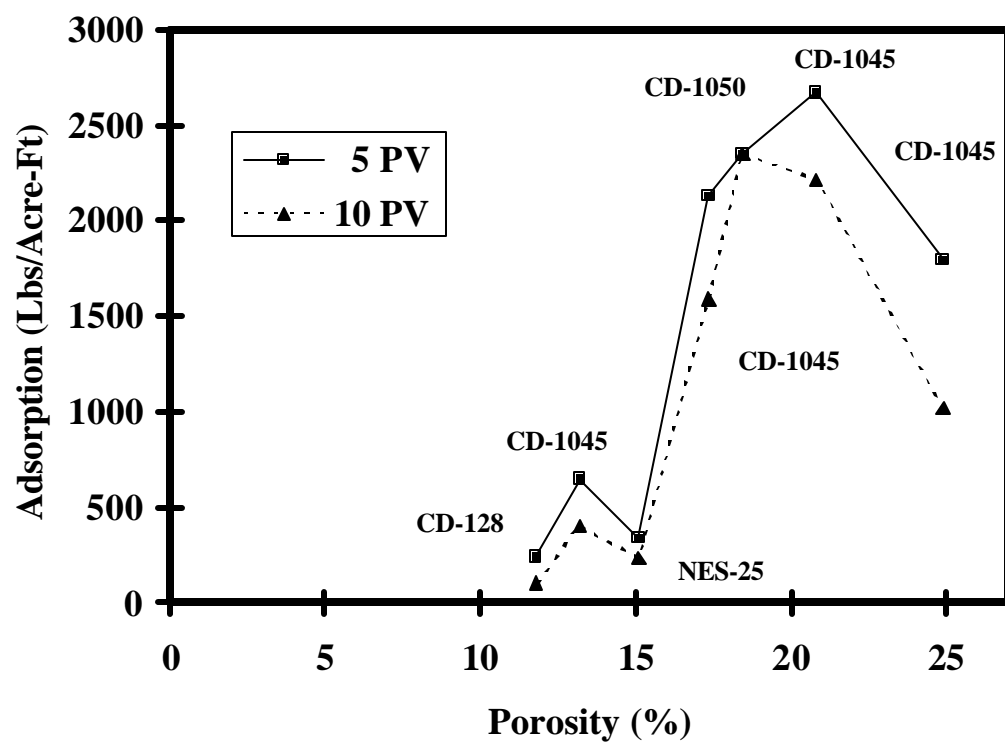


Figure 3 - Dependence of Adsorption on Porosity

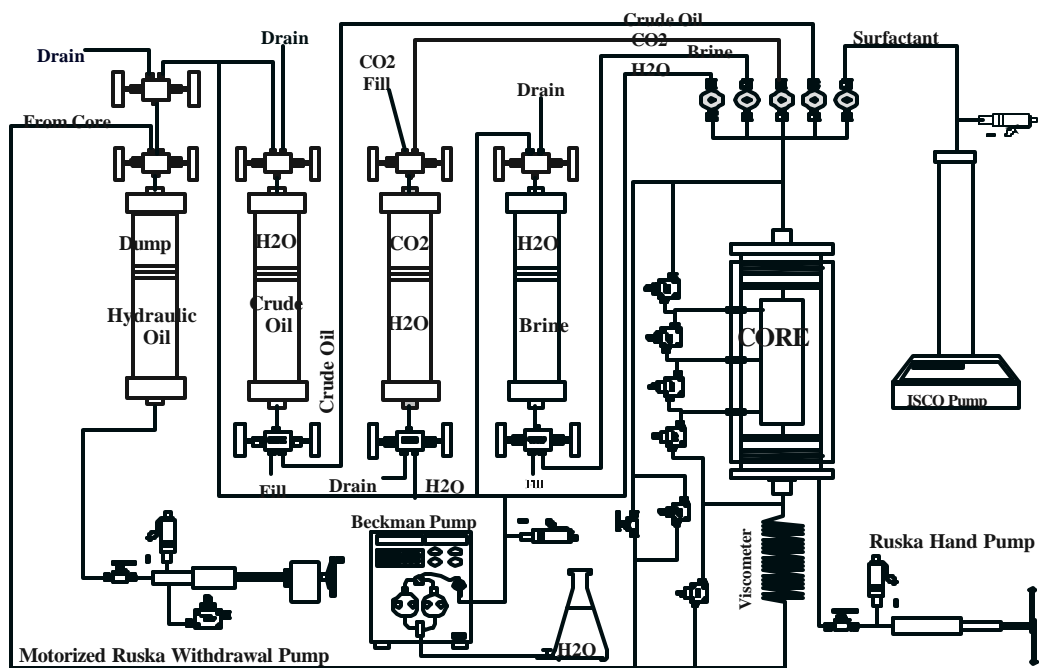
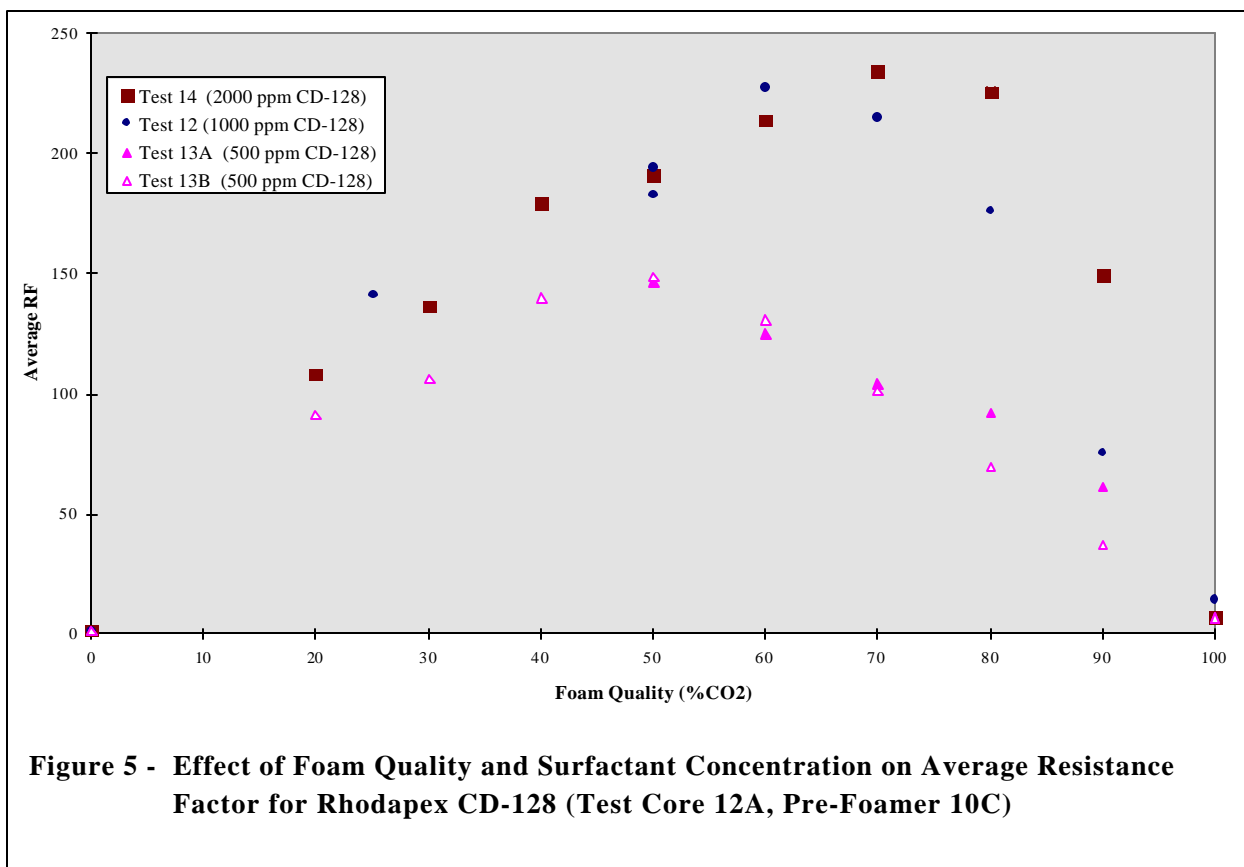
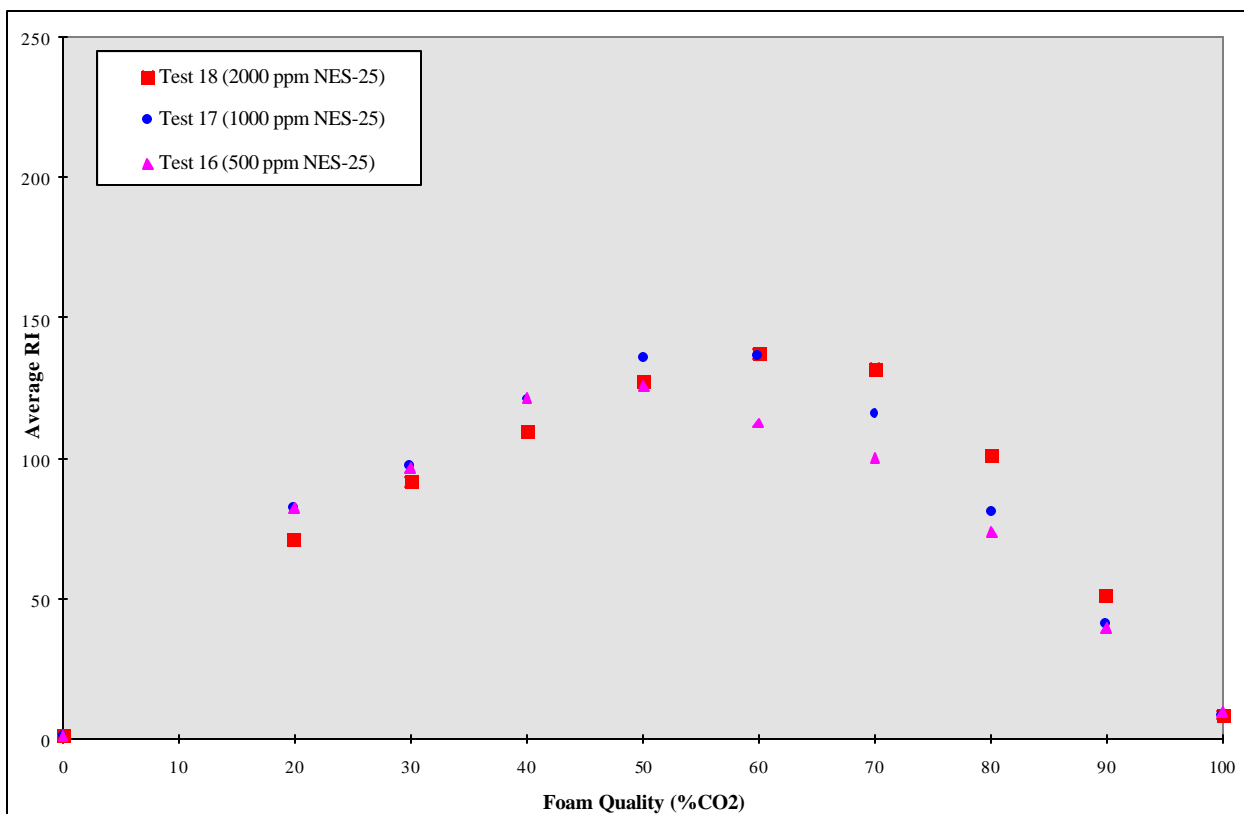


Figure 4 - Core Test Setup

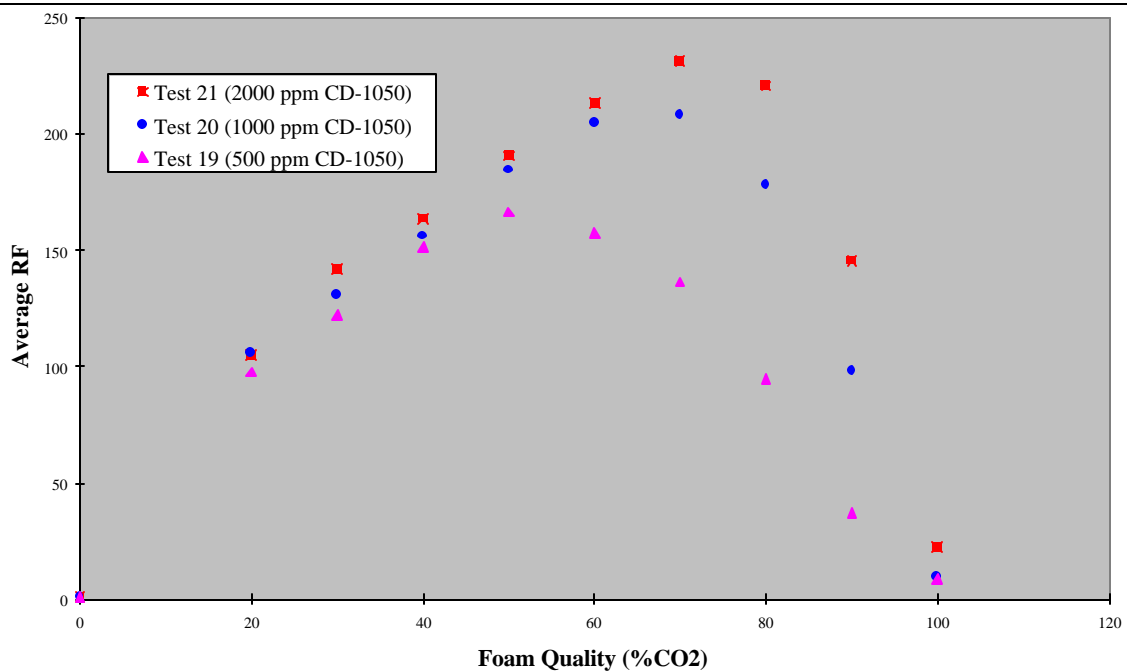
C:\BOWS-COWDEN\STOPIG-4\_101795



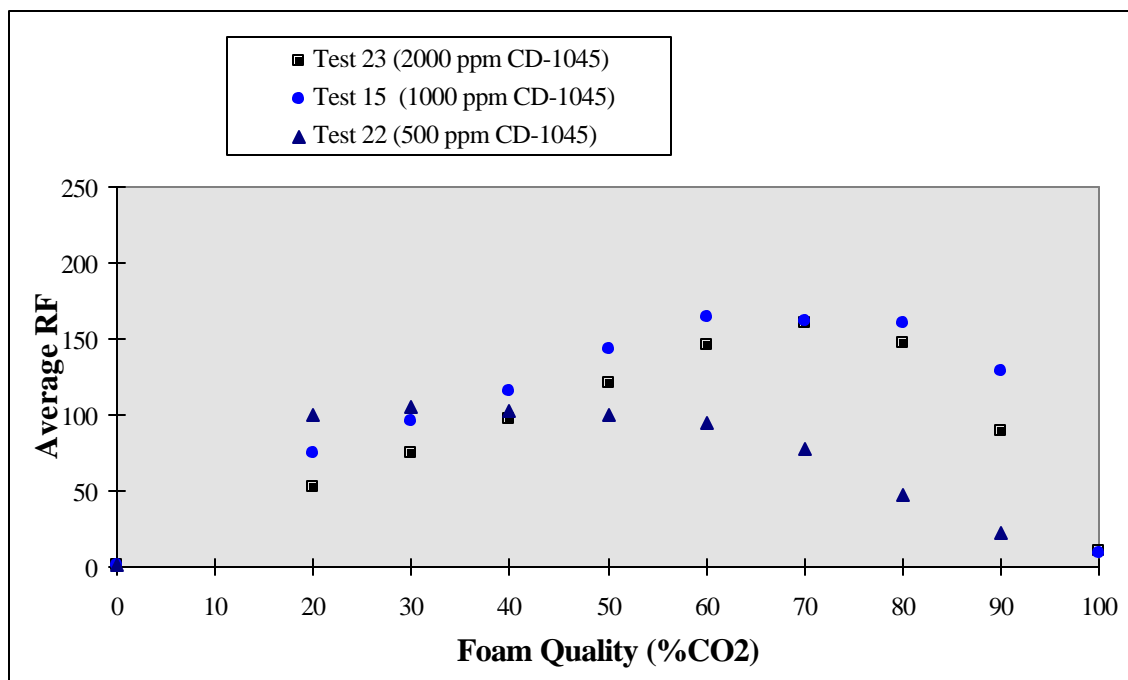




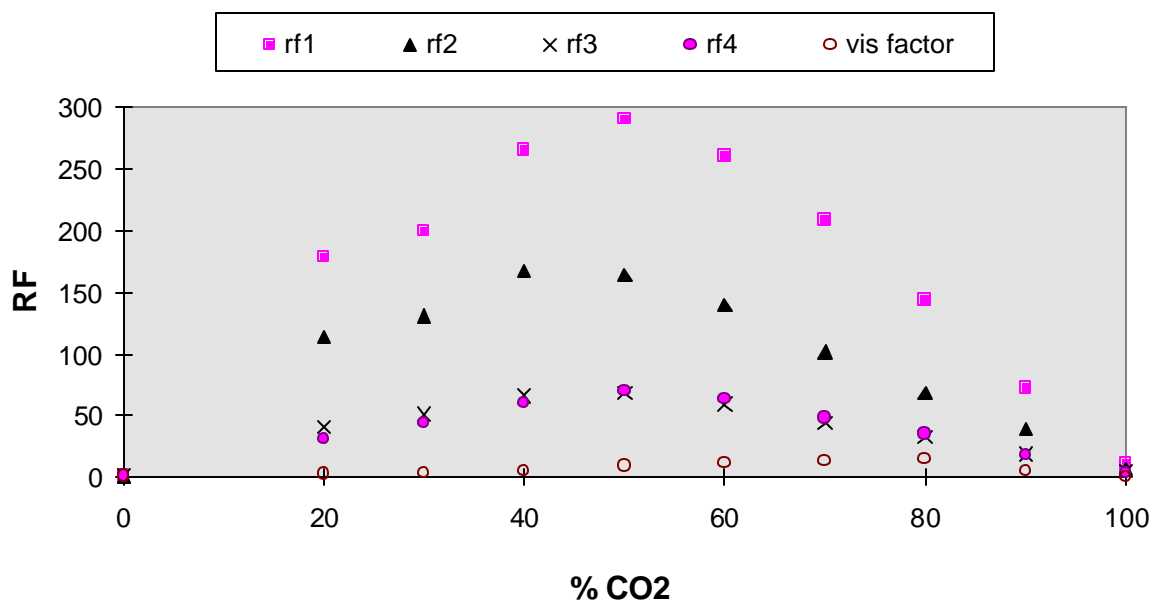
**Figure 6 - Effect of Foam Quality and Surfactant Concentration on Average Resistance Factor for Foamer NES-25 (Test Core 12A, Pre-Foamer 10C)**



**Figure 7 - Effect of Foam Quality and Surfactant Concentration on Average Resistance Factor for Chaser CD-1050 (Test Core 12A, Pre-Foamer 10C)**



**Figure 8 - Effect of Foam Quality and Surfactant Concentration on Average Resistance Factor for Chaser CD-1045 (Test Core 12A, Pre-Foamer 10C)**



**Figure 9 - Effect of Foam Quality on Resistance Factor for Each Section of the Test Core (12A) for 500 ppm Rhodaplex CD-128 in South Cowden Brine**

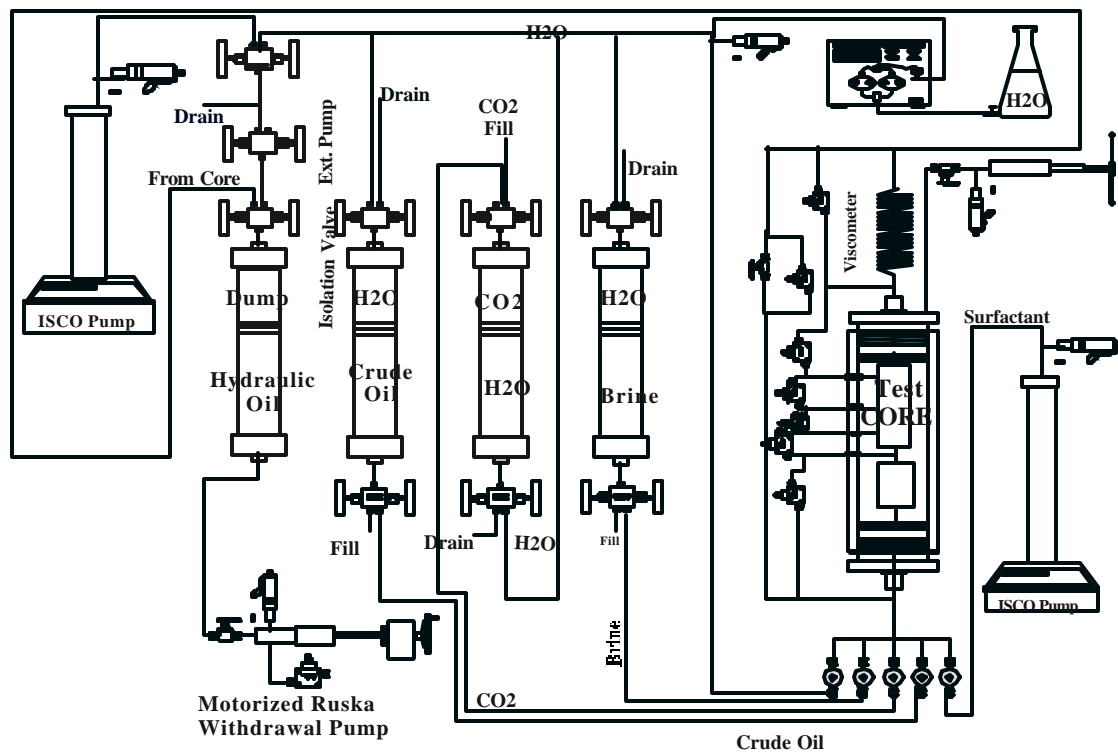
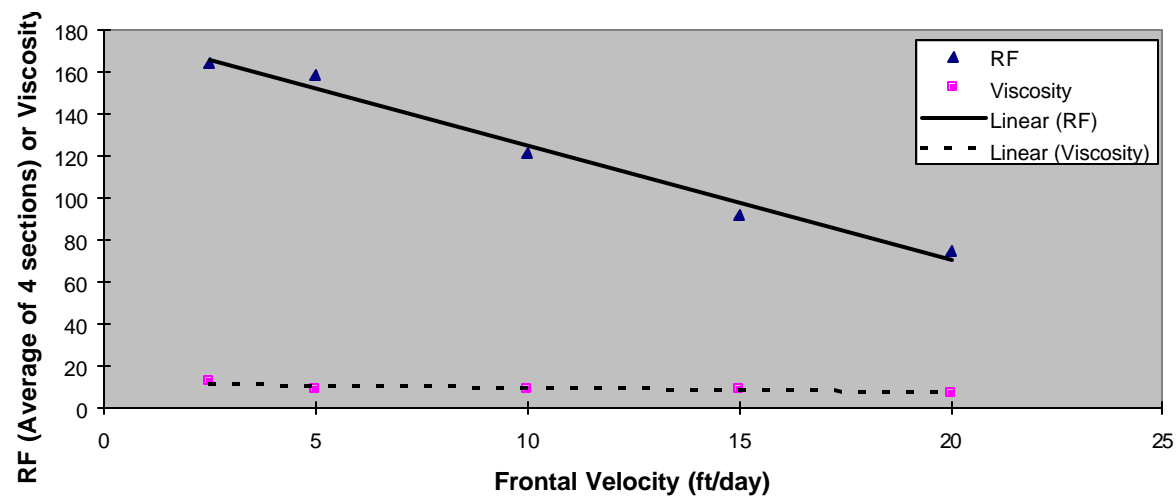


Figure 10 Modified Core Test Setup



**Figure 11 - Dependence of Resistance Factor and Viscosity on Frontal Velocity for CO<sub>2</sub>-Foam Produced with 500 ppm Chaser CD-1045 (Pre-Foamer Core 3C, Test Core 10C)**

## **SPECIAL LABORATORY STUDIES**

### **SCREENING STUDIES TO IDENTIFY SUITABLE GELLED POLYMERS FOR PROFILE MODIFICATION**

#### **OBJECTIVE**

Gels produced by an *in situ* cross-linking reaction of water-soluble polymers are used to block water intrusion into producing wells<sup>1-2</sup>. These are also effective in injection profile modification, i.e., redirecting the injection fluid flow to a less permeable zone containing oil by placing gels in high permeable streaks or fractures near the injection wells<sup>2-6</sup>.

A gel is a three-dimensional polymer network, produced by cross-linking of polymer chains, swollen with a solvent. It typically possesses mechanical properties similar to those of natural rubber, with high deformability and nearly complete recoverability. Gels used in oil recovery applications are hydrogels, i.e., the polymer networks that possess the ability to swell in water and retain a significant fraction of water within their structures, but these will not dissolve in water. These gels typically consist of about 0.5-3% of cross linked water-soluble polymers that hold 99.5-97% water in an equilibrated state. Exposure of the gel to forces such as temperature, pressure, pH etc. that might alter the nature or the degree of cross linking can disrupt this equilibrium which usually results in shrinkage with expulsion of water from the gel<sup>7</sup>. This phenomenon is called syneresis and is often observed in many oilfield gel systems. For instance, when polyacrylamide gel is exposed to hard brine at elevated temperatures for an extended period of time, the gel shrinks to small particles which are brittle. Thus, there is no single polymer gel system for every reservoir application.

The primary objective of this subtask was, therefore, to identify one or more suitable polymer systems for possible use at the So. Cowden Unit for fluid diversion as well as for water shut-off applications. The gels should be stable and effective under anticipated CO<sub>2</sub> injection conditions. The polymer gel systems will be considered for use in the planned horizontal injection wells to improve injection conformance as/if needed. This report summarizes the results and details procedures of laboratory work completed through the Phase I time period.

#### **EXPERIMENTAL**

**Polymer Solution:** The polymers used for this screening study are emulsion as well as solid materials. The emulsion polymer, OFXC<sup>®</sup>1163, was received at 30% active concentration from American Cyanamid. Approximately 6100 ppm polymer stock solution was prepared by inverting 6.58 g of emulsion in 300 ml produced brine containing 0.276 ml of Activator 478<sup>®</sup> (American Cyanamid) in a blender (Osterizer) running at high speed for 30 seconds. The polymer stock solution was allowed to stand at room temperature until all air bubbles disappeared. The test solutions were prepared using the homogeneous stock solution.

The polymer stock solution using solid material was prepared by adding a measured quantity of a solid polymer to the vortex which was produced by stirring a measured amount of solvent with a magnetic stirrer bar. The stirring was continued until the polymer particles were completely dissolved which usually varied 8-24 hours.

The aqueous cross-linker solutions were also diluted to a convenient concentration level with distilled water before using in the preparation of test solutions. The test solutions were prepared by adding aliquot for desired concentration of cross-linker to the measured aliquot of polymer stock solution. Any necessary makeups for obtaining desired concentrations of polymer and cross-linker were done with produced brine. The test solutions were shaken well before placing them into the oven for aging at reservoir temperature.

**Gel Evaluation:** About 20 ml aliquot of gelling mixture are placed in a series of glass ampules (OD=2.2 cm, Length= 22.5 cm) and sealed. The ampules are then placed vertically in a metal container and aged in the oven at the desired temperature. For the first 12-24 hours of aging the ampules are checked frequently for gelation by placing the ampule horizontally behind a shield and the gelling mixture is allowed to flow to equilibrium and its tongue length (TL) is measured. This tongue length usually decreases with aging times. The Percent Gel Strength (%GS) is then calculated from Equation 1 and is determined as a function of time<sup>8</sup>.

$$\%GS = (22.5 - TL) \times 100 / 22.5 \quad (1)$$

Percent Gel Strength as defined by Equation 1 is based on an ampule length of 22.5 cm.

A high pressure apparatus was designed and fabricated for evaluation of gel stability under 2000 psi of CO<sub>2</sub> pressure to simulate field use in a CO<sub>2</sub> pilot. The schematic of the apparatus is shown in Fig. 1. Two high pressure stainless steel vessels were equipped with a pressure gauge and a rupture disk safety relief valve. These vessels were connected to an LDC Bio pump and a booster pump to pressurize the vessels. A programmable ISCO syringe pump was used to depressurize the test vessels at a uniform rate. The pressurized vessels were housed in a thermostatted chamber. A series of preformed full strength gels in glass ampules was placed vertically inside the vessels. The vessels contained produced brine just enough to hold the samples without floating in it. The ampules were opened and about 10 ml produced brine was added on top of each gel sample. Then the lids were tightly screwed and the vessels were pressurized at 2000 psi with CO<sub>2</sub>. The vessels with contents were aged for three weeks at

the reservoir temperature of 98° F. Then, the ISCO syringe pump was programmed to release the pressure at a rate to depressurize the system over the period of six days to avoid creating a strong pressure turbulence which might shatter the gels.

## **RESULTS AND DISCUSSION**

The Phillips files on the past polymer work at the So. Cowden Unit were reviewed first. The previous laboratory work was conducted using simulated brines. Two different simulated brine compositions were found. Total dissolved solid (TDS) contents in these two formulations differed by 2 wt%. Thus, it was decided to analyze So. Cowden produced water. Since this formation water is high in H<sub>2</sub>S content, we felt that we might have to use a simulated brine for polymer/gel screening studies. Three samples of produced water collected from different points in the unit were analyzed, see Table 1. These samples were not significantly different from each other and the TDS was about 7.8 wt%. An aerated sample of produced water did not differ with respect to Na<sup>+</sup>, K<sup>+</sup>, Ca<sup>++</sup>, Mg<sup>++</sup>, and Cl<sup>-</sup> ions from the original sample. However, sulfate ions in the aerated sample were found to be about 1000 ppm higher than that of the original sample. The aerated sample was again analyzed twice for sulfate and the sulfate content was found to be about 3700 ppm both times which was within 100 ppm compared to one of the original samples. The previous large discrepancy was perhaps due to an instrumental error. The aerated produced brine did not have any significant odor. Therefore, polymer gel work was conducted in aerated So. Cowden produced water instead of a simulated brine.

Table 2 lists the polymers and crosslinkers that were studied. Two commercially available acrylamide polymers and three cross-linkers were studied. The first system studied was with a high molecular weight (10-15x10<sup>6</sup>) anionic (5-7 mole%) polyacrylamide (in emulsion), OFXC<sup>®</sup>1163 (American Cyanamid) and a low toxicity zirconium cross-linker, Zirtech<sup>®</sup> LA110 from Benchmark R&T Inc.. Since the pH of a carbon dioxide flood is in the range of 3.9 to 4.2 and the gelled polymer will be also used for diverting the fluid of a planned carbon dioxide flood in So. Cowden Unit the system was studied in So. Cowden produced water at an adjusted pH of 4.2. The pH of aerated sample of So. Cowden produced water measured about 6.5. The results of the studies are given in Tables 3 and 4. The progress of gelation was monitored by measuring the tongue length<sup>8</sup> of the gelling mixture. The tongue length develops when the gelling solution begins to form a crosslinked three dimensional structure strong enough to hold fluids within its structure. The tongue length decreases as the gel strength increases. Thus, the tongue length gives a measure of gel quality. As can be seen from Tables 3 and 4 the gelation rate is slightly faster at an adjusted pH of 4.2 in all crosslinker concentrations studied. It is also noticeable that the gelation rate decreases with increasing crosslinker concentration and developed significantly weaker gel beyond 750 ppm zirconium concentration. This observation is consistent with our previous studies in other brines. Since the system of OFXC<sup>®</sup>1163 and Zirtech<sup>®</sup> LA110 were recently successfully field-tested at the North Burbank Unit (NBU) in Oklahoma and at the C. B. Long Unit in Texas, the gels produced with 500 ppm Zr in So. Cowden water are compared with those produced in NBU or in C. B. Long produced waters as shown in Table 5. Although the gelation rate in So. Cowden produced water was slightly slower compared to the other two produced waters, the system developed acceptable gels at So. Cowden reservoir conditions.



The second system consisted of a low molecular weight ( $3-5 \times 10^5$ ) solid anionic (5 or < 5 mole%) polyacrylamide, Alcoflood<sup>®</sup> 254S (Allied Colloids) and Zirtech<sup>®</sup> LA110. This system was studied at the adjusted pH of 4.2 only. The results are shown in Tables 6 and 7. This system produced acceptable strong bulk gels at much higher concentrations of 20,000-30,000 ppm polymer and 500 ppm Zr level. However, the gelation rate of this system is significantly slower making the system suitable for near well bulk gel treatment. The gels produced by both polymer systems were found stable after prolonged aging for more than 200 days.

The polymer/gel screening studies described above were conducted at 120° F temperature. However, the reservoir temperature of the So. Cowden Unit is said to vary from 98° to 120° F, therefore, the bulk gel tests using both polymers with zirconium crosslinker were repeated in pH adjusted (3.9-4.2) So. Cowden produced water at 98° F. In addition to these screening tests both polymers were also tested with widely used MARCIT<sup>®</sup> chrome acetate as well as another low toxicity titanium crosslinking system in So. Cowden produced water (pH adjusted) at both temperatures. All these screening test results are summarized in Figure 2.

Both polymers with Zr crosslinker developed acceptable gels at 98° F. There is no significant difference in the gelation rate for high molecular weight polymer (OFXC<sup>®</sup> 1163) at both temperatures. However, in the case of low molecular weight polymer (Alcoflood<sup>®</sup> 254S), the gelation rate is significantly slower at 98° F and the system utilizes higher polymer and crosslinker concentrations. The OFXC<sup>®</sup> 1163 with chromium acetate crosslinking system developed gels at much slower rate than that of zirconium system. For example, the system containing 5000 ppm OFXC<sup>®</sup> 1163 and 250 ppm Cr developed only 68% gel strength at 120° F or 0% gel strength at 98° F after 3.12 hr aging. These compare to the percent gel strengths of 81% and 80% at 120° F and 98° F, respectively developed by Zr containing system at the same concentration levels after only 2.5 hours of aging. However, although chromium acetate resulted in strong gels at 120° F the gels at both temperatures are loosening up by expelling water from the gels after 42 days of aging whereas no separated water in zirconium gels after 206 days of aging at the similar conditions. On the other hand, the low molecular weight polymer (Alcoflood<sup>®</sup> 254S) with chromium system developed gels at a faster but more uniform rate than that with zirconium system and the gels are stable with no sign of separated water after 115 days of aging.

The third low toxicity titanium crosslinker with OFXC<sup>®</sup> 1163 developed gels at a slower rate with no sign of gel forming characteristics until after 6 hours and measurable gel strength after 23 hours of aging at 98° F. The system developed about 85% gel strength after 5 days of aging and after 57 days of aging the gel strength is increased to about 95% indicating a long term gel stability. This system utilizes low concentrations of polymer and crosslinker making the system economically attractive.

The next phase of bulk gel work involved gel stability tests under 2000 psi CO<sub>2</sub> pressure to simulate field use in a CO<sub>2</sub> pilot. Two systems, the low toxicity OFXC<sup>®</sup> 1163 with Zirtech<sup>®</sup> LA110 system and Alcoflood<sup>®</sup> 254S with MARCIT<sup>®</sup> chrome acetate system were tested. The testing gels were prepared first using 1% OFXC<sup>®</sup> 1163 with 250-1500 ppm Zr in pH unadjusted So. Cowden produced water

and 2% Alcoflood<sup>®</sup> 254S with 250-1500 ppm Cr in pH adjusted (4.2) produced water. It is interesting to note that Alcoflood<sup>®</sup> 254S even at 4% concentration level did not produce gels with Cr in pH unadjusted produced water. The preformed gels were then exposed to 2000 psi pressure of CO<sub>2</sub> (See Experimental) and aged at 98° F for three weeks. The results are given Table 8. The gels of both systems are stable with no sign of deterioration or water phase separation. However, since the MARCIT<sup>®</sup> chrome acetate gels are produced in pH adjusted water, these gels may not withstand the CO<sub>2</sub> pressure for a very long time due to the possibility of over cross-linking which will cause syneresis.

## CONCLUSIONS

- 1) The system of high molecular weight ( $10\text{--}15 \times 10^6$ ) anionic (5–7 mole%) polyacrylamide, OFXC<sup>®</sup>1163 and low toxicity zirconium cross-linker, Zirtech<sup>®</sup> LA110 makes strong gels in So. Cowden produced water and gels are stable at the reservoir temperature under anticipated CO<sub>2</sub> injection conditions.
- 2) The low molecular weight ( $3\text{--}5 \times 10^5$ ) anionic (5 or < 5 mole%) polyacrylamide, Alcoflood<sup>®</sup> 254S and low toxicity zirconium cross-linker, Zirtech<sup>®</sup> LA110 system also makes strong and stable gels. This system is attractive particularly for its significantly slower gelation rate. However, the system utilizes much higher polymer and cross-linker concentrations making it a somewhat more expensive system.
- 3) The high molecular weight polymer, OFXC<sup>®</sup>1163 with another low toxicity titanium cross-linker, RIX:98 develops acceptable gels at much slower rate than the OFXC<sup>®</sup>1163/Zirconium system. It is also important to note that this system utilizes lower cross-linker concentration.
- 4) Although MARCIT<sup>®</sup> chrome acetate with Alcoflood<sup>®</sup> 254S produces strong gels at the desired rate, the system utilizes much higher concentrations of polymer and cross-linker. The system also produces gels only at a lower pH so that the gels may not withstand CO<sub>2</sub> pressure for a very long time.

## REFERENCES

1. Gruenenfelder, M. A., Zaitoun, A., Ali, S. A. and Linser, T. M., *SPE/DOE Paper 27770* [SPE/DOE 9th Symposium on Improved Oil Recovery Proceedings, vol. 1, Tulsa, Oklahoma, USA], 387 (1994).
2. Southwell, G. P., and Posey, S. M., *SPE/DOE Paper 27779* [SPE/DOE 9th Symposium on Improved Oil Recovery Proceedings, vol. 1, Tulsa, Oklahoma, USA], 513 (1994).
3. Moffitt, P. D. and Zornes, D. R., *SPE Paper 24933* [67th Annual SPE Technical Conference and Exhibition, Washington, DC, USA], 813 (1992).
4. Zornes, D. R., Long, H. Q. and Cornelius, A. J., *SPE Paper 14113* [International Meeting on Petroleum Engineering, Beijing, China], 311 (1986).
5. Doll, T. E. and Hanson, M. T., *SPE Paper 15162* [Rocky Mountain Regional Meeting of the SPE, Billings, MT, USA], 281 (1986).
6. Mack, J. C. and Warren, J., *J. Pet. Tech.*, 36, 1145 (1984).

7. DiGiacomo, P. M. and Schram, C. M., *SPE Paper 11787*, [International Symposium on Oilfield and Geothermal Chemistry, Denver, CO, USA], 165 (1983).
8. Moradi-Araghi, A., Bjornson, G. and Doe, P. H., *SPE Paper 18500* [SPE International Symposium on Oilfield Chemistry, Houston, Texas, USA], 367 (1989).

**Table 1**  
**So. Cowden Water Analyses**

Water Sample	%TDS	N	K	Ca	Mg	Sr	Cl	SO4
		ppm						
Tract2-Trans, Pump	7.27	22800	388	2500	619	55.8	36200	3593
Tract6-FWKO	7.84	25100	441	2490	633	55.0	39900	3238
Tract6-IPD	7.84	25200	513	2490	650	55.3	39400	3237
Tract6-FWKO (Aerated and filtered)	7.72	24900	442	2420	636	53.4	40500	4173

**Table 2**  
**Polymer and Crosslinker Systems**

OFXC <sup>®</sup> 1163 (American Cyanamid)	High Molecular Weight (10-15x10 <sup>6</sup> ) Anionic (5-7 mole%) Polyacrylamide in Emulsion	
Alcoflood <sup>®</sup> 254S (Allied Colloids)	Low Molecular Weight (3-5x10 <sup>5</sup> ) Anionic (5 or < 5mole%)	Polyacrylan
Zirtech <sup>®</sup> LA110 (Benchmark R&T)	Organically Complexed Zirconium Compound in Aqueous	
RIX:98 (Benchmark R&T)	Organically Complexed Titanium Compound in Aqueous	
Water-Cut <sup>®</sup> 684 (Tiorco, Inc.)	Organically Complexed Chromium(III) Compound in	

**Table 3**  
**Bulk Gel Test With OFXC®1163 and Zirtech® LA110 in Aerated FWKO Water at 120°F**

Polymer Conc. ppm	Zr Conc. ppm	0hr	1hr	2hr	3.4hr	4.5hr	24hr	15d	224d
		Tongue Length (TL), cm							
5000	250	T	PG	7.0	6.0	5.3	4.7	4.8	4.7
5000	500	T	PG	6.4	4.8	4.4	3.2	2.5	2.2
5000	750	T	PG	8.3	6.4	5.6	3.3	2.2	1.7
5000	1000	T	PG	PG	7.6	6.8	4.6	2.6	1.2
5000	1500	T	SG	PG	PG	8.2	5.1	3.3	0.9
5000	2000	T	VT	SG	PG	PG	6.8	3.6	2.9

NG= No gel, T= Thick, VT= Very thick, SG= Slight gel, PG= Partial gel

**Table 4**  
**Bulk Gel Test With OFXC®1163 and Zirtech® LA110 in Aerated and pH Adjusted (4.2) FWKO Water at 120° F**

Polymer Conc. ppm	Zr Conc. ppm	0hr	1hr	2.6hr	4.2hr	5.4hr	22.6hr	13.9d	206d
		Tongue Length (TL), cm							
5000	250	T	6.7	4.4	3.7	3.1	3.0	2.0	1.8
5000	500	T	PG	5.5	4.5	4.0	2.9	1.8	2.7
5000	750	T	PG	6.6	5.1	4.5	3.1	1.8	1.3
5000	1000	T	PG	8.2	6.5	5.1	3.6	1.8	0.7
5000	1500	T	PG	PG	PG	7.8	5.2	2.9	3.5
5000	2000	T	SG	PG	PG	PG	6.5	4.0	4.2

NG= No gel, T= Thick, VT= Very thick, SG= Slight gel, PG= Partial gel

**Table 5**  
**Comparison of Bulk Gels Prepared With 5000 ppm Polymer and 500 ppm Zr in So.**

Polymer/X-linker/Water	0hr	1hr	2hr	3hr	4hr	24hr		
<hr/>								
Tongue Length (TL), cm								
<hr/>								
OFXC <sup>®</sup> /LA110/FWKO	T	PG	6.4	4.8	4.4	3.2	2.5(15d)	
OFXC <sup>®</sup> /LA110/FWKO (pH 4.2)	T	PG	5.5	--	4.5	2.9	1.8(13d)	
OFXC <sup>®</sup> /LA110/NBU TB-57	T	3.9	3.2	--	2.4	2.2	1.6(6d)	
OFXC <sup>®</sup> /LA110/CBLong(pump dis.)	T	4.1	2.2	2.1	--	1.8	1.2(6d)	

NG= No gel, T= Thick, VT= Very thick, SG= Slight gel, PG= Partial gel

**Table 6**  
**Bulk Gel Test With Alcoflood<sup>®</sup> 254S and Zirtech<sup>®</sup> LA110 in Aerated and pH Adjusted (4.2) FWKO Water at 120° F**

Polymer Conc'n. ppm	Zr Conc'n. ppm	0hr	1hr	2.6hr	4.2hr	5.4hr	22.7hr	13.9d	206d
Tongue Length (TL), cm									
20000	250	NG	NG	NG	NG	T	T	4.0	0.9
20000	500	NG	NG	NG	NG	T	T	1.5	0.7
20000	750	NG	NG	NG	NG	NG	T	1.7	0.7
20000	1000	NG	NG	NG	NG	NG	T	2.8	0.6
20000	1500	NG	NG	NG	NG	NG	NG	8.0	0.7
20000	2000	NG	NG	NG	NG	NG	NG	S-PG	0.5

NG= No gel, T= Thick, VT= Very thick, SG= Slight gel, PG= Partial gel

**Table 7**  
**Bulk Gel Test With Alcoflood<sup>®</sup> 254S and Zirtech<sup>®</sup> LA110 in Aerated and pH Adjusted (4.2) FWK**

Polymer Conc'n. ppm	Zr Conc'n. ppm	0hr	1hr	3hr	4.4hr	6.5hr	23hr	13d	196d
		Tongue Length (TL), cm							
30000	250	NG	NG	NG	NG	T	S-PG	2.3	0.7
30000	500	NG	NG	NG	NG	T	S-PG	0.8	0.7
30000	750	NG	NG	NG	NG	T	SG	0.8	0.8
30000	1000	NG	NG	NG	NG	T	T	1.0	0.7
30000	1500	NG	NG	NG	NG	T	T	2.7	0.8
30000	2000	NG	NG	NG	NG	T	T	7.9	0.6

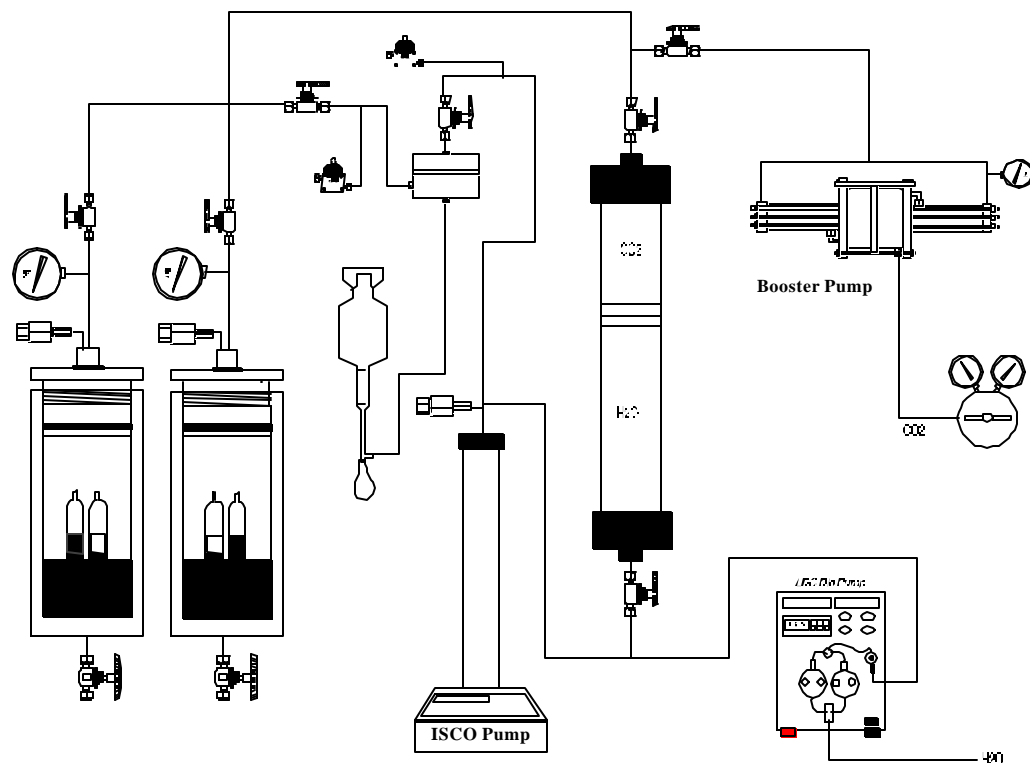
NG= No gel, T= Thick, VT= Very thick, SG= Slight gel, PG= Partial gel

**Table 8**  
**Gel Stability Tests at 98° F Under 2000 psi Pressure of CO<sub>2</sub>**

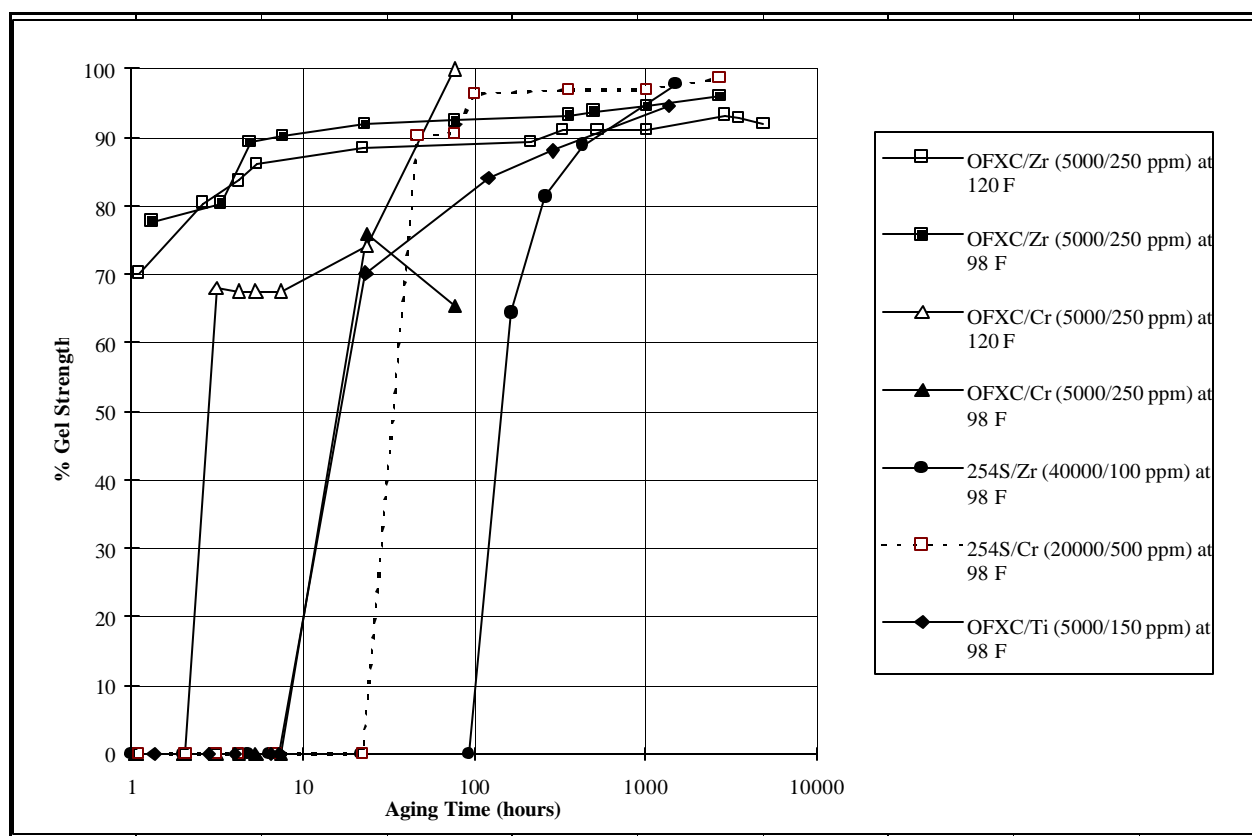
Gel System	Cross-linker Conc'n. ppm	%Gel Strength Before Exposure to CO <sub>2</sub>	%Gel Strength After Exposure to CO <sub>2</sub>
1% OFXC <sup>®</sup> 1163 and Zr in pH unadjusted FWKO water	250	70	70
	500	93	93
	750	98	98
	1000	98	98
	1500	97	97
2% Alcoflood <sup>®</sup> 254S and Cr pH adjusted (4.2) FWKO water	250	95	95
	500	97	97
	750	98	98
	1000	98	98
	1500	97	97



**Figure 1. High Strength Gel Stability Test Apparatus**



**Figure 2. Gel Strength as a Function of Aging Time for Various Polymer/Cross-linker Systems at different Concentrations and Temperatures.**



**PRESSURE BUILDUP TESTS  
& RFT PRESSURE MEASUREMENTS**

Field: SOUTH COWDEN  
Rsvr : SAN ANDRES  
Well : SO. COWDEN UNIT 6-23  
Test : BUILDUP TEST

Well Test Database  
Summary Report  
Evt. 01, Buildup

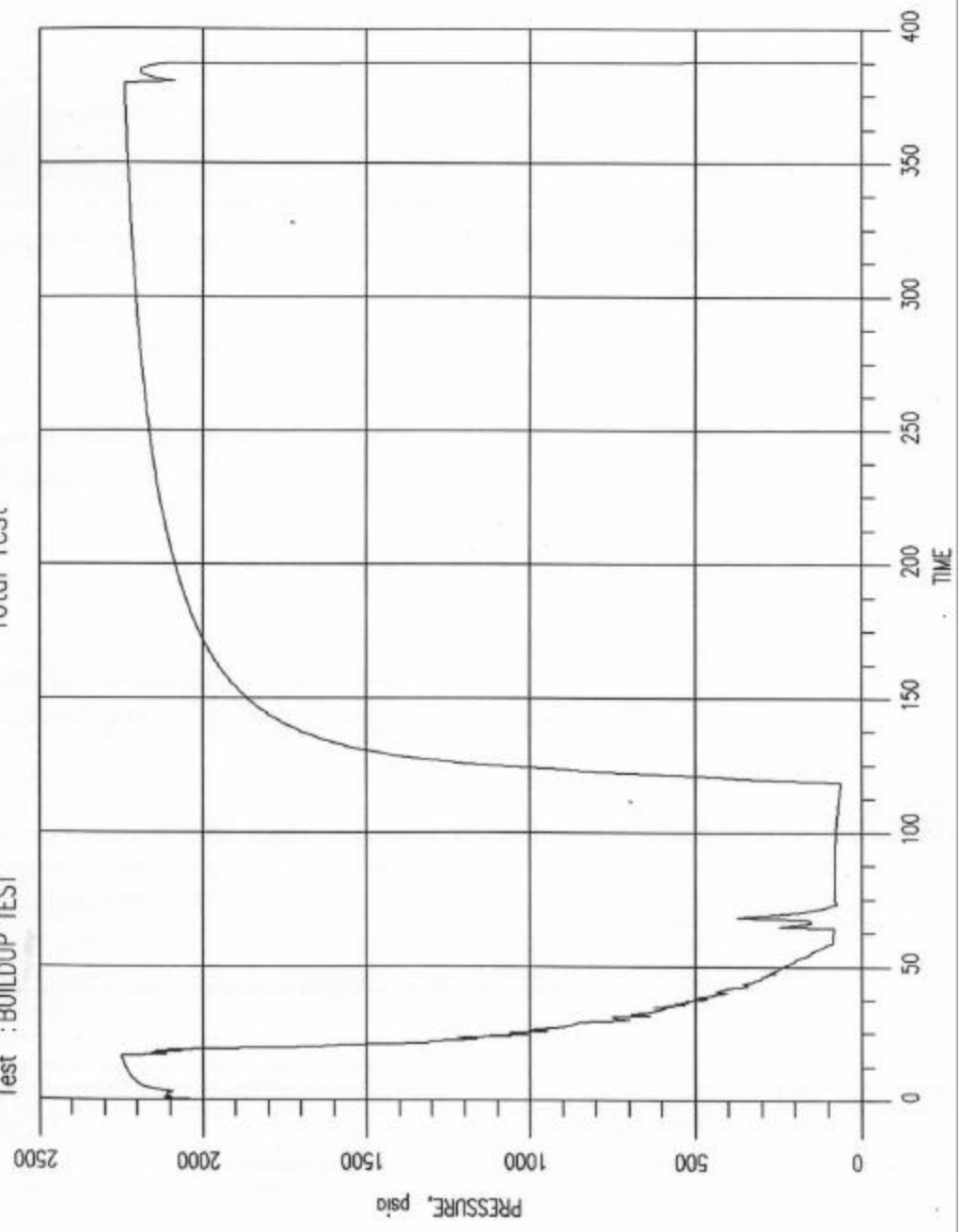
	Start -----	End ---	
Date :	07/26/94	08/06/94	
Time :	22:42:00	19:34:59	
Delta time :	118.700	379.583	hours
Pressure :	62.19	2239.69	psia
Temperature:	96.16	96.13	F
Rate :	0.00	0.00	BBL/DAY

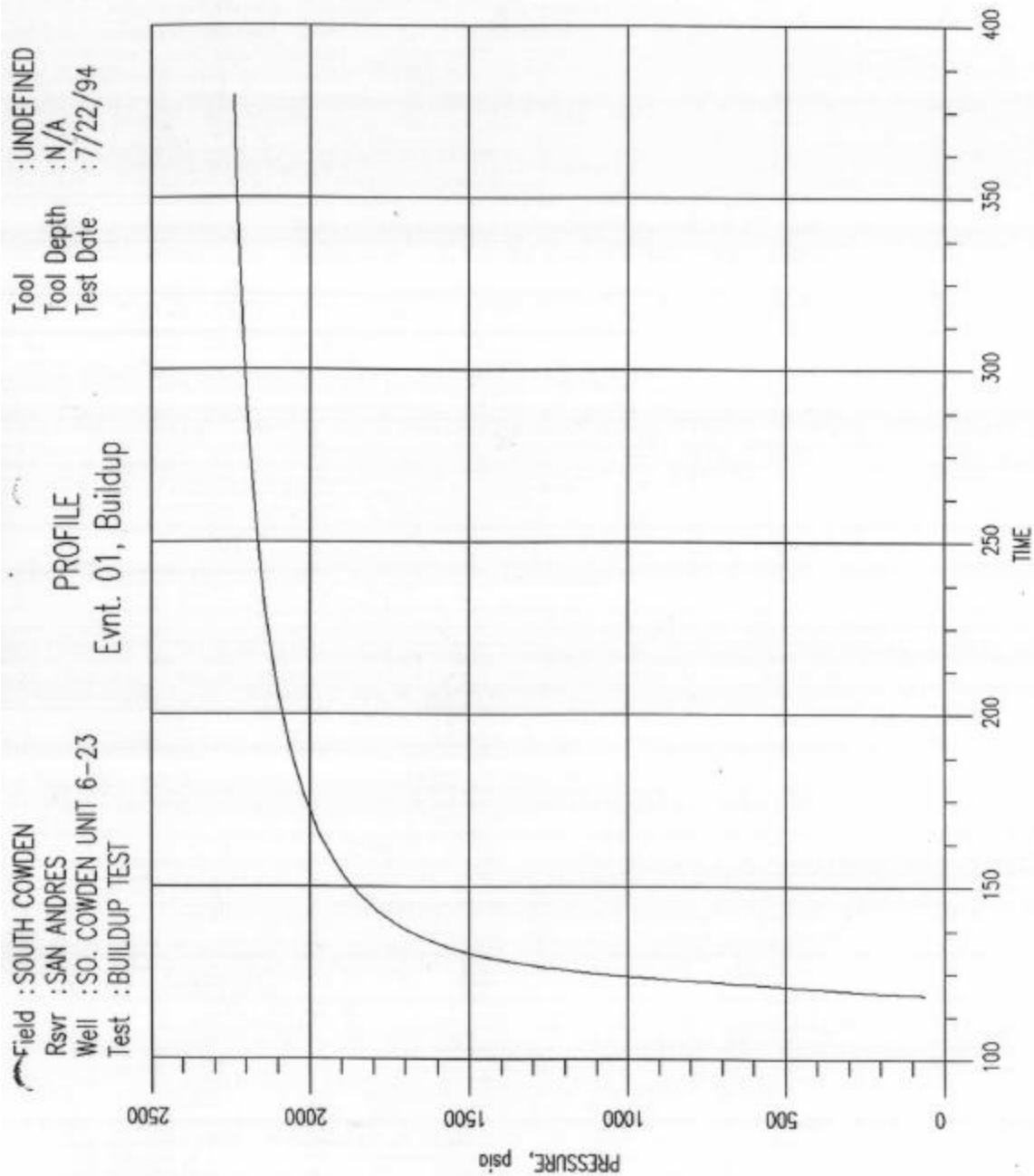
No of Points : 86

Field : SOUTH COWDEN  
Rsvr : SAN ANDRES  
Well : SO. COWDEN UNIT 6-23  
Test : BUILDUP TEST

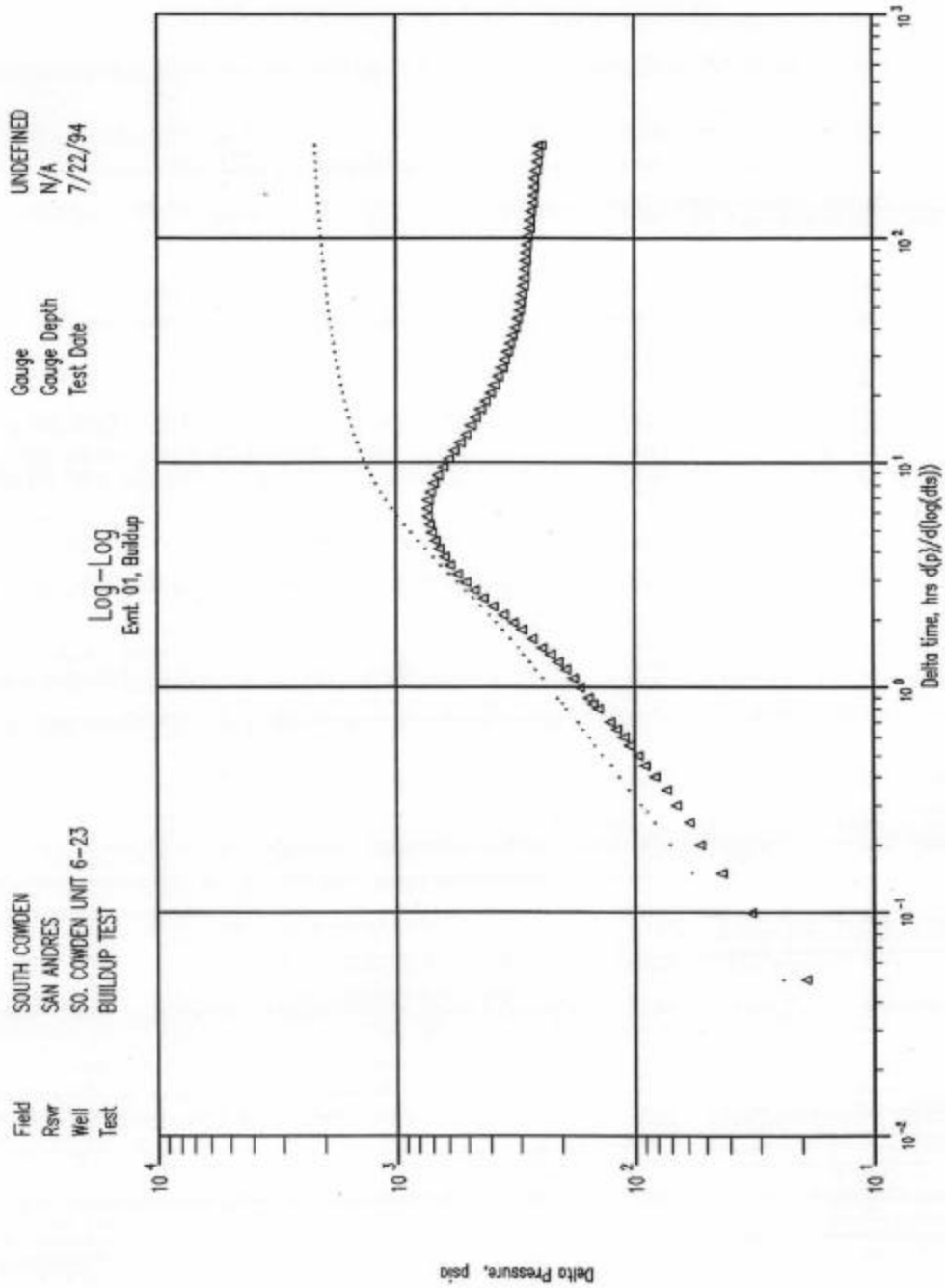
Tool : UNDEFINED  
Tool Depth : N/A  
Test Date : 7/22/94

PROFILE  
Total Test



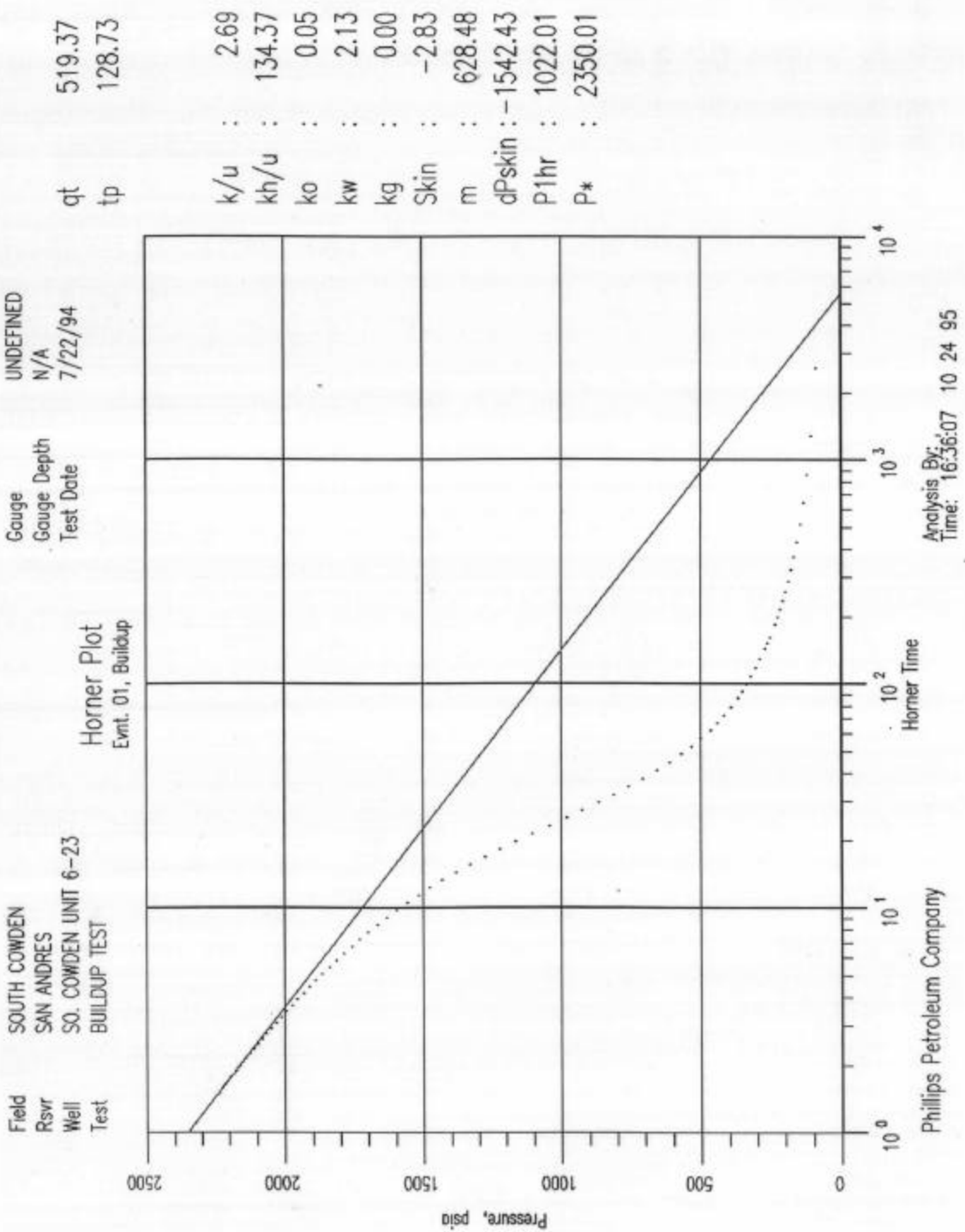


qt 519.37  
tp 128.73



Analysis By: .  
Time: 16:33:25 10/24/95

Phillips Petroleum Company





Evnt. 01, Buildup

FIELD :	SOUTH COWDEN	GAUGE :	UNDEFINED
RSVR :	SAN ANDRES	GAUGE DEPTH:	N/A
WELL :	SO. COWDEN UNIT 6-23	TEST DATE:	7/22/94
TEST :	BUILDUP TEST		

SEMI-LOG ANALYSIS REPORT

Horner Plot

GENERAL INFORMATION

Y-Func:	Pressure, . psia	Phase:	MULTI, OIL
X-Func:	Horner Time		

SEMI-LOG STRAIGHT LINE

pzero =	62.19 psia	pavg =	2200.00 psia
Slope =	628.47620	Plhr =	1022.01 psia
Pstar =	2350.01 psia		

De-superposition

Slope =	0.00	Duration =	1.00000 hrs
Cons. =	62.2 psia		
(from Log Delta Time Plot of Preceding Event)			

Calculated Results

kh/u =	134.4 md.ft/cp	ko =	0.04729 md
k/u =	2.687 k/u	kw =	2.131 md
		kg =	0 md
Skin =	-2.826	Skin,o =	-0.77
dp s =	-1542.42542 psia	Skin,g =	0.00
ri =	795 ft (t = 260.9 hrs)	Skin,w =	-2.82

Calculated Vs. Measured qt

qt(calc) =	295.3 BBL/D	qt(meas) =	519.4 BBL/D
deviation =	-43.14 %		

RESTRAN II ANALYSIS

Field: SOUTH COWDEN  
 Rsvr : SAN ANDRES  
 Well : SO. COWDEN UNIT 6-21  
 Test : INITIAL TEST

Well Test Database  
 Summary Report  
 Evnt. 01, Buildup

	Start -----	End ---	
Date :	08/20/94	08/31/94	
Time :	13:32:00	08:36:59	
Delta time :	120.250	379.333	hours
Pressure :	345.97	1959.84	psia
Temperature:	97.57	97.16	F
Rate :	0.00	0.00	BBL/DAY

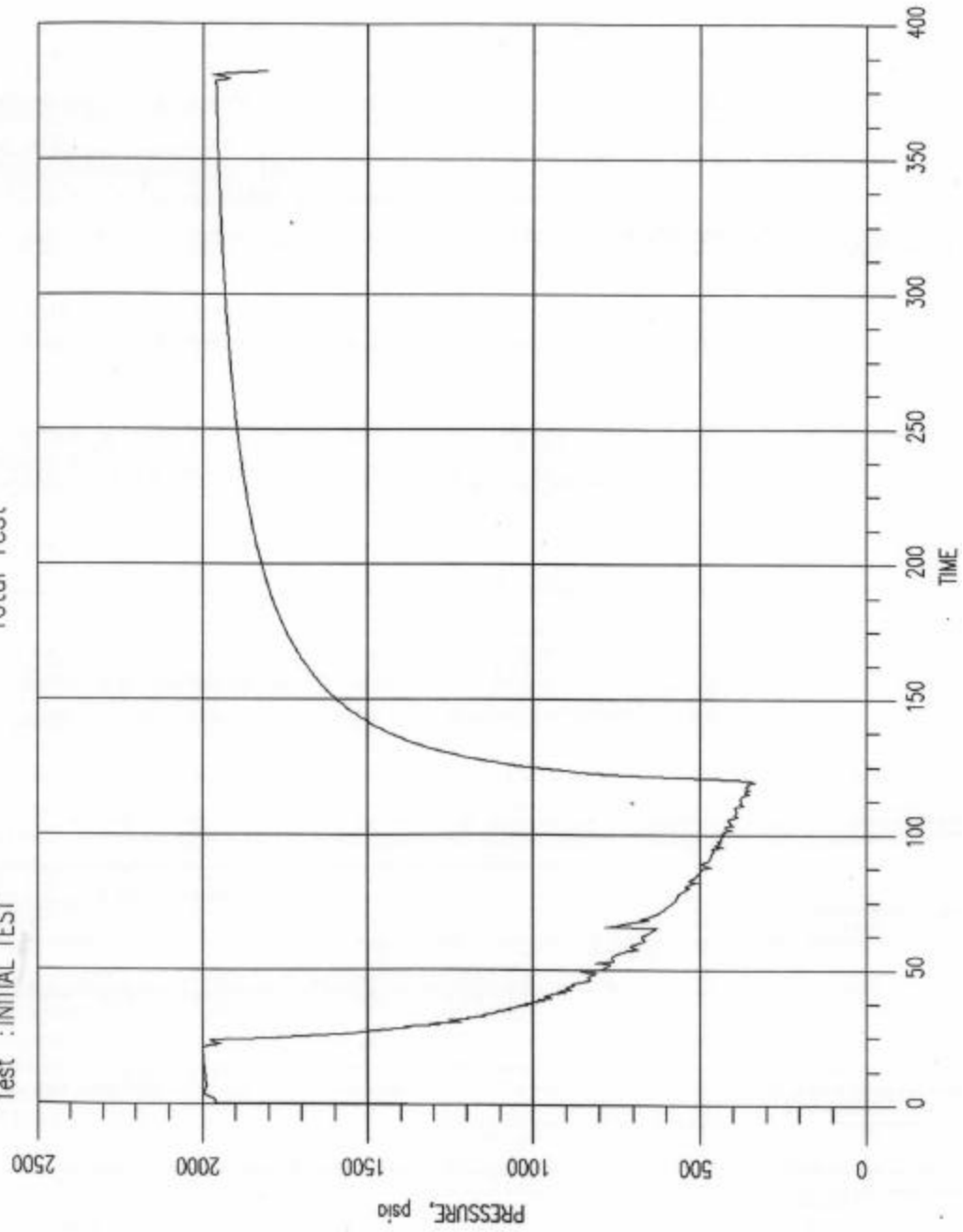
No of Points : 86

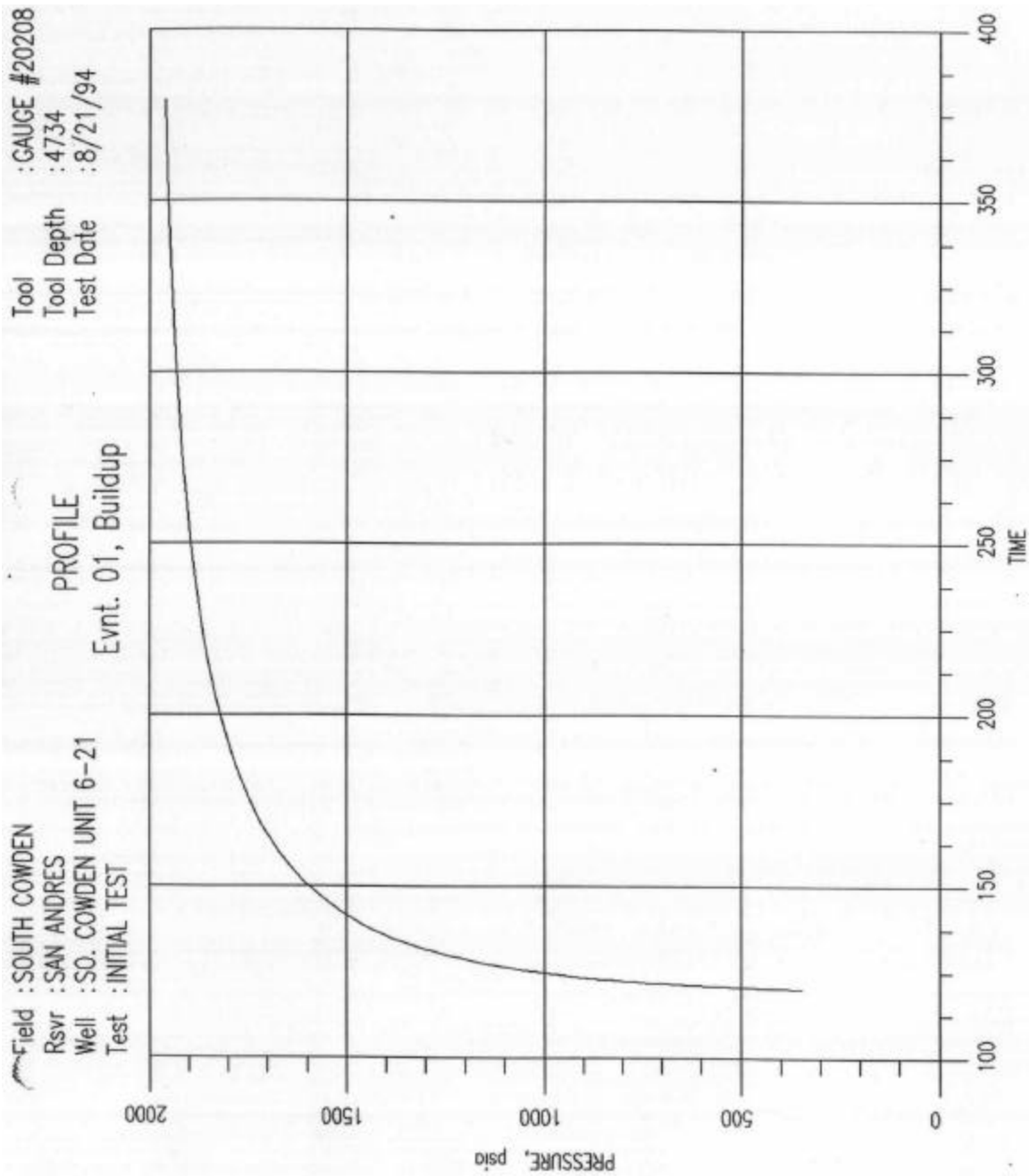
Results:

	Log-Log delta p Delta t No Model	Semi-Log Pressure Horner t
y-func		
x-func		
MODEL		
k/u	1.17 md/cp	1.18 md/cp
ko	0.00 md	0.00 md
kg	0.00 md	0.00 md
kw	0.00 md	0.77 md
xf	1.00 ft	
s	-4.01	-3.81
p*		2090.92 psia
cd	2988.70	

Field : SOUTH COWDEN  
Rsvr : SAN ANDRES  
Well : SO. COWDEN UNIT 6-21  
Test : INITIAL TEST

PROFILE  
Total Test





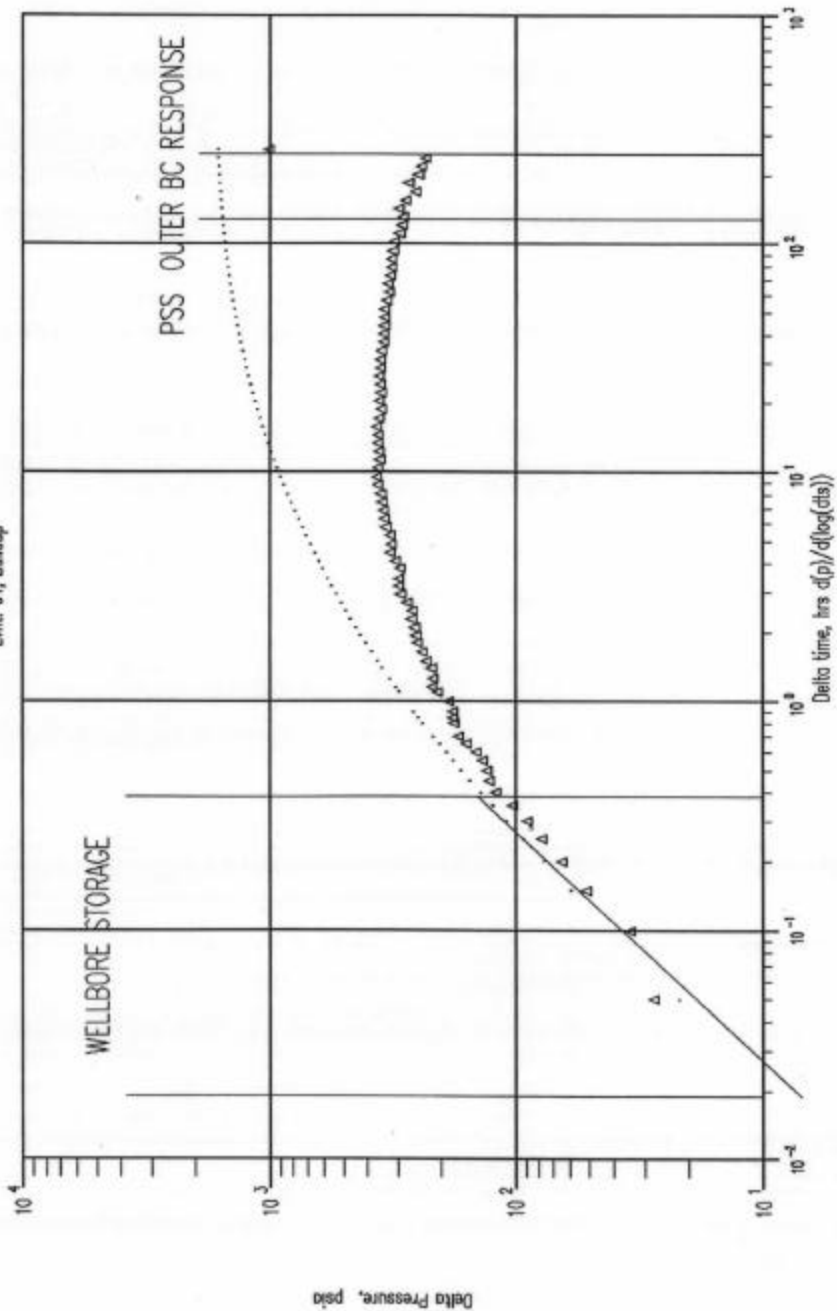
qt	446.97
tp	99.48
kh/u	93.43
ko	0.00
Cs	0.05
Cd	2988.70
PbarM	0.000

Gauge #20208  
4734  
8/21/94

SOUTH COWDEN  
SAN ANDRES  
SO. COWDEN UNIT 6-21  
INITIAL TEST

Field  
Rsvr  
Well  
Test

Log-Log  
Evrnt. 01, Buildup



Phillips Petroleum Company

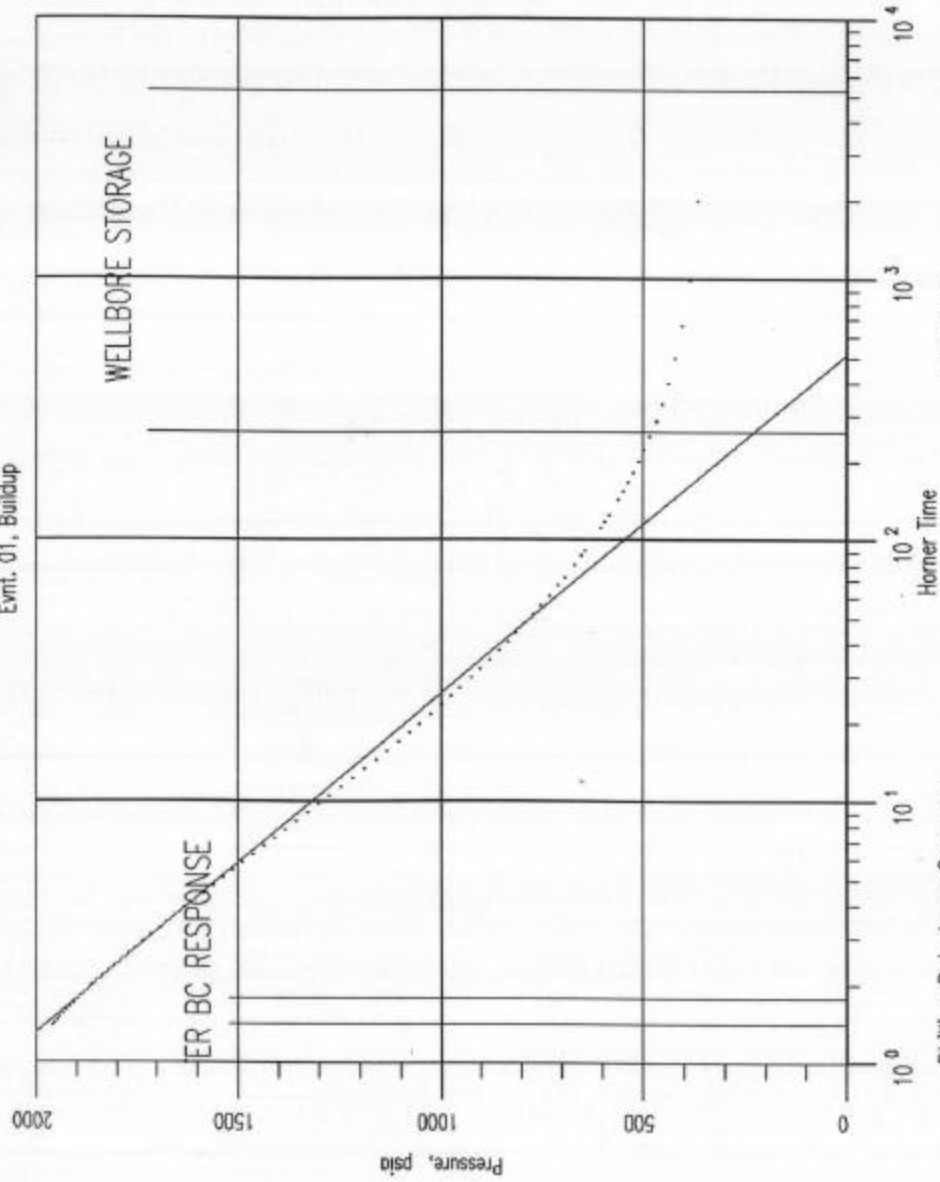
Analysis By .  
Time: 16:07:37 10/24/95

Field SOUTH COWDEN  
 Rsvr SAN ANDRES  
 Well SO. COWDEN UNIT 6-21  
 Test INITIAL TEST

Horner Plot  
 Evtl. 01, Buildup

Gauge Gauge #20208  
 Gauge Depth 4734  
 Test Date 8/21/94

qt 446.97  
 tp 99.48



k/u : 1.18  
 kh/u : 94.16  
 ko : 0.00  
 kw : 0.77  
 kg : 0.00  
 Skin : -3.81  
 m : 771.83  
 dPskin : -2550.66  
 P1hr : 545.67  
 P\* : 2090.93

Analysis By:  
 Time: 06:52:35 10 25 95

Phillips Petroleum Company

Evnt. 01, Buildup

FIELD :	SOUTH COWDEN	GAUGE :	GAUGE #20208
RSVR :	SAN ANDRES	GAUGE DEPTH:	4734
WELL :	SO. COWDEN UNIT 6-21	TEST DATE:	8/21/94
TEST :	INITIAL TEST		

SEMI-LOG ANALYSIS REPORT

Horner Plot

GENERAL INFORMATION

Y-Func: Pressure, .psia      Phase: MULTI, OIL  
X-Func: Horner Time

SEMI-LOG STRAIGHT LINE

pzero =	345.97 psia	pavg =	1152.91 psia
Slope =	771.82770	Plhr =	545.67 psia
Pstar =	2090.93 psia		

De-superposition

Slope = 0.00      Duration = 1.00000 hrs  
Cons. = 346.0 psia  
(from Log Delta Time Plot of Preceding Event)

Calculated Results

kh/u =	94.16 md.ft/cp	ko =	0.002804 md
k/u =	1.177 k/u	kw =	0.7664 md
		kg =	0.0001146 md
Skin =	-3.806	Skin,o =	-1.22
dp s =	-2550.66309 psia	Skin,g =	-1.66
ri =	490 ft (t = 259.1 hrs)	Skin,w =	-3.80

Calculated Vs. Measured qt

qt(calc) =	168.0 BBL/D	qt(meas) =	447.0 BBL/D
deviation =	-62.40 %		

RESTRAN II ANALYSIS

## RFT Pressure Data

**Well: 8-19**

**Date: 1992**

<u>Depth (msl)</u>	<u>Zone</u>	<u>Pressure</u>
-1702 ft	G	2255 psia
-1721 ft	F	2170 psia
-1723 ft	F	2171 psia
-1738 ft	E	2159 psia
-1745 ft	E	2156 psia
-1762 ft	E	2147 psia
-1777 ft	E	2175 psia
-1807 ft	D	2543 psia (?)
-1821 ft	D	2321 psia
-1842 ft	C	2241 psia
-1873 ft	B	2378 psia

---

Average = 2247 psia



## RFT Pressure Data

**Well: 6-23**

**Date: August, 1994**

<u>Depth (msl)</u>	<u>Zone</u>	<u>Pressure</u>
-1678 ft	F	2364 psia
-1696 ft	E	2318 psia
-1705 ft	E	2348 psia
-1715 ft	E	2338 psia
-1722 ft	E	2341 psia
-1763 ft	D	2369 psia
-1788 ft	C	2443 psia

---

Average = 2360 psia

## **FIGURE VII**

**FIGURE VII**  
**ENVIRONMENTAL INFORMATION**

**?? Surface elevation**

The Unit varies from 2900'-2950' above sea level.

**?? Surface conditions**

The surface area occupied by the South Cowden Unit is relatively flat and arid. There is one small area called a "buffalo Wallow" which is lower than the surrounding area and tends to stay green part of the year.

**?? Distance from navigable surface water (if < 5 mi.)**

The Unit is greater than 5 miles to navigable waters.

**?? Distance from air quality non-attainment area (if < 20 mi.)**

The closest non-attainment area is Dallas, Texas.

**?? Location (depth) of groundwater < 10,000 TDS**

The State of Texas requires that usable-quality ground water be protected from surface to 250' and from 1000' to 1400'.

**?? Depth of surface casing**

New wells have surface casing set at 1450'; however, some earlier wells only have 200'-300' of surface casing.

**?? Volume of produced water**

The Unit produced an average of 5400 BPD of water during the six month period prior to project start-up.

**?? Produced water quality (if state requires tests)**

The State of Texas does not require such tests.

**?? Produced water treatment/disposal methods used**

The produced water is skimmed to remove residual oil and treated for corrosion inhibition.

**?? Volume of drilling wastes from new wells**

Wastes from drilling wells are minimal. Nearly all of the fluids used on the new wells will be exempt under RCRA. However, trash generated and engine fluid drilling will require off-site disposal.

**?? Drilling mud content for new wells**

The mud system used for new wells will be water-based mud with the generic components being water, barite, bentonite, polymer, starch, bicarbonate, caustic soda, calcium chloride, lime, lignosulfonate, defoamer, soda ash, and lost circulation materials of cedar fiber, ground paper, mica, and walnut hulls.

**?? Drilling mud handling practice (closed system, lined pit, unlined pit)**

The wells will be drilled utilizing a lined pit. The pit will be left open to dry and then be filled.

**?? Location, size, purpose of any surface impoundments at site**

There are no impoundments at the South Cowden Unit.

**?? Results of recent mechanical integrity tests**

Recent mechanical integrity tests have found some leaks in the casing. Wells with leaks are being repaired or temporarily abandoned as appropriate as the mechanical problems are found. Approximately 40% of the wells (production and injection) have been tested recently.

**?? Results of area of review studies for injection wells**

No Results